THE ROLE OF COMPLEMENT IN MICROBIAL INFECTIONS

EDITED BY: Heribert Stoiber, Nicole Thielens, Iara De Messias Reason and Reinhard Würzner

PUBLISHED IN: Frontiers in Immunology

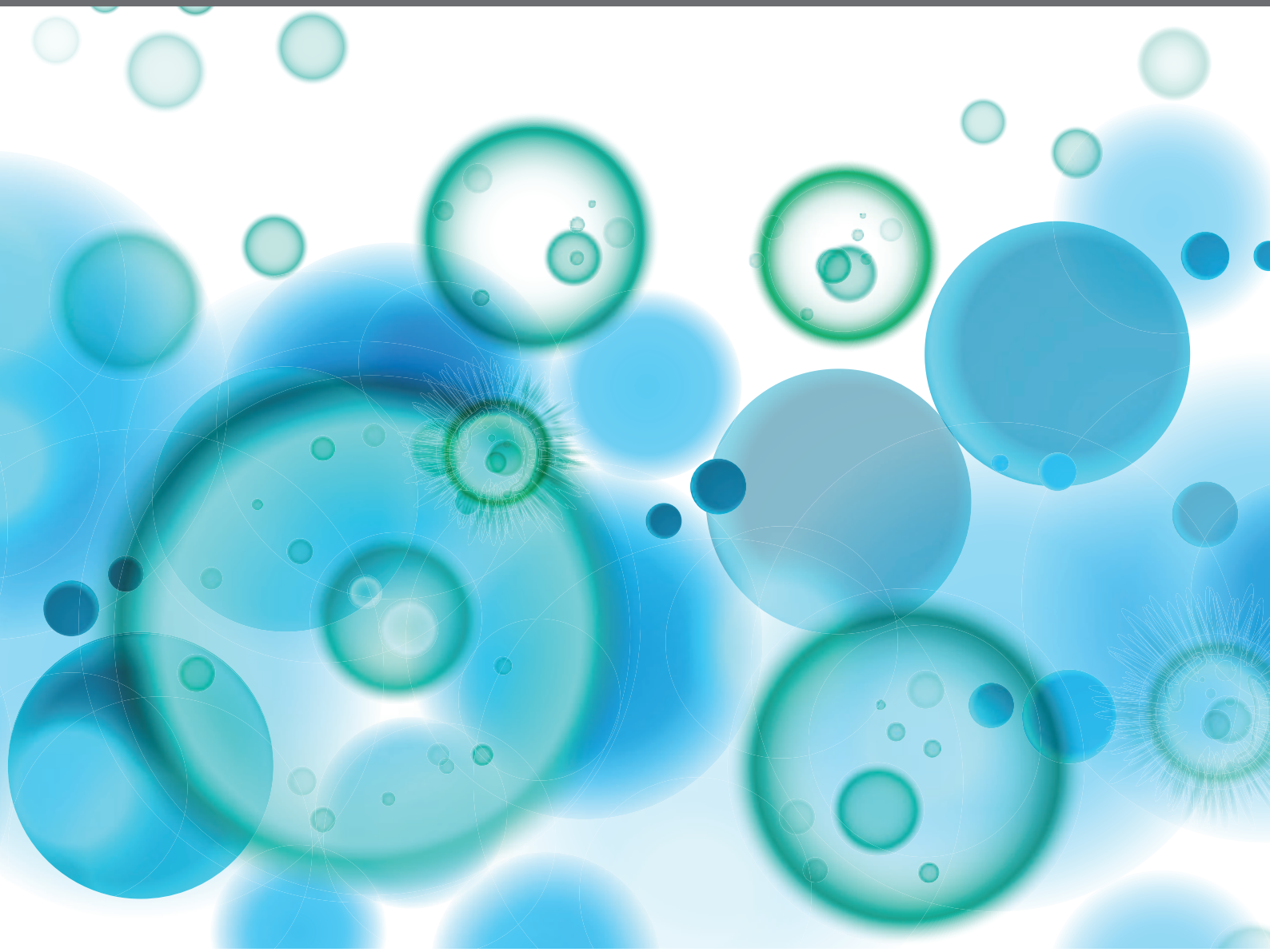

frontiers Research Topics

frontiers

ISSN 1664-8714
ISBN 978-2-88966-690-4
DOI 10.3389/978-2-88966-690-4

About Frontiers

Frontiers is more than just an open-access publisher of scholarly articles: it is a pioneering approach to the world of academia, radically improving the way scholarly research is managed. The grand vision of Frontiers is a world where all people have an equal opportunity to seek, share and generate knowledge. Frontiers provides immediate and permanent online open access to all its publications, but this alone is not enough to realize our grand goals.

Frontiers Journal Series

The Frontiers Journal Series is a multi-tier and interdisciplinary set of open-access, online journals, promising a paradigm shift from the current review, selection and dissemination processes in academic publishing. All Frontiers journals are driven by researchers for researchers; therefore, they constitute a service to the scholarly community. At the same time, the Frontiers Journal Series operates on a revolutionary invention, the tiered publishing system, initially addressing specific communities of scholars, and gradually climbing up to broader public understanding, thus serving the interests of the lay society, too.

Dedication to Quality

Each Frontiers article is a landmark of the highest quality, thanks to genuinely collaborative interactions between authors and review editors, who include some of the world's best academicians. Research must be certified by peers before entering a stream of knowledge that may eventually reach the public - and shape society; therefore, Frontiers only applies the most rigorous and unbiased reviews.
Frontiers revolutionizes research publishing by freely delivering the most outstanding research, evaluated with no bias from both the academic and social point of view. By applying the most advanced information technologies, Frontiers is catapulting scholarly publishing into a new generation.

What are Frontiers Research Topics?

Frontiers Research Topics are very popular trademarks of the Frontiers Journals Series: they are collections of at least ten articles, all centered on a particular subject. With their unique mix of varied contributions from Original Research to Review Articles, Frontiers Research Topics unify the most influential researchers, the latest key findings and historical advances in a hot research area! Find out more on how to host your own Frontiers Research Topic or contribute to one as an author by contacting the Frontiers Editorial Office: frontiersin.org/about/contact

THE ROLE OF COMPLEMENT IN MICROBIAL INFECTIONS

Topic Editors:
Heribert Stoiber, Innsbruck Medical University, Austria
Nicole Thielens, UMR5075 Institut de Biologie Structurale (IBS), France
Iara De Messias Reason, Federal University of Paraná, Brazil
Reinhard Würzner, Innsbruck Medical University, Austria

Citation: Stoiber, H., Thielens, N., De Messias Reason, I., Würzner, R., eds. (2021). The Role of Complement in Microbial Infections. Lausanne: Frontiers Media SA. doi: 10.3389/978-2-88966-690-4

Table of Contents

frontiers in Immunology

EDITORIAL
published: 04 March 2021
doi: 10.3389/fimmu.2021.640092

Editorial: The Role of Complement in Microbial Infections

Heribert Stoiber[1]*, *Nicole Thielens*[2], *Reinhard Würzner*[3] and *Iara De Messias Reason*[4]

[1] Institute of Virology, Innsbruck Medical University, Innsbruck, Austria, [2] Université Grenoble Alpes, CNRS, CEA, IBS, Grenoble, France, [3] Institute of Hygiene and Medical Microbiology, Innsbruck Medical University, Innsbruck, Austria, [4] Laboratório de Imunopatologia Molecular, Universidade Federal do Paraná, Curitiba, Brazil

Keywords: complement, pathogens, bacteria, viruses, fungi, parasites

Editorial on the Research Topic

The Role of Complement in Microbial Infections

Complement plays a major role in immune defense against all different types of pathogens, namely bacteria, viruses, fungi, and parasites. All these pathogens try to evade complement attack by numerous mechanisms. The 14 articles of this themed collection highlight the latest advances regarding this complement-pathogen relationship. A theme, which is found frequently is the binding of complement regulator proteins on the surface of pathogens to avoid complement-mediated destruction. A major regulator is hereby factor H (fH), which is recruited from fluid phase. The group of Marc Thilo Figge provided a sophisticated mathematical model, which allows quantifying fH mediated discrimination to self vs. non-self in fluid phase and steady state (Tille et al.). This dynamic model may be used to not only define critical fH concentrations on the surface of pathogens, but also to model interactions of fH mutants and their effect under pathophysiological conditions (Tille et al.).

Kristensen et al. from Copenhagen, Denmark show in a prospective, observational study that different complement factors and complement activation products could be potential prognostic markers for necrotizing soft-tissue infection (NSTI), a life-threatening condition whose early diagnosis is mandatory for successful outcome. The authors found that both complement lectin and classical pathway were depleted during NSTI due to complement activation and that complement could be a good predictor of mortality in patients with NSTI, being a promising novel prognostic tool for the disease (Kristensen et al.).

Three contributions focus on bacteria. The first by Röttgerding and Kraiczy from Frankfurt, Germany, is summarizing immune evasion strategies of relapsing fever spirochetes. Relapsing fever, a neglected arthropod-borne disease, is caused by a number of diverse human pathogenic *Borrelia* species which all inactivate complement by recruiting distinct regulatory proteins, e.g., C1 esterase inhibitor (C1-INH), C4b-binding protein (C4BP), factor H (FH), FH-like protein-1 (FHL-1), and factor H-related proteins FHR-1 and FHR-2, or by binding to individual complement components (Röttgerding and Kraiczy).

The second paper by the group of Lourdes Isaac, Sao Paolo, Brazil, is focusing on the role of properdin in immune defense against *Leptospira biflexa*. Properdin (P) is a positive regulatory protein of the complement alternative pathway (AP), recently been implicated to directly bind to the surface of certain pathogens regardless of the presence of C3bBb (Martinez et al.). In that paper the authors demonstrate direct binding of P to saprophytic *Leptospira*. Most importantly, this microorganism survives in P-depleted human serum while the addition of purified P to P-depleted human serum decreases the number of viable leptospires (Martinez et al.).

Edited by:
Ulrich Emil Schaible, Research Center Borstel (LG), Germany

Reviewed by:
David M. Mosser, University of Maryland, College Park, United States

***Correspondence:**
Heribert Stoiber
heribert.stoiber@i-med.ac.at

Specialty section:
This article was submitted to Microbial Immunology, a section of the journal Frontiers in Immunology

Received: *10 December 2020*
Accepted: *29 January 2021*
Published: *04 March 2021*

Citation:
Stoiber H, Thielens N, Würzner R and De Messias Reason I (2021) Editorial: The Role of Complement in Microbial Infections. Front. Immunol. 12:640092. doi: 10.3389/fimmu.2021.640092

The third paper from the group of Jeane Eliete Laguila Visentainer from Maringa, Brazil assesses the association of MBL2 exon 1 polymorphisms with multibacillary leprosy (Tiyo et al.). Mannose-binding lectin (MBL), a recognition protein of the lectin pathway, plays a major role in innate anti-microbial immunity. Different variants on exon 1 of the gene coding for MBL (*MBL2*) influence MBL serum level. In a case-control study including 350 leprosy patients from Southern Brazil, the authors found an association of *MBL2* B variant with a higher risk for development of multibacillary (MB) leprosy. In addition, the TGG and CAG haplotypes presented an increased susceptibility to develop leprosy in general and MB disease, in women, which was not observed in the male population (Tiyo et al.).

Four contributions deal with viruses. The first two by the group of Posch et al., Innsbruck, Austria; in Bermejo-Jambrina et al. they investigated the effect of complement opsonization of HIV-1, which has been shown to enhance infection of dendritic cells (DCs) while enhancing anti-viral immune response. Here they further deciphered the underlying mechanisms by studying the individual role of complement receptors CR3 and CR4. THP-1 cells knocked-out for CD11b (CR3) and CD11c (CR4) were generated using the CRISPR-Cas9 technology and differentiated into THP1-DCs. Evidence is provided for distinct and opposite roles of CR3 and CR4, the latter playing a major role in the inflammatory and anti-viral responses triggered by complement-opsonized HIV (Bermejo-Jambrina et al.). The role of complement receptors was summarized in an additional contribution of this group (Posch et al.) focusing on HIV and DCs. This comprehensive review discussed recent finding and gave a summary of the high potential of DCs primed with complement-opsonized HIV to initiates efficient antiviral and cytotoxic anti-HIV immunity (Posch et al.).

The second review, which focuses on complement-virus interactions was provided by the group of John Bernet Johnson, Thiruvananthapuram, India and addressed the interaction of complement with RNA viruses from a more general point of view (Kumar et al.). The authors discussed all aspects of complement RNA virus interactions from complement activation, to interactions of opsonized RNA viruses with complement receptors and mechanisms to escape from complement-mediated lysis (Kumar et al.).

Malekshahi et al. from Innsbruck, Austria provided evidence that the envelope (E) protein of Zika virus directly bind to proteins of the terminal pathway of complement and interferes with the formation of the membrane-attack complex (MAC). The authors showed that both NS1 and the E proteins work synergistically to protect the virus by limiting MAC formation and thus reducing complement-mediated damage (Malekshahi et al.).

Two contributions focus on fungi. Deshmukh et al. from Innsbruck, Austria, investigated the interaction of Aspergillus-derived galactosaminogalactan (GAG) with platelets and the subsequent complement activation. This effect was exclusively induced by GAG from A. fumigatus and not observed with other Aspergillus species or several Mucorales tested. The induction of C3a and C5a, pro-inflammatory cytokines and the detection of C5b-C9 complexes on platelets might contribute to the reduced number of these cells and this might provide an explanation for the excessive inflammation, thrombocytopenia, and thrombosis observed in infected patients (Deshmukh et al.). The group of Cornelia Speth, Innsbruck, Austria added a further paper to the Research Topic focusing on new aspects on the interaction of Candida and complement (Harpf et al.). Beside reviewing several escape mechanisms from the activated complement system by *C. albicans*, recent findings on the interplay between non-albicans C.-species such as *C. auris* were highlighted (Harpf et al.).

Parasites were the final group of pathogens, which were addressed by three contributions. The group of Jörg Köhl, Lübeck, Germany, investigated the role of C5a/C5aR1 axis activation for early immune responses in a mouse model of *Toxoplasma gondii* (*T. gondii*) infection. *C5ar1–/–* mice suffered from more severe disease progression, which was associated with reduced concentrations of IL-12, IL-27, and IFN-γ in serum (Briukhovetska et al.). This resulted not only in decreased frequency of IFN-γ+ NK cells in the spleen, but also reduced IL12 production by splenic DCs, which is important for IFN-γ production and subsequent iNOS expression in the brain to control acute *T. gondii* infection (Briukhovetska et al.).

Among the virulence factors of *Trypanosoma cruzi* (*T. cruzi*) with a capacity to inhibit complement activation is T. cruzi calreticulin (TcCalr). Ramirez-Toloza et al., Santiago, Chile, and colleagues reviewed the mechanisms by which TcCalr blocks either, the classical or lectin pathway. In addition, they addressed recent findings indicating that TcCalr inhibits angiogenesis, promotes wound healing and reduces tumor growth. As other parasites express Calr, too, the detailed understanding of the role of this virulence factor may provide new strategies to develop anti-parasite therapies and prophylaxis (Ramirez-Toloza et al.).

The manuscript presented by Shao et al. adds a piece of interesting data on the modulation of complement activation by a helminth parasite. The authors showed that a calreticulin protein secreted by *Trichinella spiralis,* TsCRT, interacts with human complement C1q through its S-domain inhibiting C1q-mediated complement activation (1). Furthermore, TsCRT-S was able to inhibit neutrophil activation as well as formation of ROS and neutrophil NETs *in vitro*. The authors suggest a potential therapeutic effect of TsCRT-S in the treatment of C1q/immune complex-related autoimmune and inflammatory diseases (1).

In summary, all published articles provide new exciting data of complement-pathogen interactions and help to elucidate additional pieces of the fascinating jigsaw.

AUTHOR CONTRIBUTIONS

All authors listed have made a substantial, direct and intellectual contribution to the work, and approved it for publication.

FUNDING

RW and HS was supporting by the FWF (W-1253 DK HOROS).

REFERENCES

1. Chen Y, Shao S, Huang J, Gu Y, Cheng Y, Zhu X. Therapeutic efficacy of a *Trichinella spiralis* paramyosin-derived peptide modified with a membrane-targeting signal in mice with antigen-induced arthritis. *Front Microbiol.* (2020) 11:608380. doi: 10.3389/fmicb.2020.608380

Conflict of Interest: The authors declare that the research was conducted in the absence of any commercial or financial relationships that could be construed as a potential conflict of interest.

frontiers in Immunology

ORIGINAL RESEARCH
published: 31 January 2020
doi: 10.3389/fimmu.2020.00017

Complement Activation Is Associated With Mortality in Patients With Necrotizing Soft-Tissue Infections—A Prospective Observational Study

Markus Korsholm Kristensen[1], *Marco Bo Hansen*[1,2], *Martin Bruun Madsen*[3], *Cecilie Bo Hansen*[1], *Katrine Pilely*[1], *Ole Hyldegaard*[2,3] *and Peter Garred*[1]*

[1] Laboratory of Molecular Medicine, Department of Clinical Immunology, Rigshospitalet, University Hospital of Copenhagen, Copenhagen, Denmark, [2] Department of Anesthesia, Center of Head and Orthopedics, Rigshospitalet, University Hospital of Copenhagen, Copenhagen, Denmark, [3] Department of Intensive Care, Rigshospitalet, University Hospital of Copenhagen, Copenhagen, Denmark

OPEN ACCESS

Edited by:
Iara De Messias Reason,
Federal University of Paraná, Brazil

Reviewed by:
Goran Zoran Stanojević,
University of Niš, Serbia
László Cervenak,
Semmelweis University, Hungary

***Correspondence:**
Peter Garred
peter.garred@regionh.dk

Specialty section:
This article was submitted to Microbial Immunology, a section of the journal Frontiers in Immunology

Received: 31 October 2019
Accepted: 07 January 2020
Published: 31 January 2020

Citation:
Kristensen MK, Hansen MB, Madsen MB, Hansen CB, Pilely K, Hyldegaard O and Garred P (2020) Complement Activation Is Associated With Mortality in Patients With Necrotizing Soft-Tissue Infections—A Prospective Observational Study. Front. Immunol. 11:17. doi: 10.3389/fimmu.2020.00017

Aim: We assessed whether different complement factors and complement activation products were associated with poor outcome in patients with necrotizing soft-tissue infection (NSTI).

Methods: We conducted a prospective, observational study in an intensive care unit where treatment of NSTI is centralized at a national level. In 135 NSTI patients and 65 control patients, admission levels of MASP-1, MASP-2, MASP-3, C4, C3, complement activation products C4c, C3bc, and terminal complement complex (TCC) were assessed.

Results: The 90-day mortality was 23%. In a Cox regression model adjusted for sex, and SAPS II, a higher than median MASP-1 (HR 0.378, CI 95% [0.164–0.872], $p = 0.0226$) and C4 (HR 0.162, 95% CI [0.060–0.438], $p = 0.0003$), C4c/C4 ratio (HR 2.290 95% CI [1.078–4.867], $p = 0.0312$), C3bc (HR 2.664 95% CI [1.195–5.938], $p = 0.0166$), and C3bc/C3 ratio (HR 4.041 95% CI [1.673–9.758], $p = 0.0019$) were associated with 90-day mortality, while MASP-2, C4c, C3, and TCC were not. C4 had the highest ROC-AUC (0.748, [95% CI 0.649–0.847]), which was comparable to the AUC for SOFA score (0.753, [95% CI 0.649–0.857]), and SAPS II (0.862 [95% CI 0.795–0.929]).

Conclusion: In adjusted analyses, high admission levels of the C4c/C4 ratio, C3bc, and the C3bc/C3 ratio were significantly associated with a higher risk of death after 90 days while high admission levels of MASP-1 and C4 were associated with lower risk. In this cohort, these variables are better predictors of mortality in NSTI than C-reactive protein and Procalcitonin. C4's ability to predict mortality was comparable to the well-established scoring systems SAPS score II and SOFA on day 1.

Keywords: necrotizing fasciitis, soft tissue infection, sepsis, amputation, survival complement activation, immune system

INTRODUCTION

Necrotizing soft-tissue infections (NSTIs) are infections with a necrotizing component involving any or all layers of the soft tissue compartment (1). They are rapidly progressive and can lead to sepsis, multisystem organ failure, and in 8–49% death (2). Surgical removal of all necrotic tissue is essential for survival and time to surgery an important determinant for the outcome (3–6). Yet it is common for patients to have additional areas of necrosis, and therefore require multiple operations with serial exploration and debridement until the infection is controlled (7). In 16% of patients, amputation is necessary (5).

If we had reliable tools to identify the patients requiring extensive surgery and discriminate them from the low-risk patients, we could improve survival rates, and avoid the extensive surgery in low-risk patients that currently leads to functional limitations in 30% of patients (8).

It is reasonable to look for such biomarkers in the complement system. Complement plays a crucial role in the microbial defense by mediating opsonization, sequestration, and lysis of pathogens (9), bridges the innate and adaptive system (10), and is activated by apoptotic and necrotic tissue (11). Uncontrolled complement activation is part of the hyperinflammatory response seen in sepsis and sepsis-related coagulopathy (12).

The complement system is divided into three converging proteolytic cascades; the classical, the lectin, and the alternative pathways. We have previously investigated the use of the lectin pathway initiator molecules and kinetic complement analyses as prognostic markers in NSTI patients (13), suggesting that pattern recognition molecules of the lectin pathway play an important role in these patients. Here, we further investigate the levels the lectin pathway associated enzymes MASP-1, MASP-2, MASP-3, the down-stream components C4, C3, the complement activation products C4c, C3bc, and the fluid phase analog of the terminal C5b-9 complement complex (TCC) in NSTI patients and a group of non-infected control patients.

MATERIALS AND METHODS

Study Design and Setting

This prospective, observational study was conducted from February 2013 to March 2015 at the Copenhagen University Hospital (Rigshospitalet) where the national treatment of NSTI has been centralized. This is a substudy of the European INFECT project (ClinicalTrials.gov Identifier: NCT01790698).

Patients were screened at arrival to Rigshospitalet. Inclusion criteria were: (1) NSTI based on surgical findings with necrosis engaging any layers of the soft tissue compartments and (2) age ≥18 years. Patients were excluded if the NSTI diagnosis could not be confirmed during surgery.

Control patients were eligible for inclusion if they were: (1) undergoing elective orthopedic surgery at Rigshospitalet; and (2) were aged ≥18 years. Patients with ongoing infection or inflammatory conditions were excluded.

Data Collection

We obtained clinical data from electronic records on age, sex, body mass index, chronic disease (diabetes, liver cirrhosis, chronic kidney disease, cardiovascular disease, chronic obstructive, pulmonary disease, peripheral vascular disease, immune deficiency, malignancy, rheumatoid disease), primary site of infection, microorganism, biochemistry, treatment, and the intensive care unit scoring systems; Simplified Acute Physiology Score II (SAPS II) and Sequential Organ Failure Assessment (SOFA) score day 1. SOFA score was altered as the Glasgow Coma Scale score was omitted. Vital status and time of death, if relevant, were extracted from the hospital database linked to the Danish Civil Registration System. The decision to amputate was based on the surgeon's evaluation. No protocol for amputation was used.

Standard blood analyses including platelet count, creatinine, leucocyte count, and C-reactive protein (CRP) levels were performed at the Department of Clinical Biochemistry, Rigshospitalet, as part of routine analyses, whereas sodium, potassium, hemoglobin, lactate, pH, base excess, pO_2, and pCO_2 were measured using an ABL 725 (Radiometer, Copenhagen, Denmark).

Upon admission, blood was drawn from an arterial line or central venous catheter into 9-mL vacuum tubes containing EDTA. For the control group, venous blood samples were drawn preoperatively. The samples were immediately put on ice until plasma was seperated from whole blood by centrifugation (within 40 min) at 2,400 G for 10 min and subsequently stored at −80°C.

MASPs, C4c, C3bc, and TCC were measured in the samples by Enzyme-linked Immunosorbent assays (ELISAs). MASP-1 and MASP-2 plasma levels were measured using commercial ELISA kits (MASP-1: USCN Life Sciences; catalog#: SEB895Hu, MASP-2: HycultBiotech Catalog #: HK326-02), as recommended by the manufacturer. Plasma levels of MASP-3, C4c, C3bc, and TCC were measured using previously described in house sandwich ELISAs (14–17). Total plasma concentrations of C4 and C3 were measured using an automated turbidimetric protein analyzer according to the manufacturer's instructions (SPAPLUS®, the Binding Site group LDT, Birmingham, UK).

Outcome Measures

Our primary analysis was the association between complement parameters measured upon admission, 90-day mortality, and disease severity. We compared patients with septic shock vs. patients without, amputated vs. non-amputated patients and survivors vs. non-survivors. Septic shock was defined according to the criteria of Bone et al. (18). Amputation was defined as any amputation of a limb or penis.

Secondarily, we dichotomized every complement parameter by its median and investigated for associations with 90-day mortality. Patients were followed from inclusion until death, loss to follow up or March 2015, whichever came first.

Abbreviations: AUC, area under the curve; CI, confidence interval; CRP, C-reactive protein; ELISA, enzyme-linked immunosorbent assays; HR, hazard ratio; IQR, interquartile range; NSTI, necrotizing soft-tissue infection; P, *p*-value; PRMs, pattern recognition molecules; ROC, Receiver Operating Characteristics; SAPS II, Simplified Acute Physiology Score II; SOFA, Sequential Organ Failure Assessment; suPAR, soluble urokinase plasminogen activator receptor; TCC, terminal C5b-9 complement complex.

Statistical Analyses

The significance level was set at 0.05. Kolmogorov-Smirnov and Shapiro-Wilk normality tests were performed for all variables. Due to non-parametric distribution, continuous data were reported as median (IQR) and compared by the Kruskal–Wallis test. For *ad-hoc* pairwise analyses, we used Dunn's test. For categorical data, we reported absolute numbers, with proportions in parentheses, and used Pearson's chi-square test or Fisher's exact test for comparisons.

The prognostic value of the complement parameters for 90-day-mortality was investigated using Cox regression. For multivariate analysis, the first model was adjusted for sex and SAPS II, the second for age, sex, chronic disease (yes/no), and SAPS II. Data from the Cox analyses were presented as hazard ratios (HR) with 95 % confidence intervals (95% CI). The proportional hazard assumption was met for all parameters in our regression models. We were unable to calculate SAPS II in five patients due to missing data. These patients were excluded from the multivariate analysis. Receiver operating characteristic (ROC) curves with area under the curve (AUC) were reported for the complement parameters for 90-day mortality. Nine patients were excluded from the ROC analyses due to missing SAPS II, pH, base excess, or lactate. Statistical analyses were performed using SAS 9.4 (SAS Institute Inc., Cary, NC).

RESULTS

We included 135 NSTI patients (**Figure 1**) and 65 control patients, matched for age and sex. Ninety-six patients (71%) had septic shock, amputation was undertaken in 27 cases (20%), and 31 patients (23%) died within 90 days. **Table 1** displays differences in the clinical data between surviving and non-surviving patients.

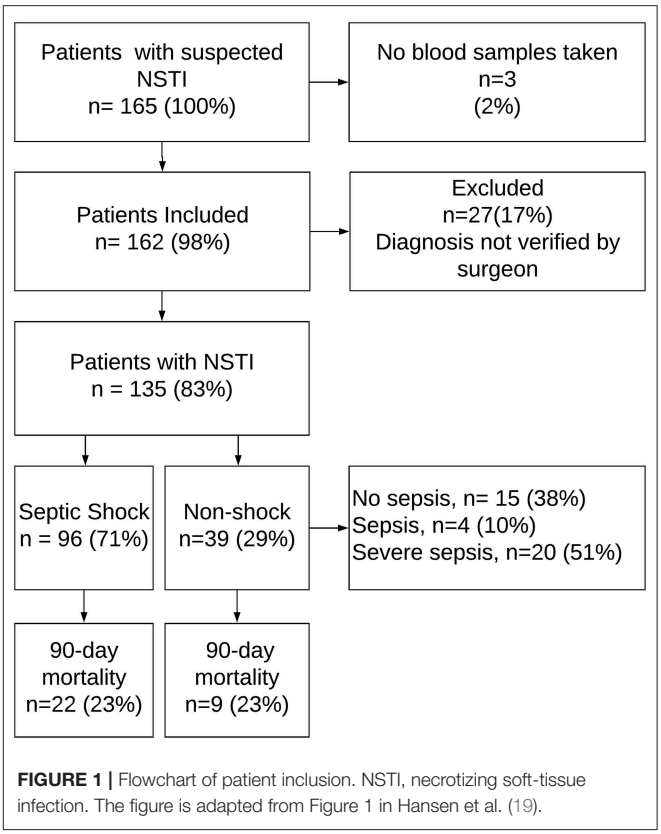

FIGURE 1 | Flowchart of patient inclusion. NSTI, necrotizing soft-tissue infection. The figure is adapted from Figure 1 in Hansen et al. (19).

Complement Levels and NSTI Severity

MASP-1, C4, C4c, C3, decreased gradually, and C3bc/C3 levels increased gradually from controls to survivors, and from survivors to non-survivors, with significant differences both overall (Kruskal Wallis, $p < 0.0003$, $p < 0.0001$, $p < 0.0001$, $p < 0.0001$, and $p < 0.0001$, respectively), and between all groups as revealed by the *ad-hoc* test (**Table 2**). MASP-2 levels differed significantly between the groups (Kruskal Wallis, $p = 0.0025$). The *ad-hoc* analysis revealed that MASP-2 was significantly lower in non-survivors compared to survivors and controls but did not differ between controls and survivors. MASP-3 and TCC differed significantly between the groups (Kruskal Wallis, $p < 0.0001$). The *ad-hoc* test showed significantly lower MASP-3 and higher TCC levels in surviving and non-surviving patients when compared to controls resulting in an overall difference between the groups (Kruskal Wallis, $p < 0.0001$).

Table 3 displays the differences in the complement parameters across control patients and NSTI patients with and without septic shock. The median MASP-1 and C4c levels differed significantly between the groups (Kruskal Wallis, $p = 0.0017$ and $p < 0.0001$), and the *ad-hoc* analyses revealed significantly lower levels in shock patients compared to controls. There was a significant difference in median MASP-2 level between controls, non-shock and shock patients (Kruskal Wallis, $p = 0.0390$), but with no differences in the pairwise *ad-hoc* analyses. The levels of MASP-3, C4, and C3bc/C3 differed significantly between the groups (Kruskal Wallis, $p < 0.0001$, $p < 0.0001$, and $p = 0.0002$, respectively), with *ad-hoc* analyses showing significantly lower levels in non-shock and shock patients compared with controls. The C3 levels decreased gradually, from controls to non-shock, and from non-shock to septic shock with significant differences both overall (Kruskal Wallis, $p < 0.0001$), and between all groups as revealed by the *ad-hoc* test. Similarly, the median TCC levels increased gradually from the control patients to non-shock and non-shock to shock patients with significant differences both overall (Kruskal Wallis, $p < 0.0001$), and between all groups as revealed by *ad-hoc* analyses.

Admission levels of C4, C4c, and C3 were lower in patients who underwent amputation vs. non-amputated ($p = 0.0081$, 0.0066, 0.0464, respectively; **Supplementary Table 1**).

Survival Analysis

Univariate Analysis

The univariate models revealed that an increase in age, SOFA score, and SAPS II were associated with a higher hazard of death before 90-days. Chronic disease and amputation were not associated with mortality (**Supplementary Table 2**). Regarding the complement parameters, significant associations with 90-day

TABLE 1 | Clinical data in survivors and non-surviving necrotizing soft-tissue infection patients.

Variable	Total NSTI patients (*N* = 135)	Survivors (*N* = 104)	Non-survivors (*N* = 31)	*p*-value
Age, years	61.0 [52.0–69.0]	61.0 [50.0–67.5]	67.0 [58.0–70.0]	0.0693
Sex, male	84 (62.2)	63 (60.6)	21 (67.7)	0.4702
Body mass index, *kg/m*^{2}[a]	26.1 [23.5–31.1]	25.6 [23.4–30.9]	27.8 [24.8–33.6]	0.0660
Active smoker	40 (29.6)	34 (32.7)	6 (19.4)	0.3023
High alcohol consumption[ab]	19 (19.6)	17 (22.4)	2 (9.5)	0.1892
Chronic disease	86 (63.7)	63 (60.6)	23 (74.2)	0.1664
Cardiovascular disease	58 (43.0)	41 (39.4)	17 (54.8)	0.1281
Chronic obstructive pulmonary disease	14 (10.4)	9 (8.7)	5 (16.1)	0.2308
Chronic kidney disease	12 (8.9)	6 (5.8)	6 (19.4)	0.0197
Diabetes	30 (22.2)	20 (19.2)	10 (32.3)	0.1257
Immune deficiency/AIDS	3 (2.2)	3 (2.9)	0 (0.0)	1.0000F
Liver cirrhosis	5 (3.7)	3 (2.9)	2 (6.5)	0.3236F
Malignancy	15 (11.1)	12 (11.5)	3 (9.7)	0.7723
Peripheral vascular disease	20 (14.8)	13 (12.5)	7 (22.6)	0.1655
Rheumatoid disease	10 (7.4)	8 (7.7)	2 (6.5)	0.8169
Hemoglobin, *mmol/L*, *lowest value*	2.2 [1.2–4.5]	1.9 [1.2–3.2]	4.3 [1.6–14.5]	0.0017
Na^{+}, *mmol/L*, *lowest value*	5.7 [4.9–6.5]	5.8 [5.0–6.6]	5.2 [4.3–6.1]	0.0216
K^{+}, *mmol/L*, *lowest value*	136.0 [132.0–138.0]	136.0 [132.0–138.0]	135.0 [131.0–139.0]	0.9979
Glucose, *mmol/L*, *highest value*	4.3 [4.0–4.9]	4.3 [4.0–4.6]	4.8 [3.8–5.5]	0.0617
Creatinine μmol/l, *highest value*[a]	8.3 [7.1–11.5]	8.3 [7.1–11.5]	8.2 [6.7–14.5]	0.8856
pO_2, *kPa, from lowest* PaO_2/FiO_2 *ratio*[a]	119.0 [77.0–205.0]	101.0 [72.0–166.0]	216.0 [128.0–262.0]	0.0003
pH, *lowest value*	13.7 [10.9–19.6]	13.2 [10.9–18.6]	14.0 [9.4–22.3]	0.8351
Base excess, *mmol/L*, *lowest value*[a]	7.3 [7.2–7.4]	7.3 [7.2–7.4]	7.2 [7.1–7.3]	0.0014
Lactate, *mmol/L*, *highest value*	−5.5 [−9.4–−1.8]	−4.8 [−7.7–−1.6]	−10.2 [−13.9–−5.1]	0.0003
Steroid treatment[a]	16 (11.9)	9 (8.7)	7 (23.3)	0.0825F
Immunosupressing drugs[a]	12 (9.0)	10 (9.6)	2 (6.7)	1.0000F
Ventilator treatment	122 (90.4)	91 (87.5)	31 (100.0)	0.0384F
Renal replacement therapy	34 (25.2)	18 (17.3)	16 (51.6)	0.0001
Amputation	27 (20.0)	18 (17.3)	9 (29.0)	0.1520
Septic shock[c]	96 (71.1)	74 (71.2)	22 (71.0)	0.9840
SAPS II[a]	45.0 [35.0–52.0]	40.5 [32.0–48.5]	59.0 [48.0–76.0]	<0.0001
SOFA score day 1[a]	7.0 [4.0–9.0]	7.0 [4.0–9.0]	10.0 [8.0–12.0]	<0.0001
Primary site of infection				
Head/neck	21 (15.6)	16 (15.4)	5 (16.1)	0.9200
Chest	5 (3.7)	3 (2.9)	2 (6.5)	0.3236F
Abdomen	11 (8.1)	8 (7.7)	3 (9.7)	0.7229
Genitals/Perineum	36 (26.7)	31 (29.8)	5 (16.1)	0.1306
Upper extremity	15 (11.1)	14 (13.5)	1 (3.2)	0.1115
Lower extremity	47 (34.8)	32 (30.8)	15 (48.4)	0.0707
Microbiology				
Positive tissue or blood cultures	102 (75.6)	78 (75.0)	24 (77.4)	0.7832
Polymicrobial infection[a]	57 (55.9)	43 (55.1)	14 (58.3)	0.7821
Staphylococcus aureus[a]	17 (16.7)	13 (16.7)	4 (16.7)	1.0000F
Group A Streptococcus[a]	36 (35.3)	32 (41.0)	4 (16.7)	0.0290
Gram negative rods[a]	27 (26.5)	18 (23.1)	9 (37.5)	0.1613
Obligate anaerobes[a]	32 (31.4)	24 (30.8)	8 (33.3)	0.8129
Other bacteria[a]	21 (20.6)	15 (19.2)	6 (25.0)	0.5410F

Values presented as Median [IQR] or N (column %) with Fisher's Exact-test (F) or Pearson's chi-square test.

[a]*Data not available for all subjects. Missing values: Body mass index (n = 5): High alcohol consumption (n = 38), creatinine (n = 4),* pO_2 *(n = 10), pH (n = 5), base excess (n = 5), lactate (n = 5), SOFA score (n = 6), steroid treatment (n = 1), Immunosuppresing drugs (n = 1), SAPS II (n = 5), SOFA score day 1 (n = 6), and positive tissue or blood cultures (n = 33).*

[b]*High alcohol consumption: >14 units of alcohol/week (women); >21 units of alcohol/week (men).*

[c]*Septic shock as defined by sepsis criteria by Bone et al. (18).*

SAPS II, Simplified Acute Physiology Score II; SOFA, Sequential Organ Failure Assessment; NSTI, Necrotizing soft tissue infection.

TABLE 2 | Complement, leukocytes, and albumin in controls, surviving and non-surviving necrotizing soft-tissue infection patients.

Variable	Total (*N* = 135)	Controls (*N* = 65)	NSTI survivors (*N* = 104)	NSTI non-survivors (*N* = 31)	*p*-value
MASP-1, *AU/L*	7.6 [6.5–8.9]	8.7 [7.5–10.2][ab]	7.8 [6.8–9.0][cb]	7.0 [5.8–8.0][ca]	0.0003
MASP-2, *AU/L*	793.4 [504.1–1121.0]	977.5 [623.3–1464.3][b]	874.5 [568.8–1182.5][b]	551.9 [404.6–849.4][ca]	0.0025
MASP-3, *AU/L*	65.4 [47.5–100.5]	109.3 [87.9–130.1][ab]	64.3 [46.5–100.1][c]	67.6 [56.6–104.8][c]	<0.0001
C4, *g/L*[d]	0.17 [0.14–0.24]	0.24 [0.20–0.31][ab]	0.19 [0.15–0.26][cb]	0.13 [0.11–0.17][ca]	<0.0001
C4c *AU/L*	134.6 [87.3–199.0]	194.7 [130.9–326.5][ab]	150.4 [96.2–210.3][cb]	99.6 [69.8–158.9][ca]	<0.0001
C4c/C4[d]	752.9 [507.1–1165.8]	855.3 [569.8–1391.0]	720.2 [496.5–1163.0]	791.5 [571.3–1250.6]	0.2793
C3, *g/L*[d]	0.93 [0.75–1.2]	1.2 [1.1–1.4][ab]	0.96 [0.79–1.2][cb]	0.79 [0.56–0.98][ca]	<0.0001
C3bc, *AU/L*	15.7 [9.2–24.2]14.7 [9.1–22.0]	12.5 [9.1–18.4]	15.2 [9.0–22.0]	17.7 [9.5–26.4]	0.1091
C3bc/C3[d]	16.5 [10.3–27.0]	10.7 [7.7, 14.7][ab]	14.9 [9.8, 21.7][cb]	24.3 [16.5, 40.6][ca]	<0.0001
TCC, *AU/L*	1.5 [1.00–2.6]	0.35 [0.26–0.46][ab]	1.5 [0.97–2.6][c]	1.5 [1.1–2.7][c]	<0.0001
Leukocyte count, *× 10/l, highest value*	16.9 [10.4–23.9]	7.2 [6.3–9.3][ab]	16.5 [11.1–23.1][c]	18.3 [8.5–27.2][c]	<0.0001
C-reactive protein, *mg/L*[d]	222.0 [141.0–298.0]	2.0 [1.00–4.0][ab]	224.5 [169.0–306.5][cb]	165.0 [83.0–259.0][ca]	<0.0001
Albumin, *g/L*	20.0 [16.0–22.0]	39.0 [36.0–41.0][ab]	20.0 [16.5–22.5][c]	19.0 [15.0–21.0][c]	<0.0001

Values presented as Median [IQR] with Kruskal-Wallis test. A significance level of 0.0167 was used for pairwise ad-hoc comparisons.
[a]*Significantly different from NSTI survivors.*
[b]*Significantly different from NSTI non-survivors.*
[c]*Significantly different from controls.*
[d]*Data not available for all subjects. Missing values: C4 (n = 4), C4c/C4 (n = 4) C3 (n = 4), C3bc/c3 (n=4), leukocyte count (n = 3), and CRP (n = 4).*
NSTI, necrotizing soft-tissue infection.

TABLE 3 | Complement, leukocytes, and albumin in controls and necrotizing soft-tissue infection patients with and without septic shock.

Variable	Total (*N* = 135)	Controls (*N* = 65)	Non-shock (*N* = 39)	Septic shock (*N* = 96)	*p*-value
MASP-1, *AU/L*	7.6 [6.5–8.9]	8.7 [7.5–10.2][a]	8.4 [6.8–9.3]	7.4 [6.3–8.7][b]	0.0017
MASP-2, *AU/L*	793.4 [504.1–1121.0]	977.5 [623.3–1464.3]	905.1 [551.9–1422.5]	717.3 [487.6–1015.0]	0.0390
MASP-3, *AU/L*	65.4 [47.5–100.5]	109.3 [87.9–130.1][ca]	65.4 [48.4–86.2][b]	65.5 [46.5–113.7][b]	<0.0001
C4, *g/L*[d]	0.17 [0.14–0.24]	0.24 [0.20–0.31][ca]	0.17 [0.14–0.26][b]	0.17 [0.13–0.24][b]	<0.0001
C4c *AU/L*	134.6 [87.3–199.0]	194.7 [130.9–326.5][a]	158.2 [106.1–261.4]	125.9 [80.7–188.8][b]	<0.0001
C4c/C4[d]	752.9 [507.1–1165.8]	855.3 [569.8–1391.0]	958.6 [522.1–1442.3]	671.5 [506.0–1086.0]	0.0828
C3, *g/L*[d]	0.93 [0.75–1.2]	1.2 [1.1–1.4][ca]	1.04 [0.82–1.4][ba]	0.89 [0.73–1.08][bc]	<0.0001
C3bc, *AU/L*	15.7 [9.2–24.2]14.7 [9.1–22.0]	12.5 [9.1–18.4]	17.0 [9.5–22.4]	15.6 [9.1–24.2]	0.2460
C3bc/C3[d]	16.5 [10.3–27.0]	10.7 [7.7,14.7][ca]	15.2 [9.3,23.0][b]	16.7 [10.4,27.3][b]	0.0002
TCC *AU/L*	1.5 [1.00–2.6]	0.35 [0.26–0.46][ca]	1.3 [0.68–1.8][ba]	1.7 [1.1–2.8][bc]	<0.0001
Leukocyte count, × 10/l, *highest value*	16.9 [10.4–23.9]	7.2 [6.3–9.3][ca]	15.5 [9.7–22.7][b]	17.6 [12.3–24.4][b]	<0.0001
C-reactive protein, *mg/L*[d]	222.0 [141.0–298.0]	2.0 [1.00–4.0][ca]	201.0 [134.0–275.0][b]	222.0 [154.0–301.5][b]	<0.0001
Albumin, *g/L*	20.0 [16.0–22.0]	39.0 [36.0–41.0][ca]	21.0 [18.0–23.0][b]	18.5 [15.0–22.0][b]	<0.0001

Values presented as Median [IQR] with Kruskal-Wallis test. A significance level of 0.0167 was used for pairwise ad-hoc comparisons. Septic shock defined by criteria of Bone et al. (18).
[a]*Significantly different from Septic Shock.*
[b]*Significantly different from controls.*
[c]*Significantly different from non-shock.*
[d]*Data not available for all subjects. Missing values: C4 (n = 4), C4c/C4 (n = 4) C3 (n = 4), C3bc/c3 (n = 4), leukocyte count (n = 3), and CRP (n = 4).*

mortality were found for MASP-1 (HR 0.372, 95% CI [0.171–0.808], $p = 0.0125$), MASP-2 (HR 0.297, 95% CI [0.133–0.666], $p = 0.0032$), C4 (HR 0.215, 95% CI [0.088–0.525], $p = 0.0007$), C4c (HR 0.371, 95% CI [0.171–0.806], $p = 0.0123$), C3 (HR 0.434, 95% CI [0.204–0.921], $p = 0.0297$), and C3bc/C3 (HR 3.283, 95% CI [1.468–7.344], $p = 0.0038$; **Table 4**).

Multivariate Analysis

When adjusting the models for sex and SAPS II a level above the median MASP-1 (HR 0.378, CI 95% [0.164–0.872], $p = 0.0226$) and C4 (HR 0.162, 95% CI [0.060–0.438], $p = 0.0003$) remained significantly associated with lower 90-day mortality (**Table 4**). Additionally, a level above the median C4c/C4 ratio (HR 2.290 95% CI [1.078–4.867], $p = 0.0312$), C3bc (HR 2.664 95% CI [1.195–5.938], $p = 0.0166$), and C3bc/C3 ratio (HR 4.041 95% CI [1.673–9.758], $p = 0.0019$) were associated with an increased mortality. The remaining complement parameters were not associated with death in the adjusted models.

In a model where we adjusted for age, sex, chronic disease, and SAPS II, the same complement parameters yielded significant

TABLE 4 | Cox regression analyses for 90-day mortality.

		Unadjusted			Adjusted for sex, SAPS II			Adjusted for age, sex, chronic disease, and SAPS II		
Variables grouped by their medians		**HR**	**95% CI**	***P*-value**	**HR**	**95% CI**	***P*-value**	**HR**	**95% CI**	***P*-value**
MASP-1	≤7.63 *AU/L*	1.000			1.000			1.000		0.0251
	>7.63 *AU/L*	0.372	[0.171–0.808]	0.0125	0.378	[0.164–0.872]	0.0226	0.368	[0.153–0.882]	
MASP-2	≤793.36 *AU/L*	1.000			1.000			1.000		0.0936
	>793.36 *AU/L*	0.297	[0.133–0.666]	0.0032	0.475	[0.202–1.119]	0.0886	0.473	[0.197–1.135]	
MASP-3	≤65.39 *AU/L*	1.000			1.000			1.000		0.3232
	>65.39 *AU/L*	1.133	[0.560–2.291]	0.7289	1.497	[0.710–3.157]	0.2896	1.466	[0.686–3.133]	
C4	≤0.17 *g/L*	1.000			1.000			1.000		0.0003
	>0.17 *g/L*	0.215	[0.088–0.525]	0.0007	0.162	[0.060–0.438]	0.0003	0.158	[0.057–0.434]	
C4c	≤134.63 *AU/L*	1.000			1.000			1.000		0.9072
	>134.63 *AU/L*	0.371	[0.171–0.806]	0.0123	1.033	[0.425–2.508]	0.9437	1.056	[0.424–2.631]	
C4c/C4	≤752.86	1.000			1.000			1.000		0.0250
	>752.86	1.473	[0.722–3.007]	0.2872	2.290	[1.078–4.867]	0.0312	2.543	[1.124–5.755]	
C3	≤0.93 *g/L*	1.000			1.000			1.000		0.9437
	>0.93 *g/L*	0.434	[0.204–0.921]	0.0297	1.005	[0.429–2.352]	0.9911	1.032	[0.433–2.460]	
C3bc	≤15.67 *AU/L*	1.000			1.000			1.000		0.0132
	>15.67 *AU/L*	1.657	[0.804–3.414]	0.1708	2.664	[1.195–5.938]	0.0166	2.841	[1.244–6.487]	
C3bc/C3	≤16.49	1.000			1.000			1.000		0.0017
	>16.49	3.283	[1.468–7.344]	0.0038	4.041	[1.673–9.758]	0.0019	4.301	[1.730–10.697]	
TCC	≤1.55 *AU/L*	1.000			1.000			1.000		0.1236
	>1.55 *AU/L*	0.961	[0.475–1.945]	0.9130	0.564	[0.267–1.192]	0.1338	0.554	[0.261–1.175]	

Values are presented as Hazard ratios (HR) with 95% confidence intervals (95% CI) and p-values. Complement factors are divided according to median values with below median group as references. SAPS II, Simplified Acute Physiology Score II.

results (**Table 4**). Adding amputation as a covariate in our models did not change our results (data not shown).

Receiver Operating Characteristics (ROC) Curves

We generated ROC curves for our explanatory variables predicting 90-day mortality and compared them to the ROC curves for SAPS II, SOFA score on day 1, and arterial blood gas values.

The ROC Area Under the Curve (AUC) for MASP-1 (AUC 0.657, [95% CI 0.544–0.770]), MASP-2 (AUC 0.683, [95% CI 0.573–0.793]), C4 (AUC 0.748, [95% CI 0.649–0.847]), C4c (AUC 0.639, [95% CI 0.526–0.751]), C3 (AUC 0.686, [95% CI 0.577–0.794]), and C3bc/C3 (AUC 0.683, [95% CI 0.570–0.796]) were significantly different from random chance (AUC 0.5) as illustrated in **Figure 2**.

The SOFA score had an AUC of 0.753, [95% CI 0.649–0.857], SAPS II had an AUC of 0.862, [95% CI 0.795–0.929]. The AUCs for the complement parameters combined with SOFA score or SAPS II were not significantly different from the AUC of SOFA or SAPS II alone (data not shown).

For pH the AUC was 0.704 [95% CI 0.589–0.818], for base excess the AUC was 0.716 [95% CI 0.603–0.829], and for lactate the AUC was 0.731 [95% CI 0.631–0.831]. The ROC curve for C4 combined with pH (AUC 0.777 [95% CI 0.674–0.880]) was significantly different than the ROC curve for pH alone ($p = 0.0374$). C4 combined with base excess or lactate was not better than base excess or lactate alone (data not shown).

Microbiology

Out of 135 patients, we could determine a responsible pathogen in 102 cases (76%). Two or more bacteria were responsible for 57 (56%) of these patients. The most common pathogen was Group A Streptococcus (GAS) with 36 infected patients (35%) (**Table 1**), but only 22 (22%) patients were only infected with GAS.

DISCUSSION

In this prospective, observational study we have shown that there's a relationship between the degree of complement activation and NSTI severity. Specifically, the levels of MASP-1, C4, C4c, C3, were significantly lower and C3bc/C3 significantly higher in non-survivors, than in survivors, who again differed significantly from controls. Similarly, the septic shock patients had significantly lower levels of C3, and higher levels of soluble TCC in their plasma, than the non-septic patients, who also differed significantly from the controls.

Interestingly, C4 and its breakdown product C4c both decreased with increasing severity. We expected an inverse proportionality between C4 and C4c, as we saw for C3 and its breakdown product C3bc. A probable explanation for this is a

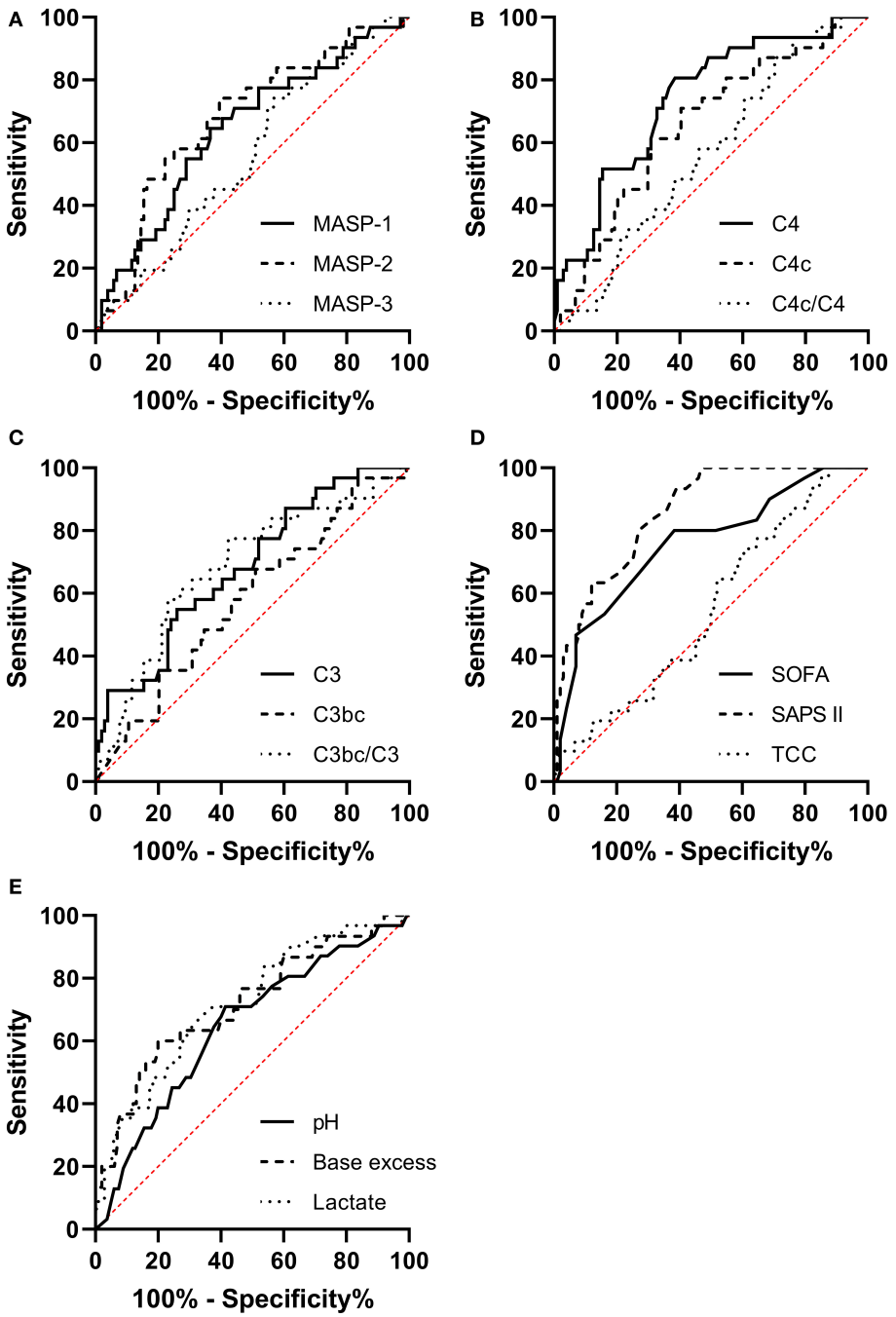

FIGURE 2 | Receiver operating characteristic curves for predicting the 90-day mortality in necrotizing soft-tissue infection patients for **(A)** MASP-1, MASP-2, and MASP-3. **(B)** C4, C4c, and C4c/C4. **(C)** C3, C3bc, and C3bc/C3. **(D)** Sequential Organ Failure Assessment and score day 1 (SOFA), Simplified Acute Physiology Score II (SAPS II), and the terminal complement complex (TCC). **(E)** Arterial pH, base excess, and lactate.

shorter half-life for C4c, leading to a faster clearance of C4c than of C3bc.

Overall, our findings are in line with studies on septic patients showing low C4 and C3 in non-survivors (20–22), and low MASP-1 in patients with disseminated intravascular coagulation (DIC) due to septic shock (23). This underlines that consumption of complement is directly linked to the pathophysiology in the hyperinflammatory reaction in NSTI as well as sepsis in general.

We have previously examined several complement system associated pattern recognition molecules (PRMs) such as CRP, Pentraxin-3, MBL, ficolin-1, ficolin-2, and ficolin-3 as biomarkers for risk stratification in the same cohort of NSTI patients (13, 19). In the survival analysis, ficolin-2 was the most promising of

the above-mentioned PRMs, but the association with mortality disappeared after adjusting for SAPS II (13). Biomarkers outside of the complement system such as Procalcitonin and soluble urokinase plasminogen activator receptor (suPAR) have also been examined and they were not associated with mortality in the adjusted analyses (19, 24).

Here, we adjusted for the same covariates as previously and found above-median admission levels of MASP-1 and C4 to be independently associated with a lower risk of death before 90-days, when compared to below or equal to median admission levels. Above median admission levels of the C4c/C4 ratio, C3bc, and the C3bc/C3 ratio were independently associated with increased risk of death before 90-days from admission when compared to below or equal to median admission levels. These findings clearly suggest that complement consumption predicts a poor outcome in NSTI and that the ability to maintain circulating complement is linked to survival.

There are several, non-exclusive theories explaining the biological mechanism behind complement consumption in hyperinflammatory states. One theory is that consumption is a result of complement deposition in the necrotic and infected tissue. In addition, the complement protein production is probably affected in multiple organ failure, and there could also be a dilution effect with fluid resuscitation, although fluid resuscitation cannot explain why TCC concentration is higher in shock or non-survivors.

We lacked statistical power to examine the pathogens in the NSTI patients, but the MASP-1 findings indicate that the lectin pathway is involved in the pathophysiology. This is also supported by our previous findings showing that the NSTI patients had significantly lower baseline MBL and ficolin levels than the non-infected controls (13), indicating that the lectin pathway PRM's are also consumed in NSTI. To better understand the role of the classical pathway in NSTI we will have to proceed with C1q measurements.

If the depleted complement in plasma is reflecting an overactivation and dysregulation of complement in the infected and necrotic tissue; complement inhibition could possibly be beneficial. Complement inhibition has already been shown to improve survival in a septic baboon model (25). We think our findings warrant further studies on the use of C1-inhibitor and C5 inhibition in animal models.

The well-established clinical SOFA score and SAPS II also predicted the risk of death in adjusted Cox analyses. Scoring systems are necessary to monitor the patients over several days, however, using scoring systems as admission triage can be problematic as the necessary variables are often available after at least 24 h of admission. At that point, many interventions have already been made (26). The new SAPS 3, can be calculated quicker since it uses data available within 1 h of ICU admission (27), but, as Polzik et al. points out; it requires more variables to calculate, many of which may be missing upon admission (24). We wanted to compare the ROC curves for our complement parameters to the ROC curves for SAPS II, SOFA score on day 1, and the quickly available pH, base excess and lactate levels.

The prognostic value of MASP-1, MASP-2, C4, C4c, C3, C3bc/C3, pH, base excess, and lactate were similar to the prognostic value of SOFA score day 1, but only the AUC for C4, base excess and lactate had 95% CI's that overlapped with the AUC for SAPS II (0.862, [95% CI 0.795–0.929]). C4 had a higher AUC (0.748, [95% CI 0.649–0.847]) than the arterial gas values. Additionally, the AUC for C4 and pH combined (AUC 0.777 [95% CI 0.674–0.880]) was significantly higher than the AUC for pH alone (0.704, [95% CI 0.589–0.818]), further underlining C4's potential as a prognostic marker.

To our knowledge, this is the first study to examine complement parameters in a large, prospective cohort of NSTI patients. The study includes all NSTI patients transferred to our tertiary care hospital during the study period, which raises external validity. Besides, there was no loss to follow up, and the investigators performing analyses were blinded. Nevertheless, it is pertinent to mention some limitations of our study. NSTI patients are a heterogeneous group, and the complement parameters could be influenced by unknown confounders, as in other observational studies. Secondly, some patients might have died, before transfer to our tertiary hospital center, increasing the risk of selection bias. Fifteen patients (11%), did not fulfill the sepsis criteria according to Bone et al. which could be a result of this selection bias but could also be due to the variable time course to fulminant disease (18). Our controls were sampled preoperatively, while the NSTI patient's primary debridement often happened before transfer to our hospital. This means that the surgery, in and of itself, could bias the differences we measure between controls and patients. In addition, the controls were all elective orthopedic surgery patients. An extremity is the primary affected site in most NSTI cases but ideally, we should also have included controls from other surgical specialties. Lastly, we did not account for varying levels of complement proteins throughout the study, although the baseline level is most important for initial risk stratification and triage.

Since MASP-1, C4, the C4c/C4 ratio, C3bc, and the C3bc/C3 ratio showed great potential as prognostic markers next steps could be verification in a randomized control trial investigate differences in mortality, where one study arm uses complement admission levels to identify high-risk patients and then investigate for differences in mortality between groups. It would also be interesting to examine whether complement levels can discriminate non-necrotizing soft-tissue patients from NSTI to elucidate whether the complement levels could play a role diagnostically.

CONCLUSIONS

We have shown that there is a relationship between the degree of complement activation and NSTI severity suggesting that consumption of complement is directly linked to the pathophysiology in NSTI. Additionally, we have shown that low levels of MASP-1, C4 and high levels of the C4c/C4 ratio, C3bc and the C3bc/C3 ratio are associated with 90-day mortality in unadjusted and adjusted survival analyses, establishing these

markers as better predictors of mortality than the currently used NSTI biomarkers C-reactive protein and Procalcitonin, at least in this cohort.

C4's ability to predict mortality was comparable to the well-established scoring systems SAPS score II and SOFA on day 1.

DATA AVAILABILITY STATEMENT

The raw data supporting the conclusions of this article will be made available by the authors, without undue reservation, to any qualified researcher.

ETHICS STATEMENT

The studies involving human participants were reviewed and approved by the Regional Ethics Committee of the Capital Region of Denmark (H-2-2014-071) and the Danish Data Protection Agency (J. no. 30-1282) and registered at ClinicalTrials.gov (NCT02180906). The patients/participants or their legal guardians provided their written informed consent to participate in this study.

AUTHOR CONTRIBUTIONS

PG and OH conceived the study. PG, MH, and MM participated in study design and coordination. MH and MM participated in data acquisition and maintain the database for analysis. MH, KP, and MK analyzed the data. MK drafted the first manuscript. PG, OH, KP, CH, MH, MM, and MK contributed to critical revision of the work.

FUNDING

This INFECT project was supported by the European Seventh Framework Programme (Grant No. 305340). For more information about the European collaborative INFECT project, please visit https://cordis.europa.eu/project/rcn/106297/factsheet/en. This substudy was also supported by the Rigshospitalet Research Funds (grant number E-22514-02), the Aase and Ejnar Danielsens Foundation (Grant No. 10-001274), the Hans and Nora Buchards Foundation (Grant No. 7334), the Director Jacob Madsen and Olga Madsens Foundation (Grant No. 5323) and the Christian Larsen and judge Ellen Larsen's Foundation, the Tryg Foundation, the Danish Hearth Foundation [16-R107-A6650-22966], the Danish Research Foundation of Independent Research [DFF-6110-00489] and the Novo Nordisk Research Foundation.

ACKNOWLEDGMENTS

We thank Jesper Andresen for help with the complement analyses and Nina Falcon Bærnthsen, Morten Hedetoft, Anna Mygind Wahl, Marie Warrer Petersen, Peter Polzik, and Isabel Guida Smidt-Nielsen for collecting blood samples. We also thank Peter Buhl Hjortrup, Matilde Jo Allingstrup, and Rasmus Müller for help with patient inclusion and the research nurses Diana Isaksen and Jette Fredlund Degn for help with data acquisition.

SUPPLEMENTARY MATERIAL

The Supplementary Material for this article can be found online at: https://www.frontiersin.org/articles/10.3389/fimmu.2020.00017/full#supplementary-material

REFERENCES

1. Sartelli M, Guirao X, Hardcastle TC, Kluger Y, Boermeester MA, Raşa K, et al. 2018 WSES/SIS-E consensus conference: recommendations for the management of skin and soft-tissue infections. *World J Emerg Surg.* (2018) 13:58. doi: 10.1186/s13017-018-0219-9
2. Hua C, Sbidian E, Hemery F, Decousser JW, Bosc R, Amathieu R, et al. Prognostic factors in necrotizing soft-tissue infections (NSTI): a cohort study. *J Am Acad Dermatol.* (2015) 73:1006–12.e8. doi: 10.1016/j.jaad.2015.08.054
3. Bilton BD, Zibari GB, McMillan RW, Aultman DF, Dunn G, McDonald JC. Aggressive surgical management of necrotizing fasciitis serves to decrease mortality: a retrospective study. *Am Surgeon.* (1998) 64:397–401.
4. Wong C-H, Chang H-C, Pasupathy S, Khin L-W, Tan J-L. Necrotizing Fasciitis: Clinical Presentation, Microbiology, and Determinants of Mortality. *J Bone Joint Surg Am.* (2003) 85:1454–60. doi: 10.2106/00004623-200308000-00005
5. Goh T, Goh LG, Ang CH, Wong CH. Early diagnosis of necrotizing fasciitis. *BJS.* (2014) 101:e119–25. doi: 10.1002/bjs.9371
6. Latifi R, Patel AS, Samson DJ, Tilley EH, Gashi S, Bergamaschi R, et al. The roles of early surgery and comorbid conditions on outcomes of severe necrotizing soft-tissue infections. *Eur J Trauma Emerg Surg.* (2018) 45:919–26. doi: 10.1007/s00068-018-0958-z
7. Garcia NM, Cai J. Aggressive soft tissue infections. *Surg Clin North Am.* (2018) 98:1097–108. doi: 10.1016/j.suc.2018.05.001
8. Pham TN, Moore ML, Costa BA, Cuschieri J, Klein MB. Assessment of functional limitation after necrotizing soft tissue infection. *J Burn Care Res.* (2009) 30:301–6. doi: 10.1097/BCR.0b013e318198a241
9. Walport MJ. Complement - first of two parts. *N Engl J Med.* (2001) 344:1140–4. doi: 10.1056/NEJM200104123441506
10. Lubbers R, van Essen MF, van Kooten C, Trouw LA. Production of complement components by cells of the immune system. *Clin Exp Immunol.* (2017) 188:183–94. doi: 10.1111/cei.12952
11. Martin M, Blom AM. Complement in removal of the dead – balancing inflammation. *Immunol Rev.* (2016) 274:218–32. doi: 10.1111/imr.12462
12. Markiewski MM, DeAngelis RA, Lambris JD. Complexity of complement activation in sepsis. *J Cell Mol Med.* (2008) 12:2245–54. doi: 10.1111/j.1582-4934.2008.00504.x
13. Hansen MB, Rasmussen LS, Pilely K, Hellemann D, Hein E, Madsen MB, et al. The lectin complement pathway in patients with necrotizing soft tissue infection. *JIN.* (2016) 8:507–16. doi: 10.1159/000447327
14. Garred P, Mollnes TE, Lea T. Quantification in enzyme-linked immunosorbent assay of a C3 neoepitope expressed on activated human complement factor C3. *Scand J Immunol.* (1988) 27:329–35. doi: 10.1111/j.1365-3083.1988.tb02354.x
15. Pilely K, Skjoedt M-O, Nielsen C, Andersen TE, Louise Aabom A, Vitved L, et al. A specific assay for quantification of human C4c by use of an anti-C4c monoclonal antibody. *J Immunol Methods.* (2014) 405:87–96. doi: 10.1016/j.jim.2014.01.011
16. Mollnes TE, Lea T, Frøland SS, Harboe M. Quantification of the terminal complement complex in human plasma by an enzyme-linked immunosorbent assay based on monoclonal antibodies against a neoantigen of the complex. *Scand J Immunol.* (1985) 22:197–202. doi: 10.1111/j.1365-3083.1985.tb01871.x
17. Skjoedt M-O, Palarasah Y, Munthe-Fog L, Jie Ma Y, Weiss G, Skjodt K, et al. MBL-associated serine protease-3 circulates in high serum

concentrations predominantly in complex with ficolin-3 and regulates ficolin-3 mediated complement activation. *Immunobiology*. (2010) 215:921–31. doi: 10.1016/j.imbio.2009.10.006
18. Bone RC, Balk RA, Cerra FB, Dellinger RP, Fein AM, Knaus WA, et al. Definitions for sepsis and organ failure and guidelines for the use of innovative therapies in sepsis. *Chest*. (1992) 101:1644–55. doi: 10.1378/chest.101.6.1644
19. Hansen MB, Rasmussen LS, Garred P, Bidstrup D, Madsen MB, Hyldegaard O. Pentraxin-3 as a marker of disease severity and risk of death in patients with necrotizing soft tissue infections: a nationwide, prospective, observational study. *Crit Care*. (2016) 20:40. doi: 10.1186/s13054-016-1210-z
20. Andaluz-Ojeda D, Iglesias V, Bobillo F, Almansa R, Rico L, Gandía F, et al. Early natural killer cell counts in blood predict mortality in severe sepsis. *Crit Care*. (2011) 15:R243. doi: 10.1186/cc10501
21. Nakae H, Endo S, Inada K, Yoshida M. Chronological changes in the complement system in sepsis. *Surg Today*. (1996) 26:225–9. doi: 10.1007/BF00311579
22. Ren J, Zhao Y, Yuan Y, Han G, Li W, Huang Q, et al. Complement depletion deteriorates clinical outcomes of severe abdominal sepsis: a conspirator of infection and coagulopathy in crime? *PLoS ONE*. (2012) 7:e47095. doi: 10.1371/journal.pone.0047095
23. Larsen JB, Laursen MA, Hvas CL, Larsen KM, Thiel S, Hvas A-M. Reduced mannose-binding lectin-associated serine protease (MASP)-1 is associated with disturbed coagulation in septic shock. *Thromb Haemost*. (2019) 119:952–61. doi: 10.1055/s-0039-1685140
24. Polzik P, Grøndal O, Tavenier J, Madsen MB, Andersen O, Hedetoft M, et al. SuPAR correlates with mortality and clinical severity in patients with necrotizing soft-tissue infections: results from a prospective, observational cohort study. *Sci Rep*. (2019) 9:5098. doi: 10.1038/s41598-019-41688-y
25. Keshari RS, Silasi R, Popescu NI, Patel MM, Chaaban H, Lupu C, et al. Inhibition of complement C5 protects against organ failure and reduces mortality in a baboon model of *Escherichia coli* sepsis. *Proc Natl Acad Sci USA*. (2017) 114:E6390–9. doi: 10.1073/pnas.1706818114
26. Awad A, Bader-El-Den M, McNicholas J, Briggs J, El-Sonbaty Y. Predicting hospital mortality for intensive care unit patients: time-series analysis. *Health Informatics J*. (2019). doi: 10.1177/1460458219850323. [Epub ahead of print].
27. Moreno RP, Metnitz PGH, Almeida E, Jordan B, Bauer P, Campos RA, et al. SAPS 3—from evaluation of the patient to evaluation of the intensive care unit. part 2: development of a prognostic model for hospital mortality at ICU admission. *Intensive Care Med*. (2005) 31:1345–55. doi: 10.1007/s00134-005-2763-5

Conflict of Interest: The authors declare that the research was conducted in the absence of any commercial or financial relationships that could be construed as a potential conflict of interest.

frontiers in Immunology

ORIGINAL RESEARCH
published: 08 July 2020
doi: 10.3389/fimmu.2020.01397

C5aR1 Activation Drives Early IFN-γ Production to Control Experimental *Toxoplasma gondii* Infection

Daria Briukhovetska[1†], Birte Ohm[1], Fabian T. Mey[1], Julio Aliberti[2†], Marie Kleingarn[1], Markus Huber-Lang[3], Christian M. Karsten[1] and Jörg Köhl[1,2*]*

[1] Institute for Systemic Inflammation Research, University of Lübeck, Lübeck, Germany, [2] Division of Immunobiology, Cincinnati Children's Hospital and College of Medicine, University of Cincinnati, Cincinnati, OH, United States, [3] Institute of Clinical and Experimental Trauma-Immunology, University Hospital of Ulm, Ulm, Germany

OPEN ACCESS

Edited by:
Heribert Stoiber,
Innsbruck Medical University, Austria

Reviewed by:
Zoltan Banki,
Medical University of Innsbruck, Austria
Tiago W. P. Mineo,
Federal University of Uberlandia, Brazil

***Correspondence:**
Christian M. Karsten
christian.karsten@uksh.de
Jörg Köhl
joerg.koehl@uksh.de

†Present address:
Daria Briukhovetska,
Division of Clinical Pharmacology, Department of Medicine IV, Member of the German Center for Lung Research, Klinikum der Ludwig-Maximilians-Universität München, Munich, Germany
Julio Aliberti,
Immunology Review Branch, National Institute of Allergy and Infectious Diseases, Rockville, MD, United States

Specialty section:
This article was submitted to Microbial Immunology, a section of the journal Frontiers in Immunology

Received: 25 March 2020
Accepted: 01 June 2020
Published: 08 July 2020

Citation:
Briukhovetska D, Ohm B, Mey FT, Aliberti J, Kleingarn M, Huber-Lang M, Karsten CM and Köhl J (2020) C5aR1 Activation Drives Early IFN-γ Production to Control Experimental Toxoplasma gondii Infection. Front. Immunol. 11:1397. doi: 10.3389/fimmu.2020.01397

Toxoplasma gondii (*T. gondii*) is a parasite infecting animals and humans. In intermediate hosts, such as humans or rodents, rapidly replicating tachyzoites drive vigorous innate and adaptive immune responses resulting in bradyzoites that survive within tissue cysts. Activation of the innate immune system is critical during the early phase of infection to limit pathogen growth and to instruct parasite-specific adaptive immunity. In rodents, dendritic cells (DCs) sense *T. gondii* through TLR11/12, leading to IL-12 production, which activates NK cells to produce IFN-γ as an essential mechanism for early parasite control. Further, C3 can bind to *T. gondii* resulting in limited complement activation. Here, we determined the role of C5a/C5aR1 axis activation for the early innate immune response in a mouse model of peritoneal *T. gondii* infection. We found that *C5ar1*$^{-/-}$ animals suffered from significantly higher weight loss, disease severity, mortality, and parasite burden in the brain than wild type control animals. Severe infection in *C5ar1*$^{-/-}$ mice was associated with diminished serum concentrations of IL-12, IL-27, and IFN-γ. Importantly, the serum levels of pro-inflammatory cytokines, including IL-1α, IL-6, and TNF-α, as well as several CXC and CC chemokines, were decreased in comparison to wt animals, whereas anti-inflammatory IL-10 was elevated. The defect in IFN-γ production was associated with diminished *Ifng* mRNA expression in the spleen and the brain, reduced frequency of IFN-γ^{+} NK cells in the spleen, and decreased *Nos2* expression in the brain of *C5ar1*$^{-/-}$ mice. Mechanistically, DCs from the spleen of *C5ar1*$^{-/-}$ mice produced significantly less IL-12 in response to soluble tachyzoite antigen (STAg) stimulation *in vivo* and *in vitro.* Our findings suggest a model in which the C5a/C5aR1 axis promotes IL-12 induction in splenic DCs that is critical for IFN-γ production from NK cells and subsequent iNOS expression in the brain as a critical mechanism to control acute *T. gondii* infection.

Keywords: complement, C5a, C5a receptor 1, *Toxoplasma gondii*, dendritic cell, NK cell, interferon-gamma, interleukin-12

INTRODUCTION

T. gondii is an obligate intracellular apicomplexan parasite capable of infecting virtually all nucleated animal cells (1). Typically, infection occurs after ingestion of oocysts or tissue cysts that release the fast-replicating form of the parasite—the tachyzoites, which multiply asexually and spread through the host [reviewed in (2)]. Following successful immune system activation, the parasite converts into the slowly replicating bradyzoites and persists asymptomatically as a latent infection in the central nervous system or muscle tissue in the form of cysts (2).

As an intracellular parasite, *T. gondii* drives the induction of typical Th1 immune responses, in which IL-12 and IFN-γ are indispensable to control the infection (3). In mice, immune recognition of *T. gondii* occurs through binding of profilin to the intracellular toll-like receptor (TLR) 11/12 dimers in CD8α$^+$ splenic DCs, which act as a primary source for IL-12 (4–8). Secreted IL-12, together with TNFα and IL-18, stimulate NK and T cells to produce IFN-γ (9–11). Such IFN-γ primes infected cells to express immunity-related GTPases (IRGs) and inducible nitric oxide synthase (iNOS, NOS2) as important effector agents [reviewed in (12)]. Reactive nitrogen species synthesized by iNOS exert microbicidal activity in macrophages and microglia and are also essential for the control of *T. gondii* in the brain during the chronic stage of infection (13).

In addition to the cellular immune system, the complement system functions as an essential arm of innate humoral immunity. Studies performed in the '80s have shown that the central complement component C3 can bind to *T. gondii* tachyzoites and activate the alternative pathway (AP). However, alternative pathway activation was shown to be inefficient and did not lead to parasite lysis. Additional activation of the classical pathway (CP) increased the formation of the membrane attack complex (MAC) and the sensitivity of the parasite to complement-mediated killing (14, 15). A recent report identified the lectin pathway (LP) in addition to AP activation in *T. gondii* type I and II strains (16). The authors further showed that *T. gondii* binds the CP and LP regulator C4 binding protein (C4BP) and the AP regulator Factor H (FH). These complement regulators inactivated C3b and limited the formation of the MAC. On the other hand, they found that C3-deficient mice were more susceptible to i.p. *T. gondii* infection resulting in higher mortality than in wt control mice due to uncontrolled parasite proliferation in several tissues. These findings demonstrate a host protective role for pathways downstream of C3. C3 is cleaved into the anaphylatoxin (AT) C3a and the opsonin C3b. C3a exerts its effector functions through activation of its cognate G protein-coupled C3a receptor (C3aR) (17) expressed on several immune cells (18). C3b and its degradation products can either activate immune cells directly through binding to complement receptors type 1 (CR1), CR2 or CR3 (19) or serve as the nucleus to form C5 convertases that cleave C5 into C5a and C5b. C5a is the second AT that exerts its pleiotropic functions through binding and activation of its cognate G protein-coupled C5a receptor 1 (C5aR1, CD88) (20), and C5a receptor 2 (C5aR2, C5L2, GPR77) (21) both of which are mainly expressed by immune cells of the myeloid lineage (18, 22, 23). Several reports have shown that C5aR1 signaling pathways intersect with TLR signaling in many ways, thereby modulating TLR-driven immune responses critical for immune sensing and resistance against several pathogens [reviewed in (24, 25)]. In this context, C5a/C5aR1 axis controls the development of Th1 immune responses in response to several viruses and intracellular parasites (26, 27) through autocrine, TLR-driven AT generation in DCs (28, 29) and subsequent C5aR1 activation resulting in DC cytokine production (29). Importantly, in the absence of C3aR1 and C5aR1, mouse splenic cells failed to produce IL-12 and IFN-γ in response to STAg (26). Our previous findings suggest that CD8α$^+$ splenic DCs express C5aR1, but neither C3aR nor C5aR2 [reviewed in (30)].

Based on these findings, we hypothesized that C5a generation during the early *T. gondii* infection and consecutive activation of C5aR1 on splenic DCs are critical for early protective innate immunity. To test this hypothesis, we infected C57BL/6 wt and *C5ar1*$^{-/-}$ mice i.p. with cysts of the *T. gondii* type II strain ME49 and determined complement activation, susceptibility to infection, and parasite burden. We also assessed the production of several pro- and anti-inflammatory cytokines *in vivo* and *in vitro* with a particular emphasis on IL-12 family cytokines and IFN-γ induction as these cytokines play crucial roles in *T. gondii* control. Here, we identified a critical role for C5a/C5aR1 axis activation in CD8α$^+$ splenic DCs resulting in IL-12 and subsequent IFN-γ production from NK cells during the first week after infection, eventually controlling parasite proliferation and persistence.

MATERIALS AND METHODS

Reagents

Monoclonal antibodies: PE anti-mouse IL-12/23 (p40; clone C15.6, BD Biosciences Cat# 554479, RRID:AB_395420), Brilliant Violet 510™ anti-mouse/human CD11b (clone M1/70, BioLegend Cat# 101245, RRID:AB_2561390), Brilliant Violet 421™ anti-mouse CD8a (clone 53-6.7, BioLegend Cat# 100737, RRID:AB_10897101), Alexa Fluor® 700 anti-mouse NK-1.1 (clone PK136, BioLegend Cat# 108729, RRID:AB_2074426), PE anti-mouse IFN-γ, eBioscience (clone XMG1.2, Thermo Fisher Scientific Cat# 12-7311-82, RRID:AB_466193), APC anti-mouse CD11c, eBioscience (clone N418, Thermo Fisher Scientific Cat# 17-0114-82, RRID:AB_469346), PE anti-mouse CD11c (clone HL3, BD Biosciences Cat#561044, RRID:AB_2033996), PerCP-Cy5.5 anti-mouse CD3e, eBioscience (clone 145-2C11, Thermo Fisher Scientific Cat# 45-0031-82, RRID:AB_1107000), eFluor450 anti-mouse CD3 (clone 17A2, Thermo Fisher Scientific Cat# 48-0032-82, RRID:AB_1272193), eFluor450 anti-mouse CD19 (clone eBio1D3, Thermo Fisher Scientific Cat# 48-0193-80, RRID:AB_2637304), APC-Cy7 anti-mouse Ly6G (clone 1A8, BioLegend Cat# 127623, RRID:AB_10645331). Cytofix/Cytoperm was from BD Biosciences. Red blood cell (RBC) lysis buffer was prepared using 155 mM NH^4Cl, 10 mM $KHCO_3$, and 0.1 mM EDTA (all from Sigma-Aldrich, Merck). DNase I (Fermentas) and the RevertAid First Strand cDNA

Synthesis Kit for mRNA generation was from Thermo Fisher Scientific. Primers for real-time RT-PCR were from Eurofins Genomics, and all other reagents for RT-PCR were from Bio-Rad. RPMI 1640 medium, Dulbecco's PBS (DPBS), L-glutamine, penicillin, and streptomycin were from Life Technologies. BSA was from Sigma-Aldrich, Merck.

Mice

Wild type C57BL/6 mice were purchased from Janvier Labs (Le Genest Saint Isle, France). *C5ar1*$^{-/-}$ (B6.129S4-*C5ar1*^{tm1Cge}, MGI:6382541) mice (31) on the C57BL/6 background were bred and housed under specific pathogen-free conditions in the animal facilities of the University of Lübeck, Germany, and Cincinnati Children's Hospital Medical Center, Cincinnati, Ohio, USA. NMRI mice were purchased from Charles River (Sülzfeld, Germany). Animals were used at 8–12 weeks of age. C57BL/6 control mice and *C5ar1*$^{-/-}$ mice were co-housed and matched by age and sex. Mixed-gender groups were used. All animal studies were reviewed and approved by local authorities of the Animal Care and Use Committee (*Ministerium für Landwirtschaft, Energiewende, Umwelt und Ländliche Räume*, Kiel, Germany) according to permission number V242-7224.122-39 (36-3/15) and IACUC according to the protocol number 2013-0144 (J. Aliberti, CCHMC, Cincinnati, Ohio, USA).

Parasites and Infection

The STAg was prepared using *T. gondii* RH tachyzoites kindly provided by A. Sher (National Institute of Allergy and Infectious Diseases (NIAID), Bethesda, USA) that were maintained on the human foreskin fibroblast cell line HS27 (ATCC CRL-1634, RRID:CVCL_0335) as previously described (32). The *T. gondii* type II strain ME49 was kindly provided by D. Schlüter (Otto von Guericke University Magdeburg, Germany). Tissue cysts were maintained through passaging in NMRI mice (Charles River) as described (33) and propagated in C57BL/6 mice 4–8 weeks before infection. C57BL/6 mice were infected by injection of 50 *T. gondii* ME49 brain cysts in 200 µl of homogenate/DPBS intraperitoneally (i.p.). The clinical course, including weight, disease severity, and survival was monitored daily.

Disease Severity Score

Each mouse was scored daily by two people. The score was defined as follows: (1) coat, appetite, gait, posture is healthy, the mouse is alert and usually responds to external stimuli (escape behavior, reactivity); (2) the mouse is active, but moves slower than average, back slightly humped, the fur starts to become dull; (3) score two plus tilted head, ataxia or delayed righting reflex; (4) the mouse is quiet, alert and responsive, but shows a strongly hunched posture, coarse fur, reacts with movement only to external stimulation; (5) the mouse no longer responds to stimuli and is apathetic, lays on the side (34). Termination criteria were defined as a score of 5 or a loss of more than 20% of the initial body weight.

RNA Extraction

For total RNA extraction, the whole organs were homogenized in RLT buffer (Qiagen) using an Ultra-Turrax™ homogenizer (IKA) according to the manufacturer's recommendations. RNA was extracted on spin columns using AllPrep DNA/RNA 96 Kit (Qiagen) according to the manufacturer's instructions. After extraction, RNA quantity, purity, and quality were determined by NanoDrop 1000 spectrophotometer (Thermo Scientific).

Real-Time RT-qPCR

Reverse transcription reaction was performed after DNase I treatment of the RNA using first-strand cDNA synthesis kit (Thermo Scientific). Real-time qPCR was done using iQ SYBR Green Supermix on a CFX96 Real-Time System (Bio-Rad) using the following primers (Eurofins, Reichenwalde, Germany): β-actin 5′-GCACCACACCTTCTACAATGAG-3′ (sense) and 5′-AAATAGCACAGCCTGGATAGCAAC-3′ (antisense), IFN-γ 5′-ATGAACGCTACACACTGCATC-3′ (sense) and 5′-CCATCCTTTTGCCAGTTCCTC-3′ (antisense), IL12p35 5′-CTGTGCCTTGGTAGCATCTATG-3′ (sense) and 5′-GCAGAGTCTCGCCATTATGATTC-3′ (antisense), IL12p40 5′-CAGAAGCTAACCATCTCCTGG-3′ (sense) and 5′-AGTCCAGTCCACCTCTACAAC-3′ (antisense), IL-18 5′-TCAAAGTGCCAGTGAACCCCA-3′ (sense) and 5′-CACAGCCAGTCCTCTTACTTCA-3′ (antisense), iNOS 5′-AGCCAAGCCCTCACCTAC-3′ (sense) and 5′-AATCT CTGCCTATCCGTC-3′ (antisense) primers. The temperature profile of the quantitative (q)PCR was a follows: 95°C for 3 min, followed by 40 cycles at 95°C for 5 s, 58°C for 5 s, and 72°C for 30 s, followed by 30 cycles for 5 s with a 1°C temperature increase starting at 65°C to confirm the expected PCR products by melting curve analysis. Real-time RT-qPCR data were analyzed using CFX Manager Software 3.1 (Bio-Rad). Relative expression was calculated using the $\Delta\Delta Ct$ method (35).

Serum Sampling

Blood was obtained from mice through the submandibular venipuncture and collected in Microtainer tubes (BD) (36). Tubes were inverted, incubated for 30 min at room temperature for complete blood clotting, and centrifuged at 12,500 g for 5 min. Separated serum was stored at −20°C until further analysis.

Determination of Cytokine, Chemokine, and C5a Serum Concentrations

IL-12p40 and IFN-γ were quantified by ELISA using commercial kits (R&D Systems). IL-12p70 was quantified using the V-PLEX Proinflammatory Panel 1 (mouse) kit (MSD, Rockville, USA according to manufacturer's instructions and measured using MESO Quick Plex SQ120 device (MSD). IL-1α, IL-6, IL-10, IL-23, IL-27, TNF-α, and IFN-γ were measured using the bead-based LEGENDplex™ assay (BioLegend) and analyzed on MACSQuant Analyzer 10 (Miltenyi Biotech). G-CSF, GM-CSF, CXCL1 (KC), CCL2 (MCP-1), CCL3 (MIP-1α), CCL4 (MIP-1β), and CCL5 (RANTES) were analyzed using bead-based Bio-Plex Pro Mouse Cytokine 23-plex Assay (Bio-Rad) according to manufacturer's instructions. C5a serum levels were determined as described (37). All samples were analyzed in duplicate.

Cell Preparation From the Spleen, Mesenteric Lymph Nodes, and Peritoneum

Mice were killed under anesthesia by cervical dislocation. Isolation of cells from the spleen was performed by mechanical disruption using a 40 μm Nylon cell strainer and the plunger of a 5 ml syringe (all BD). The cell strainer was flushed three times, with 5 ml of DPBS. Cells were then incubated with RBC lysis buffer for 3 min, washed with DPBS, and used for flow cytometry analysis or DC isolation (22). $CD11c^+$ cells were purified using CD11c MicroBeads, followed by MACS column separation (Miltenyi Biotech, Gladbach, Germany. Cells were cultured in complete RPMI 1640 medium (10% FBS, heat-inactivated, 100 unit/ml penicillin, 100 μg/ml streptomycin, 2 mM L-Glutamine) overnight at 37°C and 5% CO_2. Supernatants were collected and stored at −20°C until cytokine analysis.

Mesenteric lymph nodes were removed and placed into 1.5 ml reaction tubes containing 1 ml DPBS and placed on ice. To obtain a single cell suspension, the same procedure as described for splenic cell isolation was used except that the red blood cell lysis was omitted.

Peritoneal cells were isolated as described (38). Briefly, a small incision was made in the outer skin of peritoneum, then the skin was gently pulled back to expose the inner skin lining of the peritoneal cavity. Then, 5ml of ice-cold DPBS were injected into the peritoneal cavity using a 27g needle. The peritoneum was then gently massaged to release attached cells into the peritoneal cavity. The cell suspension was carefully aspirated with the same syringe and transferred into 15 ml Falcon tube. The tube was centrifuged for 5 min at 450 g, 4°C. The supernatant was discarded and the cell pellet was used for analysis. Cells were kept on ice between manipulations.

Brain Preparation and *T. gondii* Cyst Counting

For the brain preparation, tissue was collected and homogenized with the addition of ice-cold DPBS in a total volume of 1 ml by repeated aspiration and ejection from a 5 ml Luer-lock syringe (BD) connected to an 18, 21 g and finally a 26 g needle. The number of cysts was then counted in 10 μl of the homogenate under the coverslip using ×40 magnification.

Flow Cytometry

Intracellular cytokine staining was performed in fixed and permeabilized cells. For cytokine accumulation, freshly isolated splenic cells were resuspended in complete RPMI medium with the addition of Brefeldin A (3 μg/ml; eBioscience) without additional stimulation. The cell suspension was incubated for 2 h (5% CO_2, 37°C). Then, cells were labeled extracellularly, fixed and permeabilized using the Cytofix/Cytoperm kit (BD Biosciences) according to manufacturer's instruction. $CD11c^+CD8a^+$ or $CD11c^+CD11b^+$ DCs were incubated with PE-labeled anti-IL-12/23p40, whereas $NK1.1^+CD3^-$ NK cells, $NK1.1^+CD3^+$ NKT, $CD3^+CD8^+$ T cells or $CD3^+CD8^-$ T cells were incubated with PE-labeled anti-IFN-γ Abs for 30 min at 4°C, washed and analyzed by BD LSRII flow cytometer. Flow cytometry data were analyzed using FlowJo 9 software (TreeStar). Cell debris was excluded from the analysis based on the SSC-A/FSC-A signal, and doublets were excluded according to the FSC-A/FSC-H signal ratio.

Statistical Analysis

Statistical analysis was performed using GraphPad Prism 6 (La Jolla, California, USA). Normal distribution of data was tested using the Kolmogorov-Smirnov test. Outliers were excluded from analysis using ROUT (robust regression and outlier removal) method with Q = 1%. An unpaired *t*-test was used to compare two sets of normally distributed data. Comparison between multiple groups were done by one-way or two-way ANOVA. Statistical differences regarding the survival of treatment groups were calculated using the log-rank Mantel-Cox test. Linear regression analysis with the Pearson correlation coefficient was performed to determine the relationship between two cytokines. A p-value < 0.05 was considered significant ($^*p < 0.05$, $^{**}p < 0.01$, $^{***}p < 0.001$).

RESULTS

C5aR1-Deficient Mice Are More Susceptible to Experimental *T. gondii* Infection Than wt Mice

The gut microbiota actively contributes to the innate immune sensing during oral *T. gondii* infection through the activation of several TLRs including TLR2, TLR4, and TLR9 at the site of invasion (39). Thus, we decided to use an intraperitoneal infection model that primarily depends on the direct sensing of parasite-derived antigens by the intracellular TLR11/12 dimers (40). We infected wt and $C5ar1^{-/-}$ mice with 50 brain cysts of the type II *T. gondii* strain ME49 i.p. and recorded the weight (**Figure 1A**), clinical score (**Figure 1B**), and survival time (**Figure 1C**) of these animals for 30 days. At the end of the experiment, we sacrificed the surviving mice and determined the parasite load by direct microscopic counting of cysts in the brain homogenate (**Figure 1D**). $C5ar1^{-/-}$ mice suffered from a significantly higher relative weight loss, disease severity during infection (**Figures 1A,B**) that was associated with a ∼20% increase in the mortality rate in the $C5ar1^{-/-}$ group as compared to control mice (**Figure 1C**). Further, the number of parasite cysts in the brain of those $C5ar1^{-/-}$ animals that survived the *T. gondii* infection for 30 days was significantly higher than that of wt mice (**Figure 1D**). Together, these data suggest that parasite-sensing by the complement system and consecutive C5a generation is critical for the development of appropriate innate immune responses during the first 30 days after *T. gondii* infection.

C5a Serum Concentrations Increase During the First 5 Days After *T. gondii* Infection

In support of this view, previous studies have demonstrated that C5 is an indispensable part of complement-mediated *T. gondii* elimination (14, 15). C5 can be cleaved into the AT C5a and C5b by canonical and non-canonical pathways

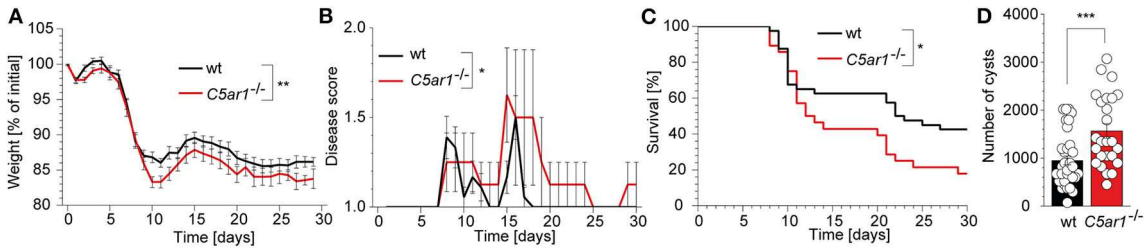

FIGURE 1 | Impact of C5aR1 activation on weight loss, disease severity, survival, and parasite burden in the brain after i.p. *T. gondii* infection. Wt and *C5ar1*$^{-/-}$ mice were infected i.p with 50 cysts of *T. gondii* type II strain ME49 and monitored for 30 days. **(A)** Relative weight change in infected wt ($n = 30$) and *C5ar1*$^{-/-}$ mice ($n = 23$). **(B)** Change of disease score during the course of infection (wt $n = 18$, *C5ar1*$^{-/-}$ $n = 9$). **(C)** Survival of wt and *C5ar1*$^{-/-}$ mice post-infection. Statistical differences in survival between wt ($n = 40$) and *C5ar1*$^{-/-}$ ($n = 28$) mice were calculated using the Log-rank Mantel-Cox test. **(D)** Cyst count in brain tissues 30 days after infection in surviving wt and *C5ar1*$^{-/-}$ mice as counted in the brain homogenate using light microscopy (wt $n = 35$, *C5ar1*$^{-/-}$ $n = 25$). Values shown in **(A,B,D)** are the mean ± SEM; differences between groups were compared by unpaired *t*-test, $^{*}p < 0.05$, $^{**}p < 0.01$, $^{***}p < 0.001$.

(41). We determined the kinetics of C5a generation in the serum of wt and *C5ar1*$^{-/-}$ mice during the acute phase of infection. Before the infection, C5a serum levels were in the range of 200-250 ng/ml (**Figure 2**) in wt and *C5ar1*$^{-/-}$ mice. During the first week after infection, C5a concentrations increased similarly in both mouse strains, peaked at day 5, and started to decline on day 7 (**Figure 2**), demonstrating significant early systemic complement activation after i.p. *T. gondii* infection.

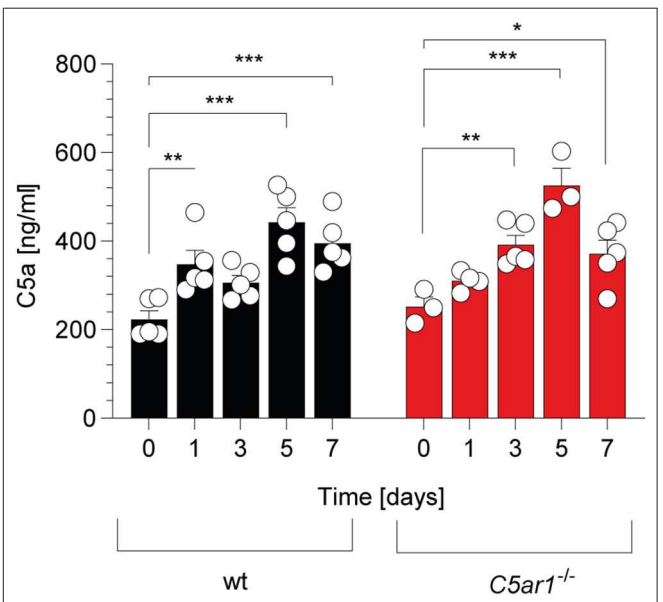

FIGURE 2 | Kinetic of C5a serum concentrations in wt and *C5ar1*$^{-/-}$ mice during the first 7 days post-i.p. *T. gondii* infection. Serum samples were obtained before and 1, 3, 5, and 7 days after infection. Cytokine levels were determined by ELISA. Values shown are the mean ± SEM, $n = 3$–5. Differences between control and infected groups were compared by ANOVA with Sidak's *post-hoc* test, $^{*}p < 0.05$, $^{**}p < 0.01$, $^{***}p < 0.001$.

T. gondii Infection Is Associated With a Lower Frequency of Neutrophils in the Peritoneal Cavity of C5aR1-Deficient Mice

Given that C5aR1-deficient mice suffered from more severe clinical symptoms, increased mortality, and higher parasite burden when compared to wt mice, we aimed to delineate the mechanisms of higher parasite susceptibility. Previously, it has been shown that neutrophils play an important role in *T. gondii* infection (9, 42). Given that neutrophils express C5aR1 at high levels and migrate strongly toward C5a (23), we determined neutrophil numbers and frequencies in the spleen, mesenteric lymph nodes (MLN), and the peritoneum in uninfected mice and 5 days after *T. gondii* infection. Neutrophils were identified as $Lin^{-}Ly6G^{+}$ in the different organs (**Supplementary Figure 1**). As shown in **Figure 3A**, neutrophil numbers significantly increased in the spleen, MLN, and peritoneum in wt and *C5ar1*$^{-/-}$ mice after infection Importantly, while neutrophil numbers were similar in the spleen and MLN of wt and *C5ar1*$^{-/-}$ mice, we found slightly lower cell numbers in the peritoneum of *C5ar1*$^{-/-}$ mice when compared to wt animals. More strikingly, the frequency of neutrophils was markedly reduced in C5aR1-deficient animals (**Figure 3B**) suggesting that C5aR1 activation contributes to the recruitment of neutrophils into the peritoneum in response to *T. gondii* infection. TLR11-independent production of IFN-γ from neutrophils has been described in response to *T. gondii* (42). However, we observed no IFN-γ production in neutrophils from spleens of wt and *C5ar1*$^{-/-}$ mice 5 days after infection (data not shown).

Low IL-12 Family Cytokine and Chemokine Serum Levels in C5aR1-Deficient Mice Are Associated With Low IFN-γ Serum Concentrations 7 Days After *T. gondii* Infection

Previously, we demonstrated that C5aR1 controls the production of cytokines and chemokines that are associated with resistance to *T. gondii* infection (43–46). Here, we focused on the impact of C5aR1 activation on IL-12 as the main driver of IFN-γ production from NK cells and the development of protective Th1 immunity (4, 10, 47). IL-12 is a heterodimer comprising the p40

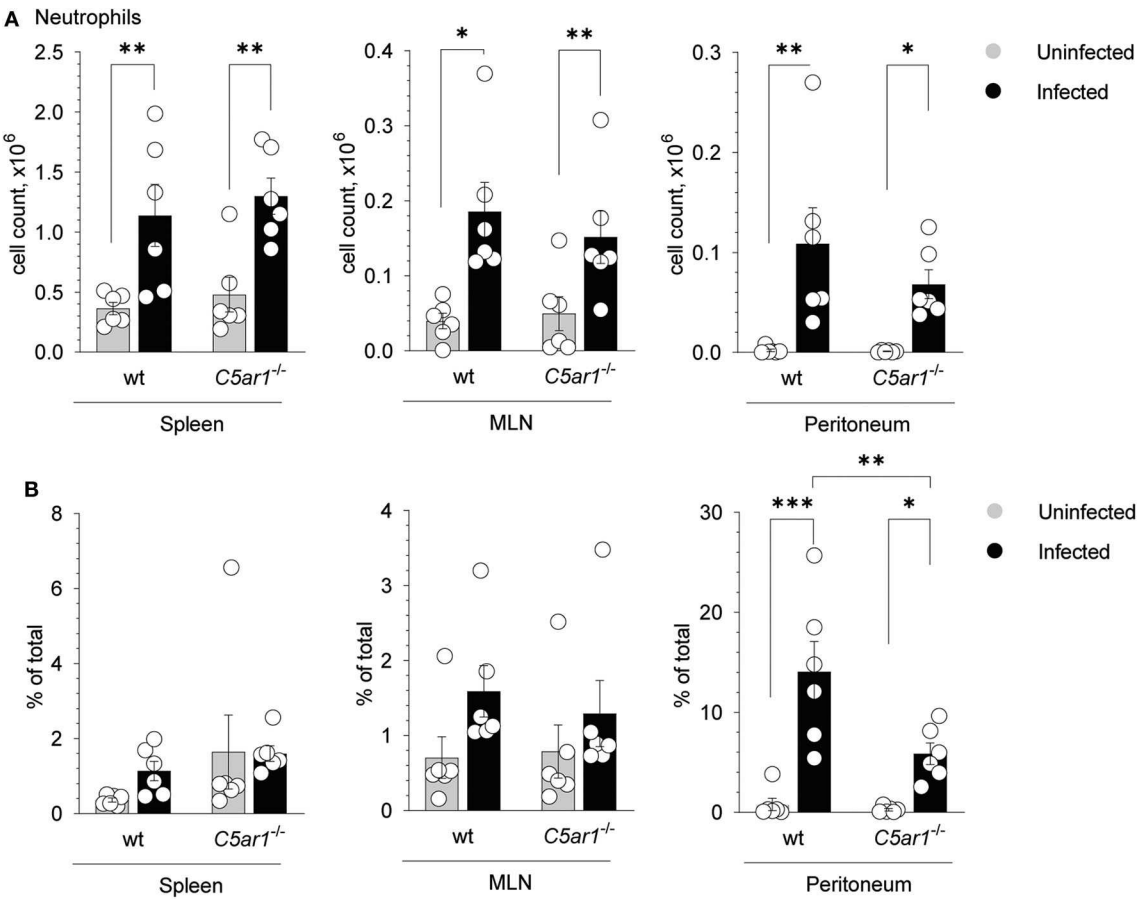

FIGURE 3 | Impact of C5aR1 activation on neutrophil recruitment into the spleen, mesenteric lymph nodes and the peritoneum. **(A,B)** Number **(A)** or frequency **(B)** of neutrophils in the spleen (left panel), mesenteric lymph nodes (MNL; middle panel) and peritoneum (right panel) of uninfected and *T. gondii*-infected wt and *C5ar1*$^{-/-}$ mice. Values shown are the mean ± SEM; $n = 6$/group. Differences between groups were determined by ANOVA and Sidak's *post-hoc* test, $^{*}p < 0.05$, $^{**}p < 0.01$, $^{***}p < 0.001$.

and p35 subunits. First, we determined the kinetics of systemic IL-12p40, and IFN-γ concentrations in wt and *C5ar1*$^{-/-}$ mice during the first 7 days after *T. gondii* infection. The IL-12p40 concentration steadily increased after infection and reached a maximum of 6.2 ± 1.96 (wt) or 6.98 ± 2.67 ng/ml (*C5ar1*$^{-/-}$) 5 days after infection in both mouse strains (**Figure 4A**). IFN-γ levels started to increase on day three and reached a maximum on day 7. Strikingly, the IFN-γ concentrations in wt mice were significantly higher than in *C5ar1*$^{-/-}$ mice on day 7 (8.68 ± 5.41 vs. 5.22 ± 2.73 ng/ml) (**Figure 4B**). Next, we determined IL-12p70 serum concentrations in wt and *C5ar1*$^{-/-}$ mice at day seven after *T. gondii*. We observed significantly higher levels of IL-12p70 in wt than in *C5ar1*$^{-/-}$ animals (**Figure 4C**), sugessting that C5a/C5aR1 axis activation controls early IFN-γ production at the level of IL-12 production. The significant correlation between IL-12 and IFN-γ serum concentrations further corroborates this view (**Figure 4D**). In addition to IL-12p70, we also determined the impact of C5aR1 activation on the production of other IL-12 family cytokines, including IL-23 and IL-27. While IL-12p70 is critical for early IFN-γ production by NK cells after primary infection, IL-23 has recently been found to contribute to protective immunity against secondary *T. gondii* infection (48). IL-23 serum levels in *T. gondii*-infected mice were minor and much lower than in naïve wt or *C5ar1*$^{-/-}$ mice, suggesting either reduced production or high consumption (**Figure 4E**). Interestingly, we found a significant increase in IL-27 serum concentrations in wt but not in *C5ar1*$^{-/-}$ mice after infection (**Figure 4E**). IL-27 is known to regulate T cell responses and has previously been shown to reduce the immunopathology in experimental murine toxoplasmosis (49). We also measured TNFα (50), IL-1α (51), IL-6 (52), and IL-10 (10, 53) as these cytokines have also been demonstrated to confer protection from acute *T. gondii* infection (**Figures 4E,F**). In particular, TNF-α is essential during early *T. gondii* infection in mice, as it is also required for NK cell priming (50). Similar to the IL-12 family cytokines, we detected significantly lower amounts of TNF-α, IL-1α, and IL-6 in the serum of C5aR1-deficient animals in comparison to the wt group (**Figure 4F**). Further, G-CSF serum levels were lower in *C5ar1*$^{-/-}$ mice, whereas GM-CSF levels were similar (**Figure 4F**). In contrast, we observed

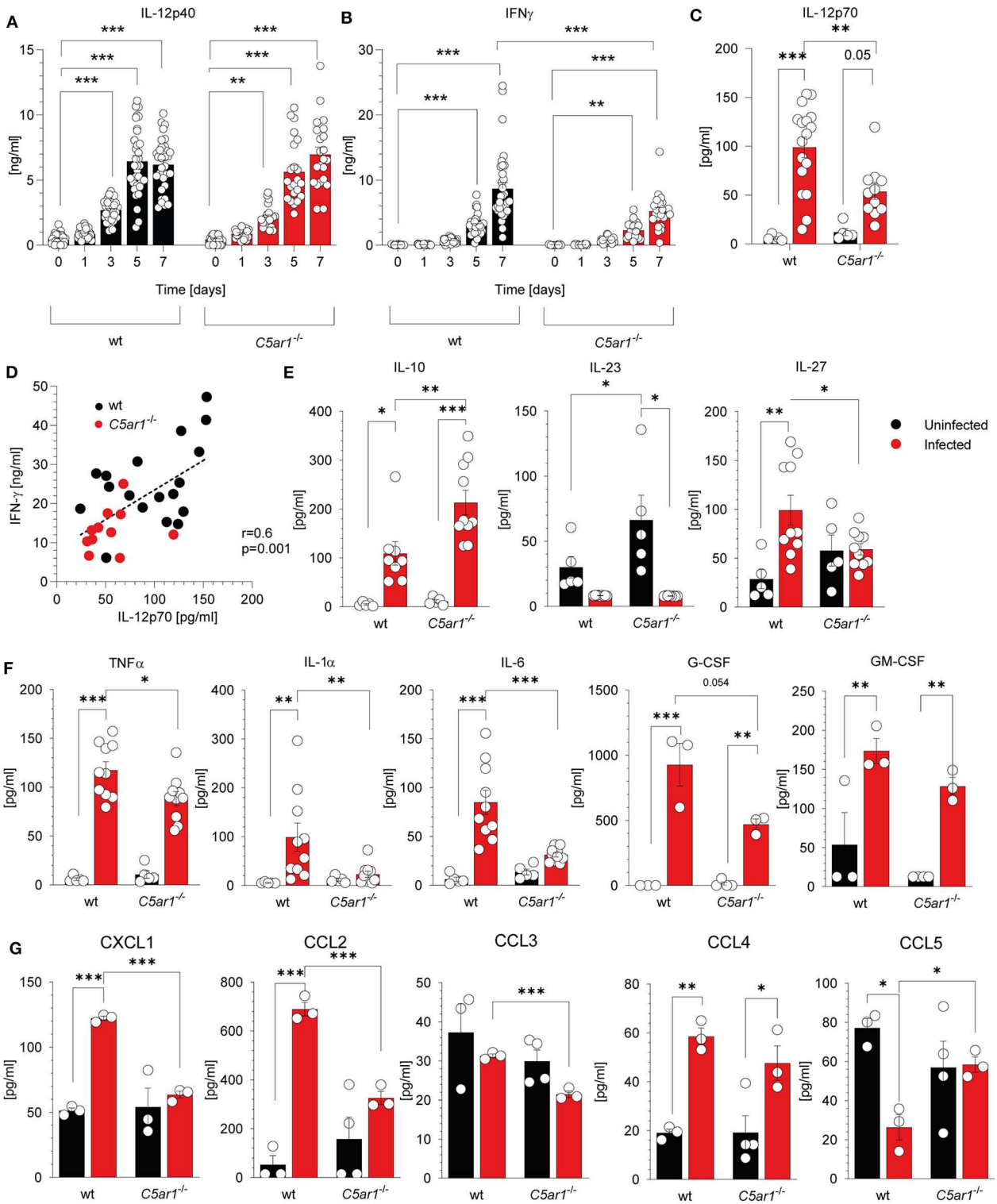

FIGURE 4 | C5aR1 activation drives systemic cytokine and chemokine production during the early phase of *T. gondii* infection. **(A)** Kinetics of IL-12p40 and **(B)** IFN-γ serum concentrations in wt and *C5ar1*$^{-/-}$ mice after *T. gondii* infection. Serum samples were obtained before and 1, 3, 5, and 7 days after infection. Cytokine levels were determined by ELISA. The data are from three independent experiments, $n = 22$–33/condition. **(C)** IL-12p70 cytokine serum concentrations in wt and *C5ar1*$^{-/-}$ mice 7 days after *T. gondii* infection as determined by bioplex assay (Meso Scale Discovery); $n = 10$–17/condition. **(D)** Linear regression analysis between IL-12p70 and IFN-γ serum concentrations 7 days after infection. The *p*-value was calculated using the Pearson's correlation coefficient, $n = 29$ pairs. **(E)** IL-10, IL-23,

(Continued)

FIGURE 4 | and IL-27 cytokine serum concentrations in wt and *C5ar1*$^{-/-}$ mice 7 days after *T. gondii* infection; $n = 10$–17/condition. **(F)** Serum concentrations of TNF-α, IL-1α, IL-6, G-CSF, and GM-CSF determined in wt and *C5ar1*$^{-/-}$ mice 7 days after infection. Cytokine concentrations were determined by LEGENDplex™ assay (BioLegend), $n = 10$/group. **(G)** Serum concentrations of CXCL1 (KC), CCL2 (MCP-1), CCL3 (MIP-1α), CCL4 (MIP-1β), CCL5 (RANTES) in wt and *C5ar1*$^{-/-}$ mice 7 days after infection. The cytokines and chemokines were determined by Bio-Plex assay (Bio-Rad), $n = 3$/group. Values shown in **(A–C)** and **(E–G)** are the mean ± SEM, Differences between groups were determined by ANOVA and Sidak's *post-hoc* test. $^{*}p < 0.05$, $^{**}p < 0.01$, $^{***}p < 0.001$.

significantly higher serum levels of IL-10 in C5aR1-deficient mice (**Figure 4E**). Of note, IL-10 induced by *T. gondii* was found to suppress acute pathological inflammation that causes tissue necrosis and early mortality (53–55). Additionally, chemokine induction was low in *C5ar1*$^{-/-}$ mice as reflected by lower serum levels of CXCL1 (KC), CCL2 (MCP-1), and CCL3 (MIP-1α) when compared to those of wt mice whereas and CCL4 (MIP-1β) levels were similar between wt and *C5ar1*$^{-/-}$ mice (**Figure 4G**). Interestingly, serum levels of CCL5 (RANTES) were elevated in *C5ar1*$^{-/-}$ animals in comparison to wt animals (**Figure 4G**).

Activation of C5aR1 Axis in the Spleen and the Brain Is Required for the Expression of IFN-γ and iNOS

It has been previously demonstrated that IL-12 and IFN-γ are essential in controlling *T. gondii* tachyzoite invasion (4) whereas inflammasome activation and IL-18 production can enhance IL-12-driven IFN-γ production (11, 56, 57). Further, nitric oxide (NO) production form IFN-g-activated macrophages in response to iNOS is a crucial effector molecule of antimicrobial activty (12). Thus, we determined whether local C5aR1 activation affects the transcription of IFN-γ (*Ifng*) in the spleen and brain as well as IL-12p35 (*Il12a*), IL-12p40 (*Il12b*), IL-18 (*Il18*), and iNOS (*Nos2*) in the brain of *T. gondii*-infected animals on day seven after infection using RT-qPCR (**Figures 5A–F**). Baseline cytokine gene and *Nos2* expression in wt and *C5ar1*$^{-/-}$ mice were similar except *Il18*, which was somewhat reduced in *C5ar1*$^{-/-}$ mice (**Supplementary Figure 2**). We observed a strong upregulation of *Ifng* expression upon infection, which was >50-fold in the spleen (**Figure 5A**) and >500-fold in the brain (**Figure 5E**) of wt mice. Consistent with our observations in the serum, the *Ifng* gene expression in the spleen and brain of *C5ar1*$^{-/-}$ mice was significantly lower than that in wt mice (**Figures 5A,E**). The markedly increased *Ifng* expression in the brain was associated with a 3-fold increase in *Il12b*, whereas *Il12a* expression was decreased, and that of *Il18* was unchanged in wt mice (**Figures 5C–F**). *Il12a*, *Il12b*, and *Il18* expression in the brain of *C5ar1*$^{-/-}$ mice was consistently lower than that in wt mice (**Figures 5C–E**). Finally, we determined *Nos2* mRNA expression in the brain, which encodes the iNOS effector molecule that is crucial for parasite control during the chronic stage of infection (13). Importantly, we found a 3-fold upregulation of *Nos2* mRNA expression in the brain of infected wt when compared to uninfected control mice, whereas *C5ar1*$^{-/-}$ mice poorly induced *Nos2* transcripts in the brain (**Figure 5F**).

C5aR1 Activation Has a Moderate Impact on the Frequency and Number of IFN-γ-Producing NK and NKT Cells in the Spleen

CD8α^{+} DCs in the spleen are critical for parasite sensing and the main source of IL-12 production during *T. gondii* infection (6, 40). Previously, we demonstrated that C5aR1 is expressed on CD8α^{+} but not on CD11b^{+} conventional DCs in the mouse spleen using a GFP-C5aR1 knock-in mouse (23). Here we used intracellular cytokine staining to determine the frequencies of IL-12p40-producing CD8α^{+} and CD11b^{+} DCs in the spleen 5 days after *T. gondii* infection (**Supplementary Figure 3**). We found upregulated IL-12p40-expression in CD8^{+} DCs and CD11b^{+} DCs from wt and *C5ar1*$^{-/-}$ mice. However, the frequencies of IL-12p40 expressing DCs were similar in wt and *C5ar1*$^{-/-}$ animals (**Figure 6A**). Next, we assessed the total numbers of IFN-γ producing NK, NKT, as well as CD8^{+} and CD8^{-} T cells in the spleens of the same animals (**Supplementary Figure 4**, **Figures 6B–D**). We found no differences in the total numbers of NK and NKT cells in wt and *C5ar1*$^{-/-}$ mice before or after *T. gondii* infection. In contrast, the number of CD8^{+} T cells and CD8^{-} T_H cells increased in *C5ar1*$^{-/-}$ but not in wt mice (**Figure 6B**). Within the group of NK cells, we observed a markedly increased frequency of IFN-γ^{+} NK cells from 0.97 ± 0.83% or 1.26 ± 0.98% in uninfected wt and *C5ar1*$^{-/-}$ mice to 9.05 ± 0.82% or 6.46 ± 2.49% in infected wt or *C5ar1*$^{-/-}$ mice (**Figure 6C**). The frequency of IFN-γ^{+} NKT cells increased modestly in response to infection in wt and C5ar1$^{-/-}$ mice (**Figure 6C**). Also, we found a moderate increase in the frequency of IFN-γ^{+} CD8^{-} or CD8^{+} T cells in wt and *C5ar1*$^{-/-}$ mice (**Figure 6C**). Of note, the frequency of IFN-γ^{+} CD8^{+} T cells was somewhat higher in wt than in *C5ar1*$^{-/-}$ mice. Importantly, the frequency of IFN-γ^{+} NK cells was significantly lower in *C5ar1*$^{-/-}$ mice as compared with wt mice, whereas the frequencies of IFN-γ-expressing NKT and CD8^{-} T_H cells were similar in wt and *C5ar1*$^{-/-}$ mice (**Figure 6C**). Interestingly, we did not detect C5aR1 expression in naïve spleen-derived NK cells using the GFP-C5aR1 knock-in mice (23), suggesting that the effect of C5a on IFN-γ production from NK is indirect and likely mediated by IL-12-producing DCs residing in the spleen.

In addition to the frequencies, we also determined the numbers of IFN-γ^{+} NK, NKT, and T cells in the spleen (**Figure 6D**). Similar to the frequency, we found a strong increase in the number of IFN-γ^{+}NK cells after infection, both in wt and in *C5ar1*$^{-/-}$ mice (**Figure 6D**). However, in contrast to the frequency, the numbers of NK cells were similar in wt and *C5ar1*$^{-/-}$ mice. The increase in NKT cell numbers was only minor in wt mice but massive in *C5ar1*$^{-/-}$ animals (**Figure 6D**) and thus significantly higher than in wt mice. However, as

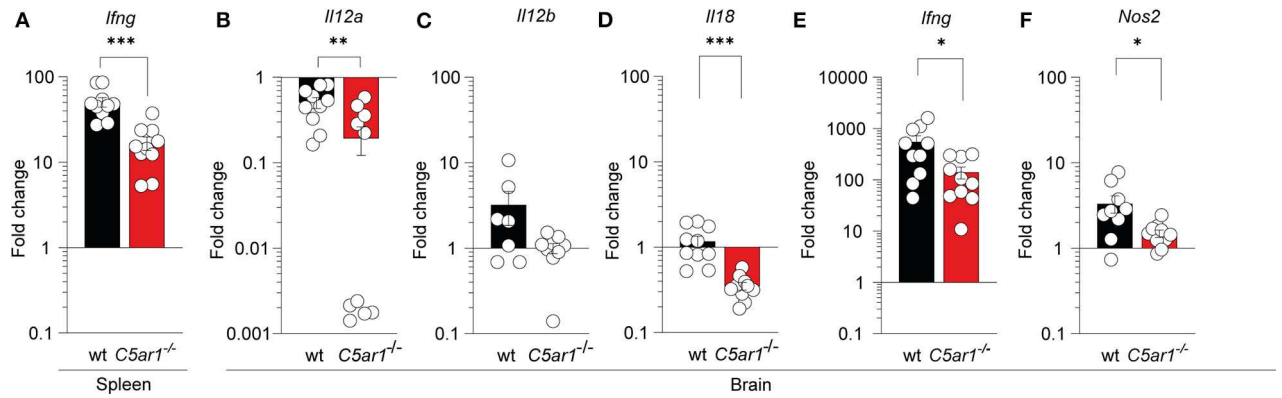

FIGURE 5 | Impact of C5aR1 deficiency on *Ifng mRNA expression in the spleen and brain and on Il12a, Il12b, Il18*, and *Nos2* mRNA expression in the brain during the early phase of *T. gondii* infection. *Ifng* mRNA transcription in the spleen **(A)**, and *Il12a* **(B)**, *Il12b* **(C)**, *Il18* **(D)**, *Ifng* **(E)**, and *Nos2* **(F)** in the brain of wt and *C5ar1*$^{-/-}$ mice 7 days after *T. gondii* infection as determined by RT-qPCR. The data show the relative change in mRNA transcripts in comparison to uninfected mice; the reference value for uninfected mice was set as 1, $n = 10$/group. Values shown are the mean ± SEM, Differences between groups were determined by unpaired *t*-test, $^{*}p < 0.05$, $^{**}p < 0.01$, $^{***}p < 0.001$.

compared to IFN-γ^+ NK or -T cells, the number of IFN-γ^+ NKT cells was much lower. The number of IFN-γ^+ CD8$^-$ T_H and CD8$^+$ T cells increased moderately, and we observed no differences between wt and *C5ar1*$^{-/-}$ mice despite the upregulation in the total cell numbers of these populations in *C5ar1*$^{-/-}$ mice (**Figures 6B,D**). The number of IFN-γ^+ CD8$^-$ T cells after infection in wt or *C5ar1*$^{-/-}$ mice was 5- to 10-fold higher than that of IFN-γ^+ NK or NKT cells and 2- to 3-fold higher than that of IFN-γ^+ CD8$^+$ T cells (**Figures 6B,D**). Thus, C5aR1 activation impacts mainly on the frequency but not the total number of IFN-γ^+ NK cells. Also, it affects the number and frequency of NKT cells but has no impact on IFN-γ^+ T cell numbers and frequencies.

C5aR1 Activation Is Critical for IL-12 Production From Spleen-Residing DCs in Response to *T. gondii* Antigen Challenge

Given that C5aR1 is expressed on DCs and that DCs are essential producers of IL-12, we assessed the potential of C5aR1 activation to drive IL-12 production in spleen-residing DCs. We used CD11c$^+$ MACS-enriched DCs, which comprised ∼10% CD8α$^+$ DCs and in total ∼90% of CD11c$^+$ cells in wt and *C5ar1*$^{-/-}$ mice as determined by flow cytometry (**Figure 7A**, **Supplementary Figure 3B**). DCs from naïve wt or *C5ar1*$^{-/-}$ mice were stimulated with either the TLR9 ligand CpG ODN1668 or STAg, both of which signal through MyD88-dependent pathways to induce their effector functions. As expected, CpG ODN1668 stimulation resulted in significant production of IL-12p40 and IL-12p70. In contrast, we found only a minor increase in IL-12p40 and IL-12p70 production in the supernatants from *C5ar1*$^{-/-}$ sDCs (**Figure 7B**). IL-12p40 as well as IL-12p70 production in wt DCs was significantly higher than in *C5ar1*$^{-/-}$ DCs (**Figure 7B**). Similar to CPG, STAg stimulation induced strong IL-12p40 and IL-12p70 production in spleen DCs (**Figure 7C**). In *C5ar1*$^{-/-}$ DCs, the STAg challenge induced increased IL-12p40 production. However, this increase did not translate into enhanced production of IL-12p70. IL-12p40 and IL-12p70 production of IL-12p40 and IL12-p70 were significantly higher in wt than in *C5ar1*$^{-/-}$ DCs (**Figure 7C**).

To assess *ex vivo* cytokine production, we injected naïve wt and *C5ar1*$^{-/-}$ mice i.p. with 100 μg of STAg. After 6 h, we took blood samples and determined IL-12p40, IL-12p70, and IFN-γ serum concentrations. Similar to what we had observed in the case of TLR9 stimulation, we found high concentrations of systemic IL-12 and IFN-γ in the serum of wt mice (**Figure 7D**). In contrast, *C5ar1*$^{-/-}$ mice failed to upregulate serum levels of IL-12p40, IL-12p70, and subsequently, IFN-γ (**Figure 7D**), which is crucial for the induction of effector mechanisms against *T. gondii* infection (9).

DISCUSSION

The biologic relevance of complement activation in *T. gondii* infection is ill-defined. The extracellular phase within the life cycle of *T. gondii* suggests that the parasite may have evolved mechanisms to evade complement-mediated sensing and attack by the MAC of the terminal pathway. Recent findings uncovered that *T. gondii* type I and II strains not only activate complement by the AP and LP but bind C4BP and FH to limit complement activation at the parasite surface to survive complement attack (16). In line with this observation, we found activation of the complement cascade, which resulted in the generation of C5a in the circulation of wt and *C5ar1*$^{-/-}$ animals peaking on day five after infection. On the other hand, the parasite seems to exploit complement activation as an essential pathway to limit the uncontrolled proliferation of tachyzoites and the killing of the host. After infection with 40 cysts of the *T. gondii* type II strain ME49 > 75% of C3-deficient mice succumbed to infection whereas all wt mice survived the observation period of 30 days suggesting that pathways downstream of C3 tip the

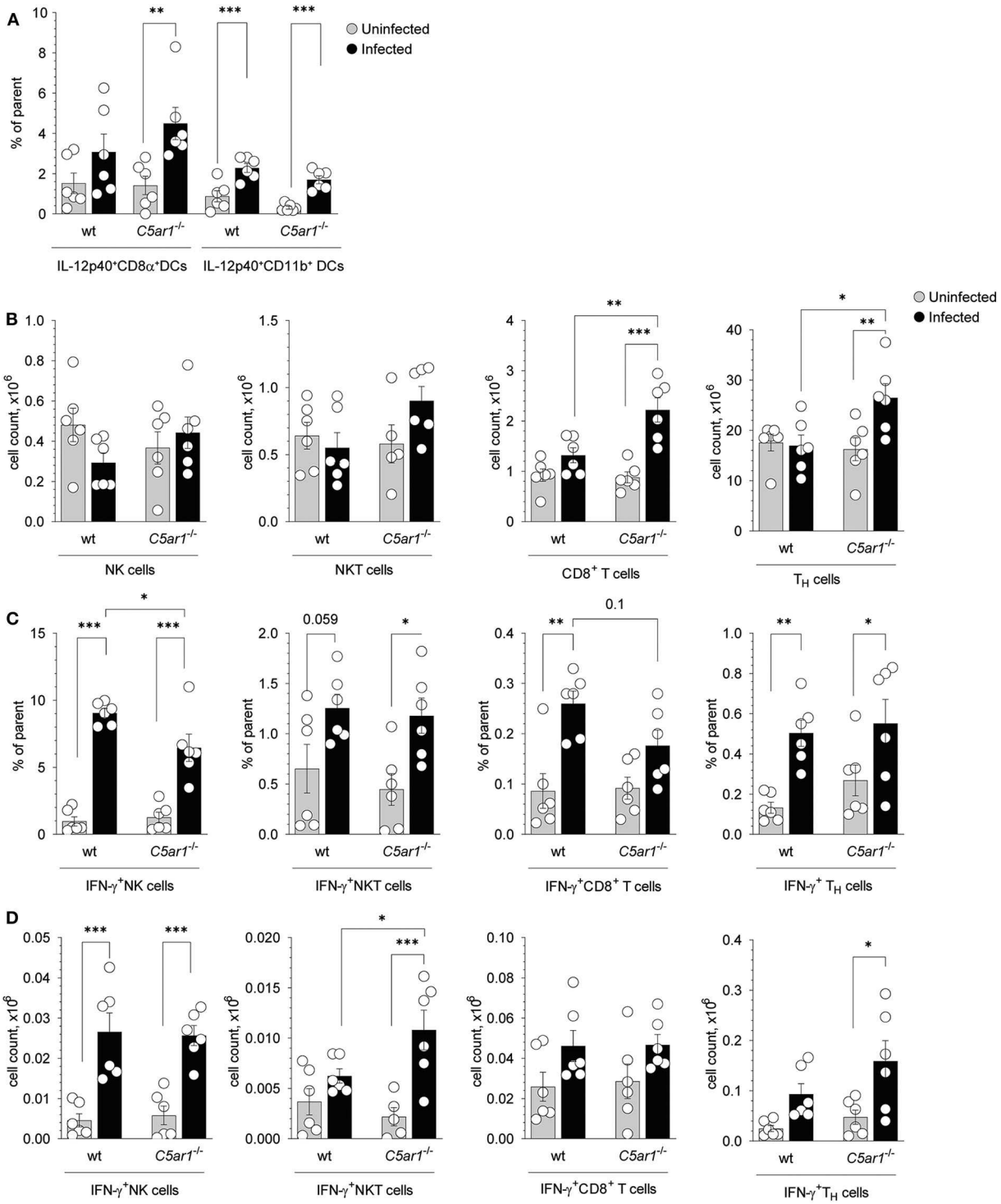

FIGURE 6 | Impact of C5aR1 activation on IL-12p40 production from splenic DCs and IFN-γ production from splenic NK, NKT, and T cells during acute *T. gondii* infection. **(A)** Frequencies of IL-12p40$^+$ CD8α$^+$ (left) and IL-12p40$^+$ CD11b$^+$ (right) DCs in the spleen of uninfected and *T. gondii*-infected wt and *C5ar1*$^{-/-}$ mice, $n =$ 6/group. **(B–D)** Total cell numbers **(B)**, frequencies **(C)**, and numbers **(D)** of IFN-γ$^+$ NK (left), NKT (middle-left), CD8$^+$ T cells (middle-right), and CD8$^-$ T_H cells (right) in the spleen of uninfected and *T. gondii* infected wt and *C5ar1*$^{-/-}$ mice, $n = 6$/group. Cytokine production was assessed at day 5 after *T. gondii* infection by the intracellular staining. Cells were incubated *ex vivo* for 2 h in the presence of 3 μg/ml of Brefeldin A without additional stimulation. Values shown are the mean ± SEM, Differences between groups were determined by ANOVA and Sidak's *post-hoc* test, $^*p < 0.05$, $^{**}p < 0.01$, $^{***}p < 0.001$.

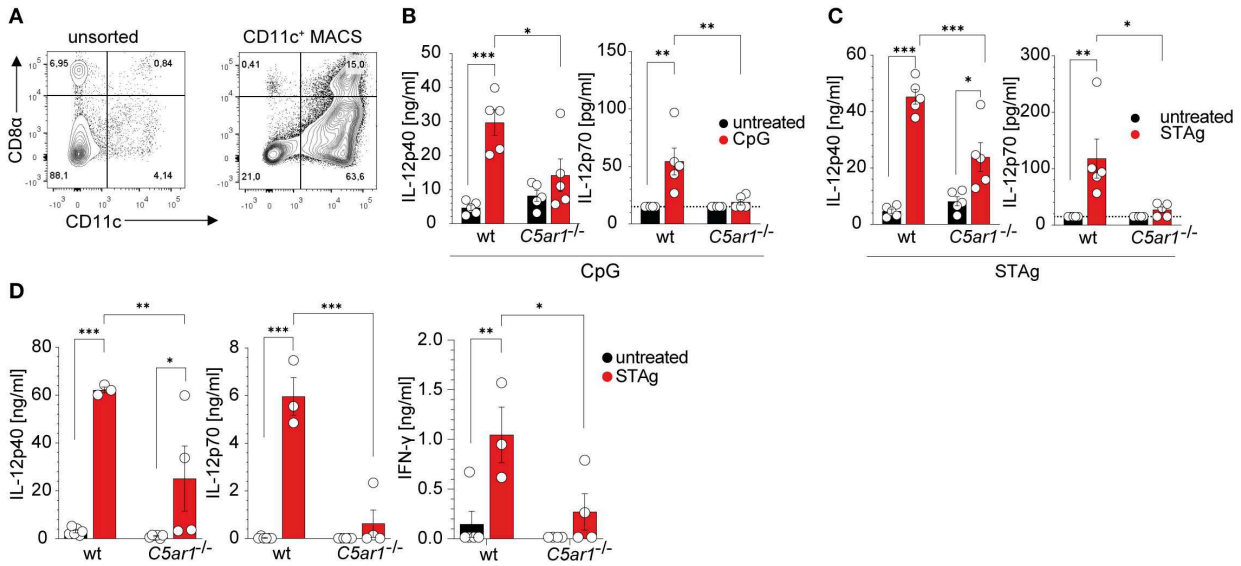

FIGURE 7 | The C5a/C5aR1 axis controls TLR9 and STAg-induced IL-12 production from spleen-residing DCs. **(A)** Dot plots showing the frequencies of unsorted (left) and CD11c$^+$ MACS positively selected (right) splenic DCs. The numbers in the four quadrants show the frequencies of the individual cell populations. **(B)** Impact of CpG ODN1668 (1 μg/ml) or **(C)** STAg (1 μg/ml) stimulation of splenic DCs (1 × 10^6) from wt or *C5ar1*$^{-/-}$ mice on IL-12p40 (left) and IL-12p70 (right) production. The dotted line depicts the detection limit of the assay, $n = 5$/group. **(D)** Impact of STAg injection (i. p., 100 μg, 6 h) on IL-12p40 (left), IL-12p70 (middle), and IFN-γ (right) serum concentrations in wt and *C5ar1*$^{-/-}$ mice. The dotted line depicts the detection limit of the assay, $n = 3$–6/group. Values shown in **(B–D)** are the mean ± SEM, differences between groups were determined by ANOVA and Sidak's *post-hoc* test, $^*p < 0.05$, $^{**}p < 0.01$, $^{***}p < 0.001$.

balance (16) between fatal acute and persistent infection which guarantees the transmission of the parasite to new hosts. Also, mice lacking C5aR1 and C3aR died 12 days after i.p. infection with 20 cysts of *T. gondii*, whereas all wt mice survived >50 days (26). The individual contribution of C3aR or C5aR1 to this effect remained unclear. We found a significantly higher disease severity score and higher weight loss in C5aR1-deficient animals, which was associated with a higher mortality rate when compared to wt controls. In 20% of *C5ar1*$^{-/-}$ mice that survived the 30 days' observation period, the parasite burden in the brain was significantly higher than that observed in the 40% of the surviving wt mice, suggesting that C5aR1 activation is an essential immune mechanism to control the parasite burden in the brain.

In the search for mechanisms underlying the impaired resistance of *C5ar1*$^{-/-}$ mice to *T. gondii* infection, we monitored IL-12p40, and IFN-γ serum levels during the first 7 days after infection. While the initial increase in IFN-γ production was similar between wt and *C5ar1*$^{-/-}$ mice, we found significantly lower IFN-γ serum concentrations 7 days after infection. Surprisingly, the difference in IFN-γ production was not matched by the IL-12p40 serum concentrations. However, when we determined IL-12p70 on day 7 after infection, we found a significantly lower cytokine production in *C5ar1*$^{-/-}$ as compared with wt mice. These data suggested that the C5a/C5aR1 axis controls early IFN-γ production at the level of IL-12p35 production. However, when we determined *Il12a* and *Il12b* gene expression in the brain, we not only observed lower *Il12a* but also *Il12b* expression in *C5ar1*$^{-/-}$ mice. Also, STAg-induced IL-12p40 and IL12p70 production was significantly lower in *C5ar1*$^{-/-}$ than in wt DCs and in *C5ar1*$^{-/-}$ mice after *in vivo* administration of STAg suggesting that C5aR1 activation controls both IL-12p35 and IL-12p40 production in *T. gondii* infection mainly through its impact on DCs. Since IL-12p40 serum levels were not affected by C5aR1 deficiency, other pathways seem to add to IL-12p40 serum production. Previously, a similar regulatory effect of C5a on the IL-12/IFN-γ axis has been shown in models of sepsis and chronic inflammatory diseases (58). When we assessed the induction of the IL-12 family cytokines IL-23 and IL-27, we detected only minor IL-23 serum concentrations in wt and *C5ar1*$^{-/-}$ mice and no IL-17 production (data not shown). The available data suggest that IL-12/23p40 and IL-12p35, but not IL-23p19, drive IFN-γ production during early primary *T. gondii* infection (59) and that IL-23 contributes to IFN-γ-dependent protection during a secondary *T. gondii* infection (48). Noteworthy, IL-12p40 homodimer formation has been described to inhibit IL-12p70-mediated IFN-γ production in a dose-dependent manner (60). The role of IL-12p40 homodimers in *T. gondii* infection has not been studied yet. In contrast to IL-23, IL-27 serum levels sharply increased after infection in wt and to a much lower extent in *C5ar1*$^{-/-}$ animals. IL-27Rα (WSX-1) signaling controls T cell proliferation and immune cell infiltration in *T. gondii* infection (61). The reduced IL-27 serum levels in *C5ar1*$^{-/-}$ animals during the acute stage of infection might explain the increased numbers of CD8$^+$ and CD8$^-$T$_H$ cells in the spleen of such mice as compared with wt animals. However, however it did not translate into higher frequencies or numbers of IFN-γ$^+$ T cells (as shown in **Figures 6B,C**).

While IL-12 is necessary and sufficient to mount an appropriate IFN-γ response to *T. gondii* infection, IL-18 can synergize and enhance IL-12-mediated resistance to the parasite (11, 56, 57). Further, in the absence of TLR11, caspase-1 and-11 drive robust IFN-γ production from Th1 cells which is critical for host survival in response to *T. gondii* infection (62). We found no increase in local *Il18* gene expression in the brain of *T. gondii*-infected wt mice and markedly reduced Il18 expression in *C5ar1*$^{-/-}$ animals, pointing toward a regulatory impact of C5aR1 activation on local IL-18 production in the brain. Of note, local *Il18* gene expression in *C5ar1*$^{-/-}$ mice was already somewhat reduced in non-infected mice indicating regulation of steady state *Il18* gene expression.

In addition to the IL-12 family cytokines, the absence of C5aR1 signaling impaired IL-1α, IL-6, and TNF-α production in acutely infected mice. TNF-α and IL-1α are critical for survival during acute murine toxoplasmosis (51). IL-6 has been shown to promote IL-17 production from NK cells during *T. gondii* infection (52). However, as already pointed out, we did not detect IL-17 in serum of infected mice (data not shown). In addition to IL-1α, IL-6 and TNF-α, systemic levels of CXCL1 (KC), CCL2 (MCP-1), and CCL3 (MIP-1α) were significantly lower in *C5ar1*$^{-/-}$ than in wt mice. CXCL1 is a strong chemotaxin for neutrophils via CXCR2. It is produced in large amounts by peritoneal mesothelial cells in response to IL-1β and TNF-α (63). In line with the reduced TNF-α and CXCL1 serum levels, we found reduced recruitment of neutrophils into the peritoneum of C5aR1-deficient mice, whereas we observed no differences in macrophage numbers in the peritoneum, spleen, or MLNs in *C5ar1*$^{-/-}$ mice (data not shown). Interestingly, CCL5 (RANTES) serum levels were higher in *C5ar1*$^{-/-}$ mice than in wt animals. CCR5, the cognate receptor for RANTES, can form heterodimers together with C5aR1 (64), which contributes to CCR5-mediated HIV entry into macrophages (65). However, the functional relevance of heterodimer formation in *T. gondii* infection remains to be determined, in particular, as CCR5 has also been described as a ligand for *T. gondii*-derived cyclophilin 18 (3). Of note, cyclophilin 18-mediated activation of CCR5 on CD8α$^+$ DCs in the spleen can also drive IL-12 production (3).

To determine the source of serum IFN-γ, we performed a transcriptional analysis of this cytokine in the spleen. We found a massive upregulation of *Ifng* mRNA in wt mice that was significantly impaired in *C5ar1*$^{-/-}$ animals suggesting that C5aR1 activation of spleen cells regulates the production of IFN-γ. Also, we assessed the mRNA expression of *Ifng* and the IFN-γ-inducing *Il12a* and *Il12b* as well as *Il18* genes in the brain. Similar to the spleen, *Ifng* gene expression was markedly increased in wt mice and to a lesser extent in wt animals. This was associated with decreased *Il12a* and *IL12b* gene expression in C5aR1-deficient mice as compared with wt animals. Also, we detected a significant downregulation of *Il18* gene transcription in the brain of *C5ar1*$^{-/-}$ but not of wt mice. However, we already noted a lower number of *Il18* gene transcripts in naïve *C5ar1*$^{-/-}$ mice. Importantly, we found upregulation of *Nos2* mRNA expression in the brain of wt but not *C5ar1*$^{-/-}$ mice during early infection in comparison to the naïve state. The reduced *Nos2* production will likely result in the lower generation of nitrogen intermediates required for parasite elimination by microglia/macrophages during bradyzoite conversion. It may cause the increased parasite burden in the brain that we have observed in *C5ar1*$^{-/-}$ mice on day 30 (13).

To identify the cellular sources of IL-12 and IFN-γ during the early phase of *T. gondii* infection, we determined intracellular IL-12p40 production in CD8α$^+$ and CD11b$^+$ DCs and IFN-γ production in NK, NKT, and T cells from wt and *C5ar1*$^{-/-}$ mice. CD8α$^+$ DCs in the spleen is the main source of IL-12 (3). Previously, we identified C5aR1, but not C3aR or C5aR2 expression on CD8α$^+$ DCs in the spleen using transgenic AT receptor reporter mice; none of these receptors was expressed on naïve or activated T cells (18, 22, 23, 30). The frequencies of IL-12p40$^+$ CD8α$^+$ and CD11b$^+$ DCs increased to a similar extent after infection in wt and *C5ar1*$^{-/-}$ mice. Interestingly, C5a downregulates the expression of IRF1 and IRF8 (ICSBP) in a *Leishmania major* model (44). IRF8 is a transcription factor essential for the development of CD8α$^+$ DCs (66), and together with NF-κB specifically mediates profilin-induced IL-12 secretion from DCs (40, 67), providing a potential link for TLR11/12 and C5aR1 cross-talk that could be explored in future studies.

Regarding the IFN-γ production, we identified 8–10% of wt NK cells as IFN-γ producers, whereas around 6% of NK cells from C5aR1-deficient mice were IFN-γ$^+$ during acute *T. gondii* infection. IFN-γ production from NK cells during acute *T. gondii* infection is critical to mount an appropriate Th1 response (10). Animals in which NK cells are depleted succumb to *T. gondii* infection (47). In line with the reduced IL-12p70 serum levels and the reduced IL-12p70 production from splenic DCs after STAg activation, these findings suggest that C5aR1 activation contributes to early activation of NK cells in response to *T gondii* infection through a paracrine mechanism, i.e., IL-12 production in spleen-residing DC, similar to the regulation of T cell differentiation (29). In support of this view, we found no detectable C5aR1 expression on murine NK cells taking advantage of GFP-C5aR1 knock-in mice (22, 30, 68). This is different from what we have recently found for C5aR2, which is expressed in a subset of splenic and blood NK cells (22). Specific activation of C5aR2 on NK cells suppressed IL-12/IL-18-induced IFN-γ production (22).

In addition to NK cells, we observed that already 0.5% of wt and *C5ar1*$^{-/-}$ CD8$^-$ T_H cells were IFN-γ producers. Although the frequency of IFN-γ-producing CD8$^-$ T_H cells was 16- to 20-fold lower than that of IFN-γ-producing NK cells, the overall number of IFN-γ-producing T cell was still 3- to 5-fold higher than that of NK cells given the much higher number of T cells in the spleen. Also, the frequency of IFN-γ$^+$ CD8$^+$ T cells from wt and *C5ar1*$^{-/-}$ mice was much lower (∼50-fold) than that of IFN-γ$^+$ NK cells, whereas the total number of IFN-γ$^+$ CD8$^+$ T cells from wt and *C5ar1*$^{-/-}$ mice was comparable to IFN-γ$^+$ NK cells. Thus, C5aR1 activation does not seem to regulate IFN-γ production from T cells in the spleen. Similarly, C5aR1 activation does not seem to affect the frequency of IFN-γ$^+$ NKT cells. IFN-γ production by NKT cells plays an important role in the initiation of the inflammatory bowel response after oral *T. gondii* infection (69). However, the contribution of NKT cells to

IFN-γ production after peritoneal *T. gondii* infection is unclear. Our data suggest that NKT cells become activated after i.p. *T. gondii* infection and add to the early IFN-γ production after acute infection.

Multiple studies showed a robust cell-specific impact of C5a/C5aR1 axis activation on the regulation of IL-12 production in different disease models (44, 70–73). C5a stimulation induces IL-12 production from activated monocytes and macrophages (71, 73, 74). However, C5a suppresses TLR-induced IL-12 production from macrophages in a dose- and time-dependent manner (44, 71, 72). Paradoxically, complete ablation of C5aR1 in genetically modified mice does not revert this effect but reduces the amount of secreted IL-12 (45, 68, 70, 71). In line with these data, *C5ar1*$^{-/-}$ DCs showed markedly reduced TLR-induced IL-12 production in response to CpG and STAg stimulation *in vitro*. This effect was also present upon STAg injection *in vivo* and was associated with a decreased IFN-γ production, which is crucial for triggering effector mechanisms that combat intracellular parasite infection (9, 75).

Collectively, we uncovered a critical protective role for C5a/C5aR1 axis activation during the early phase of *T. gondii* infection. We propose a model, in which early C5a generation activates the C5aR1/C5a axis on spleen-residing CD8α^{+} DCs to synergize with *T. gondii* antigen-driven IL-12 production. This IL-12 production is critical to activate NK cells for IFN-γ production eventually activating phagocytic cells for iNOS production, required for the conversion from an acute tachyzoite-driven to a persistent bradyzoite infection in tissue cysts and host survival.

DATA AVAILABILITY STATEMENT

The raw data supporting the conclusions of this article will be made available by the authors, without undue reservation.

ETHICS STATEMENT

The animal study was reviewed and approved by Ministerium für Landwirtschaft, Energiewende, Umwelt und Ländliche Räume, Kiel, Germany and the Institutional Animal Care and Use Committee of Cincinnati Children's Hospital, Cincinnati, OH, USA.

AUTHOR CONTRIBUTIONS

DB, CK, JK, and JA contributed to the conception and design of the study. DB, FM, BO, MK, and MH-L performed the experiments and analyzed the data. DB and JK wrote the manuscript. All authors contributed to the article and approved the submitted version.

FUNDING

This work was supported by the German Research Foundation International Research Training Group 1911 Projects B1 and B2 (to JK and CK, respectively). The funders had no role in study design, data collection, and interpretation, or the decision to submit the work for publication.

ACKNOWLEDGMENTS

We thank Lana Pohle, Nathaniel Shryock, and Gabriele Köhl for their excellent technical assistance.

SUPPLEMENTARY MATERIAL

The Supplementary Material for this article can be found online at: https://www.frontiersin.org/articles/10.3389/fimmu.2020.01397/full#supplementary-material

REFERENCES

1. Werk R, Fischer S. Attempts to infect plant protoplasts with *Toxoplasma gondii*. *J Gen Microbiol.* (1982) 128:211–3. doi: 10.1099/00221287-128-1-211
2. Blader IJ, Coleman BI, Chen CT, Gubbels MJ. Lytic cycle of *Toxoplasma gondii*: 15 years later. *Annu Rev Microbiol.* (2015) 69:463–85. doi: 10.1146/annurev-micro-091014-104100
3. Aliberti J. Host persistence: exploitation of anti-inflammatory pathways by *Toxoplasma gondii*. *Nat Rev Immunol.* (2005) 5:162–70. doi: 10.1038/nri1547
4. Gazzinelli RT, Wysocka M, Hayashi S, Denkers EY, Hieny S, Caspar P, et al. Parasite-induced IL-12 stimulates early IFN-gamma synthesis and resistance during acute infection with *Toxoplasma gondii*. *J Immunol.* (1994) 153:2533–43.
5. Liu CH, Fan YT, Dias A, Esper L, Corn RA, Bafica A, et al. Cutting edge: dendritic cells are essential for *in vivo* IL-12 production and development of resistance against *Toxoplasma gondii* infection in mice. *J Immunol.* (2006) 177:31–5. doi: 10.4049/jimmunol.177.1.31
6. Mashayekhi M, Sandau MM, Dunay IR, Frickel EM, Khan A, Goldszmid RS, et al. CD8alpha(+) dendritic cells are the critical source of interleukin-12 that controls acute infection by *Toxoplasma gondii* tachyzoites. *Immunity.* (2011) 35:249–59. doi: 10.1016/j.immuni.2011.08.008
7. Scanga CA, Aliberti J, Jankovic D, Tilloy F, Bennouna S, Denkers EY, et al. Cutting edge: MyD88 is required for resistance to *Toxoplasma gondii* infection and regulates parasite-induced IL-12 production by dendritic cells. *J Immunol.* (2002) 168:5997–6001. doi: 10.4049/jimmunol.168.12.5997
8. Yarovinsky F, Zhang D, Andersen JF, Bannenberg GL, Serhan CN, Hayden MS, et al. TLR11 activation of dendritic cells by a protozoan profilin-like protein. *Science.* (2005) 308:1626–9. doi: 10.1126/science.1109893
9. Sturge CR, Yarovinsky F. Complex immune cell interplay in the gamma interferon response during Toxoplasma gondii infection. *Infect Immun.* (2014) 82:3090–7. doi: 10.1128/IAI.01722-14
10. Hunter CA, Subauste CS, Van Cleave VH, Remington JS. Production of gamma interferon by natural killer cells from *Toxoplasma gondii*-infected SCID mice: regulation by interleukin-10, interleukin-12, and tumor necrosis factor alpha. *Infect Immun.* (1994) 62:2818–24. doi: 10.1128/IAI.62.7.2818-2824.1994
11. Cai G, Kastelein R, Hunter CA. Interleukin-18 (IL-18) enhances innate IL-12-mediated resistance to *Toxoplasma gondii*. *Infect Immun.* (2000) 68:6932–8. doi: 10.1128/IAI.68.12.6932-6938.2000
12. Gazzinelli RT, Mendonca-Neto R, Lilue J, Howard J, Sher A. Innate resistance against *Toxoplasma gondii*: an evolutionary tale of mice, cats, and men. *Cell Host Microbe.* (2014) 15:132–8. doi: 10.1016/j.chom.2014.01.004

13. Scharton-Kersten TM, Yap G, Magram J, Sher A. Inducible nitric oxide is essential for host control of persistent but not acute infection with the intracellular pathogen *Toxoplasma gondii*. *J Exp Med.* (1997) 185:1261–73. doi: 10.1084/jem.185.7.1261
14. Fuhrman SA, Joiner KA. *Toxoplasma gondii*: mechanism of resistance to complement-mediated killing. *J Immunol.* (1989) 142:940–7.
15. Schreiber RD, Feldman HA. Identification of the activator system for antibody to Toxoplasma as the classical complement pathway. *J Infect Dis.* (1980) 141:366–9. doi: 10.1093/infdis/141.3.366
16. Sikorski PM, Commodaro AG, Grigg ME. *Toxoplasma gondii* recruits factor H and C4b-binding protein to mediate resistance to serum killing and promote parasite persistence *in vivo*. *Front Immunol.* (2019) 10:3105. doi: 10.3389/fimmu.2019.03105
17. Crass T, Raffetseder U, Martin U, Grove M, Klös A, Kohl J, et al. Expression cloning of the human C3a anaphylatoxin receptor (C3aR) from differentiated U-937 cells. *Eur J Immunol.* (1996) 26:1944–50. doi: 10.1002/eji.1830260840
18. Quell KM, Karsten CM, Kordowski A, Almeida LN, Briukhovetska D, Wiese AV, et al. Monitoring C3aR expression using a floxed tdTomato-C3aR reporter knock-in mouse. *J Immunol.* (2017) 199:688–706. doi: 10.4049/jimmunol.1700318
19. Verschoor A, Kemper C, Köhl J. *Complement Receptors*. John Wiley & Sons, Ltd. (2017). p. 1–17. doi: 10.1002/9780470015902.a0000512.pub3
20. Gerard NP, Gerard C. The chemotactic receptor for human C5a anaphylatoxin. *Nature.* (1991) 349:614–7. doi: 10.1038/349614a0
21. Okinaga S, Slattery D, Humbles A, Zsengeller Z, Morteau O, Kinrade MB, et al. C5L2, a nonsignaling C5A binding protein. *Biochemistry.* (2003) 42:9406–15. doi: 10.1021/bi034489v
22. Karsten CM, Wiese AV, Mey F, Figge J, Woodruff TM, Reuter T, et al. Monitoring C5aR2 expression using a floxed tdTomato-C5aR2 knock-in mouse. *J Immunol.* (2017) 199:3234–48. doi: 10.4049/jimmunol.1700710
23. Karsten CM, Laumonnier Y, Eurich B, Ender F, Broker K, Roy S, et al. Monitoring and cell-specific deletion of C5aR1 using a novel floxed GFP-C5aR1 reporter knock-in mouse. *J Immunol.* (2015) 194:1841–55. doi: 10.4049/jimmunol.1401401
24. Köhl J. The role of complement in danger sensing and transmission. *Immunol Res.* (2006) 34:157–76. doi: 10.1385/IR:34:2:157
25. Hawlisch H, Köhl J. Complement and toll-like receptors: key regulators of adaptive immune responses. *Mol Immunol.* (2006) 43:13–21. doi: 10.1016/j.molimm.2005.06.028
26. Strainic MG, Liu J, Huang D, An F, Lalli PN, Muqim N, et al. Locally produced complement fragments C5a and C3a provide both costimulatory and survival signals to naive $CD4^+$ T cells. *Immunity.* (2008) 28:425–35. doi: 10.1016/j.immuni.2008.02.001
27. Klos A, Tenner AJ, Johswich KO, Ager RR, Reis ES, Köhl J. The role of the anaphylatoxins in health and disease. *Mol Immunol.* (2009) 46:2753–66. doi: 10.1016/j.molimm.2009.04.027
28. Schmitz V, Almeida LN, Svensjo E, Monteiro AC, Köhl J, Scharfstein J. C5a and bradykinin receptor cross-talk regulates innate and adaptive immunity in *Trypanosoma cruzi* infection. *J Immunol.* (2014) 193:3613–23. doi: 10.4049/jimmunol.1302417
29. Sheen JH, Strainic MG, Liu J, Zhang W, Yi Z, Medof ME, et al. TLR-induced murine dendritic cell (DC) activation requires DC-intrinsic complement. *J Immunol.* (2017) 199:278–91. doi: 10.4049/jimmunol.1700339
30. Laumonnier Y, Karsten CM, Köhl J. Novel insights into the expression pattern of anaphylatoxin receptors in mice and men. *Mol Immunol.* (2017) 89:44–58. doi: 10.1016/j.molimm.2017.05.019
31. Höpken UE, Lu B, Gerard NP, Gerard C. The C5a chemoattractant receptor mediates mucosal defence to infection. *Nature.* (1996) 383:86–9. doi: 10.1038/383086a0
32. Grunvald E, Chiaramonte M, Hieny S, Wysocka M, Trinchieri G, Vogel SN, et al. Biochemical characterization and protein kinase C dependency of monokine-inducing activities of *Toxoplasma gondii*. *Infect Immun.* (1996) 64:2010–8. doi: 10.1128/IAI.64.6.2010-2018.1996
33. Parlog A, Harsan LA, Zagrebelsky M, Weller M, von Elverfeldt D, Mawrin C, et al. Chronic murine toxoplasmosis is defined by subtle changes in neuronal connectivity. *Dis Model Mech.* (2014) 7:459–69. doi: 10.1242/dmm.014183
34. Linkenhoker JR, Linton CG. Effect of nesting material on body weights of mice infected with *Toxoplasma gondii*. *J Am Assoc Lab Anim Sci.* (2013) 52:531–3.
35. Livak KJ, Schmittgen TD. Analysis of relative gene expression data using real-time quantitative PCR and the 2(-Delta Delta C(T)) method. *Methods.* (2001) 25:402–8. doi: 10.1006/meth.2001.1262
36. Golde WT, Gollobin P, Rodriguez LL. A rapid, simple, and humane method for submandibular bleeding of mice using a lancet. *Lab Anim (NY).* (2005) 34:39–43. doi: 10.1038/laban1005-39
37. Huber-Lang M, Younkin EM, Sarma JV, Riedemann N, McGuire SR, Lu KT, et al. Generation of C5a by phagocytic cells. *Am J Pathol.* (2002) 161:1849–59. doi: 10.1016/S0002-9440(10)64461-6
38. Bröker K, Figge J, Magnusen AF, Manz RA, Köhl J, Karsten CM. A novel role for C5a in B-1 cell homeostasis. *Front Immunol.* (2018) 9:258. doi: 10.3389/fimmu.2018.00258
39. Wilhelm CL, Yarovinsky F. Apicomplexan infections in the gut. *Parasite Immunol.* (2014) 36:409–20. doi: 10.1111/pim.12115
40. Raetz M, Kibardin A, Sturge CR, Pifer R, Li H, Burstein E, et al. Cooperation of TLR12 and TLR11 in the IRF8-dependent IL-12 response to *Toxoplasma gondii* profilin. *J Immunol.* (2013) 191:4818–27. doi: 10.4049/jimmunol.1301301
41. Hajishengallis G, Reis ES, Mastellos DC, Ricklin D, Lambris JD. Novel mechanisms and functions of complement. *Nat Immunol.* (2017) 18:1288–98. doi: 10.1038/ni.3858
42. Sturge CR, Benson A, Raetz M, Wilhelm CL, Mirpuri J, Vitetta ES, et al. TLR-independent neutrophil-derived IFN-gamma is important for host resistance to intracellular pathogens. *Proc Natl Acad Sci USA.* (2013) 110:10711–6. doi: 10.1073/pnas.1307868110
43. Godau J, Heller T, Hawlisch H, Trappe M, Howells E, Best J, et al. C5a initiates the inflammatory cascade in immune complex peritonitis. *J Immunol.* (2004) 173:3437–45. doi: 10.4049/jimmunol.173.5.3437
44. Hawlisch H, Belkaid Y, Baelder R, Hildeman D, Gerard C, Köhl J. C5a negatively regulates toll-like receptor 4-induced immune responses. *Immunity.* (2005) 22:415–26. doi: 10.1016/j.immuni.2005.02.006
45. Weaver DJJr, Reis ES, Pandey MK, Kohl G, Harris N, Gerard C, et al. C5a receptor-deficient dendritic cells promote induction of Treg and Th17 cells. *Eur J Immunol.* (2010) 40:710–21. doi: 10.1002/eji.200939333
46. Antoniou K, Ender F, Vollbrandt T, Laumonnier Y, Rathmann F, Pasare C, et al. Allergen-induced C5a/C5aR1 axis activation in pulmonary CD11b(+) cDCs promotes pulmonary tolerance through downregulation of CD40. *Cells.* (2020) 9:300. doi: 10.3390/cells9020300
47. Goldszmid RS, Caspar P, Rivollier A, White S, Dzutsev A, Hieny S, et al. NK cell-derived interferon-gamma orchestrates cellular dynamics and the differentiation of monocytes into dendritic cells at the site of infection. *Immunity.* (2012) 36:1047–59. doi: 10.1016/j.immuni.2012.03.026
48. Ivanova DL, Mundhenke TM, Gigley JP. The IL-12- and IL-23-dependent NK cell response is essential for protective immunity against secondary *Toxoplasma gondii* infection. *J Immunol.* (2019) 203:2944–58. doi: 10.4049/jimmunol.1801525
49. Hunter CA, Villarino A, Artis D, Scott P. The role of IL-27 in the development of T-cell responses during parasitic infections. *Immunol Rev.* (2004) 202:106–14. doi: 10.1111/j.0105-2896.2004.00213.x
50. Sher A, Oswald IP, Hieny S, Gazzinelli RT. *Toxoplasma gondii* induces a T-independent IFN-gamma response in natural killer cells that requires both adherent accessory cells and tumor necrosis factor-alpha. *J Immunol.* (1993) 150:3982–9.
51. Chang HR, Grau GE, Pechere JC. Role of TNF and IL-1 in infections with *Toxoplasma gondii*. *Immunology.* (1990) 69:33–7.
52. Passos ST, Silver JS, O'Hara AC, Sehy D, Stumhofer JS, Hunter CA. IL-6 promotes NK cell production of IL-17 during toxoplasmosis. *J Immunol.* (2010) 184:1776–83. doi: 10.4049/jimmunol.0901843
53. Gazzinelli RT, Wysocka M, Hieny S, Scharton-Kersten T, Cheever A, Kuhn R, et al. In the absence of endogenous IL-10, mice acutely infected with *Toxoplasma gondii* succumb to a lethal immune response dependent on $CD4^+$ T cells and accompanied by overproduction of IL-12, IFN-gamma and TNF-alpha. *J Immunol.* (1996) 157:798–805.
54. Neyer LE, Grunig G, Fort M, Remington JS, Rennick D, Hunter CA. Role of interleukin-10 in regulation of T-cell-dependent and T-cell-independent mechanisms of resistance to *Toxoplasma gondii*. *Infect Immun.* (1997) 65:1675–82. doi: 10.1128/IAI.65.5.1675-1682.1997

55. Khan IA, Matsuura T, Kasper LH. IL-10 mediates immunosuppression following primary infection with *Toxoplasma gondii* in mice. *Parasite Immunol.* (1995) 17:185–95. doi: 10.1111/j.1365-3024.1995.tb00888.x
56. Yap GS, Ortmann R, Shevach E, Sher A. A heritable defect in IL-12 signaling in B10.Q/J mice. II. Effect on acute resistance to *Toxoplasma gondii* and rescue by IL-18 treatment. *J Immunol.* (2001) 166:5720–5. doi: 10.4049/jimmunol.166.9.5720
57. Gorfu G, Cirelli KM, Melo MB, Mayer-Barber K, Crown D, Koller BH, et al. Dual role for inflammasome sensors NLRP1 and NLRP3 in murine resistance to *Toxoplasma gondii*. *MBio.* (2014) 5:e01117-13. doi: 10.1128/mBio.01117-13
58. Grailer JJ, Bosmann M, Ward PA. Regulatory effects of C5a on IL-17A, IL-17F, and IL-23. *Front Immunol.* (2012) 3:387. doi: 10.3389/fimmu.2012.00387
59. Lieberman LA, Cardillo F, Owyang AM, Rennick DM, Cua DJ, Kastelein RA, et al. IL-23 provides a limited mechanism of resistance to acute toxoplasmosis in the absence of IL-12. *J Immunol.* (2004) 173:1887–93. doi: 10.4049/jimmunol.173.3.1887
60. Gillessen S, Carvajal D, Ling P, Podlaski FJ, Stremlo DL, Familletti PC, et al. Mouse interleukin-12 (IL-12) p40 homodimer: a potent IL-12 antagonist. *Eur J Immunol.* (1995) 25:200–6. doi: 10.1002/eji.1830250133
61. Villarino A, Hibbert L, Lieberman L, Wilson E, Mak T, Yoshida H, et al. The IL-27R (WSX-1) is required to suppress T cell hyperactivity during infection. *Immunity.* (2003) 19:645–55. doi: 10.1016/S1074-7613(03)00300-5
62. Lopez-Yglesias AH, Camanzo E, Martin AT, Araujo AM, Yarovinsky F. TLR11-independent inflammasome activation is critical for $CD4^+$ T cell-derived IFN-gamma production and host resistance to *Toxoplasma gondii*. *PLoS Pathog.* (2019) 15:e1007872. doi: 10.1371/journal.ppat.1007872
63. Visser CE, Tekstra J, Brouwer-Steenbergen JJ, Tuk CW, Boorsma DM, Sampat-Sardjoepersad SC, et al. Chemokines produced by mesothelial cells: huGRO-alpha, IP-10, MCP-1 and RANTES. *Clin Exp Immunol.* (1998) 112:270–5. doi: 10.1046/j.1365-2249.1998.00592.x
64. Huttenrauch F, Pollok-Kopp B, Oppermann M. G protein-coupled receptor kinases promote phosphorylation and beta-arrestin-mediated internalization of CCR5 homo- and hetero-oligomers. *J Biol Chem.* (2005) 280:37503–15. doi: 10.1074/jbc.M500535200
65. Moreno-Fernandez ME, Aliberti J, Groeneweg S, Kohl J, Chougnet CA. A novel role for the receptor of the complement cleavage fragment C5a, C5aR1, in CCR5-mediated entry of HIV into macrophages. *AIDS Res Hum Retroviruses.* (2016) 32:399–408. doi: 10.1089/aid.2015.0099
66. Aliberti J, Schulz O, Pennington DJ, Tsujimura H, Reis e Sousa C, Ozato K, et al. Essential role for ICSBP in the *in vivo* development of murine CD8alpha + dendritic cells. *Blood.* (2003) 101:305–10. doi: 10.1182/blood-2002-04-1088
67. Scharton-Kersten T, Contursi C, Masumi A, Sher A, Ozato K. Interferon consensus sequence binding protein-deficient mice display impaired resistance to intracellular infection due to a primary defect in interleukin 12 p40 induction. *J Exp Med.* (1997) 186:1523–34. doi: 10.1084/jem.186.9.1523
68. Fusakio ME, Mohammed JP, Laumonnier Y, Hoebe K, Köhl J, Mattner J. C5a regulates NKT and NK cell functions in sepsis. *J Immunol.* (2011) 187:5805–12. doi: 10.4049/jimmunol.1100338
69. Ronet C, Darche S, Leite de Moraes M, Miyake S, Yamamura T, Louis JA, et al. NKT cells are critical for the initiation of an inflammatory bowel response against *Toxoplasma gondii*. *J Immunol.* (2005) 175:899–908. doi: 10.4049/jimmunol.175.2.899
70. Zhang X, Kimura Y, Fang C, Zhou L, Sfyroera G, Lambris JD, et al. Regulation of Toll-like receptor-mediated inflammatory response by complement *in vivo*. *Blood.* (2007) 110:228–36. doi: 10.1182/blood-2006-12-063636
71. Lalli PN, Strainic MG, Lin F, Medof ME, Heeger PS. Decay accelerating factor can control T cell differentiation into IFN-gamma-producing effector cells via regulating local C5a-induced IL-12 production. *J Immunol.* (2007) 179:5793–802. doi: 10.4049/jimmunol.179.9.5793
72. Wittmann M, Zwirner J, Larsson VA, Kirchhoff K, Begemann G, Kapp A, et al. C5a suppresses the production of IL-12 by IFN-gamma-primed and lipopolysaccharide-challenged human monocytes. *J Immunol.* (1999) 162:6763–9.
73. Li K, Fazekasova H, Wang N, Peng Q, Sacks SH, Lombardi G, et al. Functional modulation of human monocytes derived DCs by anaphylatoxins C3a and C5a. *Immunobiology.* (2012) 217:65–73. doi: 10.1016/j.imbio.2011.07.033
74. Karp CL, Grupe A, Schadt E, Ewart SL, Keane-Moore M, Cuomo PJ, et al. Identification of complement factor 5 as a susceptibility locus for experimental allergic asthma. *Nat Immunol.* (2000) 1:221–6. doi: 10.1038/79759
75. Suzuki Y, Orellana MA, Schreiber RD, Remington JS. Interferon-gamma: the major mediator of resistance against *Toxoplasma gondii*. *Science.* (1988) 240:516–8. doi: 10.1126/science.3128869

Conflict of Interest: The authors declare that the research was conducted in the absence of any commercial or financial relationships that could be construed as a potential conflict of interest.

frontiers in Immunology

REVIEW
published: 14 July 2020
doi: 10.3389/fimmu.2020.01471

Candida and Complement: New Aspects in an Old Battle

*Verena Harpf, Günter Rambach, Reinhard Würzner, Cornelia Lass-Flörl and Cornelia Speth**

Institute of Hygiene and Medical Microbiology, Medical University of Innsbruck, Innsbruck, Austria

Candida is a dominant fungal pathogen in immunocompromised hosts, leading to opportunistic infections. Complement with its multifaceted functions is involved in the immune defense against this yeast, and recently several novel aspects have emerged in this old battle. It is clear that *Candida* can adopt both roles as a colonizer or as a pathogen. In our article, we focus on the molecular mechanisms of the *Candida*-complement interplay, which occur in disseminated disease as well as locally on skin or on mucous membranes in mouth and vagina; the mechanisms can be supposed to be the same. Activation of the complement system by *Candida* is facilitated by directly triggering the three dominant pathways, but also indirectly via the coagulation and fibrinolysis systems. The complement-mediated anti-*Candida* effects induced thereby clearly extend chemotaxis, opsonization, and phagocytosis, and even the membrane attack complex formed on the fungal surface plays a modulatory role, although lysis of the yeast *per se* cannot be induced due to the thick fungal cell wall. In order to avoid the hostile action of complement, several evasion mechanisms have evolved during co-evolution, comprising the avoidance of recognition, and destruction. The latter comes in many flavors, in particular the cleavage of complement proteins by yeast enzymes and the exploitation of regulatory proteins by recruiting them on the cell wall, such as factor H. The rationale behind that is that the fluid phase regulators on the fungal cell surface down-regulate complement locally. Interestingly, however, evasion protein knockout strains do not necessarily lead to an attenuated disease, so it is likely more complex *in vivo* than initially thought. The interactions between complement and non-*albicans* species also deserve attention, especially *Candida auris*, a recently identified drug-resistant species of medical importance. This is in particular worth investigating, as deciphering of these interactions may lead to alternative anti-fungal therapies directly targeting the molecular mechanisms.

Keywords: *Candida*, complement, evasion, innate immunity, factor H, invasive fungal infections

OPEN ACCESS

Edited by:
Markus M. Heimesaat, Charité—Universitätsmedizin Berlin, Germany

Reviewed by:
Shanshan Luo, Huazhong University of Science and Technology, China
Heather Conti, University of Toledo, United States

****Correspondence:***
Cornelia Speth
cornelia.speth@i-med.ac.at

Specialty section:
This article was submitted to Microbial Immunology, a section of the journal Frontiers in Immunology

Received: *09 April 2020*
Accepted: *05 June 2020*
Published: *14 July 2020*

Citation:
Harpf V, Rambach G, Würzner R, Lass-Flörl C and Speth C (2020) Candida and Complement: New Aspects in an Old Battle. Front. Immunol. 11:1471. doi: 10.3389/fimmu.2020.01471

THE COMPLEMENT SYSTEM AND ITS MULTIFACETED FUNCTIONS

The complement system is an ancient and effective multicomponent bodily system for antimicrobial defense, homeostasis, and immunomodulation [reviewed in (1, 2)]. These functions are elicited by a system of soluble and membrane-bound effector, regulator, and receptor molecules, and form a tightly regulated cascade. Complement detects invading microbes and

modified self-surfaces (e.g., on apoptotic cells) using various pattern recognition molecules. Via different effector molecules of the cascade, this detection results in opsonization with subsequent phagocytic clearance, formation of the lytic C5b-9 complex of the terminal pathway, induction of inflammation, and modulation of other innate, and adaptive immune weapons.

Three activation pathways can push this system: the classical pathway (mainly induced by binding of immunoglobulins on target surfaces), the alternative pathway (triggered by deposition of spontaneously formed C3b on foreign surfaces with subsequent amplification loop), and the lectin pathway (elicited by foreign or aberrant carbohydrate structures on surfaces). The consequence of all three pathways is the covalent deposition of complement on the foreign surface and the generation of a C3-convertase that cleaves complement factor C3 into the larger C3b fragment and the smaller C3a anaphylatoxin. The composition of the C3-convertase varies upon the activation pathway (C4b2b for the classical and lectin pathway and C3bBb for the alternative pathway). The newly formed C3b either can amplify the alternative pathway by generating new C3-convertase molecules or can form a complex with the existing C3-convertases to generate a C5-convertase. The enzymatic function of the C5-convertases (cleavage of complement protein C5 into C5a anaphylatoxin and the C5b fragment) initiates the sequence of the terminal pathway. Several aggregation events finally result in generation of the C5b-9 complex. Inserted into the target membrane, C5b-9 is called membrane attack complex (MAC) and induces lysis of the pathogen or altered cell (3). If soluble, C5b-9 (called terminal complement complex TCC) harbors further functions such as cell activation and pro-inflammatory immune activation (4, 5).

The presence of such a powerful tool in the body requires the tight control by numerous regulators. Major soluble controller of the alternative pathway is factor H (FH), which is a single chained 150 kDa plasma glycoprotein (6). This protein is composed of 20 homologous domains known as short consensus repeats (SCR) or complement control protein (CCP) modules, each of which is made of 60 amino acids and stabilized by two internal disulfide-bonds (7, 8). The SCRs bear different functions. While the C-terminal domains SCRs 19 and 20 are essential for the target recognition, the N-terminal domains SCRs 1–4 mediate the diverse complement regulator functions (9–11) (**Figure 1**). Complement regulation by FH can be divided into three parts: First, FH competes with factor B for the C3b binding and therefore inhibits the assembly of the alternative pathway C3- and C5-convertases. Second, the protein exhibits a "decay accelerating activity," as it enhances the disassembly of these convertases by displacing bound factor Bb; and third, FH is used as a cofactor for the serine protease factor I in cleaving and inactivating C3b (8, 12, 13). An alternatively spliced transcript of the FH gene is factor H-like protein 1 (FHL-1) (14, 15). This 43 kDa plasma glycoprotein consists of the N-terminal domains SCRs 1–7 with four additional amino acids added at the C-terminus (16) (**Figure 1**). Compared to FH, the truncated form FHL-1 is less abundant in plasma (500 vs. 50 μg/ml, respectively) (17). FHL-1 still bears the same complement regulatory functions as FH and is therefore an important protein of the alternative pathway (8, 12, 13). The classical and lectin pathway, however, are mainly controlled by C4b binding protein (C4BP) [reviewed in (18)]. It binds to and inhibits the function of the activated complement compound C4b. C4BP acts as a cofactor of factor I (FI)-mediated cleavage

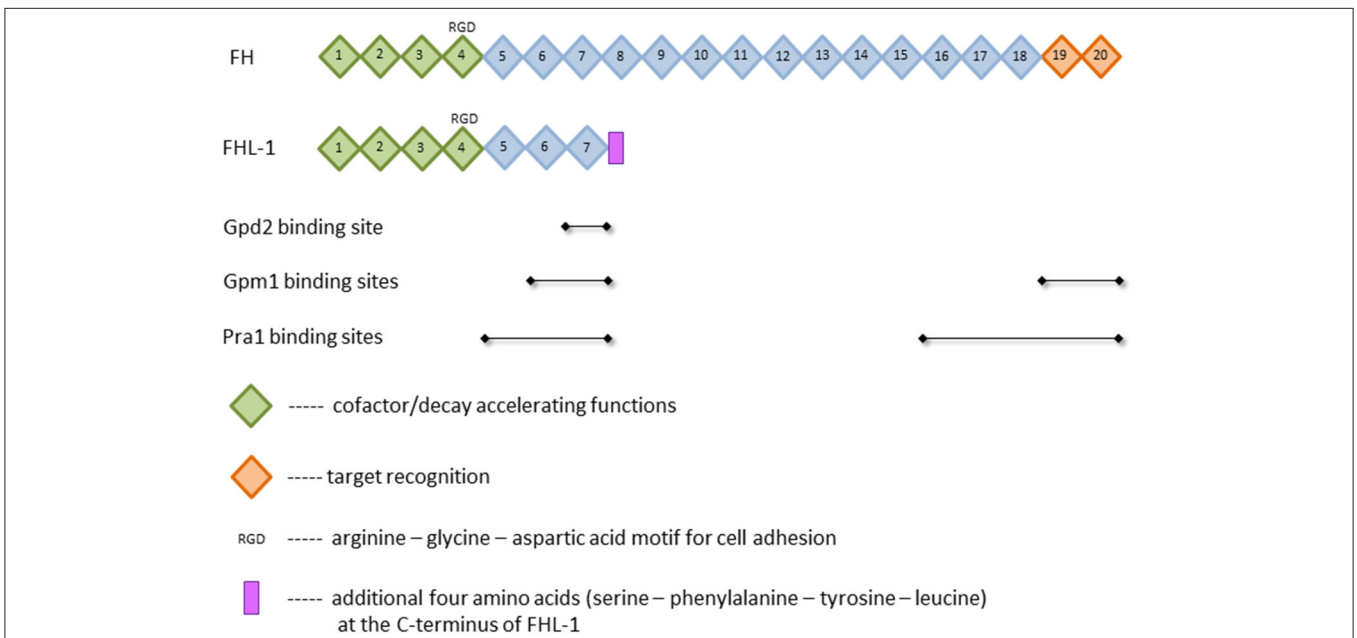

FIGURE 1 | Structure of factor H (FH) and factor H-like protein 1 (FHL-1). Depicted are selected functions of short consensus repeats (SCR), illustrated as squares, and the known binding sites of the FH-binding proteins phosphoglycerate mutase 1 (Gpm1), pH-regulated antigen 1 (Pra1), and glycerol-3-phosphate dehydrogenase 2 (Gpd2). For further details and references, see text.

and inactivation of soluble and cell-bound C4b, thus preventing the assembly of the C3-convertase C4b2b. In addition, C4BP accelerates the decay of functional C4b2b. Although FH is the main controller of the alternative pathway, C4BP also affects this pathway since it acts as a cofactor of FI in the proteolytic cleavage of C3b (18, 19).

A similar cofactor activity is attributed to the cell surface-expressed regulator molecule membrane cofactor protein (MCP; CD46). MCP and a further surface regulator, decay accelerating factor (DAF, CD55), accelerate the decay of both C3 convertases (3). Important regulators of the terminal pathway are CD59 (protectin) and vitronectin. Both molecules interfere with assembly of the C5b-9 complex and thus prevent its insertion into the membrane to form a lytic pore (20, 21).

CANDIDA AS COLONIZER AND PATHOGEN

Candida spp. are common members of the human mycobiome, but also opportunistic fungal pathogens [reviewed in (22, 23)]. In healthy individuals, *Candida* resides on the skin or as colonizer of the oral cavity, the gastrointestinal and the urogenital tract. When shifting from a colonizer to a pathogen, it causes cutaneous and mucocutaneous candidiasis as well as life-threatening invasive infections of inner organs and the bloodstream. The shift is enabled by changes in the host microbiota (e.g., by antibiotics), impairment of the host immune response (e.g., by immunosuppressive therapy), or alterations in the local conditions (e.g., shifts in nutrients or pH) (23, 24). The most common manifestation is vulvovaginal candidiasis affecting millions of women worldwide (25). The growing number of immunocompromised patients with intravenous catheters, cancer chemotherapy, or organ transplantations contributes to the boost in *Candida*-induced bloodstream infections (26).

The genus *Candida* includes at least 30 species of clinical importance; the most frequent one is *Candida albicans*, but non-*albicans* species become more and more common and are often associated with reduced antifungal susceptibility and outbreaks (22). *Candida auris* is a recently discovered emerging multidrug-resistant species that is responsible for an increasing number of nosocomial outbreaks.

Understanding of anti-*Candida* host defense mechanisms remains an urgent need. One focus is the interaction with the complement system as a universal and fast-acting immune weapon. The relevance of this interaction is accentuated by the fact that local production of complement is revealed for most organs, indicating a role in both superficial candidiasis and in *Candida* sepsis. The picture of *Candida*—complement interplay is complex and multifaceted and will be depicted in the following. Most knowledge exists about *Candida albicans*, but also non-*albicans* species are included, particularly *Candida auris*.

CANDIDA SPP. TRIGGER COMPLEMENT ACTIVATION BY MULTIPLE PATHWAYS

Various pathways are capable to mediate complement activation by *Candida*, underlining the relevance of this innate immune system in the case of infection.

The direct mechanisms of complement activation include the classical, lectin, and alternative pathway, which all were described to be triggered by *Candida* (27–29). Early experiments already showed that classical and alternative pathway are activated with different kinetics (30). The classical pathway might not only be triggered by interaction between the pattern recognition molecule C1q and specific anti-*Candida* antibodies: a recent report described that serum amyloid P (SAP) component, a member of the pentraxin family, binds to the *Candida albicans* surface (31). Although this report shows reduced phagocytosis after SAP binding, other authors described that SAP is able to activate the classical complement pathway (32, 33).

The efficiency of complement to react on the presence of *Candida* strongly depends on the surface composition of the yeast. On intact *Candida albicans* cells, β-glucan is located, together with chitin, in the inner fungal cell wall. However, during C. *albicans* infection or by treatment with caspofungin, the inner β-glucan components become exposed (34) and can initiate the alternative pathway of the complement system (35). Similarly, purified β-glucan triggered the alternative pathway when co-incubated with the purified AP proteins (35).

The lectin pathway is an evident candidate for *Candida*-triggered complement activation, since mannans represent about 40% of the total polysaccharide yeast cell wall content (36). Neth et al. (29) found diverse *Candida* species to strongly bind MBL (mannan-binding lectin), a starter molecule of the lectin pathway, with subsequent C4 deposition on the yeast surface. Another pattern recognition molecule of the lectin pathway, collectin-11, also bound to carbohydrate residues on *Candida albicans* and triggered complement activation with C4b and C3b deposition on the surface (37). Blocking of MBL in a mouse model increased C. *albicans* colonization, and MBL-deficient animals had a higher level of colonization than wild-type mice (38).

More recent findings imply that *Candida* activates the complement system not only via classical, lectin, or alternative pathway. More and more indirect mechanisms were discovered, involving molecules of the contact system, the fibrinolysis system, and the coagulation system. This complex pattern of *Candida*-induced complement activation is summarized in **Figure 2**.

The human plasma contact system represents a powerful immune surveillance tool that is activated by negatively charged surfaces, (e.g., on fungi). The contact of factor XII (FXII) to these surfaces triggers autoactivation with subsequent conversion to the active serine protease FXIIa. This process is also induced by contact with the cell walls of *Candida albicans* and *C. tropicalis* (39). In addition, previous work revealed that *Candida*-derived proteinases also activate factor XII (40), which appears to be a multifunctional molecule in innate immunity (41). Active FXIIa, either generated by *Candida* surface contact or by *Candida* proteases, cleaves prekallikrein to form kallikrein. Kallikrein reciprocally activates FXIIa, thus increasing rapidly the plasma level of both enzymes (41, 42). Furthermore, a *Candida albicans* proteinase directly converts plasma prekallikrein to active kallikrein (43). Kallikrein was shown to cleave the central complement protein C3 to yield the active fragments C3b and

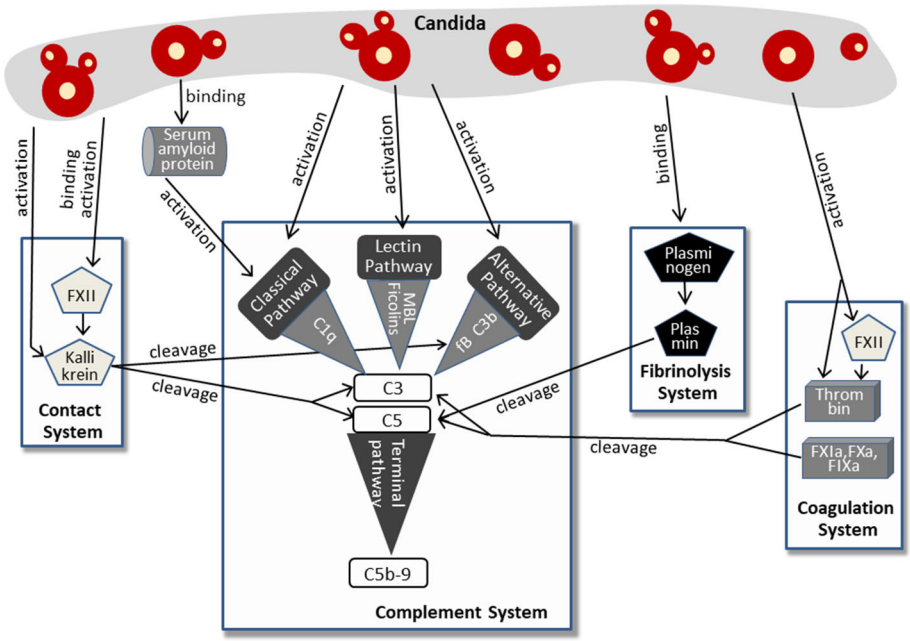

FIGURE 2 | Pathways of complement activation by *Candida*, either directly or by affecting the contact system, fibrinolysis system, or coagulation system. For further details, see text.

C3a. The proteolytic cleavage site used by kallikrein corresponds to that used by the C3 convertase, and the kallikrein-generated fragment C3b forms C3-convertase, thus triggering the C3 amplification loop. In addition, the C3a fragment resulting from kallikrein cleavage was determined to be biologically active and to harbor antimicrobial activity (44). The link from the contact system to complement activation in *Candida* infection is strengthened by findings that kallikrein also cleaves factor B, yielding Bb and Ba and thereby triggering the alternative pathway (44). Furthermore, contact system and complement system share regulator mechanisms, since C1INH, the regulator of the proteases of all three complement pathways, also represents the primary plasma control for FXIIa and kallikrein [reviewed in (45, 46)].

A second system that is activated by *Candida* and that cross-triggers complement activation is the coagulation system (**Figure 2**), a complex set of enzymes that mediates blood clotting. FXII, described above to be activated by *Candida* surfaces or *Candida* proteinases, also plays a central role in this system and promotes the generation of active thrombin (47), a key enzyme of coagulation (48). Active thrombin also results directly from the enzymatic function of *Candida* proteases (40). Thrombin effectively cleaves C3 to generate C3a that was capable to induce a chemotactic response of neutrophils (49, 50). In addition, thrombin is able to cleave C5 and thereby generates biologically active C5a and a functional C5-convertase even in the absence of C3 (51). Thrombin-generated C5 products also support triggering of the terminal complement pathway (52). Other components of the coagulation system, the factors IXa, Xa, and XIa, were also capable to cleave C3 and C5 (49).

The third system triggered by *Candida* and contributing to *Candida*-induced complement activation is the fibrinolysis system (**Figure 2**). Here, plasminogen/plasmin represent the central molecules. Urokinase-type plasminogen activator cleaves the plasma protein plasminogen to form plasmin, a serine protease that lyses fibrin clots and promotes degradation of the extracellular matrix. *Candida albicans* binds plasminogen to its surface via the proteins Gpm1 and Pra1 (53, 54). After conversion into proteolytically active plasmin, the subsequent degradation of extracellular matrix proteins and cell junction proteins might favor dissemination of the yeast. However, plasmin also mediates complement activation by cleaving C3 and C5 (49), and the plasmin-activated C5 was capable to yield a functional membrane attack complex (MAC) (55, 56). It must be mentioned that the role of plasminogen/plasmin in complement activation seems to be ambiguous, since other reports also describe an inhibitory role and list plasminogen as a complement inhibitor (see below).

COMPLEMENT-MEDIATED ANTI-*CANDIDA* EFFECTS

The infection-induced complement activation leads in general to opsonization and lysis of invading pathogens, initiation of inflammation, guidance of immune cells to the site of infection, and last but not least to stimulation of the adaptive immune response (57). The central role of complement in the host defense against *Candida* infection has been clearly demonstrated in a variety of experimental models with various deficiencies for complement proteins. C3-depleted guinea pigs showed higher

susceptibility to lethal *Candida* infections than untreated control animals (58). Tsoni et al. revealed a higher susceptibility to develop systemic and lethal infections with *C. albicans* and *C. glabrata* in C3 deficient mice compared to immunocompetent animals (59). Mice congenitally deficient in C5, such as DBA/2 or A/J, were highly susceptible to C. *albicans* infection (60–62). Furthermore, mice deficient in MBL, or double knockout mice lacking factor B and C2, showed highly increased mortality and elevated fungal load in the tissues after infection with *C. albicans* (63). The central role of complement in *Candida* infection has also been investigated in vaginal candidiasis. Notably, MBL as pattern recognition molecule plays a predominant role to determine severity and recurrence of disease. MBL was demonstrated to bind to *Candida* colonizing the vaginal cavity (64). The gene coding for MBL protein is polymorphic. A polymorphism associated with unstable MBL protein and thus decreased MBL concentrations is more prevalent in women developing primary vulvar vestibulitis syndrome than in control groups (65). Other reports confirm the relation of MBL polymorphism with recurrent vulvovaginal candidiasis and therapy resistance (36, 66–68). Similarly, cutaneous candidiasis was described to be strongly associated with complement. Mice with deficiency in C5 were less efficient in clearing experimental cutaneous *Candida* infection (69). Complement activation and deposition of C3 and factor B on *Candida* surface was demonstrated in an *in vitro* model of cutaneous candidiasis and were suggested to inhibit *Candida* adherence to corneocytes (70).

One predominant role of complement factor C3 is the opsonization of foreign structures to facilitate their uptake by complement receptor-bearing phagocytes (71). Opsonization of the *Candida* surface with C3 fragments is a very fast and efficient process, underlining the relevance of this mechanism particularly in early stages of infection (28). The most prominent receptor for C3b and iC3b deposited on the *Candida* surface is complement receptor 3 (CR3), widely expressed in professional phagocytes. Interestingly, *Candida* exposes a CR3-like molecule on its surface (72) that binds the negative complement regulator factor H and thus contributes to complement evasion, as described below.

Phagocytosis of *Candida* is not only facilitated by deposition of C3 fragments, but is further supported by an MBL-mediated "shortcut." Besides being the main pattern recognition molecule of the lectin pathway, MBL was shown to possess opsonic functions itself to bridge the *Candida* surface to the cellular complement receptor CR1 (CD35) expressed on monocytes and neutrophils (73). MBL-mediated opsonophagocytosis of *Candida albicans* by neutrophils is independent from complement activation and stimulates the intracellular expression of Dectin-1 with subsequent production of reactive oxygen species (ROS) (74). Since generation of toxic ROS represents an important fungicidal mechanism employed by innate immune cells, MBL acts as a dual complement effector molecule that utilizes both complement activation and activation-independent techniques for antifungal protection.

The pro-inflammatory anaphylatoxins C3a and C5a, which are generated by cleavage of complement factors C3 and C5, support these anti-*Candida* effects by chemotactically attracting phagocytes to the site of infection (75). C5a is particularly potent to attract neutrophils and monocytes; by binding to the corresponding receptors on neutrophils, C5a also increases their antimicrobial effector functions toward *Candida albicans* such as phagocytosis, oxidative burst, and degranulation (76). The induction of the release of the pro-inflammatory cytokines IL-6 and IL-1β by human peripheral blood mononuclear cells (PBMCs) completes the antifungal armamentarium of C5a (75, 77).

Similarly, the anaphylatoxin C3a exerts a broad spectrum of antimicrobial effects including chemotaxis and immune cell activation (78). However, C3a-like peptides were also shown to act directly as antifungal weapons by binding to the *Candida* surface and inducing membrane perturbations (79).

In contrast, the influence of the terminal complement cascade on host defense against yeasts is less clear. In any case, the progress of the terminal pathway will lead to formation of the C5b-9 complex on the yeast cell surface. Although C5b-9 is also termed membrane attack complex (MAC), the thick fungal cell wall inhibits its lytic activity against fungal cells (unlike for gram-negative bacteria or erythrocytes) (3). However, deposited MAC may cause immune modulatory effects, as it induces a higher fungal mitochondrial activation and augments phagocytosis (80).

COMPLEMENT EVASION BY *CANDIDA*

Masking

As described above, β-glucan molecules from the inner part of the *Candida* cell wall become exposed during infection or by treatment with the echinocandin caspofungin (34). Triggering of the alternative pathway of the complement system is a consequence of β-glucan exposure on the surface (35). Intact *Candida albicans* cells, however, are covered by a sheath of mannan that masks the complement-activating β-glucan layer (81) (**Table 1**). This mannan sheath provides resistance against alternative pathway activation (see **Figure 3**); conversion of mannose polysaccharides to polyalcohols or chemical removal of the surface mannan was shown to overcome this resistance (35). Specific antibodies against *C. albicans* mannan are a further tool to overcome this masking mechanism and to improve the outcome in experimental disseminated candidiasis (97). Interestingly, antibodies specifically recognizing β-mannans were protective against candidiasis, whereas α-mannan antibodies turned out to be non-protective. This difference perfectly correlated with the capacity of the antibodies to bind complement factor C3 on the yeast surface, a process that is much more efficient for the protective antibodies (97). The potency of mannan antibodies to overcome complement resistance is of particular interest, as most individuals have naturally occurring antibodies reactive with *Candida* mannan epitopes. However, these antibodies vary considerably regarding quantity and epitope specificity (98).

Cleavage and Blocking of Complement Proteins by *Candida*-Derived Proteases

Candida albicans produces a family of 10 related secreted aspartyl proteases (Sap proteins) that are considered to contribute

TABLE 1 | Overview of the different types of complement evasion performed by *Candida* species and the underlying mechanisms. For further details, see text.

Type of complement evasion	Mechanism	*Candida* species	References
Masking	Sheath of mannan covering β-glucan layer providing resistance against alternative pathway activation	*C. albicans*	(81)
Cleavage and blocking of complement proteins	Sap1-Sap3 degrade C3b, C4b, and C5 inhibiting opsonization by C3b and generation of anaphylatoxin C5a	*C. albicans*	(82)
	Sap2 cleaves FH, eliminating FH-mediated bridge between pathogen and neutrophils	*C. albicans*	(83, 84)
	Sap2 interferes with CR3 and CR4 expression on macrophages	*C. albicans*	(83)
	Sapp1 and Sapp2 cleave C3b, C4b and FH	*C. parapsilosis*	(85)
	Sapp2 degrades FHR5	*C. parapsilosis*	(85)
	Pra1 cleaves C3 at a unique site; the resulting C3a-like fragment has no effector functions and the C3b-like fragment is also not active and further degraded by FI and FH	*C. albicans*	(86)
	Pra1 blocks C3a derived from the action of C3 convertases	*C. albicans*	(86)
Recruitment of complement regulators	Acquisition of FH, FHL-1 by • Gpm1 • Pra1 • Hgt1 • Gpd2 – Competing with FB for C3b binding and inhibiting the assembly of the alternative pathway C3- and C5-convertases – Accelerating the decay of alternative pathway C3- and C5-convertases by displacing bound factor Bb – Enhancing FI-mediated cleavage and inactivation of C3b	*C. albicans*	(54, 72, 87–89)
	Acquisition of vitronectin by Gpm1 inhibiting C5b-7 insertion and C9 polymerization	*C. albicans*	(90, 91)
	Acquisition of C4BP by • Pra1 • Hgt1 – Acting as a cofactor of FI-mediated cleavage and inactivation of the soluble and cell-bound C4b and preventing the assembly of the C3 convertase C4b2b – Enhancing FI-mediated C3b degradation	*C. albicans*	(72, 92, 93)
	Acquisition of plasminogen by • Gpm1 • Gpd2 • Other proteins – Enhancing FI-mediated C3b degradation – Cleaving C3b and C5, when activated to plasmin	*C. albicans* *C. parapsilosis*	(54, 94–96)

substantially to pathogenicity by favoring adhesion, invasion, and tissue damage (99, 100). Furthermore, Sap proteins are of central relevance for pathogen survival in the host, since they destroy molecules of the immune system (antibodies, complement factors, cytokines) and thus limit microbicidal attacks (101). In this respect, elimination of an effective complement cascade as first-line defense is of special importance (**Figure 3**). Three members of the Sap family (Sap1-Sap3) were proven to bind and proteolytically degrade the complement proteins C3b, C4b, and C5 (82) and thereby subsequently inhibit complement activation (**Table 1**).

The functionality of this process was demonstrated by the findings that Sap proteins inhibit the opsonization of *C. albicans* by C3b and the generation of the anaphylatoxin C5a (82). A second complement-evading mechanism could be attributed to Sap2. It cleaves factor H (FH), a regulator of complement activity and, in addition, a putative bridging molecule between the pathogen and complement receptor CR3 (83) (**Table 1**). Losse et al. (84) revealed that FH, factor H-like protein (FHL-1) and factor H-related protein-1 (FHR-1) bind to *C. albicans* as well as to neutrophils. CR3 (CD11b/CD18) was identified to be the major receptor on neutrophils and thus facilitates the attachment of neutrophils to FH-bound *Candida*. When attached to *Candida* surface, FH and FHR1 enhanced the antimicrobial activity of the granulocytes and increased the killing of the pathogen (84). Secretion of Sap2 by *Candida* thus can contribute to immune evasion by proteolytically eliminating the FH-mediated bridge between pathogen and neutrophils. Furthermore, Sap2 interferes with CR3 and CR4 expression on macrophages (83) (**Table 1**).

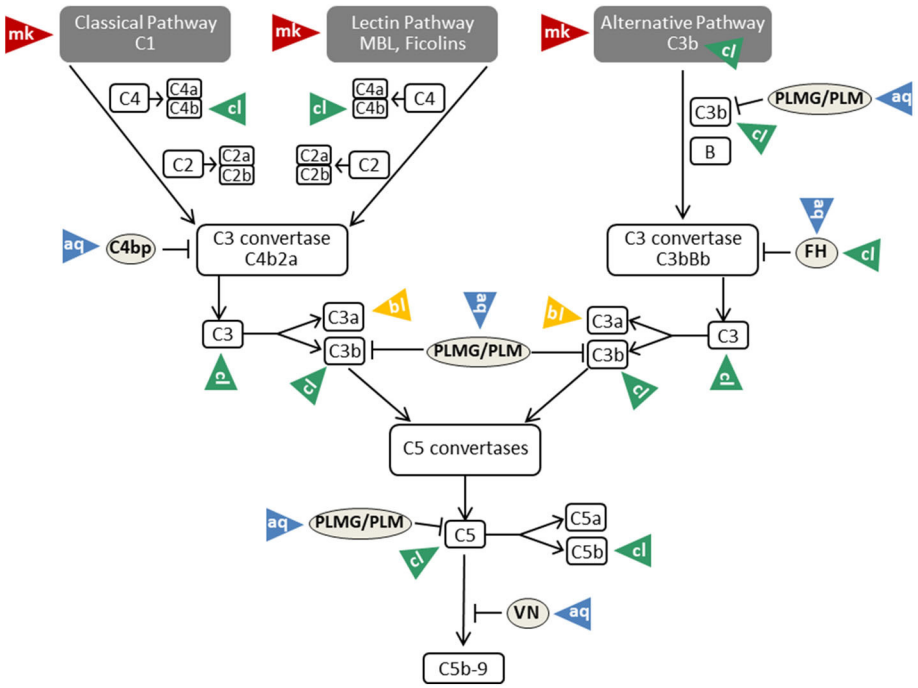

FIGURE 3 | Mechanisms of complement evasion by *Candida*. The different evasion mechanisms affecting the complete flow of the complement cascade are indicated by triangles and labeled with mk (masking; red triangles), aq (acquisition; blue triangles), cl (cleavage; green triangles), and bl (blocking; yellow triangles). VN, vitronectin; PLMG, Plasminogen; PLM, Plasmin; FH, factor H. For further details and references, see text.

The relevance of Sap proteins as virulence factors is not limited to *C. albicans*. A recent paper describes the functional characterization of Saps produced by *Candida parapsilosis* (85). *C. parapsilosis* possesses three secreted aspartyl protease-encoding genes (Sapp1-Sapp3). The purified enzymes Sapp1 and Sapp2 were demonstrated to efficiently cleave the complement components C4b, C3b, and FH; Sapp2 additionally degraded factor H-related protein 5 (FHR5) (**Table 1**). Macrophages phagocytosed and killed *C. parapsilosis* sapp1/2/3-/- deletion mutants more efficiently than wild type strains, indicating that Sap-mediated complement evasion is not limited to *C. albicans* (85). Two additional species that possess Sap genes, namely *C. tropicalis* (Sapt1-Sapt4) and *C. dubliniensis* (Sapcd1-Sapcd4, Sapcd7-Sapcd10), might also utilize Saps to modulate the complement system due to the high similarity of their Sap genes with those of *C. albicans* and *C. parapsilosis* (102, 103).

Saps are not the only *Candida*-derived proteases that contribute to virulence. The pH-regulated antigen 1 (Pra1) is described to interfere with complement-mediated antimicrobial functions by several mechanisms. Besides recruiting in its surface-bound form the complement inhibitors FH and C4BP to the *Candida* surface (see below), it is also released by *C. albicans* yeast and hyphal forms (87). Recombinant Pra1 was identified as a C3-degrading protease, cleaving C3 at a unique site (**Table 1**). Pra1 blocks effector functions of the resulting C3a fragment, whereas the Pra1-generated C3b-like fragment is processed and thus inactivated by the complement regulators factor I and factor H. Furthermore, Pra1 can also block C3a derived from the action of the C3 convertases (86) (**Table 1**).

Recruitment of Complement Regulators FH and FHL-1 on the *Candida* Surface

Although factor H (FH) and factor H-like protein 1 (FHL-1), beside others, should prevent the detrimental effect of the complement system on endogenous cells, such proteins are frequently used by pathogens to avoid recognition or destruction by complement. Regarding FH and FHL-1, it is known so far that *Candida albicans* expresses four different so-called FH-binding proteins, namely phosphoglycerate mutase 1 (Gpm1), pH-regulated antigen 1 (Pra1), high affinity glucose transporter 1 (Hgt1), and glycerol-3-phosphate dehydrogenase 2 (Gpd2) (53, 54, 72, 88) (**Table 1**).

Gpm1 was the first protein shown to bind FH (54). The native protein has a mass of 27.5 kDa and regulates the catalytic conversion of 3-phosphoglycerate to 2-phosphoglycerate in glycolysis and the reverse reaction in gluconeogenesis in the cytoplasm (54, 90). Beside the localization in the cytoplasm, Gpm1 is present in the cell wall of yeast cells and hyphae, latter especially on the tip of the hyphae. The lack of classical signal and transport sequences implies that export from the cytoplasm to the yeast surface circumvents endoplasmic reticulum and Golgi, but rather occurs via a non-conventional transport mechanism (54). When located on the cell wall, Gpm1 binds different complement regulators, namely FH, FHL-1 as well as vitronectin and plasminogen (see below). Regarding FH, Gpm1 bears two binding sites for this protein, which are located at SCRs 6-7 and SCRs 19–20 (**Figure 1**), the former is shared with FHL-1. These regulators stay active when Gpm1 binds them to *Candida* (54). Even though this moonlighting protein was detected on the

cell surface of different *Candida* species, namely *C. albicans*, *C. parapsilosis*, and *C. glabrata*, only little is known on the functions of Gpm1 in non-*albicans* species (104).

In 2009, 2 years after the first FH-binding molecule was described, Pra1 was discovered to bind FH to *Candida albicans*. In its monomeric form, Pra1 has a mass of 68 kDa and is composed of 299 amino acids (53, 105). It was initially described as a fibrinogen binding protein, which is localized on the cell wall of yeast and hyphae (105). The concentration is enhanced on the hyphal surface and notably high on the tips (53). Pra1 can either act as a pH-dependent zincophore, or manipulate complement to *Candida's* favor, as described above (53, 87, 106). Additionally, Pra1 binds directly or indirectly to different immune cells, resulting in contradictory effects. On the one hand, it can bind to $CD4^+$ T-cells and inhibit cytokine secretion; on the other hand, it serves as a ligand for the integrin $\alpha_M\beta_2$ (CD11b/CD18, CR3) expressed on neutrophilic granulocytes and therefore enables enhanced phagocytosis (107–109). FH is bound to Pra1 by two binding sites, namely SCRs 16–20, distinct for FH, and SCRs 5–7 (**Figure 1**), which is also a binding site for FHL-1. As the first four SCRs, mediating the complement regulator functions, are not affected by these different binding sites, pathogen-bound FH and FHL-1 stay functionally active (53).

In 2011, another FH-binding molecule named Hgt1 was discovered (72). This protein belongs to a large gene family of glucose transporters (20 proteins are described by now) and consists of 12 transmembrane domains, 545 amino acids, and weighs 60.67 kDa (110). Hgt1 can also be found in the cell wall of yeast cells and hyphae, where it can serve, in addition to its function as glucose transporter, as a binding molecule for the complement regulators FH and C4b-binding protein (C4BP) (72, 89). With binding of FH as main regulator of alternative pathway and of C4BP as main inhibitor of the classical and lectin pathway, Hgt1 has the capacity to comprehensively interfere with complement activation.

Gpd2, the fourth and by now last protein realized to bind FH, is made up of 371 amino acids, weighs 52 kDa and is localized on the surface of both yeast cells and hyphae (88). Initially, this protein was described as a nicotinamide adenine dinucleotide (NAD+)-dependent enzyme contributing to the degradation of glycerol (111). Gpd2 on *Candida* was shown to bind to human epithelial and endothelial cells, which might support *Candida* infection and dissemination in the host. In addition, Gpd2 controls the complement system by binding plasminogen via lysine residues (like Gpm1) and FH/FHL-1 by an amino acid sequence in SCR 7 (88) (**Figure 1**). FH/FHL-1 derived from individuals with a known human polymorphism on SCR7 (112, 113) may be unable to attach to Gpd2; it is interesting to speculate if these individuals show a better outcome in *Candida* infections.

Factor H binding by *Candida* might, however, also represent a double-edged sword for the pathogen. Since FH was described to also serve as a ligand for CR3 (114), *Candida*-bound FH might interact with CR3 on neutrophils and macrophages, thus bridging the pathogen to professional phagocytes and supporting clearance of the invader.

Recruitment of Other Complement Regulators on the *Candida* Surface

The family of factor H, factor H-like proteins, and factor H-related proteins are not the only complement regulators that are exploited by *Candida* to evade from complement. The soluble plasma proteins C4BP, plasminogen and vitronectin were also described to attach to *Candida* surface, to retain their complement regulatory functions and to assist in complement evasion (19, 87, 115) (**Figure 3**).

Acquisition of vitronectin on the surfaces of pathogens is a common complement evasion mechanism that was described for bacterial and viral pathogens (116, 117). As mentioned above, vitronectin is an inhibitor of the terminal pathway of complement; by inhibiting the membrane insertion of C5b-7 and the polymerization of C9, it interferes with assembly of the C5b-9 complex and formation of a lytic pore [reviewed in (19, 118)]. Vitronectin was shown to be a ligand for the *Candida albicans* surface protein Gpm1 (90). Acquisition of vitronectin to *Candida* leaves its terminal pathway regulatory domain accessible, thus enabling inhibition of C5b-7 insertion and C9 polymerization (91) (**Table 1**). Furthermore, vitronectin also binds to *C. parapsilosis* and *C. tropicalis* pseudohyphae via various surface compounds (119), implying that a similar complement evasion mechanism might be possible for these *Candida* species.

To limit complement activation for survival in the presence of innate immunity, *Candida* exploits the efficacy of the main regulator of the classical and lectin pathway, C4BP. For this purpose, both the yeast and the hyphal forms of *Candida albicans* are capable of binding C4BP to the fungal surface (92, 120). Preferential binding sites are located on the tips of the germ tubes. The surface-attached C4BP retains its regulatory capacity, inactivates C4b and thus limits the flow of the complement cascade (92) (**Table 1**). The pH-regulated antigen 1 (Pra1) and high affinity glucose transporter 1 (Hgt1) of *Candida albicans* were described to be the corresponding C4BP-binding molecules that enable this mechanism of fungal complement evasion (72, 87). Pra1 expression levels of different clinical *Candida albicans* isolates correlated with C4BP binding activity, increased fungal virulence and enhanced survival of the pathogen in the presence of complement (93). The acquisition of C4BP on the fungal surface is not limited to *Candida albicans*. Meri et al. also proved the binding of this protein to the yeast form of *C. tropicalis*, *C. glabrata*, and *C. krusei*, but it is not known whether the bound C4BP remains regulatory active in these species (92).

The third usage of complement regulators for *Candida albicans* survival concerns plasminogen. *C. albicans* acquires plasminogen on its surface via attachment to Gpm1, and bound plasminogen can be converted into the active protease plasmin by urokinase-type plasminogen activator (54). A recent report even lists eight plasminogen-binding proteins on *Candida albicans* and four proteins in *Candida parapsilosis* (94, 95). As mentioned above, some reports describe plasminogen/plasmin as a trigger for complement activation with generation of active C5 fragments. However, various reports show opposing results and picture plasminogen as complement inhibitor. Barthel et al.

mention plasminogen as a complement inhibitor that enhances FI-mediated C3b degradation and, activated to plasmin, cleaves C3b and C5 (96) (**Table 1**).

AN EMERGING FIELD: *CANDIDA AURIS* AND COMPLEMENT

In the last decade, *Candida auris* emerged as a multidrug-resistant yeast with severe cases of nosocomial infections. Outbreaks were observed all around the world in more than 30 countries (121, 122). The new species is intrinsically resistant to fluconazole and shows variable susceptibility to other azoles, echinocandins, and amphotericin B (122, 123). The genetic relation is closer to rarer *Candida* species such as *C. haemulonii* than to common species such as *C. albicans* and *C. glabrata* (123). Meanwhile, four distinct clades were distinguished with considerable inter-clade variation, implying independent emergence in multiple geographic regions.

The multidrug resistance strongly asks for deeper insights as a basis to develop immune-based supporting therapies. However, the knowledge about the interaction of *C. auris* with innate immunity is still limited. Xin et al. described that a mouse strain deficient in complement protein C5 (ΔC5) showed a high susceptibility for disseminated *C. auris* infection, compared to strains expressing C5. Immunosuppression with cyclophosphamide further substantially increased this susceptibility in ΔC5 mice, whereas treatment of animals with intact C5 gene had only minor effect. Detailed analysis of fungal burden in different organs revealed that expression of C5 is essential to limit the dissemination of *C. auris* into kidney, heart, and brain in infected mice (124).

Mimicry of complement receptors on the fungal surface is another link between *C. auris* and the complement system. The *Candida* complement receptor 3-related protein (CR3-RP) is a surface protein expressed by various *Candida* species during biofilm formation. CR3-RP is functionally and structurally related to the human CR3 (Mac-1, CD11b/CD18) expressed on neutrophils, monocytes, and macrophages. CR3-RP binds the human complement fragment iC3b and plays an important role in adherence to epithelial cells and in biofilm formation of different *Candida* species (125). Recent analysis confirmed the presence of CR3-RP also on the surface of *C. auris*. Blocking of CR3-RP with an antibody in the adherence phase inhibited *C. auris* biofilm formation. Furthermore, a polyclonal anti-CR3-RP antibody decreased the metabolic activity of pre-formed *C. auris* biofilms (126). Future work concerning *C. auris*-triggered complement activation, opsonization, and evasion mechanisms are necessary to get deeper insight into the interplay between this multidrug-resistant pathogen and the complement cascade.

CONCLUSION AND OUTLOOK: CURRENT AND FUTURE ASPECTS OF *CANDIDA*-COMPLEMENT RESEARCH

As described in our review, complement as a fast-acting immune weapon with nearly overall presence in the body and a broad spectrum of pathogen recognition is of central relevance for local and invasive *Candida* infections.

Although comprehensive views on this interesting mutual interplay between a pathogen and the corresponding innate immune response already exist, some aspects ask for further studies. Only limited precise data are available on complement and local *Candida* lesions in mouth, gut, skin, and vagina. Since many complement proteins are acute-phase proteins, the extent of the topical synthesis of single complement proteins in different stages of disease would be interesting. Furthermore, the contribution of excessive complement activation to development and severity of local lesions is a relevant aspect to be clarified.

Another emphasis should be a broader insight into non-*albicans* species. Although some data are available on the expression of Saps or plasminogen-binding proteins for non-*albicans*, (e.g., for *C. parapsilosis* or *C. glabrata*, an overview about the relevance of single complement aspects for the different species is lacking). A special focus in this respect should be laid on *Candida auris*. The relevance of complement for the defense against this species is emphasized by the susceptibility of complement-deficient animals. However, it is unclear which activation pathway has the highest impact to trigger the cascade. The rather small number of patients makes it difficult to weight the role of MBL polymorphism for the susceptibility against *C. auris*. Furthermore, the evasion mechanisms of *C. auris* are still completely unknown. Here, the acquisition of factor H, a central evasion mechanism for other *Candida* species, deserves particular attention.

Exploitation of complement molecules by *Candida* to down-regulate inflammatory immune responses is another aspect that should be expanded to non-*albicans* species. *C. albicans* was described to secrete soluble β-glucan that binds to complement receptor CR3 on host monocytes. Consequently, monocytes form and release vesicles that transport TGF-β1. TGF-β1-transporting extracellular vesicles down-modulate inflammation in whole-blood cells and amplify the anti-inflammatory reaction of endothelial cells (127). This fascinating mechanism might also play a role for other *Candida* species. The battle between *Candida* and complement is old, but still reveals many new aspects.

AUTHOR CONTRIBUTIONS

VH wrote the section Recruitment of Complement Regulators FH and FHL-1 on the *Candida* Surface. GR wrote chapter AN EMERGING FIELD: *CANDIDA AURIS* AND COMPLEMENT and references. RW wrote section COMPLEMENT-MEDIATED ANTI-*CANDIDA* EFFECTS. CS wrote the other chapters. CL-F did proofreading and corrections. All authors contributed to the article and approved the submitted version.

FUNDING

RW, VH, CS, and CL-F were supported by the Austrian Science Fund (FWF) Doctoral Program of Excellence HOROS (W1253).

REFERENCES

1. Bordron A, Bagacean C, Tempescul A, Berthou C, Bettacchioli E, Hillion S, et al. Complement system: a neglected pathway in immunotherapy. *Clin Rev Allergy Immunol*. (2019) 58:155–71. doi: 10.1007/s12016-019-08741-0
2. Vignesh P, Rawat A, Sharma M, Singh S. Complement in autoimmune diseases. *Clin Chim Acta*. (2017) 465:123–30. doi: 10.1016/j.cca.2016.12.017
3. Speth C, Prodinger W, Würzner R, Stoiber H, Dierich MP. Complement. In: Paul WE, editor. *Fundamental Immunology*. 6th ed. Philadelphia, PA: Lippincott Williams & Wilkins (2008). p. 1047–78.
4. Chen Y, Yang C, Jin N, Xie Z, Tang Y, Fei L, et al. Terminal complement complex C5b-9-treated human monocyte-derived dendritic cells undergo maturation and induce Th1 polarization. *Eur J Immunol*. (2007) 37:167–76. doi: 10.1002/eji.200636285
5. Nicholson-Weller A, Halperin JA. Membrane signaling by complement C5b-9, the membrane attack complex. *Immunol Res*. (1993) 12:244–57. doi: 10.1007/BF02918256
6. Rodriguez de Cordoba S, Esparza-Gordillo J, Goicoechea de Jorge E, Lopez-Trascasa M, Sanchez-Corral P. The human complement factor H: functional roles, genetic variations and disease associations. *Mol Immunol*. (2004) 41:355–67. doi: 10.1016/j.molimm.2004.02.005
7. Klickstein LB, Wong WW, Smith JA, Weis JH, Wilson JG, Fearon DT. Human C3b/C4b receptor (CR1). Demonstration of long homologous repeating domains that are composed of the short consensus repeats characteristics of C3/C4 binding proteins. *J Exp Med*. (1987) 165:1095–112. doi: 10.1084/jem.165.4.1095
8. Kopp A, Hebecker M, Svobodova E, Jozsi M. Factor h: a complement regulator in health and disease, and a mediator of cellular interactions. *Biomolecules*. (2012) 2:46–75. doi: 10.3390/biom2010046
9. Gordon DL, Kaufman RM, Blackmore TK, Kwong J, Lublin DM. Identification of complement regulatory domains in human factor H. *J Immunol*. (1995) 155:348–56.
10. Kuhn S, Skerka C, Zipfel PF. Mapping of the complement regulatory domains in the human factor H-like protein 1 and in factor H1. *J Immunol*. (1995) 155:5663–70.
11. Pangburn MK. Cutting edge: localization of the host recognition functions of complement factor H at the carboxyl-terminal: implications for hemolytic uremic syndrome. *J Immunol*. (2002) 169:4702–6. doi: 10.4049/jimmunol.169.9.4702
12. Farries TC, Seya T, Harrison RA, Atkinson JP. Competition for binding sites on C3b by CR1, CR2, MCP, factor B and factor H. *Complement Inflamm*. (1990) 7:30–41. doi: 10.1159/000463124
13. Meri T, Hartmann A, Lenk D, Eck R, Wurzner R, Hellwage J, et al. The yeast *Candida albicans* binds complement regulators factor H and FHL-1. *Infect Immun*. (2002) 70:5185–92. doi: 10.1128/IAI.70.9.5185-5192.2002
14. Zipfel PF, Hellwage J, Friese MA, Hegasy G, Jokiranta ST, Meri S. Factor H and disease: a complement regulator affects vital body functions. *Mol Immunol*. (1999) 36:241–8. doi: 10.1016/S0161-5890(99)00038-3
15. Zipfel PF, Jokiranta TS, Hellwage J, Koistinen V, Meri S. The factor H protein family. *Immunopharmacology*. (1999) 42:53–60. doi: 10.1016/S0162-3109(99)00015-6
16. Schwaeble W, Zwirner J, Schulz TF, Linke RP, Dierich MP, Weiss EH. Human complement factor H: expression of an additional truncated gene product of 43 kDa in human liver. *Eur J Immunol*. (1987) 17:1485–9. doi: 10.1002/eji.1830171015
17. Friese MA, Hellwage J, Jokiranta TS, Meri S, Peter HH, Eibel H, et al. FHL-1/reconectin and factor H: two human complement regulators which are encoded by the same gene are differently expressed and regulated. *Mol Immunol*. (1999) 36:809–18. doi: 10.1016/S0161-5890(99)00101-7
18. Ermert D, Blom AM. C4b-binding protein: the good, the bad and the deadly. Novel functions of an old friend. *Immunol Lett*. (2016) 169:82–92. doi: 10.1016/j.imlet.2015.11.014
19. Zipfel PF, Skerka C. Complement regulators and inhibitory proteins. *Nat Rev Immunol*. (2009) 9:729–40. doi: 10.1038/nri2620
20. Defendi F, Thielens NM, Clavarino G, Cesbron JY, Dumestre-Perard C. The immunopathology of complement proteins and innate immunity in autoimmune disease. *Clin Rev Allergy Immunol*. (2020) 58:229–51. doi: 10.1007/s12016-019-08774-5
21. Mathern DR, Heeger PS. Molecules great and small: the complement system. *Clin J Am Soc Nephrol*. (2015) 10:1636–50. doi: 10.2215/CJN.06230614
22. Eggimann P, Garbino J, Pittet D. Epidemiology of *Candida* species infections in critically ill non-immunosuppressed patients. *Lancet Infect Dis*. (2003) 3:685–702. doi: 10.1016/S1473-3099(03)00801-6
23. Nobile CJ, Johnson AD. *Candida albicans* biofilms and human disease. *Annu Rev Microbiol*. (2015) 69:71–92. doi: 10.1146/annurev-micro-091014-104330
24. Romo JA, Kumamoto CA. On commensalism of *Candida*. *J Fungi*. (2020) 6:e10016. doi: 10.3390/jof6010016
25. Sobel JD. Vulvovaginal candidosis. *Lancet*. (2007) 369:1961–71. doi: 10.1016/S0140-6736(07)60917-9
26. Sardi JC, Scorzoni L, Bernardi T, Fusco-Almeida AM, Mendes Giannini MJ. *Candida* species: current epidemiology, pathogenicity, biofilm formation, natural antifungal products and new therapeutic options. *J Med Microbiol*. (2013) 62:10–24. doi: 10.1099/jmm.0.045054-0
27. Cheng SC, Joosten LA, Kullberg BJ, Netea MG. Interplay between *Candida albicans* and the mammalian innate host defense. *Infect Immun*. (2012) 80:1304–13. doi: 10.1128/IAI.06146-11
28. Kozel TR. Activation of the complement system by pathogenic fungi. *Clin Microbiol Rev*. (1996) 9:34–46. doi: 10.1128/CMR.9.1.34
29. Neth O, Jack DL, Dodds AW, Holzel H, Klein NJ, Turner MW. Mannose-binding lectin binds to a range of clinically relevant microorganisms and promotes complement deposition. *Infect Immun*. (2000) 68:688–93. doi: 10.1128/IAI.68.2.688-693.2000
30. Kozel TR, Weinhold LC, Lupan DM. Distinct characteristics of initiation of the classical and alternative complement pathways by *Candida albicans*. *Infect Immun*. (1996) 64:3360–8. doi: 10.1128/IAI.64.8.3360-3368.1996
31. Behrens NE, Lipke PN, Pilling D, Gomer RH, Klotz SA. Serum amyloid P component binds fungal surface amyloid and decreases human macrophage phagocytosis and secretion of inflammatory cytokines. *MBio*. (2019) 10:19. doi: 10.1128/mBio.00218-19
32. Roy N, Ohtani K, Hidaka Y, Amano Y, Matsuda Y, Mori K, et al. Three pentraxins C-reactive protein, serum amyloid p component and pentraxin 3 mediate complement activation using Collectin CL-P1. *Biochim Biophys Acta General Subjects*. (2017) 1861:1–14. doi: 10.1016/j.bbagen.2016.11.023
33. Ying SC, Gewurz AT, Jiang H, Gewurz H. Human serum amyloid P component oligomers bind and activate the classical complement pathway via residues 14–26 and 76–92 of the A chain collagen-like region of C1q. *J Immunol*. (1993) 150:169–76.
34. Wheeler RT, Kombe D, Agarwala SD, Fink GR. Dynamic, morphotype-specific *Candida albicans* beta-glucan exposure during infection and drug treatment. *PLoS Pathog*. (2008) 4:e1000227. doi: 10.1371/journal.ppat.1000227
35. Boxx GM, Kozel TR, Nishiya CT, Zhang MX. Influence of mannan and glucan on complement activation and C3 binding by *Candida albicans*. *Infect Immun*. (2010) 78:1250–9. doi: 10.1128/IAI.00744-09
36. Hammad NM, El Badawy NE, Ghramh HA, Al Kady LM. Mannose-binding lectin: a potential therapeutic candidate against *Candida* infection. *Biomed Res Int*. (2018) 2018:2813737. doi: 10.1155/2018/2813737
37. Ma YJ, Skjoedt MO, Garred P. Collectin-11/MASP complex formation triggers activation of the lectin complement pathway–the fifth lectin pathway initiation complex. *J Innate Immun*. (2013) 5:242–50. doi: 10.1159/000345356
38. Choteau L, Parny M, Francois N, Bertin B, Fumery M, Dubuquoy L, et al. Role of mannose-binding lectin in intestinal homeostasis and fungal elimination. *Mucosal Immunol*. (2016) 9:767–76. doi: 10.1038/mi.2015.100
39. Karkowska-Kuleta J, Kozik A, Rapala-Kozik M. Binding and activation of the human plasma kinin-forming system on the cell walls of *Candida albicans* and *Candida tropicalis*. *Biol Chem*. (2010) 391:97–103. doi: 10.1515/bc.2009.145
40. Kaminishi H, Hamatake H, Cho T, Tamaki T, Suenaga N, Fujii T, et al. Activation of blood clotting factors by microbial proteinases. *FEMS Microbiol Lett*. (1994) 121:327–32. doi: 10.1111/j.1574-6968.1994.tb07121.x
41. Renne T, Stavrou EX. Roles of factor XII in innate immunity. *Front Immunol*. (2019) 10:2011. doi: 10.3389/fimmu.2019.02011
42. Raghunathan V, Zilberman-Rudenko J, Olson SR, Lupu F, McCarty OJT, Shatzel JJ. The contact pathway and sepsis. *Res Practice Thrombosis Haemostasis*. (2019) 3:331–9. doi: 10.1002/rth2.12217

43. Kaminishi H, Tanaka M, Cho T, Maeda H, Hagihara Y. Activation of the plasma kallikrein-kinin system by *Candida albicans* proteinase. *Infect Immun*. (1990) 58:2139–43. doi: 10.1128/IAI.58.7.2139-2143.1990
44. Irmscher S, Doring N, Halder LD, Jo EA. H., Kopka I, Dunker C, et al. Kallikrein cleaves C3 and activates complement. *J Innate Immun*. (2018) 10:94–105. doi: 10.1159/000484257
45. Davis AE 3rd. The pathophysiology of hereditary angioedema. *Clin Immunol*. (2005) 114:3–9. doi: 10.1016/j.clim.2004.05.007
46. Longhurst HJ, Bork K. Hereditary angioedema: an update on causes, manifestations and treatment. *Br J Hosp Med*. (2019) 80:391–8. doi: 10.12968/hmed.2019.80.7.391
47. Gailani D, Bane CE, Gruber A. Factor XI and contact activation as targets for antithrombotic therapy. *J Thromb Haemost*. (2015) 13:1383–95. doi: 10.1111/jth.13005
48. Negrier C, Shima M, Hoffman M. The central role of thrombin in bleeding disorders. *Blood Rev*. (2019) 38:100582. doi: 10.1016/j.blre.2019.05.006
49. Amara U, Flierl MA, Rittirsch D, Klos A, Chen H, Acker B, et al. Molecular intercommunication between the complement and coagulation systems. *J Immunol*. (2010) 185:5628–36. doi: 10.4049/jimmunol.0903678
50. Amara U, Rittirsch D, Flierl M, Bruckner U, Klos A, Gebhard F, et al. Interaction between the coagulation and complement system. *Adv Exp Med Biol*. (2008) 632:71–9. doi: 10.1007/978-0-387-78952-1_6
51. Huber-Lang M, Sarma JV, Zetoune FS, Rittirsch D, Neff TA, McGuire SR, et al. Generation of C5a in the absence of C3: a new complement activation pathway. *Nat Med*. (2006) 12:682–7. doi: 10.1038/nm1419
52. Krisinger MJ, Goebeler V, Lu Z, Meixner SC, Myles T, Pryzdial EL, et al. Thrombin generates previously unidentified C5 products that support the terminal complement activation pathway. *Blood*. (2012) 120:1717–25. doi: 10.1182/blood-2012-02-412080
53. Luo S, Poltermann S, Kunert A, Rupp S, Zipfel PF. Immune evasion of the human pathogenic yeast *Candida albicans*: Pra1 is a Factor H, FHL-1 and plasminogen binding surface protein. *Mol Immunol*. (2009) 47:541–50. doi: 10.1016/j.molimm.2009.07.017
54. Poltermann S, Kunert A, von der Heide M, Eck R, Hartmann A, Zipfel PF. Gpm1p is a factor H-, FHL-1-, and plasminogen-binding surface protein of *Candida albicans*. *J Biol Chem*. (2007) 282:37537–44. doi: 10.1074/jbc.M707280200
55. Foley JH, Walton BL, Aleman MM, O'Byrne AM, Lei V, Harrasser M, et al. Complement activation in arterial and venous thrombosis is mediated by plasmin. *EBioMedicine*. (2016) 5:175–82. doi: 10.1016/j.ebiom.2016.02.011
56. Leung LL, Morser J. Plasmin as a complement C5 convertase. *EBioMedicine*. (2016) 5:20–1. doi: 10.1016/j.ebiom.2016.03.015
57. Merle NS, Noe R, Halbwachs-Mecarelli L, Fremeaux-Bacchi V, Roumenina LT. Complement system part II: role in immunity. *Front Immunol*. (2015) 6:257. doi: 10.3389/fimmu.2015.00257
58. Bottger EC, Metzger S, Bitter-Suermann D, Stevenson G, Kleindienst S, Burger R. Impaired humoral immune response in complement C3-deficient guinea pigs: absence of secondary antibody response. *Eur J Immunol*. (1986) 16:1231–5. doi: 10.1002/eji.1830161008
59. Tsoni SV, Kerrigan AM, Marakalala MJ, Srinivasan N, Duffield M, Taylor PR, et al. Complement C3 plays an essential role in the control of opportunistic fungal infections. *Infect Immun*. (2009) 77:3679–85. doi: 10.1128/IAI.00233-09
60. Ashman RB, Fulurija A, Papadimitriou JM. Strain-dependent differences in host response to *Candida albicans* infection in mice are related to organ susceptibility and infectious load. *Infect Immun*. (1996) 64:1866–9. doi: 10.1128/IAI.64.5.1866-1869.1996
61. Ashman RB, Papadimitriou JM, Fulurija A, Drysdale KE, Farah CS, Naidoo O, et al. Role of complement C5 and T lymphocytes in pathogenesis of disseminated and mucosal candidiasis in susceptible DBA/2 mice. *Microb Pathog*. (2003) 34:103–13. doi: 10.1016/S0882-4010(02)00211-5
62. Hector RF, Domer JE, Carrow EW. Immune responses to *Candida albicans* in genetically distinct mice. *Infect Immun*. (1982) 38:1020–8. doi: 10.1128/IAI.38.3.1020-1028.1982
63. Held K, Thiel S, Loos M, Petry F. Increased susceptibility of complement factor B/C2 double knockout mice and mannan-binding lectin knockout mice to systemic infection with *Candida albicans*. *Mol Immunol*. (2008) 45:3934–41. doi: 10.1016/j.molimm.2008.06.021
64. Pellis V, De Seta F, Crovella S, Bossi F, Bulla R, Guaschino S, et al. Mannose binding lectin and C3 act as recognition molecules for infectious agents in the vagina. *Clin Exp Immunol*. (2005) 139:120–6. doi: 10.1111/j.1365-2249.2005.02660.x
65. Babula O, Linhares IM, Bongiovanni AM, Ledger WJ, Witkin SS. Association between primary vulvar vestibulitis syndrome, defective induction of tumor necrosis factor-alpha, and carriage of the mannose-binding lectin codon 54 gene polymorphism. *Am J Obstet Gynecol*. (2008) 198:101.e101–104. doi: 10.1016/j.ajog.2007.05.037
66. Babula O, Lazdane G, Kroica J, Ledger WJ, Witkin SS. Relation between recurrent vulvovaginal candidiasis, vaginal concentrations of mannose-binding lectin, and a mannose-binding lectin gene polymorphism in Latvian women. *Clin Infect Dis*. (2003) 37:733–7. doi: 10.1086/377234
67. Donders GG, Babula O, Bellen G, Linhares IM, Witkin SS. Mannose-binding lectin gene polymorphism and resistance to therapy in women with recurrent vulvovaginal candidiasis. *BJOG*. (2008) 115:1225–31. doi: 10.1111/j.1471-0528.2008.01830.x
68. Hammad NM, El Badawy NE, Nasr AM, Ghramh HA, Al Kady LM. Mannose-binding lectin gene polymorphism and its association with susceptibility to recurrent vulvovaginal candidiasis. *Biomed Res Int*. (2018) 2018:7648152. doi: 10.1155/2018/7648152
69. Wilson BD, Sohnle PG. Neutrophil accumulation and cutaneous responses in experimental cutaneous candidiasis of genetically complement-deficient mice. *Clin Immunol Immunopathol*. (1988) 46:284–93. doi: 10.1016/0090-1229(88)90190-0
70. Ray TL, Digre KB, Payne CD. Adherence of *Candida* species to human epidermal corneocytes and buccal mucosal cells: correlation with cutaneous pathogenicity. *J Invest Dermatol*. (1984) 83:37–41. doi: 10.1111/1523-1747.ep12261661
71. Densen P. Human complement deficiency states and infection. In: Whaley K, Loos M, Weiler JM, editors. *Complement in Health and Disease*. Dordrecht: Springer Netherlands (1993). p. 173–97. doi: 10.1007/978-94-011-2214-6_6
72. Lesiak-Markowicz I, Vogl G, Schwarzmuller T, Speth C, Lass-Florl C, Dierich MP, et al. *Candida albicans* Hgt1p, a multifunctional evasion molecule: complement inhibitor, CR3 analogue, and human immunodeficiency virus-binding molecule. *J Infect Dis*. (2011) 204:802–9. doi: 10.1093/infdis/jir455
73. Ghiran I, Barbashov SF, Klickstein LB, Tas SW, Jensenius JC, Nicholson-Weller A. Complement receptor 1/CD35 is a receptor for mannan-binding lectin. *J Exp Med*. (2000) 192:1797–808. doi: 10.1084/jem.192.12.1797
74. Li D, Dong B, Tong Z, Wang Q, Liu W, Wang Y, et al. MBL-mediated opsonophagocytosis of *Candida albicans* by human neutrophils is coupled with intracellular Dectin-1-triggered ROS production. *PLoS ONE*. (2012) 7:e50589. doi: 10.1371/journal.pone.0050589
75. Zipfel PF, Skerka C. Complement, *Candida*, and cytokines: the role of C5a in host response to fungi. *Eur J Immunol*. (2012) 42:822–5. doi: 10.1002/eji.201242466
76. Hunniger K, Bieber K, Martin R, Lehnert T, Figge MT, Loffler J, et al. A second stimulus required for enhanced antifungal activity of human neutrophils in blood is provided by anaphylatoxin C5a. *J Immunol*. (2015) 194:1199–210. doi: 10.4049/jimmunol.1401845
77. Cheng SC, Sprong T, Joosten LA, van der Meer JW, Kullberg BJ, Hube B, et al. Complement plays a central role in *Candida albicans*-induced cytokine production by human PBMCs. *Eur J Immunol*. (2012) 42:993–1004. doi: 10.1002/eji.201142057
78. Nordahl EA, Rydengard V, Nyberg P, Nitsche DP, Morgelin M, Malmsten M, et al. Activation of the complement system generates antibacterial peptides. *Proc Natl Acad Sci USA*. (2004) 101:16879–84. doi: 10.1073/pnas.0406678101
79. Sonesson A, Ringstad L, Nordahl EA, Malmsten M, Morgelin M, Schmidtchen A. Antifungal activity of C3a and C3a-derived peptides against *Candida*. *Biochim Biophys Acta*. (2007) 1768:346–53. doi: 10.1016/j.bbamem.2006.10.017
80. Triebel T, Grillhosl B, Kacani L, Lell CP, Fuchs A, Speth C, et al. Importance of the terminal complement components for immune defence against *Candida*. *Int J Med Microbiol*. (2003) 292:527–36. doi: 10.1078/1438-4221-00211
81. Suzuki S. Immunochemical study on mannans of genus *Candida*. I. Structural investigation of antigenic factors 1, 4, 5, 6, 8, 9, 11, 13, 13b, and 34. *Curr Top Med Mycol*. (1997) 8:57–70.

82. Gropp K, Schild L, Schindler S, Hube B, Zipfel PF, Skerka C. The yeast *Candida albicans* evades human complement attack by secretion of aspartic proteases. *Mol Immunol*. (2009) 47:465–75. doi: 10.1016/j.molimm.2009.08.019
83. Svoboda E, Schneider AE, Sandor N, Lermann U, Staib P, Kremlitzka M, et al. Secreted aspartic protease 2 of *Candida albicans* inactivates factor H and the macrophage factor H-receptors CR3 (CD11b/CD18) and CR4 (CD11c/CD18). *Immunol Lett*. (2015) 168:13–21. doi: 10.1016/j.imlet.2015.08.009
84. Losse J, Zipfel PF, Jozsi M. Factor H and factor H-related protein 1 bind to human neutrophils via complement receptor 3, mediate attachment to *Candida albicans*, and enhance neutrophil antimicrobial activity. *J Immunol*. (2010) 184:912–21. doi: 10.4049/jimmunol.0901702
85. Singh DK, Nemeth T, Papp A, Toth R, Lukacsi S, Heidingsfeld O, et al. Functional characterization of secreted aspartyl proteases in *Candida parapsilosis*. *mSphere*. (2019) 4:19. doi: 10.1128/mSphere.00484-19
86. Luo S, Dasari P, Reiher N, Hartmann A, Jacksch S, Wende E, et al. The secreted *Candida albicans* protein Pra1 disrupts host defense by broadly targeting and blocking complement C3 and C3 activation fragments. *Mol Immunol*. (2018) 93:266–77. doi: 10.1016/j.molimm.2017.07.010
87. Luo S, Blom AM, Rupp S, Hipler UC, Hube B, Skerka C, et al. The pH-regulated antigen 1 of *Candida albicans* binds the human complement inhibitor C4b-binding protein and mediates fungal complement evasion. *J Biol Chem*. (2011) 286:8021–9. doi: 10.1074/jbc.M110.130138
88. Luo S, Hoffmann R, Skerka C, Zipfel PF. Glycerol-3-phosphate dehydrogenase 2 is a novel factor H-, factor H-like protein 1-, and plasminogen-binding surface protein of *Candida albicans*. *J Infect Dis*. (2013) 207:594–603. doi: 10.1093/infdis/jis718
89. Kenno S, Speth C, Rambach G, Binder U, Chatterjee S, Caramalho R, et al. *Candida albicans* factor H binding molecule Hgt1p—a low glucose-induced transmembrane protein is trafficked to the cell wall and impairs phagocytosis and killing by human neutrophils. *Front Microbiol*. (2018) 9:3319. doi: 10.3389/fmicb.2018.03319
90. Lopez CM, Wallich R, Riesbeck K, Skerka C, Zipfel PF. *Candida albicans* uses the surface protein Gpm1 to attach to human endothelial cells and to keratinocytes via the adhesive protein vitronectin. *PLoS ONE*. (2014) 9:e90796. doi: 10.1371/journal.pone.0090796
91. Hallstrom T, Singh B, Kraiczy P, Hammerschmidt S, Skerka C, Zipfel PF, et al. Conserved patterns of microbial immune escape: pathogenic microbes of diverse origin target the human terminal complement inhibitor vitronectin via a single common motif. *PLoS ONE*. (2016) 11:e0147709. doi: 10.1371/journal.pone.0147709
92. Meri T, Blom AM, Hartmann A, Lenk D, Meri S, Zipfel PF. The hyphal and yeast forms of *Candida albicans* bind the complement regulator C4b-binding protein. *Infect Immun*. (2004) 72:6633–41. doi: 10.1128/IAI.72.11.6633-6641.2004
93. Luo S, Hipler UC, Munzberg C, Skerka C, Zipfel PF. Sequence variations and protein expression levels of the two immune evasion proteins Gpm1 and Pra1 influence virulence of clinical *Candida albicans* isolates. *PLoS ONE*. (2015) 10:e0113192. doi: 10.1371/journal.pone.0113192
94. Crowe JD, Sievwright IK, Auld GC, Moore NR, Gow NA, Booth NA. *Candida albicans* binds human plasminogen: identification of eight plasminogen-binding proteins. *Mol Microbiol*. (2003) 47:1637–51. doi: 10.1046/j.1365-2958.2003.03390.x
95. Karkowska-Kuleta J, Zajac D, Bras G, Bochenska O, Rapala-Kozik M, Kozik A. Binding of human plasminogen and high-molecular-mass kininogen by cell surface-exposed proteins of *Candida parapsilosis*. *Acta Biochim Pol*. (2017) 64:391–400. doi: 10.18388/abp.2017_1609
96. Barthel D, Schindler S, Zipfel PF. Plasminogen is a complement inhibitor. *J Biol Chem*. (2012) 287:18831–42. doi: 10.1074/jbc.M111.323287
97. Han Y, Kozel TR, Zhang MX, MacGill RS, Carroll MC, Cutler JE. Complement is essential for protection by an IgM and an IgG3 monoclonal antibody against experimental, hematogenously disseminated candidiasis. *J Immunol*. (2001) 167:1550–7. doi: 10.4049/jimmunol.167.3.1550
98. Zhang MX, Bohlman MC, Itatani C, Burton DR, Parren PW, St. Jeor SC, et al. Human recombinant antimannan immunoglobulin G1 antibody confers resistance to hematogenously disseminated candidiasis in mice. *Infect Immun*. (2006) 74:362–9. doi: 10.1128/IAI.74.1.362-369.2006
99. Naglik J, Albrecht A, Bader O, Hube B. *Candida albicans* proteinases and host/pathogen interactions. *Cell Microbiol*. (2004) 6:915–26. doi: 10.1111/j.1462-5822.2004.00439.x
100. Rapala-Kozik M, Bochenska O, Zajac D, Karkowska-Kuleta J, Gogol M, Zawrotniak M, et al. Extracellular proteinases of *Candida* species pathogenic yeasts. *Mol Oral Microbiol*. (2018) 33:113–24. doi: 10.1111/omi.12206
101. Monika S, Malgorzata B, Zbigniew O. Contribution of aspartic proteases in *Candida* virulence. Protease inhibitors against *Candida* infections. *Curr Protein Peptide Sci*. (2017) 18:1050–62. doi: 10.2174/1389203717666160809155749
102. Parra-Ortega B, Cruz-Torres H, Villa-Tanaca L, Hernández-Rodríguez C. Phylogeny and evolution of the aspartyl protease family from clinically relevant *Candida* species. *Mem Inst Oswaldo Cruz*. (2009) 104:505–12. doi: 10.1590/S0074-02762009000300018
103. Zaugg C, Borg-Von Zepelin M, Reichard U, Sanglard D, Monod M. Secreted aspartic proteinase family of *Candida tropicalis*. *Infect Immun*. (2001) 69:405–12. doi: 10.1128/IAI.69.1.405-412.2001
104. Karkowska-Kuleta J, Satala D, Bochenska O, Rapala-Kozik M, Kozik A. Moonlighting proteins are variably exposed at the cell surfaces of *Candida glabrata*, *Candida parapsilosis* and *Candida tropicalis* under certain growth conditions. *BMC Microbiol*. (2019) 19:149. doi: 10.1186/s12866-019-1524-5
105. Sentandreu M, Elorza MV, Sentandreu R, Fonzi WA. Cloning and characterization of PRA1, a gene encoding a novel pH-regulated antigen of *Candida albicans*. *J Bacteriol*. (1998) 180:282–9. doi: 10.1128/JB.180.2.282-289.1998
106. Loboda D, Rowinska-Zyrek M. Zinc binding sites in Pra1, a zincophore from *Candida albicans*. *Dalton Trans*. (2017) 46:13695–703. doi: 10.1039/C7DT01675A
107. Bergfeld A, Dasari P, Werner S, Hughes TR, Song WC, Hortschansky P, et al. Direct binding of the pH-regulated protein 1 (Pra1) from *Candida albicans* inhibits cytokine secretion by mouse CD4(+) T cells. *Front Microbiol*. (2017) 8:844. doi: 10.3389/fmicb.2017.00844
108. Soloviev DA, Fonzi WA, Sentandreu R, Pluskota E, Forsyth CB, Yadav S, et al. Identification of pH-regulated antigen 1 released from *Candida albicans* as the major ligand for leukocyte integrin alphaMbeta2. *J Immunol*. (2007) 178:2038–46. doi: 10.4049/jimmunol.178.4.2038
109. Soloviev DA, Jawhara S, Fonzi WA. Regulation of innate immune response to *Candida albicans* infections by alphaMbeta2-Pra1p interaction. *Infect Immun*. (2011) 79:1546–58. doi: 10.1128/IAI.00650-10
110. Fan J, Chaturvedi V, Shen SH. Identification and phylogenetic analysis of a glucose transporter gene family from the human pathogenic yeast *Candida albicans*. *J Mol Evol*. (2002) 55:336–46. doi: 10.1007/s00239-002-2330-4
111. Ansell R, Granath K, Hohmann S, Thevelein JM, Adler L. The two isoenzymes for yeast NAD+-dependent glycerol 3-phosphate dehydrogenase encoded by GPD1 and GPD2 have distinct roles in osmoadaptation and redox regulation. *EMBO J*. (1997) 16:2179–87. doi: 10.1093/emboj/16.9.2179
112. Ormsby RJ, Ranganathan S, Tong JC, Griggs KM, Dimasi DP, Hewitt AW, et al. Functional and structural implications of the complement factor H Y402H polymorphism associated with age-related macular degeneration. *Invest Ophthalmol Vis Sci*. (2008) 49:1763–70. doi: 10.1167/iovs.07-1297
113. Weismann D, Hartvigsen K, Lauer N, Bennett KL, Scholl HP, Charbel Issa P, et al. Complement factor H binds malondialdehyde epitopes and protects from oxidative stress. *Nature*. (2011) 478:76–81. doi: 10.1038/nature10449
114. DiScipio RG, Daffern PJ, Schraufstatter IU, Sriramarao P. Human polymorphonuclear leukocytes adhere to complement factor H through an interaction that involves alphaMbeta2 (CD11b/CD18). *J Immunol*. (1998) 160:4057–66.
115. Behnsen J, Hartmann A, Schmaler J, Gehrke A, Brakhage AA, Zipfel PF. The opportunistic human pathogenic fungus *Aspergillus fumigatus* evades the host complement system. *Infect Immun*. (2008) 76:820–7. doi: 10.1128/IAI.01037-07
116. Conde JN, da Silva EM, Allonso D, Coelho DR, Andrade IDS, de Medeiros LN, et al. Inhibition of the membrane attack complex by dengue virus NS1 through Interaction with vitronectin and terminal complement proteins. *J Virol*. (2016) 90:9570–81. doi: 10.1128/JVI.00912-16
117. Singh B, Su, Y.-C., Riesbeck K. Vitronectin in bacterial pathogenesis: a host protein used in complement escape and cellular invasion.

Mol Microbiol. (2010) 78:545–60. doi: 10.1111/j.1365-2958.2010.07373.x
118. Blom AM, Hallstrom T, Riesbeck K. Complement evasion strategies of pathogens-acquisition of inhibitors and beyond. *Mol Immunol*. (2009) 46:2808–17. doi: 10.1016/j.molimm.2009.04.025
119. Kozik A, Karkowska-Kuleta J, Zajac D, Bochenska O, Kedracka-Krok S, Jankowska U, et al. Fibronectin-, vitronectin- and laminin-binding proteins at the cell walls of *Candida parapsilosis* and *Candida tropicalis* pathogenic yeasts. *BMC Microbiol*. (2015) 15:197. doi: 10.1186/s12866-015-0531-4
120. Blom AM, Villoutreix BO, Dahlback B. Complement inhibitor C4b-binding protein-friend or foe in the innate immune system? *Mol Immunol*. (2004) 40:1333–46. doi: 10.1016/j.molimm.2003.12.002
121. Chaabane F, Graf A, Jequier L, Coste AT. Review on antifungal resistance mechanisms in the emerging pathogen *Candida auris*. *Front Microbiol*. (2019) 10:2788. doi: 10.3389/fmicb.2019.02788
122. Rhodes J, Fisher MC. Global epidemiology of emerging *Candida auris*. *Curr Opin Microbiol*. (2019) 52:84–9. doi: 10.1016/j.mib.2019.05.008
123. Snyder GM, Wright SB. The epidemiology and prevention of *Candida auris*. *Curr Infect Dis Rep*. (2019) 21:19. doi: 10.1007/s11908-019-0675-8
124. Xin H, Mohiuddin F, Tran J, Adams A, Eberle K. Experimental mouse models of disseminated *Candida auris* infection. *mSphere*. (2019) 4:19. doi: 10.1128/mSphere.00339-19
125. Bujdakova H, Paulovicova E, Paulovicova L, Simova Z. Participation of the *Candida albicans* surface antigen in adhesion, the first phase of biofilm development. *FEMS Immunol Med Microbiol*. (2010) 59:485–92. doi: 10.1111/j.1574-695X.2010.00713.x
126. Dekkerova J, Lopez-Ribot JL, Bujdakova H. Activity of anti-CR3-RP polyclonal antibody against biofilms formed by *Candida auris*, a multidrug-resistant emerging fungal pathogen. *Eur J Clin Microbiol Infect Dis*. (2019) 38:101–8. doi: 10.1007/s10096-018-3400-x
127. Halder LD, Jo EAH, Hasan MZ, Ferreira-Gomes M, Krüger T, Westermann M, et al. Immune modulation by complement receptor 3-dependent human monocyte TGF-β1-transporting vesicles. *Nat Commun*. (2020) 11:2331. doi: 10.1038/s41467-020-16241-5

Conflict of Interest: The authors declare that the research was conducted in the absence of any commercial or financial relationships that could be construed as a potential conflict of interest.

frontiers in Immunology

MINI REVIEW
published: 23 July 2020
doi: 10.3389/fimmu.2020.01561

The Interactions of Parasite Calreticulin With Initial Complement Components: Consequences in Immunity and Virulence

Galia Ramírez-Toloza[1], Lorena Aguilar-Guzmán[2], Carolina Valck[3], Viviana P. Ferreira[4]* and Arturo Ferreira[3]**

[1] Department of Preventive Veterinary Medicine, Faculty of Veterinary Medicine and Livestock Sciences, University of Chile, Santiago, Chile, [2] Department of Pathology, Faculty of Veterinary Medicine and Livestock Sciences, University of Chile, Santiago, Chile, [3] Department of Immunology, ICBM, Faculty of Medicine, University of Chile, Santiago, Chile, [4] Department of Medical Microbiology and Immunology, College of Medicine and Life Sciences, University of Toledo, Toledo, OH, United States

OPEN ACCESS

Edited by:
Heribert Stoiber,
Innsbruck Medical University, Austria

Reviewed by:
Marcel I. Ramirez,
Oswaldo Cruz Foundation (Fiocruz), Brazil
Debora Decote-Ricardo,
Universidade Federal Rural do Rio de Janeiro, Brazil

***Correspondence:**
Galia Ramírez-Toloza
galiaram@uchile.cl
Viviana P. Ferreira
viviana.ferreira@utoledo.edu
Arturo Ferreira
aferreir@med.uchile.cl

Specialty section:
This article was submitted to Microbial Immunology, a section of the journal Frontiers in Immunology

Received: 29 April 2020
Accepted: 12 June 2020
Published: 23 July 2020

Citation:
Ramírez-Toloza G, Aguilar-Guzmán L, Valck C, Ferreira VP and Ferreira A (2020) The Interactions of Parasite Calreticulin With Initial Complement Components: Consequences in Immunity and Virulence. Front. Immunol. 11:1561. doi: 10.3389/fimmu.2020.01561

Because of its capacity to increase a physiologic inflammatory response, to stimulate phagocytosis, to promote cell lysis and to enhance pathogen immunogenicity, the complement system is a crucial component of both the innate and adaptive immune responses. However, many infectious agents resist the activation of this system by expressing or secreting proteins with a role as complement regulatory, mainly inhibitory, proteins. *Trypanosoma cruzi*, the causal agent of Chagas disease, a reemerging microbial ailment, possesses several virulence factors with capacity to inhibit complement at different stages of activation. *T. cruzi* calreticulin (TcCalr) is a highly-conserved, endoplasmic reticulum-resident chaperone that the parasite translocates to the extracellular environment, where it exerts a variety of functions. Among these functions, TcCalr binds C1, MBL and ficolins, thus inhibiting the classical and lectin pathways of complement at their earliest stages of activation. Moreover, the TcCalr/C1 interaction also mediates infectivity by mimicking a strategy used by apoptotic cells for their removal. More recently, it has been determined that these Calr strategies are also used by a variety of other parasites. In addition, as reviewed elsewhere, TcCalr inhibits angiogenesis, promotes wound healing and reduces tumor growth. Complement C1 is also involved in some of these properties. Knowledge on the role of virulence factors, such as TcCalr, and their interactions with complement components in host–parasite interactions, may lead toward the description of new anti-parasite therapies and prophylaxis.

Keywords: *Trypanosoma cruzi*, complement, calreticulin, C1q, host-parasite interaction, host immune evasion

INTRODUCTION

The complement system (C), essential in both the innate and adaptive immune responses, increases physiologic inflammation, stimulates microbial phagocytosis and their lysis, and promotes the elimination of a large variety of aggressive microorganisms by enhancing their immunogenicity. Some activated C components and derived molecules, opsonize a variety of microorganisms and apoptotic cells promoting their phagocytosis and destruction inside the phagocyte (1).

However, pathogens such as viruses, bacteria, fungi and parasites, utilize some surface proteins and receptors to evade C during its activation (1).

Trypanosoma cruzi calreticulin (TcCalr), similar to calreticulin from other species, including human (HuCALR), is a multifunctional endoplasmic reticulum-resident chaperone, that the parasite translocates to the extracellular environment, where TcCalr participates in C evasion and infection, with important consequences in virulence. Thus, TcCalr is a *bona fide* virulence factor. Calr from other important parasite species shares several of these properties with TcCalr. These issues are reviewed herein. TcCalr also participates in the control of angiogenesis and tumor growth, as reviewed elsewhere (2).

COMPLEMENT ACTIVATION AND REGULATION: A BRIEF OVERVIEW

C consists of soluble and membrane-bound molecules that are activated through a stringently regulated proteolytic cascade (3). Activation may occur through the classical (CP), alternative (AP), and lectin (LP) pathways. The CP is initiated by the recognition, by C1, of antibodies aggregated on foreign antigens, or by acute phase proteins identifying danger signals on a microbial aggressor. The LP is activated by mannose-binding lectin (MBL) or by ficolins recognizing a variety of bacterial motifs. Conversely, spontaneous hydrolysis of C3, near cell surfaces, produces a constitutive AP activation, which is tightly controlled by C regulatory proteins present on host cells (Factor I, C4-binding protein, decay-accelerating factor, membrane co-factor protein, C receptor 1) or in plasma (Factor H, C1-inhibitor, S-protein, clusterin, CD59). These proteins limit amplification of the downstream cascade (3, 4).

C activation generates split products with opsonizing, pro-inflammatory and immune-stimulating properties (3). The three activation pathways converge in the generation of C3 convertases that continuously cleave C3 into C3a and C3b, as well as C5 convertases that produce the split products C5a and C5b. C5b, in conjunction with C6–C9, form the membrane attack complex (MAC) and lyse the pathogen (3).

C1 AND CALRETICULIN INTERACTION PROMOTES PHAGOCYTOSIS

In mammals, C1 is a highly complex protein, composed by eighteen polypeptide chains, grouped in six heterotrimeric units, each carrying the products of 3 genes, A, B, C. Each trimer has several functional sites located on both a collagen-like (cC1q) and a globular head (gC1q) regions (5). Each globular head (ghA, ghB, and ghC) has special affinity for the CH2 and CH3 domains of IgG and IgM molecules, respectively, or for other unrelated molecules (5).

Beyond its role as a pattern recognition receptor (PRR), C1 binds to a wide variety of phagocytic cells, resulting in the induction of cell-specific responses such as phagocytosis, cellular activation, release of biological mediators and expression of adhesion molecules, promoting inflammation (6). At least four C1q binding cell surface receptors have been identified: CR1 (CD35), receptor for C3b; C1q-Rp (CD93), a 120 kDa O-sialoglycoprotein; gC1q-R/p33, a 33kDa homotrimeric protein, and cC1q-R/CR, a 60 kDa protein (5, 6). The 33 kDa molecule has high affinity for the globular heads while the 60 kDa molecule, also known as collectin receptor, binds to the collagenous tails and its N-terminal sequence is 100% identical with Calr (5).

Calr is a 46 kDa multifunctional protein, mainly located in the endoplasmic reticulum (ER) and highly conserved in all species, including plants and microorganisms (2, 7, 8). Calr is involved in Ca^{2+} homeostasis and in other important functions inside and outside the cell, including: cardiogenesis, adipocyte differentiation, cellular stress responses, wound healing and immunity (9). Its structure comprises three main domains: N-terminal globular, flexible proline-rich P intermediate arm-like and C-carboxyl terminal (7, 9).

Both, C1q and MBL bind to apoptotic cells and stimulate phagocytosis by ligation of Calr on the phagocyte surface, which binds to the endocytic receptor protein CD91 (10). Phagocytic cells, monocyte-derived macrophages and dendritic cells express and secrete Calr as a C1q receptor. On the cell, Calr bridges the phagocytic cell and the target (apoptotic cell or an immune complex), promoting removal (6). Activated macrophages secrete Calr, which binds to the surface of viable target cells and marks them for removal by programmed cell phagocytosis (11). Additionally, Calr is found on the surface of apoptotic cells acting as a damage-associated molecular pattern (DAMP), responsible for the immunogenicity of apoptotic cancerous cells (12–14). Binding of C1q to cell-bound Calr results in opsonization (15). Most important, the pro-phagocytic Calr/C1q/C1qR interaction is used by different parasites to promote infectivity.

TRYPANOSOMA CRUZI EVADES THE COMPLEMENT SYSTEM: THE ROLE OF CALRETICULIN

Chagas disease, is a zoonotic and chronic parasitic illness affecting 7–8 million people worldwide, that may be symptomatic in about 30% of those infected, leading to incapacitating situations in some of them. The disease is currently endemic in 21 Latin-American countries and, due to migration of chronically infected individuals, is now a global concern (16). Its causal agent, the flagellated protozoan *T. cruzi*, is an obligatory intracellular infectious agent transmitted by triatomine vectors, but also by congenital route, blood transfusions, organ transplantation or by ingesting contaminated food and beverages (17). In all these routes of infection, once trypomastigotes (infective form in mammalian host) reach the bloodstream, the parasite, using different proteins and mechanisms, bypasses C-mediated lysis (18), and disseminates to many tissues during the acute phase (19). There are a variety of molecules involved in C immune evasion in *T. cruzi*. Among them, TcCalr plays an important role.

Bloodstream trypomastigotes, amastigotes (intracellular replicative stage in host cells) and metacyclic trypomastigotes (infective forms present in vector dejections) are resistant to the C-mediated lysis (20). Instead, epimastigotes, the replicative and

non-infective form of the parasite, are highly susceptible (21–23). The ability to resist C differs among the parasite developmental stage (24) and strains (21).

Several molecules present on the parasite have been identified as resistance mediators, at different levels of the C cascade. Moreover, trypomastigotes capture inhibitory host components, which are used to inhibit the C activation on the parasite surface, such as: plasma-membrane derived-vesicles (PMV) (25, 26), *T. cruzi* trypomastigotes-decay accelerating factor (T-DAF) (27, 28), *T. cruzi* C regulatory protein (CRP) (29–32); Factor H (FH) (33), gp58/68 (34), and C2 receptor inhibitor trispanning (CRIT) (21, 35) (**Table 1**). The molecular inhibitory mechanisms of these proteins are only partially known. Some of these molecules play a central role in the inhibition of C3 and/or C5 convertases. The inhibition of these key enzymes may have important biological consequences, such as: (i) inhibition of C-mediated lysis, (ii) a decrease in the C3a and C5a (anaphylotoxins) generation (these small C fragments are essential in the recruitment of blood cells to the infection site), and (iii) a decreased opsonization, which mediates phagocytosis of pathogens during infection (25).

TcCalr, similar to its human counterpart, resides in the ER, where it modulates Ca^{2+} homeostasis and participates as a chaperone protein (39). However, TcCalr is also located in the Golgi, reservosomes, flagellar pocket, cell surface, cytosol, nucleus and kinetoplast. Large quantities of TcCalr accumulate in the kinetoplast, apparently as a previous step to its translocation to the parasite exterior (36, 39, 40). This parasitic protein shares 50% of homology with HuCALR (41) and with its three domains (42): N, P, and C. Within the N and P domains, TcCalr has an S-domain (aa 159–281) that specifically interacts with C1 (43, 44) (**Figure 1**).

The TcCalr/C1 interaction promotes important functions in the host-parasite interplay. TcCalr competes with the $(C1r\text{-}C1s)_2$ tetrameric complex for binding to the collagenous tails of C1q, interfering with the C1s-mediated cleavage of C4 and C2 and thus CP activation (36). TcCalr binds both serine-proteases, C1r and C1s, but only TcCalr-C1r binding inhibits the C4-activating function (37). Additionally, TcCalr competes with the serine proteases, but does not displace them from preformed C1 (37). This fact may be explained by the strong interaction between the enzymatic tetramer ($C1r_2$, $C1s_2$) and C1q (45). TcCalr inhibits C more efficiently than HuCALR and these functional differences may be explained, at least in part, by comparative crystallographic studies that have identified conformational rearrangements in TcCalr and HuCALR (46) and some aminoacidic substitutions that confer differences in polarity and spatial stability (47). TcCalr not only inhibits the CP; it also binds MBL and Ficolins, inhibiting the LP (38). L-, but not H-Ficolin binds to TcCalr, but this binding does not interfere with lipoteichoic acid binding to L-Ficolin and its activation. Moreover, L-Ficolin binds preferentially to trypomastigotes, rather than to epimastigotes, which translocate significantly lower amounts of TcCalr to their surfaces (38). All these facts have been corroborated *in vivo* by using genetically modified parasites carrying a monoallelic

TABLE 1 | Regulatory proteins playing a role in *Trypanosoma cruzi* complement system immune evasion.

Complement regulatory protein	Specific functions	Complement pathway affected	References
COMPLEMENT REGULATORY PROTEINS PRESENT ON THE *T. CRUZI* SURFACE			
Trypanosoma cruzi calreticulin (TcCalr)	TcCalr is a 45 kDa protein that binds to C1 (C1q, C1r, and C1s), and also binds to MBL and ficolins (L-Ficolin).	CP and AP	(36–38)
Trypomastigote Decay-Accelerating Factor (T-DAF)	T-DAF is a 87–93 kDa glycoprotein that interferes with assembly of the C3 and C5 convertase of both CP and AP.	CP, LP (probably) and AP	(27, 28)
Trypanosoma cruzi Complement C2 Receptor Inhibitor Trispanning Protein (CRIT)	CRIT is a 32 kDa protein that inhibits the C2 cleavage by C1s and MASP2 and impairs C3 convertase formation.	CP and LP	(21, 35)
Trypanosoma cruzi Complement Regulatory Protein (TcCRP)	TcCRP is a surface-anchored glycoprotein also named gp160 that binds C3b and C4b, inhibiting the CP and AP C3 convertase.	CP, LP (probably) and AP	(29–32)
Glycoprotein 58/68 (Gp58/68)	GP58/68 is a 58-68 kDa protein that inhibits the C3 convertase formation by binding factor B.	AP	(34)
COMPLEMENT REGULATORY PROTEIN FROM THE HOST USED BY *T. CRUZI*			
Factor H (FH)	FH binds to trypomastigotes covered by sialic acid probably accelerating the decay of C3 convertase.	AP	(33)
OTHER PROTEINS WITH COMPLEMENT REGULATORY FUNCTIONS IN *T. CRUZI*			
T. cruzi induced membrane-derived vesicles from host cells or microvesicles (MV)	MVs from different types of cells interact with C3 convertase	CP and LP	(25, 26)

CP, Classical pathway; LP, Lectin pathway; AP, Alternative pathway; C, Complement system.

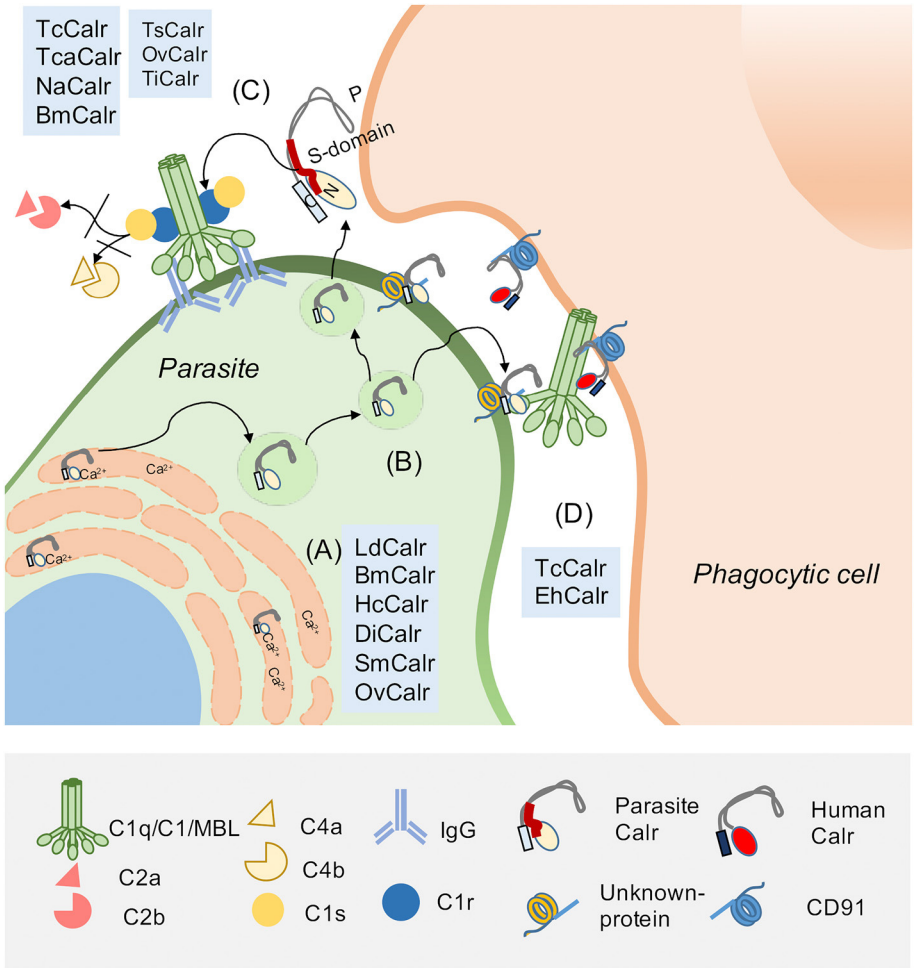

FIGURE 1 | Parasite Calreticulin participates in complement (C) evasion and in infectivity. Calreticulin (Calr), highly conserved and pleiotropic, is mainly found in the endoplasmic reticulum (ER), but also in the extracellular environment. (A) In the ER, Calr is a chaperone and Ca^{2+} binding protein. These properties are also described for Calrs from other parasites, such as: *L. donovani* (LdCalr), *B. malayi* (BmCalr), *H. contortus* (HcCalr), *D. immitis* (DiCalr), *S. mansoni* (SmCalr) and *O. viverrini (OvCalr).* (B) Extracellularly, the Calr S-domain (a fragment located between N and P domains) interacts with C system molecules such as (C) C1q, C1 complex and MBL, inhibiting C activation. This property has been described for human Calr (HuCALR) and parasitic Calrs such as *T. cruzi calreticulin* (TcCalr), *T. carassii* (TcaCalr), *N. americanum* (NaCalr), BmCalr, *T. spiralis* (TsCalr), OvCalr, and *T. infestans* (TiCalr). Additionally, the C1/Calr interaction on the parasite is used by *T. cruzi* and *E. histolytica* to promote infectivity. (D) TcCalr and *E. histolytica* Calr (EhCalr) on the parasite surface bind C1q. This interaction is recognized by HuCALR present on phagocytes as an "eat me" signal. This Calr/C1q/HuCALR interaction, that promotes phagocytosis, was previously described as a mechanism to promote the clearance of apoptotic cells, which overexpress Calr as a damage-associated molecular pattern (DAMP) on their surface. This Calr on apoptotic cells is recognized by the pattern-recognition receptor (PRR) C1q, which is recognized by a C1q receptor on the phagocytic cells, identified as HuCALR. Calr, which does not have a transmembrane tail, binds to CD91 on the phagocyte.

deletion of the *TcCRT* gene or a transgenic version, expressing an extra copy of the gene. The parasites expressing less TcCalr are significantly more susceptible to C-mediated lysis and those overexpressing TcCRT are significantly more resistant to both CP and LP-mediated lysis (48, 49).

TcCALR/C1 INTERACTION: ROLE IN PROMOTING INFECTIVITY

Another important role of the TcCalr/C1 interaction is to promote infectivity. TcCalr is expressed mainly on the trypomastigote flagellum emergence area, where it recruits C1q/C1 (36). This interaction correlates with a TcCalr mRNA level increase in the early infection steps (50). This is corroborated since anti-TcCalr $F(ab')_2$ antibody fragments (unable to bind C1 because they lack their Fc domains) inhibit the TcCalr/C1 interaction, thus decreasing infectivity *in vitro* and *in vivo* (50). Non-infective epimastigotes express less TcCalr on their surface (36, 51), which may contribute to their high sensitivity to C and lack of infectivity. In agreement with this notion, when exogenous TcCalr is added, epimastigotes are internalized by fibroblasts, in a C1q-dependent manner (52).

As mentioned, the capacity of the TcCalr/C1q interaction to mediate phagocytosis was originally described for apoptotic

cells. C1q and MBL bind to these cells, exposing HuCALR, and stimulating their ingestion by ligation on the phagocyte surface in a HuCALR/C1q-mediated manner (10). We have proposed that the TcCalr/C1q complex is recognized as an *"eat me"* signal on the parasite by host Calr on phagocytes and other cellular types, thus promoting infectivity (**Figure 1**). In agreement with these findings, Calr-deficient fibroblasts are unable to internalize these parasites (52). Moreover, in mice inoculated with trypomastigotes, carrying a monoallelic *TcCalr* deletion, no parasitemia, nor anti-*T. cruzi* IgG levels are detected, demonstrating that these mutants have a potent restriction in their capacity to infect host cells, due to insufficient Calr expression and consequent reduced resistance to C (49).

Calr is also important in infectivity, as determined in an *ex vivo* model using human placenta explants, which express high HuCALR levels (53–55). In these explants, the TcCalr/C1q/HuCALR synapsis mediates the first stages of *T. cruzi* infection (56). This fact is particularly relevant due to the current high impact of congenital Chagas disease transmission.

TcCalr also binds MBL and Ficolins (36, 37), but the role of TcCalr/MBL or TcCalr/Ficolins interactions in *T. cruzi* infectivity processes has not yet been demonstrated. However, in C-resistant *T. cruzi* strains, MBL seems to participate in the infectivity process while the parasite deactivates the LP (57). However, the ligand for MBL on the parasite surface remains unknown.

CALRETICULIN IN OTHER PARASITIC INFECTIONS

Several functions are shared and conserved, to differing extents, by Calr from different species (41, 58). Calr, is a surprisingly pleiotropic protein, present in all nucleated cells in different organisms including parasites, where it was first described in *Schistosoma mansoni* (59, 60), *Dirofilaria immitis* (61) and *Necator americanus* (62). More recently, Calr has been characterized in *Entamoeba histolytica* (63, 64), *Leishmania donovani* (65), *Trypanosoma carassii* (66), and in the helminths *Brugia malayi* (67), *Haemonchus contortus* (68), *Opisthorchis viverrini* (69, 70), and *Trichinella spiralis* (71).

Structurally, Calr from different species possesses a broad spectrum of sequence conservations and differences (46). *L. donovani* Calr (LdCalr) binds $Ca^{2+}$and RNA sequences (65) and its P-domain is implicated in ER chaperone functions, since a modulation of its expression affects the targeting of proteins associated with virulence, during their trafficking through the parasite secretory pathway (72). Additionally, proteomic approaches indicate LdCalr is an immunostimulatory protein (73, 74). However, its specific role in host-parasite interactions is still unknown.

In *E. histolytica*, a protozoan parasite that causes amebiasis, Calr (EhCalr) participates in several roles related to the host-immune modulation. Quantitative proteomic analysis and an *ex vivo* modeling indicates that EhCalr is an abundant membrane protein expressed in virulent variants (75, 76). EhCalr, from pathogenic and non-pathogenic species, binds C1 and inhibits the CP activation (63). Additionally, EhCalr is exported from the ER to the phagolysosome, where it favors phagocytosis in a C1q-dependent manner (64, 77). EhCalr also interferes in the pathogenesis and host immune response modulation. Thus, *in vitro*, EhCalr acts as an immunogen for the specific activation of peripheral blood mononuclear cells, inducing a Th2 cytokine profile, during the acute phase, and a Th1 profile in the resolution phase (78).

T. carassii, a flagellated bloodstream parasite of cyprinid fish, produces anemia during peak parasitemias and it is highly resistant to C-mediated lysis (79, 80). Its Calr (TcaCalr) is a surface protein that binds C1 and inhibits the CP activation (66), but its role in infectivity has not yet been elucidated. *Trypanosoma congolense* Calr (TcoCalr) is an immunogen in mice, delaying parasitemia and increasing survival in challenged animals (81).

In nematodes Calr is also important in immune evasion (2). *Necator americanus* Calr (NaCalr) was first described as a hookworm allergen in infected patients (62). NaCalr does not bind Ca^{2+}, but interacts with C1 and inhibits the CP (82). Calr from *B. malayi* (BmCalr), a parasite causing lymphatic filariasis, binds Ca^{2+} and Zinc (67) and interacts with host C1, inhibiting the CP (83). *Haemonchus contortus* is a gastrointestinal parasite of small ruminants that feeds on blood. The N-domain of HcCalr mediates Ca^{2+} binding and blood clotting inhibition. It also binds C1 (68) and C-reactive protein (84), thus inhibiting the CP. The C1 binding sites reside in two sequences present in its N-domain (85). *Trichinella spiralis* activates C in infective larvae, adults and newborn larvae. However, C is primarily activated by the AP (86) and none of these stages bind C1 (87). *T. spiralis* expresses two proteins that bind C1 and inhibit the CP: paramyosin (88) and Calr (TsCalr) (71). Additionally, TsCalr/C1q binding inhibits the C1-induced non-C activation of macrophages (71). In the nematode *Dirofilaria immitis*, a Ca^{2+} binding protein, similar to Calr, was isolated and shown to be immunogenic in chronically-infected microfilaremic dogs (61).

Calrs from the trematodes *Schistosoma mansoni* (SmCalr) and *Schistosoma japonicum* (SjCalr) have been characterized (59, 60, 89, 90). SmCalr is a Ca^{2+} binding protein, mainly present in miracidia and genital organs (59), that participates as T and B cell antigen (60). Both C1 (91) and MBL (92) bind to *S. mansoni*, but the role of SmCalr in this binding or C evasion is unknown. SjCalr participates as an immunomodulatory protein, activating dendritic cells and inducing a Th1 immune response (89). Calr from *Opisthorchis viverrini* (OvCalr), a trematode parasite affecting humans, with carcinogenic effects, is mainly expressed in the reproductive system and its C-domain binds Ca^{2+} (70). OvCalr also binds C1 and inhibits the CP and, additionally, OvCalr is released from the parasite, interfering with cell proliferation, cell migration and sprouting, and stimulates specific antibody production (69).

Hematophagous arthropods also use these Calr-mediated mechanisms to evade C. Thus, Calr from *Triatoma infestans* (TiCalr), the principal vector of Chagas disease (93), also binds C1 and inhibits the CP. Most likely TiCalr in saliva helps to control the activation of host C, present in the blood meal

and consequent digestive tract tissue damage (93). Another example is the tick *Amblyomma americanum,* which secretes Calr (AaCalr) while feeding (94). AaCalr also binds C1, but this interaction does not inhibit C activation (94). In ticks, such as *Boophilus micropus*, Calr (BmCalr) is present in saliva, is immunogenic in tick-infested bovines (95) and, similar to *Haemaphysalis qinghaiensis* Calr (HqCalr), it is secreted in their host during blood sucking, promoting a humoral response (96).

OTHER TcCALR FUNCTIONS IN THE HOST-PARASITE INTERPLAY

As reviewed elsewhere (2), in addition to their roles in C evasion and infectivity, TcCalr and its N-terminal domain are anti-angiogenic in several experimental set ups (97–99). The anti-tumor effect of *T. cruzi* infection has been fully reproduced by exogenously administrated rTcCalr (97) and reverted by polyclonal anti-rTcCalr $F(ab')_2$ antibodies (51). Native endogenous TcCalr, in the context of the parasite, also has an anti-tumor effect on *T. cruzi* infection, since mice inoculated with TA3-MTXR tumor cells, infected with *T. cruzi* trypomastigotes and treated with anti-TcCalr antibodies neutralize the anti-tumor effect of the infection (51). Most recently, we have proposed that TcCalr binds to canine transmissible venereal tumor (CTVT) cells and to a canine mammary carcinoma cell line, improving the immunogenicity of both tumors. These cells can be engulfed by macrophages and dendritic cells co-cultured with rTcCalr, accelerating its maturation and activating T cells (100). Similar to its human counterpart, TcCalr promotes wound healing in rats (101); however, whether this property correlates with the known anti-complement capacity of the parasite chaperone, is unknown.

SUMMARY

Calr is a multifunctional chaperone, resident in the ER, where it controls Ca^{+2} homeostasis. However, Calr has important roles outside the cells, because it is also secreted (58). Calr is highly conserved among plants and mammals and some of its functions are significant in host-pathogen interactions (2). Thus, an important function of Calr in microorganisms is its capacity to bind C1, with consequent inhibition of the CP of C (4) and promotion of infectivity (1, 4). More recently, these two important effects have also been described for Calr from a variety of protozoan and metazoan parasites (2). C1 binding allows the parasite to evade the C system and to promote engulfment of the parasite by mimicking a strategy used by apoptotic cells (12). TcCalr also has important functions related with the inhibition of angiogenesis and tumor growth, as revised elsewhere (51, 97, 98). Progress in the knowledge of Calr functions in different parasitic infections may be useful in the design of new therapies and/or vaccines.

AUTHOR CONTRIBUTIONS

GR-T, VF, and AF contributed equally to the generation of this review. GR-T prepared the figure. GR-T, VF, and AF edited the text. All authors contributed substantially to the writing and with published previous research included herein. All authors contributed to the article and approved the submitted version.

FUNDING

The University of Toledo Biomedical Research Innovation Program (VF), Toledo, Ohio, USA; VID, University of Chile (AF); FONDECYT-Chile 1130099 (AF), and CONICYT-REDES 170126 (GR-T).

REFERENCES

1. Lukácsi S, Mácsik-Valent B, Nagy-Baló Z, Kovács KG, Kliment K, Bajtay Z, et al. Utilization of complement receptors in immune cell–microbe interaction. *FEBS Lett.* (2020) doi: 10.1002/1873-3468.13743. [Epub ahead of print].
2. Ramírez-Toloza G, Sosoniuk-Roche E, Valck C, Aguilar-Guzmán L, Ferreira VP, Ferreira A. Trypanosoma cruzi calreticulin: immune evasion, infectivity, and tumorigenesis. *Trends Parasitol.* (2020) 36:368–381. doi: 10.1016/j.pt.2020.01.007
3. Andrighetto S, Leventhal J, Zaza G, Cravedi P. Complement and complement targeting therapies in glomerular diseases. *Int J Mol Sci.* (2019) 20:6336. doi: 10.3390/ijms20246336
4. Ramírez-Toloza G, Ferreira A. Trypanosoma cruzi evades the complement system as an efficient strategy to survive in the mammalian host: the specific roles of host/parasite molecules and Trypanosoma cruzi calreticulin. *Front Microbiol.* (2017) 8:1667. doi: 10.3389/fmicb.2017.01667
5. Ghebrehiwet B, Geisbrecht BV, Xu X, Savitt AG, Peerschke EI. *The C1q Receptors: Focus on gC1qR/p33 (C1qBP, p32, HABP-1). Semin Immunol.* (2019) 5:101338. doi: 10.1016/j.smim.2019.101338
6. Ghebrehiwet B, Peerschke EI. cC1q-R (calreticulin) and gC1q-R/p33: ubiquitously expressed multi-ligand binding cellular proteins involved in inflammation and infection. *Mol Immunol.* (2004) 41:173–83. doi: 10.1016/j.molimm.2004.03.014
7. Schcolnik-Cabrera A, Oldak B, Juárez M, Cruz-Rivera M, Flisser A, Mendlovic F. Calreticulin in phagocytosis and cancer: opposite roles in immune response outcomes. *Apoptosis.* (2019) 24:245–55. doi: 10.1007/s10495-019-01532-0
8. Joshi R, Paul M, Kumar A, Pandey D. Role of calreticulin in biotic and abiotic stress signalling and tolerance mechanisms in plants. *Gene.* (2019) 714:144004. doi: 10.1016/j.gene.2019.144004
9. Wang W-A, Groenendyk J, Michalak M. Calreticulin signaling in health and disease. *Int J Biochem Cell Biol.* (2012) 44:842–6. doi: 10.1016/j.biocel.2012.02.009
10. Ogden CA, deCathelineau A, Hoffmann PR, Bratton D, Ghebrehiwet B, Fadok VA, et al. C1q and mannose binding lectin engagement of cell surface calreticulin and CD91 initiates macropinocytosis and uptake of apoptotic cells. *J Exp Med.* (2001) 194:781–96. doi: 10.1084/jem.194.6.781
11. Feng M, Marjon KD, Zhu F, Weissman-Tsukamoto R, Levett A, Sullivan K, et al. Programmed cell removal by calreticulin in tissue homeostasis and cancer. *Nat Commun.* (2018) 9:3194. doi: 10.1038/s41467-018-05211-7
12. Galluzzi L, Buqué A, Kepp O, Zitvogel L, Kroemer G. Immunogenic cell death in cancer and infectious disease. *Nat Rev Immunol.* (2017) 17:97–111. doi: 10.1038/nri.2016.107
13. Obeid M, Tesniere A, Ghiringhelli F, Fimia GM, Apetoh L, Perfettini J-L, et al. Calreticulin exposure dictates the immunogenicity of cancer cell death. *Nat Med.* (2007) 13:54–61. doi: 10.1038/nm1523

14. Krysko DV, Garg AD, Kaczmarek A, Krysko O, Agostinis P, Vandenabeele P. Immunogenic cell death and DAMPs in cancer therapy. *Nat Rev Cancer.* (2012) 12:860–75. doi: 10.1038/nrc3380
15. Verneret M, Tacnet-Delorme P, Osman R, Awad R, Grichine A, Kleman J-P, et al. Relative contribution of c1q and apoptotic cell-surface calreticulin to macrophage phagocytosis. *J Innate Immun.* (2014) 6:426–34. doi: 10.1159/000358834
16. Bivona AE, Alberti AS, Cerny N, Trinitario SN, Malchiodi EL. Chagas disease vaccine design: the search for an efficient trypanosoma cruzi immune-mediated control. *Biochim Biophys Acta Mol Basis Dis.* (2020) 1866:165658. doi: 10.1016/j.bbadis.2019.165658
17. Vos T, Barber RM, Bell B, Bertozzi-Villa A, Biryukov S, Bolliger I, et al. Global, regional, and national incidence, prevalence, and years lived with disability for 301 acute and chronic diseases and injuries in 188 countries, 1990–2013: a systematic analysis for the global burden of disease study 2013. *Lancet.* (2015) 386:743–800. doi: 10.1016/S0140-6736(15)60692-4
18. Pangburn MK. Host recognition and target differentiation by factor H, a regulator of the alternative pathway of complement. *Immunopharmacology.* (2000) 49:149–57. doi: 10.1016/S0162-3109(00)80300-8
19. Cardoso MS, Reis-Cunha JL, Bartholomeu DC. Evasion of the immune response by trypanosoma cruzi during acute infection. *Front Immunol.* (2015) 6:659. doi: 10.3389/fimmu.2015.00659
20. Iida K, Whitlow MB, Nussenzweig V. Amastigotes of trypanosoma cruzi escape destruction by the terminal complement components. *J Exp Med.* (1989) 169:881–91. doi: 10.1084/jem.169.3.881
21. Cestari Idos S, Evans-Osses I, Freitas JC, Inal JM, Ramirez MI. Complement C2 receptor inhibitor trispanning confers an increased ability to resist complement-mediated lysis in trypanosoma cruzi. *J Infect Dis.* (2008) 198:1276–83. doi: 10.1086/592167
22. Muniz J, Borriello A. Etudo sobre a agao htica de diferentes soros sobre as formas de cultura e sanguicolas do schizotrypanum cruzi en crithidias. *Rev Brasil Med.* (1945) 2:994–8.
23. Rubio M. Actividad lítica de sueros normales sobre formas de cultivo y sanguíneas de Trypanosoma cruzi. *Bol Chil Parasitol.* (1956) 11:62–9.
24. Anziano DF, Dalmasso AP, Lelchuk R, Vasquez C. Role of complement in immune lysis of trypanosoma cruzi. *Infect Immun.* (1972) 6:860–4. doi: 10.1128/IAI.6.5.860-864.1972
25. Cestari I, Ansa-Addo E, Deolindo P, Inal JM, Ramirez MI. Trypanosoma cruzi immune evasion mediated by host cell-derived microvesicles. *J Immunol (Baltimore, Md: 1950).* (2012) 188:1942–52. doi: 10.4049/jimmunol.1102053
26. Ramirez MI, Deolindo P, de Messias-Reason IJ, Arigi EA, Choi H, Almeida IC, et al. Dynamic flux of microvesicles modulate parasite-host cell interaction of trypanosoma cruzi in eukaryotic cells. *Cell Microbiol.* (2017) 19:e12672. doi: 10.1111/cmi.12672
27. Kipnis TL, Joiner KA, da Silva WD, Rimoldi MT, Hammer CH, Sher A. Identification of membrane components of trypanosoma cruzi modulators of complement system. *Mem Inst Oswaldo Cruz.* (1988) 83(Suppl. 1):571–5. doi: 10.1590/S0074-02761988000500069
28. Tambourgi DV, Kipnis TL, da Silva WD, Joiner KA, Sher A, Heath S, et al. A partial cDNA clone of trypomastigote decay-accelerating factor (T-DAF), a developmentally regulated complement inhibitor of trypanosoma cruzi, has genetic and functional similarities to the human complement inhibitor DAF. *Infect Immun.* (1993) 61:3656–63. doi: 10.1128/IAI.61.9.3656-3663.1993
29. Norris KA, Bradt B, Cooper NR, So M. Characterization of a trypanosoma cruzi C3 binding protein with functional and genetic similarities to the human complement regulatory protein, decay-accelerating factor. *J Immunol (Baltimore, Md: 1950).* (1991) 147:2240–7.
30. Norris KA, Schrimpf JE. Biochemical analysis of the membrane and soluble forms of the complement regulatory protein of Trypanosoma cruzi. *Infect Immun.* (1994) 62:236–43. doi: 10.1128/IAI.62.1.236-243.1994
31. Beucher M, Meira WS, Zegarra V, Galvao LM, Chiari E, Norris KA. Expression and purification of functional, recombinant trypanosoma cruzi complement regulatory protein. *Protein Expr Purif.* (2003) 27:19–26. doi: 10.1016/S1046-5928(02)00562-4
32. Norris KA. Stable transfection of trypanosoma cruzi epimastigotes with the trypomastigote-specific complement regulatory protein cDNA confers complement resistance. *Infect Immun.* (1998) 66:2460–5. doi: 10.1128/IAI.66.6.2460-2465.1998
33. Schenkman S, Guther ML, Yoshida N. Mechanism of resistance to lysis by the alternative complement pathway in trypanosoma cruzi trypomastigotes: effect of specific monoclonal antibody. *J Immunol (Baltimore, Md: 1950).* (1986) 137:1623–8.
34. Fischer E, Ouaissi MA, Velge P, Cornette J, Kazatchkine MD. gp 58/68, a parasite component that contributes to the escape of the trypomastigote form of T. cruzi from damage by the human alternative complement pathway. *Immunology.* (1988) 65:299–303.
35. Cestari Idos S, Krarup A, Sim RB, Inal JM, Ramirez MI. Role of early lectin pathway activation in the complement-mediated killing of trypanosoma cruzi. *Mol Immunol.* (2009) 47:426–37. doi: 10.1016/j.molimm.2009.08.030
36. Ferreira V, Valck C, Sanchez G, Gingras A, Tzima S, Molina MC, et al. The classical activation pathway of the human complement system is specifically inhibited by calreticulin from trypanosoma cruzi. *J Immunol (Baltimore, Md: 1950).* (2004) 172:3042–50. doi: 10.4049/jimmunol.172.5.3042
37. Valck C, Ramirez G, Lopez N, Ribeiro CH, Maldonado I, Sanchez G, et al. Molecular mechanisms involved in the inactivation of the first component of human complement by trypanosoma cruzi calreticulin. *Mol Immunol.* (2010) 47:1516–21. doi: 10.1016/j.molimm.2010.01.019
38. Sosoniuk E, Vallejos G, Kenawy H, Gaboriaud C, Thielens N, Fujita T, et al. Trypanosoma cruzi calreticulin inhibits the complement lectin pathway activation by direct interaction with L-Ficolin. *Mol Immunol.* (2014) 60:80–5. doi: 10.1016/j.molimm.2014.03.014
39. Gonzalez A, Valck C, Sanchez G, Hartel S, Mansilla J, Ramirez G, et al. Trypanosoma cruzi calreticulin topographical variations in parasites infecting murine macrophages. *Am J Trop Med Hygiene.* (2015) 92:887–97. doi: 10.4269/ajtmh.14-0497
40. Souto-Padron T, Labriola CA, de Souza W. Immunocytochemical localisation of calreticulin in trypanosoma cruzi. *Histochem Cell Biol.* (2004) 122:563–9. doi: 10.1007/s00418-004-0724-7
41. Ramirez G, Valck C, Ferreira VP, Lopez N, Ferreira A. Extracellular trypanosoma cruzi calreticulin in the host-parasite interplay. *Trends Parasitol.* (2011) 27:115–22. doi: 10.1016/j.pt.2010.12.007
42. Michalak M, Groenendyk J, Szabo E, Gold LI, Opas M. Calreticulin, a multi-process calcium-buffering chaperone of the endoplasmic reticulum. *Biochem J.* (2009) 417:651–66. doi: 10.1042/BJ20081847
43. Stuart GR, Lynch NJ, Lu J, Geick A, Moffatt BE, Sim RB, et al. Localisation of the C1q binding site within C1q receptor/calreticulin. *FEBS Lett.* (1996) 397:245–9. doi: 10.1016/S0014-5793(96)01156-8
44. Stuart GR, Lynch NJ, Day AJ, Schwaeble WJ, Sim RB. The C1q and collectin binding site within C1q receptor (cell surface calreticulin). *Immunopharmacology.* (1997) 38:73–80. doi: 10.1016/S0162-3109(97)00076-3
45. Wallis R, Mitchell DA, Schmid R, Schwaeble WJ, Keeble AH. Paths reunited: Initiation of the classical and lectin pathways of complement activation. *Immunobiology.* (2010) 215:1–11. doi: 10.1016/j.imbio.2009.08.006
46. Moreau C, Cioci G, Iannello M, Laffly E, Chouquet A, Ferreira A, et al. Structures of parasite calreticulins provide insights into their flexibility and dual carbohydrate/peptide-binding properties. *IUCrJ.* (2016) 3(Pt 6):408–19. doi: 10.1107/S2052252516012847
47. Álvarez JP, Teneb J, Maldonado I, Weinberger K, Rosas C, Lemus D, et al. Structural bases that underline trypanosoma cruzi calreticulin proinfective, antiangiogenic and antitumor properties. *Immunobiology.* (2020) 225:151863. doi: 10.1016/j.imbio.2019.10.012
48. Sanchez Valdez FJ, Perez Brandan C, Zago MP, Labriola C, Ferreira A, Basombrio MA. Trypanosoma cruzi carrying a monoallelic deletion of the calreticulin (TcCRT) gene are susceptible to complement mediated killing and defective in their metacyclogenesis. *Mol Immunol.* (2013) 53:198–205. doi: 10.1016/j.molimm.2012.08.001
49. Sanchez-Valdez FJ, Perez Brandan C, Ramirez G, Uncos AD, Zago MP, Cimino RO, et al. A monoallelic deletion of the TcCRT gene increases the attenuation of a cultured trypanosoma cruzi strain, protecting against an *in vivo* virulent challenge. *PLoS Neglect Trop Dis.* (2014) 8:e2696. doi: 10.1371/journal.pntd.0002696
50. Ramirez G, Valck C, Molina MC, Ribeiro CH, Lopez N, Sanchez G, et al. Trypanosoma cruzi calreticulin: a novel virulence factor that

binds complement C1 on the parasite surface and promotes infectivity. *Immunobiology.* (2011) 216:265–73. doi: 10.1016/j.imbio.2010.04.001
51. Abello-Caceres P, Pizarro-Bauerle J, Rosas C, Maldonado I, Aguilar-Guzman L, Gonzalez C, et al. Does native trypanosoma cruzi calreticulin mediate growth inhibition of a mammary tumor during infection? *BMC Cancer.* (2016) 16:731. doi: 10.1186/s12885-016-2764-5
52. Sosoniuk-Roche E, Vallejos G, Aguilar-Guzmán L, Pizarro-Bäuerle J, Weinberger K, Rosas C, et al. Exogenous calreticulin, incorporated onto non-infective trypanosoma cruzi epimastigotes, promotes their internalization into mammal host cells. *Immunobiology.* (2017) 222:529–35. doi: 10.1016/j.imbio.2016.10.020
53. Houen G, Koch C. Human placental calreticulin: purification, characterization and association with other proteins. *Acta Chem Scan.* (1994) 48:905–11. doi: 10.3891/acta.chem.scand.48-0905
54. Crawford K, Kalionis B, Stevenson J, Brennecke S, Gude N. Calreticulin has opposing effects on the migration of human trophoblast and myometrial endothelial cells. *Placenta.* (2012) 33:416–23. doi: 10.1016/j.placenta.2012.02.003
55. Gu V, Wong M, Stevenson J, Crawford K, Brennecke S, Gude N. Calreticulin in human pregnancy and pre-eclampsia. *Mol Hum Reprod.* (2008) 14:309–15. doi: 10.1093/molehr/gan017
56. Castillo C, Ramirez G, Valck C, Aguilar L, Maldonado I, Rosas C, et al. The interaction of classical complement component C1 with parasite and host calreticulin mediates trypanosoma cruzi infection of human placenta. *PLoS Neglect Trop Dis.* (2013) 7:e2376. doi: 10.1371/journal.pntd.0002376
57. Evans-Osses I, Mojoli A, Beltrame MH, da Costa DE, DaRocha WD, Velavan TP, et al. Differential ability to resist to complement lysis and invade host cells mediated by MBL in R4 and 860 strains of trypanosoma cruzi. *FEBS Lett.* (2014) 588:956–61. doi: 10.1016/j.febslet.2014.01.054
58. Eggleton P, Bremer E, Dudek E, Michalak M. Calreticulin, a therapeutic target? *Expert Opin Ther Targets.* (2016) 20:1137–47. doi: 10.1517/14728222.2016.1164695
59. Khalife J, Liu J, Pierce R, Porchet E, Godin C, Capron A. Characterization and localization of schistosoma mansoni calreticulin Sm58. *Parasitology.* (1994) 108:527–32. doi: 10.1017/S0031182000077398
60. El Gengehi N, El Ridi R, Tawab NA, El Demellawy M, Mangold BL. A schistosoma mansoni 62-kDa band is identified as an irradiated vaccine T-cell antigen and characterized as calreticulin. *J Parasitol.* (2000) 86:993–1000. doi: 10.1645/0022-3395 (2000) 086[0993:ASMKBI]2.0.CO;2
61. Tsuji N, Morales T, Ozols V, Carmody A, Chandrashekar R. Molecular characterization of a calcium-binding protein from the filarial parasite dirofilaria immitis. *Mol Biochem Parasitol.* (1998) 97:69–79. doi: 10.1016/S0166-6851(98)00131-5
62. Brown A, Kasper G, Mcelroy P, Loukas A, Hewitt C, Berry C, et al. A hookworm allergen which strongly resembles calreticulin. *Parasite Immunol.* (1999) 21:439–50. doi: 10.1046/j.1365-3024.1999.00238.x
63. Ximénez C, González E, Nieves ME, Silva-Olivares A, Shibayama M, Galindo-Gómez S, et al. Entamoeba histolytica and E. dispar calreticulin: inhibition of classical complement pathway and differences in the level of expression in amoebic liver abscess. *BioMed Res Int.* (2014) 2014:127453. doi: 10.1155/2014/127453
64. González E, de Leon MdCG, Meza I, Ocadiz-Delgado R, Gariglio P, Silva-Olivares A, et al. Entamoeba histolytica calreticulin: an endoplasmic reticulum protein expressed by trophozoites into experimentally induced amoebic liver abscesses. *Parasitol Res.* (2011) 108:439–49. doi: 10.1007/s00436-010-2085-6
65. Joshi M, Pogue GP, Duncan RC, Lee NS, Singh NK, Atreya CD, et al. Isolation and characterization of leishmania donovani calreticulin gene and its conservation of the RNA binding activity. *Mol Biochem Parasitol.* (1996) 81:53–64. doi: 10.1016/0166-6851(96)02676-X
66. Oladiran A, Belosevic M. Trypanosoma carassii calreticulin binds host complement component C1q and inhibits classical complement pathway-mediated lysis. *Dev Comp Immunol.* (2010) 34:396–405. doi: 10.1016/j.dci.2009.11.005
67. Yadav S, Prakash J, Saxena JK. Metal binding study of calreticulin: an immunomodulatory protein of human filarial parasite brugia malayi. *Int J Biol Macromol.* (2018) 117:1157–68. doi: 10.1016/j.ijbiomac.2018.06.011
68. Suchitra S, Joshi P. Characterization of haemonchus contortus calreticulin suggests its role in feeding and immune evasion by the parasite. *Biochim Biophys Acta Gen Subjects.* (2005) 1722:293–303. doi: 10.1016/j.bbagen.2004.12.020
69. Chaibangyang W, Geadkaew-Krenc A, Smooker PM, Tesana S, Grams R. Evaluation of opisthorchis viverrini calreticulin for potential host modulation. *Acta Trop.* (2018) 187:175–81. doi: 10.1016/j.actatropica.2018.08.009
70. Chaibangyang W, Geadkaew-Krenc A, Vichasri-Grams S, Tesana S, Grams R. Molecular and biochemical characterization of opisthorchis viverrini calreticulin. *Korean J Parasitol.* (2017) 55:643. doi: 10.3347/kjp.2017.55.6.643
71. Zhao L, Shao S, Chen Y, Sun X, Sun R, Huang J, et al. Trichinella spiralis calreticulin binds human complement C1q as an immune evasion strategy. *Front Immunol.* (2017) 8:636. doi: 10.3389/fimmu.2017.00636
72. Debrabant A, Lee N, Pogue GP, Dwyer DM, Nakhasi HL. Expression of calreticulin P-domain results in impairment of secretory pathway in leishmania donovani and reduced parasite survival in macrophages. *Int J Parasitol.* (2002) 32:1423–34. doi: 10.1016/S0020-7519(02)00134-0
73. Gupta SK, Sisodia BS, Sinha S, Hajela K, Naik S, Shasany AK, et al. Proteomic approach for identification and characterization of novel immunostimulatory proteins from soluble antigens of leishmania donovani promastigotes. *Proteomics.* (2007) 7:816–23. doi: 10.1002/pmic.200600725
74. Kumari S, Samant M, Misra P, Khare P, Sisodia B, Shasany AK, et al. Th1-stimulatory polyproteins of soluble Leishmania donovani promastigotes ranging from 89.9 to 97.1 kDa offers long-lasting protection against experimental visceral leishmaniasis. *Vaccine.* (2008) 26:5700–11. doi: 10.1016/j.vaccine.2008.08.021
75. Ng YL, Olivos-García A, Lim TK, Noordin R, Lin Q, Othman N. Entamoeba histolytica: quantitative proteomics analysis reveals putative virulence-associated differentially abundant membrane proteins. *Am J Trop Med Hygiene.* (2018) 99:1518–29. doi: 10.4269/ajtmh.18-0415
76. Ximénez C, González E, Nieves M, Magaña U, Morán P, Gudiño-Zayas M, et al. Differential expression of pathogenic genes of entamoeba histolytica vs E. dispar in a model of infection using human liver tissue explants. *PLoS ONE.* (2017) 12:e0181962. doi: 10.1371/journal.pone.0181962
77. Vaithilingam A, Teixeira JE, Miller PJ, Heron BT, Huston CD. Entamoeba histolytica cell surface calreticulin binds human c1q and functions in amebic phagocytosis of host cells. *Infect Immun.* (2012) 80:2008–18. doi: 10.1128/IAI.06287-11
78. Gonzalez Rivas E, Ximenez C, Nieves-Ramirez ME, Moran Silva P, Partida-Rodríguez O, Hernandez EH, et al. Entamoeba histolytica calreticulin induces the expression of cytokines in peripheral blood mononuclear cells isolated from patients with amebic liver abscess. *Front Cell Infect Microbiol.* (2018) 8:358. doi: 10.3389/fcimb.2018.00358
79. McAllister M, Phillips N, Belosevic M. Trypanosoma carassii infection in goldfish (Carassius auratus L.): changes in the expression of erythropoiesis and anemia regulatory genes. *Parasitol Res.* (2019) 118:1147–58. doi: 10.1007/s00436-019-06246-5
80. Plouffe D, Belosevic M. Enzyme treatment of trypanosoma danilewskyi (Laveran & Mesnil) increases its susceptibility to lysis by the alternative complement pathway of goldfish, Carassius auratus (L.). *J Fish Dis.* (2004) 27:277–85. doi: 10.1111/j.1365-2761.2004.00541.x
81. Bossard G, Grébaut P, Thévenon S, Séveno M, Berthier D, Holzmuller P. Cloning, expression, molecular characterization and preliminary studies on immunomodulating properties of recombinant Trypanosoma congolense calreticulin. *Infect Genet Evol.* (2016) 45:320–31. doi: 10.1016/j.meegid.2016.09.020
82. Kasper G, Brown A, Eberl M, Vallar L, Kieffer N, Berry C, et al. A calreticulin-like molecule from the human hookworm necator americanus interacts with C1q and the cytoplasmic signalling domains of some integrins. *Parasite Immunol.* (2001) 23:141–52. doi: 10.1046/j.1365-3024.2001.00366.x
83. Yadav S, Gupta S, Selvaraj C, Doharey PK, Verma A, Singh SK, et al. *In silico* and *in vitro* studies on the protein-protein interactions between Brugia malayi immunomodulatory protein calreticulin and human C1q. *PLoS ONE.* (2014) 9:e106413. doi: 10.1371/journal.pone.0106413
84. Suchitra S, Anbu K, Rathore D, Mahawar M, Singh B, Joshi P. Haemonchus contortus calreticulin binds to C-reactive protein of its host, a novel

survival strategy of the parasite. *Parasite Immunol.* (2008) 30:371–4. doi: 10.1111/j.1365-3024.2008.01028.x
85. Naresha S, Suryawanshi A, Agarwal M, Singh B, Joshi P. Mapping the complement C1q binding site in haemonchus contortus calreticulin. *Mol Biochem Parasitol.* (2009) 166:42–6. doi: 10.1016/j.molbiopara.2009.02.007
86. Hong Y, Kim CW, Ghebrehiwet B. Trichinella spiralis: activation of complement by infective larvae, adults, and newborn larvae. *Exp Parasitol.* (1992) 74:290–9. doi: 10.1016/0014-4894(92)90152-Z
87. Näreaho A, Saari S, Meri S, Sukura A. Complement membrane attack complex formation and infectivity of trichinella spiralis and T. nativa in rats. *Vet Parasitol.* (2009) 159:263–7. doi: 10.1016/j.vetpar.2008.10.037
88. Sun R, Zhao X, Wang Z, Yang J, Zhao L, Zhan B, et al. Trichinella spiralis paramyosin binds human complement C1q and inhibits classical complement activation. *PLoS Neglect Trop Dis.* (2015) 9:e004310. doi: 10.1371/journal.pntd.0004310
89. Ma L, Li D, Yuan C, Zhang X, Ta N, Zhao X, et al. SjCRT, a recombinant schistosoma japonicum calreticulin, induces maturation of dendritic cells and a Th1-polarized immune response in mice. *Parasites Vectors.* (2017) 10:570. doi: 10.1186/s13071-017-2516-7
90. Huggins MC, Gibbs J, Moloney NA. Cloning of a schistosoma japonicum gene encoding an antigen with homology to calreticulin. *Mol Biochem Parasitol.* (1995) 71:81–7. doi: 10.1016/0166-6851(95)00038-3
91. Santoro F, Ouaissi MA, Pestel J, Capron A. Interaction between schistosoma mansoni and the complement system: binding of C1q to schistosomula. *J Immunol.* (1980) 124:2886–91.
92. Klabunde J, Berger J, Jensenius JC, Klinkert M-Q, Zelck UE, Kremsner PG, et al. Schistosoma mansoni: adhesion of mannan-binding lectin to surface glycoproteins of cercariae and adult worms. *Exp Parasitol.* (2000) 95:231–9. doi: 10.1006/expr.2000.4539
93. Weinberger K, Collazo N, Aguillón JC, Molina MC, Rosas C, Peña J, et al. Triatoma infestans calreticulin: gene cloning and expression of a main domain that interacts with the host complement system. *Am J Trop Med Hygiene.* (2017) 96:295–303. doi: 10.4269/ajtmh.16-0642
94. Kim TK, Ibelli AMG, Mulenga A. Amblyomma americanum tick calreticulin binds C1q but does not inhibit activation of the classical complement cascade. *Ticks Tick-Borne Dis.* (2015) 6:91–101. doi: 10.1016/j.ttbdis.2014.10.002
95. Ferreira CAS, Vaz IDS Jr, da Silva SS, Haag KL, Valenzuela JG, Masuda A. Cloning and partial characterization of a boophilus microplus (acari: ixodidae) calreticulin. *Exp Parasitol.* (2002) 101:25–34. doi: 10.1016/S0014-4894(02)00032-2
96. Gao J, Luo J, Fan R, Fingerle V, Guan G, Liu Z, et al. Cloning and characterization of a cDNA clone encoding calreticulin from haemaphysalis qinghaiensis (acari: ixodidae). *Parasitol Res.* (2008) 102:737–46. doi: 10.1007/s00436-007-0826-y
97. Lopez NC, Valck C, Ramirez G, Rodriguez M, Ribeiro C, Orellana J, et al. Antiangiogenic and antitumor effects of trypanosoma cruzi calreticulin. *PLoS Neglect Trop Dis.* (2010) 4:e730. doi: 10.1371/journal.pntd.0000730
98. Molina MC, Ferreira V, Valck C, Aguilar L, Orellana J, Rojas A, et al. An *in vivo* role for trypanosoma cruzi calreticulin in antiangiogenesis. *Mol Biochem Parasitol.* (2005) 140:133–40. doi: 10.1016/j.molbiopara.2004.12.014
99. Toledo V, Ramírez G, Valck C, López N, Ribeiro CH, Maldonado I, et al. Comparative *in vivo* antiangiogenic effects of calreticulin from trypanosoma cruzi and Homo sapiens. *Biol Res.* (2010) 43:287–9. doi: 10.4067/S0716-97602010000300004
100. Cruz P, Sosoniuk-Roche E, Maldonado I, Torres C, Ferreira A. Trypanosoma cruzi calreticulin: *in vitro* modulation of key immunogenic markers of both canine tumors and relevant immune competent cells. *Immunobiology.* (2019) 225:151892. doi: 10.1016/j.imbio.2019.12.001
101. Arias JI, Parra N, Beato C, Torres CG, Hamilton-West C, Rosas C, et al. Different trypanosoma cruzi calreticulin domains mediate migration and proliferation of fibroblasts *in vitro* and skin wound healing *in vivo*. *Arch Dermatol Res.* (2018) 310:639–50. doi: 10.1007/s00403-018-1851-7

Conflict of Interest: The authors declare that the research was conducted in the absence of any commercial or financial relationships that could be construed as a potential conflict of interest.

frontiers in Immunology

MINI REVIEW
published: 23 July 2020
doi: 10.3389/fimmu.2020.01560

Immune Evasion Strategies of Relapsing Fever Spirochetes

*Florian Röttgerding and Peter Kraiczy**

Institute of Medical Microbiology and Infection Control, University Hospital of Frankfurt, Goethe University Frankfurt, Frankfurt, Germany

Relapsing fever (RF) is claimed a neglected arthropod-borne disease caused by a number of diverse human pathogenic *Borrelia* (*B.*) species. These RF borreliae are separated into the groups of tick-transmitted species including *B. duttonii, B. hermsii, B. parkeri, B. turicatae*, *B. hispanica*, *B. persica, B. caucasica,* and *B. myiamotoi*, and the louse-borne *Borrelia* species *B. recurrentis*. As typical blood-borne pathogens achieving high cell concentrations in human blood, RF borreliae (RFB) must outwit innate immunity, in particular complement as the first line of defense. One prominent strategy developed by RFB to evade innate immunity involves inactivation of complement by recruiting distinct complement regulatory proteins, e.g., C1 esterase inhibitor (C1-INH), C4b-binding protein (C4BP), factor H (FH), FH-like protein-1 (FHL-1), and factor H-related proteins FHR-1 and FHR-2, or binding of individual complement components and plasminogen, respectively. A number of multi-functional, complement and plasminogen-binding molecules from distinct *Borrelia* species have previously been identified and characterized, exhibiting considerable heterogeneity in their sequences, structures, gene localization, and their capacity to bind host-derived proteins. In addition, RFB possess a unique system of antigenic variation, allowing them to change the composition of surface-exposed variable major proteins, thus evading the acquired immune response of the human host. This review focuses on the current knowledge of the immune evasion strategies by RFB and highlights the role of complement-interfering and infection-associated molecules for the pathogenesis of RFB.

Keywords: spirochetes, *Borrelia*, relapsing fever, immune evasion, complement, antigenic variation, innate immunity, adaptive immunity

OPEN ACCESS

Edited by:
Reinhard Würzner,
Innsbruck Medical University, Austria

Reviewed by:
Taru Meri,
University of Helsinki, Finland
Job E. Lopez,
Baylor College of Medicine, United States

****Correspondence:***
Peter Kraiczy
kraiczy@em.uni-frankfurt.de

Specialty section:
This article was submitted to Microbial Immunology, a section of the journal Frontiers in Immunology

Received: *09 April 2020*
Accepted: *12 June 2020*
Published: *23 July 2020*

Citation:
Röttgerding F and Kraiczy P (2020) Immune Evasion Strategies of Relapsing Fever Spirochetes. Front. Immunol. 11:1560. doi: 10.3389/fimmu.2020.01560

INTRODUCTION

Relapsing fever (RF), an ectoparasite-borne bacterial disease caused by *Borrelia* species is characterized by recurrent episodes of high fever and spirochetemia in the blood of infected individuals (1–4). RF is a neglected and emerging bacterial disease in the Americas and certain African countries, especially in regions with a high incidence of infected argasid and ixodid ticks of the genus *Ornithodoros* and *Ixodes*, respectively, or the human body louse *Pediculus humanus* (2, 4). While soft tick-borne RF (STBRF) is mainly found along the West coast of North America and endemic in the temperate and tropical African territories, the occurrence of hard tick-borne RF (HTBRF) directly correlates with the distribution of ixodid ticks in the northern hemisphere (5, 6). In contrast, LBRF is geographically restricted to countries along the Horn of Africa, in particular Eritrea, Ethiopia, and South-Sudan (4). Despite its focal distribution, LBRF has the potential to dramatically re-emerge when sociodemographic factors such as war, famine, political

turmoil, and precarious hygiene conditions in overcrowding camps change (7–11). Clinical signs of STBRF and LBRF appear abruptly between 2 and 18 days after infection with high fever, often accompanied by rigors, headache, chills, nausea, vomiting, myalgia, and diarrhea (2, 4). More severe clinical manifestations affect different organs such the liver (hepatosplenomegaly, liver dysfunction, hepatic failure), spleen (rupture), gastrointestinal tract (bleeding), lung (acute pulmonary edema, acute respiratory distress syndrome), heart (myocardial failure), and the central nervous system (meningism, facial paresis, vertigo, rigidity) (4). Concerning HTBRF, fever, headache, chills, arthralgia, fatigue, and malaise have been reported as the most common symptoms and severe neurological manifestations such as meningoencephalitis occur predominantly in immunocompromised patients (6, 12, 13). Like Lyme disease spirochetes, RFB exploit diverse immune evasion strategies to avoid recognition, and circumvent the innate and adaptive immune responses. Herein, we summarize the current knowledge of potential pathogenic factors identified in diverse RFB that counteract complement and humoral immune responses of the human host.

THE COMPLEMENT SYSTEM AT A GLANCE

Complement operates as a first line of defense against intruding pathogens and consists of numerous fluid-phase and membrane-bound regulators, inhibitors and inactive precursor molecules, most of which act in concert upon activation to eliminate microbes (14). Just like a domino effect, the complement cascade can independently be activated through three distinct pathways: the alternative (AP), the classical (CP), and the lectin pathway (LP) (15, 16).

The AP is spontaneously activated by a so-called tick-over-process leading to the covalent attachment of activated C3b molecules to microbial surfaces and thus allowing a continuous monitoring for invasive human pathogens (opsonization) (17, 18). Activation of the CP is triggered by binding of C1q to surface-bound IgM or IgG clusters and the LP utilizes mannose-binding lectin (MBL), collectins, and ficolins to recognize carbohydrate moieties on bacterial cell surfaces (15, 16, 19–21). Upon activation, either the C3 convertases C3bBb (AP) or C4b2a (CP and LP) are formed, leading to a massive generation of activated C3b that covalently binds to foreign surfaces. Further downstream activation is driven by binding of C3b to the C3 convertases, resulting in the formation of the C5 convertases C3bBb3b or C4b2a3b. By engendering the C5 convertase, C5 is cleaved to C5a and C5b, which covalently binds to the target surface. This critical activation step initializes the terminal sequence (TS) and the assembly of the pore-forming membrane attack complex C5b-9 or MAC. The MAC, a ring-like structure, is composed of numerous C9 molecules, all of which integrate into the microbial membrane and ultimately cause lysis (22–24).

To protect self surfaces from excessive activation, complement is tightly controlled by a variety of soluble and cell-bound complement regulatory proteins (25). Concerning soluble regulators, the AP is regulated by factor H (FH) and the factor H-like protein 1 (FHL-1) (generated by alternative splicing of the *cfh* gene). Both regulators inactivate C3b to iC3b by acting as co-factors for factor I, thereby accelerating the decay of the membrane-bound C3 convertase. In contrast to FH and FHL-1, the factor H-related protein 1 (FHR-1) is supposed to be a regulator of the TS and appears to block the cleavage activity of the C5 convertases by inhibiting the generation of C5a (26). The role of the additional four FHR proteins in complement regulation is as yet unclear. Recent data provide some evidence that these proteins may enhance complement activation and, thus possess an opposite regulatory function compared to FH and FHL-1 (27). Initial activation of the CP and LP is controlled by C1 esterase inhibitor (C1-INH) by inactivation of the serine proteases C1r, C1s, MASP-1, and MASP-2, respectively. In addition, the downstream activation steps of the CP are terminated by binding of the C4b-binding protein (C4BP) to C4b. This soluble regulator acts as cofactor for the Factor I-mediated degradation of C4b. The TS is blocked by preventing the integration of the soluble preforming sC5b-9 complexes into the target membrane via vitronectin and clusterin (16).

RECRUITMENT OF COMPLEMENT REGULATORY PROTEINS, AN EFFICIENT STRATEGY OF RFB FOR ESCAPING COMPLEMENT-MEDIATED KILLING

Immediately upon entry into the mammalian host, RFB face complement as the first line of defense. However, the role of complement in spirochete clearance has controversially been discussed. It has been shown that IgM is able to efficiently kill *B. hermsii* in the course of bacteremia in infected C3- and C5-deficient mice by a complement-independent mechanism, while B cell-deficient mice showed very high loads of spirochetes in their blood (28, 29). These findings led to the assumption that innate immunity plays a subordinate role in the pathobiology of these pathogens. On the other hand, RFB produce complement-binding proteins, most of which operate on different activation levels to protect spirochetes from complement-mediated bacteriolysis (30–37). This includes proteins of *B. hermsii*, *B. parkeri*, *B. duttonii*, *B. miyamotoi*, and *B. recurrentis*, respectively. An overview of the characteristics of these suspected, infection-relevant surface proteins are given below.

Abbreviations: BpcA, *B. parkeri* complement regulator-binding protein A; BtcA, *B. turicatae* plasminogen-binding protein; CbiA, complement binding and inhibitory protein A; CihC, complement inhibition via C4BP; C1-INH, C1 esterase inhibitor; C4BP, C4b binding protein; FhbA, FH-binding protein A; FH, Factor H; FHL-1, FH-like protein-1; FHR, FH-related protein; HcpA, human complement regulator and plasminogen-binding protein A; HTBRF, hard tick-borne relapsing fever; GAG, glycosaminoglycans; LBRF, louse-borne relapsing fever; MAC, membrane attack complex; RCA, regulators of complement activation; RF, relapsing fever; RFB, relapsing fever borreliae; SCR, short consensus repeats; STBRF, soft tick-borne relapsing fever; Vlp, variable large protein; Vmp, variable major protein; Vsp, variable small protein.

TABLE 1 | Characteristics of complement-binding proteins of relapsing fever borreliae.

Complement binding protein	Genospecies	Strain	Gene localization	Gene locus	Gene name/ ORF	Synonyms/ other designations	Size (kDa)	Interacting complement regulator	Binding regions of complement regulator	Binding of complement component(s)	Interacting with specific host-derived proteins	Complement resistance (GOF)	Complement inhibition	References
STBRF														
BhCRASP-1	*B. hermsii*	HS1	lp174	BHA008	*cspH*	FhbA1	21.5	FH FHR-1	SCR20	n.d.	Plasminogen	Yes	n.d.	(33, 36)
FhbA	*B. hermsii*	YOR HS1	lp174	n.d.[a]	*fhbA, bha008*	FHBP19 FhbA2	24	FH FHL-1	n.d.	n.d.	n.d.	n.d.	n.d.	(30, 31, 41)
FHBP28	*B. parkeri*	RML	n.d.	n.d.	n.d.	none	28	FH	n.d.	n.d.	n.d.	n.d.	n.d.	(30, 42)
BpcA	*B. parkeri*	RML	lp150	n.d.	n.d.	none	17	FH FHR-1	SCRs 19-20 SCRs 3-5	n.d.	Plasminogen	n.d.	n.d.	(36)
BtcA	*B. turicatae*	91E135	lp159	A7978_ 04350	n.d.	none	20.5	none	n.d.	n.d.	Plasminogen	n.d.	n.d.	(36)
BHA007	*B. hermsii*	HS1	lp174	BHA007	*bhA007*	none	39	C4BP	n.d.	n.d.	Fibronectin	n.d.	n.d.	(43)
HTBRF														
CbiA	*B. miyamotoi*	FR64b	lp70	CNO09_ 05070	*cbiA*	none	21	FH	SCRs 8-20 SCRs 15-20 SCRs 19-20	C3, C3b, C4b, C5	Plasminogen	Yes	CP, TS	(37, 44)
LBRF														
HcpA	*B. recurrentis*	A1 A17	lp124	n.d.	*hcpA*	none	21	FH FHR-1	SCRs 19-20 SCRs 3-5	C3, C3b, C4b	Plasminogen	Yes	TS	(34)
CihC	*B. recurrentis*	A1 A17	lp124	n.d.	*cihC*	none	40	C4BP C1-INH	n.d.	n.d.	Fibronectin	Yes	n.d.	(35)
CihC	*B. duttonii*	La	lp165	BDU_ RSO4550	*cihC*	BDU_1	40	C4BP C1-INH	n.d.	n.d.	Fibronectin	Yes	n.d.	(35, 45)

n.d.; not determined.

GOF, protein produced in a gain-of-function background; AP, alternative pathway; CP, classical pathway; TS, terminal sequence.

[a]*Sequence of the fhbA gene could not be detected on lp200 of B. hermsii YOR and lp174 of B. hermsii HS1, respectively, by BLAST searches.*

Inactivation of the Alternative Pathway by Binding of Complement Regulator FH

Acquisition of regulators of complement activation is one of the most common strategies exploited by many human pathogenic microorganisms to evade complement (38–40). At least seven FH-interacting proteins have been described among RFB species including BhCRASP-1 (FhbA1) of *B. hermsii* HS1 and FhbA2 (FhbA, FHBP19) of *B. hermsii* YOR, FHBP28 and BpcA of *B. parkeri*, CbiA of *B. miyamotoi*, and HcpA of *B. duttonii* and *B. recurrentis* (30, 31, 33, 34, 36, 37) (**Table 1**). All FH-interacting proteins have in common binding to the C-terminal domains implicating that the regulatory domains located at the N-terminus of FH are accessible to retain their Factor I-mediated C3b degradation activity (33, 34, 36, 37) (**Table 1**). Moreover, BhCRASP-1, HcpA, BpcA, and CbiA, respectively, facilitate complement resistance when ectopically produced in genetically manipulated spirochetes (gain-of-function strains) (33, 34, 36, 37).

Within a *Borrelia* species, the FH-binding proteins are highly conserved, exhibiting sequence identity values of >93% (32) but among RFB, the percentages are quite low (36–45%). Whether the lack of sequence similarity might account for a different fold, appears to be somewhat questionable, in particular in the light of missing three dimensional structures. Interestingly, at least four conserved motifs (LDxNQKQALIxF, LGN-KxKQFLQxLH, SFSSxNFxD, and LEQKKExAL) could be identified in all seven proteins, raising the possibility of a non-continuous FH-binding site. Further studies investigating variants of FhbA2, FHBP28, HcpA, and BpcA also provide evidence that multiple regions are involved in the interaction with FH (30, 34, 36, 41). Of importance, infection studies utilizing a *fhbA* deletion mutant demonstrated that FhbA2 is the only FH-binding protein of *B. hermsii* and the absence of FhbA did not have an impact on serum resistance or infectivity of spirochetes, indicating functionally redundant roles played by other complement-interacting proteins as discussed below (46).

Inactivation of the Classical and Lectin Pathway by Binding of C1-INH and C4BP

To date, CihC of *B. recurrentis* is the soley protein displaying complement-inactivating properties on the CP and LP by binding to C1-INH and C4BP-binding protein (35). Orthologous proteins exhibiting sequence identities between 44 and 91% have been detected in *B. duttonii* Ly (BDU_1026), *B. hermsii* (BHA007), *B. turicatae* (BTA001), *B. parkeri* (BpA001), and *B. crocidurae* Achema and DOU (BCD_1370) but no homologous sequences could be found in LD spirochetes (42, 43). Functional analyses revealed that, like FH, C4BP bound to the borrelial

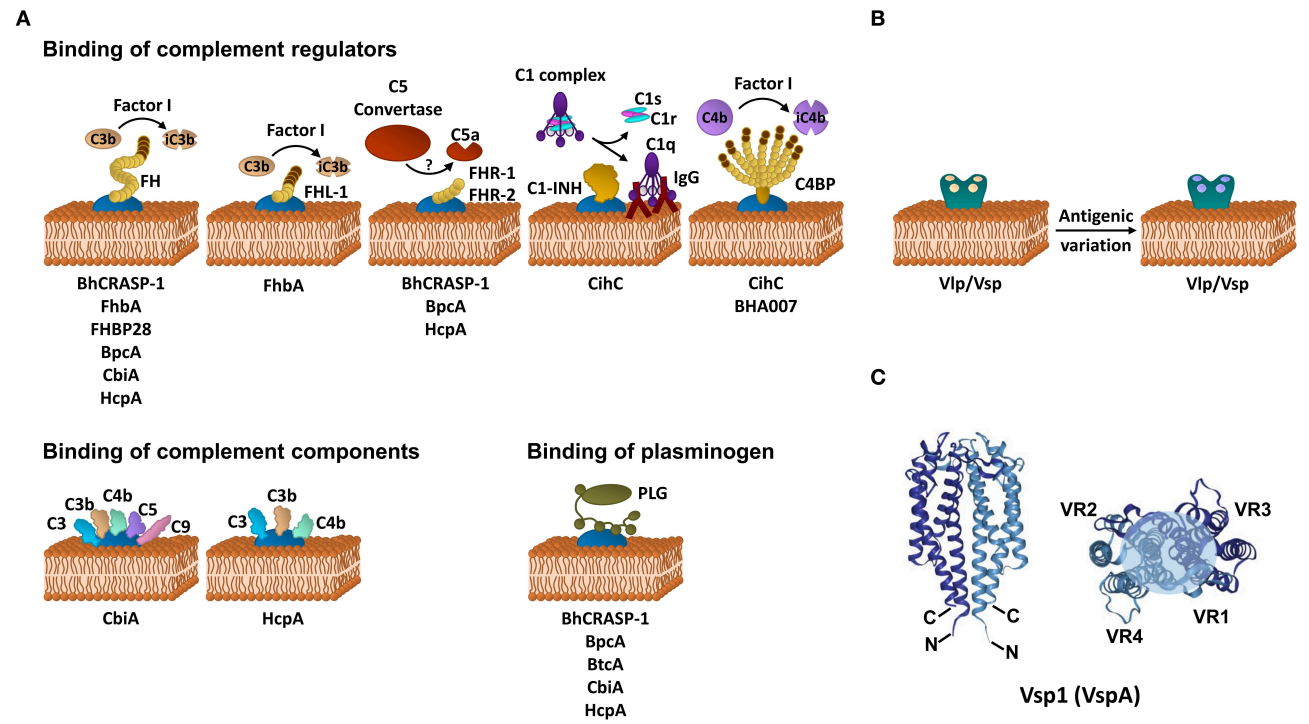

FIGURE 1 | Immune evasion strategies of RFB. **(A)** Inhibition of complement by distinct borrelial proteins acting at certain levels of the activation cascade. **(B)** Immune evasion of RFB by multiphasic antigenic variation. **(C)** Schematic representation of the structure of the Vsp1 (VspA) dimer of *B. turicatae* [PDB 2GA0, adapted from (47)]. The monomeric units are represented in dark or light blue. The variable sequences are distributed within the second and third α-helices as well as all loop regions and summarize in variable region (VR) 1–4. The light blue circle at the top of the dimer indicates the region with the highest variability. FH, factor H; FHL-1, factor H-like protein 1; FHR, factor H-related protein; C4BP, C1-INH, C1 esterase inhibitor; C4b binding protein; iC3b, inactivated C3b; iC4b, inactivated C4b, IgG, immunoglobulin G.

surface retained its complement-inhibitory activity for factor I-mediated C4b degradation, thus targeting activation of the CP and LP (**Figure 1A**, **Table 1**). Previously, Meri et al. also demonstrated inactivation of the CP by binding of functional active C4BP to the surface of *B. recurrentis* and *B. duttonii* (45). In addition, CihC also promotes termination of the CP at the initial activation steps by binding of C1-INH, indicating that this borrelial molecule displays multi-functional complement-inhibitory properties. Deletions at the N- and C-terminus of CihC did not abrogate binding of C4BP or C1-INH leading to the assumption that central regions might be responsible for binding (**Table 1**). A crucial role of CihC in mediating serum resistance of RFB was evidenced by employing *cihC*-expressing gain-of-function strains which displayed a resistant phenotype upon serum challenge (35). In contrast to CihC, the BHA007 protein of *B. hermsii* only bound C4BP but not C1-INH (42). Owing to their functional properties to interact with fibronectin, these molecules have generically been named as "fibronectin-binding proteins" and clustered together with the fibronectin-binding BBK32 protein of Lyme disease spirochetes (42). Despite their low sequence similarity, the finding that BBK32 confers bloodstream survival of spirochetes (48) supports the possibility that CihC orthologs might also play a role during infection of the human host. Concerning CP inactivation, CbiA of *B. miyamotoi* has previously been shown to strongly inhibit activation of the CP, independently from interaction with C4BP by a yet unknown mechanism (37) (**Figure 1A**, **Table 1**). It is tempting to speculate whether binding of C4b to CbiA restricts downstream activation of the CP by terminating formation of the C3 convertase (37).

Inhibition of the Terminal Sequence and MAC Assembly

Terminating the final activation steps by binding to pore-forming complexes or late complement components negatively affects assembling of the MAC as demonstrated for CbiA and HcpA (37) (**Figure 1A**, **Table 1**). In particular, CbiA strongly inhibits the TS, probably through the binding of C5 and C9 whereas HcpA moderately influences complement on this level and BpcA and BtcA, respectively, did not have an impact at all. Interference with the TS enhance the process of complement inactivation mediated by distinct outer surface proteins.

Inactivation of Complement by Acquisition of Plasminogen

Distinct complement-interacting proteins including BhCRASP-1, HcpA, and CbiA exhibit multiple binding specificities to host-derived fluid phase proteins such as plasminogen (33, 34, 36, 44) (**Figure 1A**, **Table 1**). Plasminogen is known to bind to C3, C3b, C3d, and C5 and upon activation to plasmin, C3 and C5 degradation takes place (49). Plasminogen is also able to enhance Factor I-mediated C3b degradation in the presence of FH (49). Previous studies demonstrated that plasmin(ogen) bound to *B. hermsii* HS1, *B. recurrentis* A1, and *B. parkeri* decreases the amount of C3b molecules deposited on the borrelial surface (33, 34, 36) or lead to degradation of C3b when purified HcpA, BpcA, and CbiA, respectively, have been employed (34, 36, 44). Thus, degradation of C3 and C5 appears an additional strategy of RFB to successful overcome host immune defenses.

Direct Interaction With Individual Complement Components

HcpA and CbiA also bind to some extent to individual complement components, namely C3, C3b, C4, and C4b, respectively, as well as C5 (CbiA) though the relevance of these interactions on complement inactivation require further investigation (37) (**Figure 1A**, **Table 1**).

In conclusion, these findings suggest an involvement of these molecules in immune evasion in particular as the inactivation of the key complement component C3b is thought to be an efficient instrument for bacterial survival and may account for the extraordinary pathogenesis of RFB in the human host.

ANTIGENIC VARIATION, A POWERFUL MECHANISM OF RFB TO ESCAPE IMMUNE AVOIDANCE

To evade clearance by the humoral immune response of the human host, RFB are capable of producing a bulk repertoire of antigenically distinct serotypes in a given cell population by a genetically driven process termed antigenic variation (50). In their pioneering work, Barbour and Stoenner revealed that the phenomenon of serotype switching is a spontaneous, reversible, and multiphasic process, creating outer surface proteins that bear serotype-specific epitopes (50) (**Figure 1B**). These immunodominant, variable major lipoproteins (Vmps) are divided into two different, highly polymorphic protein families: the variable small proteins, Vsp (∼20 kDa) and the variable large proteins, Vlp (∼36 kDa) that are subdivided in additional four subfamilies: α, β, γ, and δ (50–52). Apparently, the molecular mechanism of antigenic variation is not a subject to a process that is under pressure of the local environment, host factors or the host immune system. Recognizing that multiple serotypes arise from a single cell, thus, theoretically plenty of variants can be generated by producing highly diverse sets of Vlps and Vmps during infection. Previous studies revealed that 60–70 antigenically distinct variants of *B. hermsii* could arise during mammalian infection (52). Such a considerable diversity is achieved by multiple rounds of genetic rearrangements of the Vmp encoding genes including (i) non-reciprocal recombination of silent or archival *vmp* genes with an active, transcribed *vmp* gene (gene conversion), (ii) intramolecular DNA rearrangement, and (iii) switching of the expression site resulting in a modification of the transcript (53, 54). The mechanism of intermolecular recombination also appears to take place in the Old World RFB *B. duttonii* (55). Variable antigen genes encoding for Vlps and Vsps have also been detected in *B. turicatae*, *B. crocidurae, B. duttonii* (56, 57), *B. miyamotoi* (58, 59), and *B. recurrentis* (60, 61). Genetically, the silent or archival *vmp* genes are dispersed on different linear plasmids of 28–53 kb whereas an active, promoter-driven expression locus is found only on a single plasmid (53, 61). Such an active *vlp* or *vsp* gene

can be exchanged by any archival or silent *vlp* and *vsp* gene but the frequency of replacement differs between these genes (62). The unceasing exchange of *vmp* genes will undoubtedly generate numerous polymorphic Vmps, allowing spirochetes to remain one step ahead of the adaptive immune response and thereby successfully evade the host's defenses. In a study using genetically modified *B. hermsii* cells that lack the ability to undergo antigenic variation, Raffel et al. clearly demonstrated that Vmps are required for inducing a high spirochetemia in the blood and for causing a relapse in infected mice whereby colonization of the ticks by these attenuated spirochetes remains unaffected (63). Interestingly, Vmp-lacking cells showed a reduce fitness compared to the WT and reconstituted spirochetes.

Crystal structure refinements of Vsp and Vlp revealed a similar fold for both groups of proteins which are predominately composed of a 2-fold-symmetric dimer. Each monomeric unit consists of four α-helical bundles connected by two loop regions (47, 64) (**Figure 1C**). The N-terminus is anchored in the spirochetal membrane while the flexible C-terminus is folded back and oriented closely to the N-terminus. The variable loop regions are exposed to the environment and serve as ligands for antibodies. Interestingly, the most conserved regions are oriented to the outside of the protein known to be targets for anti-Vmp antibodies elicited during infection. Of note, OspC, the major outer surface protein of *B. burgdorferi* is phylogenetically and structurally related, and shares a common helical fold to the Vsps suggesting that these proteins might display similar roles in immune evasion (47, 65).

CONCLUDING REMARKS

Over the last decades, a number of complement-interacting molecules have been described, all of which touch the first line of host defense in certain ways by obstructing activation of complement. In synergy with the antigenic variation system, RFB are able to repeatedly circumvent both, the innate immune system as well as the acquired immune response. Understanding the molecular principles of how these molecules interfere with innate immunity may pave the way for developing new therapeutics for the treatment of RF patients or patients suffering from complement deficiencies, and might even serve as preventive measures for infectious diseases in general. Surface-exposed molecules may also be part of a new vaccine or can be used for the generation of novel immunoassays (32). Undoubtedly, future studies should unravel important questions addressing the role of functionally redundant, anti-complement proteins in the pathogenesis of these new-emerging pathogens.

AUTHOR CONTRIBUTIONS

FR and PK wrote the manuscript and prepared the figure and table. All authors contributed to the article and approved the submitted version.

FUNDING

This work was supported by the LOEWE Center DRUID (Novel Drug Targets against Poverty-Related and Neglected Tropical Infectious Diseases), project C3 (PK).

ACKNOWLEDGMENTS

We thank Arno Koenigs and Yi-Pin Lin for critical reading and helpful suggestions on the manuscript. We also would like to thank the two reviewers for their careful reading of our manuscript and their valuable and insightful comments.

REFERENCES

1. Dworkin MS, Schwan TG, Anderson DE Jr, Borchardt SM. Tick-borne relapsing fever. *Infect Dis Clin North Am.* (2008) 22:449–68. doi: 10.1016/j.idc.2008.03.006
2. Lopez JE, Krishnavahjala A, Garcia MN, Bermudez S. Tick-borne relapsing fever spirochetes in the Americas. *Vet Sci.* (2016) 3:16. doi: 10.3390/vetsci3030016
3. Talagrand-Reboul E, Boyer PH, Bergstrom S, Vial L, Boulanger N. Relapsing fevers: neglected tick-borne diseases. *Front Cell Infect Microbiol.* (2018) 8:98. doi: 10.3389/fcimb.2018.00098
4. Warrell DA. Louse-borne relapsing fever (*Borrelia recurrentis* infection). *Epidemiol Infect.* (2019) 147:e106. doi: 10.1017/S0950268819000116
5. Wagemakers A, Staarink PJ, Sprong H, Hovius JW. *Borrelia miyamotoi*: a widespread tick-borne relapsing fever spirochete. *Trends Parasitol.* (2015) 31:260–9. doi: 10.1016/j.pt.2015.03.008
6. Stone BL, Brissette CA. Host immune evasion by Lyme and relapsing fever borreliae: findings to lead future studies for *Borrelia miyamotoi*. *Front Immunol.* (2017) 8:12. doi: 10.3389/fimmu.2017.00012
7. Hoch M, Wieser A, Loscher T, Margos G, Purner F, Zuhl J, et al. Louse-borne relapsing fever (*Borrelia recurrentis*) diagnosed in 15 refugees from northeast Africa: epidemiology and preventive control measures, Bavaria, Germany, July to October 2015. *Euro Surveill.* (2015) 20. doi: 10.2807/1560-7917.ES.2015.20.42.30046
8. Antinori S, Mediannikov O, Corbellino M, Raoult D. Louse-borne relapsing fever among East African refugees in Europe. *Travel Med Infect Dis.* (2016) 14:110–4. doi: 10.1016/j.tmaid.2016.01.004
9. Cutler SJ. Refugee crisis and re-emergence of forgotten infections in Europe. *Clin Microbiol Infect.* (2016) 22:8–9. doi: 10.1016/j.cmi.2015.10.018
10. Darcis G, Hayette MP, Bontems S, Sauvage AS, Meuris C, Van Esbroeck M, et al. Louse-borne relapsing fever in a refugee from Somalia arriving in Belgium. *J Travel Med.* (2016) 23. doi: 10.1093/jtm/taw009
11. Grecchi C, Zanotti P, Pontarelli A, Chiari E, Tomasoni LR, Gulletta M, et al. Louse-borne relapsing fever in a refugee from Mali. *Infection.* (2017) 45:373–6. doi: 10.1007/s15010-017-0987-2
12. Platonov AE, Karan LS, Kolyasnikova NM, Makhneva NA, Toporkova MG, Maleev VV, et al. Humans infected with relapsing fever spirochete *Borrelia miyamotoi*, Russia. *Emerg Infect Dis.* (2011) 17:1816–23. doi: 10.3201/eid1710.101474
13. Hovius JW, de Wever B, Sohne M, Brouwer MC, Coumou J, Wagemakers A, et al. A case of meningoencephalitis by the relapsing fever spirochaete *Borrelia miyamotoi* in Europe. *Lancet.* (2013) 382:658. doi: 10.1016/S0140-6736(13)61644-X
14. Ricklin D, Hajishengallis G, Yang K, Lambris JD. Complement: a key system for immune surveillance and homeostasis. *Nat Immunol.* (2010) 11:785–97. doi: 10.1038/ni.1923
15. Walport MJ. Complement - First of two parts. *N Engl J Med.* (2001) 344:1058–66. doi: 10.1056/NEJM200104053441406

16. Merle NS, Church SE, Fremeaux-Bacchi V, Roumenina LT. Complement system part I - molecular mechanisms of activation and regulation. *Front Immunol*. (2015) 6:262. doi: 10.3389/fimmu.2015.00262
17. Pangburn MK, Schreiber RD, Muller-Eberhard HJ. Formation of the initial C3 convertase of the alternative complement pathway. Acquisition of C3b-like activities by spontaneous hydrolysis of the putative thioester in native C3. *J Exp Med*. (1981) 154:856–67. doi: 10.1084/jem.154.3.856
18. Bexborn F, Andersson PO, Chen H, Nilsson B, Ekdahl KN. The tick-over theory revisited: formation and regulation of the soluble alternative complement C3 convertase. (C3(H_2O)Bb). *Mol Immunol*. (2008) 45:2370–9. doi: 10.1016/j.molimm.2007.11.003
19. Fujita T, Matsushita M, Endo Y. The lectin-complement pathway–its role in innate immunity and evolution. *Immunol Rev*. (2004) 198:185–202. doi: 10.1111/j.0105-2896.2004.0123.x
20. Kishore U, Ghai R, Greenhough TJ, Shrive AK, Bonifati DM, Gadjeva MG, et al. Structural and functional anatomy of the globular domain of complement protein C1q. *Immunol Lett*. (2004) 95:113–28. doi: 10.1016/j.imlet.2004.06.015
21. Kjaer TR, Thiel S, Andersen GR. Toward a structure-based comprehension of the lectin pathway of complement. *Mol Immunol*. (2013) 56:413–22. doi: 10.1016/j.molimm.2013.05.007
22. Carroll MC. The complement system in regulation of adaptive immunity. *Nat Immunol*. (2004) 5:981–6. doi: 10.1038/ni1113
23. Aleshin AE, DiScipio RG, Stec B, Liddington RC. Crystal structure of C5b-6 suggests structural basis for priming assembly of the membrane attack complex. *J Biol Chem*. (2012) 287:19642–52. doi: 10.1074/jbc.M112.361121
24. Hadders MA, Bubeck D, Roversi P, Hakobyan S, Forneris F, Morgan BP, et al. Assembly and regulation of the membrane attack complex based on structures of C5b6 and sC5b9. *Cell Rep*. (2012) 1:200–7. doi: 10.1016/j.celrep.2012.02.003
25. Zipfel PF, Skerka C. Complement regulators and inhibitory proteins. *Nat Rev Immunol*. (2009) 9:729–40. doi: 10.1038/nri2620
26. Heinen S, Hartmann A, Lauer N, Wiehl U, Dahse HM, Schirmer S, et al. Factor H-related protein 1. (CFHR-1) inhibits complement C5 convertase activity and terminal complex formation. *Blood*. (2009) 114:2439–47. doi: 10.1182/blood-2009-02-205641
27. Cserhalmi M, Papp A, Brandus B, Uzonyi B, Jozsi M. Regulation of regulators: role of the complement factor H-related proteins. *Semin Immunol*. (2019) 45:101341. doi: 10.1016/j.smim.2019.101341
28. Newman K Jr, Johnson RC. *In vivo* evidence that an intact lytic complement pathway is not essential for successful removal of circulating *Borrelia turicatae* from mouse blood. *Infect Immun*. (1981) 31:465–9. doi: 10.1128/IAI.31.1.465-469.1981
29. Connolly SE, Benach JL. Cutting edge: the spirochetemia of murine relapsing fever is cleared by complement-independent bactericidal antibodies. *J Immunol*. (2001) 167:3029–32. doi: 10.4049/jimmunol.167.6.3029
30. McDowell JV, Tran E, Hamilton D, Wolfgang J, Miller K, Marconi RT. Analysis of the ability of spirochete species associated with relapsing fever, avian borreliosis, and epizootic bovine abortion to bind factor H and cleave c3b. *J Clin Microbiol*. (2003) 41:3905–10. doi: 10.1128/JCM.41.8.3905-3910.2003
31. Hovis KM, McDowell JV, Griffin L, Marconi RT. Identification and characterization of a linear-plasmid-encoded factor H-binding protein. (FhbA) of the relapsing fever spirochete *Borrelia hermsii*. *J Bacteriol*. (2004) 186:2612–8. doi: 10.1128/JB.186.9.2612-2618.2004
32. Hovis KM, Jones JP, Sadlon T, Raval G, Gordon DL, Marconi RT. Molecular analyses of the interaction of *Borrelia hermsii* FhbA with the complement regulatory proteins factor H and factor H-like protein 1. *Infect Immun*. (2006) 74:2007–14. doi: 10.1128/IAI.74.4.2007-2014.2006
33. Rossmann E, Kraiczy P, Herzberger P, Skerka C, Kirschfink M, Simon MM, et al. Dual binding specificity of a *Borrelia hermsii*-associated complement regulator-acquiring surface protein for factor H and plasminogen discloses a putative virulence factor of relapsing fever spirochetes. *J Immunol*. (2007) 178:7292–301. doi: 10.4049/jimmunol.178.11.7292
34. Grosskinsky S, Schott M, Brenner C, Cutler SJ, Kraiczy P, Zipfel PF, et al. Borrelia recurrentis employs a novel multifunctional surface protein with anti-complement, anti-opsonic and invasive potential to escape innate immunity. *PLoS ONE*. (2009) 4:e4858. doi: 10.1371/journal.pone.0004858
35. Grosskinsky S, Schott M, Brenner C, Cutler SJ, Simon MM, Wallich R. Human complement regulators C4b-binding protein and C1 esterase inhibitor interact with a novel outer surface protein of *Borrelia recurrentis*. *PLoS Negl Trop Dis*. (2010) 4:e698. doi: 10.1371/journal.pntd.0000698
36. Schott M, Grosskinsky S, Brenner C, Kraiczy P, Wallich R. Molecular characterization of the interaction of *Borrelia parkeri* and *Borrelia turicatae* with human complement regulators. *Infect Immun*. (2010) 78:2199–208. doi: 10.1128/IAI.00089-10
37. Röttgerding F, Wagemakers A, Koetsveld J, Fingerle V, Kirschfink M, Hovius JW, et al. Immune evasion of *Borrelia miyamotoi*: CbiA, a novel outer surface protein exhibiting complement binding and inactivating properties. *Sci Rep*. (2017) 7:303. doi: 10.1038/s41598-017-00412-4
38. Kraiczy P, Wurzner R. Complement escape of human pathogenic bacteria by acquisition of complement regulators. *Mol Immunol*. (2006) 43:31–44. doi: 10.1016/j.molimm.2005.06.016
39. Lambris JD, Ricklin D, Geisbrecht BV. Complement evasion by human pathogens. *Nat Rev Microbiol*. (2008) 6:132–42. doi: 10.1038/nrmicro1824
40. Hovingh ES, van den Broek B, Jongerius I. Hijacking complement regulatory proteins for bacterial immune evasion. *Front Microbiol*. (2016) 7:2004. doi: 10.3389/fmicb.2016.02004
41. Hovis KM, Freedman JC, Zhang H, Forbes JL, Marconi RT. Identification of an antiparallel coiled-coil/loop domain required for ligand binding by the *Borrelia hermsii* FhbA protein: additional evidence for the role of FhbA in the host-pathogen interaction. *Infect Immunity*. (2008) 76:2113–22. doi: 10.1128/IAI.01266-07
42. Lewis ER, Marcsisin RA, Campeau Miller SA, Hue F, Phillips A, Aucoin DP, et al. Fibronectin-binding protein of *Borrelia hermsii* expressed in the blood of mice with relapsing fever. *Infect Immun*. (2014) 82:2520–31. doi: 10.1128/IAI.01582-14
43. Miller SC, Porcella SF, Raffel SJ, Schwan TG, Barbour AG. Large linear plasmids of *Borrelia* species that cause relapsing fever. *J Bacteriol*. (2013) 195:3629–39. doi: 10.1128/JB.00347-13
44. Nguyen NTT, Rottgerding F, Devraj G, Lin YP, Koenigs A, Kraiczy P. The complement binding and inhibitory protein CbiA of *Borrelia miyamotoi* degrades extracellular matrix components by interacting with plasmin(ogen). *Front Cell Infect Microbiol*. (2018) 8:23. doi: 10.3389/fcimb.2018.00023
45. Meri T, Cutler SJ, Blom AM, Meri S, Jokiranta TS. Relapsing fever spirochetes *Borrelia recurrentis* and *B. duttonii* acquire complement regulators C4b-binding protein and factor H. *Infect Immun*. (2006) 74:4157–63. doi: 10.1128/IAI.00007-06
46. Fine LM, Miller DP, Mallory KL, Tegels BK, Earnhart CG, Marconi RT. The *Borrelia hermsii* factor H binding protein FhbA is not required for infectivity in mice or for resistance to human complement *in vitro*. *Infect Immun*. (2014) 82:3324–32. doi: 10.1128/IAI.01892-14
47. Lawson CL, Yung BH, Barbour AG, Zuckert WR. Crystal structure of neurotropism-associated variable surface protein 1. (Vsp1) of *Borrelia turicatae*. *J Bacteriol*. (2006) 188:4522–30. doi: 10.1128/JB.00028-06
48. Caine JA, Coburn J. A short-term *Borrelia burgdorferi* infection model identifies tissue tropisms and bloodstream survival conferred by adhesion proteins. *Infect Immun*. (2015) 83:3184–94. doi: 10.1128/IAI.00349-15
49. Barthel D, Schindler S, Zipfel PF. Plasminogen is a complement inhibitor. *J Biol Chem*. (2012) 287:18831–42. doi: 10.1074/jbc.M111.323287
50. Barbour AG, Tessier SL, Stoenner HG. Variable major proteins of *Borrellia hermsii*. *J Exp Med*. (1982) 156:1312–24. doi: 10.1084/jem.156.5.1312
51. Restrepo BI, Kitten T, Carter CJ, Infante D, Barbour AG. Subtelomeric expression regions of *Borrelia hermsii* linear plasmids are highly polymorphic. *Mol Microbiol*. (1992) 6:3299–311. doi: 10.1111/j.1365-2958.1992.tb02198.x
52. Dai Q, Restrepo BI, Porcella SF, Raffel SJ, Schwan TG, Barbour AG. Antigenic variation by *Borrelia hermsii* occurs through recombination between extragenic repetitive elements on linear plasmids. *Mol Microbiol*. (2006) 60:1329–43. doi: 10.1111/j.1365-2958.2006.05177.x
53. Kitten T, Barbour AG. Juxtaposition of expressed variable antigen genes with a conserved telomere in the bacterium *Borrelia hermsii*. *Proc Natl Acad Sci USA*. (1990) 87:6077–81. doi: 10.1073/pnas.87.16.6077
54. Restrepo BI, Carter CJ, and Barbour AG. Activation of a vmp pseudogene in *Borrelia hermsii*: an alternate mechanism of antigenic variation during relapsing fever. *Mol Microbiol*. (1994) 13:287–99. doi: 10.1111/j.1365-2958.1994.tb00423.x

55. Takahashi Y, Cutler SJ, Fukunaga M. Size conversion of a linear plasmid in the relapsing fever agent *Borrelia duttonii*. *Microbiol Immunol*. (2000) 44:1071–4. doi: 10.1111/j.1348-0421.2000.tb02605.x
56. Pennington PM, Cadavid D, Barbour AG. Characterization of VspB of *Borrelia turicatae*, a major outer membrane protein expressed in blood and tissues of mice. *Infect Immun*. (1999) 67:4637–45. doi: 10.1128/IAI.67.9.4637-4645.1999
57. Shamaei-Tousi A, Martin P, Bergh A, Burman N, Brannstrom T, Bergstrom S. Erythrocyte-aggregating relapsing fever spirochete *Borrelia crocidurae* induces formation of microemboli. *J Infect Dis*. (1999) 180:1929–38. doi: 10.1086/315118
58. Hamase A, Takahashi Y, Nohgi K, Fukunaga M. Homology of variable major protein genes between *Borrelia hermsii* and *Borrelia miyamotoi*. *FEMS Microbiol Lett*. (1996) 140:131–7. doi: 10.1111/j.1574-6968.1996.tb08326.x
59. Wagemakers A, Koetsveld J, Narasimhan S, Wickel M, Deponte K, Bleijlevens B, et al. Variable major proteins as targets for specific antibodies against *Borrelia miyamotoi*. *J Immunol*. (2016) 196:4185–95. doi: 10.4049/jimmunol.1600014
60. Vidal V, Scragg IG, Cutler SJ, Rockett KA, Fekade D, Warrell DA, et al. Variable major lipoprotein is a principal TNF-inducing factor of louse-borne relapsing fever. *Nat Med*. (1998) 4:1416–20. doi: 10.1038/4007
61. Lescot M, Audic S, Robert C, Nguyen TT, Blanc G, Cutler SJ, et al. The genome of Borrelia recurrentis, the agent of deadly louse-borne relapsing fever, is a degraded subset of tick-borne Borrelia duttonii. *PLoS Genet*. (2008) 4:e1000185. doi: 10.1371/journal.pgen.1000185
62. Stoenner HG, Dodd T, Larsen C. Antigenic variation of *Borrelia hermsii*. *J Exp Med*. (1982) 156:1297–311. doi: 10.1084/jem.156.5.1297
63. Raffel SJ, Battisti JM, Fischer RJ, Schwan TG. Inactivation of genes for antigenic variation in the relapsing fever spirochete *Borrelia hermsii* reduces infectivity in mice and transmission by ticks. *PLoS Pathog*. (2014) 10:e1004056. doi: 10.1371/journal.ppat.1004056
64. Zückert WR, Lloyd JE, Stewart PE, Rosa PA, Barbour AG. Cross-species surface display of functional spirochetal lipoproteins by recombinant *Borrelia burgdorferi*. *Infect Immun*. (2004) 72:1463–9. doi: 10.1128/IAI.72.3.1463-1469.2004
65. Eicken C, Sharma V, Klabunde T, Owens RT, Pikas DS, Hook M, et al. Crystal structure of Lyme disease antigen outer surface protein C from *Borrelia burgdorferi*. *J Biol Chem*. (2001) 276:10010–5. doi: 10.1074/jbc.M010062200

Conflict of Interest: The authors declare that the research was conducted in the absence of any commercial or financial relationships that could be construed as a potential conflict of interest.

frontiers in Immunology

ORIGINAL RESEARCH
published: 14 August 2020
doi: 10.3389/fimmu.2020.02010

CR4 Signaling Contributes to a DC-Driven Enhanced Immune Response Against Complement-Opsonized HIV-1

Marta Bermejo-Jambrina[1,2], Michael Blatzer[3], Paula Jauregui-Onieva[1], Teodor E. Yordanov[4], Paul Hörtnagl[5], Taras Valovka[4,6], Lukas A. Huber[4], Doris Wilflingseder[1] and Wilfried Posch[1]**

[1] Institute of Hygiene and Medical Microbiology, Medical University of Innsbruck, Innsbruck, Austria, [2] Department of Experimental Immunology, Amsterdam Infection and Immunity Institute, Academic Medical Center, University of Amsterdam, Amsterdam, Netherlands, [3] Experimental Neuropathology Unit, Infection and Epidemiology Department, Institute Pasteur, Paris, France, [4] Institute of Cell Biology, Biocenter, Medical University of Innsbruck, Innsbruck, Austria, [5] Central Institute for Blood Transfusion and Immunological Department, Innsbruck, Austria, [6] Department of Pediatrics I, Medical University of Innsbruck, Innsbruck, Austria

OPEN ACCESS

Edited by:
Nicole Thielens,
UMR 5075 Institut de Biologie Structurale (IBS), France

Reviewed by:
Karlhans Fru Che,
Karolinska Institutet (KI), Sweden
Olivier Schwartz,
National Institute of Health (Peru), Peru
Jeremy Dufloo,
Institut Pasteur, France,
in collaboration with reviewer OS

***Correspondence:**
Doris Wilflingseder
doris.wilflingseder@i-med.ac.at
Wilfried Posch
wilfried.posch@i-med.ac.at

Specialty section:
This article was submitted to Microbial Immunology, a section of the journal Frontiers in Immunology

Received: 15 May 2020
Accepted: 24 July 2020
Published: 14 August 2020

Citation:
Bermejo-Jambrina M, Blatzer M, Jauregui-Onieva P, Yordanov TE, Hörtnagl P, Valovka T, Huber LA, Wilflingseder D and Posch W (2020) CR4 Signaling Contributes to a DC-Driven Enhanced Immune Response Against Complement-Opsonized HIV-1. Front. Immunol. 11:2010. doi: 10.3389/fimmu.2020.02010

Dendritic cells (DCs) possess intrinsic cellular defense mechanisms to specifically inhibit HIV-1 replication. In turn, HIV-1 has evolved strategies to evade innate immune sensing by DCs resulting in suboptimal maturation and poor antiviral immune responses. We previously showed that complement-opsonized HIV-1 (HIV-C) was able to efficiently infect various DC subsets significantly higher than non-opsonized HIV-1 (HIV) and therefore also mediate a higher antiviral immunity. Thus, complement coating of HIV-1 might play a role with respect to viral control occurring early during infection via modulation of DCs. To determine in detail which complement receptors (CRs) expressed on DCs was responsible for infection and superior pro-inflammatory and antiviral effects, we generated stable deletion mutants for the α-chains of CR3, CD11b, and CR4, CD11c using CRISPR/Cas9 in THP1-derived DCs. We found that CD11c deletion resulted in impaired DC infection as well as antiviral and pro-inflammatory immunity upon exposure to complement-coated HIV-1. In contrast, sole expression of CD11b on DCs shifted the cells to an anti-inflammatory, regulatory DC type. We here illustrated that CR4 comprised of CD11c and CD18 is the major player with respect to DC infection associated with a potent early pro-inflammatory immune response. A more detailed characterization of CR3 and CR4 functions using our powerful tool might open novel avenues for early therapeutic intervention during HIV-1 infection.

Keywords: HIV-1, dendritic cell, complement, CD11c, CD11b

INTRODUCTION

Dendritic cells (DCs) play a pivotal role in the defense against invading pathogens, acting as the most potent antigen-presenting cells (APCs) of the innate immune system (1–3). They reside in the peripheral tissue, where they capture antigens and present them to naïve T cells in the lymph nodes. Hence, DCs orchestrate immune responses, serving as critical links between innate and

adaptive immunity. DCs are among the first cells to encounter HIV-1 at mucosal sites (2, 4). At the same time, HIV-1 spontaneously activates the classical complement (C-) pathway (5), even in seminal fluid (6), through direct binding of C1q to the viral surface. Therefore, complement-opsonized HIV-1 (HIV-C) accumulates at mucosal sites early during HIV-1 infection (7, 8). HIV-1 poorly replicates in DCs due to the activity of SAMHD1 [Sterile Alpha Motif (SAM) domain and histidine/aspartic acid (HD) domain containing protein 1] and effectively evades DC-mediated antiviral immunity (9). When SAMHD1 restriction of HIV-1 was abrogated by degradation of HIV-2/SIVsm viral protein Vpx, DCs demonstrated a potent type I IFN response, maturation and co-stimulatory function (10). Further, phosphorylation of the T592 residue of SAMHD1 in DCs after exposure to HIV-C overcame this restriction mechanism and initiated an effective antiviral immune response (9). The low-Beside hiding from DC-mediated immunity by low-level infection, the virus additionally exploits DCs as shuttles to promote its own dissemination (11, 12).

In previous studies we demonstrated that HIV-C has the ability to bypass SAMHD1 restriction in DCs, which resulted in more pronounced maturation and significantly higher co-stimulatory capacity compared to DCs exposed to non-opsonized HIV (9).

Additionally, complement coating of HIV-1 further activated highly functional HIV-1 specific cellular immunity as well as pro-inflammatory and type I IFN responses (9, 13, 14). Thus, enhanced DC infection was associated with an increased quality and quantity of virus-specific immune responses (9, 10, 15, 16). We could also show that HIV-C interacts with the abundantly expressed CR3 and CR4 on immature DCs (iDCs), whereas non-opsonized HIV binds via gp120 to DC-SIGN (9, 17). Taken together, these already published results clearly indicate that triggering CR3 and CR4 by HIV-C influences infection of DCs and strongly shapes immunity driven by DCs.

Here, we analyzed in detail the specific roles of CR3 and CR4 in modulating the immune response of HIV-1-infected DCs by generating knock-out (KO) cell lines lacking CD11b, CD11c, and CD18, respectively. For this we performed CRISPR/Cas9 to generate stable and irreversible deletions of these receptors in THP1 monocytes. Furthermore, we optimized the differentiation protocol to generate THP1 derived DCs and to use these THP1-differentiated DCs (THP1-DCs), comprising an iDC phenotype, as an operative model for primary DC infection. After detailed comparison of THP1-DCs with primary DCs at phenotypic and phagocytic properties, we characterized the specific tasks of CR3 and CR4 on THP1-KO DCs with respect to HIV-1 infection and antiviral immune induction using differentially opsonized HIV-1. Here we identified CR4 as potent inducer of early antiviral immunity. Further, the importance of CR3 and CR4 fine-tuning on DCs with respect to controlling viremia during the acute phase of HIV-1 infection by CR4 or down-modulating type I IFNs during chronic phase by CR3 was highlighted.

MATERIALS AND METHODS

Ethics Statement

Written informed consent was obtained from all participating blood donors by the Central Institute for Blood Transfusion and Immunological Department, Innsbruck, Austria. The use of anonymized leftover specimens for research on host/pathogen interactions was approved by the Ethics Committee of the Medical University of Innsbruck (ECS 1166/2018, PI: DW).

Generation of Human Monocyte-Derived DCs and THP1-DCs

Blood for the monocyte isolation was received by the Central Institute for Blood Transfusion and Immunological Department, Innsbruck, Austria. Briefly, PBMCs (peripheral blood mononuclear cells) were isolated from blood of healthy donors (8, 16) obtained by a density gradient centrifugation using a Ficoll Paque Premium (GE Healthcare) gradient. After washing, $CD14^+$ monocytes were isolated from PBMCs using anti-human CD14 Magnetic Beads (BD) – the purity of the isolated cells was at least 98%. Monocytes were stimulated by addition of IL-4 (200 U/ml) and GM-CSF (300 U/ml) for 5 days to generate iDCs, which were used for all further experiments. Non-stimulated iDCs were used as controls for all experiments using DCs. THP1-WT and KO DCs were generated from the respective THP1 cells by addition of IL-4 (200 U/ml), GM-CSF (300 U/ml) and TNF-α (10 ng/ml) for 5 days.

Genome Editing Using CRISPR/Cas9-Mediated Depletion of CD11b, CD11c, and CD18

For CRISPR/Cas9-mediated depletion, three guide RNA (gRNA) targeting sequences for CD11b, CD11c, and CD18 as depicted in **Table 1** were selected using an online prediction tool—CRISPR Design; Zhang Lab (18). Out of the three constructs, only one clone for each target [CD11b (5′-GCCGTAGGTTGGATCCAAACAGG-3′), CD11c (5′-GTAGAGGCCACCCGTTTGGTTGG-3′) and CD18 (5′-TGGCCGGTGTCGCSGCGSSTGG-3′)] was used for further analyses. gRNAs were cloned into a lentiCRISPRv2 vector via *Bsm*BI restriction sites. lentiCRISPRv2 was a gift from F. Zhang (Massachusetts Institute of Technology, Cambridge, MA, United States; Addgene plasmid 52961 (19).

Lentiviral Transduction

Lentiviral plasmids were co-transfected with Lipofectamine LTX (Invitrogen, cat 15338100) together with pMDG, psPAX2 and lentiCRISPRv2 into the HEK293T producer cell line. Supernatants containing viral particles were harvested 48 and 72 h post transfection, filtered using a 0.2 μm filter and directly used to transduce target THP1 cells with 5 μg/ml Polybrene (Sigma-Aldrich, cat TR-1003-G). After 7 days, transduced cells were selected using puromycin (5 μg/ml, Sigma-Aldrich, cat SBR00017). After selection, the depletion efficiency of CD11b, CD11c, and CD18 was analyzed by flow cytometry. Single-cell clones of the specific KO cells were generated after FACS

TABLE 1 | CRISPR/Cas9 gRNA sequences used to produces the THP-1 CD11b KO, THP-1 CD11c KO, and THP-1 CD18 KO.

Number	Target gene	Sequence
1	CD11b exon5	GCCGTAGGTTGGATCCAAACAGG
2	CD11b exon6	TCATCCGCCGAAAGTCATGTGGG
3	CD11b exon6	TTCATCCGCCGAAAGTCATGTGG
4	CD11c exon3	GTAGAGGCCACCCGTTTGGTTGG
5	CD11c exon3	ACTGGTAGAGGCCACCCGTTTGG
6	CD11c exon4	GACATGTTCACGGCCTCCGGGGG
7	CD18 exon3	GCCGGGAATGCATCGAGTCGGGG
8	CD18 exon3	TGCCGGGAATGCATCGAGTCGGG
9	CD18 exon4	TGGCCGGGTGTCGCAGCGAATGG

Indicated sequences target different exons of the CD11b, CD11c, and CD18 genes. One clone out of the three was used for further analyses.

sorting by the Core Facility FACS Sorting at the Medical University of Innsbruck.

Virus Production

Primary isolates as 92BR030 (subtype B/B, R5-tropic) and the laboratory strain BaL were obtained by the National Institutes of Health AIDS (available through World Health Organization depositories). Virus was propagated in PHA-L and IL-2 stimulated PBMCs. 93BR020 (subtype B/F, X4/R5-tropic) and the laboratory strain NL43 both from National Institutes of Health AIDS (available through World Health Organization depositories) were produced in the M8166 cell line. HEK293T cells were transfected with YU- 2-, and R9Bal (kindly provided by Prof. Thomas Hope, Northwestern University) plasmids using the $CaCl_2$ method (9). Vpx expression construct pcDNA3.1Vpx SIVmac239-Myc was used to obtain Vpx-carrying HIV virus preparations (20). Viral supernatants were collected on several days post infection (dpi) and cleared by filtration through 0.22 μm pore-size filters and concentrated by ultracentrifugation at 20,000 rpm for 90 min at 4°C (Beckham Coulter). The virus pellet was re-suspended in RPMI1640 without supplements and stored in small aliquots at −80°C to avoid multiple thawing. One aliquot was taken to determine the virus concentration by p24 ELISA (21) and the 50% tissue culture infective dose of the viral stock.

Opsonization of Viral Stocks

To mimic opsonization *in vitro*, purified HIV-1 and VLP stocks were incubated for 1 h at 37°C with human complement (C) serum (Quidel) in a 1:10 dilution. As negative control the virus was incubated under the same conditions in commercially available C3-deficient serum (Sigma) or in culture medium. After opsonization, the virus was thoroughly washed to remove unbound components, pelleted by ultracentrifugation (20,000 rpm/90 min/4°C), re-suspended in culture medium without supplements and virus concentrations were determined using p24 ELISA. The opsonization pattern was analyzed using a virus capture assay (VCA) described below.

Virus Capture Assay

The opsonization pattern was determined by virus capture assay (VCA) as described (8). Briefly, 96-well high-binding plates were coated with anti-human C3c, C3d, or IgG antibodies. Mouse IgG antibody was used as a control for background binding. Plates were then incubated overnight at 4°C with the differentially opsonized virus preparations (10 ng p24/well) at 4°C. After extensive washing, virus was lysed and p24 ELISA was performed to confirm the opsonization pattern.

p24 ELISA

p24 ELISA was performed as described (21). Antibodies used for p24 ELISA were kindly provided by Polymun Scientific, Vienna, Austria.

DC Infection

Cells were infected in triplicates using differentially opsonized HIV-1 as described before (8, 17). Briefly, cells (1×10^5/100 μl) were incubated for 3 h with HIV or HIV-C (25 ng p24/ml) or left uninfected and virus concentrations from supernatants were measured on several dpi. To confirm productive infection by HIV-1 and not cell-associated virus, we thoroughly washed the cells after overnight incubation with different viruses and cultured the cells at 37°C/5% CO_2. By ELISA we measured the p24 concentrations of the supernatants following spinning down the plate to pellet cells on several dpi. The following antibodies were used for blocking experiments (all anti-human): LEAF purified CD11b-Antibody (Biolegend, San Diego, CA, United States), LEAF purified CD11c-Antibody (Biolegend, San Diego, CA, Untied States).

Immunoblot Analyses of Phosphorylated Proteins

THP1-DCs were starved in RPMI 1640 containing 0.5% FCS and 1% L-Glutamine for 3 h. Starving of cells was performed to set their phosphorylation to background levels. Following starvation, THP1-DCs were incubated with the differentially opsonized HIV-1 particles. After 4 h co-incubation, cells were lysed with RIPA Buffer (Sigma-Aldrich) containing protease and phosphates inhibitors and EDTA (Thermo Fisher Scientific) for 20 min at 4°C. The protein content was determined by BCA (Thermo Fisher Scientific). Lysates were separated using 10% SDS-PAGE gels, transferred to PVDF membranes and incubated with anti-human a-tubulin as loading control as well as anti-human phospho-IRF3 (1:1000, Cell Signaling Technology) and developed with the Lass 4000 Image Quant. For this, the peak values of the target protein were divided by the peak values of the loading control before doing a relative comparison. Quantification was performed using values from three to six different experiments.

Relative Quantification by Real-Time RT-PCR

THP1-DCs (WT and KOs) were infected with the differentially opsonized HIV-1 particles at different time-points from 1–12 h at 37°C with a p24 concentration of 350 ng/mL for

0.5×10^6 cells. Cells were lysed with RLT Buffer (Qiagen) and total RNA was purified according to the manufacturer's instructions. RNA was then quantified (NanoVue) and reverse transcribed into cDNA (iScript Reverse Transcription Supermix for RT-qPCR, BioRad). The cDNA was then used for multiplex qPCR (iQ Multiplex Powermix, BioRad) amplification, using PrimePCR™ Probes for IL-10, IL-6, IL-1B, and IL23A (all from BioRad Laboratories). The RT-qPCR was run in the BioRad CFX96 Real Time PCR System. The cycling conditions were as follows: 3 min at 95°C, 44 cycles: 15 s at 95°C, 60 s at 60°C. For mRNA expression of IFNB1 real-time PCR using Sybr green qPCR (EvaGreen, BioRad) amplification and gene-specific primer pairs (BioRad) were used. The cycling conditions were: 30 s at 95°C, 39 cycles: 5 s at 95°C, 10 s at 60°C with a melt curve 65–95°C with an increment of 0.5°C for 5 s. A GAPDH (human) PCR using specific primer/probe pairs (BioRad) served as internal control to quantify the relative gene expression of target genes. Data were analyzed with the BioRad CFX Manager Software ($\Delta\Delta$CT method) and values were exported to GraphPad Prism.

Cytokine Analyses by ELISA

THP1-DCs were plated in a 12-well tissue culture-plate at 0.5×10^6 cells/well. Cells were infected with R5-tropic virus (R9Bal) for 12, 24, and 48 h. Supernatants were collected and inactivated with Igepal 5% (1:2). The amounts of IL-1β were measured by ELISA (eBioscience).

Multicolor FACS Analyses

Differentiation of THP1 into DCs exposed to cytokine cocktail (IL-4, GM-CSF, TNF-α) was analyzed by using anti-human CD11b-PE, CD11c-AlexaFluor488, CD18-APC, HLA-ABC-PerCP/Cy5.5, HLA-DR-APC-Cy7, DC-SIGN-PE, CD86-FITC, CD83-APC, CD1a-FITC, CD4-APC, CCR-PerCP/Cy5.5 and CXCR4-PE as described (16) on a FACS Verse flow cytometer (BD Biosciences). Data were analyzed using FACS DIVA software (BD Biosciences).

Statistical Analysis

Differences were analyzed by using GraphPad Prism software (GraphPad Software Inc.) and one-way ANOVA with Bonferroni post-test for multiple comparisons or Unpaired Student's t test depending on the analyses performed.

RESULTS

WT THP1-DCs and KO THP1-DCs Resemble Primary DCs Regarding Their Phenotypic and Phagocytic Capacities

To characterize CR3 and CR4 with respect to DC modulation upon exposure to differentially opsonized HIV-1, we generated CD11b-, CD11c-, and CD18 KO THP1-DCs. Since THP1 monocytes constitute an immortalized cell line and are of tumorigenic origin derived from the peripheral blood of a one-year-old male with acute monocytic leukemia, we wanted to make sure to generate an appropriate model for KO DCs. Therefore, we first characterized by multi-parameter flow cytometric analyses in detail WT-THP1 cells after optimized differentiation to DCs for their expression of characteristic DC markers, CR3 and CR4 and HIV-1 receptor and co-receptors CD4, CCR5, and CXCR4.

We found that THP1-DCs differentiated *in vitro* into a functional DC-like phenotype (**Figure 1A** and **Supplementary Figure S1** >monocyte-derived iDCs, moDCs), expressing high levels of both CRs, CR3, and CR4, as analyzed by the expression of CD11b, CD11c, and CD18. HLA-ABC, HLA-DR, and DC-SIGN were also found to be expressed on WT-THP1 DCs, and also on moDCs as illustrated by Posch et al. (9) and in **Supplementary Figure S1**. No expression of CD1a was detected. Importantly, low levels of CD83 and CD86 were indicative of an iDC state and displayed a mature phenotype upon LPS stimulation (not shown). The profile of characteristic markers CD11b, CD11c, CD18, DC-SIGN, CD83, CD86, CD4, CXCR4, and HLA-DR on immature moDCs is illustrated in **Supplementary Figure S1**. Entry of HIV-1 into target cells requires formation of a complex between the viral envelope protein gp120, the primary receptor CD4 and a chemokine co-receptor (CCR5, CXCR4). We found that THP1-DCs expressed similar amounts of CD4, CCR5, and CXCR4 as primary DCs.

THP1-DCs further illustrated a similar phagocytic capacity as their primary counterparts (**Figure 1B**). Phagocytosis of non- and complement-opsonized beads (Beads, Beads-C) was low in THP1 monocytes, while WT THP1-DCs demonstrated a similar phagocytosis of Beads/Beads-C compared to monocyte-derived DCs.

Next we investigated the expression of CD11b, CD11c, and CD18 on KO THP1-DCs generated by CRISPR-Cas9 technology. CD11b expression on single-cell clones of CD11b KO THP1-DCs was reduced to 0.81% compared to 63.43% on WT THP1-DCs (**Figure 2A**). CD11c was only slightly affected on CD11b KO THP1-DCs (**Supplementary Figure S2**). Expression of CD11c on CD11c KO THP1-DCs was also reduced from 50.53% on WT THP1-DCs to 0.81% (**Figure 2A**), while CD11b was expressed on CD11c KO THP1-DCs (**Supplementary Figure S2**). In contrast, CD18 KO resulted in significant down-modulation of CD11b as well as CD11c (**Supplementary Figure S2**) and in addition, also CD11a disappeared from the surface of CD18 KO THP1-DCs, but not on CD11b- and CD11c KO THP1-DCs (**Supplementary Figure S3**). Phagocytosis of the various KO THP1-DCs revealed that in CD11b KO cells the levels of Beads or Beads-C internalized slightly decreased compared to WT THP1-DCs (**Figure 2B**), while CD11c KO had a highly decreased phagocytosis of Beads-C, but not Beads (**Figure 2B**). KO CD18 severely reduced the amounts of Beads ingested and completely abrogated internalization of Beads-C (**Figure 2B**). We further focused on CD11b- and CD11c KO THP1-DCs throughout the manuscript and CD18 KO-THP1 DCs were used in some experiments as controls. Phenotypic and phagocytic characterization of WT and KO THP1-DCs revealed these cells as a good DC model to study

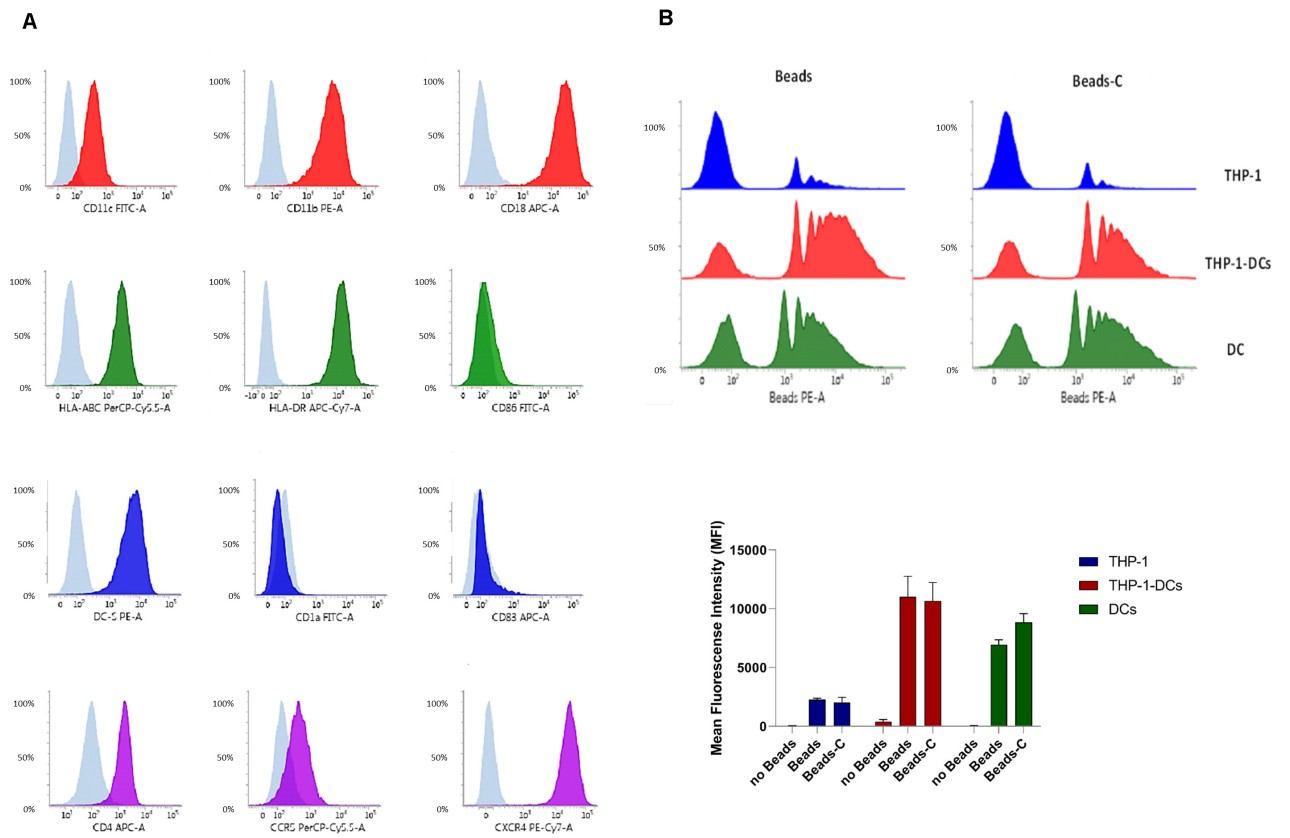

FIGURE 1 | THP1 monocytes can be differentiated into functional DCs. **(A)** WT THP1 cells were differentiated into DCs and expression of characteristic DC markers CD11c, CD11b, CD18, HLA-ABC, HLA-DR, CD86, DC-SIGN, CD1a, CD83, and HIV-1 receptors CD4, CCR5, and CXCR4 was analyzed using flow cytometry. A representative flow cytometry analysis is shown out of five independent experiments. **(B)** Phagocytosis of non- and complement-opsonized Beads (Beads, Beads-C) was analyzed in WT THP1 monocytes (blue), WT THP1-DCs (red), and monocyte-derived DCs (green). THP1-DCs (red) exerted similar phagocytosis capacities with respect to Beads and Beads-C compared to monocyte-derived DCs (green), while THP1 monocytes had a very low phagocytic activity (blue). Panel **(B)** illustrates a FACS analysis from one representative experiment (upper panel) and data from three independent experiments are summarized in panel **(B)** (lower panel).

distinct roles of CR3 and CR4 during the very early steps of HIV-1 infection.

CR4 Plays a Major Role With Respect to HIV-C Infection of DCs

Efficient antiviral T cell responses are initiated when DCs are productively infected by HIV-1 after their resistance to infection is bypassed (10, 13). In contrast, the inability of DCs to become infected is supposed to be an evasion strategy for HIV-1 survival. As previously shown by our group and also herein in **Supplementary Figure S4**, DCs are efficiently infected by complement-opsonized HIV-1 (HIV-C), while only low-level productive infection was mediated by HIV-1 (HIV) (8, 9). To unravel the specific roles of CR3 and CR4 with respect to productive DC infection, we first analyzed infection of WT THP1-DCs after exposure to HIV or HIV-C. As previously demonstrated, virus concentrations of WT THP1-DCs were similar to the ones obtained in primary DCs (13). Thus, low-level productive infection was only monitored in WT THP1-DCs exposed to HIV, whereas infection was significantly enhanced using HIV-C (**Figure 3A**). Non-infected and therefore immature THP1-DCs were used as negative controls (**Figure 3A**, uninfected or UI). Consistently with Posch et al. (9) using monocyte-derived DCs (moDCs), we could also illustrate that infection of WT THP1-DCs with Vpx-carrying HIV illustrated a similar pattern compared to HIV-C by enhancing productive infection compared to non-opsonized HIV. In addition, complement opsonization of HIV-Vpx (HIV-C Vpx) improved infection even more (**Figure 3B**). Since same infection patterns could be displayed in THP1-DCs, moDCs and BDCA1$^+$ DCs (9), we continued the next steps using WT THP1-DCs and their CD11b- and CD11c KO THP1-DCs counterparts to characterize in detail the specific roles of CR3 and CR4 during HIV-1 infection. We found that infection of CD11b- or CD11c KO THP1-DCs with non-opsonized HIV (HIV, **Figure 3C**) or non-opsonized Vpx-carrying HIV (HIV-Vpx, **Figure 3D**) was similar to infection levels of WT THP1 DCs. Vpx-carrying HIV-1 mediated a more than fivefold enhanced infection compared to the low-level productive infection induced by non-opsonized HIV-1. In contrast, infection

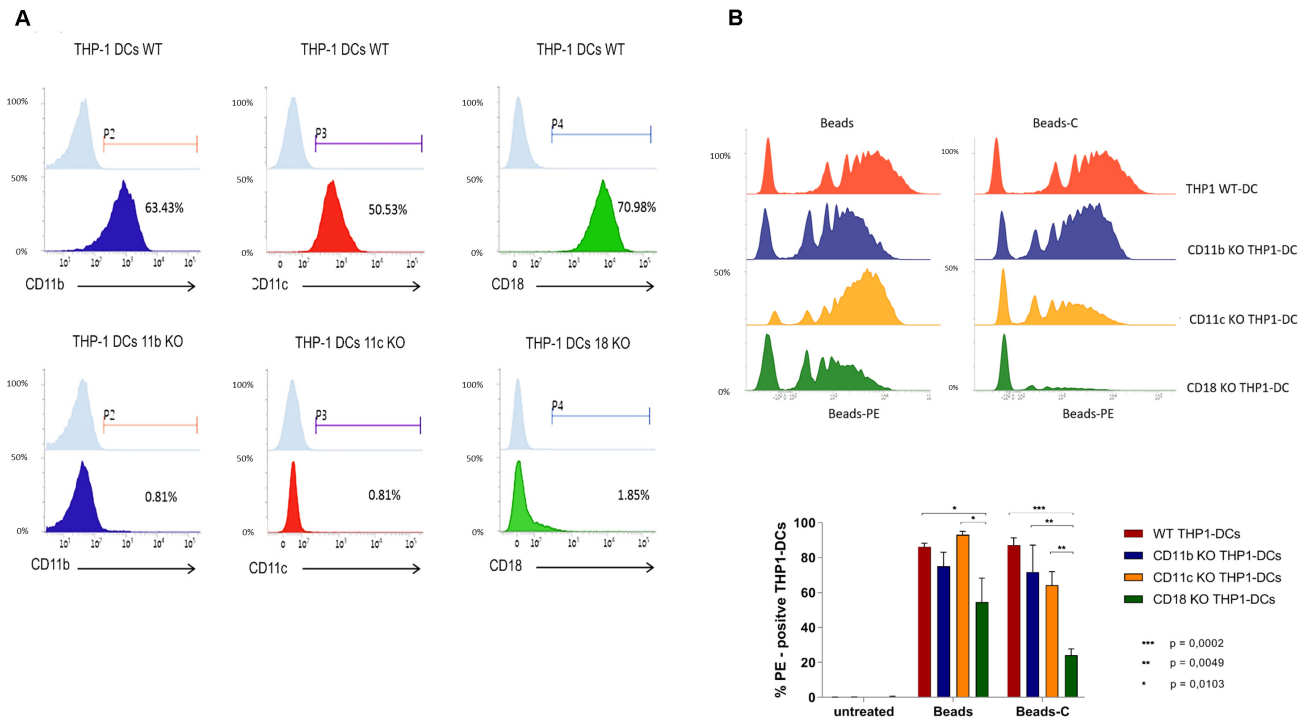

FIGURE 2 | CD11b-, CD11c-, and CD18 KO THP1 DCs comprise a novel tool to decrypt distinct functions of CR3 and CR4. **(A)** CD11b, CD11c, or CD18 were stably deleted by using the CRISPR/Cas9 genome editing technology. Top panel: WT THP1 cells differentiated to DCs were used as controls for monitoring expression of CD11b (blue), CD11c (red), and CD18 (green). Bottom panel: CD11b KO THP1-DCs do not express CD11b (blue), CD11c KO THP1-DCs are devoid of CD11c (red), and no CD18 is expressed on CD18 KO THP1-DCs (green). A representative flow cytometric analysis from one out of five experiments is illustrated. **(B)** Phagocytosis of C-opsonized Beads is hampered in CD11c- (yellow) and CD18 KO (green) THP1-DCs compared to WT (red) and CD11b KO (blue) THP1-DCs. Lowest phagocytosis using non-opsonized Beads was monitored in CD18 KO THP1 DCs (green). A representative flow cytometric analysis out of three independent experiments is depicted.

of WT- or CD11b KO THP1-DCs with complement-opsonized HIV (HIV-C, **Figure 3C**) was significantly enhanced similar to moDCs (**Supplementary Figure S4A**). This was also the case for complement-opsonized Vpx-carrying HIV (HIV-C Vpx, **Figure 3D**).

In contrast, CD11c KO-THP1 DCs showed similar p24 levels between HIV and HIV-C or HIV-Vpx and HIV-C Vpx (**Figures 3C,D**, yellow), and productive infection using HIV-C or HIV-C Vpx was significantly reduced when compared to CD11b KO or WT THP1-DCs (**Figures 3C,D**, HIV-C, yellow vs. blue and red bars). Uninfected iDCs and LPS-exposed THP1-DCs were used as controls. Using blocking antibodies against CD11b and CD11c and moDCs revealed similar results as the THP1 KO DC models. While CD11b blocking significantly enhanced productive DC infection upon exposure to HIV-C, blocking CD11c significantly decreased productive infection as seen also in CD11c KO THP1 DCs (**Supplementary Figure S4B**). This reduction was in part rescued when combining the CD11b/CD11c blocking Abs (**Supplementary Figure S4B**), highlighting the cross-talk of these two receptors.

These experiments demonstrated that THP1-DCs represent a valid model for DC infection, due to the similar infection kinetics observed in WT THP1-DCs compared to primary DCs and also because complement opsonization of HIV-1 significantly enhanced productive DC infection. Furthermore, our data revealed that CR3 is not involved in infection of DCs by HIV-C, since CD11b KO THP1-DCs or CD11b blocking using a blocking anti-human CD11b mAb showed a significant HIV-C-mediated enhancement of DC infection (**Figure 3** and **Supplementary Figure S4B**). In contrast, deleting CD11c (CR4) had a severe effect on DC infection, which caused a low-level productive DC infection with complement-opsonized HIV-1, comparable to the low-level infection observed using non-opsonized HIV-1 (**Figure 3** and **Supplementary Figure S4B**). To summarize, abrogation of CR3 does not impact productive infection with HIV-C, while CR4 KO results in low-level DC infection comparable to HIV.

CR4 KO Diminishes Antiviral Signaling Pathways and Mediates an Anti-inflammatory DC Type

To determine, whether CR4 KO also impacts the antiviral and inflammatory DC profile induced by HIV-C, we studied antiviral signaling pathway IRF3 and type I IFN expression, IL-1β production and mRNA level expression of IL6, IL10, and IL23A.

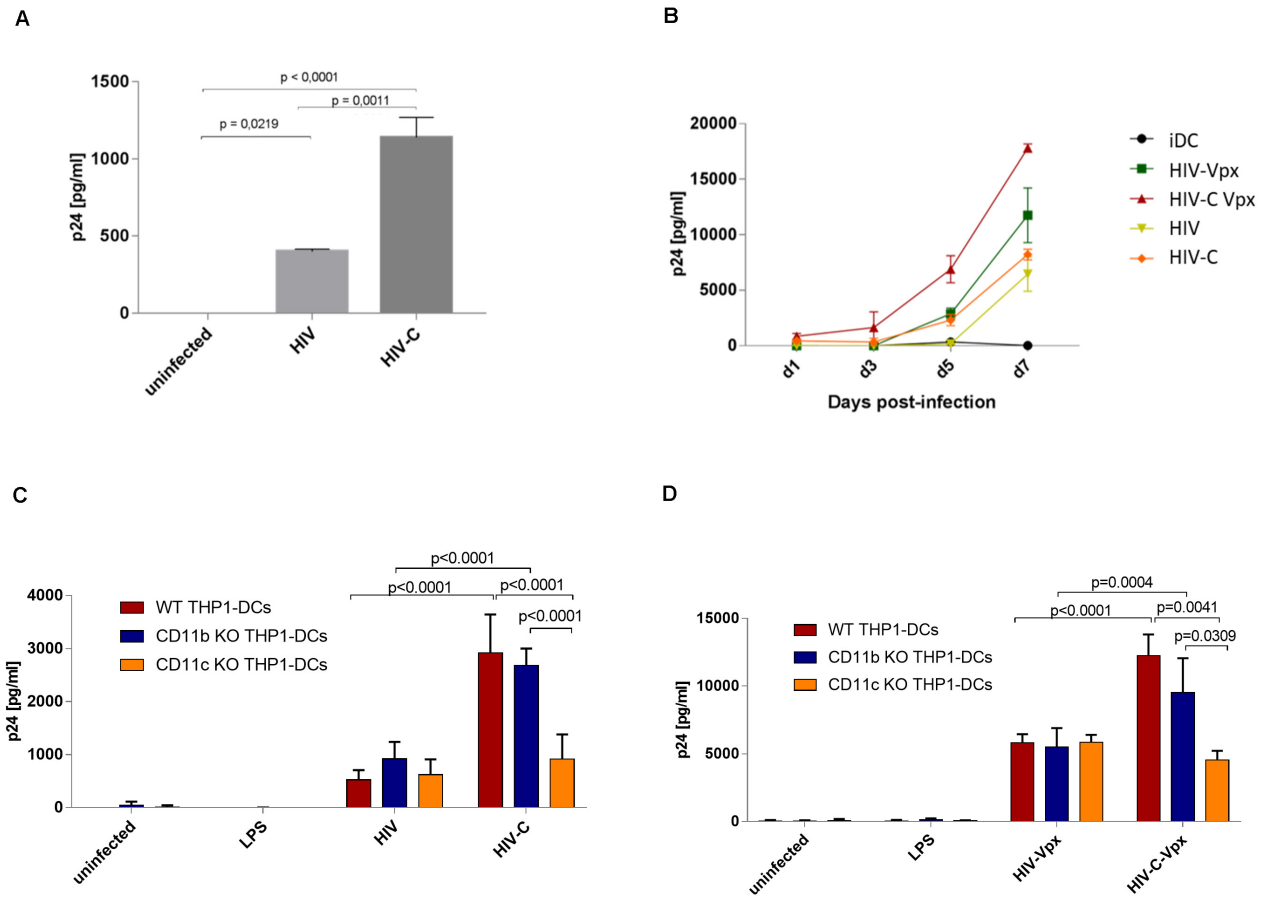

FIGURE 3 | Complement-opsonized HIV-1 effectively infects WT- and CD11b KO THP1-DCs, while productive HIV-1 infection is impaired in CD11c KO THP1-DCs. **(A,B)** Upon infection of WT THP1 DCs with HIV or HIV-C (25 ng p24/ml) a significantly enhanced productive infection was monitored using HIV-C. Means ± SD from three independent experiments in duplicates are depicted in **(A)**. Differences were analyzed using Unpaired Student's *t*-test. In **(B)** a time-course of WT THP1-DC infection exposed to HIV (lime), HIV-C (orange), HIV-Vpx (green), and HIV-Vpx-C (red) is illustrated. Experiments were repeated three times in duplicates. **(C,D)** WT- (red), CD11b KO (blue), and CD11c KO (yellow) THP1-DCs were infected with HIV or HIV-C (C) and HIV-Vpx or HIV-C-Vpx. Uninfected and LPS-incubated THP1-DCs served as controls. Infection experiments were performed in three independent experiments performed in triplicates. Differences were analyzed using GraphPad Prism and one-way ANOVA with Bonferroni post-test.

Antiviral signaling pathways involving TANK Binding Kinase 1 (TBK1) and Interferon regulatory factor 3 (IRF3) are associated with induction of an early type I IFN response. Upon analyzing IRF3 phosphorylation after exposure of DCs to HIV or HIV-C (**Figure 4A**), we found significantly increased activation levels in CD11b KO THP1-DCs upon stimulation with both, HIV- and HIV-C (**Figure 4A**). Stimulation of CD11c KO THP1-DCs with HIV, too, increased IRF3 phosphorylation, while in HIV-C-exposed CD11c KO THP1-DCs the levels were significantly decreased compared to CD11b KO THP1-DCs and reduced in comparison to WT THP1-DCs (**Figure 4A**). This enhanced activation of pIRF3 in CD11b KO THP1-DCs by HIV-C was further associated with a significantly increased expression of type I interferon IFNB, but not in case of HIV-exposed DCs (**Figure 4B**). In contrast, CD11c KO cells did not show any change on IFNB mRNA expression levels compared to WT- and CD11b KO-THP1 DCs (**Figure 4B**).

Next, we studied pro-inflammatory cytokine induction as measured by IL-1β production and IL6, IL10, and IL23A mRNA levels, since in monocyte- and blood-derived DCs we previously found that HIV-C significantly increased production of Th17-polarizing cytokines, such as IL-1β, IL-6, and IL-23, while IL-10 expression was even decreased (14). Strikingly, we found a significantly increased IL-1β secretion in HIV-C-exposed WT THP1-DCs compared to HIV-loaded or iDCs (**Figure 5A**, WT), corroborating what has already been published in primary DCs. CD11b KO THP1-DCs mediated an augmented IL-1β production, upon exposure to non-opsonized HIV, similar to HIV-C-loaded WT- and CD11b KO THP1-DCs (**Figure 5A**, CD11b and WT). In contrast, CR4 KO significantly decreased IL-1β levels secreted in HIV-C-exposed CD11c KO THP1-DCs (**Figure 5A**, CD11c). IL6 and IL23A mRNA expression were significantly enhanced in WT THP1-DCs upon exposure to HIV-C as described in primary DCs (14). In case of CD11c KO THP1-DCs, IL23A was significantly reduced in HIV-C-exposed

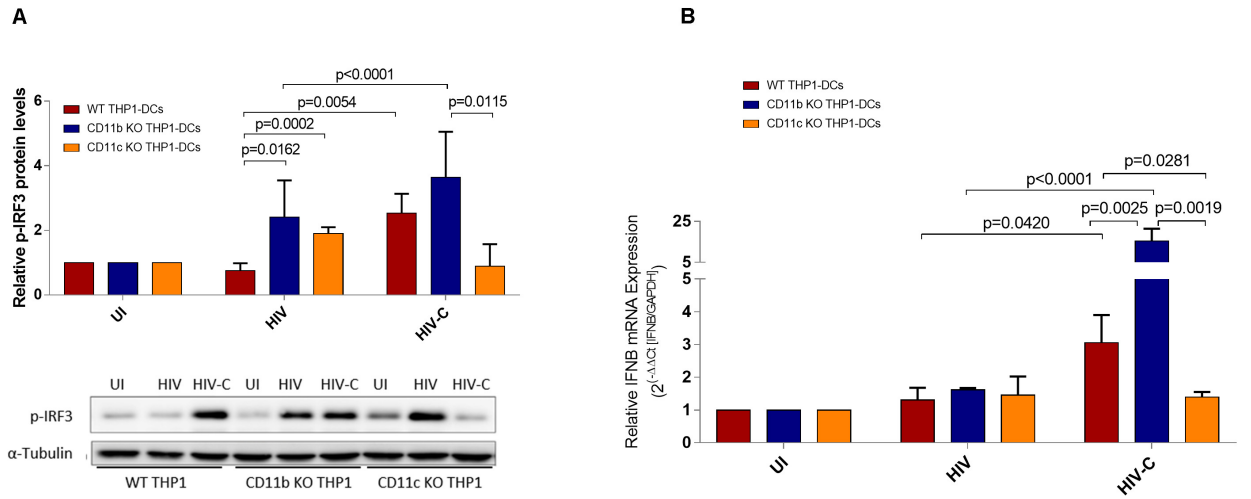

FIGURE 4 | Antiviral signaling pathways are impeded in CD11c-deleted THP1 DCs. **(A)** Relative p- p-IRF3 protein levels were assessed in WT- (red), CD11b KO (blue), and CD11c KO (yellow) THP1-DCs. Experiments were repeated four times independently and a summary as well as a representative immunoblot are depicted. UI, uninfected. **(B)** RT-PCR analyses of type I IFN (IFNB) levels in WT-, CD11b KO-, and CD11c KO-THP1 DCs after infection with HIV or HIV-C (BaL, YU-2). Non-infected iDC were used as controls. Data are mean ± SD from four different donors in duplicates. Differences were analyzed by using one-way ANOVA with Bonferroni post-test.

DCs to levels mediated by HIV (**Figure 5C**). In addition, IL6 mRNA expression was reduced, although not significantly, as for CD11c KO THP1-DCs (**Figure 5B**). A different picture was observed for IL-10 expression, since this cytokine was expressed at similar levels in all treatments (iDCs, HIV, HIV-C) using WT-, CD11b-, and CD18 KO-THP1 DCs (**Figure 5D**, WT, CD11b). In contrast, CD11c KO-THP1 DCs significantly increased expression of this anti-inflammatory cytokine upon exposure to HIV-C, but not HIV (**Figure 5D**, CD11c). Thereby, abolishing CD11c on DCs diminishes the antiviral profile in DCs, while IL-10-producing DCs (DC-10) were induced by knocking out CR4. These data point to a role of CR3 (CD11b/CD18) as regulator of dampening immune responses and CR4 (CD11c/CD18) as inducer of pro-inflammatory and antiviral immune responses.

DISCUSSION

Integrins are crucial components linking intra- and extracellular environments and thereby coordinating vital features of cellular behavior, such as adhesion, cell contact formation, signaling, immune activation. Among an array of PRRs, DCs abundantly express integrin receptors CR3 (CD11b/CD18) and CR4 (CD11c/CD18), composed of α-M (CD11b) or α-X (CD11c) and the common β2-subunit CD18. Emerging evidence suggests that integrins play an important role in immune activation and inflammation. We recently showed that complement-opsonized HIV-1 (HIV-C) overcomes restriction in DCs by efficiently activating SAMHD1 phosphorylation, and this was associated with a higher DC maturation and co-stimulatory potential, aberrant type I interferon and signaling as well as a stronger induction of pro-inflammatory and cellular immune responses (9, 14). This was not the case for non-opsonized HIV-1 (HIV), which was restricted by SAMHD1 in DCs. Therefore, we here defined in more detail the involvement of the α integrins CD11b and CD11c in this increased DC activation during HIV-1 infection, when the virus was C-opsonized. With this purpose, we generated stable CD11b- and CD11c-KO THP1 DCs using CRISPR/Cas9 technology and characterized them in detail with respect to their similarity to primary monocyte-derived DCs.

Coating of HIV-1 with complement (C-) fragments and binding of HIV-C to CRs might contribute to protecting virus particles from immediate and extensive degradation in intracellular compartments as illustrated for non-opsonized HIV-1 (22). We and others (8, 9, 17, 23, 24) found a significant enhancement of productive DC infection by HIV-C associated with the above mentioned improved antiviral immune responses as well as an adjuvant role with respect to induction of HIV-specific CTLs. This C-mediated, significantly enhanced productive HIV-1 infection was also detected in WT THP1-DCs. After detailed evaluation of WT THP1-DCs on additional characteristics exerted by primary DCs, we proved this cell line to be a suitable model, since similar expression of specific receptors were confirmed. In addition, WT THP1-DCs showed same HIV-1 infection kinetics as primary DCs, since HIV-1 subverts complement for productive infection compared to non-opsonized HIV-1 (9, 13). This complement-mediated enhancement in DC infection was further confirmed using Vpx-carrying HIV and HIV-C Vpx preparations. Productive infection of primary DCs was shown to be limited due to the restriction of SAMHD1, which is not counteracted by non-opsonized HIV-1. However, our group previously illustrated that bypassing SAMHD1 by phosphorylation through HIV-C in iDCs significantly enhanced productive HIV-1 infection and subsequent antiviral humoral and cellular immunity *in vitro* (9).

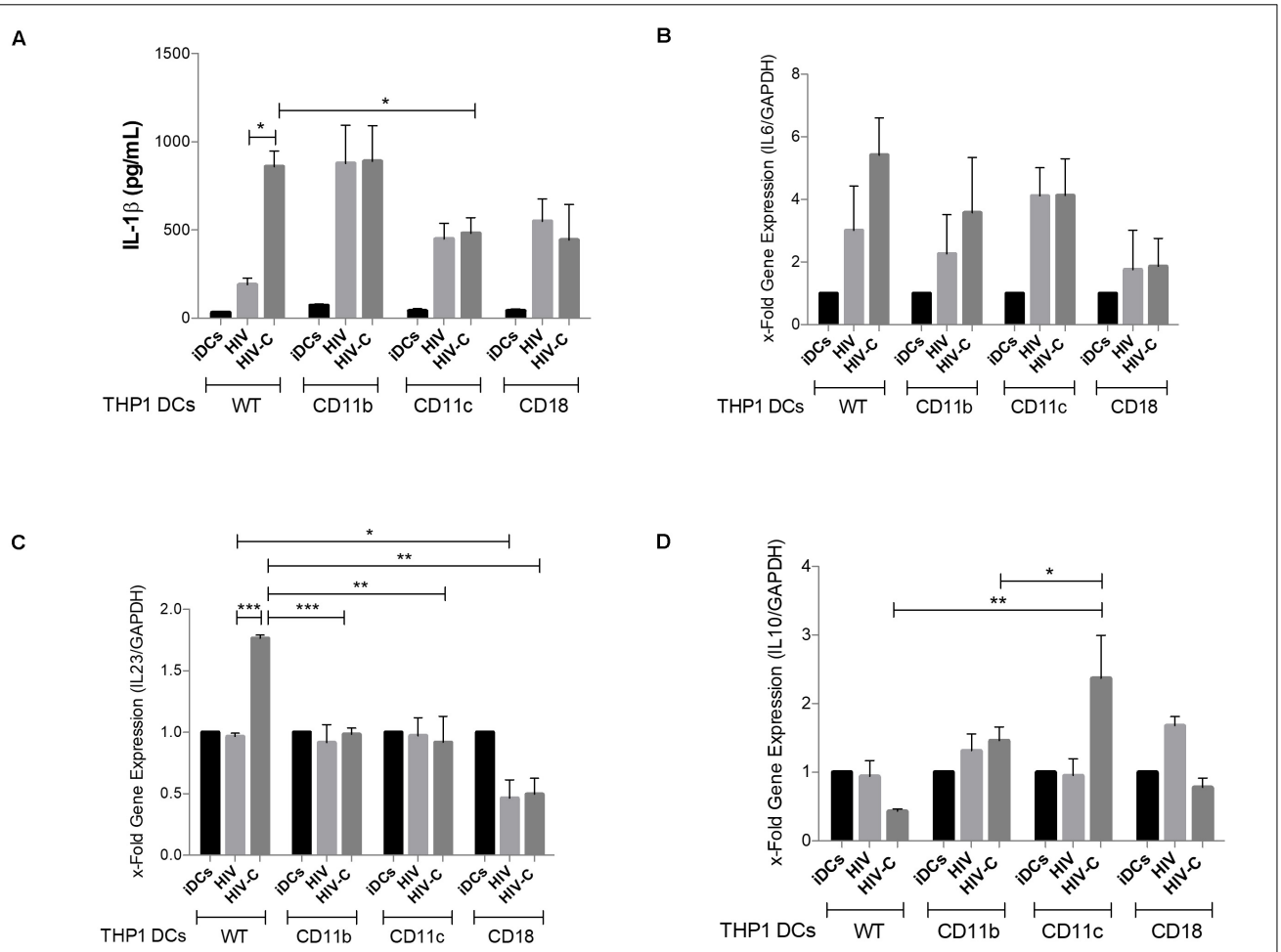

FIGURE 5 | CD11c deletion significantly modifies the cytokine profile by decreasing IL-1β production and IL23 expression, while up-regulating IL10 levels. IL-1β production **(A)**, IL6 **(B)**, IL23A **(C)**, and IL10 **(D)** expression levels were analyzed in WT-, CD11b KO-, CD11c KO-, and CD18 KO THP1-DCs as indicated following infection with HIV or HIV-C. UI cells served as controls. Experiments were repeated thrice in duplicates and RT-PCR analyses were performed. Differences were analyzed by using GraphPad Prism software and one-way ANOVA with Bonferroni post-test. *$p < 0.01$, **$p < 0.001$, ***$p < 0.0001$.

Despite significantly higher SAMHD1 levels in THP1 monocytes (11), HIV-C- and Vpx-mediated effects were also seen in WT THP1-DCs, which proves them to be a valuable model for studying functions of CR3 and CR4 in relation to HIV-1 infection in more detail.

To characterize the KO CD11b and CD11c cells, we infected WT-, CD11b-, and CD11c KO-THP1 DCs using HIV and HIV-C. In CD11b KO-THP1 DCs, HIV-C mediated a significantly enhanced productive infection similar to primary DCs and WT-THP1 DCs. However, the considerably augmented productive infection was lost in CD11c KO-THP1 DCs or upon blocking CD11c on moDCs and infection levels were comparable to the low-level productive infection mediated by HIV. Complement-mediated effects in presence of Vpx were also lost in CD11c KO THP1-DCs only, but not in CD11b KO THP1-DCs. Similar results to CD11c KO THP1-DCs were observed in CD18 KO cells, devoid of both CR3 and CR4.

Our data represent the first evidence of the major role of CR4 in DC infection with complement-opsonized HIV-1, and is in controversy to findings from Tjomsland et al. (25), who illustrated that blocking CR3 significantly decreased infection of emigrating DCs from cervical mucosal tissues. These authors used a combination of blocking antibodies against CD11b and CD18, which could cause CR3 and CR4 blocking due to the shared integrin beta chain-2 (CD18) of both CRs. Thus, effects seen in this study might not rely on CR3 blocking, but probably on blocking CR4-mediated signaling.

IRF3 and IRF7 are the main regulators of type I IFN expression (26). IRF3, localized in the cytoplasm in a latent form, gets activated by phosphorylation via TBK1 or IKKε and translocates to the nucleus. Once in the nucleus, IRF3 dimerizes with NFκB and activating transcription factor 2 (ATF2)–c-jun to recruit CREB-binding protein to the IFNB promoter to form a functional beta interferon "enhanceosome" (27). We found this IRF3/NFκB "enhanceosome" also in primary DCs exposed to HIV-C (9) and within this study we unraveled the CR responsible for this axis using the CD11b/CD11c KO THP1-DCs. In line with the results obtained from the infection analyses, we detected that the p-IRF3 signaling is significantly disrupted upon CD11c KO, but intact in WT- and CD11b KO-THP1 DCs. Disturbance

of IRF3 activation was associated with a significantly impaired *IFNB* mRNA level expression in CD11c KO THP1-DCs. These results confirm the findings, that abolishment of IFN-β was observed in DCs deficient of *Irf3* upon LPS stimulation or significantly impaired upon Poly(I:C) treatment (28) and also upon virus infection of $Irf3^{-/-}$ mouse embryonic fibroblasts (MEFs) (29). Additionally, these activated cascades contribute to the type I IFN positive feedback loop. We observed in WT THP1-DCs that type I *IFNB* mRNA significantly increased in HIV-C infection, leading to a better antiviral response. These findings are consistent with our other study (9) finding elevated levels of *IFNB* mRNA and ISGs in HIV-C exposed primary DCs. Our findings differ from results published by Ellegård et al. (30), who showed that complement opsonization of HIV-1 resulted in a decreased antiviral immune response in DCs. In contrast to that finding, the authors illustrated in line with our data, that DCs are infected to significantly higher levels when the virus was complement-opsonized (30, 31). Furthermore, they illustrated considerably enhanced IRF3 activation in DCs upon HIV-C treatment, which point to induction of an efficient antiviral immune response by DCs. Nonetheless the authors concluded that complement-opsonized HIV dampens immune responses via DCs compared to non-opsonized HIV-1. In contrast, we found, enhanced productive infection of DCs exposed to HIV-C also increases IRF3 activation and phosphorylation of TBK1 only in WT-THP1-DCs and CD11b KO THP1-DCs, but not CD11c KO THP1-DCs. In addition, CD11b KO resulted in an overshooting type I IFN response.

Since CD11b plays a key role in phagocytosis of apoptotic cells, ligation of this member of the heterodimeric β2 integrin family results in production of anti-inflammatory cytokines such as TGF-β or IL-10 (32). At the same time ligation of CD11b negatively regulates pro-inflammatory signals via e.g., TLRs or FcγR (33–35). Our data confirm this anti-inflammatory, IL-10-inducing role of CD11b, which does not only seem to negatively regulate TLR or FcγR signaling pathways (32), but also signaling pathways initiated via CD11c. A role for anti-inflammatory signaling via CD11b was also observed in CD11c KO THP1-DCs that solely express CR3, since in these cells significantly increased IL-10 expression levels were detected similar to DC-10, a human subset of tolerogenic DCs endowed with the ability to spontaneously release IL-10 as described by Comi et al. (36).

Our results nicely reflect the distinct roles of CD11b and CD11c with respect to inflammatory or antiviral host responses, but also point to the importance of balanced levels regarding either elevated, overshooting induction of antiviral signaling pathways (CD11b KO) or dampening via pIRF3/IFNB reduction and IL-10 induction (CD11c KO). Our results in WT- and CD11b KO THP1-DCs showed an enhanced antiviral type I IFN signaling pathway, comparable to the one seen in primary DCs, e.g., $BDCA1^{+}$ DCs (9). The contradictory data seen in our experiments compared to Ellegard et al. (30) might rely on diverse monocyte isolation and differentiation protocols or cell sources to work on and thereby differential expression levels of either CR3 or CR4 on generated DCs.

Our data suggest an important and distinct role for β2 integrins, CR3 and CR4, in myeloid cells. Beyond initial binding of complement-opsonized particles, myeloid cells encounter ligands within the extracellular matrix while en route to their intended targets. Here, these ligands are modified by local inflammatory mediators (37). Dependent on interaction with either CR3 or CR4, inflammatory cytokine production is restricted to minimize damage of the host via CD11b, while CD11c seems to take action with respect to efficient antiviral immune responses in a type I interferon autocrine-paracrine manner. Cooperation of the NFκB-dependent pathway leading to inflammatory cytokine secretion and the IFN-dependent pathway mediating type I IFN and ISGs was also described upon TLR7/8 triggering in DCs (38) and this type I IFN autocrine-paracrine loop seems to also play an important role in CR4-signaling, which has to be confirmed in more detail. Nevertheless, specific targeting of either CD11b or CD11c might be an innovative tool to regulate pro- and anti-inflammatory processes during infectious diseases such as HIV-1.

DATA AVAILABILITY STATEMENT

All datasets presented in this study are included in the article/**Supplementary Material**.

ETHICS STATEMENT

The Ethics Committee of the Medical University of Innsbruck approved the study. The study number is ECS 1166/2018, and the PI is the corresponding author DW. The patients/participants provided their written informed consent to participate in this study.

AUTHOR CONTRIBUTIONS

DW and WP: conceptualization and funding acquisition. MB-J, MB, PJ-O, TY, TV, LH, WP, and DW: investigation. DW, WP, and MB-J: writing – original draft. DW, MB-J, MB, TV, LH, and WP: writing – review and editing. DW: project administration. All authors contributed to the article and approved the submitted version.

FUNDING

This work was funded by the Austrian National Bank (OeNB) Jubiläumsfonds: 17614 to WP and the Austrian Science Fund (FWF): W11 and P-33510B to DW.

ACKNOWLEDGMENTS

We thank our technicians Karolin Thurnes and Christina Witting for their valuable help and support regarding this manuscript, and also Profs. Oliver Keppler, Nathaniel Landau, and Thomas J. Hope for providing reagents and virus plasmids. We also thank Prof. Sieghart Sopper from the FACS Sort Core Facility

of the Medical University of Innsbruck and Polymun Scientific, Donaustrasse 99, Klosterneuburg, Austria who provided all reagents for p24 ELISA. The reagents ARP118 (HIV-BaL) and ARP177.8 (HIV-92UG037) were obtained from the Centre for AIDS Reagents, NIBSC HPA UK, supported by the EC FP6/7 Europrise Network of Excellence, and NGIN consortia and the Bill and Melinda Gates GHRC-CAVD Project and were donated by Dr. S. Gartner, Dr. M. Popovic, Dr. R. Gallo [Courtesy of the NIH AIDS Research and Reference Reagent Program (BaL)], and the WHO UN AIDS Network for HIV-isolation and characterization (92UG037).

SUPPLEMENTARY MATERIAL

The Supplementary Material for this article can be found online at: https://www.frontiersin.org/articles/10.3389/fimmu.2020.02010/full#supplementary-material

REFERENCES

1. Fernandez NC, Lozier A, Flament C, Ricciardi-Castagnoli P, Bellet D, Suter M, et al. Dendritic cells directly trigger NK cell functions: cross-talk relevant in innate anti-tumor immune responses in vivo. *Nat Med*. (1999) 5:405–11. doi: 10.1038/7403
2. Steinman RM, Hemmi H. Dendritic cells: translating innate to adaptive immunity. *Curr Top Microbiol Immunol*. (2006) 311:17–58. doi: 10.1007/3-540-32636-7_2
3. Steinman RM. Decisions about dendritic cells: past, present, and future. *Annu Rev Immunol*. (2012) 30:1–22. doi: 10.1146/annurev-immunol-100311-102839
4. Shen R, Richter HE, Smith PD. Early HIV-1 target cells in human vaginal and ectocervical mucosa. *Am J Reprod Immunol*. (2011) 65:261–7. doi: 10.1111/j.1600-0897.2010.00939.x
5. Ebenbichler CF, Thielens NM, Vornhagen R, Marschang P, Arlaud GJ, Dierich MP. Human immunodeficiency virus type 1 activates the classical pathway of complement by direct C1 binding through specific sites in the transmembrane glycoprotein gp41. *J Exp Med*. (1991) 174:1417–24. doi: 10.1084/jem.174.6.1417
6. Bouhlal H, Chomont N, Haeffner-Cavaillon N, Kazatchkine MD, Belec L, Hocini H. Opsonization of HIV-1 by semen complement enhances infection of human epithelial cells. *J Immunol*. (2002) 169:3301–6. doi: 10.4049/jimmunol.169.6.3301
7. Stoiber H, Soederholm A, Wilflingseder D, Gusenbauer S, Hildgartner A, Dierich MP. Complement and antibodies: a dangerous liaison in HIV infection? *Vaccine*. (2008) 26(Suppl. 8):I79–85. doi: 10.1016/j.vaccine.2008.11.050
8. Wilflingseder D, Banki Z, Garcia E, Pruenster M, Pfister G, Muellauer B, et al. IgG opsonization of HIV impedes provirus formation in and infection of dendritic cells and subsequent long-term transfer to T cells. *J Immunol*. (2007) 178:7840–8. doi: 10.4049/jimmunol.178.12.7840
9. Posch W, Steger M, Knackmuss U, Blatzer M, Baldauf H-M, Doppler W, et al. Complement-opsonized HIV-1 overcomes restriction in dendritic cells. *PLoS Pathog*. (2015) 11:e1005005. doi: 10.1371/journal.ppat.1005005
10. Manel N, Hogstad B, Wang Y, Levy DE, Unutmaz D, Littman DR. A cryptic sensor for HIV-1 activates antiviral innate immunity in dendritic cells. *Nature*. (2010) 467:214–7. doi: 10.1038/nature09337
11. Laguette N, Sobhian B, Casartelli N, Ringeard M, Chable-Bessia C, Segeral E, et al. SAMHD1 is the dendritic- and myeloid-cell-specific HIV-1 restriction factor counteracted by Vpx. *Nature*. (2011) 474:654–7. doi: 10.1038/nature10117
12. Lahouassa H, Daddacha W, Hofmann H, Ayinde D, Logue EC, Dragin L, et al. SAMHD1 restricts the replication of human immunodeficiency virus type 1 by depleting the intracellular pool of deoxynucleoside triphosphates. *Nat Immunol*. (2012) 13:223–8. doi: 10.1038/ni.2236
13. Banki Z, Posch W, Ejaz A, Oberhauser V, Willey S, Gassner C, et al. Complement as an endogenous adjuvant for dendritic cell-mediated induction of retrovirus-specific CTLs. *PLoS Pathog*. (2010) 6:e1000891. doi: 10.1371/journal.ppat.1000891
14. Wilflingseder D, Schroll A, Hackl H, Gallasch R, Frampton D, Lass-Florl C, et al. Immediate T-helper 17 polarization upon triggering CD11b/c on HIV-exposed dendritic cells. *J Infect Dis*. (2015) 212:44–56. doi: 10.1093/infdis/jiv014
15. Manel N, Littman DR. Hiding in plain sight: how HIV evades innate immune responses. *Cell*. (2011) 147:271–4. doi: 10.1016/j.cell.2011.09.010
16. Posch W, Cardinaud S, Hamimi C, Fletcher A, Muhlbacher A, Loacker K, et al. Antibodies attenuate the capacity of dendritic cells to stimulate HIV-specific cytotoxic T lymphocytes. *J Allergy Clin Immunol*. (2012) 130:1368–74.e2. doi: 10.1016/j.jaci.2012.08.025
17. Pruenster M, Wilflingseder D, Banki Z, Ammann CG, Muellauer B, Meyer M, et al. C-type lectin-independent interaction of complement opsonized HIV with monocyte-derived dendritic cells. *Eur J Immunol*. (2005) 35:2691–8. doi: 10.1002/eji.200425940
18. Hsu PD, Scott DA, Weinstein JA, Ran FA, Konermann S, Agarwala V, et al. DNA targeting specificity of RNA-guided Cas9 nucleases. *Nat Biotechnol*. (2013) 31:827–32. doi: 10.1038/nbt.2647
19. Sanjana NE, Shalem O, Zhang F. Improved vectors and genome-wide libraries for CRISPR screening. *Nat Methods*. (2014) 11:783–4. doi: 10.1038/nmeth.3047
20. Baldauf HM, Pan XY, Erikson E, Schmidt S, Daddacha W, Burggraf M, et al. SAMHD1 restricts HIV-1 infection in resting CD4(+) T cells. *Nat Med*. (2012) 18:1682–7. doi: 10.1038/nm.2964
21. Purtscher M, Trkola A, Gruber G, Buchacher A, Predl R, Steindl F, et al. A broadly neutralizing human monoclonal antibody against gp41 of human immunodeficiency virus type 1. *AIDS Res Hum Retroviruses*. (1994) 10:1651–8. doi: 10.1089/aid.1994.10.1651
22. Moris A, Nobile C, Buseyne F, Porrot F, Abastado JP, Schwartz O. DC-SIGN promotes exogenous MHC-I-restricted HIV-1 antigen presentation. *Blood*. (2004) 103:2648–54. doi: 10.1182/blood-2003-07-2532
23. Bajtay Z, Speth C, Erdei A, Dierich MP. Cutting edge: productive HIV-1 infection of dendritic cells via complement receptor type 3 (CR3, CD11b/CD18). *J Immunol*. (2004) 173:4775–8.
24. Bouhlal H, Chomont N, Requena M, Nasreddine N, Saidi H, Legoff J, et al. Opsonization of HIV with complement enhances infection of dendritic cells and viral transfer to CD4 T cells in a CR3 and DC-SIGN-dependent manner. *J Immunol*. (2007) 178:1086–95.
25. Tjomsland V, Ellegard R, Kjolhede P, Wodlin NB, Hinkula J, Lifson JD, et al. Blocking of integrins inhibits HIV-1 infection of human cervical mucosa immune cells with free and complement-opsonized virions. *Eur J Immunol*. (2013) 43:2361–72. doi: 10.1002/eji.201243257
26. Taniguchi T, Ogasawara K, Takaoka A, Tanaka N. IRF family of transcription factors as regulators of host defense. *Annu Rev Immunol*. (2001) 19:623–55. doi: 10.1146/annurev.immunol.19.1.623
27. Falvo JV, Parekh BS, Lin CH, Fraenkel E, Maniatis T. Assembly of a functional beta interferon enhanceosome is dependent on ATF-2-c-jun heterodimer orientation. *Mol Cell Biol*. (2000) 20:4814–25. doi: 10.1128/mcb.20.13.4814-4825.2000
28. Sakaguchi S, Negishi H, Asagiri M, Nakajima C, Mizutani T, Takaoka A, et al. Essential role of IRF-3 in lipopolysaccharide-induced interferon-beta gene expression and endotoxin shock. *Biochem Biophys Res Commun*. (2003) 306:860–6. doi: 10.1016/s0006-291x(03)01049-0
29. Sato M, Suemori H, Hata N, Asagiri M, Ogasawara K, Nakao K, et al. Distinct and essential roles of transcription factors IRF-3 and IRF-7 in response to viruses for IFN-alpha/beta gene induction. *Immunity*. (2000) 13:539–48.
30. Ellegard R, Crisci E, Burgener A, Sjowall C, Birse K, Westmacott G, et al. Complement opsonization of HIV-1 results in decreased antiviral and inflammatory responses in immature dendritic cells via CR3. *J Immunol*. (2014) 193:4590–601. doi: 10.4049/jimmunol.1401781

31. Tjomsland V, Ellegard R, Burgener A, Mogk K, Che KF, Westmacott G, et al. Complement opsonization of HIV-1 results in a different intracellular processing pattern and enhanced MHC class I presentation by dendritic cells. *Eur J Immunol*. (2013) 43:1470–83. doi: 10.1002/eji.201242935
32. Amarilyo G, Verbovetski I, Atallah M, Grau A, Wiser G, Gil O, et al. iC3b-opsonized apoptotic cells mediate a distinct anti-inflammatory response and transcriptional NF-kappaB-dependent blockade. *Eur J Immunol*. (2010) 40:699–709. doi: 10.1002/eji.200838951
33. Faridi MH, Khan SQ, Zhao W, Lee HW, Altintas MM, Zhang K, et al. CD11b activation suppresses TLR-dependent inflammation and autoimmunity in systemic lupus erythematosus. *J Clin Invest*. (2017) 127:1271–83. doi: 10.1172/JCI88442
34. Means TK, Luster AD. Integrins limit the Toll. *Nat Immunol*. (2010) 11:691–3. doi: 10.1038/ni0810-691
35. Han C, Jin J, Xu S, Liu H, Li N, Cao X. Integrin CD11b negatively regulates TLR-triggered inflammatory responses by activating Syk and promoting degradation of MyD88 and TRIF via Cbl-b. *Nat Immunol*. (2010) 11:734–42. doi: 10.1038/ni.1908
36. Comi M, Amodio G, Gregori S. Interleukin-10-producing DC-10 is a unique tool to promote tolerance via antigen-specific T regulatory type 1 cells. *Front Immunol*. (2018) 9:682. doi: 10.3389/fimmu.2018.00682
37. dair-Kirk TLA, Senior RM. Fragments of extracellular matrix as mediators of inflammation. *Int J Biochem Cell Biol*. (2008) 40:1101–10. doi: 10.1016/j.biocel.2007.12.005
38. Gautier G, Humbert M, Deauvieau F, Scuiller M, Hiscott J, Bates EE, et al. A type I interferon autocrine-paracrine loop is involved in Toll-like receptor-induced interleukin-12p70 secretion by dendritic cells. *J Exp Med*. (2005) 201:1435–46. doi: 10.1084/jem.20041964

Conflict of Interest: The authors declare that the research was conducted in the absence of any commercial or financial relationships that could be construed as a potential conflict of interest.

frontiers in Immunology

ORIGINAL RESEARCH
published: 02 September 2020
doi: 10.3389/fimmu.2020.01911

Quantification of Factor H Mediated Self vs. Non-self Discrimination by Mathematical Modeling

Alexander Tille[1,2], *Teresa Lehnert*[1], *Peter F. Zipfel*[2,3] *and Marc Thilo Figge*[1,2]*

[1] *Applied Systems Biology, Leibniz Institute for Natural Product Research and Infection Biology—Hans Knöll Institute, Jena, Germany,* [2] *Faculty of Biological Sciences, Institute of Microbiology, Friedrich-Schiller-University Jena, Jena, Germany,* [3] *Infection Biology, Leibniz Institute for Natural Product Research and Infection Biology—Hans Knöll Institute, Jena, Germany*

The complement system is part of the innate immune system and plays an important role in the host defense against infectious pathogens. One of the main effects is the opsonization of foreign invaders and subsequent uptake by phagocytosis. Due to the continuous default basal level of active complement molecules, a tight regulation is required to protect the body's own cells (self cells) from opsonization and from complement damage. A major complement regulator is Factor H, which is recruited from the fluid phase and attaches to cell surfaces where it effectively controls complement activation. Besides self cells, pathogens also have the ability to bind Factor H; they can thus escape opsonization and phagocytosis causing severe infections. In order to advance our understanding of the opsonization process at a quantitative level, we developed a mathematical model for the dynamics of the complement system—termed *DynaCoSys model*—that is based on ordinary differential equations for cell surface-bound molecules and on partial differential equations for concentration profiles of the fluid phase molecules in the environment of cells. This hybrid differential equation approach allows to model the complement cascade focusing on the role of active C3b in the fluid phase and on the cell surface as well as on its inactivation on the cell surface. The *DynaCoSys model* enables us to quantitatively predict the conditions under which Factor H mediated complement evasion occurs. Furthermore, investigating the quantitative impact of model parameters by a sensitivity analysis, we identify the driving processes of complement activation and regulation in both the self and non-self regime. The two regimes are defined by a critical Factor H concentration on the cell surface and we use the model to investigate the differential impact of complement model parameters on this threshold value. The dynamic modeling on the surface of pathogens are further relevant to understand pathophysiological situations where Factor H mutants and defective Factor H binding to target surfaces results in pathophysiology such as renal and retinal disease. In the future, this DynaCoSys model will be extended to also enable evaluating treatment strategies of complement-related diseases.

Keywords: complement system, complement regulator factor H, non-self recognition, immune evasion, self-tolerance, mathematical modeling, hybrid differential equation approach

OPEN ACCESS

Edited by:
Heribert Stoiber, Innsbruck Medical University, Austria

Reviewed by:
Rachel LeCover, Cornell University, United States
Zoltan Banki, Medical University of Innsbruck, Austria

***Correspondence:**
Marc Thilo Figge
thilo.figge@leibniz-hki.de

Specialty section:
This article was submitted to Microbial Immunology, a section of the journal Frontiers in Immunology

Received: *27 March 2020*
Accepted: *16 July 2020*
Published: *02 September 2020*

Citation:
Tille A, Lehnert T, Zipfel PF and Figge MT (2020) Quantification of Factor H Mediated Self vs. Non-self Discrimination by Mathematical Modeling. Front. Immunol. 11:1911. doi: 10.3389/fimmu.2020.01911

INTRODUCTION

The complement system plays a key role in defending the host against invading pathogens (1–5). Its main task is the recognition, subsequent opsonization and lysis of invading microbes, foreign particles, or altered self cells (6, 7). The central molecule of the complement system is the protein C3b, which binds to cell surfaces, opsonizes the surface and allows subsequent phagocytosis or induction of the lytic terminal complement pathway. C3b results from the cleavage of the intact molecule C3 via three distinct pathways. The classical pathway and lectin pathway are activated, respectively, in the presence of antigen-antibody immune complexes and microbial carbohydrate patterns (8, 9) whereas, the alternative pathway is activated by a spontaneous hydrolysis of C3. Due to this spontaneous emergence of active molecules there is always a basal level of active complement molecules present in blood circulation. Activation and recognition by the complement systems is a double-edged sword. On the one hand, it has to be very sensitive in order to find as many infectious microbes or foreign cells as possible, so that even small fluctuations from the self-state should result into an immediate and corrective response. On the other hand, a tight regulation is required to avoid any unwanted activation and damage to the host. Balance in the host can be disturbed in various ways, such as overshooting complement activation in the context of infectious agents or diseases like sepsis (5, 10), reduced host defense against complement activation caused by genetic defects or autoantibodies (11, 12) or host cells that induce complement activation (e.g., ischemia/reperfusion, burns, apoptotic/necrotic cells). Besides diseases causing complement dysfunction, pathogenic microbes are able to evade the complement system by recruiting complement regulators like Factor H to their surface (13–18). This leads to alterations in the immune response against the pathogen and thus can be associated with serious infections.

For a better understanding of the system's balance, mathematical models can make important contributions to the quantitative understanding of the complex dynamics of the complement system. To study the process of recognizing self vs. non-self cells we here apply a systems biology approach by formulating a mathematical model that is compared to published experimental data. We refer to our newly established model, which describes the dynamics of the complement systems by a set of differential equations, as the *DynaCoSys model*. A main challenge of any quantitative complement model is the estimation of the model parameters. Quantitative time resolved data, especially of surface bound molecules are rare, which in general makes the identification of large mechanistic models difficult. Thus we focus on the main component C3b and introduce effective rates that represent the dynamics of the intermediate products contributing to the formation and decay of C3b. We are able to quantify the complements molecule concentrations on the cell surface and in the surrounding fluid in steady state as well as for the full systems dynamics. Most importantly, in order to arrive at quantitative predictions, we screen model parameters for their differential impact on the critical Factor H concentration that distinguishes between the self and non-self regimes. Our quantitative results are discussed in the light of literature knowledge and in view of applying the model to monitoring treatment of complement-associated diseases.

RESULTS

Complement Dynamics of C3b-Opsonization Requires Hybrid Differential Equation Approach

Mathematical models that aim to represent the complement system as a whole by a system of coupled ordinary differential equations (ODEs) are faced with its high complexity and the tremendous number of unknown parameter values (19–21). In addition, ODEs do not account for spatial inhomogeneities in the dynamics and interaction of complement molecules. The spatial distributions of complement molecules are induced by the local accumulation of surface-bound molecules on the cell and decrease in solution as a function of the distance from the cell. This requires a representation by partial differential equations (PDEs) (22, 23); however, modeling complement dynamics by a system of coupled PDEs instead of ODEs would increase the number of unknown parameter values even further. The *DynaCoSys model* is based on a hybrid differential equation (hDE) approach that combines ODEs and PDEs and deliberately reduces the complexity of the system by focusing on the most important complement molecules and by considering spatial inhomogeneities only where necessary. A detailed overview of the *DynaCoSys model* is given in the **Supplementary Material Section 1**, while in what follows we will only focus on the most relevant aspects.

The *DynaCoSys model* focuses on the derivatives of the central complement molecule C3 as the most important molecules (see **Figure 1A**): in the fluid phase, C3 occurs with concentration $C3^f$ and becomes cleaved into $C3a^f$ and $C3b^f$. The latter molecule has a highly reactive thioester that enables the molecule to bind covalently to any surface (24). We denote the concentration of surface-bound molecules by $C3b^s$; these molecules opsonize cells and allow phagocytosis, but may become inactivated and are then contributing to the concentration $iC3b^s$. $C3b^s$ can form complexes with other complement components, like Factor B and thereby generate an active enzyme, C3-convertase. This enzyme is able to cleave $C3^f$ and to newly generate $C3b^f$ molecules driving a massive amplification loop (2). The C3-convertase complex of the alternative pathway dominates the amplification of $C3b^s$ and is responsible for 80–90 % of the total complement activation, even if the complement reaction was initially triggered by the classical or lectin pathway (8). This opsonization process is strictly controlled by regulators (25) usually ensuring that only non-self cells become opsonized (3, 9). The regulators are either present in the fluid phase, attached to cell surfaces or integrated into cell membranes (3). They control the fluid phase activation, the amplification on the surface and they mediate the decay of surface bound $C3b^s$ molecules. The soluble regulator Factor H plays a major role in protecting also cells that do not have membrane-bound inhibitors (26). It mediates regulation in the fluid phase as well as on membranes

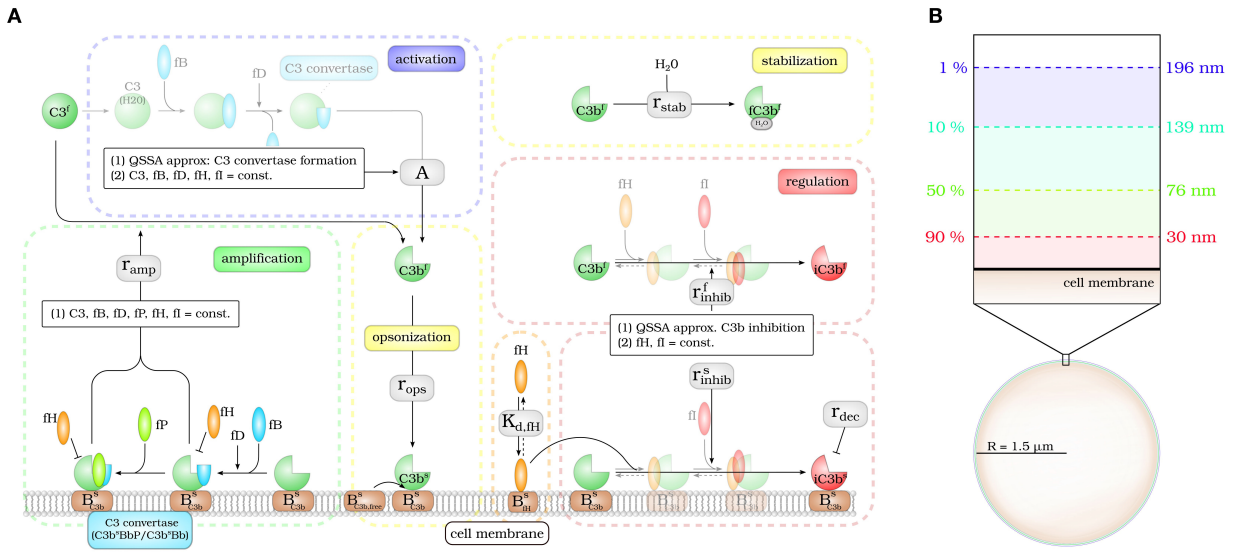

FIGURE 1 | Hybrid differential equation model of the complement system. Complement activation can be divided into five parts: (i) activation, (ii) opsonization, (iii) stabilization, (iv) amplification, and (v) regulation. **(A)** The model focuses on the dynamics of the central component *C3b*: Active *C3b* in the fluid phase, $C3b^f$, results from cleavage of precursor molecule $C3^f$. The interaction of the fluid phase molecule $C3b^f$ with the cell surface is modeled by the interaction with free surface binding sites $B^s_{C3b,free}$ and binding sites B^s_{C3b} that are occupied with molecules $C3b^s$ on the surface. $C3b^f$ that does not bind to the cell surface gets inactivated via a Factor H mediated inhibition process, or gets stabilized by water molecules and is no longer able to bind to the cell surface. Surface-bound $C3b^s$ can form C3-convertase molecules—$C3b^sBb$ and $C3b^sBbP$–that cleave $C3^f$ molecules to $C3b^f$ molecules in the vicinity of the cell surface. $C3b^s$ can be inactivated via an inhibition process that is mediated by surface-bound Factor H, whose concentration depends on the concentration of binding sites on the cell surface $B^s_{fH,max}$. **(B)** The lifetime of active $C3b^f$ is short such that, depending on the distance from the cell surface, the fraction of molecules that reach the cell surface is small; for example, only 1% at a distance of 196 nm within a simple decay model.

by slowing down the amplification process by cleavage of C3-convertase and acting as a cofactor for $C3b^s$ inactivation (27, 28). The ability of binding fluid phase Factor H and the resulting regulation of the complement cascade are the main reasons why host cells are usually not targeted by the complement system (26). As schematically shown in **Figure 1A**, our *DynaCoSys model* comprises all these features of $C3^f$ and its derivatives: (i) activation, (ii) opsonization (iii) stabilization, (iv) amplification, and (v) regulation.

The molecule concentrations of the active $C3b^s$ and inactive $iC3b^s$ molecules at the cell surface are described by ODEs:

$$\frac{d}{dt}C3b^s = r_{ops} \cdot B_{C3b,free}\left(C3b^s, iC3b^s\right) \cdot C3b^f(R)^* - r^s_{inhib}\left(fH^s\right) \cdot C3b^s, \quad (1)$$

$$\frac{d}{dt}iC3b^s = r^s_{inhib}\left(fH^s\right) \cdot C3b^s - r_{dec} \cdot iC3b^s \quad (2)$$

As can be seen in Equation (1), the dynamic increase of $C3b^s$ molecules depends on the steady state concentration of soluble $C3b^f(R)^*$ molecules at the cell surface, which are binding with rate r_{ops} to free binding sites at the cell surface that are present with concentration $B_{C3b,free}$. $C3b^s$ turns into its inactivated form $iC3b^s$ with the rate r^s_{inhib} – a process that is mediated by Factor H molecules at the cell surface that are present with concentration fH^s. The decay of inactive $iC3b^s$ molecules occurs spontaneously with rate r_{dec}. All parameters used in this study are summarized in the **Supplementary Material Section 2** and the analysis results of the steady state are given in the **Supplementary Material Section 3**. In particular, we show that tuning the fH^s concentration, the functions $C3b^s(fH^s)$ and $iC3b^s(fH^s)$ exhibit a removable singularity at Factor H concentration $fH^s_{th} = 230$ molecules/µm^2, where the amplification process with rate r_{amp} and the inhibition process with rate r^s_{inhib} of $C3b^s$ balance out ($r_{amp} = r^s_{inhib}$; see **Supplementary Figure S6**). This threshold value coincides with the maximum change in all kinds of $C3b^s$ molecule concentrations as a function of fH^s (see **Supplementary Figure S7C**) and corresponds to a relative usage of 0.41 % of all possible Factor H binding sites on the surface. Two regimes can be distinguished: for $fH^s < fH^s_{th}$ concentrations of $C3b^s$ reach high values up to the complete coverage of the cell surface. We refer to this regime as the *non-self* regime; on the other hand, for $fH^s > fH^s_{th}$ only relatively low $C3b^s$ concentrations are realized and we refer to this regime as *self* regime.

Modeling the interaction of cell surfaces with complement molecules in the fluid phase requires PDEs, because spatial concentration differences are expected in the surrounding volumes of activating surfaces. A simple decay model for $C3b^f$ allows to estimate the interaction radius of a cell with these molecules in its environment (see **Figure 1B**). In this decay model, the active thioester bond $C3b^f$ in aqueous solutions is assumed to be stabilized with a relatively short half-life time of 60 µs by water molecules (29). This stabilization process renders molecules inactive for subsequent opsonization

of cell surfaces. The volume in which activated molecules can diffuse before they are deactivated can be estimated by calculating the molecules' mean square displacement (see **Supplementary Material Section 1**). We find that the radius of a spherical volume around a cell where the concentration of $C3b^f$ is still 1% of the typical value at the cell surface is not larger than 200 nm (see **Figure 1B**). In other words, $C3b^f$ molecules that are able to reach a cell's surface are diffusing within a shell around the cell that is much smaller than the typical distance between cells in blood. For example, a concentration of 10^{10} $cells/l$, which is clearly above the cell count of typical infection scenarios in human blood, have a center-to-center distance of about 46 μm (see **Supplementary Material Section 1**). It can be concluded that it is sufficient to consider a single cell in our hDE model. The reaction-diffusion equation for $C3b^f$ is described by the PDE:

$$\frac{\partial C3b^f(r,t)}{\partial t} = D_{C3b}\cdot\Delta_r C3b^f(r,t) - \left(r^f_{inhib} + r_{stab}\right)\cdot C3b^f(r,t) + A \quad (3)$$

with $R \leq r < \infty$.

Here, D_{C3b} denotes the diffusion constant, A is the spontaneous $C3b^f$ formation and the rates r^f_{inhib} and r_{stab} refer to the inactivation of $C3b^f$ (see **Supplementary Material Section 1**). The boundary condition at the cell surface ($r = R$) corresponds to Fick's first law, where the diffusion flux is calculated from the molecules that are formed at the surface (r_{amp}) and bind (r_{ops}) to the surface:

$$\frac{\partial C3b^f(r,t)}{\partial r}|_{r=R} = \frac{r_{amp}\left(fH^s\right)\cdot C3b^s - r_{ops}\cdot B_{C3b,free}\left(C3b^s, iC3b^s\right)\cdot C3b^f(R)}{D_{C3b}} \quad (4)$$

Far away from the cell surface ($r \to \infty$) the boundary condition is given by:

$$C3b^f(r\to\infty)^* = \frac{A}{r^f_{inhib} + r_{stab}} \quad (5)$$

As shown in detail in the **Supplementary Material Section 1**, it is appropriate to assume steady state conditions, i.e., solving Equation (3) for $\partial C3b^f(r,t)/\partial t = 0$, because the reaction-diffusion dynamics equilibrates within milliseconds and by that much faster than the $C3b^s$ dynamics on the cell surface.

The impact of surface-bound Factor H on the concentration of $C3b^f$ in steady state is shown in **Figure 2A** as a function of the distance from the cell surface. As noted before, the threshold value fH^s_{th} divides the cell surfaces into two regimes. For $fH^s < fH^s_{th}$, $C3b^f$ molecules are formed to a larger extent than they are recruited and bound at the cell surface, and the opposite is true in the limit $fH^s > fH^s_{th}$. It follows that the net amount of diffused $C3b^f$ increases with decreasing fH^s concentrations; for vanishingly small values of fH^s, the concentration profile of $C3b^f$ molecules decreases by almost six orders of magnitude. Regardless of the fH^s concentration, the $C3b^f$ concentration profile reaches the equilibrium concentration at a distance from the cell surface of < 0.5 μm. This distance is more than twice as large as estimated by our simple decay model (see **Figure 1B**), which yields a maximum distance of 0.2 μm. However, this estimation did not include any cell surface, which restricts molecule diffusion to a half-space and by that effectively increases $C3b^f$ concentration in the remaining volume. The obvious dependency of the spatial $C3b^f$ concentration on fH^s confirms in retrospect that combining PDE and ODE in our hDE approach is required for a correct description of $C3b^f$ concentrations on the cell surface as well as in the fluid phase.

Similarly, we compute the spatial distribution of $C3a^f$ (see **Figure 2B**), which is affected by the amplification process but is not involved in cell surface opsonization. The steady state solution of the corresponding reaction-diffusion equation is given in **Supplementary Material Section 1**. The concentration of $C3a^f$ molecules increases proportional to the concentration of C3-convertase molecules $C3b^sBb$ and $C3b^sBbP$ with decreasing concentration of fH^s. The relatively small $C3a^f$ molecules diffuse up to 100 times further away from the cell surface than $C3b^f$ molecules, due to a decay rate

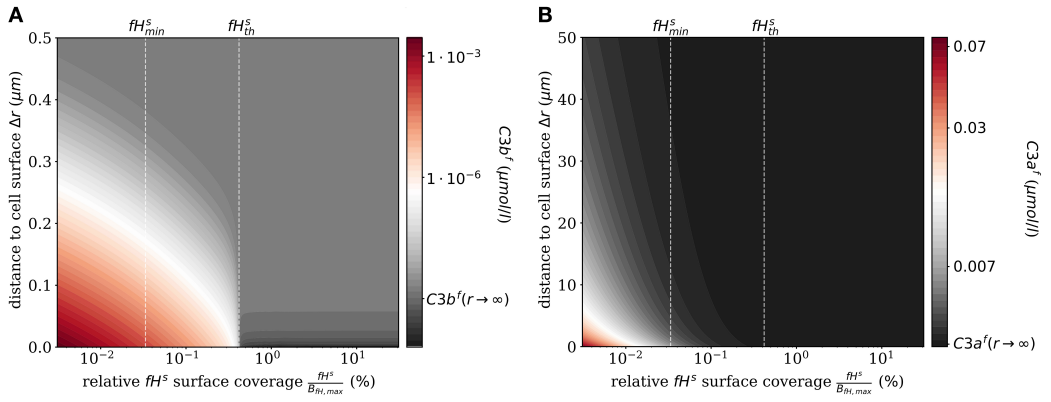

FIGURE 2 | Steady states of the molecules $C3b^f$ and $C3a^f$ in the fluid phase for varying surface-bound Factor H concentrations. **(A)** Radial steady state concentration profile of the fluid-phase $C3b^f$ concentration. **(B)** Radial steady state concentration profile of the fluid-phase $C3a^f$ concentration. Mind the different scales in **(A,B)**.

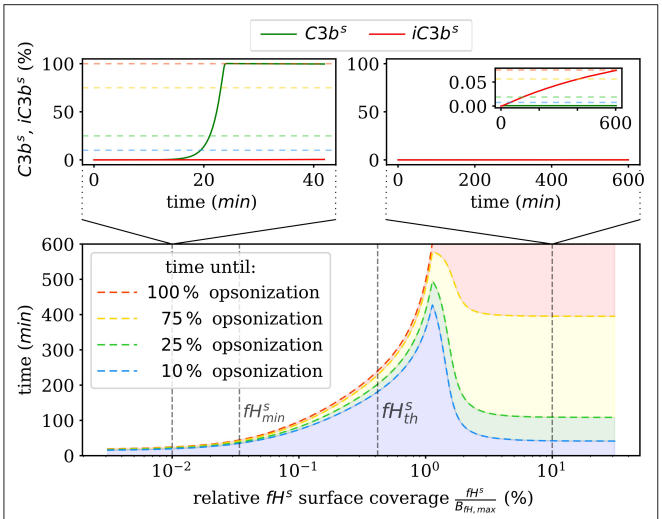

FIGURE 3 | Summary of the numerical integration of 1,000 simulations for varied fH^s concentrations. The time intervals indicate how much time passes until a certain amount of $C3b^s$ is attached to the cell surface. Two typical molecular concentration dynamics are shown for small fH^s concentrations (top left) and high fH^s concentrations (top right).

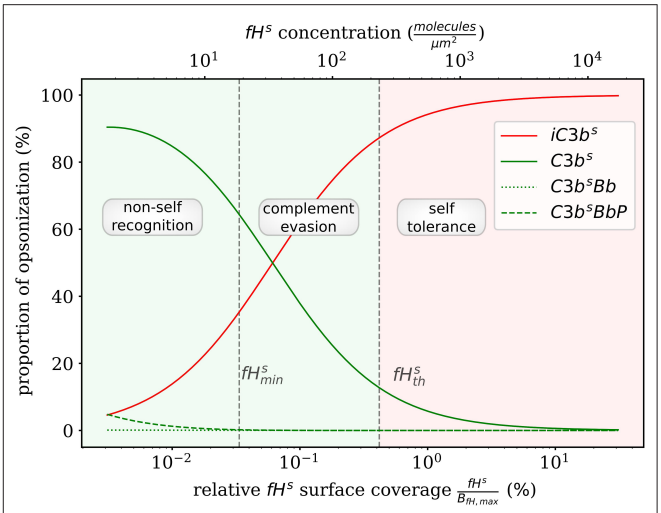

FIGURE 4 | Proportion of *C3b* molecules at the cell surface. Based on the dominating types of *C3b* molecules, we distinguish the two extreme regimes for non-self recognition and self-tolerance that are separated by a transition regime where complement evasion takes place.

of $C3a^f$ molecules that is six orders of magnitude smaller than that of $C3b^f$.

We also numerically integrate the dynamics of the hDE model for $C3b^s$ and $iC3b^s$ according to Equations (1, 2) as well as the dynamics of the amplification process on the surface as given in **Supplementary Material Equations (S41–S44)** of the **Supplementary Material Section 1**. This shows that the steady state is reached within times that are in agreement with the time scales of experimental data. The analysis of the time scales of all processes shows that, with the exception of the amplification process, they can be simplified within a quasi-steady state analysis (QSSA; see **Supplementary Material Section 3**). The resulting time scales are summarized in **Figure 3**, where it can be observed that increasing the fH^s concentration increases the time duration of opsonization. In the DynaCoSys model, cell surfaces with very low $fH^s << fH^s_{th}$ concentrations exhibit the saturation of all binding sites by $C3b^s$ molecules, i.e., about one million $C3b^s$ molecules are bound at the cell surface within 5 min. Sheep erythrocytes, which activate the complement system because of a lack of factor H molecules (30, 31), get opsonized with more than one million $C3b^s$ molecules within this time (29). Thus our model can reproduce the fast opsonization processes on complement activating surfaces. The corresponding opsonization dynamics follow a sigmoidal-shaped curve with a lag-phase of 15 min and a log phase of 5 min (see upper-left inset of **Figure 3**). Cell surfaces with $fH^s < fH^s_{th}$ concentrations reach the steady state in time durations comparable to a variety of pathogens, such as baker's yeast cells ($\sim$ 20 min) and *Escherichia coli* or *Staphylococcus aureus* ($\sim$ 120 min) (32). For fH^s concentrations close to fH^s_{th} the complete opsonization process lasts about 200 min with a maintained ratio of lag to log phase. In the case $fH^s > fH^s_{th}$, the time duration of the opsonization process increases continuously and may be reached after only 6 h with vanishingly small $C3b^s$ concentrations in steady state. Newly bound $C3b^s$ molecules are immediately inactivated. Comparable dynamics are found for sheep erythrocytes (33), where the alternative pathway is not activated due to a high affinity to Factor H (30). Thus the time duration of our simulated data is in agreement with experimental observations. However, our simulated data for $fH^s < fH^s_{th}$ exhibits longer lag phases than experimental data, as for example in (32).

Quantitative Prediction of Factor H Mediated Complement Evasion

Complement evasion is mediated by the level of Factor H concentration at cell surfaces. The level of fH^s governs the opsonization of the cell surface by $C3b^s$ and $iC3b^s$ as well as the C3-convertase products $C3b^sBb$ and $C3b^sBbP$. Our mathematical hDE model enables us to quantify the existence of various regimes. In **Figure 4**, we plot the relative amount of these four molecule concentrations as a function of fH^s for the steady state solution of the *DynaCoSys model*. In the self-regime, the opsonization by $C3b^s$ is strongly suppressed by Factor H yielding a high concentration of inactive derivative $iC3b^s$. However, the non-self regime is subdivided into a regime where non-self recognition takes place and a regime where complement evasion is possible. The latter regime is an intermediate regime with $fH^s_{\min} < fH^s < fH^s_{th}$. The concentration $fH^s_{\min}$ is defined by the minimal number of Factor H molecules that is required that each point on the whole cell surface is within the radius of action of at least one Factor H molecule. This radius is defined by the length of the Factor H molecule chain of about 70 nm (3). Interestingly, our hDE model predicts that this Factor H concentration is associated with values of

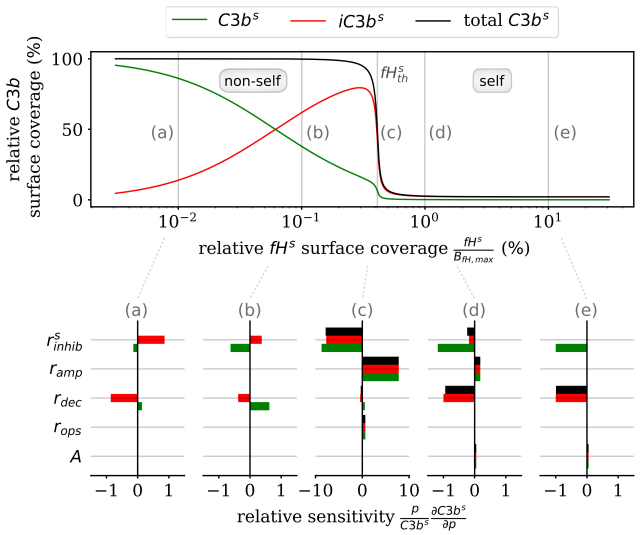

FIGURE 5 | Sensitivity analysis of the model parameters for the steady state of surface-bound *C3b* molecules. The upper plot shows the relative concentration of complement molecules on the cell surface. The lower plots for selected Factor H concentrations give the relative local sensitivity of the complement molecules with respect to a parameter p that is individually varied. Positive sensitivities correlate with increasing molecule concentration. The non-self regime is sensitive to the rates r_{dec} and r^s_{inhib} (see a,b). The transition region (c) is dominated by r^s_{inhib} and r_{amp} and the self-regime is dominated by the parameters A, r_{dec}, r^s_{inhib}, and r_{amp} (see d,e).

$70\% > C3b^s > 10\%$ as well as $30\% < iC3b^s < 90\%$. We refer to this regime as "complement evasion" regime since comparable value ranges have been reported for immune evasive pathogens, such as *E. coli*, *S. aureus*, *Haemophilus influenzae*, *Streptococcus pneumoniae*, and *Streptococcus pyogenes* (32). Except for *S. aureus*, which provides its own membrane molecule taking over Factor H functionality (8, 14), all the other previously mentioned pathogens have been shown to evade complement via Factor H recruitment (16, 34–38). Furthermore, the non-self regime with low Factor H concentrations, $fH^s < fH^s_{\min}$, is associated with $C3b^s$ concentration dominating $iC3b^s$ concentration. In this limit, we also observe increased C3-convertase products $C3b^sBb$ and $C3b^sBbP$ indicating the successful recognition of non-self. This increase in C3-convertase also induces a higher $C3b^f(R)$ concentration at the cell surface (**Figure 2A**). This in turn reduces the duration of the opsonization process, which is up to one order of magnitude shorter compared to the regime of complement evasion (**Figure 3**). As can be seen in **Figure 2B**, in this regime the *C3a* concentration is increased accordingly by the higher C3-convertase.

Furthermore, the *DynaCoSys model* enables us to dissect the individual impact of specific processes on the quantitative prediction of the opsonization level. In **Figure 5**, we plot the $C3b^s$ surface coverage in steady state. Next, we performed a local sensitivity analysis by individually varying model parameters and monitoring their effects on the opsonization level as a function of fH^s. The complete analysis is provided in the **Supplementary Material Section 3**, while **Figure 5** summarizes the results for selected values of fH^s and for the following processes: (i) inhibition on surface with rate r^s_{inhib} (see **Supplementary Material Equation S32**), (ii) amplification with rate r_{amp} (see **Supplementary Material Equation S54**), (iii) $iC3b^s$ decay with rate r_{dec} (see Equation 2), (iv) opsonization with rate r_{ops} (see **Supplementary Material Equation S13**), and (v) spontaneous emergence of $C3b^f$ with flux parameter A (see **Supplementary Material Equation S11**). The basic parameter values are given in the **Supplementary Tables S10, S11** and in the **Supplementary Figure S6**.

In the non-self regime (see **Figures 5**a,b) the two rates r^s_{inhib} and r_{dec} affect $C3b^s$ (green) and $iC3b^s$ (red) in an opposite fashion leaving the total opsonization level (black) unchanged. The total opsonization level in the non-self regime is generally quite constant, i.e., small changes in the model parameters do not have large effects on the close-to-maximal opsonization level. In contrast, the transition between the non-self and self regime (see **Figure 5**c) exhibits the highest relative sensitivities for all model parameters. The system is most sensitive to changes in the two model parameters r^s_{inhib} and r_{amp}, which underlines the importance of these two rates for the transition region. Both effective rates have approximately the same influence on the active as well as the inactive $C3b^s$ molecules and this also affects the total opsonization level at fH^s_{th}. Interestingly, increasing r_{amp} will lead to a right-shift of the transition while increasing r^s_{inhib} will lead to a left-shift of the transition region. The self-regime (see **Figures 5**d,e) is sensitive to the spontaneous activation A, the decay of the inactive $iC3b^s$ molecules r_{dec} as well as r^s_{inhib} and r_{amp}. While the influence of amplification r_{amp} decreases with increasing fH^s concentration, the sensitivity to the spontaneous activation A is constant throughout the regime. In particular, for a relative Factor H surface coverage above $fH^s = 1.72\%$, the spontaneous activation A is the only responsible factor for increasing $C3b^s$ concentrations at the cell surface. In contrast, the non-self regime is not sensitive to the spontaneous activation A pointing toward opsonization that is induced by the amplification process at the cell surface. In general, while $C3b^s$ and $iC3b^s$ are similarly sensitive for A and r_{amp} and thus change the total opsonization level, the rates r_{dec} and r^s_{inhib} change in addition the ratio between $C3b^s$ and $iC3b^s$. Finally, we find that the steady state of the cell surface concentrations does not depend on variations in the opsonization rate r_{ops}. It can thus be concluded that this rate only affects the system dynamics.

Complement Model Parameters Have Differential Impact on Critical Factor H Concentration

We investigate how the steady state of the DynaCoSys model behaves by screening various model parameters around their standard values given in **Supplementary Tables S8–S11**. Of particular interest are the molecule concentrations in the fluid phase, which can change depending on disease conditions as well as on medical treatments. The results are plotted for the concentration of all C3b molecules on the cell surface relative

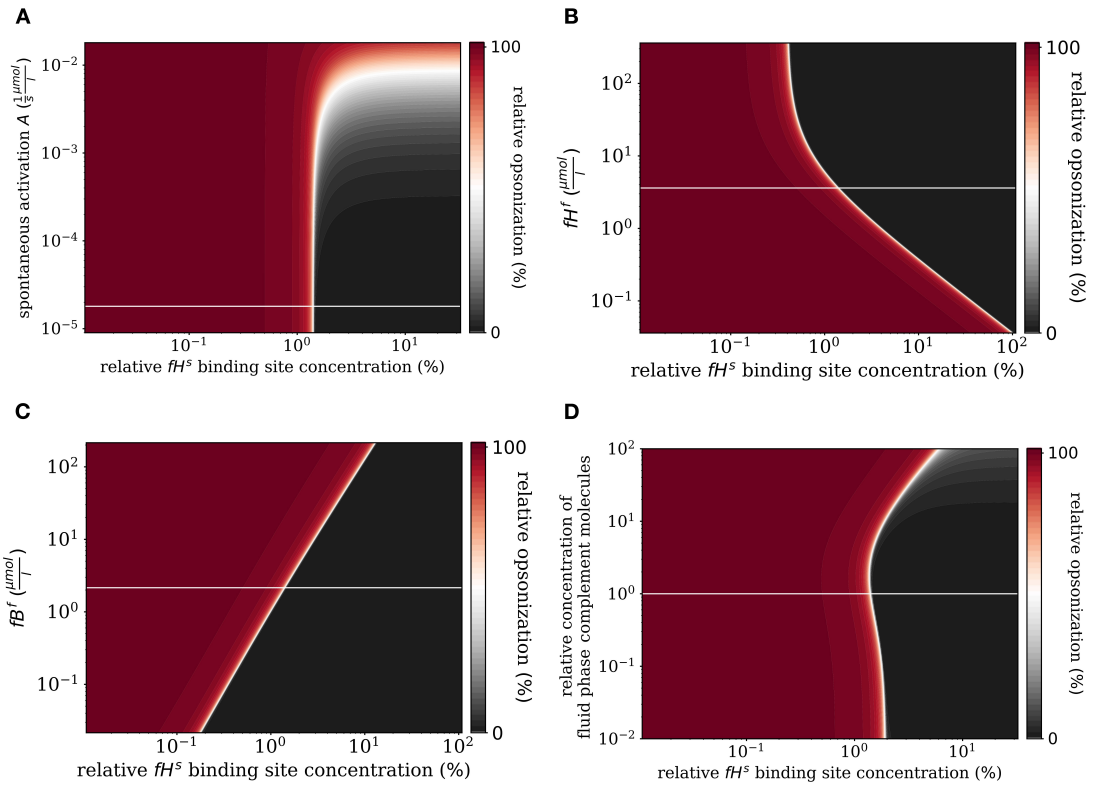

FIGURE 6 | Relative opsonization in the steady state for varied system parameters as a function of the relative Factor H binding site concentration. The white line indicates the *DynaCoSys model* for standard parameter values. **(A)** Variation of the spontaneous $C3b^f$ activation A, **(B)** variation of the fH^f concentration, **(C)** variation of the fB^f concentration, and **(D)** variation of the relative concentration of complement molecules in the fluid phase.

to the binding site concentration and as a function of the relative Factor H binding site concentration, i.e., the ratio of the concentration of binding sites for Factor H relative to its maximal concentration.

First, we varied the spontaneous $C3b^f$ activation A (see Equation 3). Increasing this parameter affects only the self-regime by increasing the molecular concentration of all C3b molecules on the cell surface (**Figure 6A**). While the threshold value fH^s_{th} remains the same, the self and non-self regime can no longer be distinguished for an increase of A by more than two orders of magnitude, since complete opsonization occurs in the self-regime. Furthermore, variation of fH^f affects the fH^s concentration on the cell surface (**Figure 6B**). With increasing fH^f concentration, more fH^s molecules bind, accelerating both the inhibition of $C3b^s$, and the decay of the C3-convertase. For increased fH^f concentrations above one order of magnitude, fH^s becomes saturated. It follows that the threshold between the non-self and self regimes is shifted toward smaller relative Factor H binding sites concentrations, i.e., for higher fH^f concentrations a cell is tolerated as self with less Factor H binding sites. In contrast, since the molecules $C3^f$, Factor B (fB^f), Factor D (fD^f), and properdin(fP^f) each enhance the amplification process positively (see **Supplementary Material Sections 1, 3**), increasing their concentrations is associated with shifts in fH^s_{th} to higher relative Factor H binding sites concentrations. In particular, fB^f shows the largest effect of these molecules involved in the amplification process (see **Figure 6C** and **Supplementary Material Section 3**). Decreasing the fluid phase concentration, i.e., the concentration of each complement molecule, is often done in experiment to slow down the dynamics of the opsonization processes. In **Figure 6D**, we scan the behavior of the system for varied fluid phase concentrations. We find that an increased serum concentration leads to increased opsonization, which is characterized by a shift of fH^s_{th} to higher binding site concentrations. The *DynaCoSys model* elucidates that, since above a certain fH^f concentration the Factor H binding sites on the cell surface are occupied, the $C3b^s$ inactivation as well as cleavage of C3-convertase by Factor H are outcompeted by the amplification process. The decrease of the fluid phase concentration by up to two orders of magnitude exhibits a fairly constant threshold value fH^s_{th}.

In addition to the variation of complement molecules, we here investigate the dissociation constant of Factor H and the cell surface ($K_{d,fH}$, see **Supplementary Material Section 1**) and the reaction rate of fH^s binding to $C3b^s$ (r^+_{fH}, see **Supplementary Material Section 1**). In the literature, both parameter values appear with large intervals of more than two orders of magnitude as well as quantitative variations depending on the type of cell surface (29). These also play a role in disease conditions caused by mutations that affect either cellular

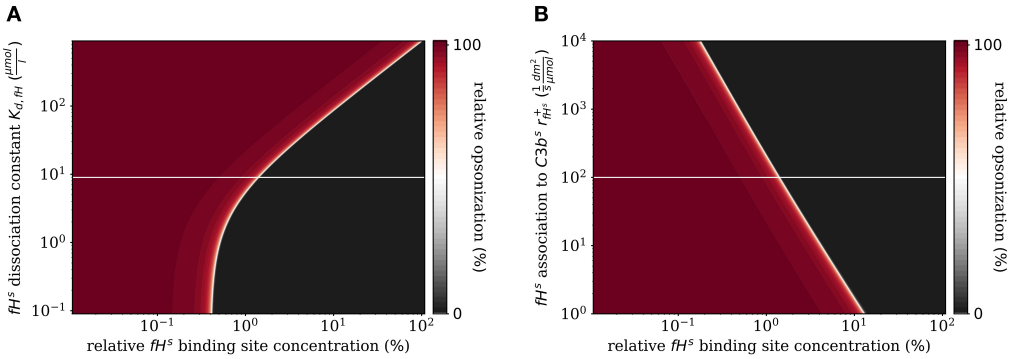

FIGURE 7 | Relative opsonization in the steady state for varied system parameters as a function of the relative Factor H binding site concentration. The white line indicates the *DynaCoSys model* for standard parameter values. **(A)** Variation of the dissociation constant for Factor H and binding sites on the cell surface. **(B)** Variation of the reaction rate for fH^s binding to $C3b^s$ molecules.

properties or the Factor H molecule binding to a cell surface (39, 40). For example, in patients with the atypic hemolytic uremic syndrome (aHUS) the dissociation constant $K_{d,fH}$ and the binding rate r^+_{fH} are, respectively, increased and decreased. The *DynaCoSys model* predicts that increasing the dissociation constant by two orders of magnitude leads to a complete opsonization of the cell surface regardless of the Factor H binding site concentration (**Figure 7A**). Thus, this implies that non-self and self cells alike will be attacked by the complement system establishing a permanent inflammatory milieu. Similarly, decreasing r^+_{fH} by two orders of magnitude causes massive shift of fH^s_{th} by a factor of ten to higher fH^s binding site concentrations (**Figure 7B**). We conclude that both the dissociation constant $K_{d,fH}$ (**Figure 7A**) and the concentration of fH^f (**Figure 6B**) have a larger influence on the steady state than r^+_{fH} if they are varied to the same extent.

DISCUSSION

In this study, we introduced the mathematical model *DynaCoSys* to simulate the dynamics of the complement system and to quantify the Factor H mediated self vs. non-self discrimination. The model focuses on the derivatives of the central complement molecule C3 and is based on a hybrid differential equation (hDE) approach, which combines ordinary differential equations (ODEs) and partial differential equations (PDEs) in one framework. To the best of our knowledge, *DynaCoSys* is the first model that models the dynamics on the cell surface using ODEs and using PDEs for the fluid phase that surrounds a cell. Previous models are typically based on ODEs only (19–21, 41–43) and do thus neglect the spatial distribution of *C3b* concentrations in the fluid phase. Compared to these models, which are trimmed for modeling details at the overwhelming costs of many parameters with large uncertainties in their unknown values (20, 21), the hDE approach of the *DynaCoSys model* allows reducing the number of model parameters by one order of magnitude. In particular, *DynaCoSys* involves only 35 model parameters of which the values for 34 parameters can be deduced from the literature (see **Supplementary Tables S8–S11**). The only remaining parameter that is unknown is the reaction rate of fH^s binding to $C3b^s$ on the cell surface (r^+_{fH}), for which we applied a screening over 4 orders of magnitude (see **Figure 7B**). Furthermore, our model reveals that the concentration difference between the cell surface and the surrounding fluid phase covers six orders of magnitude confirming the importance of pursuing the hDE approach. Moreover, our analysis revealed for typical cell concentrations in blood, that these cells can be considered as independent with regard to the concentration $C3b^s$ on cell surfaces and $C3b^f$ in the fluid phase. In the future, *DynaCoSys* may be used as a starting point for modeling complement dynamics in aggregates of cells.

We applied a quasi-steady-state-approximation (QSSA) that enables reducing the full dynamics of the *DynaCoSys model* by five ODEs including twelve model parameters. These simplifications are made at the expense of some loss of accuracy in describing the complement dynamics. In the **Supplementary Figure S9**, we analyze the applicability of QSSAs and conclude that the QSSA for the dynamics of $C3b^f$, the complement activation of the fluid phase as well as the regulation on the cell surface are well suited, because the time scales of these processes are at least one order of magnitude small than the time scale of the $C3b^s$ dynamics. However, this argument does not hold for the amplification process, because its time scale is of the same order of magnitude compared to the $C3b^s$ dynamics for $fH^s < fH^s_{th}$. In this case, the complete dynamics of the amplification process must be considered. By performing numerical simulations we showed that our model does provide quantitative results comparable to other models (20) and to experimental data. For example, complement activation in the non-self regime shows the typical sigmoidal shape with in the order of one million C3b molecules being bound within minutes as described by Pangburn et al. (29). In addition, the time durations for which the steady state is reached in the case of non-self cells are comparable to those measured for a variety of pathogens, such as *E. coli* or *S. aureus* (32). As expected, for the self-regime our model predicts significantly slower as well as lower opsonization due to the immediate

deactivation of C3b on the cell surface by complement regulator Factor H.

Apart from these agreements between the mathematical model and experimental measurements, we also observe two differences. The first difference is with regard to the duration of the lag phase, which our simulations predict to be more extended than typically found in experiment. However, experiments also show that cells are very heterogenous regarding their C3b concentration during the lag phase (29). The lag phase is largely determined by the time it takes until the amplification loop on the cell surface has started (29). Spontaneously formed C3b molecules originating from the tick over process attach randomly on cell surfaces (5, 29), such that C3b amplification will start on some cells earlier than on others. This discrepancy can be explained by the fact that our hDE approach is based on differential equations and, thus, on the implicit assumption that molecules are present at high concentration levels. Similar deviations from experiment with regard to the lag phase are observed for the ODE-based model by Zewde et al. (20) supporting the interpretation that modeling the lag phase is inaccurate where only a few molecules exist on the cell surface. The limit of only a few molecules on the cell surfaces also affects the interaction of $C3b^s$ and fH^s, since the distribution of molecules are no longer representative for a homogeneous distribution on the cell surface. In order to model this limit correctly, a spatial agent-based approach may be used. However, an agent-based approach is associated with substantially higher computational load as well as additional parameters for the motion of each molecule. Another simplification of our model concerns the binding strength of Factor H, which for the sake of simplicity we set to a fixed value. Thus, even though the polymorphism of Factor H induces different binding strengths to the cell surface (27, 44), we considered the mean value of the associated distribution in terms of a constant dissociation constants ($K_{d,fH}$). Taking a distribution for the binding strengths into account would broaden the relatively sharp transition between the self and non-self regime as a function of fH^s in the vicinity of fH^s_{th} (see e.g., **Figure 5**, upper panel).

The second difference between the dynamics predicted by *DynaCoSys* and the dynamics in experiment is the abrupt saturation of the $C3b^s$ concentration. On surfaces with high $C3b^s$ concentrations, the C3-convertase molecule changes its affinity from a C3 substrate toward a C5 substrate (5, 45). Cleavage of C5 results into the molecules C5a and C5b. Here, the anaphylatoxin C5a is a proinflammatory protein that activates immune cells (5), while the fragment C5b initiates the terminal pathway of the complement system involving the formation of membrane attack complexes (MACs) on the cell surface (5). Associated with the C5 convertase, which is not part of the current version of *DynaCoSys*, less C3 molecules are cleaved and the $C3b^s$ amplification loop slows down in experiment. In other words, our model overestimates the amplification of $C3b^s$: while the flux of new $C3b^s$ molecules is expected to decrease with increasing $C3b^s$ concentration, the flux decreases abruptly when the surface is almost completely occupied. We decided against including the dynamics of the C5-convertase in the first version of the model, because—in contrast to the C3-convertase—no experimentally measured rates can be deduced from the literature. Related to this, opinions in the literature are divided about the affinity shifting of the convertase: in some studies it is concluded that an additional $C3b^s$ molecule binds to the C3-convertase (46, 47), while other experiments seem to suggest that the increased concentration of $C3b^s$ may cause a shift from the C3 substrate toward the C5 substrate (45). Since neither the reactions nor their rates can be unambiguously deduced from the literature, we decided against including the C5 cascade and the terminal pathway in a first version of the model.

In addition to C3b opsonization, complement modulates the immune response of the innate and adaptive immune system (3, 5). However, while the complement system responds to acute infections within a few minutes up to a maximum of a few hours, the innate and adaptive immune responses react on time scales of several hours and days to weeks, respectively. Therefore, the steady state of the complement system is of particular importance for the immune response on longer time scales. For this reason, models that study the interaction of immune cells with pathogens often consider the complement system to be in steady state (48, 49). Furthermore, the steady state offers the possibility to analyze predictions of the model analytically. While other models typically distinguish only between pathogens and host cells (20), the low computational effort of our analytical steady state solution allows for screening the whole space of unknown parameters, including also aspects like the binding site concentration of Factor H. The possibility to apply an in-depth screening enables identifying regimes by characteristic complement concentrations on the cell surface. Furthermore, we can observe transitions between such regimes and define thresholds derived from the analytical solution of our model in steady state. In this way, we identified the self-regime by nearly absent C3b molecules for high Factor H concentrations on the cell surface as well as the non-self regime, with an almost completely opsonized cells surface for relatively low Factor H concentrations. While the ratio of $iC3b^s$ to $C3b^s$ changes only slightly in the self-regime, a strong shift of this ratio is observed in the non-self regime. For pathogens this shift is of vital importance, even if the absolute number of complement molecules on the surface does not change. Non-active $iC3b^s$ molecules imply a lower concentration of $C3a^f$ and $C3b^f$ molecules. As a consequence, the opsonization process is slower and the inflammatory milieu caused by $C3a^f$ is much less pronounced, which increases the chance of the pathogens to survive the attack of the complement system. The transition between the regimes of non-self recognition and of self-tolerance is associated with the mathematically defined threshold fH^s_{th}, which marks the maximum change in the opsonization of the cell surface with respect to the Factor H concentration. Nevertheless, the transition between the non-self and self regimes is smooth and leaves room for an intermediate regime. In this regime, pathogens can evade the attack of the complement system by strongly lowering their opsonization level and by that protecting themselves from the immune response (50). On the other hand, self-cells can also fall below the threshold value fH^s_{th} and become more recognizable for the complement system, e.g.,

dying cells undergoing apoptosis (5). Apoptosis is associated by the induction of specific intracellular pathways that also affect the cell surface (51) and is characterized by decreased Factor H concentrations (51) as well as a relatively large iC3b ratio (52), which renders apoptotic cells more recognizable by phagocytes for removal. Our sensitivity analysis revealed that the inhibition rate r^s_{inhib}, which is responsible for the inactivation of $C3b^s$ to $iC3b^s$, has a clear effect on surface molecule concentrations in both the non-self and self regime. This result supports the hypothesis that the recognition function of the complement system is in the interaction between surface-bound C3b and Factor H (28, 29, 50).

The *DynaCoSys model* of the complement system enables screening for the impact of various parameters and evaluating changes in the recognition of the cell surface in steady state. In particular, we can analyze pathological conditions that are directly associated with the complement system for three different reasons (24): (i) excessive complement activation exhausting the regular defense against complement damage, e.g., in the context of sepsis and immune complex disease (53, 54), (ii) lowered host defense against complement activation, e.g., syndromes like atypical hemolytic uremic syndrome (aHUS) that are caused by mutations (9), and (iii) altered host cells that activate the complement system, e.g., ischemia/reperfusion, burns, apoptotic/necrotic cells (55). The excessive complement activation can be associated with an increased $C3b^f$ level. This can lead to an extreme increase in the opsonization level, even within the regime of self-tolerance. In particular, self-cells that are in close contact with complement-activating non-self cells during an immune response are exposed to this potential threat and may no longer be able to avoid their opsonization (56). This is another motivation to extend the *DynaCoSys model* to several interacting cells in contact, where also therapies that focus on the suppression of the activation of the alternative pathway may be simulated. Various approaches may be considered: (i) inhibition of C3 activation, (ii) inhibition of convertases, and (iii) inhibition of activating enzymes like Factor B or Factor D (12, 57). Our results show that the reduction of individual complement molecules, like Factor B, has a large impact on the opsonization of cell surfaces.

The treatment of diseases caused by immune evasive pathogenic microbes becomes more and more important due to increasing case numbers (58) and rising mortality (59). One of these pathogens with increasing case numbers is *Candida albicans*, which evades opsonization by the complement system through various mechanisms (60). Firstly, *C. albicans* can express several surface molecules with high affinity to Factor H (61). By including this effective increase of binding sites, the *DynaCoSys model* may be used to identify the most important binding sites. Secondly, *C. albicans* releases proteins that prevent the cleavage of C3 in the fluid phase and thus reduce C3b production in the vicinity of the cell surface (62). Our *DynaCoSys model* may be applied to monitor the dynamics in the fluid phase in order to elucidate this evasion mechanism. Taken together, the here established *DynaCoSys model* will be very well suited for detailed investigations of mechanisms of immune evasion in the future.

METHODS

The *DynaCoSys model* focuses on the three consecutive states of the central complement molecule *C3b*: the fluid phase molecule $C3b^f$, the surface-bound molecule $C3b^s$ and the inactivated surface-bound molecule $iC3b^s$. The dynamics of other complement molecules are lumped into processes that are represented by effective rates under the following assumptions:

(i) Complement cofactor molecule concentrations can be considered as being constant in the fluid phase, because their consumption is negligibly small compared to their absolute concentrations. This reasonable assumption was also used in previous models of the complement system (20, 41, 42).
(ii) The quasi steady state approximation can be applied to the dynamics of complement molecules with concentrations that equilibrate relatively fast compared to the main dynamics of the complement system (29, 63, 64).

In the next sections we summarize the main processes included in the *DynaCoSys model*. The model is described in full detail in the **Supplementary Material Section 1**. There we introduce the 37 reactions that are considered for the differential equations, we introduce the coupling between ODEs on the cell surface and PDEs in the fluid around the cell and we explain the simplifications that are done to obtain the Equations (1–5).

Binding of Factor H to Cell Surface

The fluid-phase complement regulator Factor H is able to bind to binding sites at the cell surface (compare **Figure 1A**, orange box) (3, 9). Since the opsonization process of cell surfaces is characterized by a lag phase (33), it can be assumed that the Factor H concentration on the surface, fH^s, is in a steady state. The concentration of surface-bound Factor H depends on the dissociation constant, $K_{d,fH}$, the fluid phase concentration of Factor H, fH^f, and the maximum concentration of binding sites, $B_{fH,\max}$, at the cell surface. The surface-bound Factor H concentration influences the Equations (1, 2, 4).

Complement Activation in Fluid Phase

The activation of the alternative pathway takes place in the fluid phase and involves the spontaneous hydrolysis of $C3^f$ (compare **Figure 1A**, blue box, activation). In the presence of the two co-Factor molecules Factor B (fB^f) and Factor D (fD^f) the initial C3-convertase $C3(H2O)Bb$ is formed, which cleaves $C3^f$ enzymatically into $C3b^f$ and $C3a^f$ (29, 65). The equilibrium concentration of the initial C3-convertase is proportional to the concentration of the precursor molecule $C3^f$. Since $C3^f$ is assumed to be constant in this model (see assumption i), there is a constant inflow of $C3b^f$ molecules into the system given by the flux parameter *A*. The influx of $C3b^f$ increases the $C3b^f$ (r) concentration as described by Equations (3, 5).

Binding of Fluid-Phase C3b to Cell Surface

Upon cleavage by C3-convertase, the $C3b^f$ molecule exposes a highly reactive thioester bond (29, 66, 67). In aqueous solutions, this binding site has a very short half-life time of 60 μs (29).

The molecule can either bind to a cell surface with high affinity (24, 68) or it is inactivated, for example, by binding to a water molecule or by complement regulators (29). This opsonization process is modeled by the effective rate r_{ops} and is associated with the consumption of free binding sites $B_{C3b,free}$ (**Figure 1A**, yellow box, opsonization). The opsonization process increases $C3b^s$ (see Equation 1) and decreases the flux of $C3b^f$ (see Equation 4). The concentration of free binding sites can be calculated using mass conservation considerations. Binding sites are occupied by active $C3b$, $C3b^s$, intermediate products like C3-convertase molecules and inactive C3b: $iC3b^s$. The inactivation process due to binding of a water molecule is modeled by an exponential decay with rate r_{stab} (**Figure 1A**, yellow box, stabilization) and appears in Equations (3, 5).

Regulation of Active C3b Molecules

The regulation of the complement system takes place both in the fluid phase and on the cell surface. Factor H promotes the cleavage of $C3b^f$ and $C3b^s$ by Factor I into $C3b^f$ and $C3b^s$ via the same molecule cascade. The effective rates r^f_{inhib} and r^s_{inhib} summarize their dynamics, respectively, in the fluid and on the surface (**Figure 1A**, red box, regulation). This is accounted for by the surface dynamics in the Equations (1, 2) as well as by the fluid-phase dynamics in Equations (3, 5).

Amplification of Surface-Bound C3b Molecules

The amplification mechanism includes the formation of C3-convertase based on surface-bound $C3b^s$ molecules and the cleavage of $C3^f$ molecules by the C3-convertase molecules resulting into the amplification of $C3b^f$ concentration close to the cell surface. As in the fluid phase, $C3b^s$ molecules react with Factor B and Factor D in order to form the C3-convertase molecule (29, 65). The formation of the C3-convertase is regulated by complement protein Factor H, which interferes sterically with C3-convertase complexes and accelerates the decay of these complexes (68, 69). The life time of a C3-convertase complex increases if properdin (fP^f) binds to the complex (70, 71). It is also known to decelerate the C3-convertase decay, driven by Factor H (69, 71–73). Cleavage of the $C3^f$ molecules to $C3b^f$ and $C3a^f$ is, as in the activation part, modeled by Michaelis-Menten kinetics. As the precursor molecules $C3^f$ do not bind to the cell membrane, the nascent $C3b$ molecule will belong to the fluid phase. The inflow of nascent $C3b^f$ molecules at the cell surface is directly proportional to the $C3b^s$ concentration with the effective rate r_{amp} (fH^s), which enters (Equation 4) of the model.

DATA AVAILABILITY STATEMENT

The original contributions presented in the study are included in the article/**Supplementary Material**, further inquiries can be directed to the corresponding author/s.

AUTHOR CONTRIBUTIONS

AT and MTF conceived and designed this study, drafted the manuscript, revised it critically for important intellectual content, and final approval of the version to be published. MTF provided computational resources. Data processing, implementation and application of the computational algorithm were done by AT and TL. AT, TL, PZ, and MTF evaluated and analyzed the results of this study, and agree to be accountable for all aspects of the work in ensuring that questions related to the accuracy or integrity of any part of the work are appropriately investigated and resolved. All authors contributed to the article and approved the submitted version.

FUNDING

This work was financially supported by the International Leibniz Research School for Microbial and Biomolecular Interactions (ILRS) and by the Deutsche Forschungsgemeinschaft through the CRC/TR124 FungiNet under DFG project number 210879364 (project B4 to MTF and project C6 to PZ).

SUPPLEMENTARY MATERIAL

The Supplementary Material for this article can be found online at: https://www.frontiersin.org/articles/10.3389/fimmu.2020.01911/full#supplementary-material

REFERENCES

1. Walport MJ. Complement. First of two parts. *N Engl J Med*. (2001) 344:1058–66. doi: 10.1056/NEJM200104053441406
2. Lachmann PJ. The amplification loop of the complement pathways. In: Alt FW, editor. *Advances in Immunology*. San Diego, CA: Elsevier (2009) 4, 115–49. doi: 10.1016/S0065-2776(08)04004-2
3. Zipfel PF, Skerka C. Complement regulators and inhibitory proteins. *Nat Rev Immunol*. (2009) 9:729–40. doi: 10.1038/nri2620
4. Flaherty D, editor. Complement. In: *Immunology for Pharmacy*. Saint Louis, MO: Mosby (2012). p. 87–96. doi: 10.1016/B978-0-323-06947-2.10011-2
5. Merle NS, Church SE, Fremeaux-Bacchi V, Roumenina LT. Complement system part I - molecular mechanisms of activation and regulation. *Front Immunol*. (2015) 6:262. doi: 10.3389/fimmu.2015.00262
6. Medzhitov R, Janeway CA Jr. Decoding the pattern of self and nonself by the innate immune system. *Science*. (2002) 296:298–300. doi: 10.1126/science.1068883
7. Ogden CA, Elkon KB. Role of complement and other innate immune mechanisms in the removal of apoptotic cells. *Curr Dir Autoimmun*. (2006) 9:120–42. doi: 10.1159/000090776
8. Ricklin D, Hajishengallis G, Yang K, Lambris JD. Complement - a key system for immune surveillance and homeostasis. *Nat Immunol*. (2010) 11:785–97. doi: 10.1038/ni.1923
9. Noris M, Remuzzi G. Overview of complement activation and regulation. *Semin Nephrol*. (2013) 33:479–92. doi: 10.1016/j.semnephrol.2013.08.001
10. Ricklin D. Manipulating the mediator: Modulation of the alternative complement pathway C3 convertase in health, disease and therapy. *Immunobiology*. (2012) 217:1057–66. doi: 10.1016/j.imbio.2012.07.016
11. Noris M, Remuzzi G. Translational mini-review series on complement factor H: therapies of renal diseases associated with complement

factor H abnormalities: atypical haemolytic uraemic syndrome and membranoproliferative glomerulonephritis. *Clin Exp Immunol.* (2007) 151:199–209. doi: 10.1111/j.1365-2249.2007.03558.x
12. Morgan PB, Harris CL. Complement, a target for therapy in inflammatory and degenerative diseases. *Nat Rev Drug Discov.* (2015) 14:857–77. doi: 10.1038/nrd4657
13. Zipfel PF, Würzner R, Skerka C. Complement evasion of pathogens: common strategies are shared by diverse organisms. *Mol Immunol.* (2007) 44:3850–7. doi: 10.1016/j.molimm.2007.06.149
14. Lambris JD, Ricklin D, Geisbrecht BV. Complement evasion by human pathogens. *Nat Rev Microbiol.* (2008) 6:132–42. doi: 10.1038/nrmicro1824
15. Zipfel P, Hallström T, Riesbeck K. Human complement control and complement evasion by pathogenic microbes–tipping the balance. *Mol Immunol.* (2013) 56:152–60. doi: 10.1016/j.molimm.2013.05.222
16. Zipfel P, Hallström T, Hammerschmidt S, Skerka C. The complement fitness factor H: role in human diseases and for immune escape of pathogens, like pneumococci. *Vaccine.* (2008) 26:I67–74. doi: 10.1016/j.vaccine.2008.11.015
17. Dasari P, Koleci N, Shopova IA, Wartenberg D, Beyersdorf N, Dietrich S, et al. Enolase from aspergillus fumigatus is a moonlighting protein that binds the human plasma complement proteins factor H, FHL-1, C4BP, and plasminogen. *Front Immunol.* (2019) 10:2573. doi: 10.3389/fimmu.2019.02573
18. Dasari P, Shopova IA, Stroe M, Wartenberg D, Martin-Dahse H, Beyersdorf N, et al. Aspf2 from aspergillus fumigatus recruits human immune regulators for immune evasion and cell damage. *Front Immunol.* (2018) 9:1635. doi: 10.3389/fimmu.2018.01635
19. Liu B, Zhang J, Tan PY, Hsu D, Blom AM, Leong B, et al. A computational and experimental study of the regulatory mechanisms of the complement system. *PLoS Comput Biol.* (2011) 7:e1001059. doi: 10.1371/journal.pcbi.1001059
20. Zewde N, Gorham RD, Dorado A, Morikis D. Quantitative modeling of the alternative pathway of the complement system. *PLoS ONE.* (2016) 11:e0152337. doi: 10.1371/journal.pone.0152337
21. Morikis NZD. A computational model for the evaluation of complement system regulation under homeostasis, disease, and drug intervention. *PLoS ONE.* (2018) 13:e019864. doi: 10.1371/journal.pone.0198644
22. Conrad EC, Hsu YY, Bortz DM, Younger JG. Spatiotemporal dynamics of complement C5a production within bacterial extracellular polymeric substance. *J Innate Immun.* (2013) 5:114–23. doi: 10.1159/000345705
23. Heinrich V, Simpson WD, Francis EA. Analytical prediction of the spatiotemporal distribution of chemoattractants around their source: theory and application to complement-mediated chemotaxis. *Front Immunol.* (2017) 8:578. doi: 10.3389/fimmu.2017.00578
24. Pangburn MK, Ferreira VP, Cortes C. Discrimination between host and pathogens by the complement system. *Vaccine.* (2008) 26(Suppl. 8):15–21. doi: 10.1016/j.vaccine.2008.11.023
25. Liszewski MK, Fang CJ, Atkinson JP. Inhibiting complement activation on cells at the step of C3 cleavage. *Vaccine.* (2008) 26(Suppl. 8):22–7. doi: 10.1016/j.vaccine.2008.11.001
26. Ferreira VP, Herbert AP, Hocking HG, Barlow PN, Pangburn MK. Critical role of the C-terminal domains of factor H in regulating complement activation at cell surfaces. *J Immunol.* (2006) 177:6308–16. doi: 10.4049/jimmunol.177.9.6308
27. Perkins SJ, Nan R, Li K, Khan S, Miller A. Complement factor H-ligand interactions: self-association, multivalency and dissociation constants. *Immunobiology.* (2012) 217:281–97. doi: 10.1016/j.imbio.2011.10.003
28. Pangburn MK. Host recognition and target differentiation by factor H, a regulator of the alternative pathway of complement. *Immunopharmacology.* (2000) 49:149–57. doi: 10.1016/S0162-3109(00)80300-8
29. Pangburn MK, Müller-Eberhard HJ. The alternative pathway of complement. *Semin Immunopathol.* (1984) 7:163–92. doi: 10.1007/BF01893019
30. Ezzell JL, Parker CJ. Cell-surface regulation of the human alternative pathway of complement. *Scand J Immunol.* (1992) 36:79–88. doi: 10.1111/j.1365-3083.1992.tb02943.x
31. Fearon D, Austen K. Activation of the alternative complement pathway with rabbit erythrocytes by circumvention of the regulatory action of endogenous control proteins. *J Exp Med.* (1977) 146:22–33. doi: 10.1084/jem.146.1.22
32. Newman SL, Mikus LK. Deposition of C3b and iC3b onto particulate activators of the human complement system. *J Exp Med.* (1985) 161:1414–31. doi: 10.1084/jem.161.6.1414
33. Pangburn MK, Schreiber RD, Müller-Eberhard HJ. C3b deposition during activation of the alternative complement pathway and the effect of deposition on the activating surface. *J Immunol.* (1983) 131:1930–5.
34. Abreu AG, Barbosa AS. How *Escherichia coli* circumvent complement-mediated killing. *Front Immunol.* (2017) 8:452. doi: 10.3389/fimmu.2017.00452
35. Hallström T, Zipfel PF, Blom AM, Lauer N, Forsgren A, Riesbeck K. Haemophilus influenzae interacts with the human complement inhibitor factor H. *J Immunol.* (2008) 181:537–45. doi: 10.4049/jimmunol.181.1.537
36. Hallström T, Riesbeck K. Haemophilus influenzae and the complement system. *Trends Microbiol.* (2010) 18:258–65. doi: 10.1016/j.tim.2010.03.007
37. Laabei M, Ermert D. Catch me if you can: *Streptococcus pyogenes* complement evasion strategies. *J Innate Immun.* (2018) 11:3–12. doi: 10.1159/000492944
38. Pathak A, Bergstrand J, Sender V, Spelmink L, Aschtgen M-S, Muschiol, et al. Factor H binding proteins protect division septa on encapsulated *Streptococcus pneumoniae* against complement C3b deposition and amplification. *Nat Commun.* (2018) 9:1–16. doi: 10.1038/s41467-018-05494-w
39. Wong EKS, Goodship THJ, Kavanagh D. Complement therapy in atypical haemolytic uraemic syndrome (aHUS). *Mol Immunol.* (2013) 56:199–212. doi: 10.1016/j.molimm.2013.05.224
40. Manuelian T, Hellwage J, Meri S, Caprioli J, Noris M, Heinen S, et al. Mutations in factor H reduce binding affinity to C3b and heparin and surface attachment to endothelial cells in hemolytic uremic syndrome. *J Clin Invest.* (2003) 111:1181–90. doi: 10.1172/JCI16651
41. Hirayama H, Yoshii K, Ojima H, Kawai N, Gotoh S, Fukuyama Y. Linear systems analysis of activating processes of complement system as a defense mechanism. *Biosystems.* (1996) 39:173–85. doi: 10.1016/0303-2647(96)01617-6
42. Korotaevskiy AA, Hanin LG, Khanin MA. Non-linear dynamics of the complement system activation. *Math Biosci.* (2009) 222:127–43. doi: 10.1016/j.mbs.2009.10.003
43. Sagar A, Dai W, Minot M, Varner JD. Reduced order modeling and analysis of the human complement system. *PLoS ONE.* (2017) 12:e187373. doi: 10.1371/journal.pone.0187373
44. Herbert AP, Uhrín D, Lyon M, Pangburn MK, Barlow PN. Disease-associated sequence variations congregate in a polyanion recognition patch on human factor H revealed in three-dimensional structure. *J Biol Chem.* (2006) 281:16512–20. doi: 10.1074/jbc.M513611200
45. Berends ETM, Gorham RD, Ruyken M, Soppe JA, Orhan H, Aerts PC, et al. Molecular insights into the surface-specific arrangement of complement C5 convertase enzymes. *BMC Biol.* (2015) 13:8. doi: 10.1186/s12915-015-0203-8
46. Hong K, Kinoshita T, Pramoonjago P, Kim YU, Seya T, Inoue K. Reconstitution of C5 convertase of the alternative complement pathway with isolated C3b dimer and factors B and D. *J Immunol.* (1991) 146:1868–73.
47. Rawal N, Pangburn MK. C5 convertase of the alternative pathway of complement. *J Biol Chem.* (1998) 273:16828–35. doi: 10.1074/jbc.273.27.16828
48. Hünniger K, Lehnert T, Bieber K, Martin R, Figge MT, Kurzai O. A virtual infection model quantifies innate effector mechanisms and candida albicans immune escape in human blood. *PLoS Comput Biol.* (2014) 10:e3479. doi: 10.1371/journal.pcbi.1003479
49. Lehnert T, Timme S, Pollmächer J, Hünniger K, Kurzai O, Figge MT. Bottom-up modeling approach for the quantitative estimation of parameters in pathogen-host interactions. *Front Microbiol.* (2015) 6:608. doi: 10.3389/fmicb.2015.00608
50. Meri S. Self-nonself discrimination by the complement system. *FEBS Lett.* (2016) 590:2418–34. doi: 10.1002/1873-3468.12284
51. Trouw LA, Blom AM, Gasque P. Role of complement and complement regulators in the removal of apoptotic cells. *Mol Immunol.* (2008) 45:1199–207. doi: 10.1016/j.molimm.2007.09.008
52. Takizawa F, Tsuji S, Nagasawa S. Enhancement of macrophage phagocytosis upon iC3b deposition on apoptotic cells. *FEBS Lett.* (1996) 397:269–72. doi: 10.1016/S0014-5793(96)01197-0
53. Markiewski MM, DeAngelis RA, Lambris JD. Complexity of complement activation in sepsis. *J Cell Mol Med.* (2008) 12:2245–54. doi: 10.1111/j.1582-4934.2008.00504.x

54. Dennhardt S, Pirschel W, Wissuwa B, Daniel C, Gunzer F, Lindig S, et al. Modeling hemolytic-uremic syndrome: in-depth characterization of distinct murine models reflecting different features of human disease. *Front Immunol.* (2018) 9:1459. doi: 10.3389/fimmu.2018.01459
55. Thorgersen EB, Barratt-Due A, Haugaa H, Harboe M, Pischke SE, Nilsson PH, et al. The role of complement in liver injury, regeneration, and transplantation. *Hepatology.* (2019) 70:725–36. doi: 10.1002/hep.30508
56. Sahu A, Lambris JD. Complement inhibitors: a resurgent concept in anti-inflammatory therapeutics. *Immunopharmacology.* (2000) 49:133–48. doi: 10.1016/S0162-3109(00)80299-4
57. Zipfel FP, Wiech T, Rudnick R, Afonso S, Person F, Skerka C. Complement inhibitors in clinical trials for glomerular diseases. *Front Immunol.* (2019) 10:2166. doi: 10.3389/fimmu.2019.02166
58. Kaur H, Chakrabarti A. Strategies to reduce mortality in adult and neonatal candidemia in developing countries. *J Fungi.* (2017) 3:1–20. doi: 10.3390/jof3030041
59. Wu P-F, Liu W-L, Hsieh M-H, Hii I-M, Lee Y-L, Lin Y-T, et al. Epidemiology and antifungal susceptibility of candidemia isolates of non-albicans Candida species from cancer patients. *Emerg Microbes Infect.* (2017) 6:1–7. doi: 10.1038/emi.2017.74
60. Singh DK, Tóth R, Gácser A. Mechanisms of pathogenic candida species to evade the host complement attack. *Front Cell Infect Microbiol.* (2020) 10:94–103. doi: 10.3389/fcimb.2020.00094
61. Meri T, Hartmann A, Lenk D, Eck R, Würzner R, Hellwage J, et al. The yeast Candida albicans binds complement regulators factor H and FHL-1. *Infect Immun.* (2002) 70:5185–92. doi: 10.1128/IAI.70.9.5185-5192.2002
62. Luo S, Hartmann A, Dahse H-M, Skerka C, Zipfel PF. Secreted pH-Regulated antigen 1 of *Candida albicans* blocks activation and conversion of complement C3. *J Immunol.* (2010) 185:2164–73. doi: 10.4049/jimmunol.1001011
63. Pangburn MK, Mueller-Eberhard HJ. Kinetic and thermodynamic analysis of the control of C3b by the complement regulatory proteins factors H and I. *Biochemistry.* (1983) 22:178–85. doi: 10.1021/bi00270a026
64. Sahu A, Pangburn MK. Covalent attachment of human complement C3 to IgG. *J Biol Chem.* (1994) 269:28997–9002.
65. Pangburn MK, Müller-Eberhard HJ. The C3 convertase of the alternative pathway of human complement. *Biochem J.* (1986) 235:723–30. doi: 10.1042/bj2350723
66. Janssen BJC, Huizinga EG, Raaijmakers HCA, Roos A, Daha MR, Nilsson-Ekdahl K, et al. Structures of complement component C3 provide insights into the function and evolution of immunity. *Nature.* (2005) 437:505–11. doi: 10.1038/nature04005
67. Pangburn MK, Müller-Eberhard HJ. Initiation of the alternative complement pathway due to spontaneous hydrolysis of the thioester of C3. *Ann N Y Acad Sci.* (1983) 421:291–8. doi: 10.1111/j.1749-6632.1983.tb18116.x
68. Dinasarapu AR, Chandrasekhar A, Sahu A, Subramaniam S. Complement C3. *Ucsd Mol Pages.* (2012) 1:1–11. doi: 10.6072/H0.MP.A004235.01
69. Hourcade DE. The role of properdin in the assembly of the alternative pathway C3 convertases of complement. *J Biol Chem.* (2006) 281:2128–32. doi: 10.1074/jbc.M508928200
70. Fearon DT. Properdin: binding to C3b and stabilization of the C3b-dependent C3 convertase. *J Exp Med.* (1975) 142:856–63. doi: 10.1084/jem.142.4.856
71. Pedersen DV, Roumenina L, Jensen RK, Marinozzi C, Picard C, Rybkine T, et al. Functional and structural insight into properdin control of complement alternative pathway amplification. *EMBO J.* (2017) 36:1084–99. doi: 10.15252/embj.201696173
72. Wu J, Wu YQ, Ricklin D, Janssen BJC, Lambris JD, Gros P. Structure of complement fragment C3b-factor H and implications for host protection by complement regulators. *Nat Immunol.* (2009) 10:728–33. doi: 10.1038/ni.1755
73. Farries TC, Lachmann RAH. Analysis of the interactions between properdin, the third component of complement (C3) and its physiological activation products. *Biochem J.* (1988) 252:47–54. doi: 10.1042/bj2520047

Conflict of Interest: The authors declare that the research was conducted in the absence of any commercial or financial relationships that could be construed as a potential conflict of interest.

frontiers in Immunology

ORIGINAL RESEARCH
published: 03 September 2020
doi: 10.3389/fimmu.2020.01927

Association of *MBL2* Exon 1 Polymorphisms With Multibacillary Leprosy

Bruna Tiaki Tiyo[1], *Evelyn Castillo Lima Vendramini*[1], *Victor Hugo de Souza*[1], *Cristiane Maria Colli*[1], *Hugo Vicentin Alves*[1], *Ana Maria Sell*[1], *Sylmara Bessani Paixão Zucoloto*[2] *and Jeane Eliete Laguila Visentainer*[1]*

[1] *Laboratory of Immunogenetics, Department of Basic Health Sciences, Maringá State University (UEM), Maringá, Brazil,* [2] *Inter-municipal Public Health Consortium (CISAMUSEP), Maringá, Brazil*

Mannose-binding lectin (MBL) is a serum protein of innate immunity, with a central role in the activation of the complement system through the lectin pathway. This protein is encoded by *MBL2* gene, and single-nucleotide polymorphisms located at exon 1, such as rs5030737 C>T (*D* variant), rs1800450 G>A (*B* variant), and rs1800451 G>A (*C* variant), may change the MBL structure and the serum concentration. *MBL2* polymorphisms have been associated with several infectious diseases, including leprosy. Host immune response has a major impact on the clinical manifestation of leprosy since only a few individuals infected with *Mycobacterium leprae* will develop the disease. Therefore, the aim of this study was to evaluate the influence of *MBL2* exon 1 polymorphisms (rs5030737, rs1800450, and rs1800451) on the MBL levels and leprosy immunopathogenesis. This case–control study included 350 leprosy patients from Southern Brazil, with 279 classified as multibacillary (MB) and 71 as paucibacillary (PB). The control group consisted of 350 non-consanguineous individuals, who were not diagnosed with leprosy or other infectious and autoimmune diseases. Genotyping was performed by PCR–sequence specific primers, and the MBL serum concentrations were evaluated by ELISA. *MBL2* exon 1 polymorphisms were analyzed individually and grouped as genotypes, considering "A" as the wild allele and "O" as the presence of at least one polymorphism (*D*, *B*, or *C* variants). Differences were not observed in the distribution of genotypic and allelic frequencies between leprosy *per se* patients and controls. However, in a haplotypic analysis, the TGG haplotype presented a risk for development of leprosy *per se* in women when compared to the wild haplotype (CGG) (OR = 2.69). Comparing patients with MB and PB, in a multivariate analysis, the *B* variant was associated with the susceptibility of developing the MB form of leprosy (OR = 2.55). Besides that, the CAG haplotype showed an increased susceptibility to develop MB leprosy in women compared to men. It was observed that the A/O genotype in women was associated with a susceptibility to leprosy development *per se* (OR = 1.66) and progression to MB leprosy (OR = 3.13). In addition, the MBL serum concentrations were in accordance with the genotyping analysis. In summary, our data suggest that *MBL2* exon 1 polymorphisms are associated with an increased risk to leprosy development and progression.

Keywords: genetic polymorphism, mannose-binding lectin, multibacillary, genetic predisposition to disease, case–control study, gene frequencies

OPEN ACCESS

Edited by:
Nicole Thielens, UMR5075 Institut de Biologie Structurale (IBS), France

Reviewed by:
Patricia Muniz Moura, Universidade de Pernambuco, Brazil
Jatinder Singh, Guru Nanak Dev University, India

***Correspondence:**
Jeane Eliete Laguila Visentainer
jelvisentainer@uem.br

Specialty section:
This article was submitted to Microbial Immunology, a section of the journal Frontiers in Immunology

Received: *28 March 2020*
Accepted: *17 July 2020*
Published: *03 September 2020*

Citation:
Tiyo BT, Vendramini ECL, de Souza VH, Colli CM, Alves HV, Sell AM, Zucoloto SBP and Visentainer JEL (2020) Association of MBL2 Exon 1 Polymorphisms With Multibacillary Leprosy. Front. Immunol. 11:1927. doi: 10.3389/fimmu.2020.01927

INTRODUCTION

Mannose-binding lectin (MBL) is a soluble protein responsible for activating the complement system *via* the lectin pathway. In addition, MBL is involved in microorganism opsonization for phagocytosis and macrophage activation (1, 2).

MBL2 gene, which encodes MBL, is located on chromosome 10 (q11.2-q21) (1). Three variants are commonly studied on *MBL2* exon 1: rs5030737 (g.52771482G>A, p.Arg52Cys), rs1800450 (g.52771475C>T, p.Gly54Asp), and rs1800451 (g.52771466C>T, p.Gly57Glu), also described as *D*, *B*, and *C* variants, respectively, in contrast to the wild type, which is termed as *A* allele (3, 4). These single-nucleotide polymorphism (SNPs) are known as structural variants since they modify the structure of the protein and the assembly of MBL oligomers, leading to the formation of smaller non-functional oligomers (5). This affects binding avidity, with a possible functional implication, since the prolonged interaction can facilitate self-activation of MASP1 to activate the complement cascade more efficiently (6). Another consequence of MBL variants is increased susceptibility to degradation by metalloproteases (7).

High MBL levels may facilitate the infection of intracellular pathogens into host cells through C3b receptors. Some studies have shown that MBL deficiency indicated protection in diseases such as leishmaniasis (8, 9), tuberculosis, and leprosy (10–12).

Leprosy is a chronic infectious disease caused mainly by *Mycobacterium leprae* and *Mycobacterium lepromatosis* (13, 14), which mainly affect the skin, peripheral nerves, upper respiratory tract mucosa, and eyes (13, 15). According to the World Health Organization (WHO) classification (1982), leprosy patients are considered paucibacillary (PB), when they present up to five cutaneous lesions, or multibacillary (MB), which includes patients with more than five lesions (13).

Regarding the epidemiology of leprosy, at the end of 2018, WHO reported an incidence of 2.74 new cases per 100,000 (208,619 cases). More than 79% of new cases refer only to three countries: India, Brazil, and Indonesia. In this case, Brazil was the second country with the largest number of new leprosy cases in the world, totaling 28,660 (16, 17).

Host immune response has a major impact on the clinical manifestation of leprosy, and according to some studies, there is an association between MBL protein and the development and the progression of this disease (4, 18–20). Thus, the objective of this work was to evaluate the influence of *MBL2* gene exon 1 polymorphisms (*D*, *B*, and *C* variants), which encodes the MBL protein, on leprosy immunopathogenesis in residents of the north/northwest regions of Paraná, Brazil.

MATERIALS AND METHODS

Study Population

This case–control study consisted of leprosy patients and controls. The leprosy patients were classified following the WHO classification, multibacillary and paucibacillary. All the participants were residents of the northern and the northwestern regions of Paraná, southern Brazil (22°29′30″-26°42′59″ S and 48°02′24″-54°37′38″W). The population was considered as mixed according to Probst et al. (21) who described the Paraná ethnic constitution as predominantly of European origin (80.6%), with a small contribution from African (12.5%) and Amerindian (7.0%) ancestry (21).

The control group in this study was composed of both non-consanguineous individuals who were in household contact with leprosy patients and individuals without previous contact with these patients. All the control subjects declared that they did not present leprosy or other infectious and autoimmune diseases. The leprosy patients were diagnosed by clinical examination, bacilloscopy, and biopsy and classified by experienced dermatologists at the CISAMUSEP (Inter-municipal Public Health Consortium).

All the individuals who accepted to participate in the research signed the informed consent form, previously approved by the State University of Maringá (UEM) Human Research Ethics Committee (2.424.046/2017).

Genotyping and Quantification of Serum MBL

Genomic DNA was extracted from peripheral blood using BIOPUR® commercial kit (Mobius Life Science, Curitiba, Paraná, Brazil) according to the manufacturer's recommendations. Subsequently, three *MBL2* exon 1 SNPs were genotyped as *D* (rs5030737), *B* (rs1800450), and *C* (rs1800451) variants by polymerase chain reaction–sequence-specific primers (PCR–SSP) according to Steffensen et al., with modifications (22). The reactions were performed in a volume of 10 μl, containing 2 ng/μl of each primer, 1X buffer, 1.0 mM $MgCl_2$ for mix D, ABC, and ACD, and 1.5 mM $MgCl_2$ for mix B, C, and ABD, 0.2 mM dNTP, GoTaq® Flexi DNA Polymerase 1U (Promega Corporation, Madison, WI, USA), and 100 ng DNA. The positive controls used in the PCR–SSP reactions were previously characterized by genomic sequencing.

DNA amplification was performed in an Applied Biosystems® Veriti Thermal Cycler (Thermo Fisher Scientific, Foster City, CA, USA). The cycling conditions used were 95°C for 10 min, followed by 30 cycles of 94°C for 20 s, 65°C for 20 s, 72°C for 30 s, and a final extension of 72°C for 5 min. For mix C, the annealing temperature was 68°C. Detection of amplified fragments was performed by DNA electrophoresis on 2% agarose gel with SYBR® Safe® (Invitrogen Life Technologies, Grand Island, NY, USA) and visualized in ultraviolet light. The primers that amplify the growth gene region (HGH) were used as internal reaction controls (22).

Quantification of serum MBL was performed using a commercial capture enzyme-linked immunosorbent assay (MBL Oligomer ELISA kit; BIOPORTO® Diagnostics, Hellerup, Denmark), according to the manufacturer's instructions. The serum or plasma of patients was diluted 1:100. Absorbances were read at 450 nm in a FlexStation® 3 Multi-Mode microplate reader (Molecular Devices, San Jose, CA, USA).

Statistical Analysis

Allelic, genotypic, and haplotypic frequencies were calculated for patients and controls, and Hardy–Weinberg equilibrium (HWE) was evaluated from a genotype distribution analysis. Multiple SNP comparisons were performed for *MBL2* exon 1 SNPs. Haplotypic analysis was performed for three *MBL2*

TABLE 1 | *MBL2* exon 1 grouped genotypes.

Grouped genotypes	Genotypes for each grouped genotype
A/A	C/C (*D* variant), G/G (*B* variant), and G/G (*C* variant)
A/O	C/T (*D* variant), G/A (*B* variant), and G/A (*C* variant)
O/O	T/T (*D* variant), A/A (*B* variant), A/A (*C* variant), C/T+G/A (*D* and *B* variants), C/T+G/A (*D* and *C* variants), and G/A+G/A (*B* and *C* variants)

exon 1 SNPs as well as the linkage disequilibrium. For the analysis of multiple SNPs, the software Haploview (23) was used. Through multiple SNP analyses, we estimated the frequency of possible haplotypes using the implementation of expectation–maximization algorithm. This analysis allows one to check if these haplotypes demonstrated an association with leprosy, including linkage disequilibrium (LD).

The allelic, genotypic, and haplotypic frequencies of the studied polymorphisms, as well as the association analyses between genetic polymorphisms and leprosy, were obtained by the SNPStats program (available at: https://www.snpstats.net/) (24). The genetic inheritance models considered were codominant, dominant, recessive, overdominant, and log additive. The best inheritance model was chosen based on the lowest value for the Akaike information criterion (AIC). Odds ratio (OR) and 95% confidence interval (CI) were calculated by logistic regression tests, after including variables such as gender and age. Logistic regression test was used to verify the association of SNPs in leprosy progression. $P < 0.05$ was considered as statistically significant. Bonferroni correction for the total number of SNPs was not required by the reason that exon 1 had a high LD.

The patient and the control groups were matched for gender and age variables. In order to obtain the minimum number of samples adequate to carry out this study with adequate statistical power ($\geq$ 80%), the quantitative calculation software QUANTO (25) was used, which takes into account the frequencies of SNPs in the population and the prevalence of the disease (leprosy *per se*). Besides that, the sample size was calculated after consideration of the minor allele frequency.

Another analysis performed in this work was grouping the three SNPs (*D*, *B*, and *C* variants) into a single allele, represented by the letter "O," with the wild allele as "A" (**Table 1**).

The serum levels of MBL were calculated with a four-parameter logistic curve using My Curve Fit (https://mycurvefit.com/), with a dilution factor of 1:100. The MBL levels were compared within gender and age of patients with Pearson correlation coefficient and also between PB and MB patients with Student's *t*-test. The concentrations correlated to polymorphisms were evaluated separately (*D*, *B*, and *C*) or grouped (*A* and *O*) using Mann–Whitney *U* test in R software, version 3.5.2., by the reason that we had evaluated the normality by Shapiro–Wilk test, and this test indicated the need of a non-parametric test. For all analyses, $P < 0.05$ was considered as statistically significant.

TABLE 2 | Genotype and allele frequency distributions for *MBL2* exon 1 polymorphisms in leprosy *per se*, paucibacillary (PB) and multibacillary (MB) patients and controls.

SNP	Allele/ genotype	Leprosy patients (*N* = 350)			Controls (*N* = 350)
		Per se (*N* = 350)	MB (*N* = 279)	PB (*N* = 71)	
		n (%)	*n* (%)	*n* (%)	*n* (%)
Codon 52	C	661 (94%)	528 (95%)	133 (94%)	669 (96%)
(rs5030737)	T	39 (6%)	30 (5%)	9 (6%)	31 (4%)
D variant	C/C	312 (89.1%)	249 (89%)	63 (89%)	319 (91%)
	C/T	37 (10.6%)	30 (11%)	7 (10%)	31 (9%)
	T/T	1 (0.3%)	0	1 (1%)	0
Codon 54	G	614 (88%)	482 (86%)	132 (93%)	617 (88%)
(rs1800450)	A	86 (12%)	76 (14%)	10 (7%)	83 (12%)
B variant	G/G	269 (77%)	208 (74.5%)	61 (86%)	270 (77%)
	G/A	76 (22%)	66 (23.5%)	10 (14%)	77 (22%)
	A/A	5 (1%)	5 (2%)	0	3 (1%)
Codon 57	G	655 (94%)	522 (94%)	133 (94%)	658 (94%)
(rs1800451)	A	45 (6%)	36 (6%)	9 (6%)	42 (6%)
C variant	G/G	308 (88%)	245 (88%)	63 (89%)	310 (88.5%)
	G/A	39 (11%)	32 (11%)	7 (10%)	38 (11%)
	A/A	3 (1%)	2 (1%)	1 (1%)	2 (0.5%)

SNP, single-nucleotide polymorphism; N, number of subjects; n, number of alleles or genotypes (frequency).

RESULTS

We included 350 leprosy patients (193 males and 157 females, mean age 54 $\pm$ 13 years) and 350 controls (180 males and 170 females, mean age 56 $\pm$ 13 years) in the study. Of the leprosy patients, 279 (79.7%) were MB and 71 (20.3%) were PB (**Supplementary Table 1**).

For all genotypic analyses, the codominant association model was considered, which allows each genotype to present a different and non-additive risk. However, for the *B* variant, the log-additive (or multiplicative) model was used, which considers that each mutated allele modifies the risk in an additive form, that is, a homozygous individual for a mutated allele has a double risk compared to a heterozygous one to the same allele. The best inheritance model was chosen based on the lowest value for the AIC (https://www.snpstats.net/tutorial.htm).

Differences were not observed in the distribution of genotypic and allelic frequencies between leprosy *per se* patients and controls (**Table 2**). However, in haplotypic analysis, TGG haplotype was associated with a susceptibility to the development of leprosy *per se* in women (OR = 2.69, 95% CI = 1.04–6.97) when compared to the wild haplotype (CGG) (**Table 3**). Among the *MBL2* gene SNPs analyzed in this study, the most frequent mutated allele was codon 54 (*B* variant) in both patients (total and their classifications) and controls. The distribution of genotypes for all SNPs was in HWE. The statistical power obtained at 0.05 level of significance, two-tailed test, $K_P = 0.0025$, for the *D*, *B*, and *C* variants were power values of 93.7, 99.9,

TABLE 3 | Haplotypic frequencies of *MBL2* exon 1 polymorphisms in leprosy patients and controls within gender.

Haplotype	Frequency[a]	Female OR (95% IC)	Male OR (95% IC)
CGG	0.77	Ref.	Ref.
CAG	0.12	1.52 (0.91–2.52)	0.84 (0.53–1.35)
CGA	0.06	1.27 (0.68–2.34)	1.01 (0.56–1.83)
TGG	0.05	2.69 (1.04–6.97)	0.96 (0.49–1.88)

OR, odds ratio (95% IC); Ref., reference.
[a]Estimated relative frequency for each haplotype. Haplotype association is evaluated by logistic regression, and the most frequent haplotype is chosen automatically. The risk for each haplotype is compared with the reference, which is the most frequent haplotype (24).

TABLE 4 | Genotypic frequency for *B* variant (rs1800450), located at codon 54 of exon 1 of *MBL2* gene, among multibacillary (MB) and paucibacillary (PB) leprosy patients.

Association model	Genotype	PB patients	MB patients	OR (95% IC)	*P*-value	AIC
Codominant	G/G	61 (85.9%)	208 (74.5%)	Ref.	0.017	335.1
	G/A	10 (14.1%)	66 (23.7%)	2.40 (1.14–5.06)		
	A/A	0 (0%)	5 (1.8%)	NP		
Dominant	G/G	61 (85.9%)	208 (74.5%)	Ref.	0.008	334.2
	G/A–A/A	10 (14.1%)	71 (25.4%)	2.56 (1.22–5.37)		
Recessive	G/G–G/A	71 (100%)	274 (98.2%)	Ref.	0.14	339.1
	A/A	0 (0%)	5 (1.8%)	NP		
Overdominant	G/G–A/A	61 (85.9%)	213 (76.3%)	Ref.	0.018	335.6
	G/A	10 (14.1%)	66 (23.7%)	2.34 (1.11–4.93)		
Log additive	–	–	–	2.55 (1.24–5.24)	0.0056	333.6

SNP, single-nucleotide polymorphism; OR, odds ratio (95% IC); ref., reference; NP, not performed; AIC, Akaike information criterion.

TABLE 5 | Haplotypic frequencies of *MBL2* exon 1 polymorphisms in multibacillary (MB) and paucibacillary (PB) leprosy patients within gender.

Haplotype	Frequency[a]	Female OR (95% IC)	Male OR (95% IC)
CGG	0.77	Ref.	Ref.
CAG	0.12	2.69 (1.04–6.97)	2.62 (0.61–11.28)
CGA	0.06	1.55 (0.57–4.23)	0.74 (0.24–2.29)
TGG	0.05	1.47 (0.50–4.29)	0.52 (0.16–1.76)

OR, odds ratio (95% IC); ref., reference.
[a]Estimated relative frequency for each haplotype. Haplotype association is evaluated by logistic regression, and the most frequent haplotype is chosen automatically. The risk for each haplotype is compared with the reference, which is the most frequent haplotype (24).

TABLE 6 | Genotypic frequency of *MBL2* exon 1 polymorphisms, analyzed by grouped genotypes, between female leprosy patients and female controls.

Genotype	Controls	Leprosy *per se*	OR (95% IC)
A/A	109	82	Ref.
A/O	53	66	1.66 (1.04–2.63)
O/O	8	9	1.58 (0.58–4.30)

OR, odds ratio (95% IC); ref., reference.

TABLE 7 | Genotypic frequency of *MBL2* exon 1 polymorphisms, analyzed by grouped genotypes, between female MB and PB leprosy patients.

Genotype	PB patients	MB patients	OR (95% IC)
A/A	33	49	Ref.
A/O	12	54	3.13 (1.45–6.75)
O/O	3	6	1.24 (0.28–5.37)

OR, odds ratio (95% IC); ref., reference.

and 98.8%, respectively, to detect a genetic effect of 2.5 under a dominant model.

Although not associated with the disease, the allelic variants were in linkage disequilibrium. In the multivariate analysis, when comparing MB and PB patients, it was observed that patients with *B* variant were more susceptible to the development of MB leprosy (OR = 2.55, 95% CI = 1.24–5.24) (**Table 4**). For these analyses, the statistical power for the less frequent allele was above 80% for a risk effect of 4.5, while for the most frequent allele (*B* variant) the risk effect was 2.5 in the log-additive model. In a haplotypic analysis, the CAG haplotype was associated with a susceptibility to the development of MB leprosy in women (OR = 2.69, 95% CI = 1.04–6.97) when compared to the wild haplotype CGG (**Table 5**).

Another analysis was performed by grouping the three SNPs (*D*, *B*, and *C* variants) into a single allele. It was observed that the *A/O* genotype in women was associated with a susceptibility to leprosy development *per se* (OR = 1.66, 95% CI = 1.04–2.63) (**Table 6**) and progression to MB leprosy (OR = 3.13, 95% CI = 1.45–6.75) (**Table 7**).

The serum levels of MBL were evaluated in 80 leprosy patients (**Supplementary Table 2**). There was no difference when comparing the serum levels of MBL with age and gender. No difference was observed between the serum levels of MBL from MB and PB patients. Comparing the MBL levels with genotypes, statistically significant differences were observed between the grouped genotypes (**Figure 1**), but not when those were evaluated separately.

DISCUSSION

The *MBL2* variants have been associated with various diseases, including leprosy (8–12). We evaluated exon 1 polymorphisms (*D*, *B*, and *C* variants) in leprosy patients and controls from Southern Brazil. In this population, the *B* variant of *MBL2* exon 1 polymorphism was associated with susceptibility in leprosy patients for progression to MB form. Moreover, the grouped genotypes were also related to different MBL levels. Patients with *A/O* and *O/O* compound genotypes presented a decrease in MBL levels compared to the wild genotype (*A/A*). Other significant associations occurred only when we evaluated the

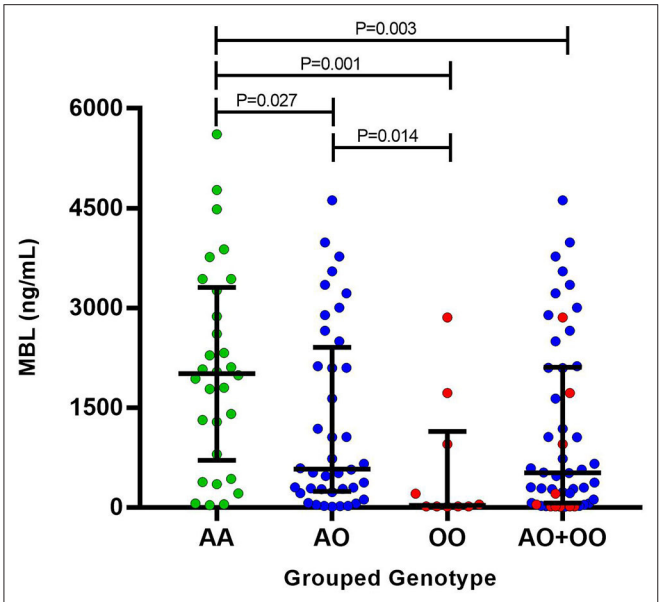

FIGURE 1 | Mannose-binding lectin serum levels between the grouped genotypes.

female population separately. In a haplotypic analysis, in women, the TGG haplotype was associated with a susceptibility to the development of leprosy *per se*; CAG haplotype was associated with susceptibility for progression to MB as well. In the grouped genotypes, a susceptibility association in female patients was also observed for both the development of leprosy *per se* and progression to MB form.

Even if it is known that men have an increased susceptibility for leprosy (26), we could not find this association. However, when we evaluated the female population separately, we found that the TGG and the CAG haplotypes increased the risk for development of leprosy and progression to MB form, respectively, when compared to women who have wild haplotype. Besides that, the grouped genotype *A/O* was also associated with a risk for development of leprosy and progression to MB form in women. On the other hand, when we evaluated only the male population, we did not find haplotype or genotype as a risk or protection factor. More studies with a greater sample size are necessary to confirm these findings.

In a northwest Brazilian population, Vasconcelos et al. (27) did not observe associations between *MBL2* exon 1 variants and leprosy (27); in contrast, Sapkota et al. (20) observed that the *MBL2 B* variant was associated with protection to the lepromatous form compared to the tuberculoid form of leprosy in a Nepalese population (20). These differences can be explained by population genetics background.

Previous studies have shown that low levels of MBL protein may influence the pathogenesis of diseases that have intracellular microorganisms as an agent (8, 9), such as leprosy (19). The deficiency of this protein has already been associated with protection against the lepromatous form of the disease, also classified as MB (18–20). Despite that we did not point an association between MBL serum levels and the development of the disease, it was observed that the presence of at least one polymorphism (*D*, *B*, or *C* variants) may decrease the MBL levels. Moreover, the *B* variant of *MBL2* exon 1 polymorphism was associated with susceptibility in leprosy patients for progression to MB. It is well known that there are other polymorphisms in the *MBL2* gene, such as in the promoter and the untranslated regions, and they also can alter the MBL serum concentration and the activity of this protein (1, 5). Although we have not studied these other polymorphisms, this limitation was not crucial in our findings, and we may confirm these results with other polymorphisms in a future study. We did not perform MBL concentration in all samples; however, we equally selected MB and PB patients, with heterogeneous genotyping in both groups. We considered a representative sample of each variant, taking into account variables such as age and gender.

Studies suggest that the binding between MBL and lipoarabinomannan, present on the cell surface of mycobacteria, promotes an increase in phagocyte ingestion of the pathogen (28). Thus, instead of this interaction between MBL and mycobacterium assisting in pathogen elimination, this may increase the uptake and the spread of the pathogen, leading to the establishment of leprosy in its most widespread form, lepromatous (18, 19). In this way, MBL deficiency would have a protective effect against pathogens that use complement-mediated opsonization to enter phagocytes, such as *M. leprae* (18), which also explains the findings of Dornelles et al. (19). Our findings indicate *MBL2* exon 1 polymorphisms to be associated to a reduction in serum protein concentration as a risk for the development of leprosy, especially in the MB form. It is noteworthy that the lectin pathway is not the only complement activation pathway and there are other evasion mechanisms (29).

Moreover, we realized that some patients showed unexpected findings, as we can see in **Supplementary Table 2**. Some patients had *O/O* genotype, but with high levels of MBL, which may be growing in response to an infection. However, for a complete characterization in high, intermediate, and low concentrations, it is necessary to evaluate other polymorphisms of the *MBL2* gene to correlate each haplotype with its respective classification. Besides that, other patients present *A/A* grouped genotype with a supposedly low concentration of MBL, even though they do not carry an exon 1 *MBL2* polymorphism. Although these findings are surprising, further studies are needed to evaluate other polymorphisms in the *MBL2* gene to better understand the role of MBL in leprosy, and we intend to continue studying these variables. We emphasize that, for all samples which had any confusing factor or bias, we certainly repeated the genotyping.

Finally, the purpose of including a select group of controls, consisting of healthy and non-consanguineous contacts of patients, was to analyze the possible genetic influence on susceptibility or resistance to leprosy (26), considering that this disease develops only in a small group of individuals infected with the bacillus (30). Thus, although these contacts were with the increased possibility of infection, they did not have the disease, suggesting that the

absence of infection is due to the immunogenetic factors of each individual.

CONCLUSION

We verify the influence of *MBL2* exon 1 polymorphisms on leprosy immunopathogenesis. The presence of the *B* variant was associated with an increased risk of developing multibacillary leprosy, as well as CAG haplotype in women. In addition, the MBL serum concentrations were in accordance with the genotyping analysis, and it was observed that the presence of at least one polymorphism (*D*, *B*, or *C* variants) may decrease the MBL levels. In summary, our data suggest that *MBL2* exon 1 polymorphisms are associated with an increased risk to leprosy development and progression. For a better understanding of the role of MBL on leprosy, more studies are necessary to evaluate other polymorphisms into the *MBL2* gene, as well as a greater sample size to confirm the findings.

DATA AVAILABILITY STATEMENT

All datasets presented in this study are included in the article/**Supplementary Material**.

ETHICS STATEMENT

The studies involving human participants were reviewed and approved by Human Research Ethics Committee of State University of Maringá (UEM). The patients/participants provided their written informed consent to participate in this study.

AUTHOR CONTRIBUTIONS

BT and EV conceived the study. BT, CC, EV, and JV participated in study design and coordination. BT, EV, and VS participated in data acquisition and maintained the database for analysis. EV and VS analyzed the data. AS, BT, CC, EV, HA, JV, SZ, and VS contributed to the critical revision of this work. All authors contributed to the article and approved the submitted version.

FUNDING

This work was supported by CAPES (Coordenação de Aperfeiçoamento de Pessoal de Nível Superior), CNPq (Conselho Nacional de Desenvolvimento Científico e Tecnológico), Fundação Araucária do Paraná, and the Laboratory of Immunogenetics at Universidade Estadual de Maringá (Proc. No.1589/2017-CSD-UEM).

ACKNOWLEDGMENTS

We thank all the volunteers and the technical staff of the Molecular Immunopathology Laboratory of Federal University of Paraná for providing control samples for the standardization of PCR–SSP reactions and CISAMUSEP in Maringá-PR, Brazil.

SUPPLEMENTARY MATERIAL

The Supplementary Material for this article can be found online at: https://www.frontiersin.org/articles/10.3389/fimmu.2020.01927/full#supplementary-material

REFERENCES

1. Madsen HO, Garred P, Thiel S, Kurtzhals JA, Lamm LU, Ryder LP, et al. Interplay between promoter and structural gene variants control basal serum level of mannan-binding protein. *J Immunol.* (1995) 155:3013–20.
2. Turner MW. The role of mannose-binding lectin in health and disease. *Mol Immunol.* (2003) 40:423–9. doi: 10.1016/S0161-5890(03)00155-X
3. Kilpatrick DC. Mannan-binding lectin and its role in innate immunity. *Transfus Med.* (2002) 12:335–52. doi: 10.1046/j.1365-3148.2002.00408.x
4. Zhang D-F, Huang X-Q, Wang D, Li Y-Y, Yao Y-G. Genetic variants of complement genes ficolin-2, mannose-binding lectin and complement factor H are associated with leprosy in Han Chinese from Southwest China. *Hum Genet.* (2013) 132:629–40. doi: 10.1007/s00439-013-1273-8
5. Auriti C, Prencipe G, Moriondo M, Bersani I, Bertaina C, Mondì V, et al. Mannose-binding lectin: biologic characteristics and role in the susceptibility to infections and ischemia-reperfusion related injury in critically Ill neonates. *J Immunol Res.* (2017) 2017:7045630. doi: 10.1155/2017/7045630
6. Teillet F, Dublet B, Andrieu J-P, Gaboriaud C, Arlaud GJ, Thielens NM. The two major oligomeric forms of human mannan-binding lectin: chemical characterization, carbohydrate-binding properties, and interaction with MBL-associated serine proteases. *J Immunol.* (2005) 174:2870–7. doi: 10.4049/jimmunol.174.5.2870
7. Butler GS, Sim D, Tam E, Devine D, Overall CM. Mannose-binding lectin (MBL) mutants are susceptible to matrix metalloproteinase proteolysis potential role in human mbl deficiency. *J Biol Chem.* (2002) 277:17511–9. doi: 10.1074/jbc.M201461200
8. Ambrosio AR, de Messias-Reason IJT. Leishmania (Viannia) braziliensis: interaction of mannose-binding lectin with surface glycoconjugates and complement activation. An antibody-independent defence mechanism. *Parasite Immunol.* (2005) 27:333–40. doi: 10.1111/j.1365-3024.2005.00782.x
9. de Miranda Santos IKF, Costa CHN, Krieger H, Feitosa MF, Zurakowski D, Fardin B, et al. Mannan-binding lectin enhances susceptibility to visceral leishmaniasis. *Infect Immun.* (2001) 69:5212–5. doi: 10.1128/IAI.69.8.5212-5215.2001
10. Areeshi MY, Mandal RK, Akhter N, Dar SA, Jawed A, Wahid M, et al. A meta-analysis of MBL2 polymorphisms and Tuberculosis risk. *Sci Rep.* (2016) 6:35728. doi: 10.1038/srep35728
11. Garred P, Harboe M, Oettinger T, Koch C, Svejgaard A. Dual role of mannan-binding protein in infections: another case of heterosis? *Eur J Immunogenet.* (1994) 21:125–31. doi: 10.1111/j.1744-313X.1994.tb00183.x
12. Remus N, Alcais A, Abel L. Human genetics of common mycobacterial infections. *Immunol Res.* (2003) 28:109–29. doi: 10.1385/IR:28:2:109
13. Eichelmann K, Gonzalez Gonzalez SE, Salas-Alanis JC, Ocampo-Candiani J. Leprosy. An update: definition, pathogenesis, classification, diagnosis, and treatment. *Actas Dermosifiliogr.* (2013) 104:554–63. doi: 10.1016/j.adengl.2012.03.028
14. Han XY, Seo Y-H, Sizer KC, Schoberle T, May GS, Spencer JS, et al. A new Mycobacterium species causing diffuse lepromatous leprosy. *Am J Clin Pathol.* (2008) 130:856–64. doi: 10.1309/AJCPP72FJZZRRVMM
15. *Leprosy*. Available online at: http://www.who.int/en/news-room/fact-sheets/detail/leprosy (accessed August 15, 2018).
16. Lastória JC, Abreu M. Hanseníase: diagnóstico e tratamento. *Diagn Trat.* (2012) 17:173–9.

17. World Health Organization. *Global Health Observatory (GHO) data | Leprosy*. WHO. World Health Organization (2019). Available online at: https://www.who.int/gho/neglected_diseases/leprosy/en/ (accessed October 13, 2019).
18. de Messias-Reason IJ, Boldt ABW, Moraes Braga AC, Von Rosen Seeling Stahlke E, Dornelles L, Pereira-Ferrari L, et al. The association between mannan-binding lectin gene polymorphism and clinical leprosy: new insight into an old paradigm. *J Infect Dis*. (2007) 196:1379–85. doi: 10.1086/521627
19. Dornelles LN, Pereira-Ferrari L, Messias-Reason I. Mannan-binding lectin plasma levels in leprosy: deficiency confers protection against the lepromatous but not the tuberculoid forms. *Clin Exp Immunol*. (2006) 145:463–8. doi: 10.1111/j.1365-2249.2006.03161.x
20. Sapkota BR, Macdonald M, Berrington WR, Misch EA, Ranjit C, Siddiqui MR, et al. Association of TNF, MBL, and VDR polymorphisms with leprosy phenotypes. *Hum Immunol*. (2010) 71:992–8. doi: 10.1016/j.humimm.2010.07.001
21. Probst CM, Bompeixe EP, Pereira NF, de O Dalalio MM, Visentainer JE, Tsuneto LT, et al. HLA polymorphism and evaluation of European, African, and Amerindian contribution to the white and mulatto populations from Paraná, Brazil. *Hum Biol*. (2000) 597–617.
22. Steffensen R, Thiel S, Varming K, Jersild C, Jensenius JC. Detection of structural gene mutations and promoter polymorphisms in the mannan-binding lectin (MBL) gene by polymerase chain reaction with sequence-specific primers. *J Immunol Methods*. (2000) 241:33–42. doi: 10.1016/S0022-1759(00)00198-8
23. Barrett JC, Fry B, Maller J, Daly MJ. Haploview: analysis and visualization of LD and haplotype maps. *Bioinformatics*. (2005) 21:263–5. doi: 10.1093/bioinformatics/bth457
24. Sole X, Guino E, Valls J, Iniesta R, Moreno V. SNPStats: a web tool for the analysis of association studies. *Bioinformatics*. (2006) 22:1928–9. doi: 10.1093/bioinformatics/btl268
25. Gauderman WJ. Sample size requirements for association studies of gene-gene interaction. *Am J Epidemiol*. (2002) 155:478–84. doi: 10.1093/aje/155.5.478
26. Pescarini JM, Strina A, Nery JS, Skalinski LM, Andrade KVF de, Penna MLF, et al. Socioeconomic risk markers of leprosy in high-burden countries: a systematic review and meta-analysis. *PLoS Negl Trop Dis*. (2018) 12:e0006622. doi: 10.1371/journal.pntd.0006622
27. Vasconcelos LRS, Fonseca JPL, do Carmo RF, de Mendonca TF, Pereira VRA, Lucena-Silva N, et al. Mannose-binding lectin serum levels in patients with leprosy are influenced by age and MBL2 genotypes. *Int J Infect Dis*. (2011) 15:e551–7. doi: 10.1016/j.ijid.2011.04.008
28. Bonar A, Chmiela M, Rudnicka W, Rozalska B. Mannose-binding lectin enhances the attachment and phagocytosis of mycobacteria in vitro. *Arch Immunol Ther Exp Ed*. (2005) 53:437.
29. Callegaro-Filho D, Shrestha N, Burdick AE, Haslett PA. A potential role for complement in immune evasion by Mycobacterium leprae. *J Drugs Dermatol*. (2010) 9:1373–82.
30. Dallmann-Sauer M, Correa-Macedo W, Schurr E. Human genetics of mycobacterial disease. *Mamm Genome*. (2018) 29:523–38. doi: 10.1007/s00335-018-9765-4

Conflict of Interest: The authors declare that the research was conducted in the absence of any commercial or financial relationships that could be construed as a potential conflict of interest.

frontiers in Immunology

REVIEW
published: 29 September 2020
doi: 10.3389/fimmu.2020.573583

In the Crosshairs: RNA Viruses OR Complement?

Nisha Asok Kumar[1,2†], Umerali Kunnakkadan[1,3†], Sabu Thomas[4] and John Bernet Johnson[1]*

[1] Viral Disease Biology, Department of Pathogen Biology, Rajiv Gandhi Center for Biotechnology, Thiruvananthapuram, India, [2] Manipal Academy of Higher Education, Manipal, India, [3] Department of Biotechnology, University of Kerala, Thiruvananthapuram, India, [4] Cholera and Biofilm Research Lab, Department of Pathogen Biology, Rajiv Gandhi Center for Biotechnology, Thiruvananthapuram, India

Complement, a part of the innate arm of the immune system, is integral to the frontline defense of the host against innumerable pathogens, which includes RNA viruses. Among the major groups of viruses, RNA viruses contribute significantly to the global mortality and morbidity index associated with viral infection. Despite multiple routes of entry adopted by these viruses, facing complement is inevitable. The initial interaction with complement and the nature of this interaction play an important role in determining host resistance versus susceptibility to the viral infection. Many RNA viruses are potent activators of complement, often resulting in virus neutralization. Yet, another facet of virus-induced activation is the exacerbation in pathogenesis contributing to the overall morbidity. The severity in disease and death associated with RNA virus infections shows a tip in the scale favoring viruses. Growing evidence suggest that like their DNA counterparts, RNA viruses have co-evolved to master ingenious strategies to remarkably restrict complement. Modulation of host genes involved in antiviral responses contributed prominently to the adoption of unique strategies to keep complement at bay, which included either down regulation of activation components (C3, C4) or up regulation of complement regulatory proteins. All this hints at a possible "hijacking" of the cross-talk mechanism of the host immune system. Enveloped RNA viruses have a selective advantage of not only modulating the host responses but also recruiting membrane-associated regulators of complement activation (RCAs). This review aims to highlight the significant progress in the understanding of RNA virus–complement interactions.

Keywords: complement activation, viral evasion strategies, RNA viruses, complement regulators, virus neutralization

OPEN ACCESS

Edited by:
Heribert Stoiber, Innsbruck Medical University, Austria

Reviewed by:
Wilfried Posch, Innsbruck Medical University, Austria
Ulf Dittmer, University of Duisburg-Essen, Germany

***Correspondence:**
John Bernet Johnson
johnbjohnson@rgcb.res.in

† These authors have contributed equally to this work

Specialty section:
This article was submitted to Microbial Immunology, a section of the journal Frontiers in Immunology

Received: *17 June 2020*
Accepted: *24 August 2020*
Published: *29 September 2020*

Citation:
Kumar NA, Kunnakkadan U, Thomas S and Johnson JB (2020) In the Crosshairs: RNA Viruses OR Complement? Front. Immunol. 11:573583. doi: 10.3389/fimmu.2020.573583

INTRODUCTION

The complement system (CS) is evolutionarily ancient and is a prime component of the innate immunity arsenal, capable of targeting a wide range of pathogens (1). Comprising of over 30 soluble and membrane-bound proteins, multiple functions besides anti-pathogenic activities have been attributed to the CS. Besides hepatocytes being the site of bulk synthesis of complement proteins in circulation, many other cell types including immune cells (2), adipocytes, fibroblasts, and endothelial cells also synthesize complement proteins locally as reviewed in Morgan and Gasque

(3) imparting their autocrine and paracrine functions (4). The CS operates via three pathways, namely, the classical pathway (CP), the lectin pathway (LP), and the alternative pathway (AP) (5), and functions like a cascade brought about by the sequential proteolytic cleavage of zymogens into their active fragments. Despite differences in the initial trigger, all three pathways converge at a common factor, C3, quintessential for the complement cascade to proceed. The activation of a specific pathway depends on the recognition of unique molecules associated with the pathogen. The CP is initiated by the binding of C1q to the Fc region of IgG or IgM in an antigen–antibody complex or directly to the pathogen. This leads to the autocatalytic activation of C1r, which activates the serine protease C1s, which can then sequentially cleave C4 into C4a and C4b and C2 into C2a and C2b (6). In contrast, binding of mannose binding lectin (MBL) or ficolins to unique carbohydrate moieties rich in D-mannose or L-fucose (7) on the pathogen surface [pathogen-associated molecular patterns (PAMPs)] activates the LP. This is facilitated by the activation of two MBL-associated serine proteases (MASP), MASP-1, and MASP-2 (8), leading to the cleavage of C4 and C2. Thus, C4 acts as the point where both the CP and LP merge, leading to the association of C4b and C2a, generating the C3 convertase (C4b2a; **Figure 1**).

The autohydrolysis of C3 to form C3(H_2O) by a mechanism known as the "tick-over" helps maintain basal levels of AP. C3(H_2O) thus formed further binds to factor B (FB) and factor D (FD). FD, being a serine protease, cleaves FB into Ba and Bb, resulting in the formation of C3(H_2O)Bb, which, like C4b2a, cleaves C3 to form C3b and C3a. The nascent C3b formed can associate with FB and, in the presence of FD, can form C3bBb, the AP C3 convertase (9). Properdin is an important component of the AP and functions by stabilizing C3bBb and increasing its half-life by 5- to 10-fold, facilitating the further cleavage of C3 into C3b (10, 11). The C3 convertase formed by all the three pathways cleaves C3 into C3a, an anaphylatoxin, and C3b, a major opsonin. The nascent C3b is central to further amplification of the pathway and is a critical component in assembling C5 convertase of the CP/LP (C4b2a3b) and the AP (C3bBb3b), essential to cleave C5 into C5a and C5b. The C5b thus formed associates with complement components C6, C7, and C8 and multiple units of C9, resulting in the formation of a multi-protein lytic complex called the membrane-attack complex (C5b-9, MAC). Apart from the membrane lytic action of complement via the MAC, CS has a wide range of other functions. Activation products, C3a, and C5a are potent anaphylatoxins, and the opsonins C3b and C4b facilitate the engagement of innate and adaptive immune cells, playing critical roles in inducing both T- and B-cell responses (12). Active cross-talk between complement proteins and various components of the adaptive arm demonstrate the role of the CS as a connecting link between the innate and the adaptive immune system (13).

Despite the decisive roles played by the CS in host immunity, the lack in memory response and its inability to distinguish between the "self" and "non-self," especially during unprecedented activation of complement, can be damaging to the host. This is largely checked by a highly concerted group of proteins called the regulators of complement activation (RCAs) (14). These proteins have unique domains called the complement control protein (CCP) or short-consensus repeats (SCRs), composed of 60–70 amino acids with complement regulatory activities. RCAs can be either membrane-associated, e.g., CD55 (decay accelerating factor, DAF), CD46 (membrane cofactor protein, MCP), CD59, and complement receptor type I (CR1, CD35) (15), or soluble in nature, e.g., C1 inhibitor (C1INH), C4b binding protein (C4BP), and factor H (fH) (14). CD55 and CD59 are attached to the cell membrane by a glycosylphosphatidylinositol (GPI) anchor while CD46 and CD35 are transmembrane proteins. CD55 has an inherent decay accelerating activity (DAA) and mediates the rapid dissociation of the C3 and C5 convertases, while CD59 prevents MAC formation by blocking the incorporation of C9 into the cell membrane. Factor H, CD35, and CD46, on the other hand, act as cofactors for the factor I (fI)-mediated inactivation of C3b into iC3b. Among the CP specific RCAs, C1INH binds to C1r and C1s and prevents their auto activation, while C4BP acts as a cofactor for the fI-mediated inactivation of C4b into C4c and C4d. CD35 is a highly potent and multifunctional RCA, since it exhibits both decay accelerating and cofactor activities. Not only does CD35 mediate the inactivation of C3b into iC3b, but it also supports an additional cleavage of iC3b into C3c and C3dg and acts as a cofactor for the inactivation of C4b by fI.

Investigation into virus-complement interactions had garnered much interest in the past, and this interest has only grown over the years to better comprehend the nature of these interactions. The knowledge acquired has enriched our insight into not only viral pathogenesis but also the underlying mechanisms of host immunity to these pathogens. Among animal viruses, RNA viruses constitute a large group of both veterinary and clinical significance. Based on the characteristics of the genetic material, they are classified into single- or double-stranded RNA viruses of positive or negative strand polarity that is either segmented or non-segmented. Human mortality of unprecedented proportions have been brought about by RNA viruses, the well documented being the pandemic H1N1 outbreak of 1918 (Spanish flu) that killed humans in millions (16). More recent outbreaks causing widespread devastation have been attributed to RNA viruses including Ebola, Nipah, and the ongoing severe acute respiratory syndrome coronavirus-2 (SARS-CoV-2). The nature of interaction of RNA viruses with the CS suggests a constant tussle for supremacy. This review focuses specifically on the effect of complement on RNA viruses, its role in disease severity, and the ingenious evasion strategies adopted by these viruses to counter complement.

COMPLEMENT ACTIVATION AND ITS EFFECTS ON RNA VIRUSES

RNA viruses have limited genome yet are pathogenic enough to cause devastating infections in both humans and animals. The CS that acts as a frontline defense against several pathogens is a potent barrier faced by RNA viruses (**Table 1**). Many characteristic features, including the molecular signatures present on the surface of RNA viruses and the presence

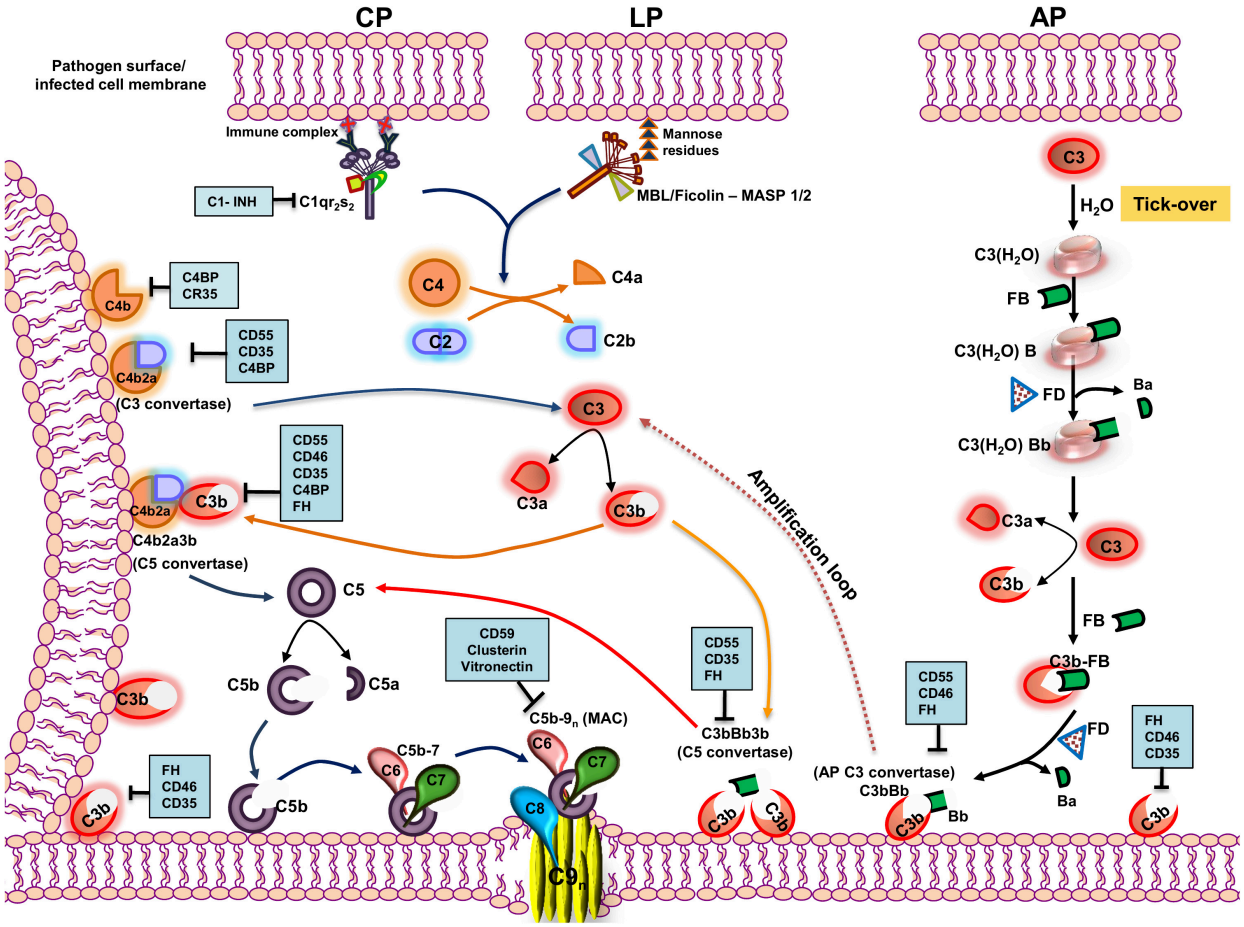

FIGURE 1 | Pathways of complement activation with complement regulators and inhibitors highlighted. The complement system is activated primarily through three pathways—classical pathway (CP), lectin pathway (LP), and alternative pathway (AP). The CP is activated by the recognition of antigen–antibody complexes formed on the surface of the pathogen or pathogen-infected cells by the C1 complex ($C1qr_2s_2$), whereas the LP is activated by the recognition of specific carbohydrate moieties present on the surface of pathogens (PAMPs) by the MBL/ficolin–MASP 1/2 complex. Upon recognition, the complexes so formed cleave C4 and C2 into C4a and C4b and C2a and C2b, respectively. The C4b so formed binds to the membrane and associates with C2a to form the C4b2a complex, the CP/LP-C3 convertase. The C3 convertase cleaves C3 into C3a and C3b. The C3b so formed further associates with C4b2a to form the C5 convertase, C4b2a3b. AP, on the other hand, is constitutively active in the plasma by a mechanism called the "tick-over," wherein the autohydrolysis of labile thioester bond in C3 forms $C3(H_2O)$. The latter binds to factor B and serine protease factor D. Factor D cleaves factor B into Ba and Bb and forms $C3(H_2O)Bb$, the initial fluid-phase AP C3 convertase. It then cleaves C3 into C3a and C3b. The C3b associates further to factor B, and factor D cleaves factor B into Ba and Bb and results in the formation of surface-bound AP C3 convertase, C3bBb, stabilized by properdin. AP C3 convertase cleaves many native C3 molecules into C3a and C3b to form a positive amplification loop, with each C3b capable of forming new AP convertases. The newly formed C3b can also bind to C3bBb and forms C3bBb3b, which is the AP C5 convertase. All the pathways converge at the terminal step where the C5 convertase cleaves C5 into C5a and C5b. The C5b binds to the cell surface to which binds C6, C7, C8, and multiple molecules of C9, inserting itself into the membrane to form a multiprotein transmembrane pore called the membrane attack complex (MAC), which ultimately results in the lysis of the cell. The events in the activation cascade are regulated at various levels by a group of host proteins called the regulators of complement activation (RCAs). The regulators either can be soluble in nature (C1INH, C4BP, and FH) or are membrane-bound (CD55, CD46, CD35, and CD59). The regulatory proteins are highlighted within blue boxes. Key: CD55 (Decay accelerating factor, DAF), CD46 (Membrane cofactor protein, MCP), C1INH (C1 inhibitor), CD35 (Complement receptor 1, CR1), and FH (factor H).

or absence of envelope and neutralizing/non-neutralizing antibodies, contribute to the nature of interaction of these viruses with the CS. Even among the enveloped RNA viruses, the surface glycoproteins contribute significantly to complement activation.

Orthomyxoviruses are enveloped viruses and the two major surface proteins hemagglutinin (HA) and neuraminidase (NA) activate complement to varying degrees, with HA being the better activator (17). Normal human serum (NHS) could readily neutralize strain A/WS/1933 H1N1 influenza virus in an antibody-dependent manner, and this neutralization was dependent on C1, C3, and C4 and thereby the CP (18). Activation of AP by this strain required antibodies and properdin stabilization, resulting in the deposition of C3. Interestingly, neither AP nor the terminal pathway components aided in virus neutralization (19). In the case of influenza viruses, the glycosylation pattern of surface proteins is a critical factor determining the pathway activated and the degree of neutralization. Studies with a series of H3N2 and H1N1

TABLE 1 | Complement activation and the effect of activation on RNA viruses.

Virus family	Pathway activated	Effect of complement activation
Orthomyxoviridae		
WS/33H1N1influenza	CP and AP	Ab – dependent, CP- mediated virus neutralization
Influenza A/Ibaraki/1/90 (H3N2)	LP	Virus neutralization
Influenza A(H1N1) pdm 009	CP and AP	Ab – dependent, C-mediated neutralization
Influenza A/PR/8/34	CP	C-deposition followed by aggregation
Paramyxoviridae		
Nipah virus	CP (Ab-dependent) and AP	Resistant to neutralization
Mumps virus	AP	Neutralization by virolysis
Parainfluenza virus 5	AP	Neutralization by virus aggregation
Parainfluenza virus 3	CP (Ab -independent)	Neutralization by virolysis
Measles virus	AP	Lysis of infected cells
Newcastle disease virus (NDV)	CP, LP, and AP	Virus neutralization
Pneumoviridae		
Human respiratory syncytial Virus (hRSV)	CP and AP	Ab-dependent, C-mediated, cytolysis
Filoviridae		
Ebola virus (Pseudotype)	LP	Neutralization
Marburg virus(Pseudotype)	LP	Neutralization
Flaviviridae		
Hepatitis C virus	LP	Neutralization
Dengue Virus	LP	Ab – dependent C-mediated Cytolysis
West Nile Virus	AP, CP and LP	Neutralization by virolysis, block in virus fusion
Zika Virus	CP	Neutralization by virolysis
Japanese Encephalitis Virus	CP	C- mediated cytolysis
Togaviridae		
Ross River virus	CP (Ab – dependent)	–––––
Chikungunya virus	––––––	Opsonization NOT leading to neutralization
Sindbis Virus	CP and AP (Ab – independent)	Neutralization
Rhabdoviridae		
Vesicular Stomatitis virus	CP	Neutralization by aggregation followed by lysis
Chandipura virus	CP	Neutralization by virus aggregation following opsonization
Retroviridae		
Human immunodeficiency virus 1	CP, LP and AP	Virolysis

Virus families with select viruses indicating the specific pathway activated and the mechanism of neutralization. Key: CP, Classical pathway, AP, Alternative pathway, LP, Lectin pathway, C, Complement, and Ab – Antibody.

mutants generated by swapping the HA and NA showed that those viruses with HA containing glycans rich in mannose oligosaccharides readily bound MBL and activated complement, leading to enhanced neutralization (20). The CP or LP activation by influenza viruses usually resulted in virus neutralization, which was enhanced many folds in the presence of binding antibodies (19). Direct binding of C1q to influenza B virus and the binding of MBL to the virus-infected cells facilitated active neutralization of the virus and lysis of infected cells by Guinea pig serum (17, 20). MBL could directly bind to influenza A/Ibaraki/1/90 (H3N2) and neutralize the virus and prevent the spread of virus in culture. The inhibition was due to the interaction of MBL with HA and NA (21). The complement-mediated neutralization of the PR8 strain of influenza A virus (influenza A virus A/PR/8/34) by mouse serum required the presence of natural IgM and the mechanism of neutralization was found to be the aggregation of the virus following complement deposition. The role of IgM was confirmed by using serum from $Rag^{-/-}$ mice (18). The role of individual pathways of complement in limiting influenza A(H1N1)pdm09 was demonstrated by the use of $C3^{-/-}$, $C4^{-/-}$, and $FB^{-/-}$ mice. Mice deficient in C3 were 100% susceptible; however, those deficient in C4 and FB were less susceptible, suggesting cross-talk between CP and AP. Simultaneous activation of both CP and AP followed by amplification through the AP enhanced the neutralization of the pandemic strain. The degree of neutralization correlated with the degree of C3b deposition and other complement components generated. Significant deposition of C3b observed on the surface of the seasonal influenza A (H3N2) compared to the pandemic virus suggest the preference of C3b for certain carbohydrates and its specificity to certain binding sites on them. The alteration in the C3b acceptor site on the surface glycoproteins, HA, and NA on the pandemic virus requires IgG to mediate the binding of C3b on them. Antagonists of C3a and C5a, and the corresponding receptor knock-out mice, showed that C5a played a less significant role in limiting the influenza A(H1N1)pdm09 virus infection (22).

Paramyxoviruses are negative-sense, single-stranded RNA viruses known to cause a number of important human diseases

including mumps, measles, and the deadly Nipah encephalitis. Nipah (NiV) and Hendra (HeV) viruses belonging to the genus *Henipavirus* of the *Paramyxoviridae* family are deadly BSL4 pathogens. Nipah virus has two major glycoproteins, the fusion protein (F), and the glycoprotein (G). Using VSV-based pseudoviruses expressing F and G glycoproteins, it was demonstrated that these glycoproteins activate the AP. However, when the pseudotypes were primed with specific antibodies, and more interestingly with the soluble EphrinB2 (the cognate receptor for NiV) linked to the Fc region of human IgG1, the CP was found to be predominantly activated (23). Among other paramyxoviruses, parainfluenza virus 5 (PIV5), and mumps virus (MuV) were found to activate the AP, while parainfluenza virus 3 (PIV3) activated CP independent of antibodies (24–28). Natural antibodies present in the NHS was found to bind to PIV5, yet CP was not activated; however, a dramatic switch from AP to CP was noticed when a single amino acid change, G3A, was engineered in the F protein (29). This clearly suggests the importance of surface glycoproteins in determining the pathway activated. Besides complement activation, the interaction of surface glycoproteins with complement proteins is critical in determining the mechanism of neutralization. The overall structure and conformation of the viral proteins and more specifically key epitopes are important factors determining the sensitivity of the virus to specific complement pathways. Although the closely related PIV5 and MuV both activated the AP, the mechanism of neutralization is quite distinct; while PIV5 aggregated in the presence of complement, significant lysis was observed in the case of MuV (27). Newcastle disease virus (NDV), an avian paramyxovirus, was found to activate complement and the neutralization was dependent on all the three pathways. C3, C4, and C5 were found to be critical components for virus neutralization (30). Apart from the importance of the complement components, the cells in which the virus is cultured and the complement source also dictated the extent of neutralization. Egg-grown NDV was readily neutralized by human complement while primate cell derived NDV resisted neutralization (30, 31). Measles virus was found to be a potent activator of the AP, where the fusion protein (F) and not the hemagglutinin protein (HA) contributed significantly toward this activation (25). Measles virus-infected cells sensitized with antibodies against the F and HA, when exposed to C4-deficient serum, were lysed, suggesting a role for the AP (26). An antibody-independent activation of AP by measles virus-infected cells has also been reported (32). Human respiratory syncytial virus (hRSV) is an enveloped virus and a member of the family *Pneumoviridae* known to cause respiratory infections in children. Deposition of antibodies IgG, IgA, IgM, and IgE bound to hRSV antigens in the nasopharyngeal cells of children with acute hRSV infection suggested a role of complement activation in hRSV infection (33). An antibody-dependent protection in hRSV infection was later confirmed in complement-deficient mice (34, 35). HeLa cells infected with hRSV activated both CP and AP; however, anti-hRSV antibodies were required for cytolysis by complement (36, 37). The importance of pulmonary macrophages and the CS in restricting hRSV replication suggests the significance of local complement production in limiting RNA viruses (34).

Flaviviruses are a family of positive-sense, single-stranded RNA viruses primarily transmitted by ticks and mosquitoes with notable exception like the hepatitis C virus (HCV). This family of viruses is distributed globally and can cause a wide range of human illnesses including dengue hemorrhagic fever (DHF), yellow fever, and West Nile encephalitis. The LP plays a critical role in the neutralization of HCV, wherein MBL binds directly to the E1 and E2 surface glycoprotein and activate LP by engaging MASP-2 (38). The NS1 protein of dengue virus (DENV) plays an important role in complement activation. It is secreted by the infected cells and accumulates in the serum of the infected patients and can also bind back to the infected cells. The NS1 protein of dengue virus can activate complement in an antibody-independent manner; however, engagement of anti-NS1 antibody with cell surface-bound NS1 further accentuates complement activation leading to cytolysis (39–41). A key feature in DENV pathogenesis is antibody-dependent enhancement (ADE) of infectivity. Low-avidity antibodies arising from a prior exposure to a specific DENV can cross-react with other DENV serotypes during a subsequent infection, resulting in ADE and disease severity. The binding of C1q to human anti-*flavivirus* antibodies results in marked reduction of ADE in an IgG subclass-dependent manner (42, 43). Among the pool of antibodies against Japanese encephalitis virus (JEV) surface proteins in the convalescent sera of patients in JEV endemic areas, only anti-NS1 antibodies supported complement-dependent cytolysis of infected cells (44). West Nile virus (WNV) transmitted mainly through the bites of infected mosquitoes can cause fatal neurological disease in humans. The role of complement in restricting WNV infectivity was also demonstrated *in vivo*. Compared to wtC57BL6 mice, $C3^{-/-}$, $CR1^{-/-}$, and $CR2^{-/-}$ mice were highly susceptible to WNV infection. Virus neutralization by complement was much enhanced in the presence of an antibody against the envelope protein (E) of WNV (45). The neutralization of WNV by serum complement was antibody dependent nevertheless; MBL was also found to directly bind to the virus, promoting opsonization by complement components and limiting virus entry (45, 46). While binding of C1q directly to the E protein of DENV could reduce virus infectivity, it was found to enhance the WNV neutralization potential of anti-WNV antibodies even at a low antibody titer (47–49). Recognition of N-linked glycans on the surface proteins of both WNV and DENV by MBL activated the LP, resulting in virus neutralization by blocking virus fusion (50, 51). Interestingly, components of all three complement pathways are essential for limiting the WNV infection (45, 50, 52). Using factor $B^{-/-}$, factor $D^{-/-}$, $C1q^{-/-}$, and $C4^{-/-}$ mice, it was clearly demonstrated that deficiency in AP components contributed significantly to neuropathogenesis, while deficiency in CP/LP components drastically affected the adaptive responses required to restrict WNV infection (52). While the neutralization of WNV and DENV by complement showed marked dependency on MBL, a less important role for the terminal pathway complement components including C5 was observed in the case of WNV (51, 53). Among the flaviviruses, the interaction of E protein–antibody complex with complement components plays a

critical role in the reduction of infectivity. Neutralization of Zika virus (ZIKV), another mosquito-borne flavivirus, associated with microencephaly in the neonates and Guillain–Barré syndrome in the adults was largely dependent on CP. Natural IgM antibodies were found to have a protective role against ZIKV. The binding of C1q to both envelope (E) and NS1 proteins followed by MAC formation resulted in virolysis (54).

The *Togaviridae* is a family of enveloped, positive-sense single-stranded RNA viruses distributed globally. This family consists of two genera, namely, *Alphavirus*, and *Rubivirus*. Extensive studies on Sindbis virus of the *Alphavirus* genus showed that while the virus was capable of activating both the AP and CP, the degree of activation of AP depended on the levels of sialic acid, with low levels being a better activator of AP (55, 56). Other alphaviruses investigated for their interactions with the CS include the Ross River virus (RRV) and Chikungunya virus (CHIKV), wherein the role of complement was rather destructive to the host than protective during virus infection. CHIKV was also found to activate complement, resulting in the deposition of complement components C3b and C4b on the surface of the virus (57).

Rhabdoviruses are negative-sense, single-stranded RNA viruses with broad tropism ranging from plants to mammals. Members of the *vesiculovirus*, *lyssavirus*, and *ephemerovirus* genera of the *Rhabdoviridae* family are known to cause infection in mammals. Vesicular stomatitis virus (VSV), a prototypic member of the genus vesiculovirus, was found to activate the CP of complement either in an antibody-dependent or -independent manner. Natural IgM present in the serum was found to enhance the complement-mediated neutralization by opsonization (58, 59). Activation of complement by VSV results in initial aggregation of the virus followed by virolysis (60). Chandipura virus (CHPV), another vesiculovirus and a potent human pathogen, has also been shown to activate the CP, which involved the direct binding of C1q to the virus. This virus was highly sensitive to complement and was neutralized effectively by complement-dependent virus aggregation (61). Although VSV and CHPV belong to the same genus with a single glycoprotein (G) in the virus envelope, marked differences were observed in the mechanism of neutralization. This suggests that the interaction of viruses even within the same genus can be quite complex, thus requiring extensive investigation. Filoviruses are negative-sense, single-stranded RNA viruses with characteristic filamentous virus particles. This family of viruses includes the highly pathogenic Marburg and Ebola (EBOV) viruses known to cause fatal hemorrhagic fever. The EBOV and Marburg virus glycoproteins were found to activate the LP; however, the binding of MBL to EBOV had a mixed effect of either promoting LP progression or promoting virus entry (62).

Human immunodeficiency virus (HIV), an enveloped retrovirus, is known to activate the CP and LP independent of antibody, with direct binding of C1q to gp41 acting as a trigger for CP activation (63–66). Interaction of gp120 of HIV with the components of the CP, LP, and AP further induces complement activation. Interestingly, the CP was activated by HIV in the sera of rabbit, mouse, and guinea pig, resulting in the lysis of both virus and virus-infected cells (67–69). Enhanced activation of CP by antibodies against HIV followed by opsonization with C3 occurs during seroconversion and after transition to chronic phase (70). Human T-cell leukemia virus type 1 (HTLV-1) binds directly to C1q via its extramembrane region of the envelope protein gp21. However, binding of C1q to the cell-free virion not only inhibited its potency to infect cells but also resisted lysis by human serum. Treatment with anti C1q antibody could, however, reverse the inhibitory effect (71).

As discussed above, complement activation by many RNA viruses results in their neutralization; however, there have been exceptions to this rule. In the case of NiV, the presence of the F and G glycoproteins was sufficient to protect the VSV pseudotypes from being neutralized by complement (23). This resistance was further confirmed with wild-type NiV, which, upon exposure to complement, was found to be completely resistant to neutralization with marked reduction in surface deposition of C3b in comparison to PIV5 (72). Interestingly, similar observations were made during our investigations with CHIKV, wherein the virus was found to resist complement-mediated neutralization. Complement activation by CHIKV did result in deposition of C3b and C4b on the virus, but to a lesser degree (57). The inherent resistance to complement observed in the case of both CHIKV and NiV alludes to a virus-associated mechanism for complement resistance discussed in much detail later. Earlier *in vitro* studies demonstrated that RRV could not independently activate the AP or CP (73). However, the role of C3 in RRV pathogenesis was established when it was observed that the disease associated with RRV infection was severe in wtC57BL6 mice compared to $C3^{-/-}$ mice (74). Extensive studies had shown that the binding of MBL to the glycans associated with the E2 glycoprotein on the RRV-infected cells enhanced the disease severity in the host (75, 76).

The outbreak of the novel SARS-CoV-2 has had a devastating effect globally. Human coronaviruses belong to the family *Coronaviridae* and primarily affect the respiratory and gastrointestinal tract of a range of animals including mammals and birds. Clinical studies based on the 2003 SARS-CoV outbreak have highlighted the significance of LP in limiting the infection. The direct binding of the spike protein (S) of SARS-CoV to the carbohydrate recognition domain of MBL resulted in complement activation and C4 deposition on virus-infected cells. The residue on the S protein that binds to MBL was identified as the N-linked glycosylation at N330 (77). This residue is close to the angiotensin-converting enzyme 2 (ACE-2) receptor binding site on the virus. The MBL-S protein interaction did not affect SARS-CoV binding to ACE-2 but blocked the binding of the virus to C-type lectin (DC-SIGN) (78). Therefore, a direct correlation of MBL versus susceptibility to virus could be drawn as most patients with SARS had MBL levels in serum significantly lower than the controls. Proteomic analysis of serum proteins from SARS patients showed significantly higher levels of C3c compared to the control sera, suggesting complement activation during SARS-CoV infection (79). Further, the N protein of SARS-CoV2 was found to activate MASP-2, leading to the aberrant complement activation and deposition of MASP-2 and C4 in the lung tissue of severely affected COVID-19 patients (80). In another study, extensive deposition of C5b-9, C4d, and MASP-2 was observed in the postmortem lungs of COVID-19 patients

(81). These findings suggest that the deposition of C3 and C4 on the SARS-CoV-2 virion may lead to their neutralization (82).

COMPLEMENT: A DRIVER OF DISEASE SEVERITY

Complement, thus, is capable of restricting virus infection to a great extent. In certain viral infections, overwhelming immune response often results in significant damage to the host. Hyper-activation of complement has also been attributed to disease severity in a number of viral infections. This is well demonstrated in the case of RRV, an arthritogenic alphavirus known to cause marked inflammation of the joints. Exacerbation in the disease severity was observed in wtC57BL6 mice infected with RRV compared to $C3^{-/-}$ mice, despite marked similarities in the level of immune cell infiltration. This clearly demonstrated the importance of C3 in promoting disease rather than limiting the virus spread (74). Further studies demonstrated that the severity in the arthritic disease is dependent on complement receptor 3 (CR3 or CD11b/CD18). $CR3^{-/-}$ mice had only mild disease symptoms; however, similar to the $C3^{-/-}$ mice, the absence of CR3 did not affect recruitment of cellular infiltrate at the localized sites of inflammation. Therefore, the CR3-dependent signaling that is required for the overall expression of proinflammatory molecules was found to be the contributing factor for disease severity (83). In addition to C3, MBL and hence the LP contributed to the disease severity in mouse models of RRV infection, as increased deposition of MBL in the muscle tissue of RRV infected wtC57BL6 compared to $MBL^{-/-}$ mouse correlated with the enhanced disease severity in the former. Interestingly, the severity of RRV-induced symptoms in $C1q^{-/-}$ and Factor $B^{-/-}$ mice were comparable to wild type, suggesting the decisive role of LP in the disease prognosis. The glycans on the E2 protein of RRV was found to be the recognition sites for MBL, as mice infected with mutant RRV lacking the glycans had less pronounced symptoms despite both the viral load and the infiltration of proinflammatory cells being comparable to mice infected with wild-type RRV (75). These findings are clinically relevant as it was also demonstrated in the same study that human patients with RRV infections had substantially higher concentrations of MBL in both serum and synovial fluids compared to that of healthy individuals (75). Hence, it is clear that complement contributes significantly to the overall disease severity during RRV infection.

The role of complement in disease enhancement has also been well documented in flaviviral infection. In severe forms of DENV infection including DHF and dengue shock syndrome (DSS), complement activation caused significant damage to the host. Complement activation markers C3a and C5a (potent anaphylatoxins) were found to promote vascular leakage, contributing directly to DSS (52, 84–89). This is further supported by the findings that prior to enhanced consumption and reduction in complement components in the plasma of DSS patients, a significant increase in C3a and C5a was observed (87, 90–92). Other key observations supporting a role for complement in the severity of DENV disease include the activation of complement followed by MAC formation in the presence of anti-DENV antibodies; enhanced levels of C5a, C3a, NS1, and soluble C5b-9 in DHF patients; and, more indirectly, the observation that CD59 was found to be up regulated in patients with less severe form of disease (39, 93, 94). The relevance of complement in disease exacerbation during WNV infection is well documented clinically as well as in mouse models. *In vitro* studies have demonstrated that complement supported WNV infection with increased virus output, which required the cross-talk between IgM and CR3. In the absence of CR3, the effect was found to be reversed (95). The memory impairment due to the elimination of presynaptic terminals, observed in the survivors of West Nile encephalitis, was attributed to complement with C3 playing a major role. Up regulation of C1q in infected neurons and microglia and also the presynaptic terminals in mouse models further validated the damaging effect of complement in WNV infection (96).

Human immunodeficiency virus-associated neurocognitive disorder (HAND) can be due to either HIV encephalitis (HIVE) or mild neurocognitive impairment (NCI), for which the neuropathological substrate has not been established. Earlier studies have suggested that the central nervous system (CNS) dysfunction in HIV infection is due to indirect effects rather than neuronal or glial infection (97). The expression of complement components including C3 was significantly higher in brain tissues of HAND patients, and marked C3 reactivity was observed in astrocytes and neurons. Exposure of human fetal astrocytes to HIV in culture induced C3 promoter activity, mRNA expression, and protein production via NF-κB and protein kinase signaling in an IL-6-dependent manner (98). Similarly, when the global gene expression profile of various brain regions from HIV-1-infected patients without substantial NCI, those with substantial NCI without HIVE, and those with substantial NCI with HIVE against uninfected controls was performed, not only was HIV-1 RNA found to be substantially higher [3log (10) units], but several complement components were significantly up regulated in the neostriatum of NCI with HIVE group. Thus, the CS has a potential role in the overall pathogenesis of HIVE-induced NCI (99). Exposure of primary astrocytes and different cell lines of astrocytic origin to HIV-1 resulted in marked up regulation of C2 and C3 expression. The up regulation of C3 transcript and protein involved HIV-1 co-receptor engagement by both laboratory and primary isolates of HIV-1. Most importantly, the C3 induced was biologically active in the complement cascade (100). These findings hold huge significance as elevated levels of C3 and C4 in the CSF of HIV-infected individuals have been reported (101). In addition to this, significant up regulation in the cerebral synthesis of complement factors, C1q and C3, was observed in a range of cell types including astrocytes, neurons, microglia, infiltrating macrophages, and multinuclear giant cells in monkeys challenged with simian immunodeficiency virus (SIV) compared to the control animals. Up regulation also led to the enhanced deposition of both C3 and C1q on neighboring neuronal cells leading to lysis (102). This could possibly account for the cellular damage in brain

observed during neuro-AIDS. Peripheral blood T-lymphocytes from HIV-infected patients had decreased levels of CD59, suggesting suppression of CD59 expression by HIV (103). Upon exposure of human neuronal (SK-N-SH) and astrocyte (T98G) cell lines to either recombinant HIV gp41 protein or an immunodominant gp41 peptide, significant reduction in CD59 mRNA and protein was observed (104). These findings further substantiate that not only CD59 but also other proteins of the complement activation pathway are modulated by HIV. This, in turn, may contribute to the neuronal and glial cell damage in HAND patients.

Persistent activation of complement is one of the causative factors in chronic HCV infections, which may further lead to liver fibrosis (105). Contribution of C5 in mediating HCV-associated hepatic fibrosis was elucidated *in vivo*, and treatment with small-molecule inhibitors against C5aR exhibited antifibrotic effects (105). Several experimental and clinical studies so far support the involvement of complement dysregulation in intra- and extrahepatic disorders like type II mixed cryoglobulinemia (MC) and B cell lymphoma (106). A higher prevalence of anti-C1q antibodies among HCV genotype IV-infected patients with extrahepatic autoimmune involvement has been reported. HCV patients with immune complex diseases like systemic lupus erythematosus, cryoglobulinemia, glomerulonephritis, vasculitis, and severe rheumatoid arthritis had significantly higher levels of anti-C1q antibodies, which correlated to decreased C4 levels (107, 108). Hence, sustained activation of complement or suppression of complement by the core protein of HCV added to the significantly high levels of anti-C1q antibodies support manifestation of HCV-associated liver diseases.

More recently, MASP-2 has been implicated as one of the factors contributing to aggravated lung injury in COVID-19 pathogenesis. It was demonstrated that the N-protein, a secreted protein of SARS-CoV, MERS-CoV, and SARS-CoV-2, binds to MASP-2 (80). The binding site for MASP-2 on the N-protein of SARS-CoV was identified to be between the amino acid residues 116–124 in the coil motif of the N-protein. Binding of MASP-2 to the N-proteins of SARS-CoV-2 and MERS-CoV was traced to N (115–123) and N (104–112) regions that shared a high level of identity with the SARS-CoV N (116–124) motif. The N-proteins of all three viruses potentiated MBL–MASP-2 interaction, resulting in aberrant complement activation and subsequent deposition of C3 and C4 component. Using an adenovirus system encoding SARS-CoV-N and MERS-CoV-N, the investigators could further substantiate the role of N protein in acute inflammation. Administration of C1INH or an antibody against MASP-2 could substantially limit the damage. These findings were further validated using MASP-2 knockout mice, wherein the disease symptoms post N-protein challenge were less severe with longer survival rates than that of the wild-type mice, suggesting the importance of MASP-2 in SARS infection (80). The immunohistochemical analysis of postmortem lung tissues from five COVID-19 patients who died of respiratory failure showed enhanced deposition of MBL, MASP-2, and other markers including C4d and C5b-9 co-localizing with S protein of SARS-CoV-2 (80, 81). The serum samples also had elevated levels of C5a, suggesting hyperactivation of complement systemically or as a result of leakage of activated fragments from diseased lung (82). SARS-CoV-2-infected A549 cells showed differential expression of C3, C1r, and other complement proteins. Serum C3 levels were reduced in ∼57% of individuals, suggesting C3 consumption followed by complement activation (109). Of much interest was the finding that the anti-C5a antibody (BDB-001) had much promise in the recovery of severe COVID-19 patients (80, 82). Thus, the overall effect of RNA virus-complement interaction can be multifaceted as these interactions can either limit or promote the severity of disease.

COMPLEMENT AT THE CROSSROADS OF INNATE AND ADAPTIVE IMMUNITY IN RNA VIRUS INFECTION

A growing body of investigation reveals that the delicate balance between complement activation and regulation is one focal point of the disease outcome in viral infections. Apart from the immense role it plays in innate immunity, ample evidence points to the existence of cross-talk between the CS and the adaptive immune system.

Increased levels of C3a and C5a in the bronchoalveolar lavage fluid (BALF) and serum from patients infected with H1N1 pandemic virus suggest their role in virus-induced acute lung injury (ALI). The increased expression of C5aR on dendritic cells (DCs) promoted $CD8^+$ T cell activation by C5a. Mice treated with C5aR-specific antagonist showed a reduction in the flu virus-specific $CD8^+$ T cells accompanied by attenuated cytolysis in the lung (110). C5a-mediated leucopenia, reduced antigen-presenting cells, and impaired T cell responses had been observed in severe H7N9 influenza infection (111, 112). C5a being a chemoattractant for neutrophils and monocytes activates these cells to generate reactive oxygen species (ROS) (113). Studies from mice infected with influenza suggested a critical role of ROS in infection-induced pneumonia (114). Treatment with antioxidants could effectively reduce the lung damage and mortality in these mice (115). Increased expression of C5aR1 in bronchial epithelial and inflammatory cells accompanied by increase in C5a levels and deposition of C3 and C5b-9 in patients points to the association of C5a-C5R1 signaling in the systemic inflammatory response and the local tissue damage. Blockade of C5aR1 restricted viral replication in lung tissue and also alleviated ALI (116). The C3d and C3a generated during influenza A(H1N1)pdm09 infection plays a crucial role in evoking B cell as well as $CD4^+$ and $CD8^+$ T cell responses, which helps to contain the virus infection (22). The role of MBL in up regulating inflammatory responses causing tissue damage was demonstrated in MBL knockout (KO) mice challenged with the pandemic H1N1 or the avian influenza H9N2/G1. The KO mice developed less severe disease as indicated by the reduced weight loss when compared to the wild type. Increased levels of proinflammatory cytokines and chemokines in the wild-type mice were also observed when compared to MBL KO mice,

suggesting a role of MBL as a contributing factor to disease severity (117).

Increased viral load in the brain of mice infected with WNV, in the absence of C3 or CR1/CR2, suggested their importance in limiting viral infection. Deficiency in the components of the CP (C4 and C1q) was associated with decreased splenic infections and impaired B and T cell responses to WNV infection as C4 generated anti-WNV IgM responses, while C4 and C1q were required for anti-WNV IgG responses (45). In mouse macrophages, a CR3 mediated complement-dependent enhancement of WNV infection was observed.

Hepatitis C virus is known to cause persistent infections in individuals which later on may lead to chronic liver diseases such as cirrhosis and hepatocellular carcinoma. Defective expansion and differentiation of HCV-specific T cells observed in chronic HCV patients suggest an impaired antiviral immune response during the early stages of infection. A role of HCV core protein in immunomodulatory functions was demonstrated in chronic HCV patients and *in vivo* (118). The interaction of HCV core protein with gC1q receptor on human monocyte-derived DCs inhibited TLR-induced IL-12 production alone and not any other cytokines induced by TLR (119). Moreover, the engagement of core protein with gCIqR on the DCs also inhibited the production of IL-12 and mediated the production of Th2-induced cytokines such as IL-4 upon co-culturing with $CD4^+$ T cells. Patients with chronic HCV infection showed persistent expression of $gC1qR^+$ $CD4^+$ T cells, impairing T cell responses (120). These results taken together suggest that HCV limits the induction of Th1 response through the binding of core protein to gC1qR on the DCs, contributing to viral persistence (119).

The binding of HIV-1 gp41 to gC1qR on uninfected $CD4^+$ T lymphocytes resulted in NK cell-mediated lysis of these cells during HIV infection (121). HIV, during its dissemination through the bloodstream, is opsonized and adheres to the erythrocyte membrane through CR1. The presence of antibodies enhances this binding (122). The absence of complement opsonins on HIV or the blockade of CR1 inhibited virus adherence to RBCs. The CR1 inactivates C3b into iC3b and C3d. The C3d-bound HIV-1 is then trapped in follicular dendritic cells (FDCs), where it remains infectious and intact, acting as a reservoir (123). Opsonized HIV can also bind to B cells expressing CR-2 and further results in B-cell-mediated transmission of the virion to HIV-negative $CD4^+$ T cells in a CR1- or CR2-dependent manner (124). CR3 also plays an important role in HIV infection via modulating TLR 8-mediated signal transduction (125). Opsonization of retroviral particles with complement proteins has been shown to enhance the ability of DCs to induce the activation, expansion, and differentiation of virus-specific cytotoxic T lymphocyte (CTL) responses, both *in vitro* and *in vivo* (126). Exposure of DCs to C-opsonized HIV was able to activate DCs, which, in turn, stimulated CTLs to elicit antiviral activity, significantly better than non-opsonized HIV (126). The presence of HIV-specific CTLs correlated with the decline in viremia during the acute phase, but not during the chronic phase of infection (127, 128). The susceptibility of monocyte-derived macrophages (MDM) to HIV-1 infection was enhanced multiple folds upon pre-exposure to C5a or $C5a^{desArg}$. This was attributed to a notable increase in the secretion of TNF- α and IL-6, suggesting the role of complement anaphylatoxin in inducing proinflammatory responses, thereby supporting virus infection (129). Thus, C5a-elicited proinflammatory cytokines and recruited DCs can indirectly promote infection of MDMs and T cells (129, 130). HIV-complement interaction results in the generation of C5a, which, besides its anaphylactic property, can exert its function by interacting with C5a receptor 1 (C5aR1; CD88) and C5a receptor 2 (C5aR2, C5L2). In myeloid cells, C5aR1 heterodimerization with CCR5, a co-receptor for HIV, was observed. C5a receptor-specific antagonist or neutralizing monoclonal antibodies against C5aR1 could limit the integration of the R5 strain of HIV in MDM by reducing the CCR5 expression. Since the levels of C5aR1 in MDM of CCR5D32 homozygous individuals were comparable to that of the normal controls, it is evident that C5aR1 works in concert with CCR5 promoting HIV entry into macrophages (131). The opsonization of HIV-1 by complement is a critical factor in driving the hyper-expression and secretion of key cytokines, transforming growth factor b (TGF β), interleukin 1b (IL-1β), interleukin 6 (IL-6), and interleukin 23 (IL-23) in DCs supporting the T helper 17 cell (TH17) induction. The opsonized HIV mediated the expression of TH17 polarizing cytokines in DCs, via the extracellular signal-related kinases (ERK) and induced C3a production in these DCs, enhancing TH17 polarization (132). The type of opsonin on HIV also determined the type of response generated in DCs. While exposure of DCs to complement-opsonized HIV supported HIV-specific $CD8^+$ T cell response, HIV opsonized with IgG dampened this response (133). DCs are known to mount potent antiviral responses that can limit HIV infection, which includes the Sterile alpha motif and HD-domain-containing protein 1 (SAMHD1)-mediated response. However, complement-opsonized HIV overcomes SAMHD1 and other restrictions mounted by DCs to productively infect these cells. Interestingly, the degradation of SAMHD1 was not observed but phosphorylation of T_{592} in SAMHD1 restricted intracellular replication of HIV-1. Not only was the virus replication restricted, complement-opsonized HIV induced multiple changes in the DCs including DC maturation and expression of co-stimulatory molecules of Type I interferon genes, thereby stimulating HIV-specific $CD4^+$ and $CD8^+$ cells (134).

The disease progression to severe pneumonia and acute respiratory distress in SARS patients has been attributed to the hyperactivation of complement (135). The systemic activation of complement mediated by MBL in SARS-CoV-2 has also been demonstrated by the co-localization of MASP2 with the spike protein (S) in the lungs of COVID-19 patients (81). Most of the disease-associated inflammation and hypercoagulability is a direct effect of the binding of the complement component C5a to its receptor, C5aR on the T cells, activating them. This binding results in a hyper-inflammatory response called the "cytokine storm" (136). C5a also promotes immune paresis and exhaustion of antigen-specific lymphocytes in cases of higher viral load. C5a-mediated IL-6 and IL-8 release in SARS-CoV-1 and MERS-CoV

infections diminishes the antigen-presenting ability of DCs to T cells. Also, declined production of antiviral cytokines like IFN-α, -β, and -γ and IL-12p40 with an up regulation in proinflammatory chemokines dictates the imbalance in the pro- and anti-inflammatory cytokines in patients with H7N9, SARS-CoV-1, MERS-CoV, and the current SARS-CoV-2 infections (137). C5a-C5aR axis thereby plays a critical role in mediating damage caused by highly pathogenic viruses.

COMPLEMENT EVASION BY RNA VIRUSES

The response of complement to RNA virus infection is potent enough to restrict these viruses. It might appear that the CS is insurmountable and can, therefore, tip the balance always in favor of the host. On the contrary, these viruses have evolved to adapt and have adopted unique strategies to limit the damaging effects of complement (**Figure 2** and **Table 2**). Again, the limited genome in the case of RNA viruses is not a handicap as these viruses coexist with the host and exploit components from the host that favor their survival. This strategy strongly works in favor of enveloped RNA viruses; nonetheless, RNA viruses that lack envelope also possess certain characteristic features that help them counter the effects of complement. The sections below discuss the strategies adopted by RNA viruses to counter the effects of complement.

Viral Proteins as Complement Inhibitors

Non-enveloped RNA viruses lack the host-derived membrane but have unique mechanisms for targeting complement. Human astroviruses are icosahedral RNA viruses known to cause gastroenteritis. The direct association of the human astrovirus type 1 (HAstV-1) coat protein with C1q, an upstream component of CP, mediated the dissociation of C1s from the protease tetramer. This arrested the C1s cleavage, limiting the progression of the pathway, resulting in the decreased levels of C3b and C4b. The coat proteins of at least two other serotypes, HAstV-2 and HAstV-4, were also found to inhibit complement activation, suggesting that this inhibition was not restricted to HAstV-1 alone (138). Further investigations revealed that the inhibitory potential of the coat protein of HAstV-1 was not restricted to the CP but also included the LP by the direct binding of coat protein to MBL. The finding that the coat protein can inhibit C5a generation leading to a substantial reduction in C5b-9 holds clinical relevance as HAstV-1 infection causes gastroenteritis with a low inflammatory status in children (139). Hence, it is evident that the structural proteins in non-enveloped viruses can have direct modulatory effects on complement activation, thus limiting virus neutralization.

Proteins of enveloped viruses are also known to interact with key complement components and inhibit complement function. HCV belonging to the family *Flaviviridae* has a unique mechanism of modulating the CP. The NS 3/4A, a non-structural protein of HCV with protease activity, could directly bind and cleave the γ-subunit of C4, abrogating the effect of complement on the virus (140). The structural protein E2 in the bovine viral diarrhea virus has also been shown to block complement-mediated cell lysis, thereby acting as a potent inhibitor of complement (141). The NS1 protein secreted from the DENV-infected insect cells contains glycans rich in mannose. This secreted form of NS1 could also be identified in the saliva of DENV-infected *A. aegypti* mosquito. Independently, while DENV-NS1 could bind to C1s, C4, and C4BP, it was also found to bind to MBL, protecting the virus from neutralization by complement at the local sites of infection (142). WNV NS1 also binds to C1s and C4 and inactivate C4, thereby attenuating complement activation (143).

The matrix protein (M1) of influenza virus (A/WSN/33 strain) is an abundantly expressed protein in virus-infected cells and is released during necrosis to protect the newly formed virus particles from complement-mediated neutralization. The N-terminal domain of M1 binds to the globular head of C1q, blocking the interaction of IgG and C1q and thereby the CP (144).

Exploitation of the Complement Pathway Proteins

The main role of proteins associated with all the three complement pathways is to target pathogens including viruses, which, upon activation, facilitate virus neutralization. In many instances, these proteins have been found to be exploited by viruses to gain entry into cells, to replicate and utilize such cells as reservoirs, and to enhance virus spread. Many viruses preferentially exploit upstream components of the CP and LP like C1q and MBL to enhance infectivity and spread. The NS1 proteins of flaviviruses WNV, DENV, and yellow fever virus (YFV) have been shown to directly interact with C4, limiting the CP and LP. The NS1 protein directly binds to C4 and recruits C1s, the protease in the C1 complex, forming the C4–NS1–C1s complex that promotes active sequestration of C4, protecting the virus from the neutralizing effects of complement (143). Interaction of HCV core protein with gC1qR was found to have major implications in the immune responses to the virus (145–147).

Mannose binding lectins were found to enhance the infectivity of a range of RNA viruses including WNV, NiV, Hendra virus, and EBOV. Using EBOV glycoprotein pseudotyped lentivirus, it has been demonstrated that specific epitopes on the N-linked glycans of EBOV glycoproteins bound specifically to the carbohydrate recognition domain on MBL. Enhancement in virus uptake and infection due to MBL binding was found to be dependent on C1QBP (gC1q receptor) (148). The binding of mucin like domain of EBOV (Zaire strain) glycoprotein to the fibrinogen-like recognition domain of ficolin-1, in the presence of limited complement, promoted virus entry rather than neutralization via the LP. The significance of this interaction is that ficolin-1 was found to enhance EBOV infection in an antibody- dependent manner (149).

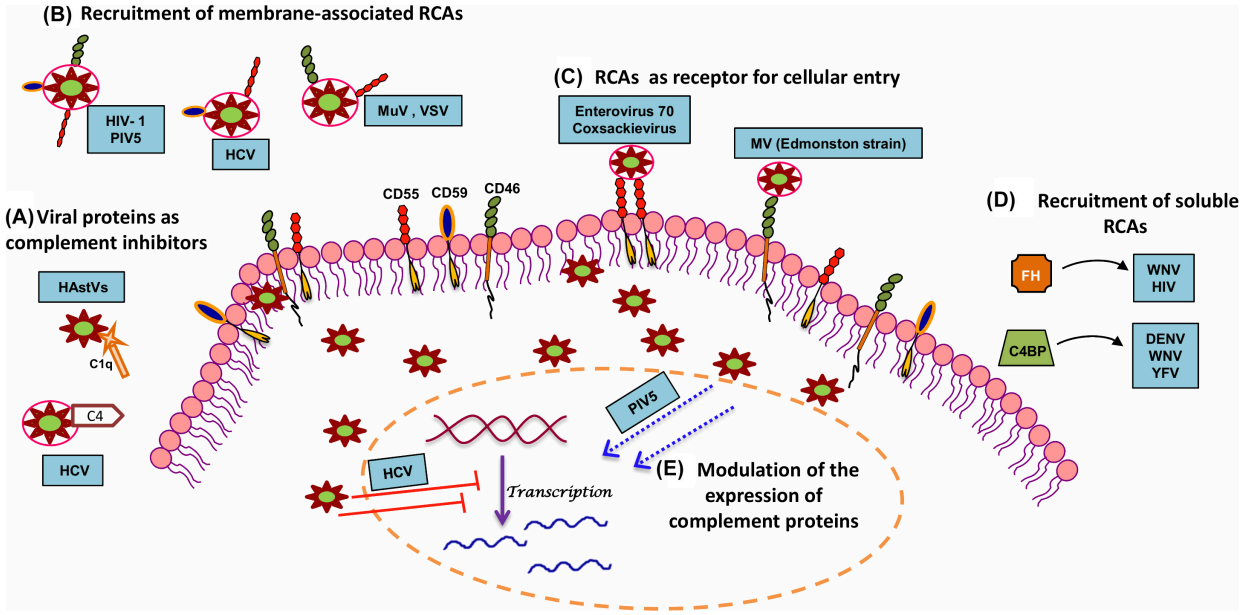

FIGURE 2 | Strategies adopted by RNA viruses to modulate complement. In order to productively infect the host, RNA viruses have adopted several strategies to subvert the neutralizing effects of complement. A few mechanisms include **(A)** utilization of viral proteins as complement inhibitors, **(B)** recruitment of membrane-associated RCAs, **(C)** utilization of complement proteins for cellular entry and propagation, **(D)** recruitment of soluble RCAs, and **(E)** modulation of host complement protein expression. Examples of RNA viruses adopting these mechanisms are highlighted in blue boxes. Key: HAstV (human astroviruses), HCV (hepatitis C virus), HIV-1 (human immunodeficiency virus type 1), MuV (mumps virus), PIV5 (parainfluenza virus type 5), VSV (vesicular stomatitis virus), MV (measles virus), WNV (West Nile virus), DENV (dengue virus), YFV (yellow fever virus), and HIV (human immunodeficiency virus).

Modulation of the Expression of Complement Components

RNA viruses have also been shown to down regulate the synthesis of complement proteins. HCV effectively puts a block in the progression of the complement pathway by transcriptionally regulating expression of critical components like C3, C4, C2, and C9 (150–153). Analysis of the liver tissue from chronic HCV patients showed a reduced expression of C4 mRNA. The NS5A protein of HCV was found to modulate the expression of two of the transcription factors, namely, upstream stimulating factor I (USF-1) and inhibiting interferon regulatory factor I (IRF-1), which are essential for either basal or IFN-γ-induced C4 expression (151). Similarly, HCV was also found to modulate C3 mRNA expression. The down regulation of farnesoid X receptor (FXR) by the HCV core protein weakly represses the C3 promoter activity, whereas NS5A protein, by inhibiting the expression of CAAT/enhancer binding protein beta (C/EBP-β), a transcription factor known to bind to the IL-1/IL-6 response element in the C3 promoter, strongly repressed IL-1β-induced C3 promoter activity. Thus, active modulation of C3 transcription factors by HCV results in the underexpression of C3 in chronic HCV patients (150). Both HCV and its core protein were found to repress C9 mRNA and protein expression. The core protein modulated T cell factor-4, the transcription factor regulating C9 promoter activity, resulting in the decreased levels of C9 mRNA in liver tissue and C5b-9 in the sera of chronic HCV patients (152). Marked decrease in C2 mRNA in chronic HCV infection also contributed to significantly low levels of CP C3 convertase (C4b2a). This resulted in a reduction of overall C3 turnover and diminished C3b deposition on target cells (153). HCV NS2 and NS5B proteins are also responsible for HCV-associated decrease in MHC class I chain-related protein A and B (MICA/B), resulting in a loss of the C3/C4 complement components. This inactivation of the CS leads to impairment of NK cell activation and attenuated adaptive immune response (154). Taken together, the potency of complement is reduced during HCV infection due to the active modulation of complement gene expression at the level of transcription. Besides modulation of complement components of the activation pathway, certain RNA viruses also modulate the expression of regulatory proteins or inhibitors of complement. Paramyxoviruses PIV5 and hRSV are known to up regulate the expression of CD55 (155) and CD59 (156). The up regulation of the regulatory proteins favors the virus as it can readily incorporate these proteins into their envelope during budding, limiting the neutralizing effect of complement.

Recruitment of Membrane-Associated Regulators

Enveloped RNA viruses acquire their envelope from the host during the process of virus egress. This, in many instances, turns out to be advantageous for the virus, as it also picks up the host proteins associated with the membrane, which can confer protection from the host complement. Widely reported host membrane-associated RCAs in the virus envelope include CD46, CD55, and CD59. RNA viruses including HIV-1, PIV5, MuV, NDV, and VSV are known to incorporate these RCAs into their

TABLE 2 | Evasion strategies adopted by RNA viruses against the complement system.

S.No.	Complement evasion strategy	Virus family and examples
1.	Recruitment of membrane-associated regulators of complement activation	***Rhabdoviridae*** Vesicular stomatitis virus (CD46, CD55) ***Paramyxoviridae*** Parainfluenza virus 5 (CD46, CD55) Newcastle disease virus (CD55, CD46) ***Flaviviridae*** Hepatitis C virus (CD59) ***Retroviridae*** Human immunodeficiency virus type 1 (CD46,CD55,CD59) Human T-cell leukemia virus type 1 (CD55,CD59)
2.	Incorporation of soluble regulators of complement activation	***Flaviviridae*** Dengue virus (C4BP, Clusterin, Vitronectin) West Nile virus (fH, C4BP) Yellow fever virus (C4BP) ***Retroviridae*** Human immunodeficiency virus type 1 (fH)
3.	Virion-associated protease activity (FI-like activity)	***Paramyxoviridae*** Nipah virus ***Togaviridae*** Chikungunya virus
4.	Exploitation of complement proteins as entry receptors	***Paramyxoviridae*** Measles virus – Edmonston strain (CD46) ***Picornaviridae*** Echoviruses (CD55) Group B coxsackieviruses (CD55)
5.	Transcriptional regulation of complement proteins	***Flaviviridae*** Hepatitis C virus (HCV down regulation of C2, C3 and C9) ***Paramyxoviridae*** Parainfluenza virus 5 (up regulation of CD59 and CD55) ***Retroviridae*** Human immunodeficiency virus type 1 (down regulation of CD59 and up regulation of C3 and C1q in the brain) ***Pneumoviridae*** Human respiratory syncytial virus (Up regulation of CD59 and CD55)
6.	Viral proteins as complement inhibitors	***Astroviridae*** Human astrovirus 1 (Coat protein binds to C1q and arrests C1s) ***Orthomyxoviridae*** Influenza virus (A/WSN/33) M1 protein binds to C1q and blocks its interaction with IgG ***Flaviviridae*** Bovine viral diarrhea virus (E2 protein) Hepatitis C virus (NS3/4A binds to C4, cleaves γ subunit)

envelope (30, 60, 155, 157, 158). Extensive studies on the virus-associated CD46 and CD55 show that they are functional, with CD46 acting as a cofactor for the fI-mediated cleavage of C3b into iC3b, and CD55, accelerating the decay of complement convertases protecting these viruses from complement (60, 159). HCV particles generated from hepatic cells were found to harbor CD59, an inhibitor of the terminal pathway of complement. CD59 associated with the virion conferred protection to the virus from antibody-dependent complement-mediated lysis. Addition of CD59 blockers to both cell line derived and plasma primary virions resulted in substantial virolysis in the presence of complement, which highlights the significance of CD59 in protecting HCV from complement (160).

Human immunodeficiency virus 1 incorporates CD46, CD55, and CD59 into the virus envelope during egress. The presence or absence of the RCAs in the virus envelope depended on the cell type in which the virus was generated. The levels of RCA incorporated into the virus envelope dictated the extent of neutralization. When sensitized with gp160 antibodies, only those viruses generated in cell lines underwent virolysis; however, primary HIV isolates required sensitization with anti-RCA antibodies to undergo virolysis by complement. Besides the primary isolates of HIV-1 and specific cell line-derived HIV, (SIV delta/B670) was also found to incorporate all three RCAs. The protective role of the RCAs in limiting the effect of complement on HIV is well evidenced from the findings that HIV cultured in CHO cells with individual RCAs was significantly protected from complement-mediated virolysis compared to those without the regulators (157, 158, 161–163). Human T cell leukemia/lymphoma oncovirus type I (HTLV-1) cultured in MT2 cells contained both CD55 and CD59 in the virus envelope. The incorporated RCAs protected the particles from complement-mediated neutralization. However, this was reversed when the particles were treated with anti-CD55 and anti-CD59 antibodies

or phospholipase C (164). Although it could well be considered that incorporation is a random process, growing evidences as in the case of HCV, RSV, and PIV5 suggest the recruitment of CD55 and/or CD59 to be more specific in nature because the respective virus infection induced up regulation of the RCAs in infected cells (155, 156, 165, 166).

Recruitment of Soluble Regulators

RNA viruses not only incorporate membrane bound RCAs but also recruit soluble RCAs. The NS1 protein of DENV, WNV, and YFV were all found to recruit C4BP, an RCA of the CP (167), while other complement regulators reported to bind to NS1 include fH (168), clusterin (169), and vitronectin (170). The secreted WNV NS1 protein recruits soluble fH either in solution or onto the cell surface, as NS1 is known to bind back to cell surface. The fH thus recruited acted as a cofactor for the factor I-mediated cleavage of C3b into iC3b. The fH bound to NS1 protein can rapidly regulate complement in solution and limit complement deposition and damage to the virus and virus-infected cells (168). It can also restrict both CP and LP by binding to C4BP and inactivating C4b, both on the cell surface and in solution (167). Recruitment of soluble RCAs by NS1 protein is not pan-flavivirus as it has been demonstrated that the NS1 protein of JEV was incapable of recruiting fH (44). As mentioned above, the NS1 protein of at least three flaviviruses binds to C4BP and acts as a cofactor for the inactivation of C4b into C4c and C4d both in solution and on the cell surface. The binding site of NS1 on C4BP was mapped to the α-chain of C4BP (167). The DENV NS1 protein can also interact with clusterin, an important regulator of the terminal pathway of complement. This interaction prevents the assembly of MAC and thereby, virolysis (169). The NS1 protein of flaviviruses, including DENV2, ZIKV, and WNV, has been shown to play a role in inhibiting the terminal pathway of complement by inhibiting C9 polymerization. Additionally, the NS1 protein of DENV-2 was found to bind to vitronectin, a regulator of the terminal complement pathway and block C9 polymerization and MAC assembly (170). Among the retroviruses, HIV is known to recruit fH with the binding target being the Env proteins gp120 and gp41 (171–173). Factor H was found to have a dominant role in protecting HIV from complement. This is highlighted by the finding that even in the presence of anti-HIV antibodies, HIV was not neutralized by NHS but was neutralized by fH-deficient serum. The neutralizing effect of complement in NHS could be restored only upon inhibiting the interaction of fH with gp41, using a specific blocking monoclonal antibody against the fH binding site on gp41 (173).

Most of the evasion strategies described above involved recruitment of either membrane-associated or soluble RCAs and inhibitors of complement. Factor I is an important and unique serine protease involved in the regulatory arm of the complement. Factor I mediates the inactivation of C3b into iC3b or C3c and C3d, and C4b into C4c and C4d in the presence of specific cofactors. Earlier we had discussed that NiV exhibits an fI-like activity that could inactivate C3b but not C4b. Only the first order of C3b inactivation, which is the conversion of C3b into iC3b, was supported by the NiV-associated fI-like activity. Conversion of C3b into iC3b occurred with the incubation of C3b, fH, or sCR1 and wtNiV without the addition of fI. CD46 was also found to be associated with wtNiV, but interestingly, the associated CD46 was incapable of inactivating C3b into iC3b even with the addition of fI (72). More recently, it was identified that CHIKV also has an fI-like activity that contributes to its complement resistance. However, a stark difference was that the CHIKV-associated fI-like activity supported only the fH and not CD35-mediated inactivation of C3b into iC3b. Like NiV, CHIKV-associated fI-like activity was incapable of inactivating C4b. Although electron microscopic analysis pointed to an association of fI to the CHIKV envelope, immunoblotting and function blocking cofactor activity assays with an antibody targeting fI protease activity showed that CHIKV-associated fI-like activity is not of host origin (57). Since the source of fI or fI-like activity is not yet determined at least in the case of CHIKV, detailed investigations are required to gain a better understanding on the precise mechanisms involved.

Complement Proteins as Tools for Virus Attachment and Entry

Receptor usage is a key factor that determines the host range in many viruses. Viruses using RCAs to attach to and infect cells have been widely reported among the members of the *Picornaviridae* family. Many subtypes of echoviruses like echo-6, -7, -11, -12, -20, and -21 bind to CD55 to gain access into the cell (174) and further studies established the binding site of echo-7 virus to CCPs 2–4 of CD55 (175). In contrast, many types of coxsackieviruses and enterovirus 70 also bind to CD55, but this attachment did not directly facilitate virus entry (176–179). Group B coxsackieviruses (CVBs) binding to CD55 on the apical surface of cells resulted in the clustering of CD55. This activated Abl kinases, resulting in actin remodeling, which delivers the virus to the tight junctions. At the tight junction, it interacts with the coxsackievirus and adenovirus receptor (CAR), leading to the internalization and the subsequent uncoating and replication (180). The Edmonston strain of measles virus uses all four isoforms of CD46 as its cellular receptor binding to CCP-1 and -2 with hemagglutinin being the interacting viral surface glycoprotein (181–185). CR3 and CR4 are used by hantavirus (186) for entry, while CR4 is exploited by rotavirus (187).

CONCLUDING REMARKS

Complement–RNA virus interactions are complex, with each remaining in the cross hairs of the other. The role of the CS is undeniably that of a barrier at all levels of virus infection, with RNA viruses facing stiff resistance from the very early stages of infection. Infection with RNA viruses mostly begins locally, involving skin (vector borne infections) or the mucosal surface. It has been well established that the CS is active at these local sites of infection (2, 3). Surface features of these viruses dictate the type of pathway activated, with some viruses even activating more than one pathway (52). These viral signatures are so critical that even slight alterations can cause switch in pathways (29) and can define the host responses to infection, which include disease severity.

These initial interactions set the stage for sequential progress of the complement cascade promoting virus neutralization. Yet again, marked variations exist even among closely related viruses with regard to the mechanism of neutralization (**Table 1**) (27, 60, 61). Although it may be anticipated that surface glycoproteins could contribute to these differences, in-depth investigations into these interactions are required to better understand their role. Another key aspect is the damaging effect the CS imparts on the host during the process of virus clearance. Hyperactivation of complement during infection by certain members of the *Togaviridae*, *Flaviviridae*, and *Coronaviridae* plays a key role in disease severity. The cross-talk between complement and other components of the immune system during RNA virus infection plays a pivotal role in the overall pathogenesis, with the latest example being complement-mediated disease enhancement in SARS-CoV-2 infection. Thus, RNA viruses appear to be in the cross hairs of complement.

The big question that arises out of RNA virus–complement interactions is how these viruses productively infect and cause diseases in the host, overcoming complement. Both enveloped and non-enveloped RNA viruses have ingenious ways of limiting complement. Many DNA viruses including poxviruses and γ-herpes viruses have a large genome that supports expression of viral homologs that mimic the functions of complement regulatory proteins. RNA viruses might appear at a disadvantage with respect to its genome size; however, they are known to thwart complement in multiple ways. One well-studied mechanism is the recruitment of the host RCAs by enveloped RNA viruses. The protective effect of these RCAs on the virus is very significant, especially at the local sites of infection. Another area requiring significant investigation is the nature of incorporation of the RCAs. Detailed investigation is required to further understand the specificity or selectivity of incorporation of these RCAs.

The evasion strategies adopted by RNA viruses bring the CS in the cross hairs of the virus. It is clear that the balance is quite delicate and can tip to any side, as is evidenced in the case of flaviviruses like DENV and more recently in SARS-CoV-2. Approaches to combat SARS-CoV-2, although not proven completely, include targeting complement activation to better manage the disease symptoms. Exploitation of RNA viruses as vaccine and oncolytic vectors is an emerging field. Viral vectors should be attenuated enough so as to not cause disease but yet be capable of productively infecting the target cells. An attenuated vector harboring RCAs would be a better candidate to bypass complement yet meet the requirements. Thus, a rational approach to develop therapeutics, inhibitors, or viral vectors should also take the role of complement into consideration. In conclusion, studies have highlighted the complexities in RNA virus–complement interactions, but with emerging viruses, a constant pursuit is required to better understand these interactions.

AUTHOR CONTRIBUTIONS

NK, UK, and JJ conceived the concept for this review article. NK, UK, ST, and JJ wrote the manuscript. NK, UK, ST, and JJ read, edited, and reviewed the manuscript. All authors contributed to the article and approved the submitted version.

FUNDING

This work was supported by the Department of Biotechnology-Ramalingaswami Fellowship, BT/RLF/Re-entry/29/2012, and Department of Biotechnology–Rajiv Gandhi Center for Biotechnology Intramural funds (to JJ). NK acknowledges funding from the Council of Scientific & Industrial Research (CSIR), India [09/716(0174)/2017-EMR-1] and UK, the University Grants Commission/Council of Scientific & Industrial Research (UGC/CSIR), India [19/06/2016(i)EU-V]

ACKNOWLEDGMENTS

We thank Prof. M. Radhakrishna Pillai, Director, RGCB, for his constant support.

REFERENCES

1. Kolev M, Kemper C. Keeping it all going-complement meets metabolism. *Front Immunol.* (2017) 8:1. doi: 10.3389/fimmu.2017.00001
2. Lubbers R, van Essen MF, van Kooten C, Trouw LA. Production of complement components by cells of the immune system. *Clin Exp Immunol.* (2017) 188:183–94. doi: 10.1111/cei.12952
3. Morgan BP, Gasque P. Extrahepatic complement biosynthesis: where, when and why? *Clin Exp Immunol.* (1997) 107:1–7. doi: 10.1046/j.1365-2249.1997.d01-890.x
4. Bajic G, Degn SE, Thiel S, Andersen GR. Complement activation, regulation, and molecular basis for complement-related diseases. *EMBO J.* (2015) 34:2735–57. doi: 10.15252/embj.201591881
5. Walport MJ. Complement. First of two parts. *N Engl J Med.* (2001) 344:1058–66.
6. Carroll MV, Sim RB. Complement in health and disease. *Adv Drug Deliv. Rev.* (2011) 63:965–75.
7. Ricklin D, Reis ES, Lambris JD. Complement in disease: a defence system turning offensive. *Nat Rev Nephrol.* (2016) 12:383–401. doi: 10.1038/nrneph.2016.70
8. Schwaeble W, Dahl MR, Thiel S, Stover C, Jensenius JC. The mannan-binding lectin-associated serine proteases (MASPs) and MAp19: four components of the lectin pathway activation complex encoded by two genes. *Immunobiology.* (2002) 205:455–66. doi: 10.1078/0171-2985-00146
9. Fearon DT, Austen KF, Ruddy S. Formation of a hemolytically active cellular intermediate by the interaction between properdin factors B and D and the activated third component of complement. *J Exp Med.* (1973) 138:1305–13. doi: 10.1084/jem.138.6.1305
10. Le GT, Abbenante G, Fairlie DP. Profiling the enzymatic properties and inhibition of human complement factor B. *J Biol Chem.* (2007) 282:34809–16. doi: 10.1074/jbc.m705646200
11. Pillemer L, Blum L, Lepow IH, Ross OA, Todd EW, Wardlaw AC. The properdin system and immunity. I. Demonstration and isolation of a new serum protein, properdin, and its role in immune phenomena. *Science.* (1954) 120:279–85. doi: 10.1126/science.120.3112.279

12. Morgan BP, Marchbank KJ, Longhi MP, Harris CL, Gallimore AM. Complement: central to innate immunity and bridging to adaptive responses. *Immunol Lett.* (2005) 97:171–9. doi: 10.1016/j.imlet.2004.11.010
13. Carrol MC, Fearon DT. *Regulation by Complement of Acquired Immunity, The Human Complement System in Health and Disease*. New York, NY: Marcel Dekker, Inc (2004). p. 327–33.
14. Zipfel PF, Skerka C. Complement regulators and inhibitory proteins. *Nat Rev Immunol.* (2009) 9:729–40. doi: 10.1038/nri2620
15. Kim DD, Song WC. Membrane complement regulatory proteins. *Clin Immunol.* (2006) 118:127–36.
16. Taubenberger JK. The origin and virulence of the 1918 "Spanish" influenza virus. *Proc Am Philos Soc.* (2006) 150:86–112.
17. Yamamoto F, Maeno K, Shibata S, Iinuma M, Miyama A, Kawamoto Y. Inactivation of influenza B virus by normal guinea-pig serum. *J Gen Virol.* (1987) 68(Pt 4):1135–41. doi: 10.1099/0022-1317-68-4-1135
18. Jayasekera JP, Moseman EA, Carroll MC. Natural antibody and complement mediate neutralization of influenza virus in the absence of prior immunity. *J Virol.* (2007) 81:3487–94. doi: 10.1128/jvi.02128-06
19. Beebe DP, Schreiber RD, Cooper NR. Neutralization of influenza virus by normal human sera: mechanisms involving antibody and complement. *J Immunol.* (1983) 130:1317–22.
20. Reading PC, Hartley CA, Ezekowitz RA, Anders EM. A serum mannose-binding lectin mediates complement-dependent lysis of influenza virus-infected cells. *Biochem Biophys Res Commun.* (1995) 217:1128–36. doi: 10.1006/bbrc.1995.2886
21. Kase T, Suzuki Y, Kawai T, Sakamoto T, Ohtani K, Eda S, et al. Human mannan-binding lectin inhibits the infection of influenza A virus without complement. *Immunology.* (1999) 97:385–92. doi: 10.1046/j.1365-2567.1999.00781.x
22. Rattan A, Pawar SD, Nawadkar R, Kulkarni N, Lal G, Mullick J, et al. Synergy between the classical and alternative pathways of complement is essential for conferring effective protection against the pandemic influenza A(H1N1) 2009 virus infection. *PLoS Pathog.* (2017) 13:e1006248. doi: 10.1371/journal.ppat.1006248
23. Johnson JB, Aguilar HC, Lee B, Parks GD. Interactions of human complement with virus particles containing the Nipah virus glycoproteins. *J Virol.* (2011) 85:5940–8. doi: 10.1128/jvi.00193-11
24. Vasantha S, Coelingh KL, Murphy BR, Dourmashkin RR, Hammer CH, Frank MM, et al. Interactions of a nonneutralizing IgM antibody and complement in parainfluenza virus neutralization. *Virology.* (1988) 167:433–41. doi: 10.1016/s0042-6822(88)90105-5
25. Devaux P, Christiansen D, Plumet S, Gerlier D. Cell surface activation of the alternative complement pathway by the fusion protein of measles virus. *J Gen Virol.* (2004) 85:1665–73. doi: 10.1099/vir.0.79880-0
26. Sissons JG, Cooper NR, Oldstone MB. Alternative complement pathway-mediated lysis of measles virus infected cells: induction by IgG antibody bound to individual viral glycoproteins and comparative efficacy of F(ab')2 and Fab' fragments. *J Immunol.* (1979) 123:2144–9.
27. Johnson JB, Capraro GA, Parks GD. Differential mechanisms of complement-mediated neutralization of the closely related paramyxoviruses simian virus 5 and mumps virus. *Virology.* (2008) 376:112–23. doi: 10.1016/j.virol.2008.03.022
28. Hirsch RL, Wolinsky JS, Winkelstein JA. Activation of the alternative complement pathway by mumps infected cells: relationship to viral neuraminidase activity. *Arch Virol.* (1986) 87:181–90. doi: 10.1007/bf01315298
29. Johnson JB, Schmitt AP, Parks GD. Point mutations in the paramyxovirus F protein that enhance fusion activity shift the mechanism of complement-mediated virus neutralization. *J Virol.* (2013) 87:9250–9. doi: 10.1128/jvi.01111-13
30. Biswas M, Johnson JB, Kumar SR, Parks GD, Elankumarana S. Incorporation of host complement regulatory proteins into Newcastle disease virus enhances complement evasion. *J Virol.* (2012) 86:12708–16. doi: 10.1128/jvi.00886-12
31. Welsh RM. Host cell modification of lymphocytic choriomeningitis virus and Newcastle disease virus altering viral inactivation by human complement. *J Immunol.* (1977) 118:348–54.
32. Sissons JG, Oldstone MB, Schreiber RD. Antibody-independent activation of the alternative complement pathway by measles virus-infected cells. *Proc Natl Acad Sci USA.* (1980) 77:559–62. doi: 10.1073/pnas.77.1.559
33. Kaul TN, Welliver RC, Ogra PL. Appearance of complement components and immunoglobulins on nasopharyngeal epithelial cells following naturally acquired infection with respiratory syncytial virus. *J Med Virol.* (1982) 9:149–58. doi: 10.1002/jmv.1890090210
34. Bukreyev A, Yang L, Collins PL. The secreted G protein of human respiratory syncytial virus antagonizes antibody-mediated restriction of replication involving macrophages and complement. *J Virol.* (2012) 86:10880–4. doi: 10.1128/jvi.01162-12
35. Corbeil S, Seguin C, Trudel M. Involvement of the complement system in the protection of mice from challenge with respiratory syncytial virus Long strain following passive immunization with monoclonal antibody 18A2B2. *Vaccine.* (1996) 14:521–5. doi: 10.1016/0264-410x(95)00222-m
36. Edwards KM, Snyder PN, Wright PF. Complement activation by respiratory syncytial virus-infected cells. *Arch Virol.* (1986) 88:49–56. doi: 10.1007/bf01310889
37. Yoder SM, Zhu Y, Ikizler MR, Wright PF. Role of complement in neutralization of respiratory syncytial virus. *J Med Virol.* (2004) 72:688–94. doi: 10.1002/jmv.20046
38. Brown KS, Keogh MJ, Owsianka AM, Adair R, Patel AH, Arnold JN, et al. Specific interaction of hepatitis C virus glycoproteins with mannan binding lectin inhibits virus entry. *Protein Cell.* (2010) 1:664–74. doi: 10.1007/s13238-010-0088-9
39. Avirutnan P, Punyadee N, Noisakran S, Komoltri C, Thiemmeca S, Auethavornanan K, et al. Vascular leakage in severe dengue virus infections: a potential role for the nonstructural viral protein NS1 and complement. *J Infect Dis.* (2006) 193:1078–88. doi: 10.1086/500949
40. Libraty DH, Young PR, Pickering D, Endy TP, Kalayanarooj S, Green S, et al. High circulating levels of the dengue virus nonstructural protein NS1 early in dengue illness correlate with the development of dengue hemorrhagic fever. *J Infect Dis.* (2002) 186:1165–8. doi: 10.1086/343813
41. Lin CF, Lei HY, Shiau AL, Liu CC, Liu HS, Yeh TM, et al. Antibodies from dengue patient sera cross-react with endothelial cells and induce damage. *J Med Virol.* (2003) 69:82–90. doi: 10.1002/jmv.10261
42. Yamanaka A, Kosugi S, Konishi E. Infection-enhancing and -neutralizing activities of mouse monoclonal antibodies against dengue type 2 and 4 viruses are controlled by complement levels. *J Virol.* (2008) 82:927–37. doi: 10.1128/jvi.00992-07
43. Mehlhop E, Ansarah-Sobrinho C, Johnson S, Engle M, Fremont DH, Pierson TC, et al. Complement protein C1q inhibits antibody-dependent enhancement of flavivirus infection in an IgG subclass-specific manner. *Cell Host Microbe.* (2007) 2:417–26. doi: 10.1016/j.chom.2007.09.015
44. Krishna VD, Rangappa M, Satchidanandam V. Virus-specific cytolytic antibodies to nonstructural protein 1 of Japanese encephalitis virus effect reduction of virus output from infected cells. *J Virol.* (2009) 83:4766–77. doi: 10.1128/jvi.01850-08
45. Mehlhop E, Whitby K, Oliphant T, Marri A, Engle M, Diamond MS. Complement activation is required for induction of a protective antibody response against West Nile virus infection. *J Virol.* (2005) 79:7466–77.
46. Fuchs A, Lin TY, Beasley DW, Stover CM, Schwaeble WJ, Pierson TC, et al. Direct complement restriction of flavivirus infection requires glycan recognition by mannose-binding lectin. *Cell Host Microbe.* (2010) 8:186–95. doi: 10.1016/j.chom.2010.07.007
47. Douradinha B, McBurney SP, Soares de Melo KM, Smith AP, Krishna NK, Barratt-Boyes SM, et al. C1q binding to dengue virus decreases levels of infection and inflammatory molecules transcription in THP-1 cells. *Virus Res.* (2014) 179:231–4. doi: 10.1016/j.virusres.2013.11.007
48. Mehlhop E, Nelson S, Jost CA, Gorlatov S, Johnson S, Fremont DH, et al. Complement protein C1q reduces the stoichiometric threshold for antibody-mediated neutralization of West Nile virus. *Cell Host Microbe.* (2009) 6:381–91. doi: 10.1016/j.chom.2009.09.003
49. Nelson S, Jost CA, Xu Q, Ess J, Martin JE, Oliphant T, et al. Maturation of West Nile virus modulates sensitivity to antibody-mediated neutralization. *PLoS Pathog.* (2008) 4:e1000060. doi: 10.1371/journal.ppat.1000060

50. Fuchs A, Pinto AK, Schwaeble WJ, Diamond MS. The lectin pathway of complement activation contributes to protection from West Nile virus infection. *Virology.* (2011) 412:101–9. doi: 10.1016/j.virol.2011.01.003
51. Avirutnan P, Hauhart RE, Marovich MA, Garred P, Atkinson JP, Diamond MS. Complement-mediated neutralization of dengue virus requires mannose-binding lectin. *mBio.* (2011) 2:e00276–11.
52. Mehlhop E, Diamond MS. Protective immune responses against West Nile virus are primed by distinct complement activation pathways. *J Exp Med.* (2006) 203:1371–81. doi: 10.1084/jem.20052388
53. Mehlhop E, Fuchs A, Engle M, Diamond MS. Complement modulates pathogenesis and antibody-dependent neutralization of West Nile virus infection through a C5-independent mechanism. *Virology.* (2009) 393:11–5. doi: 10.1016/j.virol.2009.08.019
54. Schiela B, Bernklau S, Malekshahi Z, Deutschmann D, Koske I, Banki Z, et al. Active human complement reduces the Zika virus load via formation of the membrane-attack complex. *Front Immunol.* (2018) 9:2177.
55. Hirsch RL, Griffin DE, Winkelstein JA. Host modification of Sindbis virus sialic acid content influences alternative complement pathway activation and virus clearance. *J Immunol.* (1981) 127:1740–3.
56. Hirsch RL, Griffin DE, Winkelstein JA. Role of complement in viral infections: participation of terminal complement components (C5 to C9) in recovery of mice from Sindbis virus infection. *Infect Immunity.* (1980) 30:899–901.
57. Nag J, Mukesh RK, Suma SM, Kunnakkadan U, Kumar NA, Johnson JB. A Factor I-Like activity associated with chikungunya virus contributes to its resistance to the human complement system. *J Virol.* (2020) 94:e2062–2019.
58. Mills BJ, Beebe DP, Cooper NR. Antibody-independent neutralization of vesicular stomatitis virus by human complement. II. Formation of VSV-lipoprotein complexes in human serum and complement-dependent viral lysis. *J Immunol.* (1979) 123:2518–24.
59. Beebe DP, Cooper NR. Neutralization of vesicular stomatitis virus (VSV) by human complement requires a natural IgM antibody present in human serum. *J Immunol.* (1981) 126:1562–8.
60. Johnson JB, Lyles DS, Alexander-Miller MA, Parks GD. Virion-associated complement regulator CD55 is more potent than CD46 in mediating resistance of mumps virus and vesicular stomatitis virus to neutralization. *J Virol.* (2012) 86:9929–40. doi: 10.1128/jvi.01154-12
61. Kunnakkadan U, Nag J, Kumar NA, Mukesh RK, Suma SM, Johnson JB. Complement-mediated neutralization of a potent neurotropic human pathogen, chandipura virus, is dependent on C1q. *J Virol.* (2019) 93:e994–919.
62. Ji X, Olinger GG, Aris S, Chen Y, Gewurz H, Spear GT. Mannose-binding lectin binds to Ebola and Marburg envelope glycoproteins, resulting in blocking of virus interaction with DC-SIGN and complement-mediated virus neutralization. *J Gen Virol.* (2005) 86:2535–42. doi: 10.1099/vir.0.81199-0
63. Ebenbichler CF, Thielens NM, Vornhagen R, Marschang P, Arlaud GJ, Dierich MP. Human immunodeficiency virus type 1 activates the classical pathway of complement by direct C1 binding through specific sites in the transmembrane glycoprotein gp41. *J Exp Med.* (1991) 174:1417–24. doi: 10.1084/jem.174.6.1417
64. Haurum JS, Thiel S, Jones IM, Fischer PB, Laursen SB, Jensenius JC. Complement activation upon binding of mannan-binding protein to HIV envelope glycoproteins. *Aids.* (1993) 7:1307–13. doi: 10.1097/00002030-199310000-00002
65. Ji X, Gewurz H, Spear GT. Mannose binding lectin (MBL) and HIV. *Mol Immunol.* (2005) 42:145–52. doi: 10.1016/j.molimm.2004.06.015
66. Spear GT, Sullivan BL, Takefman DM, Landay AL, Lint TF. Human immunodeficiency virus (HIV)-infected cells and free virus directly activate the classical complement pathway in rabbit, mouse and guinea-pig sera; activation results in virus neutralization by virolysis. *Immunology.* (1991) 73:377–82.
67. Prohaszka Z, Hidvegi T, Ujhelyi E, Stoiber H, Dierich MP, Susal C, et al. Interaction of complement and specific antibodies with the external glycoprotein 120 of HIV-1. *Immunology.* (1995) 85:184–9.
68. Susal C, Kirschfink M, Kropelin M, Daniel V, Opelz G. Identification of complement activation sites in human immunodeficiency virus type-1 glycoprotein gp120. *Blood.* (1996) 87:2329–36. doi: 10.1182/blood.v87.6.2329.bloodjournal8762329
69. Susal C, Kirschfink M, Kropelin M, Daniel V, Opelz G. Complement activation by recombinant HIV-1 glycoprotein gp120. *J Immunol.* (1994) 152:6028–34.
70. Stoiber H, Kacani L, Speth C, Wurzner R, Dierich MP. The supportive role of complement in HIV pathogenesis. *Immunol Rev.* (2001) 180:168–76. doi: 10.1034/j.1600-065x.2001.1800115.x
71. Ikeda F, Haraguchi Y, Jinno A, Iino Y, Morishita Y, Shiraki H, et al. Human complement component C1q inhibits the infectivity of cell-free HTLV-I. *J Immunol.* (1998) 161:5712–9.
72. Johnson JB, Borisevich V, Rockx B, Parks GD. A novel factor I activity in Nipah virus inhibits human complement pathways through cleavage of C3b. *J Virol.* (2015) 89:989–98. doi: 10.1128/jvi.02427-14
73. Aaskov JG, Hadding U, Bitter-Suermann D. Interaction of Ross River virus with the complement system. *J Gen Virol.* (1985) 66(Pt 1):121–9. doi: 10.1099/0022-1317-66-1-121
74. Morrison TE, Fraser RJ, Smith PN, Mahalingam S, Heise MT. Complement contributes to inflammatory tissue destruction in a mouse model of Ross River virus-induced disease. *J Virol.* (2007) 81:5132–43. doi: 10.1128/jvi.02799-06
75. Gunn BM, Jones JE, Shabman RS, Whitmore AC, Sarkar S, Blevins LK, et al. Ross River virus envelope glycans contribute to disease through activation of the host complement system. *Virology.* (2018) 515:250–60. doi: 10.1016/j.virol.2017.12.022
76. Gunn BM, Morrison TE, Whitmore AC, Blevins LK, Hueston L, Fraser RJ, et al. Mannose binding lectin is required for alphavirus-induced arthritis/myositis. *PLoS Pathog.* (2012) 8:e1002586. doi: 10.1371/journal.ppat.1002586
77. Ip WK, Chan KH, Law HK, Tso GH, Kong EK, Wong WH, et al. Mannose-binding lectin in severe acute respiratory syndrome coronavirus infection. *J Infect Dis.* (2005) 191:1697–704.
78. Zhou Y, Lu K, Pfefferle S, Bertram S, Glowacka I, Drosten C, et al. A single asparagine-linked glycosylation site of the severe acute respiratory syndrome coronavirus spike glycoprotein facilitates inhibition by mannose-binding lectin through multiple mechanisms. *J Virol.* (2010) 84:8753–64. doi: 10.1128/jvi.00554-10
79. Pang RT, Poon TC, Chan KC, Lee NL, Chiu RW, Tong YK, et al. Serum proteomic fingerprints of adult patients with severe acute respiratory syndrome. *Clin Chem.* (2006) 52:421–9. doi: 10.1373/clinchem.2005.061689
80. Gao T, Hu M, Zhang X, Li H, Zhu L, Liu H, et al. Highly pathogenic coronavirus N protein aggravates lung injury by MASP-2-mediated complement over-activation. *MedRxiv.* [Preprint]. (2020). doi: 10.1101/2020.03.29.20041962
81. Magro C, Mulvey JJ, Berlin D, Nuovo G, Salvatore S, Harp J, et al. Complement associated microvascular injury and thrombosis in the pathogenesis of severe COVID-19 infection: a report of five cases. *Transl Res.* (2020) 220:1–13. doi: 10.1016/j.trsl.2020.04.007
82. Noris M, Benigni A, Remuzzi G. The case of complement activation in COVID-19 multiorgan impact. *Kidney Int.* (2020) 98:314–22. doi: 10.1016/j.kint.2020.05.013
83. Morrison TE, Simmons JD, Heise MT. Complement receptor 3 promotes severe ross river virus-induced disease. *J Virol.* (2008) 82:11263–72. doi: 10.1128/jvi.01352-08
84. Malasit P. Complement and dengue haemorrhagic fever/shock syndrome. *Southeast Asian J Trop Med Public Health.* (1987) 18:316–20.
85. Bokisch VA, Muller-Eberhard HJ, Dixon FJ. The role of complement in hemorrhagic shock syndrome (dengue). *Trans Assoc Am Phys.* (1973) 86:102–10.
86. Bokisch VA, Top FH Jr., Russell PK, Dixon FJ, Muller-Eberhard HJ. The potential pathogenic role of complement in dengue hemorrhagic shock syndrome. *N Engl J Med.* (1973) 289:996–1000. doi: 10.1056/nejm197311082891902

87. Nishioka K. Serum complement level in dengue hemorrhagic fever. *Allergie Immunol.* (1974) 20-21:385–92.
88. Nascimento EJ, Silva AM, Cordeiro MT, Brito CA, Gil LH, Braga-Neto U, et al. Alternative complement pathway deregulation is correlated with dengue severity. *PLoS One.* (2009) 4:e6782. doi: 10.1371/journal.pone.0006782
89. Pinto AK, Ramos HJ, Wu X, Aggarwal S, Shrestha B, Gorman M, et al. Deficient IFN signaling by myeloid cells leads to MAVS-dependent virus-induced sepsis. *PLoS Pathog.* (2014) 10:e1004086. doi: 10.1371/journal.ppat.1004086
90. Churdboonchart V, Bhamarapravati N, Futrakul P. Crossed immunoelectrophoresis for the detection of split products of the third complement in dengue hemorrhagic fever. I. Observations in patients' plasma. *Am J Trop Med Hygiene.* (1983) 32:569–76. doi: 10.4269/ajtmh.1983.32.569
91. Churdboonchart V, Bhamarapravati N, Yoksan S. Crossed immunoelectrophoresis for the detection of split products of the third complement component in dengue hemorrhagic fever. II. In vitro activation by dengue viral antigen. *Am J Trop Med Hygiene.* (1984) 33:1239–47. doi: 10.4269/ajtmh.1984.33.1239
92. Shaio MF, Chang FY, Hou SC. Complement pathway activity in serum from patients with classical dengue fever. *Trans R Soc Trop Med Hygiene.* (1992) 86:672–5. doi: 10.1016/0035-9203(92)90186-g
93. Avirutnan P, Malasit P, Seliger B, Bhakdi S, Husmann M. Dengue virus infection of human endothelial cells leads to chemokine production, complement activation, and apoptosis. *J Immunol.* (1998) 161:6338–46.
94. Ubol S, Masrinoul P, Chaijaruwanich J, Kalayanarooj S, Charoensirisuthikul T, Kasisith J. Differences in global gene expression in peripheral blood mononuclear cells indicate a significant role of the innate responses in progression of dengue fever but not dengue hemorrhagic fever. *J Infect Dis.* (2008) 197:1459–67. doi: 10.1086/587699
95. Cardosa MJ, Porterfield JS, Gordon S. Complement receptor mediates enhanced flavivirus replication in macrophages. *J Exp Med.* (1983) 158:258–63. doi: 10.1084/jem.158.1.258
96. Vasek MJ, Garber C, Dorsey D, Durrant DM, Bollman B, Soung A, et al. A complement-microglial axis drives synapse loss during virus-induced memory impairment. *Nature.* (2016) 534:538–43. doi: 10.1038/nature18283
97. Wiley CA, Schrier RD, Nelson JA, Lampert PW, Oldstone MB. Cellular localization of human immunodeficiency virus infection within the brains of acquired immune deficiency syndrome patients. *Proc Natl Acad Sci USA.* (1986) 83:7089–93. doi: 10.1073/pnas.83.18.7089
98. Nitkiewicz J, Borjabad A, Morgello S, Murray J, Chao W, Emdad L, et al. HIV induces expression of complement component C3 in astrocytes by NF-kappaB-dependent activation of interleukin-6 synthesis. *J Neuroinflamm.* (2017) 14:23.
99. Gelman BB, Chen T, Lisinicchia JG, Soukup VM, Carmical JR, Starkey JM, et al. National Neuro, The National NeuroAIDS Tissue Consortium brain gene array: two types of HIV-associated neurocognitive impairment. *PLoS One.* (2012) 7:e46178. doi: 10.1371/journal.pone.0046178
100. Speth C, Stockl G, Mohsenipour I, Wurzner R, Stoiber H, Lass-Florl C, et al. Human immunodeficiency virus type 1 induces expression of complement factors in human astrocytes. *J Virol.* (2001) 75:2604–15. doi: 10.1128/jvi.75.6.2604-2516.2001
101. Jongen PJ, Doesburg WH, Ibrahim-Stappers JL, Lemmens WA, Hommes OR, Lamers KJ. Cerebrospinal fluid C3 and C4 indexes in immunological disorders of the central nervous system. *Acta Neurol Scand.* (2000) 101:116–21. doi: 10.1034/j.1600-0404.2000.101002116.x
102. Speth C, Williams K, Hagleitner M, Westmoreland S, Rambach G, Mohsenipour I, et al. Complement synthesis and activation in the brain of SIV-infected monkeys. *J Neuroimmunol.* (2004) 151:45–54. doi: 10.1016/j.jneuroim.2004.02.013
103. Weiss L, Okada N, Haeffner-Cavaillon N, Hattori T, Faucher C, Kazatchkine MD, et al. Decreased expression of the membrane inhibitor of complement-mediated cytolysis CD59 on T-lymphocytes of HIV-infected patients. *Aids.* (1992) 6:379–85. doi: 10.1097/00002030-199204000-00004
104. Chong YH, Lee MJ. Expression of complement inhibitor protein CD59 in human neuronal and glial cell lines treated with HIV-1 gp41 peptides. *J Neurovirol.* (2000) 6:51–60. doi: 10.3109/13550280009006382
105. Stoermer KA, Morrison TE. Complement and viral pathogenesis. *Virology.* (2011) 411:362–73. doi: 10.1016/j.virol.2010.12.045
106. El-Shamy A, Branch AD, Schiano TD, Gorevic PD. The complement system and C1q in chronic hepatitis C virus infection and mixed cryoglobulinemia. *Front immunol.* (2018) 9:1001.
107. Fadda SH, Bassyouni IH, Hamdy A, Foad NA, Wali IE. Anti-C1q in chronic hepatitis C virus genotype IV infection: association with autoimmune rheumatologic manifestations. *Immunol Invest.* (2015) 44:45–55. doi: 10.3109/08820139.2014.932378
108. Saadoun D, Sadallah S, Trendelenburg M, Limal N, Sene D, Piette JC, et al. Anti-C1q antibodies in hepatitis C virus infection. *Clin Exp Immunol.* (2006) 145:308–12. doi: 10.1111/j.1365-2249.2006.03153.x
109. Bosmann M. Complement activation during critical illness: current findings and an outlook in the Era of COVID-19. *Am J Respir Crit Care Med.* (2020) 202:163–5. doi: 10.1164/rccm.202005-1926ed
110. Kim AH, Dimitriou ID, Holland MC, Mastellos D, Mueller YM, Altman JD, et al. Complement C5a receptor is essential for the optimal generation of antiviral CD8+ T cell responses. *J Immunol.* (2004) 173:2524–9. doi: 10.4049/jimmunol.173.4.2524
111. Chen Y, Li X, Tian L, Zheng S, Yang S, Dong Y, et al. Dynamic behavior of lymphocyte subgroups correlates with clinical outcomes in human H7N9 infection. *J Infect.* (2014) 69:358–65. doi: 10.1016/j.jinf.2014.05.006
112. Diao H, Cui G, Wei Y, Chen J, Zuo J, Cao H, et al. Severe H7N9 infection is associated with decreased antigen-presenting capacity of CD14+ cells. *PLoS One.* (2014) 9:e92823. doi: 10.1371/journal.pone.0092823
113. Guo RF, Ward PA. Role of C5a in inflammatory responses. *Annu Rev Immunol.* (2005) 23:821–52.
114. Domej W, Oettl K, Renner W. Oxidative stress and free radicals in COPD–implications and relevance for treatment. *Int J Chronic Obstructive Pulm. Dis.* (2014) 9:1207–24. doi: 10.2147/copd.s51226
115. Akaike T, Ando M, Oda T, Doi T, Ijiri S, Araki S, et al. Dependence on O2-generation by xanthine oxidase of pathogenesis of influenza virus infection in mice. *J Clin Invest.* (1990) 85:739–45. doi: 10.1172/jci114499
116. Song N, Li P, Jiang Y, Sun H, Cui J, Zhao G, et al. C5a receptor1 inhibition alleviates influenza virus-induced acute lung injury. *Int Immunopharm.* (2018) 59:12–20. doi: 10.1016/j.intimp.2018.03.029
117. Ling MT, Tu W, Han Y, Mao H, Chong WP, Guan J, et al. Mannose-binding lectin contributes to deleterious inflammatory response in pandemic H1N1 and avian H9N2 infection. *J Infect Dis.* (2012) 205:44–53. doi: 10.1093/infdis/jir691
118. Polyak SJ, Klein KC, Shoji I, Miyamura T, Lingappa JR. Assemble and interact: pleiotropic functions of the HCV core protein. In: Tan SL editor. *Hepatitis C Viruses: Genomes and Molecular Biology*. Norfolk: Horizon Bioscience (2006).
119. Waggoner SN, Hall CH, Hahn YS. HCV core protein interaction with gC1q receptor inhibits Th1 differentiation of CD4+ T cells via suppression of dendritic cell IL-12 production. *J Leukoc Biol.* (2007) 82:1407–19. doi: 10.1189/jlb.0507268
120. Cummings KL, Rosen HR, Hahn YS. Frequency of gC1qR+CD4+ T cells increases during acute hepatitis C virus infection and remains elevated in patients with chronic infection. *Clin Immunol.* (2009) 132:401–11. doi: 10.1016/j.clim.2009.05.002
121. Fausther-Bovendo H, Vieillard V, Sagan S, Bismuth G, Debre P. HIV gp41 engages gC1qR on CD4+ T cells to induce the expression of an NK ligand through the PIP3/H2O2 pathway. *PLoS Pathog.* (2010) 6:e1000975. doi: 10.1371/journal.ppat.1000975
122. Montefiori DC, Graham BS, Zhou JY, Zhou JT, Ahearn JM. Binding of human immunodeficiency virus type 1 to the C3b/C4b receptor CR1 (CD35) and red blood cells in the presence of envelope-specific antibodies and complement. National Institutes of Health AIDS Vaccine Clinical Trials Networks. *J Infect Dis.* (1994) 170:429–32. doi: 10.1093/infdis/170.2.429
123. Jakubik JJ, Saifuddin M, Takefman DM, Spear GT. Immune complexes containing human immunodeficiency virus type 1 primary isolates bind to lymphoid tissue B lymphocytes and are infectious for T lymphocytes. *J Virol.* (2000) 74:552–5. doi: 10.1128/jvi.74.1.552-555.2000
124. Moir S, Malaspina A, Li Y, Chun TW, Lowe T, Adelsberger J, et al. B cells of HIV-1-infected patients bind virions through CD21-complement interactions and transmit infectious virus to activated T cells. *J Exp Med.* (2000) 192:637–46. doi: 10.1084/jem.192.5.637

125. Bajtay Z, Speth C, Erdei A, Dierich MP. Cutting edge: productive HIV-1 infection of dendritic cells via complement receptor type 3 (CR3, CD11b/CD18). *J Immunol.* (2004) 173:4775–8. doi: 10.4049/jimmunol.173.8.4775
126. Banki Z, Posch W, Ejaz A, Oberhauser V, Willey S, Gassner C, et al. Complement as an endogenous adjuvant for dendritic cell-mediated induction of retrovirus-specific CTLs. *PLoS Pathog.* (2010) 6:e1000891. doi: 10.1371/journal.ppat.1000891
127. Borrow P, Lewicki H, Hahn BH, Shaw GM, Oldstone MB. Virus-specific CD8+ cytotoxic T-lymphocyte activity associated with control of viremia in primary human immunodeficiency virus type 1 infection. *J Virol.* (1994) 68:6103–10. doi: 10.1128/jvi.68.9.6103-6110.1994
128. Koup RA, Safrit JT, Cao Y, Andrews CA, McLeod G, Borkowsky W, et al. Temporal association of cellular immune responses with the initial control of viremia in primary human immunodeficiency virus type 1 syndrome. *J Virol.* (1994) 68:4650–5. doi: 10.1128/jvi.68.7.4650-4655.1994
129. Kacani L, Banki Z, Zwirner J, Schennach H, Bajtay Z, Erdei A, et al. C5a and C5a(desArg) enhance the susceptibility of monocyte-derived macrophages to HIV infection. *J Immunol.* (2001) 166:3410–5. doi: 10.4049/jimmunol.166.5.3410
130. Soederholm A, Banki Z, Wilflingseder D, Gassner C, Zwirner J, Lopez-Trascasa M, et al. HIV-1 induced generation of C5a attracts immature dendriticcells and promotes infection of autologous T cells. *Eur J Immunol.* (2007) 37:2156–63. doi: 10.1002/eji.200636820
131. Moreno-Fernandez ME, Aliberti J, Groeneweg S, Kohl J, Chougnet CA. A novel role for the receptor of the complement cleavage fragment C5a, C5aR1, in CCR5-mediated entry of HIV into macrophages. *AIDS Res Human Retroviruses.* (2016) 32:399–408. doi: 10.1089/aid.2015.0099
132. Wilflingseder D, Schroll A, Hackl H, Gallasch R, Frampton D, Lass-Florl C, et al. Immediate T-helper 17 polarization upon triggering CD11b/c on HIV-exposed dendritic cells. *J Infect Dis.* (2015) 212:44–56. doi: 10.1093/infdis/jiv014
133. Posch W, Cardinaud S, Hamimi C, Fletcher A, Muhlbacher A, Loacker K, et al. Antibodies attenuate the capacity of dendritic cells to stimulate HIV-specific cytotoxic T lymphocytes. *J Allergy Clin Immunol.* (2012) 130:1368–74e2.
134. Posch W, Steger M, Knackmuss U, Blatzer M, Baldauf HM, Doppler W, et al. Complement-opsonized HIV-1 overcomes restriction in dendritic cells. *PLoS Pathog.* (2015) 11:e1005005. doi: 10.1371/journal.ppat.1005005
135. Sun S, Zhao G, Liu C, Wu X, Guo Y, Yu H, et al. Inhibition of complement activation alleviates acute lung injury induced by highly pathogenic avian influenza H5N1 virus infection. *Am J Respir Cell Mol Biol.* (2013) 49:221–30. doi: 10.1165/rcmb.2012-0428oc
136. Chauhan AJ, Wiffen LJ, Brown TP. COVID-19: a collision of complement, coagulation and inflammatory pathways. *J Thromb Haemostasis.* (2020) 18:2110–7. doi: 10.1111/jth.14981
137. Wang R, Xiao H, Guo R, Li Y, Shen B. The role of C5a in acute lung injury induced by highly pathogenic viral infections. *Emerging Microbes Infect.* (2015) 4:e28.
138. Bonaparte RS, Hair PS, Banthia D, Marshall DM, Cunnion KM, Krishna NK. Human astrovirus coat protein inhibits serum complement activation via C1, the first component of the classical pathway. *J Virol.* (2008) 82:817–27. doi: 10.1128/jvi.01847-07
139. Hair PS, Gronemus JQ, Crawford KB, Salvi VP, Cunnion KM, Thielens NM, et al. Human astrovirus coat protein binds C1q and MBL and inhibits the classical and lectin pathways of complement activation. *Mol Immunol.* (2010) 47:792–8. doi: 10.1016/j.molimm.2009.10.006
140. Mawatari S, Uto H, Ido A, Nakashima K, Suzuki T, Kanmura S, et al. Hepatitis C virus NS3/4A protease inhibits complement activation by cleaving complement component 4. *PLoS One* (2013) 8:e82094. doi: 10.1371/journal.pone.0082094
141. Ostachuk A. Bovine viral diarrhea virus structural protein E2 as a complement regulatory protein. *Arch Virol.* (2016) 161:1769–82. doi: 10.1007/s00705-016-2835-6
142. Thiemmeca S, Tamdet C, Punyadee N, Prommool T, Songjaeng A, Noisakran S, et al. Secreted NS1 protects dengue virus from mannose-binding lectin-mediated neutralization. *J Immunol.* (2016) 197:4053–65. doi: 10.4049/jimmunol.1600323
143. Avirutnan P, Fuchs A, Hauhart RE, Somnuke P, Youn S, Diamond MS, et al. Antagonism of the complement component C4 by flavivirus nonstructural protein NS1. *J Exp Med.* (2010) 207:793–806. doi: 10.1084/jem.20092545
144. Zhang J, Li G, Liu X, Wang Z, Liu W, Ye X. Influenza A virus M1 blocks the classical complement pathway through interacting with C1qA. *J Gen Virol.* (2009) 90:2751–8. doi: 10.1099/vir.0.014316-0
145. Yao ZQ, Ray S, Eisen-Vandervelde A, Waggoner S, Hahn YS. Hepatitis C virus: immunosuppression by complement regulatory pathway. *Viral Immunol.* (2001) 14:277–95. doi: 10.1089/08828240152716547
146. O'Beirne J, Mitchell J, Farzaneh F, Harrison PM. Inhibition of major histocompatibility complex Class I antigen presentation by hepatitis C virus core protein in myeloid dendritic cells. *Virology.* (2009) 389:1–7. doi: 10.1016/j.virol.2009.03.035
147. Zhang Y, Ma CJ, Ni L, Zhang CL, Wu XY, Kumaraguru U, et al. Cross-talk between programmed death-1 and suppressor of cytokine signaling-1 in inhibition of IL-12 production by monocytes/macrophages in hepatitis C virus infection. *J Immunol.* (2011) 186:3093–103. doi: 10.4049/jimmunol.1002006
148. Brudner M, Karpel M, Lear C, Chen L, Yantosca LM, Scully C, et al. Lectin-dependent enhancement of Ebola virus infection via soluble and transmembrane C-type lectin receptors. *PLoS One.* (2013) 8:e60838. doi: 10.1371/journal.pone.0060838
149. Favier AL, Gout E, Reynard O, Ferraris O, Kleman JP, Volchkov V, et al. Enhancement of ebola virus infection via Ficolin-1 interaction with the mucin domain of GP glycoprotein. *J Virol.* (2016) 90:5256–69. doi: 10.1128/jvi.00232-16
150. Mazumdar B, Kim H, Meyer K, Bose SK, Di Bisceglie AM, Ray RB, et al. Hepatitis C virus proteins inhibit C3 complement production. *J Virol.* (2012) 86:2221–8. doi: 10.1128/jvi.06577-11
151. Banerjee A, Mazumdar B, Meyer K, Di Bisceglie AM, Ray RB, Ray R. Transcriptional repression of C4 complement by hepatitis C virus proteins. *J Virol.* (2011) 85:4157–66. doi: 10.1128/jvi.02449-10
152. Kim H, Meyer K, Di Bisceglie AM, Ray R. Hepatitis C virus suppresses C9 complement synthesis and impairs membrane attack complex function. *J Virol.* (2013) 87:5858–67. doi: 10.1128/jvi.00174-13
153. Kim H, Meyer K, Di Bisceglie AM, Ray R. Inhibition of c3 convertase activity by hepatitis C virus as an additional lesion in the regulation of complement components. *PLoS One.* (2014) 9:e101422. doi: 10.1371/journal.pone.0101422
154. Kim H, Bose SK, Meyer K, Ray R. Hepatitis C virus impairs natural killer cell-mediated augmentation of complement synthesis. *J Virol.* (2014) 88:2564–71. doi: 10.1128/jvi.02988-13
155. Li Y, Johnson JB, Parks GD. Parainfluenza virus 5 upregulates CD55 expression to produce virions with enhanced resistance to complement-mediated neutralization. *Virology.* (2016) 497:305–13. doi: 10.1016/j.virol.2016.07.030
156. Li Y, Parks GD. Relative contribution of cellular complement inhibitors CD59, CD46, and CD55 to parainfluenza Virus 5 inhibition of complement-mediated neutralization. *Viruses.* (2018) 10:219. doi: 10.3390/v10050219
157. Marschang P, Sodroski J, Wurzner R, Dierich MP. Decay-accelerating factor (CD55) protects human immunodeficiency virus type 1 from inactivation by human complement. *Eur J Immunol.* (1995) 25:285–90. doi: 10.1002/eji.1830250147
158. Saifuddin M, Hedayati T, Atkinson JP, Holguin MH, Parker CJ, Spear GT. Human immunodeficiency virus type 1 incorporates both glycosyl phosphatidylinositol-anchored CD55 and CD59 and integral membrane CD46 at levels that protect from complement-mediated destruction. *J Gen Virol.* (1997) 78(Pt 8):1907–11. doi: 10.1099/0022-1317-78-8-1907
159. Johnson JB, Grant K, Parks GD. The paramyxoviruses simian virus 5 and mumps virus recruit host cell CD46 to evade complement-mediated neutralization. *J Virol.* (2009) 83:7602–11. doi: 10.1128/jvi.00713-09
160. Amet T, Ghabril M, Chalasani N, Byrd D, Hu N, Grantham A, et al. CD59 incorporation protects hepatitis C virus against complement-mediated destruction. *Hepatology.* (2012) 55:354–63. doi: 10.1002/hep.24686
161. Montefiori DC, Cornell RJ, Zhou JY, Zhou JT, Hirsch VM, Johnson PR. Complement control proteins, CD46, CD55, and CD59, as common surface constituents of human and simian immunodeficiency viruses and possible

targets for vaccine protection. *Virology.* (1994) 205:82–92. doi: 10.1006/viro.1994.1622
162. Saifuddin M, Parker CJ, Peeples ME, Gorny MK, Zolla-Pazner S, Ghassemi M, et al. Role of virion-associated glycosylphosphatidylinositol-linked proteins CD55 and CD59 in complement resistance of cell line-derived and primary isolates of HIV-1. *J Exp Med.* (1995) 182:501–9. doi: 10.1084/jem.182.2.501
163. Schmitz J, Zimmer JP, Kluxen B, Aries S, Bogel M, Gigli I, et al. Antibody-dependent complement-mediated cytotoxicity in sera from patients with HIV-1 infection is controlled by CD55 and CD59. *J Clin Invest.* (1995) 96:1520–6. doi: 10.1172/jci118190
164. Spear GT, Lurain NS, Parker CJ, Ghassemi M, Payne GH, Saifuddin M. Host cell-derived complement control proteins CD55 and CD59 are incorporated into the virions of two unrelated enveloped viruses. Human T cell leukemia/lymphoma virus type I (HTLV-I) and human cytomegalovirus (HCMV). *J Immunol.* (1995) 155:4376–81.
165. Mazumdar B, Kim H, Meyer K, Bose SK, Di Bisceglie AM, Ray RB, et al. Hepatitis C virus infection upregulates CD55 expression on the hepatocyte surface and promotes association with virus particles. *J Virol.* (2013) 87:7902–10. doi: 10.1128/jvi.00917-13
166. Kwon YC, Kim H, Meyer K, Di Bisceglie AM, Ray R. Distinct CD55 isoform synthesis and inhibition of complement-dependent cytolysis by Hepatitis C virus. *J Immunol.* (2016) 197:1127–36. doi: 10.4049/jimmunol.1600631
167. Avirutnan P, Hauhart RE, Somnuke P, Blom AM, Diamond MS, Atkinson JP. Binding of flavivirus nonstructural protein NS1 to C4b binding protein modulates complement activation. *J Immunol.* (2011) 187:424–33. doi: 10.4049/jimmunol.1100750
168. Chung KM, Liszewski MK, Nybakken G, Davis AE, Townsend RR, Fremont DH, et al. West Nile virus nonstructural protein NS1 inhibits complement activation by binding the regulatory protein factor H. *Proc Natl Acad Sci USA.* (2006) 103:19111–6. doi: 10.1073/pnas.0605668103
169. Kurosu T, Chaichana P, Yamate M, Anantapreecha S, Ikuta K. Secreted complement regulatory protein clusterin interacts with dengue virus nonstructural protein 1. *Biochem Biophys Res Commun.* (2007) 362:1051–6. doi: 10.1016/j.bbrc.2007.08.137
170. Conde JN, da Silva EM, Allonso D, Coelho DR, Andrade IDS, de Medeiros LN, et al. Inhibition of the membrane attack complex by dengue virus NS1 through interaction with vitronectin and terminal complement proteins. *J Virol.* (2016) 90:9570–81. doi: 10.1128/jvi.00912-16
171. Pinter C, Siccardi AG, Longhi R, Clivio A. Direct interaction of complement factor H with the C1 domain of HIV type 1 glycoprotein 120. *AIDS Res Human Retroviruses.* (1995) 11:577–88. doi: 10.1089/aid.1995.11.577
172. Pinter C, Siccardi AG, Lopalco L, Longhi R, Clivio A. HIV glycoprotein 41 and complement factor H interact with each other and share functional as well as antigenic homology. *AIDS Res Human Retroviruses.* (1995) 11:971–80. doi: 10.1089/aid.1995.11.971
173. Stoiber H, Pinter C, Siccardi AG, Clivio A, Dierich MP. Efficient destruction of human immunodeficiency virus in human serum by inhibiting the protective action of complement factor H and decay accelerating factor (DAF, CD55). *J Exp Med.* (1996) 183:307–10. doi: 10.1084/jem.183.1.307
174. Bergelson JM, Chan M, Solomon KR, St John NF, Lin H, Finberg RW. Decay-accelerating factor (CD55), a glycosylphosphatidylinositol-anchored complement regulatory protein, is a receptor for several echoviruses. *Proc Natl Acad Sci USA.* (1994) 91:6245–8.
175. Williams P, Chaudhry Y, Goodfellow IG, Billington J, Powell R, Spiller OB, et al. Mapping CD55 function. The structure of two pathogen-binding domains at 1.7 A. *J Biol Chem.* (2003) 278:10691–6.
176. Shafren DR, Bates RC, Agrez MV, Herd RL, Burns GF, Barry RD. Coxsackieviruses B1, B3, and B5 use decay accelerating factor as a receptor for cell attachment. *J Virol.* (1995) 69:3873–7.
177. Shafren DR, Dorahy DJ, Ingham RA, Burns GF, Barry RD. Coxsackievirus A21 binds to decay-accelerating factor but requires intercellular adhesion molecule 1 for cell entry. *J Virol.* (1997) 71:4736–43.
178. Karnauchow TM, Dawe S, Lublin DM, Dimock K. Short consensus repeat domain 1 of decay-accelerating factor is required for enterovirus 70 binding. *J Virol.* (1998) 72:9380–3.
179. Karnauchow TM, Tolson DL, Harrison BA, Altman E, Lublin DM, Dimock K. The HeLa cell receptor for enterovirus 70 is decay-accelerating factor (CD55). *J Virol.* (1996) 70:5143–52.
180. Coyne CB, Bergelson JM. Virus-induced Abl and Fyn kinase signals permit coxsackievirus entry through epithelial tight junctions. *Cell.* (2006) 124:119–31.
181. Dorig RE, Marcil A, Chopra A, Richardson CD. The human CD46 molecule is a receptor for measles virus (Edmonston strain). *Cell.* (1993) 75:295–305.
182. Naniche D, Varior-Krishnan G, Cervoni F, Wild TF, Rossi B, Rabourdin-Combe C, et al. Human membrane cofactor protein (CD46) acts as a cellular receptor for measles virus. *J Virol.* (1993) 67:6025–32.
183. Manchester M, Gairin JE, Patterson JB, Alvarez J, Liszewski MK, Eto DS, et al. Measles virus recognizes its receptor, CD46, via two distinct binding domains within SCR1-2. *Virology.* (1997) 233:174–84.
184. Manchester M, Liszewski MK, Atkinson JP, Oldstone MB. Multiple isoforms of CD46 (membrane cofactor protein) serve as receptors for measles virus. *Proc Natl Acad Sci USA.* (1994) 91:2161–5.
185. Nussbaum O, Broder CC, Moss B, Stern LB, Rozenblatt S, Berger EA. Functional and structural interactions between measles virus hemagglutinin and CD46. *J Virol.* (1995) 69:3341–9.
186. Raftery MJ, Lalwani P, Krautkrmer E, Peters T, Scharffetter-Kochanek K, Kruger R, et al. beta2 integrin mediates hantavirus-induced release of neutrophil extracellular traps. *J Exp Med.* (2014) 211:1485–97.
187. Coulson BS, Londrigan SL, Lee DJ. Rotavirus contains integrin ligand sequences and a disintegrin-like domain that are implicated in virus entry into cells. *Proc Natl Acad Sci USA.* (1997) 94:5389–94.

Conflict of Interest: The authors declare that the research was conducted in the absence of any commercial or financial relationships that could be construed as a potential conflict of interest.

frontiers in Immunology

ORIGINAL RESEARCH
published: 06 October 2020
doi: 10.3389/fimmu.2020.550827

Aspergillus-Derived Galactosaminogalactan Triggers Complement Activation on Human Platelets

Hemalata Deshmukh[1], *Cornelia Speth*[1,2*], *Donald C. Sheppard*[3], *Magdalena Neurauter*[1], *Reinhard Würzner*[1], *Cornelia Lass-Flörl*[1,2] *and Günter Rambach*[1,2]

[1] *Institute of Hygiene and Medical Microbiology, Medical University of Innsbruck, Innsbruck, Austria,* [2] *Christian Doppler Laboratory for Invasive Fungal Infections, Innsbruck, Austria,* [3] *Department of Microbiology and Immunology, McGill University, Montréal, QC, Canada*

Invasive fungal infections caused by *Aspergillus* (*A.*) and Mucorales species still represent life-threatening diseases in immunocompromised individuals, and deeper knowledge about fungal interactions with elements of innate immunity, such as complement and platelets, appears essential for optimized therapy. Previous studies showed that galactosaminogalactan secreted by *A. fumigatus* and *A. flavus* is deposited on platelets, thereby inducing their activation. Since the altered platelet surface is a putative trigger for complement activation, we aimed to study the interplay of platelets with complement in the presence of fungal GAG. Culture supernatants (SN) of *A. fumigatus* and *A. flavus* both induced not only GAG deposition but also subsequent deposition of complement C3 fragments on the platelet surface. The SN of a Δ*uge3* mutant of *A. fumigatus*, which is unable to synthesize GAG, did not induce complement deposition on platelets, nor did the SN of other *Aspergillus* species and all tested Mucorales. Detailed analysis revealed that GAG deposition itself triggered the complement cascade rather than the GAG-induced phosphatidylserine exposure. The lectin pathway of complement could be shown to be crucially involved in this process. GAG-induced complement activation on the platelet surface was revealed to trigger processes that might contribute to the pathogenesis of invasive aspergillosis by *A. fumigatus* or *A. flavus*. Both pro-inflammatory anaphylatoxins C3a and C5a arose when platelets were incubated with SN of these fungal species; these processes might favor excessive inflammation after fungal infection. Furthermore, platelets were stimulated to shed microparticles, which are also known to harbor pro-inflammatory and pro-coagulant properties. Not only did early processes of the complement cascade proceed on platelets, but also the formation of the terminal complement C5b-9 complex was detected on platelets after incubation with fungal SN. Subsequently, reduced viability of the platelets could be shown, which might contribute to the lowered platelet numbers found in infected patients. In summary, fungal GAG initiates an interplay between complement and platelets that can be supposed to contribute to excessive inflammation, thrombocytopenia, and thrombosis, which are important hallmarks of fatal invasive mycoses.

Keywords: aspergillosis, galactosaminogalactan, platelets, complement, innate immunity, invasive fungal infections

OPEN ACCESS

Edited by:
Eric Pearlman,
University of California, Irvine,
United States

Reviewed by:
Joshua J. Obar,
Dartmouth College, United States
Caroline N. Jones,
Virginia Tech, United States

****Correspondence:***
Cornelia Speth
cornelia.speth@i-med.ac.at

Specialty section:
This article was submitted to Microbial Immunology, a section of the journal Frontiers in Immunology

Received: *10 April 2020*
Accepted: *21 August 2020*
Published: *06 October 2020*

Citation:
Deshmukh H, Speth C, Sheppard DC, Neurauter M, Würzner R, Lass-Flörl C and Rambach G (2020) Aspergillus-Derived Galactosaminogalactan Triggers Complement Activation on Human Platelets. Front. Immunol. 11:550827. doi: 10.3389/fimmu.2020.550827

INTRODUCTION

Although invasive fungal infections are rare in immunocompetent individuals, they remain a significant cause of morbidity and mortality in immunocompromised patients. Medical progress leads to improved survival of chronically immunosuppressed patients, but the reverse of the medal is an increasing number of patients at risk for fungal infections (1, 2).

Lung infections due to *Aspergillus* species are caused by inhalation of ubiquitously present airborne conidia, with *Aspergillus fumigatus* and *Aspergillus flavus* as predominant human pathogenic species (3). Invasion of *Aspergillus* hyphae into the pulmonary arterioles initiates hematogenic dissemination, as it occurs in approximately one-third of patients with pulmonary aspergillosis. Consequences include thrombosis, hemorrhagic infarctions, and involvement of distant organs (4, 5). Mortality rates up to 40–50% are reported in patients with acute leukemia and recipients of hematopoietic stem cell transplantation suffering from invasive aspergillosis (6).

Various secreted fungal components have been described as relevant virulence factors, thus essentially contributing to the pathogenesis of invasive infections. One of these components is the heteropolysaccharide galactosaminogalactan (GAG), which is secreted by actively growing hyphae of *A. fumigatus* and *A. flavus* (7). Other *Aspergillus* species or Mucorales do not produce GAG. Fungal GAG fulfills multiple roles in the interaction between pathogen and host [reviewed in (8)]. Many of these roles concern an interference with the immune system, including neutrophils, cytokine production, and T-cell response. Recent results revealed that GAG acts as an activator of platelets (9). This aspect is of particular interest, since platelets show a broad spectrum of immunological competences and thus might at least partly replace other immune weapons that are down-modulated by GAG (8, 10, 11). Platelets, acaryote cell fragments derived by megakaryocytes, are endowed with a comprehensive panel of pathogen detection molecules. When pathogen-associated molecular patterns are sensed, platelets can act both autonomously to fight the invaders, and they can collaborate with other soluble or cellular immune elements in a complex network (10, 12).

The complement system is a key collaboration partner of platelets within the immune network. Complement represents a multi-component cascade made of about 30 soluble and membrane-bound factors, regulators, and receptors. Similar to platelets, complement represents a fast-acting part of the innate immunity with a comprehensive spectrum of pathogen sensors and a versatile armamentarium to fight against invaders. Classical pathway, alternative pathway, and lectin pathway all differ in protein composition and their mechanisms to recognize foreign structures. However, they all converge at the level of the central complement factor C3; processing of C3 constitutes the starter reaction of the common terminal pathway. Numerous complement activation products are central immunological effector molecules. Opsonins derived from C3 cleavage act as natural adjuvants, supporting effective phagocytosis and contributing to a proper B-cell reaction (13, 14). The anaphylatoxins C3a and C5a modulate many immunological processes, mainly in a pro-inflammatory manner and via binding to their corresponding receptors that are expressed on a broad range of cell types (15). The C5b-9 complex, also called membrane attack complex (MAC) or terminal complement complex (TCC), is the final product of the terminal pathway. As a cytolytic effector, it forms a pore in the membrane of pathogens or targeted cells and thus induces osmolysis. Besides this function, C5b-9 can trigger intracellular signaling cascades and cell activation [reviewed in (16)].

Our previous studies showed that secreted GAG activates platelets and is deposited on their surface (9). Both platelet activation, with exposition of phosphatidylserine from the inner to the outer side of the plasma membrane, and deposition of foreign GAG polysaccharide onto the platelet membrane might stimulate the complement system to recognize these platelets as foreign. Putative consequences would be their opsonization, generation of pro-inflammatory complement products, and platelet loss by direct lysis or by stimulation of complement receptor-bearing phagocytes. Both features, excessive inflammation, and thrombocytopenia, are characteristics of invasive fungal infections. For that reason, we tested the hypothesis that GAG-triggered platelet modifications lead to complement activation in invasive fungal infections with platelet loss and pro-inflammatory reactions as putative respective consequences.

MATERIALS AND METHODS

Antibodies, Chemicals, and Media

Most of the antibodies were from BioLegend (San Diego, CA, USA), C3c antibody was from Dako (Glostrup, Denmark), and C5b-9 antibody was ordered from Hycult Biotech (Uden, The Netherlands). Soybean agglutinin (SBA) lectin was from Vector labs (Burlingame, CA, USA), and the synthetic peptides sunflower MASP inhibitor peptides SFMI-1 and SFMI-2 were from Metabion (Planegg, Germany). Human C3a and C5a ELISA kits were purchased from BD Biosciences (San Diego, CA, USA), calcein blue AM was from Thermo-Fisher Scientific (Waltham, MA, USA), and thrombin was from Sigma-Aldrich (St. Louis, MO, USA).

RPMI1640 medium (R6504, Sigma-Aldrich) was supplemented with 19.8 g/L glucose and 34.5 g/L MOPS and adjusted to pH 7.0 with NaOH. Sabouraud glucose medium came from BD Diagnostic Systems (Heidelberg, Germany). Supplemented minimal medium (SUP) was prepared with yeast extract (Roth, Karlsruhe, Germany), supplemented with glucose, NH_4Cl, KH_2PO_4, K_2HPO_4 (Roth), and $MgSO_4$ (Merck, Darmstadt, Germany) (17).

Fungal Isolates and Preparation of Fungal Culture Supernatants

Clinical isolates of most *Aspergillus* and all mucormycete species were obtained from patients with proven invasive aspergillosis or mucormycosis with various underlying diseases; three *A. versicolor* isolates were environmental strains. The *A. fumigatus*

mutant strain Δ*uge3* was constructed from the parental strain *AF293* (18); this deletion of *uge3* completely abolishes GAG synthesis. This mutant was described to show normal growth and morphology, but lower adherence to a variety of substrates including pulmonary epithelia cells, and attenuated virulence in mouse models (19). The Δ*uge3* strain was routinely included in the experiments as negative control. A detailed table of all used strains of *Aspergillus* spp. and Mucorales species is shown elsewhere (9).

Aspergillus spp. isolates were cultured on Sabouraud glucose agar (SAB), and mucormycetes on Supplemented Minimal Medium (SUP) agar, for 3–5 days at 37°C, until sporulation was clearly visible. *A. versicolor* was grown at 30°C, and *Mucor* spp. was cultured at 28°C. Spores were rinsed off with phosphate buffered saline (PBS, supplemented with 0.05% Tween-20) and filtered through a 40-μm and a 10-μm cell strainer (BD Biosciences). The conidial suspension was counted in a hemocytometer, adjusted to a concentration of 1×10^8/ml in PBS and kept at 4°C. To obtain fungal culture supernatants (SN), 1×10^4 spores of *Aspergillus* or mucormycetes strains were inoculated in 500 μl of RPMI medium with high glucose content and incubated at 37°C for 2 days. Fungal elements were removed by centrifugation, and SN was obtained by filtration using Spin-X filters (Corning Life Sciences, Corning, NY, USA). The fungal SN was used freshly or kept frozen at −20°C for further use.

Preparation of Human Platelets

All studies were approved by the local ethics committee (Nr. AN5170 328/4.1 342/5.2). Whole blood from healthy volunteers with informed consent was collected in a trisodium citrate blood collection system (Sarstedt, Nürnbrecht, Germany) with avoidance of shear stress; for one experiment, the anticoagulant citrate-theophylline-adenosine-dipyridamole (CTAD; Greiner Bio-One, Kremsmünster, Austria) was used instead of citrate. Platelet-rich plasma (PRP) was obtained by centrifugation of blood at 135 × *g* for 15 min (slow deceleration) at room temperature (RT). A concentration of 2×10^5 platelets/μl in RPMI medium was adjusted after counting in a hemocytometer. All steps were performed in low-binding tubes with inert surfaces to avoid spontaneous platelet activation.

Platelet concentrates were provided from the local Department of Immunology and Blood Transfusion. Platelets were collected from healthy blood donors and prepared by thrombocytapheresis with Amicus cell separator (Baxter, Deerfield, IL, USA). The platelet number was routinely determined with a hemocytometer and adjusted to a concentration of $1.2–1.4 \times 10^6$/μl in RPMI medium.

To obtain human serum, whole blood of healthy volunteers was collected without anticoagulants and centrifuged for 15 min at 1,500 × *g* at RT. Serum from at least five donors was pooled and stored at −80°C for further use.

Analysis of Platelet Parameters by Flow Cytometry and Confocal Microscopy

Platelets (PRP or platelet concentrates) were pre-incubated with RPMI medium, 0.1 IU/ml thrombin, or SN (20% v/v, unless otherwise stated) of different fungal isolates for 30 min at 37°C, followed by addition of 40% v/v (unless otherwise stated) human serum (or PBS control) as complement source. For analysis of C3c deposition, incubation was continued for further 30 min. To detect C5b-9 formation and deposition on platelets, the further incubation time was 120 min.

Samples were fixed with 1% formalin for 30 min (RT), washed with PBS by centrifugation at 1,100 × *g*, and incubated for 30 min (RT) with fluorescence-labeled specific antibodies. To quantify GAG deposition, platelets were stained with FITC-labeled SBA lectin, as previously described elsewhere (9). All samples were analyzed by flow cytometry (FACSVerse^{TM}, BD Diagnostics). Platelets were gated by forward and side scatter and by the use of a labeled antibody against the platelet marker CD41 (BioLegend). Secretion of α-granules during platelet activation results in surface exposure of CD62P (P-selectin), which was detected by a specific fluorescence-labeled antibody (BioLegend). Complement deposition was measured by the use of a C3c antibody, which detects both the C3c fragment of the C3 protein and the C3c part of C3b. The C5b-9 antibody binds to a C9 neoantigen of the TCC; this neoantigen is absent from native C9 prior to complex formation. To assess budding of platelet-derived microparticles, the platelets were incubated in the presence or absence of fungal SN and human serum for 90 min as described above and fixated with 1% formalin. The microparticles were analyzed by flow cytometry by gating of the adequate size and binding of labeled CD41 antibody. Furthermore, microparticles were visualized by confocal microscopy.

For confocal microscopy, the samples were prepared as described above and, after washing, embedded in liquid mounting medium (Mowiol, Sigma-Aldrich), followed by visualization employing a confocal microscope (PerkinElmer).

Determination of Platelet Viability by Calcein Blue

Calcein blue AM, a cell-permeant esterase substrate, measures both enzymatic activity and cell-membrane integrity. Calcein blue AM is only weakly fluorescent. Upon cleavage by intracellular esterases, this tracer becomes polar and stays intracellular when the membrane is intact. Furthermore, its fluorescence intensity increases and its fluorescence spectra shift to longer excitation/emission maxima. Calcein blue AM was used according to the manufacturer's instructions. Briefly, 10 μM calcein stain was added to each sample along with the addition of serum or buffer to the platelets that were pre-incubated with medium or different concentrations of fungal SN. After fixation in 1% formalin and washing with PBS, the calcein signal was quantified by flow cytometry.

C3a and C5a ELISA

The anaphylatoxins C3a and C5a are generated upon complement activation and rapidly cleaved to the C3a-desArg and C5a-desArg form, respectively, by the endogenous serum carboxypeptidase N enzyme. The commercially available kits are solid phase sandwich ELISAs and quantify C3a-desArg and C5a-desArg in biological samples. The kits were used according to the manufacturer's instructions (BD Biosciences). Briefly, platelets were pre-incubated for 30 min with medium, 0.1 IU/ml

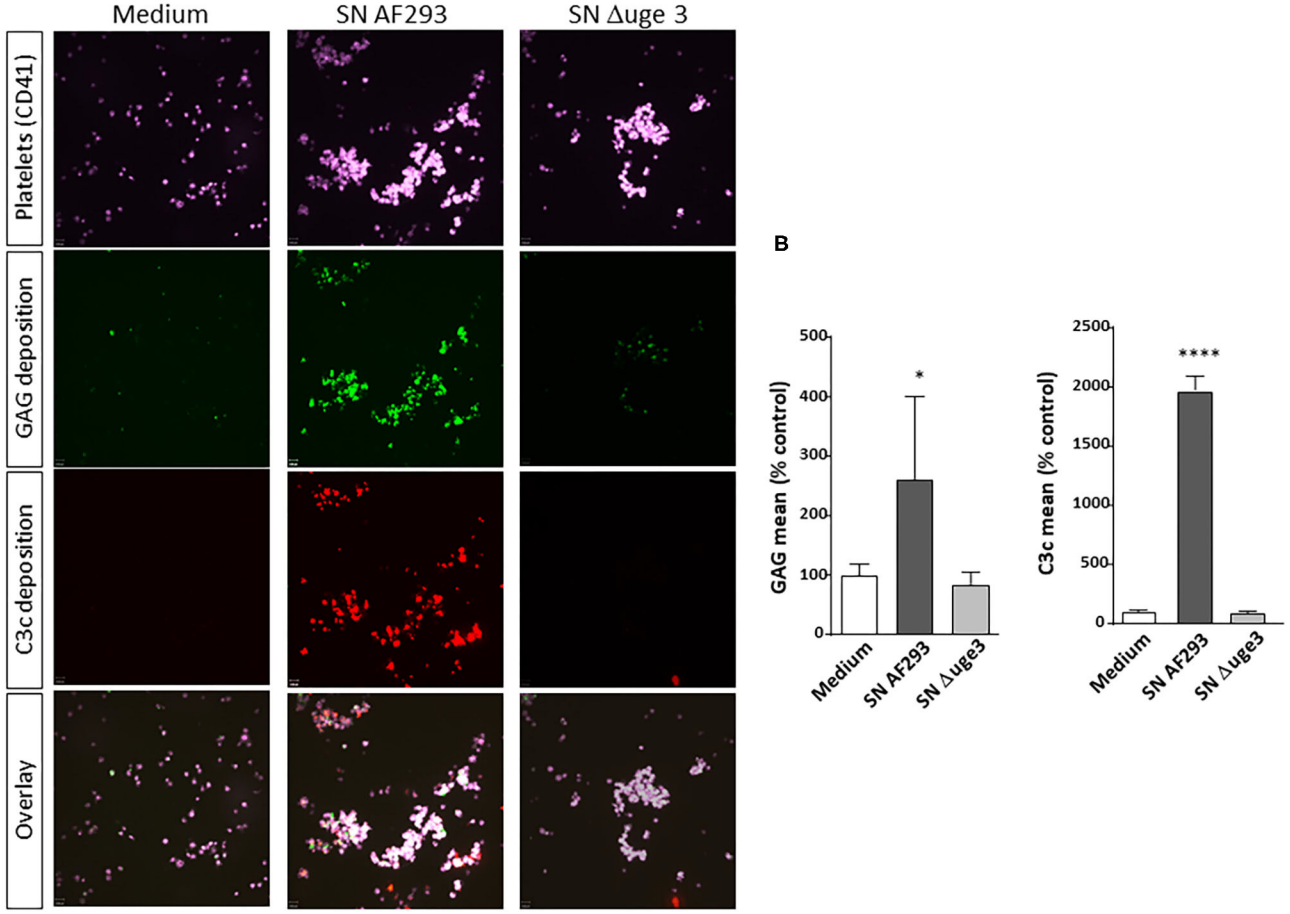

FIGURE 1 | GAG-dependent complement deposition on platelets. Platelets, labeled with a fluorescent αCD41 antibody (purple), were pre-incubated with medium or with 20% supernatant (SN) of *A. fumigatus* wild-type strain (AF293), or the GAG mutant Δ*uge3*, followed by addition of serum as complement source. Deposition of GAG was detected using SBA lectin (green), and opsonization of platelets was investigated by using an αC3c antibody (red). Samples were analyzed by confocal microscopy **(A)** and by flow cytometry **(B)**. Results in **(B)** are analyzed in comparison with the medium sample, which was set to 100%. $^{****}p < 0.001$, $^{*}p < 0.05$.

thrombin, or 20% fungal SN derived from different species, followed by addition of serum as complement source for another 30 min. Platelets were removed by centrifugation, and the SN samples were transferred to the pre-coated ELISA wells. After washing the wells with PBS, the respective biotinylated detection antibodies and the substrate were added and the color signals were quantified in an ELISA reader at 450 nm.

Statistical Analysis

All assays were performed with platelets from at least three different donors in triplicates. Results are presented as the mean ± standard deviation of representative experiments. Statistical analyses were performed with GraphPad Prism 7 software, using one-way ANOVA with Dunnett's multiple comparison test to check statistically significant values relative to controls. In addition, also unpaired *t*-tests were done to evaluate significant differences between two specified groups. Values of $p < 0.05$ are considered as statistically significant.

RESULTS

GAG Deposition on Platelet Surface Induces Opsonization of the Platelets by Complement

Previous studies demonstrated that GAG was secreted by *A. fumigatus*, deposited on the surface of platelets, and subsequently induced their activation (9). We therefore analyzed whether GAG deposition leads to the recognition of the platelet surface by the complement system as foreign and thus triggers complement activation. Platelets were incubated with fungal culture SN derived from *A. fumigatus* strain AF293 and, as control, from the GAG-deficient mutant strain Δ*uge3*. GAG deposition on platelets and deposition of complement factor C3 fragments as marker for complement activation were quantified in parallel (**Figure 1**). Fluorescence microscopy clearly revealed that deposition of GAG and C3c on the platelet surface both occurred with the SN of AF293, whereas SN of the Δ*uge3* mutant induced neither

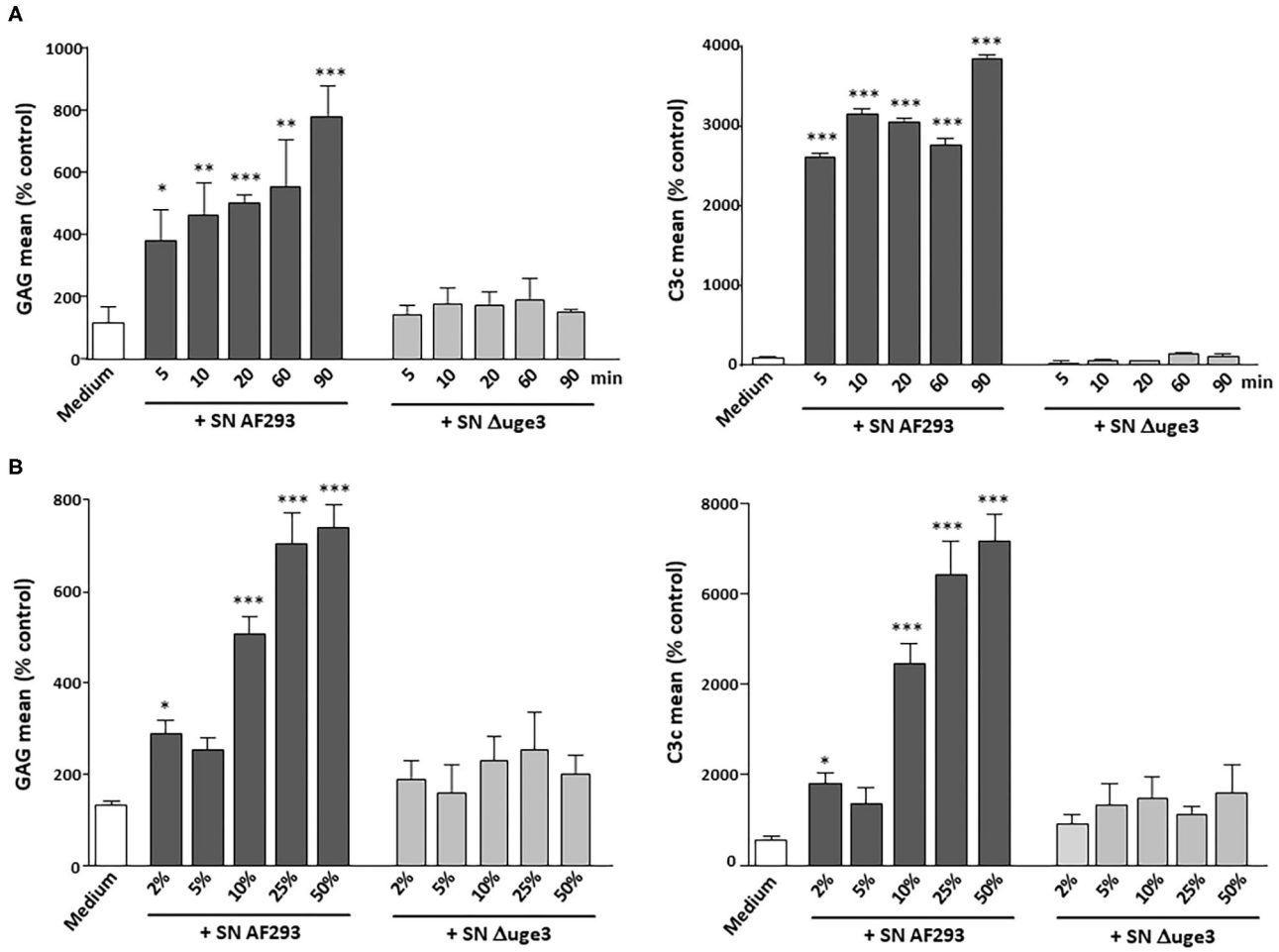

FIGURE 2 | Time and dose curve of GAG-dependent complement deposition on platelets. **(A)** Platelets were incubated for 5–90 min with serum as complement source in the presence of either medium, 20% supernatant (SN) of AF293, or 20% SN of Δ*uge3*. **(B)** Platelets were incubated for 90 min with serum as complement source in the presence of 2–50% SN of AF293 or Δ*uge3*. GAG deposition and opsonization were evaluated by flow cytometry. Each experiment was repeated at least three times with different platelet donors and with triplicate samples. Results are analyzed in comparison with the medium sample, which was set to 100%. ***$p < 0.005$, **$p < 0.01$, *$p < 0.05$.

of these processes (**Figure 1A**). Flow cytometry confirmed and quantified these results; whereas the SN of the Δ*uge3* mutant induced the same background signal for GAG and C3c as medium, the incubation of platelets with SN of AF293 resulted in significant deposition of both GAG and C3c (**Figure 1B**).

In addition, time kinetics of GAG deposition on platelets and opsonization by C3 fragments were evaluated and compared. GAG deposition on platelets was a very fast process with a significant signal already 5 min after the start of incubation (**Figure 2A**). Dose dependence was measured by incubating the platelets with 2–50% SN of AF293 (**Figure 2B**). A small increase of the GAG signal and of opsonization was visible already with 2% SN. A clear deposition with GAG and opsonization could be achieved with 10% SN. Incubation with SN derived from the Δ*uge3* mutant did not induce any effect, not even at the longest incubation time or at the highest concentration.

To strengthen the correlation between deposition of GAG on platelets and their opsonization by complement, further SN derived from other fungal species were included in the tests. SN from the clinical *A. fumigatus* isolate A22 as well as from two *A. flavus* strains that all had previously been shown to induce GAG deposition (9) could be demonstrated to also trigger opsonization with C3c on the platelet surface. All other Aspergillus species (*A. niger*, *A. nidulans*, *A. terreus*, and *A. versicolor*), negative for GAG secretion, had no effect on C3c deposition (**Figures 3A,B**). Similarly, the SN of the tested GAG-negative Mucorales species (*Lichtheimia corymbifera*, *L. ramosa*, *Rhizopus arrhizus, R. microsporus, Rhizomucor pusillus, and Mucor circinelloides*) lacked the capacity to induce complement deposition on the platelets (**Figures 3C,D**).

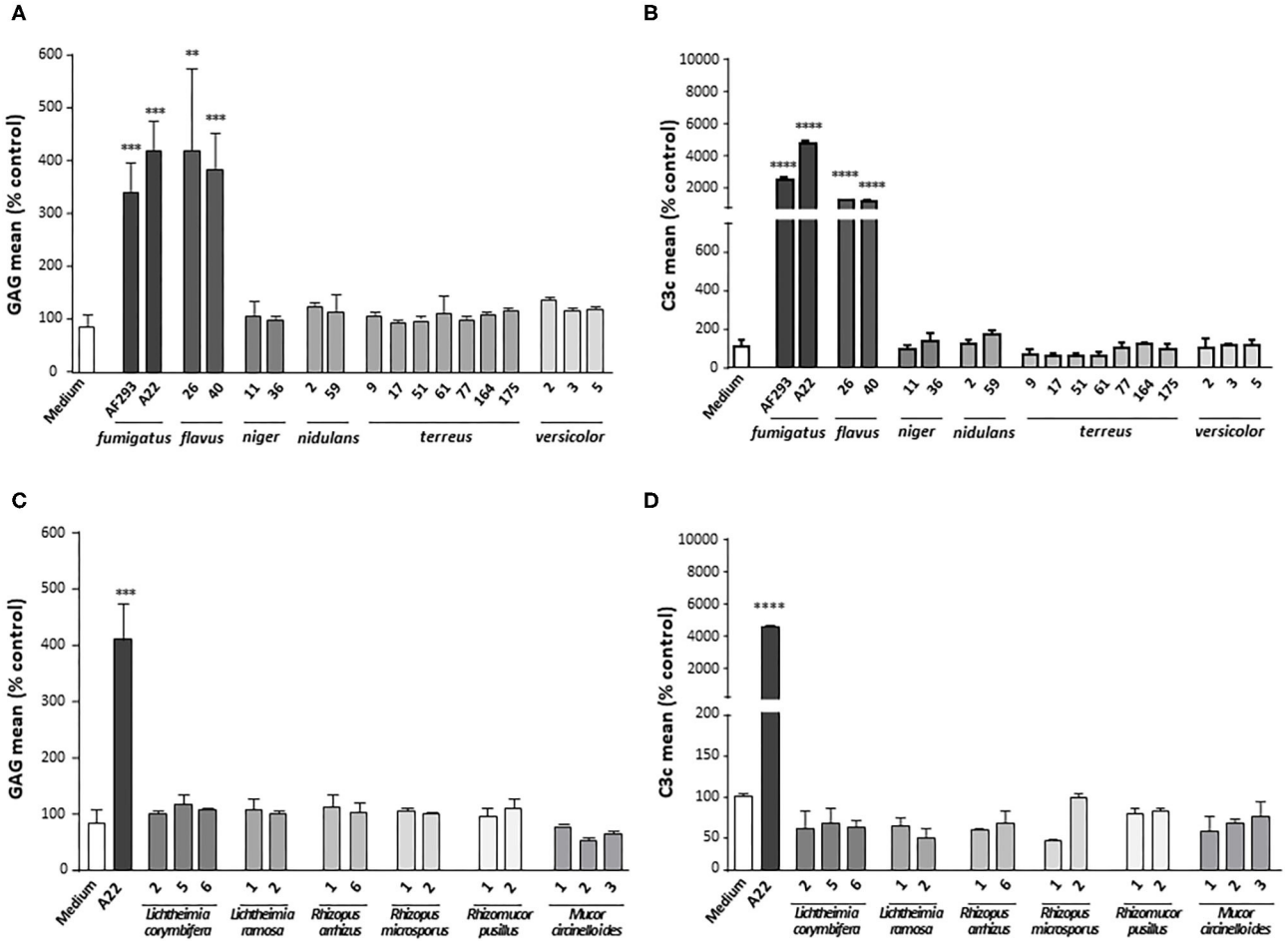

FIGURE 3 | Complement deposition on platelets incubated with different fungal supernatants. Platelets were pre-treated with medium or supernatants (SN) of different isolates of *Aspergillus* species **(A,B)** or Mucorales species **(C,D)**, followed by addition of serum as complement source. GAG deposition **(A,C)** and opsonization **(B,D)** of platelets were quantified by flow cytometry using SBA lectin or an αC3c antibody, respectively. Each experiment was repeated at least three times with different platelet donors and with triplicate samples. Results were shown and statistically analyzed in comparison to medium as a negative control, which was set to 100%. $^{****}p < 0.001$, $^{***}p < 0.005$, $^{**}p < 0.01$.

Relevant Mechanisms of GAG-Induced Platelet Opsonization

In a next step, we aimed to differentiate whether the complement system is triggered by GAG deposition itself or by GAG-induced platelet activation with exposure of phosphatidylserine on the outer leaflet of the plasma membrane (9). For that purpose, platelets were stimulated with thrombin, a well-known strong platelet activator. Whereas, incubation with the fungal SN increased both the activation marker CD62P and the opsonization marker C3c on the platelets, thrombin stimulated only platelet activation but not opsonization (**Figures 4A,B**). The SN derived from the Δ*uge3* mutant did alter activation or C3c deposition. In addition, CTAD was tested as an alternative anticoagulant for platelet isolation; in contrast to the routinely used citrate, CTAD is known to inhibit platelet activation. Usage of CTAD as an anticoagulant interfered with the SN-induced platelet activation but still allowed the opsonization of platelets with complement fragments (**Figures 4A,B**). The deposition of GAG on the platelets was similar with both anticoagulants (**Figure 4C**). These results imply that platelet activation is not a prerequisite for GAG-induced opsonization, and complement recognizes the GAG sheath itself as foreign rather than the GAG-induced phosphatidylserine exposure.

To get deeper insight into the mechanism of GAG-induced complement activation, we aimed to identify the involved activation pathways. Serum as complement source was supplemented with either EDTA or EGTA before incubation with the platelets and the fungal SN. EDTA blocked all three activation pathways and completely abolished all GAG-triggered C3c deposition on the platelets. EGTA, which blocks the classical and lectin pathway, had a similar effect, indicating that the alternative pathway plays only a minor role (**Supplementary Figure 1**). Since GAG is a polysaccharide, we hypothesized that the lectin pathway might be the more likely candidate than the classical

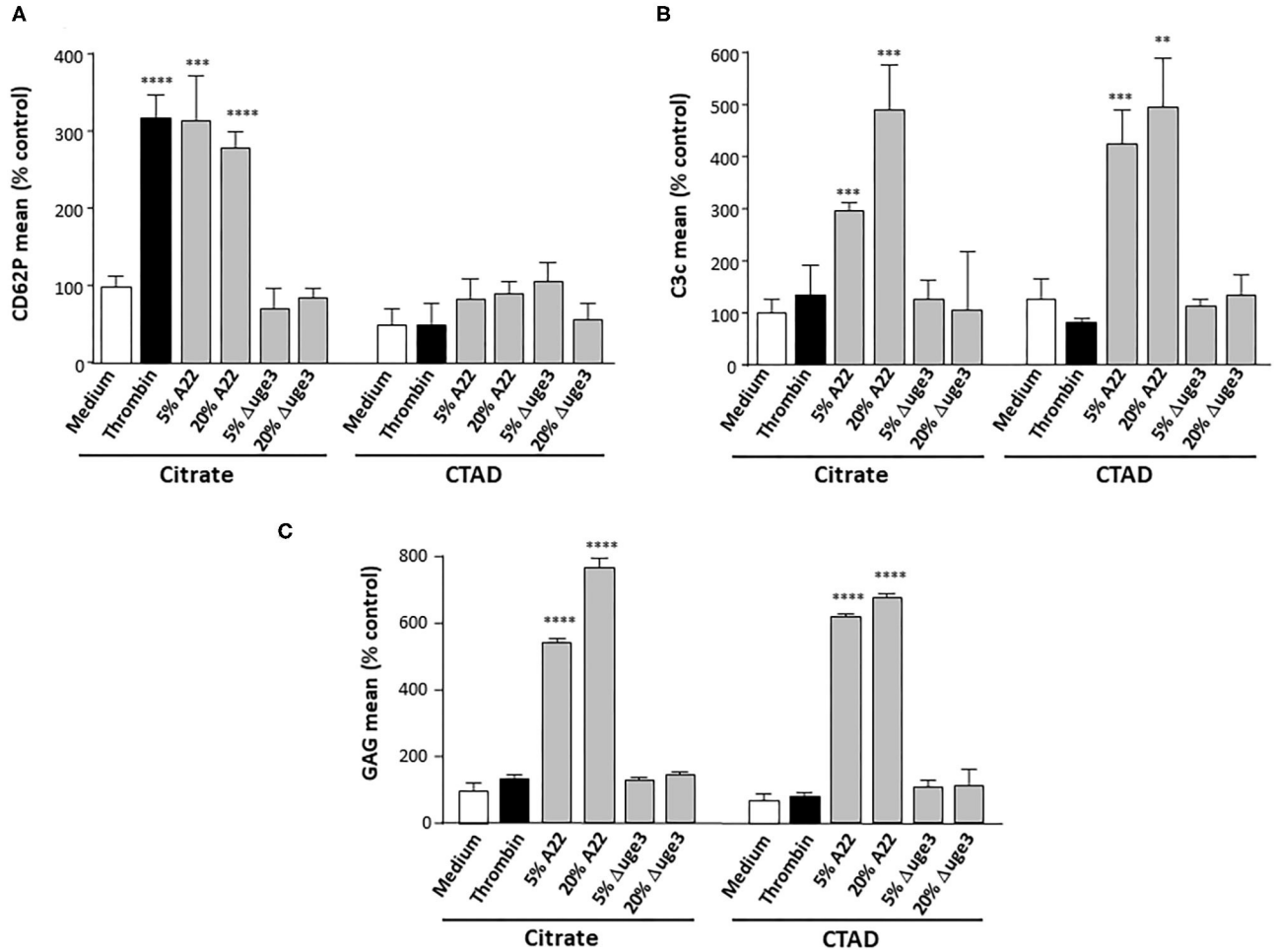

FIGURE 4 | Evaluation of a necessity of platelet activation for GAG-induced platelet opsonization. Blood samples were taken using either citrate or CTAD as anticoagulants, and platelets were isolated. Platelets were pre-treated with medium, thrombin, or 5–20% of supernatant (SN) of *Aspergillus fumigatus* A22 or the Δ*uge3* mutant, followed by addition of serum as complement source. Platelet activation and opsonization were quantified by flow cytometry using an αCD62P antibody as activation marker **(A)** or an αC3c antibody **(B)** to quantify opsonization. Deposition of GAG on the platelets was controlled using SBA lectin **(C)**. Each experiment was repeated at least three times with different platelet donors and with triplicate samples. Results were shown and statistically analyzed in comparison to medium as a negative control, which was set to 100%. $^{****}p < 0.001$, $^{***}p < 0.005$, $^{**}p < 0.01$.

pathway. To investigate this thesis, we used synthetic peptides that specifically inhibit the lectin pathway by preventing the binding of ficolins or MBL to MASPs. The peptide SFMI-1 inhibits both MASP-1 and MASP-2 binding, whereas peptide SFMI-2 is more potent to inhibit binding of MASP-2. Addition of one of the peptides to the serum as complement source induced a significant reduction of GAG-triggered platelet opsonization, and the effect was even more pronounced when both peptides were added (**Figure 5A**). This effect was confirmed with SN of the *A. fumigatus* wild-type strain AF293, whereas the C3c signal was negative for the SN of the GAG mutant Δ*uge3*, irrespective of presence or absence of the peptides (**Figure 5B**). The deposition of GAG was not affected by the peptides (**Figure 5C**). Since *A. flavus* was the only non-*fumigatus* species that secreted GAG and triggered platelet opsonization, the *A. flavus* SN was also tested with the peptides. Again, the peptides at least partly interfered with the opsonization process, and the effect was most profound when both peptides were added to the serum (**Figure 5D**). These results indicate that the lectin pathway might play a dominant role in GAG-induced complement opsonization of the platelet surface.

GAG-Induced Complement Activation on Platelets Triggers Inflammation

To monitor the physiological relevance of GAG-induced complement activation on platelets, formation of the complement factors C3a and C5a after contact of platelets with fungal SN was quantified. These pro-inflammatory anaphylatoxins are putative mediators of thrombosis and inflammation (20, 21) and thus might essentially contribute to these hallmarks of invasive fungal infections. Respective ELISAs demonstrated a significantly higher formation of both anaphylatoxins when platelets were incubated in the presence of serum with SN of *A. fumigatus* and *A. flavus* than in medium

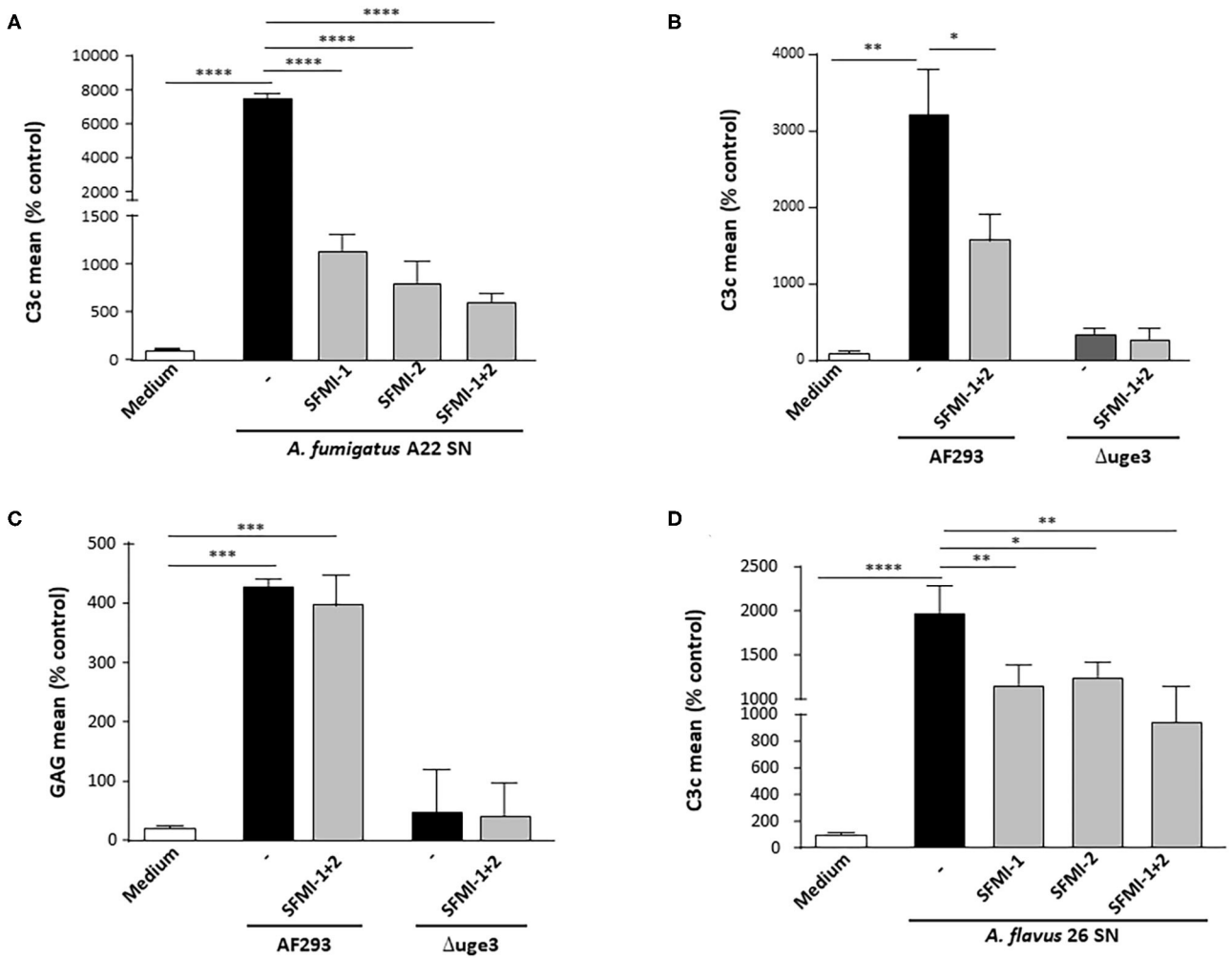

FIGURE 5 | Contribution of lectin pathway to GAG-induced platelet opsonization. Platelets were pre-incubated with medium or 20% supernatant (SN) of *A. fumigatus* A22 **(A)**, *AF293*, and the GAG mutant Δ*uge3* **(B,C)** or *A. flavus* 26 **(D)**. Serum as complement source was added, supplemented with buffer (–) or with the lectin-inhibiting peptides SFMI-1, SFMI-2, or the combination thereof (SFMI-1 + SFMI-2). Complement deposition **(A,B,D)** and deposition of GAG (**C**) on platelets was measured by flow cytometry using an αC3c antibody or SBA lectin, respectively. Results are shown in comparison to medium as a negative control, which was set to 100%. Each experiment was repeated at least three times with different platelet donors and with triplicate samples. $^{****}p < 0.001$, $^{***}p < 0.005$, $^{**}p < 0.01$, $^{*}p < 0.05$.

or thrombin controls (**Figures 6A,B**). In contrast, the SN of *A. terreus* or the Δ*uge3* mutant, which were not able to produce or secrete GAG, did not induce generation of C3a or C5a.

Budding of microparticles is another mechanism how platelets can contribute to inflammation, since they can contribute to dissemination of pro-inflammatory signals (cytokines and chemokines) (22). We evaluated whether GAG-induced platelet opsonization might trigger microparticle formation. As described previously, incubation of platelets with SN of GAG-secreting *A. fumigatus* enhanced the percentage of microparticles (**Figure 7A**). When incubation of platelets with SN was performed in the presence of serum, the percentage of microparticles was five times higher than with SN alone (**Figure 7A**). Confocal microscopy confirmed the enhanced SN-induced microparticle formation in the presence of serum (**Figure 7B**). In contrast to the wild type, SN of the Δ*uge3* mutant did not significantly alter the percentage of microparticles compared to the medium control (**Figure 7A**).

GAG-Induced Complement Activation on Platelets Triggers Platelet Loss

The complement cascade ends in the terminal pathway with formation of the C5b-9 complex. Whereas, the soluble form (TCC) contributes to immune cell activation, the membrane-bound form (MAC) forms a pore to induce membrane disintegration and lysis. We therefore monitored whether secreted GAG leads to C5b-9 formation on the platelet surface. Incubation of platelets with fungal SN of *A. fumigatus* A22 triggered formation of the C5b-9 complex on the surface, whereas the signal was negative with SN of *Lichtheimia corymbifera* LC-2 (**Figure 8A**). A broad screening and quantitative analysis of different isolates and species confirmed that GAG-secreting

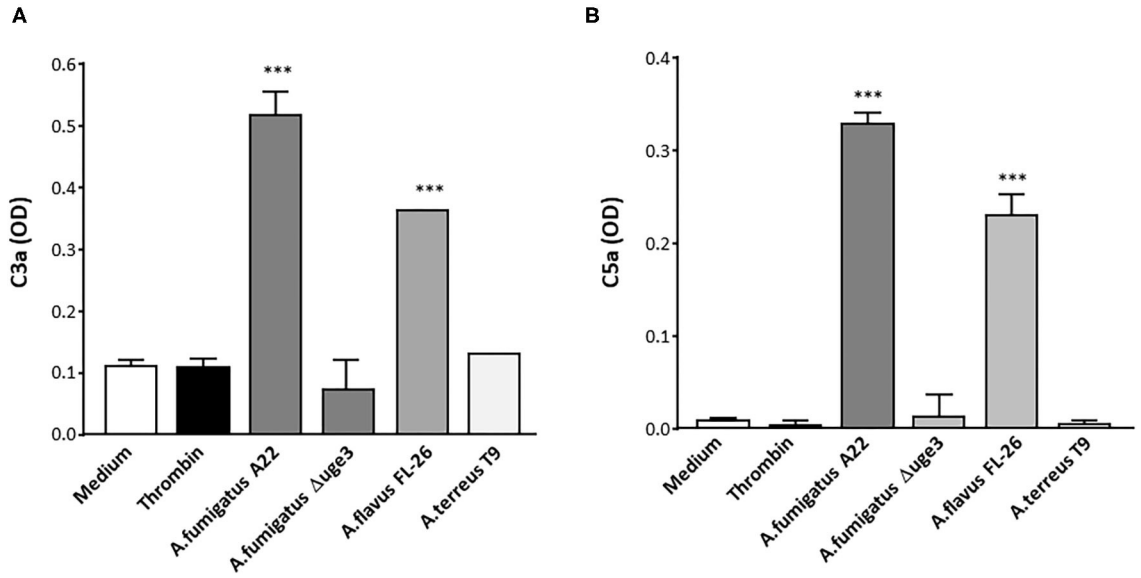

FIGURE 6 | Generation of anaphylatoxins C3a and C5a by GAG-triggered complement activation. Platelets were pre-incubated with medium, thrombin, or 20% supernatant (SN) of *A. fumigatus* (isolate A22), Δ*uge3* mutant *A. flavus* (isolate FL-26), or *A. terreus* (isolate T9), followed by addition of serum as complement source. Formation of C3a **(A)** and C5a **(B)** was quantified by ELISA and is given as optical density (OD). Each experiment was repeated at least three times with different platelet donors and with triplicate samples. Results were statistically analyzed in comparison to medium as a negative control. ***$p < 0.005$.

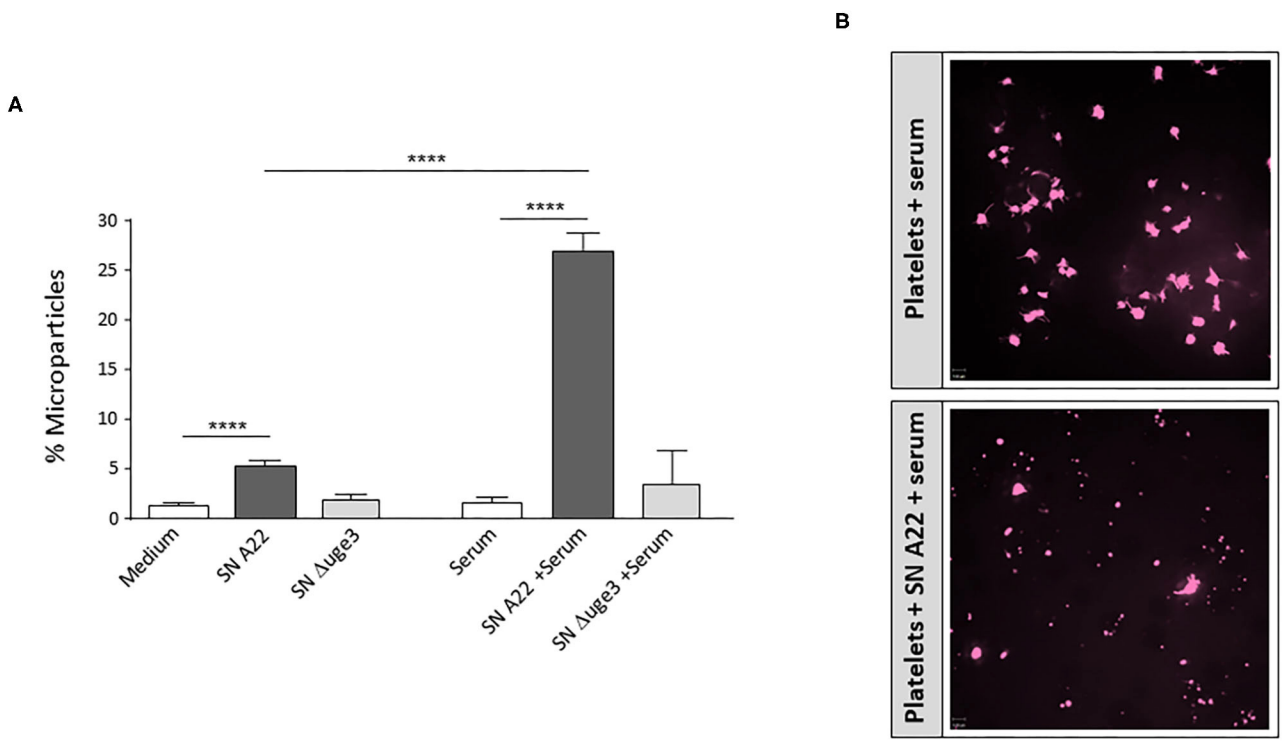

FIGURE 7 | Formation of microparticles upon GAG-induced platelet opsonization. **(A)** Platelets, labeled with a fluorescent αCD41 antibody, were incubated with medium, 20% supernatant (SN) of *A. fumigatus* strain A22 or Δ*uge3* mutant, serum, or 20% fungal supernatants plus serum. Newly formed microparticles were gated in flow cytometry according to their size and are expressed as percentage of all CD41-positive events. **(B)** Microparticle formation was also visualized by confocal microscopy. Each experiment was repeated at least three times with different platelet donors and with triplicate samples. ****$p < 0.001$.

isolates of *A. fumigatus* and *A. flavus* all induced C5b-9 formation on platelets, while species without GAG secretion, such as *A. terreus L. corymbifera*, or the Δ*uge3* mutant, did not (**Figure 8B**).

GAG-induced formation of C5b-9 could also be correlated with loss of platelet viability. Platelets were incubated with increasing concentrations of SN of *A. fumigatus* A22, in the presence or absence of serum as complement source. Calcein blue, a cell-permeant esterase substrate, serves as a viability probe that measures both activity of intracellular esterases and cell-membrane integrity. Incubation of platelets with fungal SN alone results in a concentration-dependent staining intensity of platelets with calcein blue, reflecting the SN-induced platelet activation (**Figure 8C**). In the presence of serum as complement source, however, the calcein blue signal decreases significantly, again in a concentration-dependent manner (**Figure 8C**). Addition of heat-inactivated serum did not affect staining with calcein blue and thereby platelet viability (data not shown).

DISCUSSION

The angioinvasive capacity of human-pathogenic *Aspergillus* species makes complement and platelets prevailing targets of interest. Both are elements of innate immunity, and both are present in the blood in high concentrations/amounts. The present study revealed that deposition of fungal GAG on the surface of platelets results in activation of the complement cascade with respective consequences of complement activity. Fungal secretory products such as GAG are commonly supposed to play a substantial role in the pathogenesis of invasive fungal infections (23). Their action is not limited to the site of infection and the presence of fungal hyphae, but they can easily disseminate in the bloodstream and exert their impact throughout the body and distant from the focus of infection. In the stage of hematogenic spreading of the invading fungi, the high concentration of platelets in the blood draws the attention on the effect of secretory compounds on platelets.

The surface-bound polysaccharide GAG, produced by *A. fumigatus* and *A. flavus*, was previously shown to mediate the interaction between hyphae and platelets (24). The spectrum of GAG–platelet interactions was expanded by findings that also secreted GAG affects platelets by binding to their surface and inducing their activation (9). In the experiments presented here, we could allocate a further function to GAG, i.e., the triggering of a complement reaction against platelets.

The close relationship between complement and platelets includes multiple axes and molecular mechanisms of mutual regulation [reviewed in (25, 26)]. Upon activation, platelets were described to expose P-selectin (CD62P) on their surface, which subsequently triggers the alternative complement pathway (27, 28). This is in contrast to our findings, which indicate that thrombin-induced activation alone is not sufficient to induce significant complement activation. Possible explanations of this discrepancy might be that these research groups used other platelet activators such as TRAP, ADP, or arachidonic acid. Only one experiment used thrombin as activator, but at 10-fold higher concentrations than in our assays (1 IU/ml vs. 0.1 IU/ml, respectively).

Furthermore, in our experiments, CTAD, which is an alternative anticoagulant inhibiting platelet activation and CD62P exposition, still enabled GAG-induced complement deposition on the platelet surface. According to this finding, the deposition of fungal GAG on platelets appears to be the main trigger of complement activation in our experimental setting. This thesis was strengthened by experiments applying lectin pathway-inhibiting peptides. Whereas, CD62P exposition was described to mainly initiate the alternative pathway (27, 28), inhibition of the lectin pathway by these peptides significantly interfered with GAG-induced complement activation. This finding is consistent with the fact that GAG is a polysaccharide and therefore a natural target for the lectin pathway specialized on the recognition of microbial carbohydrates. The relevance of the lectin pathway for GAG-stimulated complement activation might also partly explain why MBL-deficient mice showed an improved survival in a mouse model of systemic aspergillosis, as reviewed elsewhere (29).

Data of mouse models indicate that platelets represent a key factor to maintain hemostasis and lung integrity in response to exposed fungal antigens. Thrombocytopenic mice exhibited severe hemorrhage into the airways in response to *A. fumigatus* challenge (30). Since platelets are versatile antifungal immune weapons (10, 11), their shutoff via the body's own complement cascade represents a perfidious mechanism of fungal immune evasion. Indications that elimination of platelet immunology affects the prognosis of infected patients came from studies showing that low baseline platelet counts predict a poor outcome of invasive aspergillosis (31). Lowered platelet count in invasive fungal disease was also described in preterm infants, and antifungal treatment significantly elevated the platelet number in blood (32). The consequence of GAG-triggered complement attack against platelets is the loss of platelet viability and, as a result, the loss of platelet-associated immune and hemostatic capacities. Platelet loss might be reinforced by interaction with neutrophils that may bind via their complement receptors to opsonized platelets and may trigger their phagocytosis and destruction.

GAG-mediated complement activation on the platelet surface might not only damage the platelets themselves but also affect "bystander" cells, thus contributing to cell loss during invasive aspergillosis. Tissue damage mediated by activated complement ("friendly fire") is evident in numerous diseases, including arthritis, cancer, stroke, and infections (33, 34). Further studies, e.g., by co-incubation of platelets and GAG with putative bystander cells, will help to confirm the relevance of this mechanism.

GAG-driven complement activation might not only induce platelet loss, thrombocytopenia, and bystander lysis in infected patients but also participate in thrombosis and inflammation. Our results show that significant amounts of complement-derived anaphylatoxins C3a and C5a are generated after triggering GAG deposition on platelets in the presence of serum as complement source. In addition, platelets were shown to

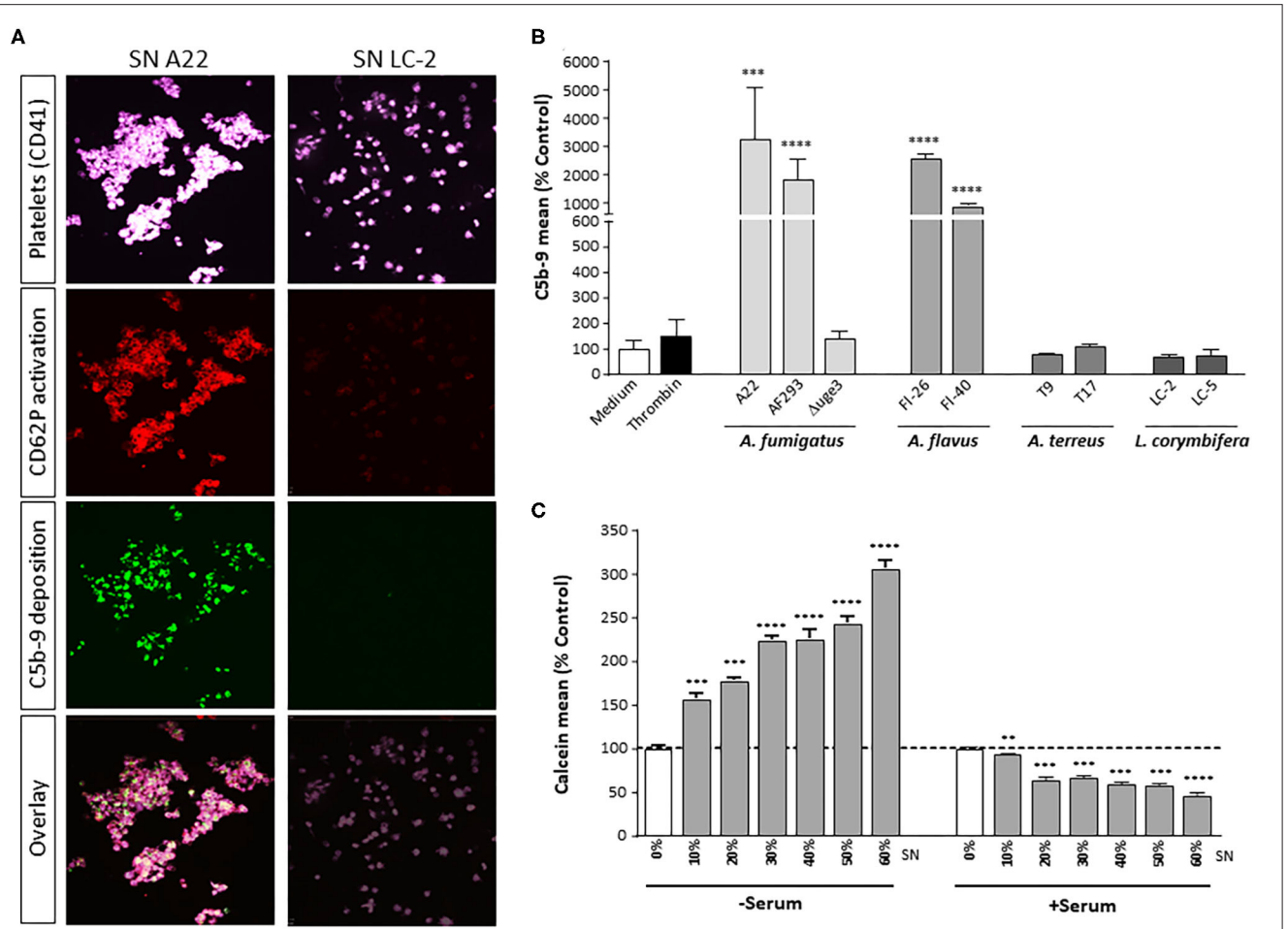

FIGURE 8 | GAG-dependent complement C5b-9 formation on platelets and platelet viability. **(A,B)** Platelets, labeled with a fluorescent αCD41 antibody (purple), were pre-incubated with medium or with 20% supernatant (SN) of different fungal species, followed by addition of serum as complement source. Activation of platelets was monitored **(A)** by a specific αCD62P antibody. Generation of C5b-9 on the platelet surface was detected by confocal microscopy **(A)** or quantified by flow cytometry **(B)**. **(C)** Platelets were pre-incubated with increasing concentrations of *A. fumigatus* A22 supernatant (SN), followed by addition of medium or serum as complement source. Platelet viability was monitored by addition of calcein blue and analyzed by flow cytometry. Each experiment was repeated at least three times with different platelet donors and with triplicate samples. Results in **(B,C)** are analyzed in comparison with the medium sample, which was set to 100%. ****$p < 0.001$, ***$p < 0.005$, **$p < 0.01$.

bear receptors for C3a and C5a (35, 36) themselves. Binding of the generated anaphylatoxins to their receptors on circulating "bystander" platelets may further enhance the participation of platelets in thrombotic and inflammatory processes (26, 36). Furthermore, C5a was described to cause profound prothrombotic perturbations on the endothelium and thus to drive macrovascular thrombosis (37). Released anaphylatoxins might also chemotactically attract other immune cells such as neutrophils and thus contribute to initiation of pro-inflammatory processes (38).

According to our results, a further amplification of thrombus formation might be provoked by GAG-driven shedding of pro-coagulant platelet microparticles. Microparticle formation might be stimulated by C5a or C5b-9 formation, which both were detected after incubation of platelets with GAG-containing fungal SN and subsequent presence of serum. These complement activation products were described to promote the shedding of microparticles (37). The released microparticles budding from the plasma membrane of platelets expose phospholipids on their surface that act as procoagulants (39). Platelet-derived microparticles are even reported to have a 50- to 100-fold higher procoagulant activity than activated platelets (40). Thus, secretion of fungal GAG with its subsequent effects on platelet-complement interaction might be a serious perpetrator for thrombosis in aspergillosis patients (41), predominantly in those with predisposing factors such as prolonged neutropenia, chronic administration of corticosteroids, insertion of prosthetic devices, or tissue damage due to prior infection or trauma (42).

Both GAG-induced anaphylatoxins and microparticles also act in a pro-inflammatory manner and thereby might mediate excessive inflammation during invasive aspergillosis. Microparticles contain chemokines (e.g., RANTES) and

cytokines (e.g., IL-1β) and thus are able to trigger inflammation distant from the site of infection (43). C5a is a well-known chemoattractant and recruits immune cells into inflamed tissue (44). C3a is mainly described as a pro-inflammatory molecule but also shows several anti-inflammatory facets (20).

Interestingly, all tested Mucorales species were unable to secrete GAG, and their culture SN did not induce activation of platelets or complement activation on the platelet surface. This is surprising, since angioinvasion and thrombosis are typical hallmarks of invasive mucormycosis, as reviewed elsewhere (45). Our results, however, indicate that the mechanism of Mucorales-induced thrombosis does not involve a pro-thrombotic activity of a secreted compound.

In summary, GAG deposition on platelets leads to complement activation and might thus support the attack against the invading fungal pathogens. The activated complement might also trigger other arms of innate and adaptive immune system. However, putative negative consequences are thrombocytopenia, thrombosis, and excessive inflammation. *In vivo* studies in a mouse model will help to assess the influence of GAG on the complement–platelet axis during invasive aspergillosis.

DATA AVAILABILITY STATEMENT

The raw data supporting the conclusions of this article will be made available by the authors, without undue reservation.

ETHICS STATEMENT

The studies involving human participants were reviewed and approved by Ethics committee of the Medical University of Innsbruck. The patients/participants provided their written informed consent to participate in this study.

AUTHOR CONTRIBUTIONS

CS, GR, DS, RW, and CL-F contributed to the conception and design of the study. HD and MN performed experiments. CS and MN made statistical analysis. CS, HD, and GR wrote sections of the manuscript. All authors contributed to the revision of the manuscript, read, and approved the submitted version.

FUNDING

This study was supported by the FWF Austrian Science Fund (Project Nr. P26117-B20). CL-F, RW, and HD were supported by the FWF doctoral program of excellence HOROS (W1253).

SUPPLEMENTARY MATERIAL

The Supplementary Material for this article can be found online at: https://www.frontiersin.org/articles/10.3389/fimmu.2020.550827/full#supplementary-material

REFERENCES

1. Mellinghoff SC, Panse J, Alakel N, Behre G, Buchheidt D, Christopeit M, et al. Primary prophylaxis of invasive fungal infections in patients with haematological malignancies: 2017 update of the recommendations of the Infectious Diseases Working Party (AGIHO) of the German Society for Haematology and Medical Oncology (DGHO). *Ann Hematol*. (2018) 97:197–207. doi: 10.1007/s00277-017-3196-2
2. Otto WR, Green AM. Fungal infections in children with haematologic malignancies and stem cell transplant recipients. *Br J Haematol*. (2020) 189:607–24. doi: 10.1111/bjh.16452
3. Latge JP, Chamilos G. Aspergillus fumigatus and Aspergillosis in 2019. *Clin Microbiol Rev Dec*. (2019) 18:33. doi: 10.1128/CMR.00140-18
4. Lehrnbecher T, Frank C, Engels K, Kriener S, Groll AH, Schwabe D. Trends in the postmortem epidemiology of invasive fungal infections at a university hospital. *J Infect*. (2010) 61:259–65. doi: 10.1016/j.jinf.2010.06.018
5. Subira M, Martino R, Rovira M, Vazquez L, Serrano D, De la Camara R. Clinical applicability of the new EORTC/MSG classification for invasive pulmonary aspergillosis in patients with hematological malignancies and autopsy-confirmed invasive aspergillosis. *Ann Hematol*. (2003) 82:80–2. doi: 10.1007/s00277-002-0599-4
6. Brown GD, Denning DW, Gow NA, Levitz SM, Netea MG, White TC. Hidden killers: human fungal infections. *Sci Transl Med*. (2012) 4:165rv113. doi: 10.1126/scitranslmed.3004404
7. Lee MJ, Liu H, Barker BM, Snarr BD, Gravelat FN, Al Abdallah Q, et al. The fungal exopolysaccharide galactosaminogalactan mediates virulence by enhancing resistance to neutrophil extracellular traps. *PLoS Pathog*. (2015) 11:e1005187. doi: 10.1371/journal.ppat.1005187
8. Speth C, Rambach G, Lass-Florl C, Howell PL, Sheppard DC. Galactosaminogalactan (GAG) and its multiple roles in *Aspergillus* pathogenesis. *Virulence*. (2019) 22:1–8. doi: 10.1080/21505594.2019.1568174
9. Deshmukh H, Rambach G, Sheppard DC, Lee M, Hagleitner M, Hermann M, et al. Galactosaminogalactan secreted from *Aspergillus fumigatus* and *Aspergillus flavus* induces platelet activation. *Microbes Infect*. (2020) 18:4. doi: 10.1016/j.micinf.2019.12.004
10. Speth C, Loffler J, Krappmann S, Lass-Florl C, Rambach G. Platelets as immune cells in infectious diseases. *Future Microbiol*. (2013) 8:1431–51. doi: 10.2217/fmb.13.104
11. Speth C, Rambach G, Lass-Florl C. Platelet immunology in fungal infections. *Thromb Haemost*. (2014) 112:632–9. doi: 10.1160/TH14-01-0074
12. McDonald B, Dunbar M. Platelets and intravascular immunity: guardians of the vascular space during bloodstream infections and sepsis. *Front Immunol*. (2019) 10:2400. doi: 10.3389/fimmu.2019.02400
13. Kumar V. The complement system, toll-like receptors and inflammasomes in host defense: three musketeers' one target. *Int Rev Immunol*. (2019) 38:131–56. doi: 10.1080/08830185.2019.1609962
14. Mongini PK, Jackson AE, Tolani S, Fattah RJ, Inman JK. Role of complement-binding CD21/CD19/CD81 in enhancing human B cell protection from Fas-mediated apoptosis. *J Immunol*. (2003) 171:5244–54. doi: 10.4049/jimmunol.171.10.5244
15. Ajona D, Ortiz-Espinosa S, Pio R. Complement anaphylatoxins C3a and C5a: Emerging roles in cancer progression and treatment. *Semin Cell Dev Biol*. (2019) 85:153–63. doi: 10.1016/j.semcdb.2017.11.023
16. Xie CB, Jane-Wit D, Pober JS. Complement membrane attack complex: new roles, mechanisms of action, and therapeutic targets. *Am J Pathol*. (2020) 16:6. doi: 10.1016/j.ajpath.2020.02.006
17. Wostemeyer J. (1985). Strain-dependent variation in ribosomal DNA arrangement in Absidia glauca. *Eur J Biochem*. 146:443–8. doi: 10.1111/j.1432-1033.1985.tb08671.x
18. Lee MJ, Gravelat FN, Cerone RP, Baptista SD, Campoli PV, Choe SI, et al. Overlapping and distinct roles of Aspergillus fumigatus UDP-glucose 4-epimerases in galactose metabolism and the synthesis of galactose-containing cell wall polysaccharides. *J Biol Chem*. (2014) 289:1243–56. doi: 10.1074/jbc.M113.522516
19. Gravelat FN, Beauvais A, Liu H, Lee MJ, Snarr BD, Chen D, et al. *Aspergillus galactosaminogalactan* mediates adherence to host constituents and conceals

hyphal beta-glucan from the immune system. *PLoS Pathog*. (2013) 9:e1003575. doi: 10.1371/journal.ppat.1003575
20. Coulthard LG, Woodruff TM. Is the complement activation product C3a a proinflammatory molecule? Re-evaluating the evidence and the myth. *J Immunol*. (2015) 194:3542–8. doi: 10.4049/jimmunol.1403068
21. Kourtzelis I, Markiewski MM, Doumas M, Rafail S, Kambas K, Mitroulis I, et al. Complement anaphylatoxin C5a contributes to hemodialysis-associated thrombosis. *Blood*. (2010) 116:631–9. doi: 10.1182/blood-2010-01-264051
22. Kapur R, Zufferey A, Boilard E, Semple JW. Nouvelle cuisine: platelets served with inflammation. *J Immunol*. (2015) 194:5579–87. doi: 10.4049/jimmunol.1500259
23. Ghannoum MA. Potential role of phospholipases in virulence and fungal pathogenesis. *Clin Microbiol Rev*. (2000) 13:122–43. doi: 10.1128/CMR.13.1.122
24. Rambach G, Blum G, Latge JP, Fontaine T, Heinekamp T, Hagleitner M, et al. Identification of *Aspergillus fumigatus* surface components that mediate interaction of conidia and hyphae with human platelets. *J Infect Dis*. (2015) 212:1140–9. doi: 10.1093/infdis/jiv191
25. Eriksson O, Mohlin C, Nilsson B, Ekdahl KN. The human platelet as an innate immune cell: interactions between activated platelets and the complement system. *Front Immunol*. (2019) 10:1590. doi: 10.3389/fimmu.2019.01590
26. Speth C, Rambach G, Wurzner R, Lass-Florl C, Kozarcanin H, Hamad OA, et al. Complement and platelets: mutual interference in the immune network. *Mol Immunol*. (2015) 67:108–18. doi: 10.1016/j.molimm.2015.03.244
27. Del Conde I, Cruz MA, Zhang H, Lopez JA, Afshar-Kharghan V. Platelet activation leads to activation and propagation of the complement system. *J Exp Med*. (2005) 201:871–9. doi: 10.1084/jem.20041497
28. Saggu G, Cortes C, Emch HN, Ramirez G, Worth RG, Ferreira VP. Identification of a novel mode of complement activation on stimulated platelets mediated by properdin and C3(H2O). *J Immunol*. (2013). 190:6457–67. doi: 10.4049/jimmunol.1300610
29. Parente R, Doni A, Bottazzi B, Garlanda C, Inforzato A. The complement system in *Aspergillus fumigatus* infections and its crosstalk with pentraxins. *FEBS Lett*. (2020) 28:13744. doi: 10.1002/1873-3468.13744
30. Tischler BY, Tosini NL, Cramer RA, Hohl TM. Platelets are critical for survival and tissue integrity during murine pulmonary *Aspergillus fumigatus* infection. *PLoS Pathog*. (2020) 16:e1008544. doi: 10.1371/journal.ppat.1008544
31. Nouer SA, Nucci M, Kumar NS, Grazziutti M, Restrepo A, Anaissie E. Baseline platelet count and creatinine clearance rate predict the outcome of neutropenia-related invasive aspergillosis. *Clin Infect Dis*. (2012) 54:e173–83. doi: 10.1093/cid/cis298
32. Zhao D, Qiu G, Luo Z, Zhang Y. Platelet parameters and (1, 3)-beta-D-glucan as a diagnostic and prognostic marker of invasive fungal disease in preterm infants. *PLoS ONE*. (2015) 10:e0123907. doi: 10.1371/journal.pone.0123907
33. Arumugam TV, Woodruff TM, Lathia JD, Selvaraj PK, Mattson MP, Taylor SM. Neuroprotection in stroke by complement inhibition and immunoglobulin therapy. *Neuroscience*. (2009) 158:1074–89. doi: 10.1016/j.neuroscience.2008.07.015
34. Koscielska-Kasprzak K, Bartoszek D, Myszka M, Zabinska M, Klinger M. The complement cascade and renal disease. *Archiv Immunol Therap Exp*. (2014) 62:47–57. doi: 10.1007/s00005-013-0254-x
35. Martel C, Cointe S, Maurice P, Matar S, Ghitescu M, Theroux P, et al. Requirements for membrane attack complex formation and anaphylatoxins binding to collagen-activated platelets. *PLoS ONE*. (2011) 6:e18812. doi: 10.1371/journal.pone.0018812
36. Patzelt J, Mueller KA, Breuning S, Karathanos A, Schleicher R, Seizer P, et al. Expression of anaphylatoxin receptors on platelets in patients with coronary heart disease. *Atherosclerosis*. (2015) 238:289–95. doi: 10.1016/j.atherosclerosis.2014.12.002
37. Noris M, Remuzzi G. Terminal complement effectors in atypical hemolytic uremic syndrome: C5a, C5b-9, or a bit of both? *Kidney Int*. (2019) 96:13–5. doi: 10.1016/j.kint.2019.02.038
38. Sadik CD, Miyabe Y, Sezin T, Luster AD. The critical role of C5a as an initiator of neutrophil-mediated autoimmune inflammation of the joint and skin. *Semin Immunol*. (2018) 37:21–9. doi: 10.1016/j.smim.2018.03.002
39. Nomura S, Shimizu M. Clinical significance of procoagulant microparticles. *J Intensive Care*. (2015) 3:2. doi: 10.1186/s40560-014-0066-z
40. Sinauridze EI, Kireev DA, Popenko NY, Pichugin AV, Panteleev MA, Krymskaya OV, et al. Platelet microparticle membranes have 50- to 100-fold higher specific procoagulant activity than activated platelets. *Thromb Haemost*. (2007) 97:425–34. doi: 10.1160/TH06-06-0313
41. Ben-Ami R. Angiogenesis at the mold-host interface: a potential key to understanding and treating invasive aspergillosis. *Future Microbiol*. (2013) 8:1453–62. doi: 10.2217/fmb.13.114
42. Gundlach JP, Gunther R, Fickenscher H, Both M, Rocken C, Becker T, et al. Lethal thrombosis of the iliac artery caused by *Aspergillus fumigatus* after liver transplantation: case report and review of the literature. *BMC Surg*. (2019) 19:200. doi: 10.1186/s12893-019-0668-4
43. Koupenova M, Clancy L, Corkrey HA, Freedman JE. Circulating platelets as mediators of immunity, inflammation, and thrombosis. *Circ Res*. (2018) 122:337–51. doi: 10.1161/CIRCRESAHA.117.310795
44. Zaal A, van Ham SM, Ten Brinke A. Differential effects of anaphylatoxin C5a on antigen presenting cells, roles for C5aR1 and C5aR2. *Immunol Lett*. (2019) 209:45–52. doi: 10.1016/j.imlet.2019.03.014
45. Ghuman H, Voelz K. Innate and adaptive immunity to mucorales. *J Fungi*. (2017) 3:48. doi: 10.3390/jof3030048

Conflict of Interest: The authors declare that the research was conducted in the absence of any commercial or financial relationships that could be construed as a potential conflict of interest.

frontiers in Immunology

ORIGINAL RESEARCH
published: 28 October 2020
doi: 10.3389/fimmu.2020.569549

Interference of the Zika Virus E-Protein With the Membrane Attack Complex of the Complement System

Zahra Malekshahi[1], Britta Schiela[1], Sarah Bernklau[1], Zoltan Banki[1], Reinhard Würzner[2] and Heribert Stoiber[1]**

[1] Institute of Virology, Medical University of Innsbruck, Innsbruck, Austria, [2] Institute of Hygiene & Medical Microbiology, Medical University of Innsbruck, Innsbruck, Austria

The complement system has developed different strategies to clear infections by several effector mechanisms, such as opsonization, which supports phagocytosis, attracting immune cells by C3 and C5 cleavage products, or direct killing of pathogens by the formation of the membrane attack complex (MAC). As the Zika virus (ZIKV) activates the classical complement pathway and thus has to avoid clearance by the complement system, we analyzed putative viral escape mechanisms, which limit virolysis. We identified binding of the recombinant viral envelope E protein to components of the terminal pathway complement (C5b6, C7, C8, and C9) by ELISA. Western blot analyses revealed that ZIKV E protein interfered with the polymerization of C9, induced on cellular surfaces, either by purified terminal complement proteins or by normal human serum (NHS) as a source of the complement. Further, the hemolytic activity of NHS was significantly reduced in the presence of the recombinant E protein or entire viral particles. This data indicates that ZIKV reduces MAC formation and complement-mediated lysis by binding terminal complement proteins to the viral E protein.

Keywords: complement, lysis, membrane attack complex, Zika virus, envelope protein, terminal complement pathway

OPEN ACCESS

Edited by:
Zvi Fishelson,
Tel Aviv University, Israel

Reviewed by:
Kenneth Reid,
University of Oxford, United Kingdom
Horea Rus,
University of Maryland, Baltimore, United States

***Correspondence:**
Heribert Stoiber
Heribert.stoiber@i-med.ac.at
Reinhard Würzner
Reinhard.wuerzner@i-med.ac.at

Specialty section:
This article was submitted to Molecular Innate Immunity, a section of the journal Frontiers in Immunology

Received: *11 June 2020*
Accepted: *05 October 2020*
Published: *28 October 2020*

Citation:
Malekshahi Z, Schiela B, Bernklau S, Banki Z, Würzner R and Stoiber H (2020) Interference of the Zika Virus E-Protein With the Membrane Attack Complex of the Complement System. Front. Immunol. 11:569549. doi: 10.3389/fimmu.2020.569549

INTRODUCTION

The complement system is an effective arm of innate immunity. It is a family of membrane-anchored and soluble proteins circulating in the blood in their inactive form (1, 2). Upon activation by harmful exogenous or endogenous ligands, one of the three complement pathways is triggered. The classical pathway is induced by immune complexes or by direct binding of C1q to the surface of pathogens, while the lectin pathway is activated by mannose binding lectin (MBL) bound to pathogen-associated molecular patterns, respectively. The third pathway, referred to as the alternative pathway, is initiated by spontaneous hydrolysis of C3 protein. All three pathways result in C3 activation and the formation of C3 convertases, and they merge in the induction of the terminal pathway. This final step generates the membrane attack complex (MAC) consisting of C5b-8 and 12–18 molecules of C9, which makes a pore on the cell surface to kill pathogens or infected cells (1, 2). To avoid destruction by the complement system, viruses have acquired strategies that can be condensed to a few successful mechanisms: 1) inactivation by enzymatic

degradation; 2) the recruitment or mimicking of complement regulators; and 3) the modulation or inhibition of complement proteins by direct interactions (3). Different viral families take advantage of at least one of the above-mentioned mechanisms. Among them are retroviruses, orthopox or herpes viruses to name only a few (4–8). In addition, flaviviridae have adapted strategies to escape complement-mediated lysis (9–11).

The flavivirus group includes several human pathogens, such as Dengue (DENV), yellow fever (JFV), West Nile (WNV), Japanese encephalitis (JEV), Zika virus (ZIKV), and the closely related hepatitis C virus (HCV), all of which share close similarities in structure (12, 13). The family belongs to enveloped viruses with a single stranded RNA with positive polarity, which is translated into a single polyprotein. This precursor protein is processed by both host and viral proteases and gives rise to three structural and seven nonstructural (NS) proteins (12, 13). The structural proteins include E protein (envelope protein) PrM, which is the precursor for membrane (M) and plays an important role in virus maturation and capsid (C). The envelope E protein mediates viral entry and modulates infection mainly in its glycosylated form (14). It binds to the different receptors on the surface of human cells and aids in the fusion and subsequent entrance of the virus *via* endocytosis (receptor-mediated endocytosis) (15). NS proteins are responsible for the regulation of RNA transcription, replication, and evasion or attenuation of the host immune response. By NS1, flaviviruses escape from complement-mediated lysis by binding complement regulator proteins such as factor H, C4bp, or vitronectin (9, 10). In line with this, Zika virus (ZIKV) takes advantage of NS1 by binding vitronectin, a regulator protein that interferes with MAC formation by binding to C5, C6, C7, and C9 (16, 17). Furthermore, NS1 may directly reduce C9 polymerization and thus prevent lysis by the terminal pathway complement (18). Although different by mechanism, HCV inhibits C9 polymerization by the acquisition and incorporation of CD59 into the viral envelope (11, 19).

Our data indicates that, similar to NS1, the E protein binds to terminal pathway complement proteins, interferes with the formation of MAC on the surface of the cells and further reduces complement-mediated lysis.

MATERIALS AND METHODS

Proteins

Purified complement proteins C5b6 (MW 285 kDa), C7 (MW 91.4 kDa), C8 (MW 151 kDa), and C9 (MW 71 kDa) were purchased from Complement Technology (Tyler, TX, USA). ZIKV recombinant E and NS1 proteins were provided by Aviva Systems Biology (San Diego, CA); E protein PMA04848-1MG and Biozol (Eching, Germany); E protein MBS596001, and Zika NS1 MBS596002). Anti-flavivirus group antigen antibody [D1-4G2-4-15 (4G2)] and goat anti-mouse antibody conjugated to horseradish peroxidase were purchased from Szabo-Scandic (Vienna, Austria).

Recombinant human vitronectin was obtained from BioLegend (Koblenz, Germany). Bovine serum albumin (BSA) was provided by Carl-Roth (Karlsruhe, Germany).

Anti-C9 (C9 neoantigen, Human, mAb WU13-15) was purchased from Hycult (Uden, NL). Normal human serum (NHS) was acquired from Dunn Labortechnik GmbH (Ansbach, Germany) and stored in aliquots at −80°C. Anti-human HLA-ABC antigen clone W6/32 was obtained from Agilent Technologies Dako (Vienna, Austria). C9 depleted serum was generated as described in detail (20).

Cells and Viruses

A549 cells for Western blot and virus production and Aedes albopictus C6/36 mosquito cells for virus propagation were kindly provided by Prof. Dr. Karin Stiasny, Medical University of Vienna. Sheep erythrocytes for the hemolysis assay were obtained from Virion (Würzburg, Germany). Two strains of the virus, MRS_OPY_Martinique_PaRi_2015 (GenBank: KU647676) and ZIKV strain MR766 (GenBank: DQ859059) were kindly provided by the European Virus Archive (Marseille, France). The virus was propagated as described elsewhere (21).

Buffers and Mediums

Cell lysates were analyzed by western blot, RIPA buffer for inducing lysis of the A549 cells was purchased from Cell Signaling Technology (Frankfurt, Germany). Veronal-buffered saline (VBS) was provided by Virion. Dulbecco's modified Eagle's medium (DMEM) and phosphate buffered saline (PBS) were purchased from Sigma-Aldrich (Vienna, Austria).

Binding Assay

Complement proteins including C5b6, C7, C8, and C9 in 1:2 dilutions starting from 5 μg/ml were coated on the microtiter 96 well ELISA plate and incubated overnight at 4°C. After washing with PBS-Tween 0.01%, E protein (10 μg/ml) was added to each well and incubated for 1 h at room temperature (RT) with slow continuous shaking. The ELISA plate was washed three times and blocked with 5% BSA for 1 h. Antibody against envelope protein (4G2) was added at a concentration of 1:500 and incubated for 1 h. Finally, horseradish peroxidase-labeled goat anti-mouse antibody was added (1:10,000). The TMB substrate from Sera Care (Tornesch, Germany) was used. The optical density (OD) was measured at a wavelength of 650 nm. To test if native C9 from NHS was also able to bind to the E protein, serial dilutions of NHS were incubated with a constant amount of E-protein (10 μg/ml coated overnight in the ELISA plate. BSA at the same concentration (10 μg/ml) or dilutions of C9-depleted serum (ΔC9 NHS) were applied as negative controls. Anti-C9 (WU 13-15) at a concentration of 1 μg per well was added. After washing, samples were incubated with secondary antibody (HRP-goat-anti-mouse Ab; 1:10,000) and finally, TMB substrate solution. Optical density (OD) was measured at a wavelength of 650 nm.

Inhibition of MAC Formation

A C9 polymerization assay was performed to study the formation of a membrane attack complex in the presence or absence of E protein. For this, A549 cells were seeded a day before the experiment at 1 × 10exp5 cells per well in 24 well plates purchased from Szabo-Scandic (Vienna, Austria) in complete

DMEM (10% fetal calf serum (FCS; Thermofisher, Vienna, Austria), 2 mM L-glutamine, 100 units/mL penicillin G, 100 µg/ml streptomycin). The next day, cells were washed three times with VBS and C5b6 protein (5 µg in 300 µl) was added to the cells and incubated for 2 h in a humidified incubator supplied with 5% CO_2 at 37°C. In parallel, the E protein was incubated with 5% NHS at 37°C for 30 min a total volume of 300 µl for each reaction). After three washing steps of the cells with VBS, the mixture of the E protein and NHS was added to the cells and incubated for 60 min at 37°C. Cells were washed again, lysed on ice with RIPA buffer for 30 min (100 µl of lysis buffer), and the lysate was loaded on an 8% acrylamide gel under non-reducing conditions. Lysates were blotted and the membrane was blocked with 5% nonfat dried milk in Tris-buffered saline with 0.1% Tween20 (TBST) for 60 min. The first antibody against C9 protein (WU 13-15) (1:2,000) was added to the blocking solution and incubated overnight at 4°C. The following day, the blot was washed three times with TBST and a horseradish peroxidase-labeled goat anti-mouse antibody was added (1:10,000). After incubation for 2 h at room temperature, the membrane was washed three times and developed using the ImageQuant LAS-4000 (GE Healthcare, Vienna, Austria). In further assays, anti-human HLA-ABC was used in a sublytic amount (1:1,000) as an activator of the classical pathway (instead of purified C5b6 protein). Ab was added to the A549 cells and incubated for 60 min at 37°C. In parallel, different amounts of E protein were incubated with 5% NHS at 37°C for 30 min. After washing the cells with VBS, the mixture of the E protein and NHS was added to the cells and incubated for 50 min at 37°C. Deposition of C9 on the cell surface was analyzed by western blotting as described above.

Hemolytic Assay

To analyze the activity of the complement system, sheep erythrocytes (1×10^8 cells/ml) resuspended in VBS were sensitized with C5b6 (1 µg) for 60 min at RT using a U-bottom microtiter plate from Greiner Bio-one (Kremsmünster, Austria). In a separate preparation, E protein (10 µg), Vn (20 µg), and mixtures of Vn-and NS1 (containing 20 µg VN and 10 µg NS1) and Vn and-E protein (containing 10 µg E protein and 20 µg Vn) were each incubated with C7-C9 (C7 (1 µg), C8 (0.5 µg), and C9 (1 µg) for 15 min at 37°C. Next, the prepared mixtures were added to the sheep erythrocytes coated with C5b6 and incubated for 30 min at 37°C in a total volume of 100 µl per reaction (9). After centrifugation, the hemolytic activity of the complement system was measured by quantitating the released hemoglobin in the supernatant at 415 nm. To test whether virus particles interfere with complement activation, a two-fold serial dilution of NHS was pre-incubated with ZIKV for 30 min on ice. Sensitized sheep erythrocytes (20 µl, 2×10^8 cells/ml) were added to the samples and the mixture was incubated for 30 min at 37°C. The amount of hemoglobin released from the lysed cells was measured by determining the absorbance of the supernatant at an optical density (OD) of 415 nm. To distinguish between the effects of NS1 or E-Protein on the reduction of hemolysis, viral proteins were incubated separately or as a mixture with NHS (1:160 in VBS) before sensitized sheep erythrocytes were added and the lysis assay was performed as described above.

Statistical Analyses

Statistical analyses were performed using the GraphPad Prism 7.0 software. All experiments were repeated at least three times always performed in duplicate. The difference between the two groups was assessed by t-test. When comparing more than two groups, ANOVA followed by Bonferroni post-hoc tests was performed. A 95% significance level ($p < 0.05$) was considered statistically significant (*<0.05, ** <0.01, ***<0.001, and ****<0.001).

RESULTS

ZIKV E Protein Binds to Components of the Terminal Pathway of Complement

As ZIKV activates the classical pathway of complement, we were interested in whether the virus adapted means to reduce virolysis. In a first attempt, we assessed whether purified C7, C8, or C9 bind ZIKV E in ELISAs. In contrast to C7, both C8 and C9 interacted with the viral recombinant E protein (**Figure 1A**). Both C8 and C9, but also C5b6 dose-dependently bound to ZIKV E protein (**Figure 1B**). Significance was reached for C8 down to 0.63 µg/ml of ZIKV E (**Figure 1B**), and for C9 and C5b6 down to 1.25 µg/ml. Finally, the binding of ZIKV E protein to the already generated terminal complement cascade (TCC) was assessed in NHS. For this, a constant amount of ZIKV E or BSA was coated onto the ELISA plates and incubated with different dilutions of NHS. As a further control, ΔC9 NHS was included. Significant interaction of TCC with the viral protein was observed up to an NHS dilution of 1:8 compared to the ΔC9 NHS (**Figure 1C**). With regard to BSA, only background binding to TCC was detected, even at the highest concentration of NHS (**Figure 1C**).

ZIKV E Protein Reduces C9 Polymerization on Cellular Surfaces

To test whether the binding of ZIKV E to components of the TCC interferes with the polymerization of C9, A549 cells were incubated with purified C5b6. As a source of C7 to C9, 5% NHS was used in the absence (**Figure 2**; 0 = no E) or the presence of different amounts of ZIKV E (**Figure 2**, 12.5 to 50 µg). The polymerization of high molecular weight C9 at the cellular surface was confirmed by western blot of the cell lysates employing the C9 neo-epitope-specific anti-C9 antibody (WU 13-15). Polymeric C9 was markedly reduced in a ZIKV E-concentration-dependent manner (**Figure 2A**), while BSA had no effect (**Figure 2B**) To further analyze the effect of ZIKV E on C9 polymerization, A549 cells were first incubated with sublytic amounts of an anti-MHC-I antibody as a trigger for the classical complement pathway. After removing the antibody by washing, NHS was added to the cells, which were pre-incubated with different amounts of ZIKV E. Cell lysates were analyzed by western blotting. C9 polymerization was reduced in a dose-dependent manner (**Figure 3**). However, in contrast to the induction of TCC by incubation of the cells with purified C5b6, which gave rise to high-molecular-weight C9 polymers, the

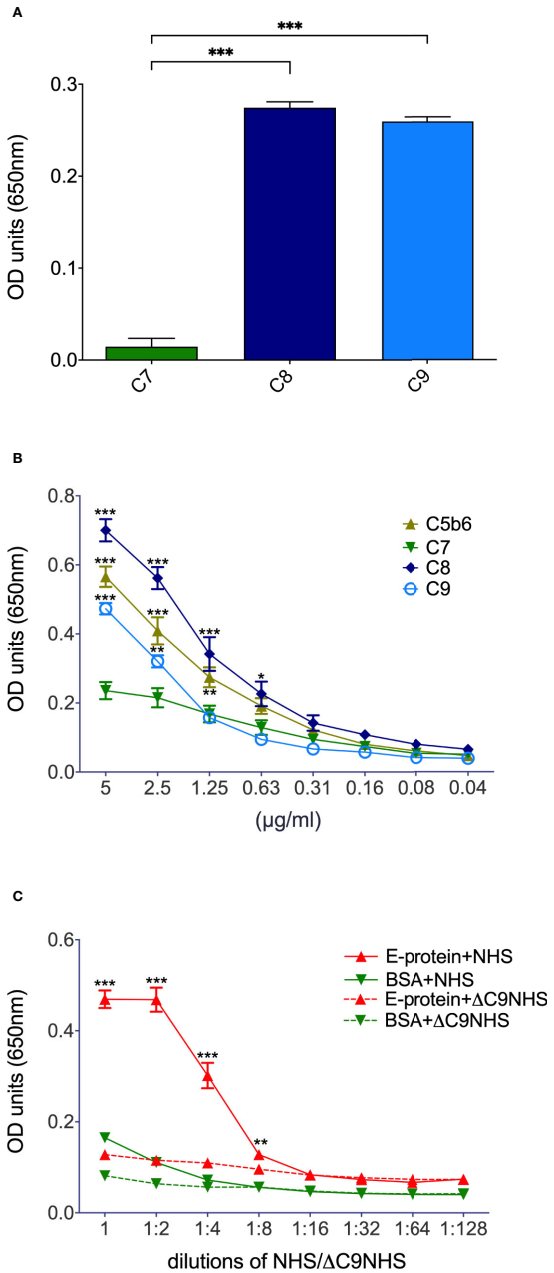

FIGURE 1 | Binding of terminal complement proteins to ZIKV E. Constant amounts (5 µg/ml; **A**) or serial dilutions (**B**, for significance – not always depicted due to limits in space – see text) of purified complement proteins were coated onto ELISA plates and incubated with 10 µg/ml ZIKV E. To visualize binding, an E-specific Ab (4G2) followed by a HRP-goat-anti-mouse Ab and TMB as a substrate were added. To test whether already generated TCC is interacting with ZIKV E too **(C)**, the recombinant viral protein was coated into ELISA plates and incubated with serial dilutions of NHS. BSA and ΔC9 NHS served as controls. Binding to TCC was determined by incubation with neoepitope-specific anti-C9 (WU 13-15) followed by HRP-goat-anti-mouse Ab. Again, TMB was used as a substrate. Optical density (OD) was measured at a wavelength of 650 nm. Experiments were repeated three times and were performed in duplicates. For statistical analysis GraphPad Prism software was used (**A**, 1-way ANOVA; **B, C**, 2-way ANOVA, respectively). *< 0.05, ** < 0.01 and *** < 0.001.

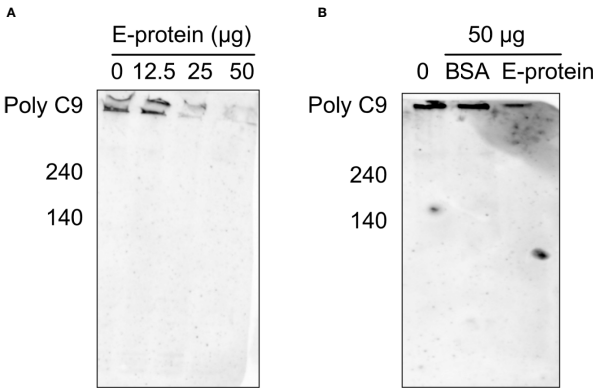

FIGURE 2 | Inhibition of C9 polymerization after induction *via* C5b6 in the presence of ZIKV E. To trigger generation of the terminal pathway of complement, A549 cells were incubated with purified C5b6 (5 µg) for 2 h at 37°C. After washing, 5% NHS was added as a source of C7 to C9 in the presence of different amounts of ZIKV E. After incubation at 37°C for 50 min and additional washing steps, cells were lysed and loaded on a SDS gels under non-reducing conditions. Lysates were blotted and visualized as described in the Material & Method section. A representative Western blot out of three independent experiments is shown **(A)**. As a control, the effect of BSA on the C9 polymerization was used **(B)**.

activation of the classical pathway of complement induced C9 oligomers of about 210 kDa in size (**Figure 3**). Again, the band observed for high molecular C9 polymers were reduced when compared to BSA.

ZIKV E Protein Inhibits the Formation of a Membrane Attack Complex

The interference of ZIKV E with the proteins of the terminal complement pathway might affect complement-mediated lysis, similar to that described for other pathogens (18, 22–24). Therefore, as sensitive functional readout, hemolytic assays with sheep erythrocytes were performed using purified TCC components. For this, ZIKV E was pre-incubated with C7, C8, and C9 and added to C5b6 pre-coated erythrocytes. When compared to lysis of the cells in the absence of viral proteins, which was set at 100% lysis, ZIKV E significantly reduced hemolysis (**Figure 4**) similar to that observed for vitronectin, a known inhibitor of the TCC (16). We confirmed that also NS1 interferes with complement-mediated hemolysis (not shown) and reproduced the data of Conde and coworkers, who showed a synergistic effect of NS1 with vitronectin (18). This synergy was not observed by combining ZIKV E with vitronectin (**Figure 4**).

Finally, we were interested in whether not only recombinant viral proteins, but also ZIKV itself interferes with hemolysis of sensitized erythrocytes. Erythrocytes were lysed by NHS in a dose-dependent manner and were not affected by the mock control, which employs the DMEM buffer used to cultivate the cells for virus propagation (**Figure 5**). In contrast, hemolysis was significantly diminished when ZIKV (2.5 × 10 exp5 PFU) was present in the system, starting from a 1:40 dilution of NHS (**Figure 5**), indicating that not only recombinant viral proteins,

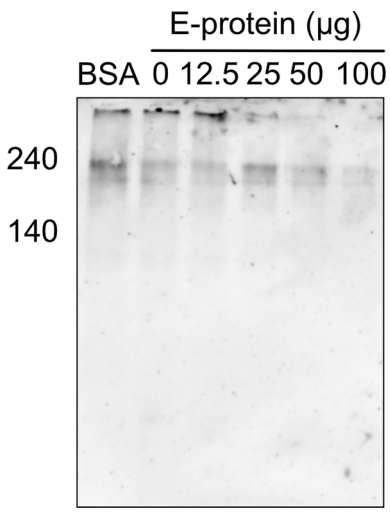

FIGURE 3 | Inhibition of C9 polymerization after induction of the classical pathway in the presence of ZIKV E. For the induction of complement activation, A549 cells were incubated with sublytic amounts of anti-MHC-1 (1:1,000). After washing, cells were incubated with 5% NHS, which was pre-incubated with different amounts of ZIKV E. After washing, cells were blotted and oligomerization of C9 was analyzed as described in **Figure 2**. A representative Western blot out of three independent experiments is shown.

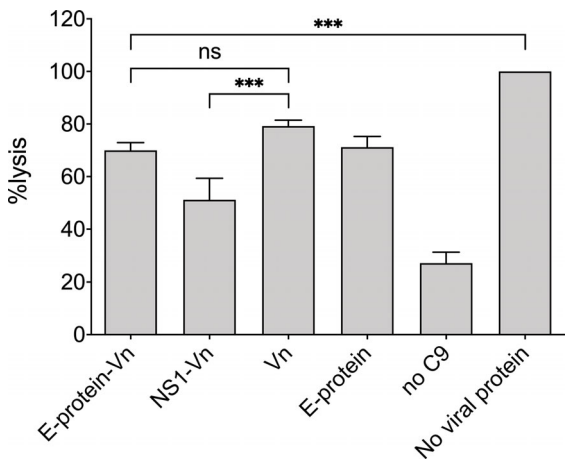

FIGURE 4 | Inhibition of MAC formation by ZIKV E: Viral proteins were pre-incubated with C7 to C9 and added to sheep erythrocytes pre-coated with C5b6. As a control vitronectin (VN) was used, a known inhibitor of the MAC. In the positive control (no viral protein) formation of the MAC was undisturbed and set at 100%. Hemolysis was determined by measuring the release of hemoglobin in the supernatant at an OD of 415 nm. Omission of C9 served as background control. Experiments were repeated three times performed in duplicates and analyzed by 1-way ANOVA. n.s., not significant. *** < 0.001.

but also viral particles interfere with MAC formation. To check whether NS1 and the E protein show additive effects, the viral protein was incubated separately and as a mixture with NHS before the erythrocytes were added. As expected, both viral proteins reduced hemolysis when compared to the buffer

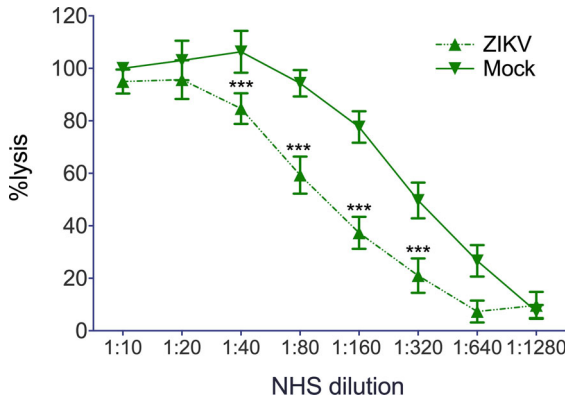

FIGURE 5 | Reduction of complement mediated lysis by ZIKV: Sensitized sheep erythrocytes were incubated for 30 min at 37°C with serial dilutions of NHS. As expected, lysis of the cell decreased with decreasing dilutions of NHS and was not affected by DMEM, the buffer used as mock control. Hemolysis was determined by measuring the release of hemoglobin in the supernatant at 415 nm. Experiments were performed three times in triplicates. Significance was calculated by 2-way ANOVA. *** < 0.001.

control (VBS). The mixture of NS1 and E further decreased cell lysis, indicating that both viral proteins contribute to the inhibition of complement-mediated lysis (**Figure 6**).

DISCUSSION

Interference with complement-mediated lysis is a common complement evasion mechanism for many viruses (9, 10).

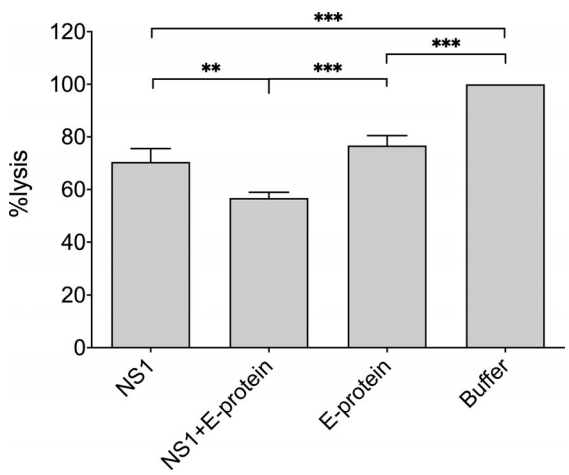

FIGURE 6 | Reduction of complement mediated lysis by recombinant viral proteins: NHS (1:160 diluted in VBS) was incubated on ice with purified recombinant viral proteins E (20 µg) or NS1 (5 µg) or a mixture of both. Sensitized sheep erythrocytes were added and incubated for 30 min at 37°C. The VBS-buffer control was set at 100%. Hemolysis was determined by measuring the release of hemoglobin in the supernatant at 415 nm. Experiments were performed three times in duplicates and analyzed by 1-way ANOVA. ** < 0.01 and *** < 0.001.

Thus, it is no surprise that members of the flavivirus family have developed strategies to escape from virolysis by interacting with proteins of the complement cascades and their regulators with NS1. WNV, for example, binds factor-H (25), a regulator of complement in the fluid phase, which interferes with the convertases and acts as a co-factor for C3b inactivation (1, 2). C4b binding protein (C4bp), a regulator of the classical and lectin pathway, is not only recruited by DENV (26), but also by WNV or YVF (27). Furthermore, the viruses' complex C4 together with C1s/proC1s in the fluid phase to decrease C4b deposition on the viral surface. Consequently, the classical pathway convertase is reduced and less MAC is induced (22). Clusterin (28) and vitronectin (18), two inhibitors of the TCC can interfere with MAC-formation by binding to NS1. In addition, flaviviral NS1, including ZIKV, can directly decrease C9 polymerization on cell surfaces and thus evade complement-induced damage (18). As mentioned above, these different strategies are attributed to the NS1 protein. Here, we report that besides NS1 also the E protein of ZIKV can directly interact with proteins of the TCC. In contrast to NS1, which also binds to C7, besides C5, C6, and C9, but not C8 (18), the viral E-protein was capable of interacting with C8, and only a poor interaction with C7 was observed. Consequently, the polymerization of C9 was reduced by the E protein in a dose-dependent manner when purified proteins were used. Of note, at basis of the molecular weight, more C9 was necessary to bind the same amount of ZIKV E. Thus, it would be interesting to check the effect of ZIKV E on the association of C8 or C5b6 during MAC formation. However this is beyond the scope of this paper. Activation of the classical pathway by antibodies bound to the cell surface resulted in a decrease of C9 oligomers in the presence of ZIKV E. Beside the bands for high molecular polymers, additional bands were identified compared to that of the experiments, in which the purified components were used. This corresponded to the size of trimerized C9 oligomers, which could be formed due to sublytic amounts of antibody used for complement activation.

According to our data, ZIKV E interfered with complement-mediated hemolysis comparable to vitronectin. Although interacting with vitronectin (data not shown), lysis induced by E protein was not further enhanced when both proteins were co-applied. In contrast, hemolysis was enhanced by vitronectin when the protein was added together with NS1, which confirms the recently published data of Conde et al. (18). As we were interested in whether lysis was impaired not only by purified complement proteins, but also in NHS as a source of complement, hemolysis assays were performed in the presence of ZIKV particles. Indeed, about four times more NHS was needed for complement-induced lysis of the cells when ZIKV was present. However, this experiment does not allow us to distinguish whether this effect is attributed to the E protein, NS1, or both. Therefore, purified recombinant viral proteins were used. Hemolysis assays showed that NS-1 and E proteins have additive effects, and thus, both proteins may contribute to the reduction in complement activity. Of note, more ZIKV E protein than NS1 was necessary to show comparable effects in the hemolysis assay, which might be due to a higher affinity of NS1 to proteins of the terminal pathway.

In summary, not only NS1, but also ZIKV E protein can reduce the formation of the MAC. As ZIKV activates the classical pathway by direct binding of C1q to the E protein and infection by this virus upregulates the expression of complement proteins (29), the virus has adopted several strategies to interfere with complement attack assembly. This corroborates the view that multiple evasion strategies are used by microorganisms, and in particular viruses, to limit damage by the complement system.

DATA AVAILABILITY STATEMENT

The original contributions presented in the study are included in the article/supplementary material. Further inquiries can be directed to the corresponding authors.

AUTHOR CONTRIBUTIONS

ZM, BS, and SB: experimental work. ZB, RW, and HS: study design, data interpretation, drafting the article, critical revision of the article, and final approval. All authors contributed to the article and approved the submitted version.

FUNDING

This study was supported by the FWF, Vienna Austria (HOROS doctoral Program, W-1253 DK HOROS).

REFERENCES

1. Merle NS, Church SE, Fremeaux-Bacchi V, Roumenina LT. Complement System Part I - Molecular Mechanisms of Activation and Regulation. *Front Immunol* (2015) 6:262. doi: 10.3389/fimmu.2015.00262
2. Merle NS, Noe R, Halbwachs-Mecarelli L, Fremeaux-Bacchi V, Roumenina LT. Complement System Part II: Role in Immunity. *Front Immunol* (2015) 6:257. doi: 10.3389/fimmu.2015.00257
3. Lambris JD, Ricklin D, Geisbrecht BV. Complement evasion by human pathogens. *Nat Rev Microbiol* (2008) 6(2):132–42. doi: 10.1038/nrmicro1824
4. Stoiber H, Pruenster M, Ammann CG, Dierich MP. Complement-opsonized HIV: the free rider on its way to infection. *Mol Immunol* (2005) 42(2):153–60. doi: 10.1016/j.molimm.2004.06.024
5. Dittmer U, Sutter K, Kassiotis G, Zelinskyy G, Bánki Z, Stoiber H, et al. Friend retrovirus studies reveal complex interactions between intrinsic, innate and adaptive immunity. *FEMS Microbiol Rev* (2019) 43(5):435–56. doi: 10.1093/femsre/fuz012
6. Rosengard AM, Liu Y, Nie Z, Jimenez R. Variola virus immune evasion design: Expression of a highly efficient inhibitor of human complement. *Proc Natl Acad Sci* (2002) 99(13):8808–13. doi: 10.1073/pnas.112220499

7. Sfyroera G, Katragadda M, Morikis D, Isaacs SN, Lambris JD. Electrostatic Modeling Predicts the Activities of Orthopoxvirus Complement Control Proteins. *J Immunol* (2005) 174(4):2143–51. doi: 10.4049/jimmunol.174.4.2143
8. Mullick J, Bernet J, Singh AK, Lambris JD, Sahu A. Kaposi's Sarcoma-Associated Herpesvirus (Human Herpesvirus 8) Open Reading Frame 4 Protein (Kaposica) Is a Functional Homolog of Complement Control Proteins. *J Virol* (2003) 77(6):3878–81. doi: 10.1128/JVI.77.6.3878-3881.2003
9. Conde JN, Silva EM, Barbosa AS, Mohana-Borges R. The Complement System in Flavivirus Infections. *Front Microbiol* (2017) 8(213). doi: 10.3389/fmicb.2017.00213
10. Avirutnan P, Mehlhop E, Diamond MS. Complement and its role in protection and pathogenesis of flavivirus infections. *Vaccine* (2008) 26 (Suppl 8):I100–7. doi: 10.1016/j.vaccine.2008.11.061
11. Ejaz A, Steinmann E, Bánki Z, Anggakusuma, Khalid S, Lengauer S, et al. Specific acquisition of functional CD59 but not CD46 or CD55 by hepatitis C virus. *PloS One* (2012) 7(9):e45770. doi: 10.1371/journal.pone.0045770
12. Lindenbach BD, Rice CM. Molecular biology of flaviviruses. *Adv Virus Res* (2003) 59:23–61. doi: 10.1016/S0065-3527(03)59002-9
13. Mukhopadhyay S, Kuhn RJ, Rossmann MG. A structural perspective of the flavivirus life cycle. *Nat Rev Microbiol* (2005) 3(1):13–22. doi: 10.1038/nrmicro1067
14. Fontes-Garfias CR, Shan C, Luo H, Muruato AE, Medeiros DBA, Mays E, et al. Functional Analysis of Glycosylation of Zika Virus Envelope Protein. *Cell Rep* (2017) 21(5):1180–90. doi: 10.1016/j.celrep.2017.10.016
15. Agrelli A, de Moura RR, Crovella S, Brandao LAC. ZIKA virus entry mechanisms in human cells. *Infect Genet Evol J Mol Epidemiol Evolution Genet Infect Dis* (2019) 69:22–9. doi: 10.1016/j.meegid.2019.01.018
16. Milis L, Morris CA, Sheehan MC, Charlesworth JA, Pussell BA. Vitronectin-mediated inhibition of complement: evidence for different binding sites for C5b-7 and C9. *Clin Exp Immunol* (1993) 92(1):114–9. doi: 10.1111/j.1365-2249.1993.tb05956.x
17. Prasada RT, Lakshmi PT, Parvathy R, Murugavel S, Karuna D, Paritosh J. Identification of second arginine-glycine-aspartic acid motif of ovine vitronectin as the complement C9 binding site and its implication in bacterial infection. *Microbiol Immunol* (2017) 61(2):75–84. doi: 10.1111/1348-0421.12468
18. Conde JN, da Silva EM, Allonso D, Coelho DR, Andrade IDS, de Medeiros LN, et al. Inhibition of the Membrane Attack Complex by Dengue Virus NS1 through Interaction with Vitronectin and Terminal Complement Proteins. *J Virol* (2016) 90 (21):9570–81. doi: 10.1128/JVI.00912-16
19. Amet T, Ghabril M, Chalasani N, Byrd D, Hu N, Grantham A, et al. CD59 incorporation protects hepatitis C virus against complement-mediated destruction. *Hepatol (Baltimore Md)* (2012) 55(2):354–63. doi: 10.1002/hep.24686
20. Orren A, O'Hara AM, Morgan BP, Moran AP, Würzner R. An abnormal but functionally active complement component C9 protein found in an Irish family with subtotal C9 deficiency. *Immunology* (2003) 108(3):384–90. doi: 10.1046/j.1365-2567.2003.01587.x
21. Schiela B, Bernklau S, Malekshahi Z, Deutschmann D, Koske I, Banki Z, et al. Active Human Complement Reduces the Zika Virus Load via Formation of the Membrane-Attack Complex. *Front Immunol* (2018) 9:2177. doi: 10.3389/fimmu.2018.02177
22. Zhang Z, Yang J, Wei J, Yang Y, Chen X, Zhao X, et al. Trichinella spiralis paramyosin binds to C8 and C9 and protects the tissue-dwelling nematode from being attacked by host complement. *PloS Neglected Trop Dis* (2011) 5(7): e1225. doi: 10.1371/journal.pntd.0001225
23. Sheehan M, Morris CA, Pussell BA, Charlesworth JA. Complement inhibition by human vitronectin involves non-heparin binding domains. *Clin Exp Immunol* (1995) 101(1):136–41. doi: 10.1111/j.1365-2249.1995.tb02289.x
24. Huang YP, Cheng J, Zhang SL, Wang L, Guo J, Liu Y, et al. Screening of hepatocyte proteins binding to F protein of hepatitis C virus by yeast two-hybrid system. *World J Gastroenterol* (2005) 11(36):5659–65. doi: 10.3748/wjg.v11.i36.5659
25. Chung KM, Liszewski MK, Nybakken G, Davis AE, Townsend RR, Fremont DH, et al. West Nile virus nonstructural protein NS1 inhibits complement activation by binding the regulatory protein factor H. *Proc Natl Acad Sci* (2006) 103(50):19111–6. doi: 10.1073/pnas.0605668103
26. Avirutnan P, Fuchs A, Hauhart RE, Somnuke P, Youn S, Diamond MS, et al. Antagonism of the complement component C4 by flavivirus nonstructural protein NS1. *J Exp Med* (2010) 207(4):793–806. doi: 10.1084/jem.20092545
27. Avirutnan P, Hauhart RE, Somnuke P, Blom AM, Diamond MS, Atkinson JP. Binding of Flavivirus Nonstructural Protein NS1 to C4b Binding Protein Modulates Complement Activation. *J Immunol* (2011) 187(1):424–33. doi: 10.4049/jimmunol.1100750
28. Kurosu T, Chaichana P, Yamate M, Anantapreecha S, Ikuta K. Secreted complement regulatory protein clusterin interacts with dengue virus nonstructural protein 1. *Biochem Biophys Res Commun* (2007) 362(4):1051–6. doi: 10.1016/j.bbrc.2007.08.137
29. Figueiredo CP, Barros-Aragão FGQ, Neris RLS, Frost PS, Soares C, Souza INO, et al. Zika virus replicates in adult human brain tissue and impairs synapses and memory in mice. *Nat Commun* (2019) 10(1):3890. doi: 10.1038/s41467-019-11866-7

Conflict of Interest: The authors declare that the research was conducted in the absence of any commercial or financial relationships that could be construed as a potential conflict of interest.

frontiers in Immunology

REVIEW
published: 03 November 2020
doi: 10.3389/fimmu.2020.572114

Role of Complement Receptors (CRs) on DCs in Anti-HIV-1 Immunity

Wilfried Posch[1†], *Marta Bermejo-Jambrina*[1,2†], *Cornelia Lass-Flörl*[1] *and Doris Wilflingseder*[1*]

[1] Institute of Hygiene and Medical Microbiology, Medical University of Innsbruck, Innsbruck, Austria, [2] Department of Experimental Immunology, Amsterdam Infection and Immunity Institute, Academic Medical Center, University of Amsterdam, Amsterdam, Netherlands

OPEN ACCESS

Edited by:
Heribert Stoiber,
Innsbruck Medical University, Austria

Reviewed by:
Yean Kong Yong,
Xiamen University, Malaysia
Sylvain Cardinaud,
Institut National de la Santé et de la Recherche Médicale (INSERM), France

***Correspondence:**
Doris Wilflingseder
doris.wilflingseder@i-med.ac.at

[†]These authors have contributed equally to this work

Specialty section:
This article was submitted to Microbial Immunology, a section of the journal Frontiers in Immunology

Received: 12 June 2020
Accepted: 06 October 2020
Published: 03 November 2020

Citation:
Posch W, Bermejo-Jambrina M, Lass-Flörl C and Wilflingseder D (2020) Role of Complement Receptors (CRs) on DCs in Anti-HIV-1 Immunity. Front. Immunol. 11:572114. doi: 10.3389/fimmu.2020.572114

Upon entry of human immunodeficiency virus 1 (HIV-1) into the host, innate immune mechanisms are acting as a first line of defense, that considerably also modify adaptive immunity by the provision of specific signals. Innate and adaptive immune responses are intimately linked and dendritic cells (DCs) together with complement (C) play an important role in regulation of adaptive immunity. Initially, the role of complement was considered to primarily support – or COMPLEMENT - cytolytic actions of antibodies or antibody-complexed antigens (immune complexes, ICs) or directly kill the pathogens by complement-mediated lysis. Recently, the role of complement was revised and found to significantly augmenting and modulating adaptive immunity, in particular against viruses. Complement and DCs are therefore predestined to open novel avenues for antiviral research and potential therapeutic interventions. Recent studies on interactions of complement-opsonized HIV-1 with DCs demonstrated a high potential of such primed DCs to initiate efficient antiviral and cytotoxic anti-HIV-1 immunity and complement-coated viral particles shift DCs functions *via* CR3 and CR4 in an antithetic manner. This review will focus on our current knowledge of CR3 and CR4 actions on DCs during HIV-1 binding and the outcome of infection influenced by entry and signaling pathways.

Keywords: complement receptors, dendritic cells, HIV-1, antiviral immunity, immune activation, SAMHD1, antigen presentation, type I IFN

INTRODUCTION

Innate immunity is the first line of defense against pathogens. It acts in a non-specific manner but is rapid and independent of antigen. The innate immune system is formed by cellular and humoral components. Complement comprises a part of the humoral innate immune system. The complement system recognizes, opsonizes and subsequently lyses the pathogens and additionally

also induces pro-inflammatory cytokines and maintains homeostasis. Immediately upon Human Immunodeficiency Virus 1 (HIV-1) entry in the body, the virus spontaneously activates the complement system even in the absence of specific antibodies. This is possible due to the complement component C1q binding site in the envelope glycoprotein gp41 of HIV-1 (1). Thus, HIV-1 is already coated with complement fragments at the initial stages of infection and during transfer. Following seroconversion, in addition to complement fragments, specific antibodies coat the viral surface. Dependent on the IgG subtype, formation of immune-complexes strongly enhances the activation of the complement system *via* the classical pathway and virus-bound antibodies dramatically increase the deposition of complement fragments (C3b) on virions (2–4). Therefore, opsonized infectious viral particles accumulate in HIV-1-positive individuals during the acute and chronic phases of infection.

Most HIV-1 particles are not killed by complement-mediated lysis but persist covered with C3 fragments in the host. This is due to the uptake of regulators of the complement activation (RCA) by the viral particles during the budding process. RCA tightly control the complement system to prevent spontaneous destruction of host cells and unfortunately they also protect HIV-1 from being lysed (5). Interestingly, opsonized HIV-1 accumulates in all so far tested compartments of HIV-1-positive individuals, for instance mucosa or seminal fluid (6). As such, it is able to interact with complement receptor (CR)-expressing cells, like dendritic cells (DCs) or macrophages. Triggering these receptors leads to cell activation and contributes to inflammation.

On one hand, complement-opsonized HIV-1 (HIV-C) increases viral infectivity and transmission *in vitro* (7). On the other hand, it strengthens cellular immunity as well as type I IFN responses (8–10). This highlights the importance of complement-mediated processes during HIV-1 pathogenesis.

One of the most important cellular components of the innate immune system are dendritic cells (DCs). They play a major role in induction of immune responses against pathogens, allergies and cancer (11, 12). Interestingly, they differ in their ability to induce an innate immune response against non-opsonized HIV-1, complement-opsonized HIV-1 and HIV type 2 (HIV-2) (9, 13, 14). Both HIV-1 and HIV-2 are causing an immunodeficiency syndrome, but differ in their genome, tropism, infectivity and pathogenicity (15). One of the most important differences is the reduced activation and infection of DCs by HIV-1, that was described to inefficiently infecting and activating DCs whereas HIV-2, and surprisingly also HIV-C, are able to efficiently infect and activate DCs (9, 10, 13, 16).

Differences between HIV-1 and HIV-2 are mainly caused by viral protein x (Vpx), the HIV-2 accessory protein that leads to SAMHD1 degradation (17–19), probably one of the most important HIV-1 restriction factors in myeloid cells. SAMHD1 is a deoxynucleoside-triphosphate (dNTP) triphosphohydrolase that restricts the replication of HIV-1 in non-cycling monocytes, monocyte-derived macrophages (MDMs), DCs, and resting T-cells (17, 19, 20). It depletes the intracellular pool of dNTPs, resulting in a blockade of virus replication at the step of reverse transcription (19, 20). Since HIV-1 lacks Vpx, it has no means to counteract the restriction. The antiviral activity of SAMHD1 is regulated by phosphorylation of amino acid T592, which results in the loss of antiviral restriction activity (21, 22). In cycling T cells, SAMHD1 is constitutively phosphorylated by cyclin dependent kinase 1 (CDK1) and does not restrict HIV-1 replication (23). In myeloid and resting lymphoid cells, where SAMHD1 exists as a mixture of phosphorylated and dephosphorylated forms, the phosphorylation is mediated by CDK2 (24). Restriction factor expression and their regulation are among the most important factors dictating HIV-1 infection of a specific cell. Specifically, after different stimuli, phosphorylation of SAMHD1 modifies its ability, leading to the inhibition of HIV-1 infection in macrophages (25, 26). Importantly, complement-opsonized HIV-1 negatively regulates SAMHD1 in DCs by inducing its phosphorylation, which results in significantly higher DC infection with HIV-C compared to non-opsonized HIV-1, even though there is no Vpx (9) (**Figure 1**). These facts illustrate that HIV-C behaves more similar in DCs to HIV-2 since the infection leads to a higher DC maturation and type I IFN expression (9). In contrast, non-opsonized HIV-1 only causes low-level productive infection of DCs due to SAMHD1 restriction and this low-level infection is associated with low-level antiviral actions and CTL induction, thus viral evasion (**Figure 2**).

These different features with respect to HIV-1 and complement-opsonized HIV-1 and previously described interactions with either complement receptor 3 (CR3, CD11b/CD18) or complement receptor 4 (CR4, CD11c/CD18) expressed on DCs is summarized below.

DC FUNCTIONS IN HIV-1 INFECTION

DCs are localized in the skin and mucosa, including oral and vaginal mucosal surfaces, and in lymphoid tissues. Because of their location through all peripheral tissues and their high abundance of pattern recognition receptors (PRRs), DCs are among the first cells to encounter a plethora of pathogens and they are also called sentinels of the immune system (12, 27). DCs capture and internalize invading pathogens and process antigens on major histocompatibility complex (MHC) class I and II to present them

Abbreviations: Ag, Antigen; AP, Alternative complement pathway; APCs, Antigen-presenting cells; C, Complement; CCR, CC- Chemokine receptor; CDK1, Cyclin dependent kinase 1; CDK2, Cyclin dependent kinase 2; cGAS, cyclic GMP-AMP Synthase; CLR(s), C-type lectin Receptor(s); CP, Classical complement pathway; CR(s), Complement receptor(s); CTLs, Cytotoxic T cells; CYPA, Cyclophilin A; CXCR, CXC chemokine receptor; DC(s), Dendritic cell(s); DC-SIGN, Dendritic cell-specific intercellular adhesion molecule-3-grabbing non-integrin; dNTPs, Deoxynucleotide triphosphate; HIV-1, Human immunodeficiency virus type 1; HIV-2, Human immunodeficiency virus type 2; HIV-C, Complement opsonized HIV; ICs, Immune Complexes; iDCs, Immature dendritic cells; IRF, Interferon regulatory factors; LCs, Langerhans cells; LP, Lectin complement pathway; MAC, Membrane attack complex; MAPKs, Mitogen-activated protein kinase; MBL, Mannose-binding lectin; MHC II, Major histocompatibility complex class II; MIDAS, Metal-ion dependent adhesion site; NF-κB, nuclear factor kappa-light-chain-enhancer of activated B cells; PAMPs, Pathogen associated molecular patterns; PLK1, Polo-like kinase 1; PRRs, Pattern Recognition Receptors; RCAs, Regulators of complement activation; SAMHD1, SAM domain- and HD domain- containing protein 1; SIV, Simian immunodeficiency virus; STAT1, Signal transducer and activator of transcription 1; STING, Stimulator of interferon genes; Vpx, Viral protein X.

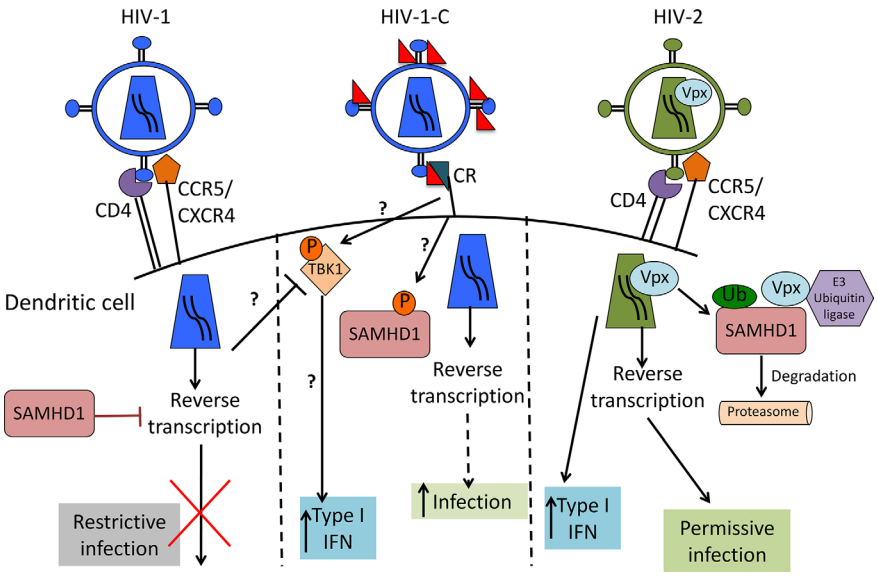

FIGURE 1 | Scheme of HIV-1, complement-opsonized HIV-1 (HIV-C) and HIV-2 restriction by SAMHD1 in DCs. HIV-1 (left) binds to CD4 and CCR5 or CXCR4 to enter the cell. SAMHD1 action inhibits HIV-1 reverse transcription and blocks infection. HIV-C (middle) binds to complement receptors (CRs), which trigger a yet unknown pathway that leads to SAMHD1 inactivation by phosphorylation. This pathway makes the virus visible for DCs by permitting reverse transcription and significantly higher DC infection as well as increased type 1 IFN induction than with HIV-1. HIV-2 (right) contains Vpx that mediates SAMHD1 degradation, thereby allowing reverse transcription to occur, productive infection and higher type 1 IFN as also seen with HIV-C.

to $CD8^+$ and $CD4^+$ T cells, respectively (28–30). DCs are key regulators of the immune system since they contribute to a broad spectrum of immune responses against infectious microbes, allergies and cancer (12, 28, 29, 31). A major function of DCs is the induction of an efficient adaptive immune response in lymph nodes (LNs); yet, DCs additionally interact with innate immune cells such as NK cells and NKT cells (32, 33). As immature DCs (iDCs), they reside in peripheral tissues, which they survey for invading pathogens. DCs express numerous PRRs that interact with PAMPs including the C-type lectin receptors (CLRs) [rev. in (34)] and the complement receptors (CRs). These PRRs not only interact with pathogens but also trigger signaling cascades (34). Upon pathogen encounter, DCs undergo maturation expressing molecules on their surface, which are important for antigen-presentation and T cell stimulation, such as CD40, CD80, CD83, CD86, and HLA. Further, they start migrating to the draining LNs *via* a chemokine gradient in a CCR7-dependent fashion (35, 36). In secondary lymphoid organs, they present the antigen to naïve $CD8^+$ and $CD4^+$ T cells, being the only antigen-presenting cells capable of activating naïve T cells (12, 29). Following the recognition of the peptide MHC, antigen-specific $CD8^+$ and $CD4^+$ T cells clonally expand and develop effector functions, such as cytokine production and cytotoxic activity. Effector T cells are recruited to the inflamed peripheral tissues and participate in the elimination of pathogens and infected cells. This very particular life cycle emphasizes to call DCs 'sentinels of the immune system' and this is why they are considered the bridge between the innate and adaptive immune system. When DCs get infected, they are able to sense HIV-1 and induce an innate immune response. One of the triggers for the innate immune activation is the recognition of nucleic acids by diverse sensors in the cytoplasm. HIV-1 DNA has been shown to be recognized by cGAS, that leads to type I IFN expression through STING activation (37). However, type I IFN expression in DCs upon HIV-1 infection is controversially discussed in the field, since many groups only find background levels of this cytokine (38). Interestingly, HIV-C or HIV-2 infection triggers a significantly higher DC maturation than non-opsonized HIV-1 (9, 13). However, the viral pathogen-associated molecular pattern (PAMP) for the higher visibility of complement-opsonized HIV-1 or HIV-2 is not known in DCs yet (9, 13, 17). The natural balance between DC infection and innate sensing in HIV-2 might contribute to the reduced pathogenicity of this virus, whereas the ability of HIV-1 to prevent sensing of its cDNA might contribute to its immune escape. Contrary to what happens during infection of DCs with non-opsonized HIV-1, complement-opsonized HIV-1 or HIV-2 strongly activate DCs, which results in activation of specific $CD4^+$ and $CD8^+$ T cells, starting an adaptive immune response.

THE ROLE OF DCs DURING HIV-1 INFECTION

By clustering and activating T cells, DCs may activate antiviral immunity as well as facilitate the spread of the virus. *In vitro* experiments indicate that DCs efficiently capture and transmit HIV-1 to T cells and initiate a vigorous infection (31, 39–41). This implies that HIV-1 exploits DCs at mucosal sites to be

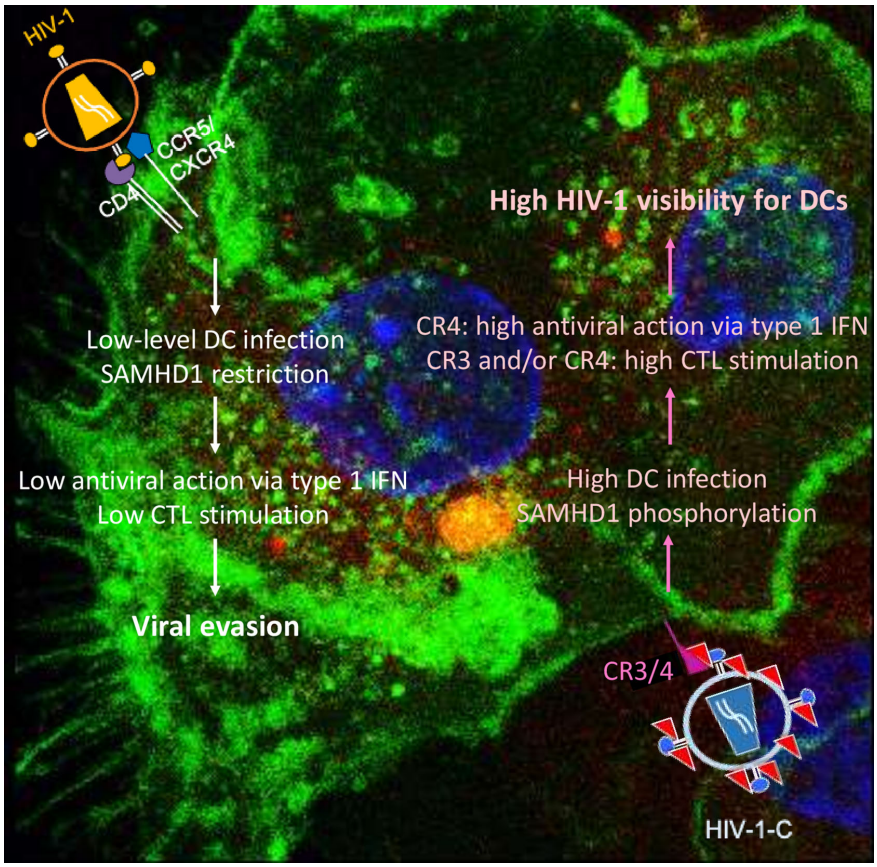

FIGURE 2 | Summary of DC functions modulated by non-opsonized HIV-1 (left) and complement-opsonized HIV-1 (HIV-C, right). Non-opsonized HIV-1 only causes low-level productive DC infection due to SAMHD1 restriction, which is associated with weak antiviral induction (left). In contrast, HIV-C overcomes SAMHD1 restriction in DCs by T592 phosphorylation—this is connected to induction of efficient type 1 IFN and CTL responses *via* DCs.

transported to $CD4^+$ T cells in the LNs *in vivo*. Virus is very efficiently transmitted from DCs to T cells either without or *via de novo* infection (41). In particular C-type lectins, such as DC-specific ICAM-3-grabbing non-integrin (DC-SIGN), expressed on DCs is implicated in the transfer of HIV-1 to T cells in the LNs (31, 42–45) [rev. in (34)]. In case of opsonized HIV, the DC-SIGN-dependent interactions play a minor role for the attachment of HIV-1 to DCs as well as the DC-mediated HIV-infection (46). However, complement-opsonization of HIV-1 significantly enhanced the productive infection of DCs compared to non-opsonized HIV-1 and additionally acted as an endogenous adjuvant for the DC-mediated induction of virus-specific cytotoxic T cells (CTLs) (8, 9). These results emphasize a role of different DC subtypes in the induction of an adaptive T cell response to complement-coated HIV-1. Indeed, a previous study revealed that complement-opsonization of HIV-1 prior to DC loading significantly enhanced the $CD8^+$ T cell-stimulatory capacity and contributed to the induction of $CD4^+$ effector function namely secretion of interleukin 17 (IL-17) (10). Overall, there is compelling evidence for the crucial role of the complement system and different subtypes of DCs in the polarized induction T cell immune responses in fighting HIV-1 and known interactions are summarized below. Nevertheless, there are still many gaps of knowledge with respect to DC processing of complement-opsonized HIV-1, which could improve current HIV-1 vaccination strategies.

COMPLEMENT ACTIVATION UPON HIV-1 INFECTION

The immune system comprises complex cellular and humoral responses, which form an interactive network to recognize and eradicate invading pathogens. Among the first humoral components activated during the innate immune response is the systemic complement (C) system. It consists of various fluid-phase and cell membrane-bound proteins and acts as a tightly regulated cascade of enzymatic reactions to defend the host against pathogens. Thus, the complement system represents a first line of host defense by opsonizing and subsequently lysing pathogens, inducing pro-inflammatory cytokines and

maintaining homeostasis. It can be activated *via* three different biochemical pathways: the classical (CP), the alternative (AP) and the lectin pathway (LP) (**Figure 3**). Activation *via* the CP occurs when the first component, C1, binds the Fc region of either natural or antigen-specific immunoglobulin G (IgG) antibody immune-complexed with its antigen (Ag). The classical pathway can also be triggered in an antibody-independent manner when C1q directly binds to pathogens or infected cells, as it is the case with HIV-1 that has a C1q-binding side in its envelope glycoprotein (47–49). The AP is activated during normal physiological conditions at very low levels and monitors for certain microbial structures. Besides direct activation the alternative pathway can also be activated spontaneously by a process known as tick-over and thereby boost the C activation initiated by the classical or the lectin pathway. The LP is activated upon recognition of terminal mannose residues on microbial glycoproteins and glycolipids by mannose-binding lectin (MBL). All three pathways converge in the cleavage of the main C component 3 (C3) into the anaphylatoxin C component 3a (C3a) and the opsonin C component 3b (C3b). This cleavage initiates a cascade of further activation events. C3b is covalently deposited on microbial surfaces and together with the C3 convertase forms the C5 convertase, which then cleaves C component 5 (C5) into the anaphylatoxin C component 5a (C5a) and the C component 5b (C5b). C5b triggers the formation of the membrane attack complex (MAC), that consists of C5b, C component 6 (C6), C component 7 (C7), C component 8 (C8) and polymeric C component 9 (C9) molecules. The formation of the MAC disrupts the microbial membrane resulting in lysis of the pathogens or infected cells (**Figure 3**).

The C system is tightly controlled by RCAs to prevent spontaneous activation or destruction of bystander cells. RCAs are present in fluid-phase and also membrane-bound to protect host cells. The anaphylatoxins C3a and C5a are small fragments, which result from the cleavage of C3 and C5 respectively—C3a and C5a promote migration of immune cells to sites of infection and thus have a critical role in the activation of immune cells. Especially complement receptors (CRs), such CR3 and CR4 expressed on dendritic cells and macrophages, are responsible for detection of C3-opsonized microbes followed by activation of the immune cells and uptake of the pathogen. Furthermore, myeloid cells express C3a and C5a receptors (C3aR and C5aR, respectively) and triggering these receptors results in cell activation and contribution to inflammation by the complement system. Since C3aR and C5aR are also expressed by non-myeloid cells like B and T lymphocytes the complement system also influences the adaptive immunity. Crosstalk of C3aR and C5aR signaling with other intra- or extracellular receptor signaling is very likely, because of mutual interaction partners such as nuclear factor kappa-light-chain-enhancer of activated B cells (NF-kB) and Mitogen-activated protein kinases (MAPKs).

C3 opsonization of pathogens is important in the induction and maintenance of B cells. Additionally, opsonized immune complexes bind to CR2 on follicular dendritic cells in germinal centers to present antigens, which results in induction of effector and memory B cells or also trapping of intact virus particles within germinal centers, i.e. HIV-1 (50).

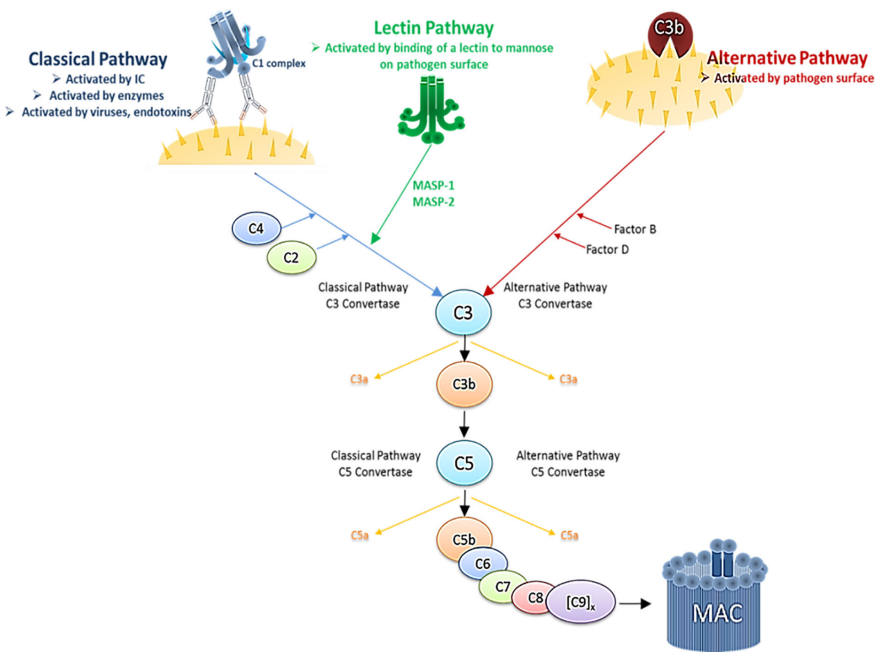

FIGURE 3 | Simplified schematic illustration of the complement cascade depicting the three activation pathways. Immune complex (IC), Mannan-binding lectin serine protease 1/2 (MASP1/2).

Besides the liver-derived systemic complement, immune cell-derived complement or cellular complement has been recently described to play a significant role in shaping immune responses (51–55). This local complement can be produced by almost all immune cells at sites of infection and is secreted by or stored inside the immune cells. Intracellular C, especially C3, is cleaved permanently by proteases such as cathepsins and binds to intracellular C3aRs on lysosomes. This engulfment regulates cell growth, cell proliferation and cell survival *via* the serine/threonine protein kinase mammalian target of rapamycin (mTOR) (56). Experiments co-culturing antigen-presenting cells (APCs) and T cells furthermore demonstrated the importance of cellular complement in terms of T helper cell development and proliferation. Interestingly, absence of cellular complement signals in these studies could not be compensated by systemic complement (52). Involvement of intra- and extracellular C has been investigated in T lymphocytes in more detail but only few studies investigating local production of C in DCs and macrophages were conducted. These studies reported that similar to T lymphocytes, DCs are also activated *via* anaphylatoxin receptors in an autocrine manner but it remains unknown which signaling pathway is affected (51, 52, 57). Therefore, also emerges as key player in regulation of cell metabolism, cell homeostasis, T cell polarization and activation (also in terms of viral infections as discussed below) and new, exciting avenues are opened if taking into account this ´old-fashioned´ component of innate immunity.

COMPLEMENT, HIV-1 AND DCs

As illustrated above, both DCs and complement comprise a bridge between innate and adaptive immunity—but which outcome does a combined action of complement and DCs exert on HIV-1 infection and antiviral activity?

DCs abundantly express CR3 and CR4—both are members of the beta-2 (CD18) integrins and in particular CR4, comprised of CD11c and CD18, is a specific marker for this cell type (58). CR3 and CR4 are involved in binding multiple ligands, participating in phagocytosis, immune synapse formation, leukocyte trafficking, and co-stimulation. Although both receptors are thought to react in a similar way because of their homology, differences with respect to their structural cellular immunology were recently reviewed by Vorup-Jensen and Jensen (2018) (59). From their structure in the metal-ion dependent adhesion site (MIDAS), CR3 mainly binds positively charged species, while in contrast CR4 strongly binds negative-charged species—therefore, also different functions with respect to CR3 and CR4 are obvious, yet neglected. Both, CR3 and CR4 with their multitude of ligands, were considered as scavenger receptors that facilitate removal of decayed material (60, 61). As such, inflammation by several types of leukocytes is down-modulated by outside-in signaling (62)—this attitude fits well in case of CR3, known to clear opsonized apoptotic cells, immune aggregates or other species present in plasma without triggering a pro-inflammatory response (63). Defects in CR3 or complement component deficiency were shown to be associated with autoimmune diseases such as systemic lupus erythematosus due to failures in cellular clearance (63). Therefore, CR4 was also put into the convenient drawer of being a scavenger receptor—but as suggested by Vorup-Jensen et al., due to its binding to polyanionic species, CR4 may serve quite different functions and act as an immune receptor to alert the immune system to microbial hazards (59). We also highlighted this versatility of CR3 and CR4 on DCs with respect to anti-HIV-1 immunity very recently (64). Among the first cells encountering HIV-1 are CR3/CR4-expressing DC subsets, such as mucosal Langerhans Cells (LCs) or dermal DCs and CR3-expressing macrophages and monocytes. Since HIV-1 spontaneously activates the classical complement pathway even in seminal fluid (2) and is very well protected against complement-mediated lysis due to acquiring RCAs during the budding process (65), interactions with these CR-expressing cells will be much more likely compared to the well described ligation of C-type lectin receptors (CLRs) at mucosal surfaces. While non-opsonized HIV-1 poorly replicates in DCs, covalently linked iC3b fragments on the HIV-1 surface were illustrated to significantly enhance *de novo (cis)* infection of CR3/CR4-expressing DC subsets (LCs, dermal DCs, blood BDCA1$^+$ DCs) and CR3-expressing monocytes and macrophages (7–10, 46, 66–71). CR3 is directly interacting with the HIV-1 envelope gp41 due to four homologous C3 regions (49, 72). Several studies have shown that semen affects the efficiency of HIV-1 transmission (2, 67, 73), and we found enhanced LC infection *in vitro* and *ex vivo* due to pre-treatment of HIV-1 with semen (unpublished). While semen was illustrated to contain components like mucin 6, that prevent transmission of HIV-1 to CD4$^+$ T cells by blocking DC-SIGN-mediated transfer of HIV-1 from DCs to T cells (74, 75), mucosal LCs were found to efficiently attract LCs to the site of the infection (76, 77) and capture semen-opsonized HIV-1 *via* CR-mediated interactions (unpublished). HIV-1 infection of monocyte-derived DCs as well as dermal and BDCA1$^+$ DCs *in vitro* and *ex vivo* was illustrated to work in a C-type lectin independent manner, when opsonized with complement, while interactions with non-opsonized HIV-1 were significantly inhibited upon blocking DC-SIGN interactions (46). The poor replication of non-opsonized HIV-1 in these DCs is mainly mediated *via* the restriction factor SAMHD1 and the non-permissiveness of DCs is suggested to go along with viral evasion (**Figure 2**). SAMHD1 restricts HIV-1 infection in DCs, myeloid cells and resting CD4$^+$ T cells by blocking reverse transcription due to limiting the dNTP pool - thus HIV-1 infection is prevented and efficient antiviral DC activation avoided (17, 20–22, 78). Other studies revealed infection of DCs with non-opsonized HIV-1 but lack of activation and type I IFN responses (79, 80). Gringhuis et al. (81) showed that low type I IFN responses in HIV-1-exposed DCs was due to DC-SIGN-dependent activation of Raf-1 and PLK1, that inhibited downstream IRF3 activation (81). When SAMHD1 restriction in DCs was revoked by Vpx of HIV-2 or SIVsm, DCs were infected to higher levels and illustrated higher maturation, co-stimulatory capacity as well as a potent type I IFN induction (13). Potent antigen presentation and initiation of antiviral immunity *via* humoral factors and T cells probably contribute to the slower pathogenesis of HIV-2 or control of SIV in natural hosts. These features could make HIV/SIV visible to the immune system,

and all—DC maturation, upregulation of co-stimulatory molecules on DCs and stimulation of antiviral immunity - were also mediated by complement-opsonized HIV-1 and interactions with CRs 3 and/or 4 on DCs (8–10, 64, 68). HIV-C was demonstrated to overcome restriction in monocyte-derived and blood BDCA1$^+$ DCs by SAMHD1 phosphorylation at the T592 residue and not due to degrading SAMHD1 similar to Vpx (9, 21). The complement-mediated SAMHD1 phosphorylation was associated with significantly enhanced DC infection, DC activation as well as aberrant type I interferon expression, pro-inflammatory responses and stronger induction of cytotoxic T cell induction by complement-HIV-exposed DCs (8–10, 68). The two major regulators of type I IFN responses comprise IRF3 and IRF7 (82). When DCs were exposed to HIV-C, Posch et al. (9) highlighted that SAMHD1 phosphorylation in DCs was associated with higher STAT1/NFκB activation and IRF3 translocation to the nucleus and the cells exerted a higher T cell stimulatory capacity and higher antiviral potential. Manel et al., also demonstrated that, if restriction to infection was relieved by addition of Vpx, newly synthesized HIV-1 capsids mediated an efficient DC activation and antiviral immune responses *via* IRF3 and CYPA (13). Also Su et al. showed that co-culture with CD4$^+$ T cells decreased SAMHD1 levels in DCs, thus enhancing HIV-1 replication accompanied by DC maturation and increased type I IFN secretion from the cells (83). In disagreement to these data, another study demonstrated that despite higher DC infection by complement-opsonized HIV-1 a decreased antiviral immune response was observed from these DCs (84). Despite an enhanced IRF3 activation was observed also in those DCs after stimulation with complement-opsonized HIV-1, a dampening of the immune response with decreased antiviral and inflammatory capacity was mediated in these studies (69, 84). The observed discrepancies might rely on differential expression of CR3 and CR4, either linked to a scavenger (CR3) or immune (CR4) function as suggested by Vorup-Jensen and Jensen (59) and lately shown in terms of HIV-C/DC interactions by Bermejo-Jambrina et al. (64). Very recently we identified CR4 as the receptor responsible for contributing to a DC-driven higher immune response to complement-opsonized HIV-1. In contrast, inflammatory cytokine production was restricted and dampened *via* CR3 (64). Therefore, either a dampening of anti-HIV-1 immune responses may be observed in DCs mainly expressing CR3, while DCs expressing both, CR3 and CR4, at high levels may initiate an inflammatory reaction. This new knowledge might be exploited to target CR3 and CR4 in an antithetic manner to switch off (CR3) or on (CR4) inflammatory and type I IFN responses.

COMPLEMENT, HIV-1 AND CHRONIC IMMUNE ACTIVATION

Little is known with respect to the role of complement in chronic immune activation. Effects during chronic disease mediated by complement are hard to investigate due to the presence of HIV-1-specific antibodies also binding to the viral surface and interacting with Fcγ receptors on DCs (68). These bound and non-neutralizing HIV-1 antibodies were demonstrated to attenuate the capacity of DCs to stimulate HIV-specific CTLs (68), but their impact on chronic immune activation still needs to be determined. We recently described a significantly enhanced type I IFN as well as pro-inflammatory immune response, when monocyte-derived or blood DCs were exposed to HIV-C (9, 10, 64). Therefore, complement coating of HIV-1 makes the virus visible for DCs, resulting in DC maturation, CTL induction and high immune activation, which is probably of advantage during the acute phase of HIV-1 pathogenesis. As shown by Gringhuis et al. (81) non-opsonized HIV-1 normally escapes immune surveillance by DCs due to blocking the DDX3-MAVS axis *via* CLR signaling. In contrast, when inhibiting DDX3-MAVS blockade an efficient type I interferon response and DC maturation were induced in HIV-1-infected monocyte-derived DCs and in infected individuals (81). Also in HIV-C-exposed DCs these features of improved early type I IFN responses, maturation and CTL-stimulation were monitored (8–10, 64), and in a yet unpublished work, we found that complement opsonization of HIV-1 mediates activation of DCs *via* MAVS. As found in rhesus macaques, blocking type I IFN responses early during SIV infection decreased expression of antiviral genes, increased SIV reservoir size and CD4$^+$ T cell depletion (85). However, permanent exposure to type I IFN responses might lead to desensitization and increase in disease progression (85). Therefore, complement is a two-edged sword - during acute HIV-1-infection, where DCs are a prominent target for HIV-1, it improves DC activation, type I IFN induction and thus limits viral replication. But type I IFNs might contribute to disease progression, if continuously activating more T cells and thus generating more targets during HIV-1 infection and thus driving progressive CD4$^+$ T cell loss (86, 87). As discussed in the paragraph above targeting either CR3 or CR4 could provide a novel strategy to specifically regulate type I IFN and pro-inflammatory immune responses.

CONCLUSIONS

Covalent complement deposition on HIV-1 particles, observed during all steps of viral pathogenesis and its subsequent interactions with DCs, comprise mixed blessing. In the acute phase of HIV-1 infection, commonly associated with a significant reduction in viral load by efficient early type I IFN induction and effective priming of HIV-specific cytotoxic T lymphocytes, complement coating of HIV-1 particles seems to be beneficial due to making the virus more visible for DCs, the most potent antigen-presenting cells of our immune system. This higher visibility may be associated with more effective DC maturation and activation *via* CR4 resulting in extensive stimulation of anti-HIV-1 immune mechanisms thereby guiding control of viral replication. A dampening of antiviral immunity at the beginning of infection *via* C-type lectins, in case of non-opsonized HIV-1, or CR3 in case of opsonized HIV-1, might subvert DC function at mucosal sites. Viral control by type I interferons may be minimized and proper activation of cytotoxic T cell responses impeded. During chronic phase, triggering the ′wrong′ signal on DCs may be associated with extensive antiviral type I interferon responses

and chronic inflammation thus driving HIV-1 pathogenesis. Overall, characterizing the versatile receptors CR3 and CR4 on DCs in the minutest detail might open new avenues of therapeutic interventions of DCs during HIV-1 infection.

AUTHOR CONTRIBUTIONS

Writing—original draft, MB-J, WP, DW. Writing—Review and editing, MB-J, WP, CL-F, DW. All authors contributed to the article and approved the submitted version.

FUNDING

We thank the Austrian National Bank (OeNB Jubiläumsfonds, number 17614 to WP) and the Austrian Science Fund FWF, project #: P33510-B (to DW).

ACKNOWLEDGMENTS

We thank Paula Jauregui-Onieva, PhD, for conceptualizing and providing **Figure 1** and discussion of this review.

REFERENCES

1. Thielens NM, Bally IM, Ebenbichler CF, Dierich MP, Arlaud GJ. Further characterization of the interaction between the C1q subcomponent of human C1 and the transmembrane envelope glycoprotein gp41 of HIV-1. *J Immunol* (1993) 151(11):6583–92. doi: 10.1016/0161-5890(93)90382-L
2. Bouhlal H, Chomont N, Haeffner-Cavaillon N, Kazatchkine MD, Belec L, Hocini H. Opsonization of HIV-1 by Semen Complement Enhances Infection of Human Epithelial Cells. *J Immunol* (2002) 169(6):3301–6. doi: 10.4049/jimmunol.169.6.3301
3. Schifferli JA. Complement and immune complexes. *Res Immunol* (1996) 147 (2):109–10. doi: 10.1016/0923-2494(96)87183-5
4. Stoiber H, Soederholm A, Wilflingseder D, Gusenbauer S, Hildgartner A, Dierich MP. Complement and antibodies: a dangerous liaison in HIV infection? *Vaccine* (2008) 26(Suppl 8):I79–85. doi: 10.1016/j.vaccine.2008.11.050
5. Saifuddin M, Parker CJ, Peeples ME, Gorny MK, Zolla-Pazner S, Ghassemi M, et al. Role of virion-associated glycosylphosphatidylinositol-linked proteins CD55 and CD59 in complement resistance of cell line-derived and primary isolates of HIV-1. *J Exp Med* (1995) 182(2):501–9. doi: 10.1084/jem.182.2.501
6. Saidi H, Jenabian MA, Belec L. Understanding factors that modulate HIV infection at the female genital tract mucosae for the rationale design of microbicides. *AIDS Res Hum Retroviruses* (2012) 28(11):1485–97. doi: 10.1089/AID.2012.0049
7. Wilflingseder D, Banki Z, Garcia E, Pruenster M, Pfister G, Muellauer B, et al. IgG opsonization of HIV impedes provirus formation in and infection of dendritic cells and subsequent long-term transfer to T cells. *J Immunol* (2007) 178(12):7840–8. doi: 10.4049/jimmunol.178.12.7840
8. Banki Z, Posch W, Ejaz A, Oberhauser V, Willey S, Gassner C, et al. Complement as an endogenous adjuvant for dendritic cell-mediated induction of retrovirus-specific CTLs. *PloS Pathog* (2010) 6(4):e1000891. doi: 10.1371/journal.ppat.1000891
9. Posch W, Steger M, Knackmuss U, Blatzer M, Baldauf HM, Doppler W, et al. Complement-Opsonized HIV-1 Overcomes Restriction in Dendritic Cells. *PloS Pathog* (2015) 11(6):e1005005. doi: 10.1371/journal.ppat.1005005
10. Wilflingseder D, Schroll A, Hackl H, Gallasch R, Frampton D, Lass-Florl C, et al. Immediate T-Helper 17 Polarization Upon Triggering CD11b/c on HIV-Exposed Dendritic Cells. *J Infect Dis* (2015) 212(1):44–56. doi: 10.1093/infdis/jiv014
11. Mildner A, Jung S. Development and function of dendritic cell subsets. *Immunity* (2014) 40(5):642–56. doi: 10.1016/j.immuni.2014.04.016
12. Steinman RM. Decisions about dendritic cells: past, present, and future. *Annu Rev Immunol* (2012) 30:1–22. doi: 10.1146/annurev-immunol-100311-102839
13. Manel N, Hogstad B, Wang Y, Levy DE, Unutmaz D, Littman DR. A cryptic sensor for HIV-1 activates antiviral innate immunity in dendritic cells. *Nature* (2010) 467(7312):214–7. doi: 10.1038/nature09337
14. Manel N, Littman DR. Hiding in plain sight: how HIV evades innate immune responses. *Cell* (2011) 147(2):271–4. doi: 10.1016/j.cell.2011.09.010
15. Nyamweya S, Hegedus A, Jaye A, Rowland-Jones S, Flanagan KL, Macallan DC. Comparing HIV-1 and HIV-2 infection: Lessons for viral immunopathogenesis. *Rev Med Virol* (2013) 23(4):221–40. doi: 10.1002/rmv.1739
16. Norton TD, Miller EA, Bhardwaj N, Landau NR. Vpx-containing dendritic cell vaccine induces CTLs and reactivates latent HIV-1 in vitro. *Gene Ther* (2015) 22(3):227–36. doi: 10.1038/gt.2014.117
17. Laguette N, Sobhian B, Casartelli N, Ringeard M, Chable-Bessia C, Segeral E, et al. SAMHD1 is the dendritic- and myeloid-cell-specific HIV-1 restriction factor counteracted by Vpx. *Nature* (2011) 474(7353):654–7. doi: 10.1038/nature10117
18. Jauregui P, Logue EC, Schultz ML, Fung S, Landau NR. Degradation of SAMHD1 by Vpx Is Independent of Uncoating. *J Virol* (2015) 89(10):5701–13. doi: 10.1128/JVI.03575-14
19. Hrecka K, Hao C, Gierszewska M, Swanson SK, Kesik-Brodacka M, Srivastava S, et al. Vpx relieves inhibition of HIV-1 infection of macrophages mediated by the SAMHD1 protein. *Nature* (2011) 474(7353):658–61. doi: 10.1038/nature10195
20. Lahouassa H, Daddacha W, Hofmann H, Ayinde D, Logue EC, Dragin L, et al. SAMHD1 restricts the replication of human immunodeficiency virus type 1 by depleting the intracellular pool of deoxynucleoside triphosphates. *Nat Immunol* (2012) 13(3):223–8. doi: 10.1038/ni.2236
21. White TE, Brandariz-Nunez A, Valle-Casuso JC, Amie S, Nguyen LA, Kim B, et al. The retroviral restriction ability of SAMHD1, but not its deoxynucleotide triphosphohydrolase activity, is regulated by phosphorylation. *Cell Host Microbe* (2013) 13(4):441–51. doi: 10.1016/j.chom.2013.03.005
22. White TE, Brandariz-Nunez A, Valle-Casuso JC, Amie S, Nguyen L, Kim B, et al. Contribution of SAM and HD domains to retroviral restriction mediated by human SAMHD1. *Virology* (2013) 436(1):81–90. doi: 10.1016/j.virol.2012.10.029
23. Cribier A, Descours B, Valadao AL, Laguette N, Benkirane M. Phosphorylation of SAMHD1 by cyclin A2/CDK1 regulates its restriction activity toward HIV-1. *Cell Rep* (2013) 3(4):1036–43. doi: 10.1016/j.celrep.2013.03.017
24. Pauls E, Ruiz A, Badia R, Permanyer M, Gubern A, Riveira-Munoz E, et al. Cell cycle control and HIV-1 susceptibility are linked by CDK6-dependent CDK2 phosphorylation of SAMHD1 in myeloid and lymphoid cells. *J Immunol* (2014) 193(4):1988–97. doi: 10.4049/jimmunol.1400873
25. Mlcochova P, Sutherland KA, Watters SA, Bertoli C, de Bruin RA, Rehwinkel J, et al. A G1-like state allows HIV-1 to bypass SAMHD1 restriction in macrophages. *EMBO J* (2017) 36(5):604–16. doi: 10.15252/embj.201696025
26. Jauregui P, Landau NR. DNA damage induces a SAMHD1-mediated block to the infection of macrophages by HIV-1. *Sci Rep* (2018) 8(1):4153. doi: 10.1038/s41598-018-22432-4
27. Steinman RM. Some active areas of DC research and their medical potential. *Eur J Immunol* (2010) 40(8):2085–8. doi: 10.1002/eji.201040733
28. Steinman RM, Hemmi H. Dendritic cells: translating innate to adaptive immunity. *Curr Top Microbiol Immunol* (2006) 311:17–58. doi: 10.1007/3-540-32636-7_2
29. Steinman RM, Banchereau J. Taking dendritic cells into medicine. *Nature* (2007) 449(7161):419–26. doi: 10.1038/nature06175
30. Banchereau J, Steinman RM. Dendritic cells and the control of immunity. *Nature* (1998) 392(6673):245–52. doi: 10.1038/32588

31. Ahmed Z, Kawamura T, Shimada S, Piguet V. The Role of Human Dendritic Cells in HIV-1 Infection. *J Invest Dermatol* (2015) 135(5):1225–33. doi: 10.1038/jid.2014.490
32. Thomas R, Yang X. NK-DC Crosstalk in Immunity to Microbial Infection. *J Immunol Res* (2016) 2016:6374379. doi: 10.1155/2016/6374379
33. Keller CW, Freigang S, Lunemann JD. Reciprocal Crosstalk between Dendritic Cells and Natural Killer T Cells: Mechanisms and Therapeutic Potential. *Front Immunol* (2017) 8:570. doi: 10.3389/fimmu.2017.00570
34. Bermejo-Jambrina M, Eder J, Helgers LC, Hertoghs N, Nijmeijer BM, Stunnenberg M, et al. C-Type Lectin Receptors in Antiviral Immunity and Viral Escape. *Front Immunol* (2018) 9:590. doi: 10.3389/fimmu.2018.00590
35. Schumann K, Lammermann T, Bruckner M, Legler DF, Polleux J, Spatz JP, et al. Immobilized chemokine fields and soluble chemokine gradients cooperatively shape migration patterns of dendritic cells. *Immunity* (2010) 32(5):703–13. doi: 10.1016/j.immuni.2010.04.017
36. Vaahtomeri K, Brown M, Hauschild R, De Vries I, Leithner AF, Mehling M, et al. Locally Triggered Release of the Chemokine CCL21 Promotes Dendritic Cell Transmigration across Lymphatic Endothelia. *Cell Rep* (2017) 19(5):902–9. doi: 10.1016/j.celrep.2017.04.027
37. Li XD, Wu J, Gao D, Wang H, Sun L, Chen ZJ. Pivotal roles of cGAS-cGAMP signaling in antiviral defense and immune adjuvant effects. *Science* (2013) 341 (6152):1390–4. doi: 10.1126/science.1244040
38. Sugawara S, Thomas DL, Balagopal A. HIV-1 Infection and Type 1 Interferon: Navigating Through Uncertain Waters. *AIDS Res Hum Retroviruses* (2019) 35 (1):25–32. doi: 10.1089/AID.2018.0161
39. Cunningham AL, Donaghy H, Harman AN, Kim M, Turville SG. Manipulation of dendritic cell function by viruses. *Curr Opin Microbiol* (2010) 13(4):524–9. doi: 10.1016/j.mib.2010.06.002
40. Mercier SK, Donaghy H, Botting RA, Turville SG, Harman AN, Nasr N, et al. The Microvesicle Component of HIV-1 Inocula Modulates Dendritic Cell Infection and Maturation and Enhances Adhesion to and Activation of T Lymphocytes. *PloS Pathog* (2013) 9(10):e100370. doi: 10.1371/journal.ppat.1003700
41. Turville SG, Santos JJ, Frank I, Cameron PU, Wilkinson J, Miranda-Saksena M, et al. Immunodeficiency virus uptake, turnover, and 2-phase transfer in human dendritic cells. *Blood* (2004) 103(6):2170–9. doi: 10.1182/blood-2003-09-3129
42. Rinaldo CR. HIV-1 Trans Infection of CD4(+) T Cells by Professional Antigen Presenting Cells. *Sci (Cairo)* (2013) 2013:164203. doi: 10.1155/2013/164203
43. Moris A, Pajot A, Blanchet F, Guivel-Benhassine F, Salcedo M, Schwartz O. Dendritic cells and HIV-specific CD4+ T cells: HIV antigen presentation, T-cell activation, and viral transfer. *Blood* (2006) 108(5):1643–51. doi: 10.1182/blood-2006-02-006361
44. Ceccaldi PE, Delebecque F, Prevost MC, Moris A, Abastado JP, Gessain A, et al. DC-SIGN facilitates fusion of dendritic cells with human T-cell leukemia virus type 1-infected cells. *J Virol* (2006) 80(10):4771–80. doi: 10.1128/JVI.80.10.4771-4780.2006
45. Geijtenbeek TB, van Kooyk Y. DC-SIGN: a novel HIV receptor on DCs that mediates HIV-1 transmission. *Curr Top Microbiol Immunol* (2003) 276:31–54. doi: 10.1007/978-3-662-06508-2_2
46. Pruenster M, Wilflingseder D, Banki Z, Ammann CG, Muellauer B, Meyer M, et al. C-type lectin-independent interaction of complement opsonized HIV with monocyte-derived dendritic cells. *Eur J Immunol* (2005) 35(9):2691–8. doi: 10.1002/eji.200425940
47. Stoiber H, Ebenbichler C, Schneider R, Janatova J, Dierich MP. Interaction of several complement proteins with gp120 and gp41, the two envelope glycoproteins of HIV-1. *AIDS* (1995) 9(1):19–26. doi: 10.1097/00002030-199501000-00003
48. Stoiber H, Ebenbichler CF, Thielens NM, Arlaud GJ, Dierich MP. HIV-1 rsgp41 depends on calcium for binding of human c1q but not for binding of gp120. *Mol Immunol* (1995) 32(5):371–4. doi: 10.1016/0161-5890(94)00156-u
49. Stoiber H, Thielens NM, Ebenbichler C, Arlaud GJ, Dierich MP. The envelope glycoprotein of HIV-1 gp120 and human complement protein C1q bind to the same peptides derived from three different regions of gp41, the transmembrane glycoprotein of HIV-1, and share antigenic homology. *Eur J Immunol* (1994) 24(2):294–300. doi: 10.1002/eji.1830240203
50. Banki Z, Kacani L, Rusert P, Pruenster M, Wilflingseder D, Falkensammer B, et al. Complement dependent trapping of infectious HIV in human lymphoid tissues. *AIDS* (2005) 19(5):481–6. doi: 10.1097/01.aids.0000162336.20439.8d
51. Arborea G, Kemper C, Kolev M. Intracellular complement - the complosome - in immune cell regulation. *Mol Immunol* (2017) 89:2–9. doi: 10.1016/j.molimm.2017.05.012
52. Liszewski MK, Kolev M, Le Friec G, Leung M, Bertram PG, Fara AF, et al. Intracellular Complement Activation Sustains T Cell Homeostasis and Mediates Effector Differentiation. *Immunity* (2013) 39(6):1143–57. doi: 10.1016/j.immuni.2013.10.018
53. Liszewski MK, Kolev M, Le Friec G, Leung M, Bertram PM, Pickering MC, et al. Evidence for intracellular complement activation vital to Th1 immunity. *Mol Immunol* (2013) 56(3):257–8. doi: 10.1016/j.molimm.2013.05.055
54. West EE, Afzali B, Kemper C. Unexpected Roles for Intracellular Complement in the Regulation of Th1 Responses. *Adv Immunol Vol 138* (2018) 138:35–70. doi: 10.1016/bs.ai.2018.02.001
55. West EE, Freeley S, Kolev M, Niyonzima N, Espevik T, Mollnes TE, et al. Auto-regulation of Th1 responses requires intracellular carboxypeptidase M-mediated complement regulation. *Mol Immunol* (2018) 102:228–8. doi: 10.1016/j.molimm.2018.06.246
56. West EE, Kunz N, Kemper C. Complement and human T cell metabolism: Location, location, location. *Immunol Rev* (2020) 295(1):68–81. doi: 10.1111/imr.12852
57. Carroll MC, Isenman DE. Regulation of humoral immunity by complement. *Immunity* (2012) 37(2):199–207. doi: 10.1016/j.immuni.2012.08.002
58. Holers VM. Complement and its receptors: new insights into human disease. *Annu Rev Immunol* (2014) 32:433–59. doi: 10.1146/annurev-immunol-032713-120154
59. Vorup-Jensen T, Jensen RK. Structural Immunology of Complement Receptors 3 and 4. *Front Immunol* (2018) 9:2716. doi: 10.3389/fimmu.2018.02716
60. Gordon S. Pattern recognition receptors: doubling up for the innate immune response. *Cell* (2002) 111(7):927–30. doi: 10.1016/s0092-8674(02)01201-1
61. Peiser L, Mukhopadhyay S, Gordon S. Scavenger receptors in innate immunity. *Curr Opin Immunol* (2002) 14(1):123–8. doi: 10.1016/s0952-7915(01)00307-7
62. Rosetti F, Mayadas TN. The many faces of Mac-1 in autoimmune disease. *Immunol Rev* (2016) 269(1):175–93. doi: 10.1111/imr.12373
63. Biermann MH, Veissi S, Maueroder C, Chaurio R, Berens C, Herrmann M, et al. The role of dead cell clearance in the etiology and pathogenesis of systemic lupus erythematosus: dendritic cells as potential targets. *Expert Rev Clin Immunol* (2014) 10(9):1151–64. doi: 10.1586/1744666X.2014.944162
64. Bermejo-Jambrina M, Blatzer M, Jauregui-Onieva P, Yordanov TE, Hörtnagl P, Valovka T, et al. CR4 Signaling Contributes to a DC-Driven Enhanced Immune Response Against Complement-Opsonized HIV-1. *Front Immunol* (2020) 11:2010. doi: 10.3389/fimmu.2020.02010
65. Frank I, Stoiber H, Godar S, Stockinger H, Steindl F, Katinger HW, et al. Acquisition of host cell-surface-derived molecules by HIV-1. *AIDS* (1996) 10 (14):1611–20. doi: 10.1097/00002030-199612000-00004
66. Bajtay Z, Speth C, Erdei A, Dierich MP. Cutting edge: productive HIV-1 infection of dendritic cells via complement receptor type 3 (CR3, CD11b/CD18). *J Immunol* (2004) 173(8):4775–8. doi: 10.4049/jimmunol.173.8.4775
67. Bouhlal H, Chomont N, Requena M, Nasreddine N, Saidi H, Legoff J, et al. Opsonization of HIV with complement enhances infection of dendritic cells and viral transfer to CD4 T cells in a CR3 and DC-SIGN-dependent manner. *J Immunol* (2007) 178(2):1086–95. doi: 10.4049/jimmunol.178.2.1086
68. Posch W, Cardinaud S, Hamimi C, Fletcher A, Muhlbacher A, Loacker K, et al. Antibodies attenuate the capacity of dendritic cells to stimulate HIV-specific cytotoxic T lymphocytes. *J Allergy Clin Immunol* (2012) 130(6):1368–1374 e2. doi: 10.1016/j.jaci.2012.08.025S0091-6749(12)01388-7[pii
69. Tjomsland V, Ellegard R, Che K, Hinkula J, Lifson JD, Larsson M. Complement opsonization of HIV-1 enhances the uptake by dendritic cells and involves the endocytic lectin and integrin receptor families. *PloS One* (2011) 6(8):e23542. doi: 10.1371/journal.pone.0023542
70. Wilflingseder D, Banki Z, Dierich MP, Stoiber H. Mechanisms promoting dendritic cell-mediated transmission of HIV. *Mol Immunol* (2005) 42(2):229–37. doi: 10.1016/j.molimm.2004.06.019

71. Thieblemont N, Haeffner-Cavaillon N, Haeffner A, Cholley B, Weiss L, Kazatchkine MD. Triggering of complement receptors CR1 (CD35) and CR3 (CD11b/CD18) induces nuclear translocation of NF-kappa B (p50/p65) in human monocytes and enhances viral replication in HIV-infected monocytic cells. *J Immunol* (1995) 155(10):4861–7.
72. Stoiber H, Schneider R, Janatova J, Dierich MP. Human complement proteins C3b, C4b, factor H and properdin react with specific sites in gp120 and gp41, the envelope proteins of HIV-1. *Immunobiology* (1995) 193(1):98–113. doi: 10.1016/s0171-2985(11)80158-0
73. Kim KA, Yolamanova M, Zirafi O, Roan NR, Staendker L, Forssmann WG, et al. Semen-mediated enhancement of HIV infection is donor-dependent and correlates with the levels of SEVI. *Retrovirology* (2010) 7:55. doi: 10.1186/1742-4690-7-55
74. Balandya E, Sheth S, Sanders K, Wieland-Alter W, Lahey T. Semen protects CD4+ target cells from HIV infection but promotes the preferential transmission of R5 tropic HIV. *J Immunol* (2010) 185(12):7596–604. doi: 10.4049/jimmunol.1002846
75. Stax MJ, van Montfort T, Sprenger RR, Melchers M, Sanders RW, van Leeuwen E, et al. Mucin 6 in seminal plasma binds DC-SIGN and potently blocks dendritic cell mediated transfer of HIV-1 to CD4(+) T-lymphocytes. *Virology* (2009) 391(2):203–11. doi: 10.1016/j.virol.2009.06.011
76. Berlier W, Bourlet T, Levy R, Lucht F, Pozzetto B, Delezay O. Amount of seminal IL-1beta positively correlates to HIV-1 load in the semen of infected patients. *J Clin Virol* (2006) 36(3):204–7. doi: 10.1016/j.jcv.2006.04.004
77. Berlier W, Cremel M, Hamzeh H, Levy R, Lucht F, Bourlet T, et al. Seminal plasma promotes the attraction of Langerhans cells via the secretion of CCL20 by vaginal epithelial cells: involvement in the sexual transmission of HIV. *Hum Reprod* (2006) 21(5):1135–42. doi: 10.1093/humrep/dei496
78. Baldauf HM, Pan X, Erikson E, Schmidt S, Daddacha W, Burggraf M, et al. SAMHD1 restricts HIV-1 infection in resting CD4(+) T cells. *Nat Med* (2012) 18(11):1682–7. doi: 10.1038/nm.2964
79. Granelli-Piperno A, Delgado E, Finkel V, Paxton W, Steinman RM. Immature dendritic cells selectively replicate macrophagetropic (M-tropic) human immunodeficiency virus type 1, while mature cells efficiently transmit both M- and T-tropic virus to T cells. *J Virol* (1998) 72(4):2733–7. doi: 10.1128/JVI.72.4.2733-2737.1998
80. Granelli-Piperno A, Golebiowska A, Trumpfheller C, Siegal FP, Steinman RM. HIV-1-infected monocyte-derived dendritic cells do not undergo maturation but can elicit IL-10 production and T cell regulation. *Proc Natl Acad Sci U S A* (2004) 101(20):7669–74. doi: 10.1073/pnas.0402431101
81. Gringhuis SI, Hertoghs N, Kaptein TM, Zijlstra-Willems EM, Sarrami-Fooroshani R, Sprokholt JK, et al. HIV-1 blocks the signaling adaptor MAVS to evade antiviral host defense after sensing of abortive HIV-1 RNA by the host helicase DDX3 (vol 18, pg 225, 2017). *Nat Immunol* (2017) 18(4):474–4. doi: 10.1038/ni0417-474c
82. Taniguchi T, Ogasawara K, Takaoka A, Tanaka N. IRF family of transcription factors as regulators of host defense. *Annu Rev Immunol* (2001) 19:623–55. doi: 10.1146/annurev.immunol.19.1.623
83. Su B, Biedma ME, Lederle A, Peressin M, Lambotin M, Proust A, et al. Dendritic cell-lymphocyte cross talk downregulates host restriction factor SAMHD1 and stimulates HIV-1 replication in dendritic cells. *J Virol* (2014) 88(9):5109–21. doi: 10.1128/JVI.03057-13
84. Ellegard R, Crisci E, Burgener A, Sjowall C, Birse K, Westmacott G, et al. Complement opsonization of HIV-1 results in decreased antiviral and inflammatory responses in immature dendritic cells via CR3. *J Immunol* (2014) 193(9):4590–601. doi: 10.4049/jimmunol.1401781
85. Sandler NG, Bosinger SE, Estes JD, Zhu RTR, Tharp GK, Boritz E, et al. Type I interferon responses in rhesus macaques prevent SIV infection and slow disease progression. *Nature* (2014) 511(7511):601–+. doi: 10.1038/nature13554
86. Fernandez S, Tanaskovic S, Helbig K, Rajasuriar R, Kramski M, Murray JM, et al. CD4+ T-cell deficiency in HIV patients responding to antiretroviral therapy is associated with increased expression of interferon-stimulated genes in CD4+ T cells. *J Infect Dis* (2011) 204(12):1927–35. doi: 10.1093/infdis/jir659
87. Fraietta JA, Mueller YM, Yang G, Boesteanu AC, Gracias DT, Do DH, et al. Type I interferon upregulates Bak and contributes to T cell loss during human immunodeficiency virus (HIV) infection. *PloS Pathog* (2013) 9(10):e1003658. doi: 10.1371/journal.ppat.1003658

Conflict of Interest: The authors declare that the research was conducted in the absence of any commercial or financial relationships that could be construed as a potential conflict of interest.

The handling editor declared a shared affiliation, though no other collaboration with the authors.

frontiers in Immunology

ORIGINAL RESEARCH
published: 10 November 2020
doi: 10.3389/fimmu.2020.572562

The Role of Properdin in Killing of Non-Pathogenic *Leptospira biflexa*

Adriana Patricia Granados Martinez[1], *Patrícia Antonia Estima Abreu*[2], *Silvio de Arruda Vasconcellos*[3], *Paulo Lee Ho*[2], *Viviana P. Ferreira*[4], *Gurpanna Saggu*[4], *Angela Silva Barbosa*[2] *and Lourdes Isaac*[1]*

[1] Department of Immunology, Institute of Biomedical Sciences, University of São Paulo, São Paulo, Brazil, [2] Laboratory of Bacteriology, Butantan Institute, São Paulo, Brazil, [3] Laboratory of Bacterial Zoonoses, Faculty of Veterinary Medicine and Animal Science, University of São Paulo, São Paulo, Brazil, [4] Department of Medical Microbiology and Immunology, College of Medicine and Life Sciences, University of Toledo, Toledo, OH, United States

Properdin (P) is a positive regulatory protein that stabilizes the C3 convertase and C5 convertase of the complement alternative pathway (AP). Several studies have suggested that properdin can bind directly to the surface of certain pathogens regardless of the presence of C3bBb. Saprophytic *Leptospira* are susceptible to complement-mediated killing, but the interaction of properdin with *Leptospira* spp. has not been evaluated so far. In this work, we demonstrate that properdin present in normal human serum, purified properdin, as well as properdin oligomers P2, P3, and P4, interact with *Leptospira*. Properdin can bind directly to the bacterial surface even in the absence of C3b. In line with our previous findings, AP activation was shown to be important for killing non-pathogenic *L. biflexa*, and properdin plays a key role in this process since this microorganism survives in P-depleted human serum and the addition of purified properdin to P-depleted human serum decreases the number of viable leptospires. A panel of pathogenic *L. interrogans* recombinant proteins was used to identify putative properdin targets. Lsa30, an outer membrane protein from *L. interrogans*, binds to unfractionated properdin and to a lesser extent to P2-P4 properdin oligomers. In conclusion, properdin plays an important role in limiting bacterial proliferation of non-pathogenic *Leptospira* species. Once bound to the leptospiral surface, this positive complement regulatory protein of the AP contributes to the formation of the C3 convertase on the leptospire surface even in the absence of prior addition of C3b.

Keywords: properdin, *Leptospira*, complement system, alternative pathway, bacteria killing ability

OPEN ACCESS

Edited by:
Reinhard Würzner, Innsbruck Medical University, Austria

Reviewed by:
Peter Kraiczy, Goethe University Frankfurt, Germany
Juha Kotimaa, University of Helsinki, Finland
Per Nilsson, University of Oslo, Norway

***Correspondence:**
Lourdes Isaac
louisaac@icb.usp.br

Specialty section:
This article was submitted to Molecular Innate Immunity, a section of the journal Frontiers in Immunology

Received: *14 June 2020*
Accepted: *05 October 2020*
Published: *10 November 2020*

Citation:
Martinez APG, Abreu PAE, de Arruda Vasconcellos S, Ho PL, Ferreira VP, Saggu G, Barbosa AS and Isaac L (2020) The Role of Properdin in Killing of Non-Pathogenic Leptospira biflexa. Front. Immunol. 11:572562. doi: 10.3389/fimmu.2020.572562

INTRODUCTION

Spirochetes of the genus *Leptospira* may cause leptospirosis, a zoonosis of worldwide distribution. The *Leptospira* genus includes pathogenic and saprophytic species, which are classified into more than 300 serovars (1). Pathogenic leptospires have evolved virulence strategies to successfully colonize a variety of hosts, but the mechanisms of pathogenesis in leptospirosis are still poorly defined. While progress has been made in this field, gaps remain in our understanding of how *Leptospira* causes disease.

One of the factors that contribute to a successful infection by spirochetes is their ability to escape the natural defense mechanisms of the human host by circumventing complement-mediated killing. Pathogenic *Leptospira* spp. control complement activation on their surfaces or in the surrounding microenvironment by *i)* hijacking soluble regulatory proteins from the host; *ii)* cleaving complement molecules of the alternative (AP), the lectin and the classical pathways through the secretion of proteases such as thermolysins; or, *iii)* the acquisition of host proteases such as plasminogen [reviewed in (2)]. In contrast, saprophyte *Leptospira* spp. are devoid of complement evasion strategies and so are highly susceptible to the bactericidal activity of human serum (2–4).

A number of surface-exposed proteins have been shown to contribute to complement immune evasion by pathogenic *Leptospira*. By binding soluble complement regulatory proteins that avoid complement activation (negative regulators) such as Factor H, C4b binding protein, and vitronectin, these bacterial proteins potentially down-regulate all three complement pathways as well as the terminal step of this cascade (3–5). While the interaction of these complement regulatory proteins with different *Leptospira* species has been well explored over the last years, binding of properdin, the only positive regulator of the complement cascade, to the surface of saprophyte and pathogenic *Leptospira* has never been evaluated.

Human properdin is a 53 kDa plasma glycoprotein composed of seven tandem repeats called thrombospondin type 1 modules (6, 7). In the circulation, identical subunits display a head to tail arrangement to form dimers, trimers and tetramers in a fixed ratio, the trimers being the most abundant form (8, 9). Properdin is synthesized primarily by neutrophils, dendritic cells, monocytes, macrophages and T cells [reviewed in (10)], and its serum concentration is approximately 5–25 μg/ml (10, 11). A number of important functions have been ascribed to properdin [reviewed in (12). The first studies assessing the role of this complement regulator date back to the 1950s when Pillemer and colleagues demonstrated that properdin could bind to a variety of targets in the absence of specific antibodies and activate the complement system (13).

In the late 1970s, properdin regained attention when a model for the assembly of C3 convertase of the AP emerged. According to this model, today known as the "standard model", C3b produced by C3 activation in the fluid-phase binds covalently to target surfaces. Subsequently, Factor B associates with C3b, and is then cleaved by Factor D. Factor B amino-terminal fragment (Ba) is released and the C3bBb complex is recognized and stabilized by properdin (14, 15). As a consequence, the C3 convertase half-life is extended by 10-fold or more (16). More recently, a series of studies indicated that physiological forms of properdin can initiate complement activation *in vitro* by directly attaching non-covalently to certain target surfaces, including *Chlamydia pneumoniae*, late apoptotic and necrotic cells, and activated platelets [reviewed in (10)]. Consistent with the "properdin-directed model", properdin binds to a target surface and recruits C3b. The C3bBb complex is then formed upon association of Factor B with C3b, as previously mentioned.

Given the importance of the AP in eliminating non-pathogenic *Leptospira*, we addressed the following questions in the present work: *i)* do pathogenic and non-pathogenic leptospiral strains interact differentially with properdin? and *ii)* does properdin bind directly to the bacterial surface or is previous binding of C3b required?

MATERIAL AND METHODS

Leptospira Strains

Saprophytic *L. biflexa* serovar Patoc strain Patoc I (non-pathogenic), *L. interrogans* serovar Pomona strain Pomona, (pathogenic, culture-attenuated), and *L. interrogans* serovar Kennewicki strain Fromm (pathogenic, virulent), were provided by the Laboratory of Bacterial Zoonoses at the Faculty of Veterinary Medicine and Animal Science, University of São Paulo. *Leptospires* were cultured at 29°C for 7 days under aerobic conditions in EMJH (Difco-USA) liquid medium supplemented with 10% *Leptospira* enrichment EMJH (BD-USA) or with 10% pre-enriched inactivated rabbit serum, L-asparagine (0.015%), sodium pyruvate (0.001%), calcium chloride (0.001%), magnesium chloride (0.001%), and peptone (0.03%). Attenuation of the strain Pomona was achieved by successive passages in culture medium and virulence of the strain Fromm was maintained by successive passages in hamsters.

Leptospira Survival in the Serum

L. biflexa serovar Patoc strain Patoc I (2–3 x 10^8 bacteria/ml) cultured in EMJH medium supplemented with bovine serum albumin (BSA) was incubated at 37°C for 2 h with 40% normal human serum (NHS), heat-inactivated NHS (HI-NHS) obtained after incubation of NHS at 56°C for 30 min; properdin-depleted (P-DS) serum (Complement Technology, Inc.) or P-DS supplemented with 5 μg, 10 μg, or 25 μg of commercial purified human properdin (Complement Technology. Inc.) to a final volume of 100 μl. After incubation, *Leptospira* survival was estimated by counting the number of viable bacteria in Petroff-Hausser's chamber using dark field microscopy, according to (4). The experiments were performed in triplicate. The survival in the presence of each serum was compared to that observed in HI-NHS (100%).

Interaction of *Leptospira* With Properdin

Cultures of *L. interrogans* serovar Kennewicki strain Fromm, *L. biflexa* serovar Patoc strain Patoc I, and *L. interrogans* serovar Pomona strain Pomona were washed twice with VBS^{++} (1.46 mM sodium barbiturate; 2.5 mM 5,5'diethyl barbituric acid; 144 mM NaCl, pH 7.4 containing 0.83 mM $MgCl_2$ and 0.25 mM $CaCl_2$). Each suspension containing 5 x 10^8 *Leptospira*/ml) was incubated with 0, 10, 25, and 50% NHS containing 10 mM EDTA (NHS-EDTA) or equivalent amounts of purified properdin (0, 2.5, 6.2, and 12.5 μg). *Leptospira* samples were also incubated with 40% C3-depleted human serum (C3-DS) (Complement Technology, Inc.) or with NHS-EDTA for 2 h at 37°C, with stirring, in a final volume of 500 μl. In parallel, *Leptospira* suspensions were

incubated with 5 µg of human properdin (Complement Technology, Inc.) or 10 µg of human C3b (Complement Technology, Inc.) for 1 h at 37°C with stirring. After three washes with VBS^{++}, 10 µg of C3b was added to the bacterial cultures that had been pre-incubated with properdin, and 5 µg of properdin was added to those that had been pre-incubated with C3b. The bacterial suspensions were then washed five times with VBS^{++} and centrifuged at 3,000 x *g* for 10 min at 4°C. The precipitates were resuspended in 0.1 M $NaHCO_3$ pH 9 and 100 µl of each sample were immobilized in duplicate on ELISA plate wells for 16 h at 4°C. Next, the wells were washed twice with PBS containing Tween 0.05% (PBS-T) and blocked with 3% BSA in PBS for 2 h at 37°C. The wells were washed three times with PBS-T. Properdin or C3b bound to the bacterial surface were detected with goat anti-properdin (1:2,000) or goat anti-C3 (1:5,000) (both antibodies were purchased from Complement Technologies, Inc.) diluted in PBS. After incubation for 1 h at 37°C and three washes with PBS-T, peroxidase-conjugated anti-goat IgG, diluted 1: 10,000 in PBS, was added for 1 h at 37°C. After three washes the reactions were developed by adding the substrate *o*-Phenylenediamine dihydrochloride (OPD; 0.04%) diluted in citrate-phosphate buffer (pH 5.0) and 0.01% H_2O_2. The plates were protected from light for 5 to 10 min and the reaction was quenched by the addition of 50 µl of 4 N H_2SO_4. The absorbance was read at 492 nm.

Interaction of Properdin Oligomers With *Leptospira* Strains and With Leptospiral Outer Membrane Proteins

We assessed binding of pure properdin oligomers, namely high molecular weight aggregates not present in serum (Pn), properdin dimer (P2), trimer (P3), and tetramer (P4) to pathogenic and non-pathogenic leptospires as well as to leptospiral membrane proteins. *L. biflexa* serovar Patoc strain Patoc I (non-pathogenic), *L. interrogans* serovar Pomona strain Pomona (culture attenuated), and *L. interrogans* serovar Kennewicki strain Fromm (virulent) suspensions containing 1 x 10^8 leptospires were incubated with 5 µg of each oligomer or with unfractionated commercial properdin (P), and the presence of properdin (total volume of 1 ml) was evaluated by ELISA as described above. In addition, with the aim of identifying putative ligands for properdin on the leptospiral membrane, a panel of recombinant proteins from *L. interrogans* serovar Copenhageni 10A [produced essentially as described in (17) was used (**Table 1**). One microgram of each protein was immobilized on ELISA plate wells and incubated with 0.5 µg of properdin. Binding was assessed as described above. Interaction of Lsa30 with properdin oligomers was also evaluated as already described. The data correspond to three independent experiments, using two separate preparations of P2, P3, P4, or Pn. Each experiment was performed in triplicate.

Detection of C3 Convertase on the *Leptospira* Surface

An ELISA-based assay with some modifications was employed. All incubations were performed in microtubes including the development of the reactions with OPD. *L. biflexa* serovar Patoc strain Patoc I and *L. interrogans* serovar Kennewicki strain Fromm cultures were centrifuged at 4,500 x *g* for 20 min at 21°C, then washed twice with PBS. Subsequently, the number of bacteria was estimated using dark field microscopy. 2 x 10^8 bacteria/ml were incubated with 5 µg/ml of commercial properdin for 1 h at 37°C with stirring. The samples were washed three times with PBS and the pellets were incubated with 10% P-DS, NHS, HI-NHS diluted in AP-CFTD (VBS buffer containing 7 mM $MgCl_2$, 10 mM EGTA, pH 7.2) buffer at 37°C for 30 min with stirring. After five washes, polyclonal goat anti-Factor B at a 1: 2,000 dilution (Complement Technology, Inc.) in PBS-T containing 1% BSA was added and incubation proceeded for 1 h at 37°C. After three washes with PBS, anti-goat IgG (KPL) diluted 1: 5,000 in PBS-T containing 1% BSA was added to the bacteria and incubated for 1 h at 37°C. Subsequently, three washes were performed, and the reaction was developed with *o*-phenylenediamine dihydrochloride (OPD) substrate (0.04%) diluted in citrate-phosphate buffer (pH 5.0) and 0.01% H_2O_2. After 5 min the reaction was stopped with 50 µl of 4N H_2SO_4, the samples were transferred to a 96-well plate and the absorbance read at 492 nm.

TABLE 1 | Recombinant Proteins from *L. Interrogans* Serovar Copenhageni 10A.

Gene	Protein	GenBank	Recombinant protein molecular mass (kDa)
LIC10325	HlyX	AAS68952.1	43
LIC11947	LcpA	AAS70529.1	20
LIC12875	EF-Tu	AAS71428.1	43
LIC10301	–	AAS68928.1	13
LIC10009	Lp25	AAS68646.1	25
LIC10507	–	AAS69128.1	22
LIC10704	–	AAS69325.1	23
LIC11352	LipL32	AAS69953.1	32
LIC10465	LigA-C	AAS69086.1	63
LIC10464	LigB-C	AAS69085.1	56
LIC10464	LigB-N	AAS69085.1	64
LIC13305	–	AAS71847.1	31
LIC11087	Lsa30	AAS69694.1	30
LIC11030	–	AAS69637.1	35

Statistical Analysis

Data was analyzed using ANOVA one-way test, using Statgraphics Centurion XVI software. Except when indicated, the variance homogeneity was assessed using Cochran test and when necessary, data logarithmic transformation was used.

RESULTS

Properdin Contributes to *Leptospira biflexa* Killing in the Serum

Considering that the AP is important for the killing of the non-pathogenic *L. biflexa* serovar Patoc strain Patoc I (3, 4, 18, 19), we evaluated survival of this strain in P-DS. Under these conditions, 70% of the bacteria survived. When purified properdin (5–25 µg/ml) was added to P-DS, bacterial survival decreased significantly as properdin concentration increased because of stabilization of

the C3 convertase (C3bBb) (**Figure 1**). These results further confirm that *L. biflexa* activates the AP, and bacterial elimination depends on the presence of properdin.

Binding of Properdin to *Leptospira* spp.

Next, we investigated if three different species of *Leptospira* including virulent (*L. interrogans* serovar Kennewicki strain Fromm), culture-attenuated (*L. interrogans* serovar Pomona strain Pomona) and non-pathogenic (*L. biflexa* serovar Patoc strain Patoc I) strains, would bind to properdin. To assess this interaction, bacterial cultures were washed and incubated with purified properdin or NHS-EDTA as a source of properdin, and binding was measured by ELISA. Our data shows that properdin, either purified or present in NHS-EDTA, interacts dose-dependently with all *Leptospira* strains tested, regardless of their virulence status (**Figures 2A–B**). Purified properdin binding to leptospires was more pronounced compared to serum properdin binding suggesting a certain degree of competition between properdin and other serum molecules. Another possibility to explain this result would be the presence of inhibitors that may interfere with the properdin binding capacity on the surface of bacteria (**Figure 2B**). Attenuated *L. interrogans* serovar Pomona tend to bind less to purified properdin than *L. interrogans* serovar Pomona and non-pathogenic *L. biflexa* serovar Patoc strain Patoc I. However, this was not statistically significant.

Leptospira spp. Binds to Purified Properdin Independently of C3b

To investigate if properdin could bind directly to *Leptospira* strains even in the absence of C3b, we incubated *L. biflexa* serovar Patoc strain Patoc I, *L. interrogans* serovar Pomona strain Pomona, and *L. interrogans* serovar Kennewicki strain Fromm with NHS-EDTA or C3-DS. Bound-properdin was detected by ELISA using anti-human properdin. As indicated in **Figure 3A**, all three *Leptospira* strains bound to serum properdin in relatively low amounts. When purified properdin was used a more pronounced interaction was observed, and properdin binding was observed in the presence or absence of C3b (**Figures 3B, C**). It is worth to mention that purified C3b is able to bind to the *Leptospira* membrane (20, 21).

These data suggest that properdin can bind directly to yet unknown leptospiral ligands regardless of the presence of C3b, which allows us to suspect that this complement regulatory protein may interact with pathogen molecular patterns and directly trigger AP activation, in addition to its known ability to act as a C3 convertase stabilizing molecule.

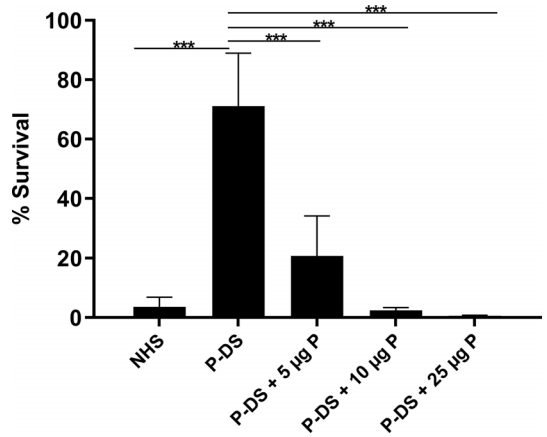

FIGURE 1 | Survival of *L. biflexa* serovar Patoc in the presence of properdin. Leptospires were incubated with normal human serum (NHS), properdin-depleted serum (P-DS) and P-DS reconstituted with 5, 10, or 25 µg of purified properdin (P) for 2 h at 37°C. The number of viable leptospires present after incubation with heat inactivated NHS was considered 100%. Data are expressed as the mean (± SD) of three independent experiments each one performed in triplicate. Statistically significant differences (ANOVA one-way test) are indicated. ***$p \leq 0.001$; confidence interval of 95%.

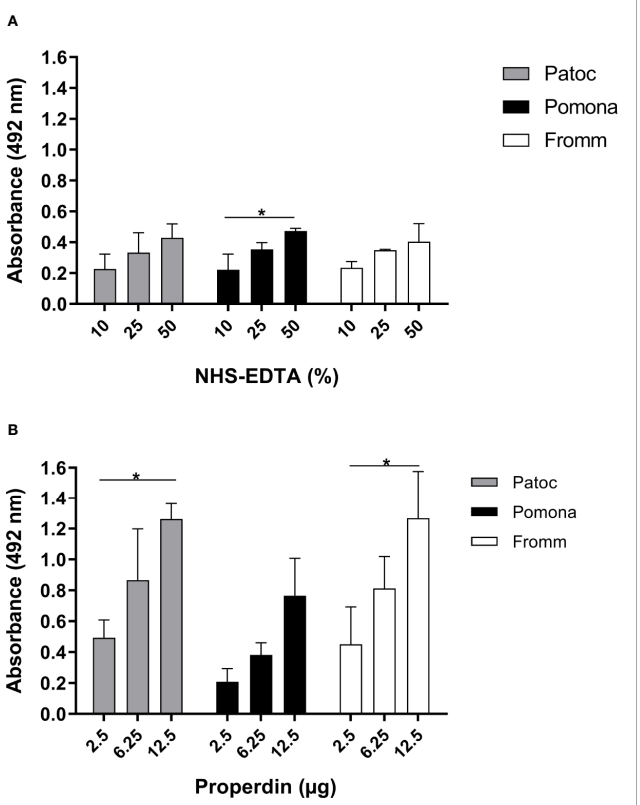

FIGURE 2 | Binding of properdin to *Leptospira*. *L. biflexa* serovar Patoc strain Patoc I (non-pathogenic), *L. interrogans* serovar Pomona strain Pomona (pathogenic, attenuated), and *L. interrogans* serovar Kennewicki strain Fromm (pathogenic, virulent) were incubated with **(A)** 10, 25, and 50% NHS-EDTA or **(B)** 2.5, 6.25, and 12.5 µg of commercial purified properdin which are equivalent to properdin concentrations found in 10, 25, and 50% NHS used above. The binding was evaluated by ELISA using polyclonal anti-human properdin. Baseline values obtained with PBS were subtracted in **(A, B)**, respectively for each type of leptospire. Data are expressed as the mean (± SD) of three independent experiments each one performed in triplicate. Statistically significant differences (ANOVA one-way test) are indicated. *$p \leq 0.05$; confidence interval of 95%. Variance homogeneity was analyzed using Bartlett.

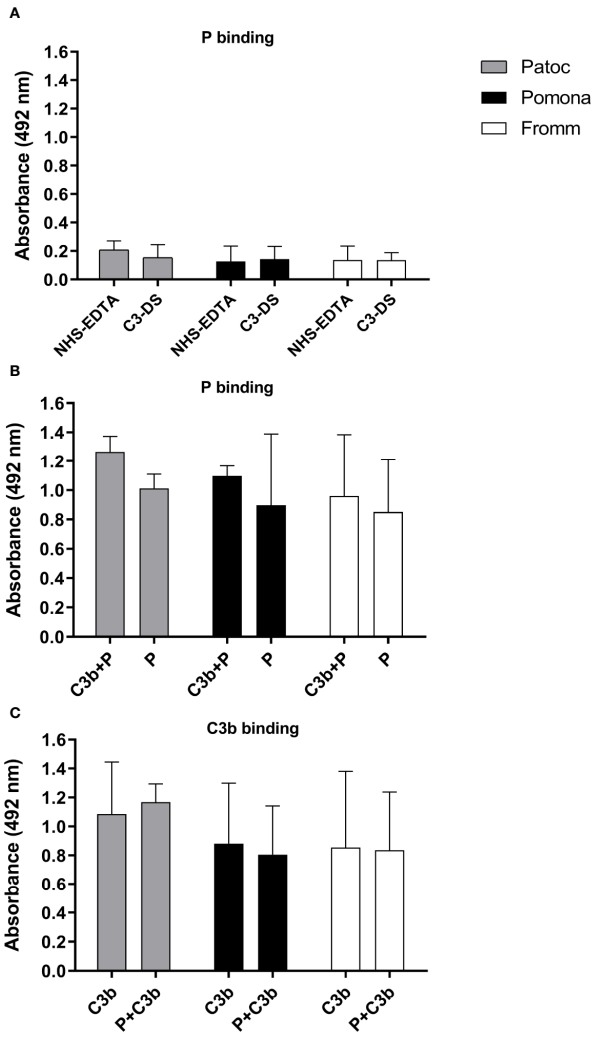

FIGURE 3 | Binding of properdin to *Leptospira* occurs even in the absence of C3b. The binding of properdin (P) on *L. biflexa* serovar Patoc strain Patoc I (non-pathogenic), *L. interrogans* serovar Pomona strain Pomona (pathogenic, attenuated), and *L. interrogans* serovar Kennewicki strain Fromm (pathogenic, virulent) was quantified by ELISA using polyclonal anti-human properdin **(A, B)** or anti-human C3 **(C)**. **(A)** *Leptospira* strains were incubated with 40% normal human serum-treated with EDTA (NHS-EDTA) or with C3 depleted serum (C3-DS). **(B)** *Leptospira* strains were incubated with purified properdin (P) for 1h at 37°C, washed, and then with C3b (C3b+P) or PBS. **(C)** *Leptospira* strains were incubated with purified C3b for 1h at 37°C, washed, and then incubated with P (P + C3b) or PBS. Baseline values obtained without any addition of P or C3b were subtracted respectively for each type of leptospire. Data are expressed as the mean (± SD) of three independent experiments each one performed in triplicate.

Binding of Different Properdin Oligomers to *Leptospira*

The interaction of *Leptospira* spp. with purified properdin oligomers (P2, P3, P4, and Pn) was investigated by comparing bacterial binding to each oligomer to that observed with commercial purified properdin. The results showed that all forms of properdin interact with the three strains of *Leptospira* tested. Virulent *L. interrogans* serovar Kennewicki strain Fromm binds less to P2 and P3 as compared to unfractionated commercial properdin (**Figure 4**). On the other hand, non-pathogenic *L. biflexa* serovar Patoc strain Patoc I and attenuated *L. interrogans* serovar Pomona strain Pomona bind similarly to unfractionated commercial properdin and to the properdin oligomers present in human serum.

Interaction of Properdin With *Leptospira* OMPs

A panel of recombinant proteins from pathogenic *L. interrogans* serovar Copenhageni 10A was used in an attempt to identify possible bacterial candidates for binding to properdin (**Table 1**). Regrettably, recombinant proteins from *L. biflexa* were not available. Among the proteins tested, Lsa30 (former LIC11087) was the only one which significantly bound to unfractionated commercial purified properdin (**Figure 5A**) as well as to P2, P3, P4, and Pn oligomers (**Figure 5B**). Binding of Lsa30 to Pn and to commercial purified properdin is more pronounced and significantly different from its binding to P2, P3 and P4.

Formation of C3 Convertase on the *L. biflexa* Surface Requires the Presence of Properdin

To assess if the formation of the C3 convertase (C3bBb) was stabilized by properdin (PC3bBb) on the leptospiral surface, *L. biflexa* serovar Patoc strain Patoc I and *L. interrogans* serovar Kennewicki strain Fromm were incubated under different serum conditions and the C3 convertase formation was detected by ELISA using anti-human Factor B antibody. As expected, C3 convertase formation on non-pathogenic *L. biflexa* serovar Patoc strain Patoc I treated with P-DS was limited and not significantly different when in the presence of HI-NHS (negative control) (**Figure 6**). However, when purified properdin was added to P-DS, a significant increase in the formation of C3bBb was observed, albeit at lower levels than that observed with NHS. With regard to the virulent *L. interrogans* serovar Kennewicki strain Fromm, no significant C3bBb formation was observed. This is probably because pathogenic leptospires bind quite well to Factor H and are able to evade complement activation (3, 5, 19).

DISCUSSION

The positive regulatory protein properdin stabilizes the C3 convertase and C5 convertase formed by the AP [(15, 16), and reviewed in (10)]. Its relevance is even more evident in immunodeficient patients that lack properdin since they are more susceptible to repeated infections caused by *Neisseria meningitidis* (22) and often results in pneumonia and otitis media (23, 24).

Since Pillemer's early work in 1954 (13), it is known that properdin can recognize pathogenic targets and thus activates the complement system (14). We are unaware of studies in the literature that decipher the role of properdin during infection with leptospires. The relevance of properdin in the elimination of non-pathogenic leptospires was confirmed in this study. As

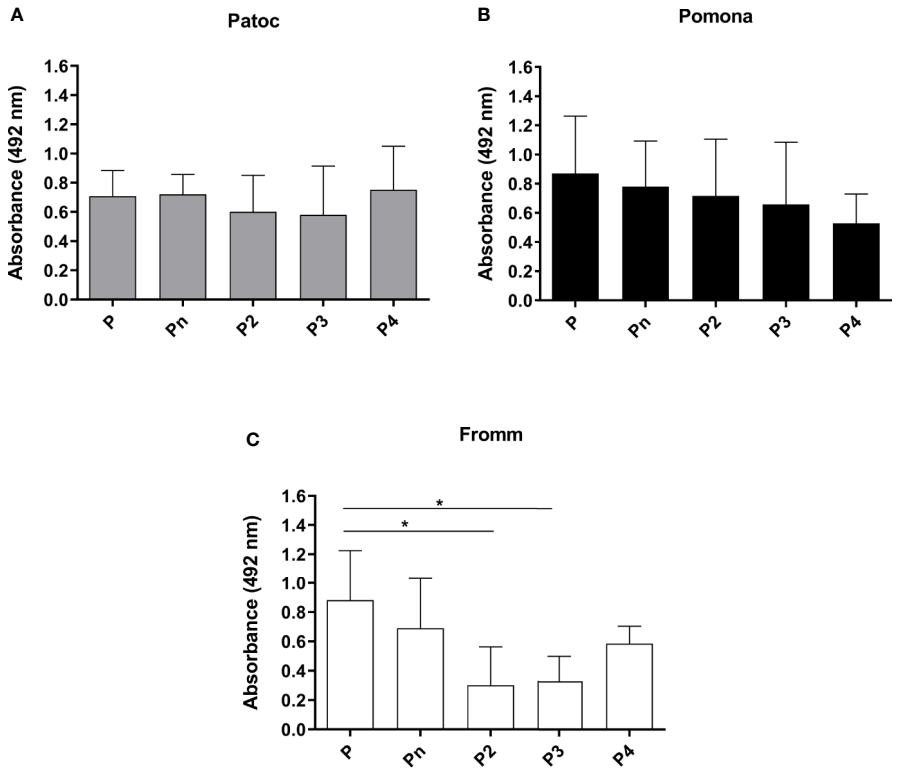

FIGURE 4 | Binding of different properdin oligomers to pathogenic and non-pathogenic *Leptospira*. Unfractionated commercial properdin (P), high molecular weight aggregate not present in serum (Pn), properdin dimer (P2), trimer (P3), and tetramer (P4) were incubated with *L. biflexa* serovar Patoc strain Patoc I (non-pathogenic) **(A)**, *L. interrogans* serovar Pomona strain Pomona (pathogenic, attenuated) **(B)**), and *L. interrogans* serovar Kennewicki strain Fromm (pathogenic, virulent) **(C)**. Five µg of each properdin form were used and the binding on the *Leptospira* surface was evaluated by ELISA using polyclonal anti-human properdin. The mean and standard deviation correspond to three independent experiments, using two independent preparations of P2, P3, P4, or Pn. Baseline values obtained with PBS were subtracted, respectively for each type of leptospire. Data are expressed as the mean (± SD) of three independent experiments each one performed in triplicate. Statistically significant differences (ANOVA one-way test) are indicated. *$p \leq 0.05$, confidence interval of 95%.

previously described (3, 4), *L. biflexa* serovar Patoc strain Patoc I is rapidly lysed in the presence of NHS. Here we have shown that approximately 70% of the cells of strain Patoc I survived in P-DS. Recently, we have demonstrated that both the Alternative and Lectin Pathways contribute to the killing of *L. biflexa* serovar Patoc (19). This could explain why, even in the absence of PC3bBb, a residual killing activity is still observed in the presence of P-DS. As purified properdin was added (up to physiological levels) to this depleted serum, the complement-mediated bactericidal activity was restored in a dose-dependent manner, confirming the importance of this regulatory protein for the control of saprophytic *Leptospira* infection. On the other hand, pathogenic *Leptospira* are more resistant to complement activation since they exhibit several immune evasion mechanisms [reviewed in (25)].

Properdin binds with similar affinity to non-pathogenic leptospires and as well to virulent or attenuated pathogenic species. In addition, purified properdin binds more efficiently to these bacteria compared to human serum properdin possibly because of competition with other serum molecules that could target the same interaction sites on the *Leptospira* surface.

Interestingly, properdin can bind directly to the surface of *Leptospira*, even in the absence of C3b fragments, suggesting that properdin may interact directly with molecular patterns present on the surface of this spirochete. Our results reinforce the existence of two models (direct and indirect) of properdin to participate in the activation of the AP, since properdin can bind to *Leptospira* before and after generation of activated C3b fragments. This observation is in agreement with previous results published by various investigators that demonstrated that properdin can directly bind to *Neisseria gonorrhoeae*, *Chlamydia pneumoniae*, apoptotic and necrotic cells, rabbit erythrocytes, and zymosan particles (26–31). Thus, we suggest that properdin may participate in the recognition of certain microorganism patterns through surface receptors not yet identified. However, this hypothesis is controversial and not completely endorsed by the work of Agarwal and colleagues (32) who did not observe direct binding to *Neisseria* when using physiological forms of properdin. In addition, the binding of physiological forms of properdin to erythrocytes or zymosan was not observed (27). No significant binding of properdin to human endothelial cells (HUVECs), zymosan from *Saccharomyces*

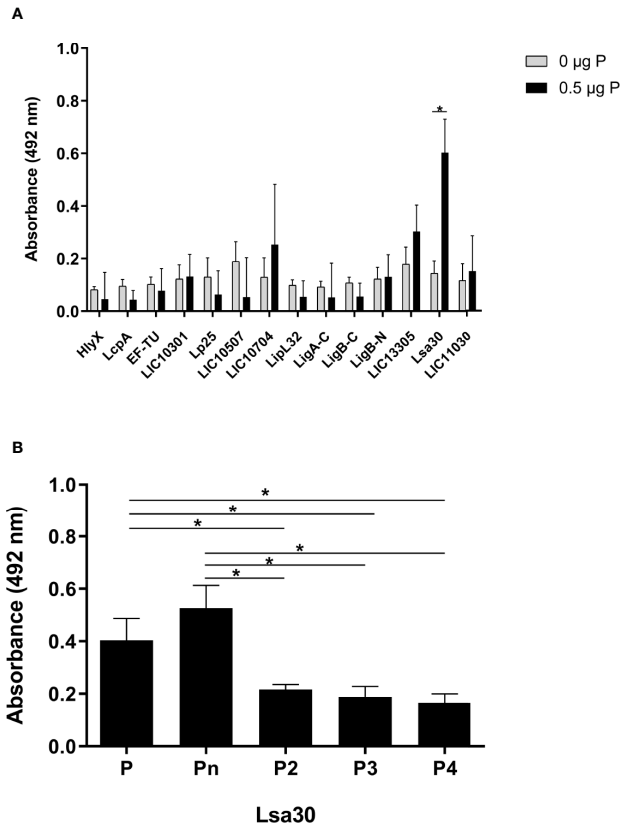

FIGURE 5 | Interaction of outer membrane proteins of *Leptospira* with properdin. **(A)** Recombinant proteins of pathogenic *L. interrogans* serovar Copenhageni 10A (listed in **Table 1**) were immobilized on ELISA plate wells and incubated with 0.5 µg of unfractionated properdin (P). Binding was assessed by ELISA using polyclonal anti-human properdin. **(B)** Recombinant Lsa30 from pathogenic *L. interrogans* was immobilized and incubated with 0.5 µg of properdin (P), P2, P3, or P4. Binding was assessed as described above in **(A)**. These data represent the average (± SD) of three independent experiments, after subtracting the basal values obtained with PBS. Each experiment was performed in triplicate, using two independent preparations of P2, P3, P4, and Pn. Statistically significant differences (ANOVA one-way test) are indicated. *$p \leq 0.05$, confidence interval of 95%.

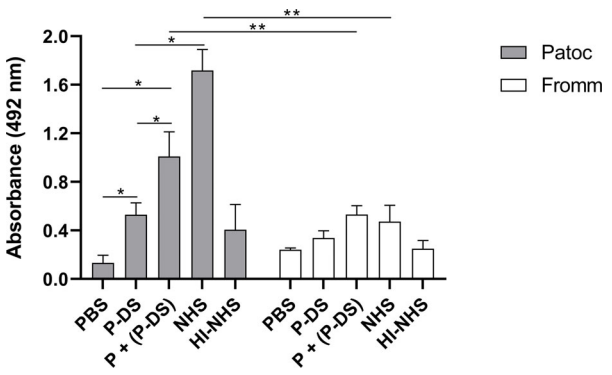

FIGURE 6 | Properdin is required for AP activation on the surface of *L. biflexa* serovar Patoc strain Patoc I. Non-pathogenic *L. biflexa* serovar Patoc strain Patoc I or pathogenic *L. interrogans* serovar Kennewicki strain Fromm were incubated with properdin-depleted human serum (P-DS), normal human serum (NHS), or heat-inactivated NHS (HI-NHS). Where indicated, leptospires were previously treated with 5 µg of purified properdin (P) before incubating with P-DS [(P + (P-DS)]. The presence of the C3 convertase was evaluated by ELISA using polyclonal anti-Factor B Data are expressed as the mean (± SD) of three independent experiments each one performed in triplicate. Statistically significant differences (ANOVA one-way test) are indicated. *$p \leq 0.05$; **$p \leq 0.001$, confidence interval of 95%.

cerevisae and *Escherichia coli* was detected in the presence of compstatin Cp40 (which inhibits C3 cleavage) or C3-DS (33).

Previous studies emphasized the importance of using isolated forms of properdin present in serum, since after the purification process there is formation of high molecular weight properdin (Pn) aggregates that are absent under physiological conditions, and these aggregates could *per se* induce complement activation in the fluid phase (26, 27). In this study, we demonstrate that non-pathogenic and pathogenic leptospires can bind to all properdin oligomers, as well as to unfractionated properdin and Pn form. However, pathogenic leptospires interacted less strongly with P2, P3, and P4 oligomers than with unfractionated properdin and its Pn form. We emphasize that the binding of P2 and P3 to pathogenic leptospires was not significantly different when compared to the negative control. Since P2 and P3 are the most abundant forms of circulating properdin, reduced binding of these two forms to pathogenic *L. interrogans* would diminish AP activation on the surface of these bacteria, thus allowing them to evade complement-mediated host defense.

The kidneys are one of the main target organs for leptospiral colonization, and it has been shown that properdin binds to renal proximal tubule HK-2 cells (34). Thus, we speculate that properdin binding to pathogenic leptospires and to renal cells could be in some extent important for invasion and subsequent dissemination through contaminated urine. This hypothesis remains to be investigated.

As we have been focusing our research efforts on characterizing *Leptospira* virulence factors over the last years, we had a panel of *L. interrogans* serovar Copenhageni 10A recombinant proteins at our disposal. Their possible interaction with properdin was then evaluated. Only Lsa30, a ~32 kDa membrane protein, also known as LIC11087, bound to properdin.

Lsa30 interacted with properdin P2, P3, and P4 as well as to the Pn form. However, the Lsa30 interaction with properdin oligomers P2, P3, and P4 was significantly lower when compared to its interaction with properdin in unfractionated form and Pn. These results are consistent with those observed for pathogenic leptospires, which did not bind significantly to fractionated properdin forms.

Once we had confirmed a direct interaction of properdin with different leptospiral strains, we evaluated whether the properdin bound on the spirochete surface would be able to promote activation of the AP. Pathogenic leptospires showed little or no activation of the AP in the presence of properdin on its surface. This effect can be attributed to: *i)* pathogenic leptospires and Lsa30 do not bind consistently to serum properdin oligomers and, *ii)* pathogenic bacteria interact with Factor H, and negatively regulate complement activation on their surface (3–5).

In response to host defense mechanisms, pathogenic microorganisms express various virulence mechanisms. *Leptospira* evasion mechanisms that directly inhibit properdin function are not yet known. However, a new mechanism was described by Tsao et al. (35) who demonstrate that exotocin B (SPE B), a pyrogenic streptococcal cysteine protease, was able to degrade properdin, impairing the activation of the AP. As a consequence, opsophagocytosis by neutrophils was affected, preventing the death of bacteria by neutrophils. This protease also contributes to the degradation of fibronectin, vitronectin and fibrinogen, and helps the pathogen to evade host defenses and increase its replication. Furthermore, S20NS protein, a tick salivary protein, interacts with properdin and, upon binding, this positive regulator dissociates from C3 convertase, inhibiting complete activation of the AP (36). Evasion of complement by pathogenic leptospires by secretion of proteases that cleave important complement components (C3, C3b, iC3b, C2, and C4) was also observed by our group (37). We evaluated whether such proteases would be able to cleave properdin, and we observed that properdin degradation only occurred under conditions of low specificity with an unsuitable substrate enzyme ratio (data not shown).

Neutrophils are phagocytes rapidly attracted in large numbers to infection sites and are considered an important source of properdin release after inflammatory stimuli such as LPS, C5a and inflammatory cytokines (28, 38). We wondered if neutrophils could internalize more leptospires when coated with properdin, effectively contributing to their elimination at the site of infection. Some studies suggest that the evasion by pathogenic bacteria of the human macrophage cell line (THP-1) from the phagolysosome may be another mechanism presented by these spirochetes to evade innate immunity and later colonize target organs of the cell host (39).

The results presented here contribute to our understanding of the role of properdin in direct interactions with leptospires. Properdin interacts directly or indirectly with pathogenic, attenuated and non-pathogenic leptospires. However, the most abundant forms of properdin present in serum (P2 and P3) do not bind pathogenic leptospires significantly. Thus, we suggest that properdin, besides being a positive regulator of the C3 convertase of the AP, could also participate in the recognition of molecular patterns of *Leptospira* and promote the activation of the complement by the AP. Studies aimed at identifying whether properdin can bind directly to leptospires *in vivo* and play a significant role in infectivity are warranted.

DATA AVAILABILITY STATEMENT

The raw data supporting the conclusions of this article will be made available by the authors, without undue reservation.

AUTHOR CONTRIBUTIONS

AG and LI designed the experiments. AG performed the experiments. GS and VF provided the fractioned purified properdin forms. SA provided the bacterial cultures. PH, PA, and AB provided the *Leptospira* recombinant proteins. AG, AB, and LI wrote the manuscript. All authors contributed to the article and approved the submitted version.

FUNDING

This work was supported by Fundação de Amparo à Pesquisa do Estado de São Paulo (FAPESP), Brazil (Proc # 2017/12924-3)). AG received student fellowships from FAPESP (2012/23708-6) and Conselho Nacional de Pesquisa e Desenvolvimento Científico (CNPq), Brazil (Proc. 141874/2012-0).

REFERENCES

1. Vincent AT, Schiettekatte O, Goarant C, Neela VK, Bernet E, Thibeaux R, et al. Revisiting the taxonomy and evolution of pathogenicity of the genus *Leptospira* through the prism of genomics. *PLoS Negl Trop Dis* (2019) 13(5): e0007270. doi: 10.1371/journal.pntd
2. Fraga TR, Isaac L, Barbosa AS. Complement Evasion by Pathogenic *Leptospira*. Front. *Immunol* (2016) 7:623:623. doi: 10.3389/fimmu.2016.00623
3. Meri T, Murgia R, Stefanel P, Meri S, Cinco M. Regulation of complement activation at the C3-level by serum resistant leptospires. *Microb Pathog* (2005) 39:139–47. doi: 10.1016/j.micpath.2005.07.003
4. Barbosa AS, Abreu PA, Vasconcellos AS, Morais ZM, Gonçales AP, Silva AS, et al. Immune evasion of *Leptospira* spp. by acquisition of human complement regulator C4BP. *Infect Immun* (2009) 77:1137–43. doi: 10.1128/IAI.01310-08
5. Castiblanco-Valencia MM, Fraga TR, Silva LB, Monaris D, Abreu PA, Strobel S, et al. Leptospiral immunoglobulin-like proteins interact with human complement regulators factor H, FHL-1, FHR-1, and C4BP. *J Infect Dis* (2012) 205(6):995–1004. doi: 10.1093/infdis/jir875
6. Goundis D, Reid KB. Properdin, the terminal complement components, thrombospondin and the circumsporozoite protein of malaria parasites contain similar sequence motifs. *Nature* (1988) 335:82–5. doi: 10.1038/335082a0
7. Higgins JM, Wiedemann H, Timpl R, Reid KB. Characterization of mutant forms of recombinant human properdin lacking single thrombospondin type I repeats. Identification of modules important for function. *J Immunol* (1995) 155(12):5777–85.
8. Nolan KF, Kaluz S, Higgins JM, Goundis D, Reid KB. Characterization of the human properdin gene. *Biochem J* (1992) 287:291–7. doi: 10.1042/bj2870291
9. Smith CA, Pangburn MK, Vogel CW, Muller-Eberhard HJ. Molecular architecture of human properdin, a positive regulator of the alternative pathway of complement. *J Biol Chem* (1984) 259(7):4582–8.
10. Chen JY, Cortes C, Ferreira VP. Properdin: A multifaceted molecule involved in inflammation and diseases. *Mol Immunol* (2018) 102:58–72. doi: 10.1016/j.molimm.2018.05.018
11. de Paula PF, Barbosa JE, Junior PR, Ferriani VP, Latorre MR, Nudelman V, et al. Ontogeny of complement regulatory proteins - concentrations of factor h, factor I, C4b-binding protein, properdin and vitronectin in healthy children of different ages and in adults. *Scand J Immunol* (2003) 58(5):572–7. doi: 10.1046/j.1365-3083.2003.01326.x
12. Kouser L, Abdul-Aziz M, Nayak A, Stover CM, Sim RB, Kishore U. Properdin and factor H: opposing players on the alternative complement

pathway "see-saw". *Front Immunol* (2013) 23:93(4):93. doi: 10.3389/fimmu.2013.00093
13. Pillemer L, Blum L, Lepow IH, Ross OA, Todd EW, Wardlaw AC. The properdin system and immunity: I. Demonstration and isolation of a new serum protein, properdin, and its role in immune phenomena. *Science* (1954) 120:279–85. doi: 10.1126/science.120.3112.279
14. Fearon DT. Regulation of the amplification C3 convertase of human complement by an inhibitory protein isolated from human erythrocyte membrane. *Proc Natl Acad Sci USA* (1979) 76(11):5867–71. doi: 10.1073/pnas.76.11.5867
15. Pangburn MK, Müller-Eberhard HJ. The alternative pathway of complement. *Springer Semin Immunopathol* (1984) 7(2-3):163–92. doi: 10.1007/BF01893019
16. Fearon DT, Austen KF. Properdin: binding to C3b and stabilization of the C3b dependent C3 convertase. *J Exp Med* (1975) 142:856–63. doi: 10.1084/jem.142.4.856
17. Barbosa AS, Abreu PA, Neves FO, Atzingen MV, Watanabe MM, Vieira ML, et al. A newly identified leptospiral adhesin mediates attachment to laminin. *Infect Immun* (2006) 74(11):6356–64. doi: 10.1128/IAI.00460-06
18. Moreno-Torres A, Malvido-Jiménez IR, Peña-Moctezuma A, Castillo Sánchez LO, Fraga TR, Barbosa AS, et al. Culture-attenuated pathogenic *Leptospira* lose the ability to survive to complement-mediated-killing due to lower expression of factor H binding proteins. *Microbes Infect* (2019) 21(8-9):377–85. doi: 10.1016/j.micinf.2019.03.001
19. Alves da Silva PYO, Midon LM, Heinemann MB, de Moraes Vasconcelos D, Barbosa AS, Isaac L. Contribution of Complement System pathways to the killing of *Leptospira* spp. *Microbes Infect* (2020) S1286-4579(20):30143–X. doi: 10.1016/j.micinf.2020.07.005
20. Choy HA. Multiple activities of LigB potentiate virulence of *Leptospira* interrogans: inhibition of alternative and classical pathways of complement. *PloS One* (2012) 7(7):e41566. doi: 10.1371/journal.pone.0041566
21. Castiblanco-Valencia MM, Fraga TR, Pagotto AH, Serrano SM, Abreu PA, Barbosa AS, et al. Plasminogen cleaves fibrinogen and the human complement proteins C3b and C5 in the presence of *Leptospira interrogans* proteins: A new role of LigA and LigB in invasion and complement immune evasion. *Immunobiology* (2016) 221(5):679–89. doi: 10.1016/j.imbio.2016.01.001
22. Sjöholm AG. Inherited complement deficiency states: implications for immunity and immunological disease. *APMIS* (1990) 98(10):861–74. doi: 10.1111/j.1699-0463.1990.tb05008.x
23. Schejbel L, Rosenfeldt V, Marquart H, Valerius NH, Garred P. Properdin deficiency associated with recurrent otitis media and pneumonia, and identification of male carrier with Klinefelter syndrome. *Clin Immunol* (2009) 131:456–62. doi: 10.1016/j.clim.2009.02.008
24. Skattum L, van Deuren M, van der Poll T, Truedsson L. Complement deficiency states and associated infections. *Mol Immunol* (2011) 48 (14):1643–55. doi: 10.1016/j.molimm.2011.05.001
25. Barbosa AS, Isaac L. Complement Immune Evasion by Spirochetes. *Curr Top Microbiol Immunol* (2018) 415:215–38. doi: 10.1007/82_2017_47
26. Cortes C, Ferreira VP, Pangburn MK. Native properdin binds to *Chlamydia pneumoniae and* promotes complement activation. *Infect Immun* (2011) 79 (2):724–31. doi: 10.1128/IAI.00980-10
27. Ferreira VP, Cortes C, Pangburn MK. Native polymeric forms of properdin selectively bind to targets and promote activation of the alternative pathway of complement. *Immunobiology* (2010) 215(11):932:40. doi: 10.1016/j.imbio.2010.02.002
28. Kemper C, Hourcade DE. Properdin: New roles in pattern recognition and target clearance. *Mol Immunol* (2008) 45(16):4048–56. doi: 10.1016/j.molimm.2008.06.034
29. Kemper C, Mitchell LM, Zhang L, Hourcade DE. The complement protein properdin binds apoptotic T cells and promotes complement activation and phagocytosis. *Proc Natl Acad Sci USA* (2008) 105(26):9023–8. doi: 10.1073/pnas.0801015105
30. Spitzer D, Mitchell LM, Atkinson JP, Hourcade DE. Properdin can initiate complement activation by binding specific target surfaces and providing a platform for de novo convertase assembly. *J Immunol* (2007) 179:2600–8. doi: 10.4049/jimmunol.179.4.2600
31. Xu W, Berger SP, Trouw LA, de Boer HC, Schlagwein N, Mutsaers C, et al. Properdin binds to late apoptotic and necrotic cells independently of C3b and regulates alternative pathway complement activation. *J Immunol* (2008) 180 (11):7613–21. doi: 10.4049/jimmunol.180.11.7613
32. Agarwal S, Ferreira VP, Cortes C, Pangburn MK, Rice PA, Ram S. An evaluation of the role of properdin in alternative pathway activation on *Neisseria meningitidis* and *Neisseria gonorrhoeae*. *J Immunol* (2010) 185 (1):507–16. doi: 10.4049/jimmunol.0903598
33. Harboe M, Johnson C, Nymo S, Ekholt K, Schjalm C, Lindstad JK, et al. Properdin binding to complement activating surfaces depends on initial C3b deposition. *Proc Natl Acad Sci USA* (2017) 114(4):E534–9. doi: 10.1073/pnas.1612385114
34. Gaarkeuken H, Siezenga MA, Zuidwijk K, van Kooten C, Rabelink TJ, Daha MR, et al. Complement activation by tubular cells is mediated by properdin binding. *Am J Physiol Renal Physiol* (2008) 295:F1397–403. doi: 10.1152/ajprenal.90313.2008
35. Tsao N, Tsai WH, Lin YS, Chuang WJ, Wang CH, Kuo CF. Streptococcal pyrogenic exotoxin B cleaves properdin and inhibits complement-mediated opsonophagocytosis. *Biochem Biophys Res Commun* (2006) 339(3):779–84. doi: 10.1016/j.bbrc.2005.11.078
36. Tyson KR, Elkins C, de Silva AM. A novel mechanism of complement inhibition unmasked by a tick salivary protein that binds to properdin. *J Immunol* (2008) 180(6):3964–8. doi: 10.4049/jimmunol.180.6.3964
37. Fraga TR, Courrol D, dos S, Castiblanco-Valencia MM, Hirata IY, Vasconcellos SA, et al. Immune evasion by pathogenic *Leptospira* strains: the secretion of proteases that directly cleave complement proteins. *J Infect Dis* (2014) 209(6):876–86. doi: 10.1093/infdis/jit569
38. Kemper C, Atkinson JP, Hourcade DE. Properdin: emerging roles of a pattern-recognition molecule. *Ann Rev Immunol* (2020) 28:131–55. doi: 10.1146/annurev-immunol-030409-101250
39. Li S, Ojcius DM, Liao S, Li L, Xue F, Dong H, et al. Replication or death: distinct fates of pathogenic Leptospira strain Lai within macrophages of human or mouse origin. *Innate Immun* (2010) 16(2):80–92. doi: 10.1177/1753425909105580

Conflict of Interest: The authors declare that the research was conducted in the absence of any commercial or financial relationships that could be construed as a potential conflict of interest.

frontiers in Immunology

ORIGINAL RESEARCH
published: 19 November 2020
doi: 10.3389/fimmu.2020.572326

Trichinella spiralis Calreticulin S-Domain Binds to Human Complement C1q to Interfere With C1q-Mediated Immune Functions

*Shuai Shao[1], Chunyue Hao[1], Bin Zhan[2], Qinghui Zhuang[1], Limei Zhao[1], Yi Chen[1], Jingjing Huang[1] and Xinping Zhu[1]**

[1] Department of Medical Microbiology and Parasitology, School of Basic Medical Sciences, Capital Medical University, Beijing, China, [2] Department of Pediatrics, National School of Tropical Medicine, Baylor College of Medicine, Houston, TX, United States

Helminths develop strategies to escape host immune responses that facilitate their survival in the hostile host immune environment. *Trichinella spiralis*, a tissue-dwelling nematode, has developed a sophisticated strategy to escape complement attack. Our previous study demonstrated that *T. spiralis* secretes calreticulin (*Ts*CRT) to inhibit host classical complement activation through binding to C1q; however, the C1q binding site in *Ts*CRT and the specific mechanism involved with complement-related immune evasion remains unknown. Using molecular docking modeling and fragment expression, we determined that *Ts*CRT-S, a 153-aa domain of *Ts*CRT, is responsible for C1q binding. Recombinant *Ts*CRT-S protein expressed in *Escherichia coli* had the same capacity to bind and inhibit human C1q-induced complement and neutrophil activation, as full-length *Ts*CRT. *Ts*CRT-S inhibited neutrophil reactive oxygen species and elastase release by binding to C1q and reduced neutrophil killing of newborn *T. spiralis* larvae. Binding of *Ts*CRT-S to C1q also inhibited formation of neutrophil extracellular traps (NETs), which are involved in autoimmune pathologies and have yet to be therapeutically targeted. These findings provide evidence that the *Ts*CRT-S fragment, rather than the full-length *Ts*CRT, is a potential target for vaccine or therapeutic development for trichinellosis, as well as for complement-related autoimmune disease therapies.

Keywords: *Trichinella spiralis*, calreticulin S-domain, binding site, complement C1q, classical complement activation, immune evasion, neutrophil, neutrophil extracellular traps

OPEN ACCESS

Edited by:
Iara De Messias Reason, Federal University of Paraná, Brazil

Reviewed by:
Lu Huang, University of Arkansas for Medical Sciences, United States
Tomabu Adjobimey, University Hospital Bonn, Germany

***Correspondence:**
Xinping Zhu
zhuxping@ccmu.edu.cn

Specialty section:
This article was submitted to Microbial Immunology, a section of the journal Frontiers in Immunology

Received: *13 June 2020*
Accepted: *20 October 2020*
Published: *19 November 2020*

Citation:
Shao S, Hao C, Zhan B, Zhuang Q, Zhao L, Chen Y, Huang J and Zhu X (2020) Trichinella spiralis Calreticulin S-Domain Binds to Human Complement C1q to Interfere With C1q-Mediated Immune Functions. Front. Immunol. 11:572326. doi: 10.3389/fimmu.2020.572326

INTRODUCTION

Trichinellosis, caused by the parasitic nematode, *Trichinella spiralis*, is a serious food-borne parasitic zoonosis affecting more than 11 million people worldwide (1). *T. spiralis* is a tissue-dwelling nematode with three life cycle stages: adult, newborn larvae (NBL), and infective muscle larvae (ML), which is encysted in host muscle tissue (2). During the life cycle, the parasite establishes orchestrated immune evasion strategies to avoid host immune attacks, from both the innate and adaptive immune systems.

The complement system is an important component of innate immunity that enhances the abilities of antibodies and phagocytic cells to clear microbes. Activated complement also directly attacks cell membranes and kills invading pathogens, including parasites (3). Over long-term evolution with their hosts, parasitic nematodes have developed sophisticated mechanisms to evade host complement attack. One mechanism used in this evasion is secretion of functional proteins that bind to different complement system components and interfere with their functions (4). *Ts*CRT is a calreticulin protein secreted by *T. spiralis* that has important roles in immunomodulation of the host immune system, including direct binding to the complement component, C1q (5), which is the initiator of the classical complement activation pathway, triggering a multistep activation cascade on binding to an immune complex (IC) (6). C1q is also involved in various cell processes by binding to its receptors on immune cells, such as macrophages, eosinophils, and neutrophils, to enhance their defensive abilities (7, 8). *T. spiralis* is a tissue-dwelling nematode, and its larvae invade intestinal epithelial cells and migrate to striated muscle, where they form an infective encysted ML. During this stage, the nematode is vulnerable to the host immune response, particularly complement attack, and *Ts*CRT is a multifunctional protein expressed by the nematode to bind to C1q and inactivate complement-mediated damage (5). Other parasites, like the intracellular protozoa *Trypanosoma cruzi*, filarial parasite *Brugia malayi*, hookworm *Necator americanus*, and nematode *Haemonchus contortus* also produce calreticulin to bind with C1q and inhibit classical complement activation on the parasite surface, thereby avoiding opsonization, immune stimulation, and lytic effects, as an immune evasion strategy (9–13).

In addition to initiating classic complement activation, C1q stimulates chemotaxis of neutrophils to the pathogen invaded region, and enhances their defense functions (14), which include production of reactive oxygen species (ROS) and neutrophil elastase (NE) (15, 16). C1q can also interact with a broad range of self and non-self ligands, such as IgG, IgM, the globular C1q receptor (gC1qR), β-amyloid peptide, lipopolysaccharide, and viral proteins, *via* its heterotrimeric globular head domain, which is composed of A (ghA), B (ghB), and C (ghC) chains (17). We previously demonstrated that *Ts*CRT can bind to host C1q; nevertheless, how the interaction of *Ts*CRT with C1q facilitates the survival of *T. spiralis* in the host under attack from complement and inflammatory cells, such as neutrophils, is not clear.

Calreticulin is a multifunctional protein with three distinct structural and functional domains: a globular N-domain, an extended proline-rich P-domain, and an acidic C-domain. The N and P domains are responsible for its chaperone function in the endoplasmic reticulum, while the C-domain contains a large number of negatively charged amino acids, responsible for high-capacity Ca^{2+} storage (18). A C1q-binding site has been located in the S-domain, which spans the intersection of the N and P domains of human calreticulin (19, 20). The tissue-dwelling filaria, *Brugia malayi*, secretes calreticulin (*Bm*CRT), that binds to host C1q through its N and P domains to inhibit the C1q-initiated classical pathway (11). Further, *Haemonchus contortus* calreticulin (*Hc*CRT) also uses its N domain to bind to C1q protein and restrict complement hemolytic activity (21). Nevertheless, the specific C1q binding site in *Ts*CRT has yet to be determined. Analysis and identification of the C1q binding site in the *Ts*CRT structure could further elucidate the mechanism involved in *T. spiralis* immune evasion and inform the development of strategies to enhance host immune responses to *Ts*CRT as a vaccine.

In addition to its functions in host defense, inappropriate activation or dysregulation of complement components can contribute to the development of autoimmune disease (22, 23). Neutrophil extracellular traps (NETs) are extracellular web-like structures, mainly comprised of DNA, histones, and granule proteins, such as elastase, and function to trap and kill invading pathogens, such as bacteria, fungi, viruses, and parasites (24, 25). IC-triggered C1q-initiated activation of the classical complement pathway can stimulate NET formation (NETosis) (26). In addition to the defense function of NETs, increasing evidence indicates that NETosis can also contribute to the pathogenesis of autoimmune disease (26, 27). Effective inhibitors of NETosis have been sought as potential therapeutic agents for autoimmune diseases (28, 29), and some complement modulators have been developed for the treatment of rheumatic diseases (30). Due to its strong C1q binding and inhibition functions, *Ts*CRT could be used to inhibit IC-C1q-initiated classical complement activation and NET formation and is, therefore, a potential therapeutic agent for autoimmune disorders, such as systemic lupus erythematosus, rheumatoid arthritis, psoriasis, and antiphospholipid syndrome (29).

In this study, the C1q binding site in *Ts*CRT was identified and shown to confer immunomodulatory functions, including inhibition of classical complement activation, C1q-mediated neutrophil functions, and NET formation. Determination of the C1q binding site in *Ts*CRT has potential to facilitate vaccine development against *T. spiralis* infection, as well as potential therapeutic targets for autoimmune diseases involving complement.

MATERIALS AND METHODS

Experimental Animals

Female BALB/c mice aged 6–8 weeks were purchased from the Laboratory Animal Services Center of Capital Medical University (Beijing China) and maintained under specific pathogen-free conditions at 20 ± 2 °C; humidity, 60 ± 10%. All animal protocols were approved by Capital Medical University Animal Care and Use Committee (approval number: AEEI-2017-133) and complied with the NIH Guidelines for the Care and Use of Laboratory Animals.

Sera

Normal human serum (NHS) was collected from the blood of healthy human volunteers, according to a protocol approved by the Institutional Review Board (IRB) of Capital Medical University (approval number: 2016SY01). Human C1q-deficient serum (C1q-D) was purchased from Merck (Darmstadt, Germany).

Parasites

T. spiralis (strain ISS 533) was maintained in female mice, and NBL were collected from fertile female adult worms cultured in phenol red-free RPMI 1640 (Gibco by Life Technologies, Carlsbad, USA) with 1× penicillin–streptomycin (Solarbio, Beijing, China) at 37°C for 48 h.

Molecular Docking

Molecular docking of *Ts*CRT with human complement C1q was performed using Discovery Studio 2017 software (Neotrident Technology Ltd., Beijing, China). The three-dimensional structure of *Ts*CRT was developed using the structure of calreticulin arm domains (PDB: 3RG0) as a template. The best *Ts*CRT structure was acquired, according to the DOPE score and PDF total energy. Alignment of the *Ts*CRT sequence (XP_003371379.1) with the template was conducted and a refined structure generated. Docking was conducted using ZDOCK and refined with RDOCK in Discovery Studio 2017.

Expression of Recombinant *Ts*CRT and Its Fragment Proteins

Based on the structure of calreticulin, full-length *Ts*CRT (*Ts*CRT, 22–413 amino acids (aa)) and its various domain fragments were expressed as recombinant proteins in *Escherichia coli*. The domain fragments included the NP-domain (22–331 aa), P-domain (*Ts*CRT-P, 172–331 aa), C-domain (*Ts*CRT-C, 332–413 aa), and S-domain, a potential C1q binding site spanning the N and P domains (*Ts*CRT-S, 135–288 aa) (**Figure 2A**). The DNA sequences encoding these fragments were subcloned into the pET-24a bacterial expression vector (Novagen, Darmstadt, Germany) using the specific primers listed in **Table 1**. Recombinant plasmids with confirmed correct sequences were transformed into *E. coli* BL21(DE3). Recombinant fragments with c-terminal His-tags (r*Ts*CRT, r*Ts*CRT-NP, r*Ts*CRT-P, r*Ts*CRT-S, and r*Ts*CRT-C) were expressed by induction using 1 mM IPTG at 37°C for 3.5 h, and then purified by Ni-affinity chromatography (Novagen, Madison, USA). Endotoxin contaminating the purified recombinant proteins was removed using Pierce High Capacity Endotoxin Removal Resin (Invitrogen, Carlsbad, CA, USA), and endotoxin removal was confirmed using the ToxinSensor Endotoxin Detection System (GenScript, Nanjing, China). The concentration of purified proteins was measured using a BCA Protein Assay Kit (Thermo Fisher, Carlsbad, USA).

Assays for *Ts*CRT and Its Human C1q Binding Fragments

ELISA

To compare the binding affinity of *Ts*CRT and its fragments to C1q, 96-well plates were coated with different amounts of human C1q (0, 0.05, 0.1, 0.2, 0.4, 0.8, 1.2, and 1.5 μg/ml) (Millipore, Darmstadt, Germany) in 100 μl/well of coating buffer (100 mM Na_2CO_3/$NaHCO_3$, pH 9.6) overnight at 4°C. The same amounts of BSA were coated in the control wells. Wells were then washed with PBS + 0.05% Tween-20 (PBST) three times, followed by blocking with 200 μl 3% BSA in PBS at 37°C for 1 h. After further washing, 100 μl of 40 nM r*Ts*CRT, r*Ts*CRT-NP, r*Ts*CRT-P, r*Ts*CRT-S, and r*Ts*CRT-C in binding buffer (100 μl of 20 mM Tris–HCl, pH 7.4, 50 mM NaCl, and 1 mM $CaCl_2$) was added to each well and incubated for 1 h at room temperature. Mouse anti-His mAb (1:10,000, Tiangen, Beijing, China) and HRP-conjugated goat anti-mouse IgG (1:10,000, BD Biosciences, Franklin Lakes, USA) were used as primary and secondary antibodies, respectively. After washing with PBST, the substrate, o-phenylenediamine dihydrochloride (Sigma, St. Louis, MO, USA) was added; colorimetric detection was performed using TMB and the absorbance measured at 450 nm using an ELISA reader (Thermo Fisher).

Far Western Blotting

Human C1q (5 μg) and BSA (5 μg) were separated on 12% SDS-PAGE gels and transferred onto nitrocellulose membranes, which were blocked with 3% BSA and then incubated with 5 μg/ml of r*Ts*CRT, r*Ts*CRT-NP, r*Ts*CRT-P, r*Ts*CRT-S, and r*Ts*CRT-C in binding buffer containing 1 mM $CaCl_2$ at 37°C for 2 h. Anti-His mAb (1:5,000) was used to detect each fragment bound to C1q, with IRDye 800CW-conjugated anti-mouse IgG (Li-COR, Lincoln, NE, USA) as the secondary antibody, followed by visualization using an Odyssey CLx Infrared Imaging System.

Immunoprecipitation

To determine whether Ca^{2+} was required for binding of *Ts*CRT-S to C1q, r*Ts*CRT-S (2 μg) was incubated with anti-His mAb (2 μg) and Protein G MicroBeads (Miltenyi Biotec, Cologne, Germany) in PBS (50 μl) with or without 1 mM $CaCl_2$ for 30 min on ice. Human C1q (3 μg) was added into the bead complex and incubated overnight at 4°C. After washing in washing buffer (1% NP40, 50 mM Tris–HCl, 50 mM NaCl, pH 8.0), the binding complex on the beads was stripped with preheated loading buffer (1× SDS, 50 mM Tris–HCl) using a magnetic field. Then, the

TABLE 1 | Primers used in expression of each fragment of *Ts*CRT.

	Forward	Reverse
***Ts*CRT**	CTAGCTAGCGAGCCGACCATTTACCTCAAG	GCCTCGAGTCAATGATGATGATGATGATGCAGCTCTTCTTTAACATTTTC
***Ts*CRT-NP**	CTAGCTAGCGAGCCGACCATTTACCTCAAG	GCCTCGAGTCAATGATGATGATGATGATGTTCAAAACCGATTGCCCCAAG
***Ts*CRT-P**	CTAGCTAGCACGCATGCGTACAAATTAATC	GCCTCGAGTCAATGATGATGATGATGATGTTCAAAACCGATTGCCCCAAG
***Ts*CRT-S**	CTAGCTAGCATGTTCGGACCTGATATATGTGGACCA	GCCTCGAGTCAATGATGATGATGATGATGATCAGGATTTGGAATTTGTTCCGGTGCCC
***Ts*CRT-C**	CTAGCTAGCCTGTATCGATACAAAGGT	GCCTCGAGTCAATGATGATGATGATGATGCAGCTCTTCTTTAACATTTTC

eluted protein complex was separated by SDS-PAGE and transferred onto a nitrocellulose membrane. Rabbit anti-human C1qA antibody (1:10,000) (Abcam, Cambridge, UK) was used to detect the C1q immunoprecipitated with r*Ts*CRT-S. Binding conditions without Ca^{2+} were used as a control.

r*Ts*CRT-S Inhibits C1q-Induced Classical Complement Activation

C4b and C3b Deposition Assay

C1q-induced classical complement activation was performed as previously described (5). Briefly, human IgM (2 μg/ml) (Millipore) was used to coat 96-well plates, which were incubated with 100 μl/well of C1q (1 μg) that had been pre-incubated with different amounts of r*Ts*CRT-S (1, 2, and 4 μg), r*Ts*CRT (2 μg), or BSA (2 μg) at 37°C for 1 h. The plates were washed with PBST and incubated with C1q-D (1:100) in $GVBS^{++}$ buffer (1× Veronal buffer, Lonza, Switzerland), containing 0.1% gelatin, 0.15 mM $CaCl_2$, and 1 mM $MgCl_2$) for 1 h at 37°C. NHS (1:50) served as a positive control. Subsequently, mouse anti-human C4b mAb and rabbit anti-human C3b polyclonal antibodies (Abcam, Cambridge, UK) at dilution of 1:5,000, were used to probe the classical complement activation intermediate products, C4b and C3b, and HRP-conjugated goat anti-mouse or goat anti-rabbit IgG (1:10,000, BD Biosciences) used to detect the deposited C4b and C3b. Absorbance was read at 450 nm using an ELISA reader.

Hemolytic Assay

To determine the inhibition effect of r*Ts*CRT-S on C1q-initiated classical complement activation-mediated hemolysis, human IgM (2 μg/ml) was coated in 96-well plates. 1 μg of C1q was incubated with different amounts of r*Ts*CRT-S, (0.5, 1, 2, 4, and 6 μg), r*Ts*CRT (4 μg), or BSA (6 μg), followed by addition of C1q-D (1:50) in 1× $HBSS^{++}$ (Hank's balanced salt solution, Thermo Fisher, containing 1 mM $MgCl_2$ and 0.15 mM $CaCl_2$) for 1 h at 37°C. Fresh sheep red blood cells (SRBC, 5×10^6 cells/ml in $HBSS^{++}$) were sensitized using rabbit anti-SRBC antibody (Sigma, USA) at 37°C for 30 min, then added into the reaction complex with C1q-D for 30 min. Hemolysis was stopped using cold $HBSS^{++}$ containing 10 mM EDTA. The mixture was then centrifuged at 1,500 × g for 10 min. Hemoglobin in the supernatant was measured at an absorbance of 412 nm. Hemolytic activity was calculated as a percentage of total hemolysis in water.

Culture and Differentiation of HL60 Cells

The human promyelocyte cell line, HL60, carries many neutrophil receptors and can be differentiated into neutrophil-like cells for studies of neutrophil function (31). HL60 cells were obtained from ATCC and maintained in RPMI 1640 medium (Invitrogen) containing 10% fetal bovine serum (FBS, Gibco) and 1× penicillin–streptomycin. Cells were stimulated with 1 μM all-trans retinoic acid (ATRA) (Sigma) for 5 days to differentiate into neutrophil-like cells (dHL60) (32, 33). To confirm dHL60 cell differentiation, ATRA-induced HL60 cells were resuspended in FBS-free RPMI 1640 medium and allowed to settle for 20 min for differentiated dHL60 cells to adhere on round glass slides in a 24-well plate, followed by fixing in 4% paraformaldehyde for 40 min (34). Adhered cells were washed with PBS and stained with DAPI dye (Zhongshanjinqiao, Beijing, China) for observation of lobulated nuclei. Differentiation of dHL60 cells was also confirmed by evaluating expression of CD11b and CD66a *via* qPCR and flow cytometry.

Neutrophil Isolation From Human Peripheral Blood

Human polymorphonuclear neutrophils (PMNs) were isolated from the peripheral blood of a healthy volunteer, using Ficoll-Paque PLUS (Solarbio) with a standard protocol. Briefly, whole fresh blood was collected in a heparin-coated tube, and PMNs were purified by density gradient centrifugation (1000 × g, 30 min) and hypotonic erythrocyte lysis on ice for 10 min. Cells were counted and suspended in RPMI 1640 medium containing 10% FBS.

r*Ts*CRT-S Inhibits C1q-Induced dHL60 Activity

C1q Binding Inhibition

To determine whether r*Ts*CRT-S or r*Ts*CRT inhibited C1q binding to C1q receptor on dHL60 cells, C1q (25 nM) was pre-incubated with different amounts of r*Ts*CRT-S (0, 0.5, 1, and 2 μM) or r*Ts*CRT (2 μM), then added to dHL60 cells that adhered on 96-well plates (5×10^4/well) or coverslips (3×10^5/well), as described above, for 1 h at 37°C. After washing, rat anti-C1q mAb (1:100, Abcam) was used to detect the binding of C1q to dHL60 cells at 4°C overnight, and DyLight 488-conjugated goat anti-rat IgG (1:100) (KPL, Milford, USA) was used as the secondary antibody. After staining, the mean fluorescence intensity (MFI) of C1q on cells in the 96-well plate was measured by High Content Analysis (Thermo Fisher). Cells containing C1q and nuclei staining were captured and analyzed by confocal laser scanning microscopy (Leica).

Transwell Chemotaxis Assay

To determine the effects of r*Ts*CRT-S and r*Ts*CRT on C1q-induced chemotactic migration of dHL60 cells, a Transwell chamber with 3-μm-pore membranes (Corning, NY, USA) was inserted in a 24-well plate. dHL60 cells (2×10^5 per well) were added to the upper chamber in 1640 medium with 5% FBS. The lower chamber was filled with C1q (50 nM) pre-incubated with different amounts of r*Ts*CRT-S or r*Ts*CRT (50 and 100 nM) in FBS-free medium to induce chemotactic migration at 37°C in a 5% CO_2 incubator for 6 h. After washing, cells that had migrated through the membrane into the lower chamber were counted using a Celigo® Image Cytometer (Nexcelom, Lawrence, MA, USA). BSA or recombinant proteins (100 nM) without C1q were used as negative controls.

Measurement of Reactive Oxygen Species

To measure the effect of *Ts*CRT on C1q-induced neutrophil activity, ROS produced by activated neutrophils was detected with 2′,7′-dichlorofluorescin diacetate (DCFH-DA, Sigma). C1q

was coated in 96-well plates (1 μg/well) at 4°C overnight, then incubated with different amounts of r*Ts*CRT-S or r*Ts*CRT (0, 0.5, 1, and 2 μM) in binding buffer at 37°C for 1 h. BSA (2 μM) was used as a control protein. PMA (160 nM) was used as a positive stimulation control. The ROS inhibitor, cysteamine (5 mM), was used as a negative control. A total of 5×10^4 dHL60 cells were added in each well. After being incubated at 37°C in a 5% CO_2 incubator overnight, ROS activity from HL60 cells was detected using 10 μM DCFH-DA. Hoechst 33342 was used to stain nuclei in living cells. ROS content was quantified as MFI using High Content Analysis.

Measurement of Neutrophil Elastase

dHL60 cells were stimulated with C1q pre-incubated with different amounts of r*Ts*CRT-S or r*Ts*CRT in 96-well plates, as described above. The NE activity of C1q-stimulated dHL60 cells was measured using a NE activity kit (Abcam) on a fluorescence microplate reader (FLx800, BioTek) at 380/500 nm. The elastase inhibitor, SPCK (60 μM), was used as a negative control.

C1q-Mediated Neutrophil Attack on NBL *In Vitro*

To determine whether r*Ts*CRT-S or r*Ts*CRT influences C1q-induced neutrophil killing on NBL, a CellTiter-Glo® Luminescent Cell Viability Assay (Promega, Madison, WI, USA) was used to measure ATP levels in parasites, to determine NBL viability (35, 36). Briefly, C1q was coated on 24-well plates (3 μg/well) at 4°C overnight, followed by incubation with different amounts of r*Ts*CRT-S or r*Ts*CRT (0, 3, and 6 μM) and BSA (6 μM) in 300 μl binding buffer at 37°C for 60 min. Next, each well was filled with PMN isolated from a healthy donor (5×10^5/500 μl), a transwell chamber added into each well, and a total of 500 NBL added to each upper chamber. After incubation at 37°C for 48 h, NBL in the upper chambers were collected and washed with phenol red-free 1640 medium. CellTiter-Glo® Reagent was added, and ATP activity in the larvae was measured, according to the manufacturer's instruction. The luminescence generated was measured using a fluorescence microplate reader (FLx800, BioTek). ATP levels were calculated using a standard curve generated from the ATP levels in untreated control NBL.

Neutrophil Extracellular Traps Assays

Quantitation of NET Formation

Cell-free extracellular DNA released by neutrophils is an important component of neutrophil extracellular traps (NETs). To determine the potential *Ts*CRT inhibition of complement-induced NETosis, through reduction of C1q function, DNA involved in net-like NET was digested using DNase I and free DNA measured using PicoGreen. IC was generated by incubating 10 μl anti-chicken egg albumin antibody (Sigma) with an equal volume of 0.25 mg/ml albumin from chicken egg (Sigma) at 37°C for 30 min. C1q (2 μg) was pre-incubated with different amounts of r*Ts*CRT-S, r*Ts*CRT (0, 0.1, 0.3, and 0.9 μM), or BSA (0.9 μM) in 50 μl binding buffer at 37°C for 60 min, followed by incubation with IC at 37°C for 30 min. Subsequently, mixtures were added to 300 μl $GVBS^{++}$ buffer with 3% C1q-D and incubated at 37°C for 30 min, to activate the complement system. For NET formation induced by activated complement, this combination was added to dHL60 or PMN cells adhered in 96-well plates (10^4/well). Cells were incubated for 6 h (dHL60) or 1 h 40 min (PMN) at 37°C in a 5% CO_2 incubator. H_2O_2 (0.05%) was further added into dHL60 cells to enhance NET formation. DNase I (200 U/ml; Roche) was added to each well to digest released extracellular DNA for 10 min in a 37°C incubator. After centrifugation, supernatants containing digested DNA were transferred into a new 96-well plate and mixed 1:1 (v/v) with PicoGreen reagent (Thermo Fisher). Fluorescence was then quantified on a BioTek microplate reader at 485 nm/528 nm.

Observation of NET Formation by Fluorescence Confocal Microscopy

dHL60 cells or PMN were adhered on 14-mm round glass slides coated with PLL (Liangyi, Dalian, China) and stimulated using activated complement complex, as described above, then fixed overnight in 2.5% glutaraldehyde at 4°C. For staining, slides were washed three times in PBS and blocked with goat serum working buffer (Zhongshanjinqiao, Beijing, China) and 2% BSA in PBS for 1 h at room temperature (RT). Rabbit anti-elastase (1:300, Merck) and mouse anti-histone H3 (1:500, Abcam) were used as primary antibodies in PBS containing 2% BSA for 1 h at RT. After washing, slides were incubated with goat anti-rabbit DyLight 488 (KPL) and goat anti-mouse Alexa Fluor 594 (Thermo) at 1:1,000 for 1 h at room temperature. Slides were then stained with DAPI and visualized using a confocal laser scanning microscope camera (Leica).

Observation of NET Formation by Scanning Electron Microscopy

dHL60 and PMN cells, treated as described above, were analyzed by scanning electron microscopy (SEM) after being fixed with 2.5% glutaraldehyde and dehydrated with gradually increased concentrations of ethanol (50, 70, 80, 90, and 100%), then dried with a critical point dryer and coated (Leica). Cells were observed using a Hitachi S-4800 scanning electron microscope (Hitachi High-Tech Corp., Tokyo, Japan).

Statistical Analysis

Results are presented as means ± standard error of the mean (SEM) and were analyzed by one-way analysis of variance using GraphPad Prism 7 software (San Diego, CA, USA); $p < 0.05$ was regarded as statistically significant.

RESULTS

Predicted Structure and C1q Binding Sites of *Ts*CRT

Homology modeling of the *T. spiralis* calreticulin structure was established using the crystal structure of human calreticulin arm domains (PDB: 3RG0) as a template; the molecules share 47.6% sequence similarity. The 3D structure of *Ts*CRT with the lowest PDF total energy was chosen (**Figure 1A**). *In silico* analysis of the *Ts*CRT amino acid sequence demonstrated that the structure of

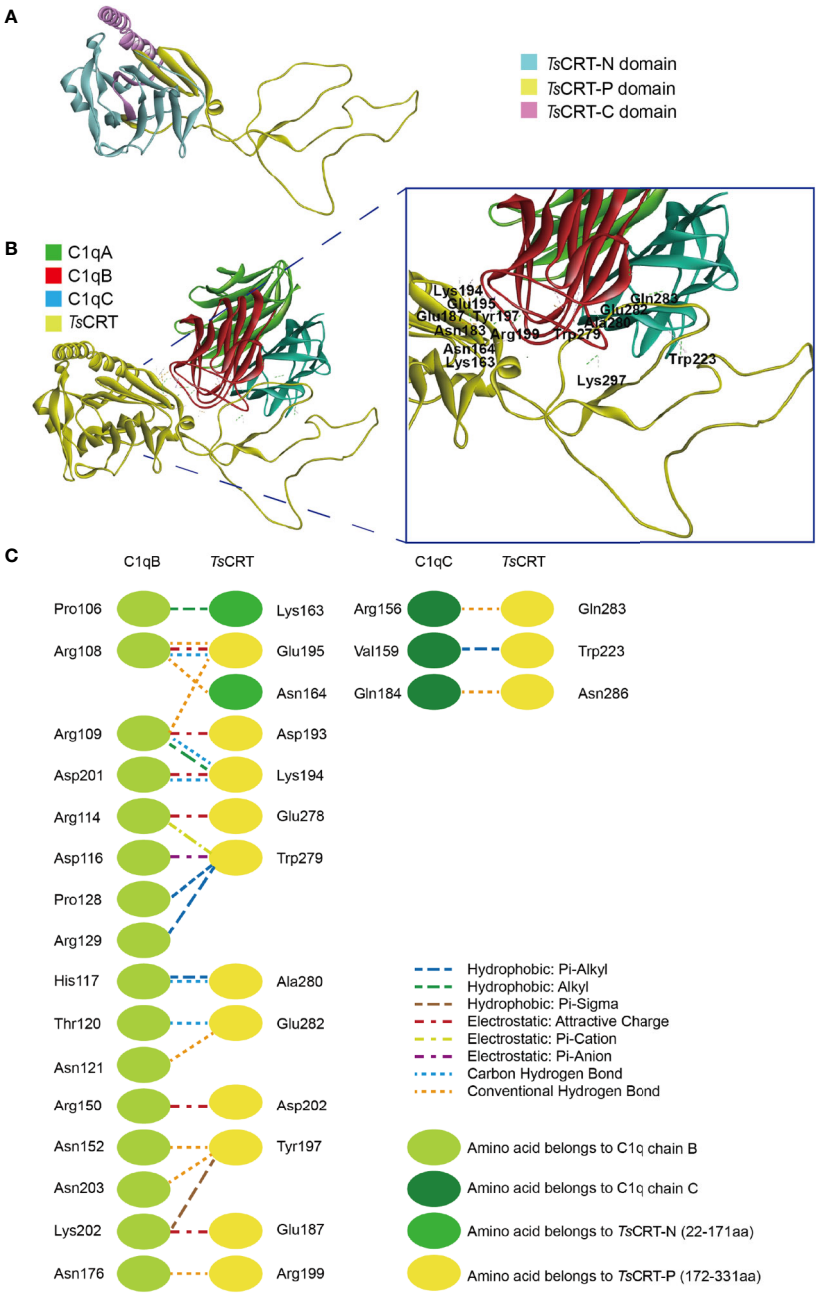

FIGURE 1 | Predicted protein–protein docking of *Ts*CRT and human C1q (1PK6) model. **(A)** Modeled 3D structure of *Ts*CRT, showing the N domain (light blue), P domain (yellow), and C domain (pink). **(B)** Predicted C1q binding site in *Ts*CRT located in the N and P domains, showing that C1qB and C1qC of C1q interact with *Ts*CRT amino acids. **(C)** Interface analysis of the C1q-*Ts*CRT binding site, showing amino acids and their bond details.

*Ts*CRT is composed of a globular domain (N-terminal β-sheet and C-terminal α-helix) and a proline-rich loop (P-domain). Analysis of the protein–protein interaction between *Ts*CRT and C1q showed that residues located within the *Ts*CRT N and P domains were involved in binding with C1q chains B and C (**Figure 1B**). Specifically, amino acids Lys^{163} and Asn^{164}, in the N-domain, and Glu^{187}, Asp^{193}, Lys^{194}, Glu^{195}, Tyr^{197}, Arg^{199}, Asp^{202}, Glu^{278}, Trp^{279}, Ala^{280}, and Glu^{282}, in the P-domain interacted with Pro^{B106}, Arg^{B108}, Arg^{B109}, Arg^{B114}, Asp^{B116}, His^{B117}, Thr^{B120}, Asn^{B121}, Pro^{B128}, Arg^{B129}, Arg^{B150}, Asn^{B152}, Asn^{B176}, Asp^{B201}, Lys^{B202}, and Asn^{B203} of the C1q B chain. Some amino acids Trp^{223}, Gln^{283}, and Asn^{286} in the P-domain are involved in interactions with Arg^{C156}, Val^{C159}, and Gln^{C184} in the C1q C chain (**Figure 1C**). The interaction between *Ts*CRT and C1q was mostly *via* hydrogen, electrostatic, and hydrophobic bonds. *In silico* docking predicted that C1q binding sites in

*Ts*CRT are mainly located between Lys^{163} in the N-domain and Asn^{286} in the P-domain.

Amino acids in human C1q involved in C1q–IgG, C1q–IgM, C1q–gC1qR, and C1q–*Ts*CRT interactions were also evaluated (17, 37, 38) (**Table 2**). The docking model suggested that C1q Arg^{B108}, Arg^{B109}, Arg^{B114}, His^{B117}, and Arg^{C156}, which were involved in interaction with C1q–*Ts*CRT, also contribute to the interactions with C1q–IgG, C1q–IgM, and C1q–gC1qR.

Expression and Characterization of Recombinant *Ts*CRT and Its Fragments

To determine the C1q binding sites and protein–protein interactions between C1q and *Ts*CRT, different fragments of *Ts*CRT, including full-length *Ts*CRT (*Ts*CRT, 22–413 aa), the NP-region (*Ts*CRT-NP, 22–331 aa), P-domain (*Ts*CRT-P, 172–331 aa), S-region (*Ts*CRT-S, 135–288 aa), and C-domain (*Ts*CRT-C, 332–413 aa) were expressed as recombinant proteins in *E. coli*. (19) (**Figure 2A**) and the His-tagged soluble recombinant proteins purified using nickel affinity chromatography. The results of SDS-PAGE showed that the purified recombinant full-length and fragment proteins of *Ts*CRT migrated at the predicted molecular weights (r*Ts*CRT 52 kDa, r*Ts*CRT-NP 46 kDa, r*Ts*CRT-P 32 kDa, r*Ts*CRT-S 27 kDa, and r*Ts*CRT-C 25 kDa) (**Figure 2B**). Endotoxin levels in the purified recombinant proteins were < 10 EU/mg.

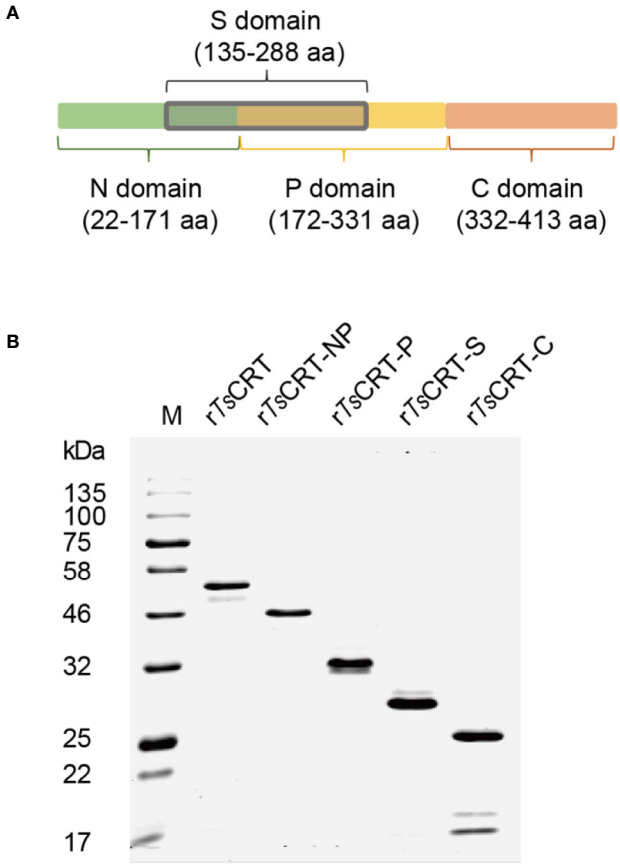

FIGURE 2 | Expression of recombinant *Ts*CRT and its fragment domains. **(A)** *Ts*CRT domain allocation. **(B)** r*Ts*CRT and its fragments (r*Ts*CRT-NP, r*Ts*CRT-P, r*Ts*CRT-S, and r*Ts*CRT-C) were expressed in *E. coli* and analyzed by SDS-PAGE.

*Ts*CRT-S Binds to Human C1q

The binding of different fragments of *Ts*CRT with C1q was confirmed using different immunological assays. ELISAs using C1q-coated plates demonstrated that r*Ts*CRT, r*Ts*CRT-NP, r*Ts*CRT-P, r*Ts*CRT-S, and r*Ts*CRT-C all bound to C1q in a C1q dose-dependent manner. When plates were coated with 0.8 μg/well of C1q, almost all fragments reached saturated binding at a protein concentration of 40 nM. Among the fragments, r*Ts*CRT-S showed the highest C1q binding capacity, with a similar level to that of r*Ts*CRT and significantly higher binding capacity than r*Ts*CRT-NP, r*Ts*CRT-P, and r*Ts*CRT-C ($p < 0.001$) (**Figure 3Aa**). There was no obvious binding of any *Ts*CRT fragment to BSA under the same conditions, indicating that r*Ts*CRT fragments bound specifically to C1q (**Figure 3Ab**).

Far western blotting with C1q transferred on to a membrane and incubated with different fragments of *Ts*CRT demonstrated that r*Ts*CRT, r*Ts*CRT-P, and r*Ts*CRT-S bound to C1qB, while r*Ts*CRT-NP mostly bound to C1qA, and r*Ts*CRT-C bound to C1qA and B, as determined by detection using anti-His antibody. From the binding density more C1q appeared to be bound to r*Ts*CRT-S and r*Ts*CRT than to r*Ts*CRT-P, r*Ts*CRT-NP, and r*Ts*CRT-C. There was no C1q bound to the BSA control (**Figure 3B**). Interestingly, C1q could not bind to denatured recombinant *Ts*CRT fragments transferred onto a membrane, indicating that C1q only binds to recombinant *Ts*CRT fragments with the correct tertiary confirmation (data not shown).

To confirm whether binding of r*Ts*CRT-S to C1q requires Ca^{2+}, an immunoprecipitation assay was performed to pull down C1q using r*Ts*CRT-S and anti-His IgG immobilized on ProteinG MicroBeads under non-denaturing conditions. C1q was only

TABLE 2 | Details of amino acids on human C1q that are involved in C1q–IgG, C1q–IgM, C1q–gC1qR and C1q–*Ts*CRT interactions.

	Amino acids	Reference
HuC1q-IgG	Arg^{A162}, Arg^{B108}, Arg^{B109}, Arg^{B114}, His^{B117}, Arg^{B129}, Arg^{B163}, Tyr^{B175}, and Arg^{C156}	(17, 37)
HuC1q-IgM	Arg^{B108}, Arg^{B109}, and Tyr^{B175}	(17)
HuC1q-gC1qR	Arg^{B114}, His^{B117}, Arg^{B163}, and Arg^{C156}	(38)
HuC1q-*Ts*CRT	Pro^{B106}, Arg^{B108}, Arg^{B109}, Arg^{B114}, Asp^{B116}, His^{B117}, Thr^{B120}, Asn^{B121}, Pro^{B128}, Arg^{B129}, Arg^{B150}, Asn^{B152}, Asn^{B176}, Asp^{B201}, Lys^{B202}, Asn^{B203}, Arg^{C156}, Val^{C159}, and Gln^{C184}	Shown in this manuscript

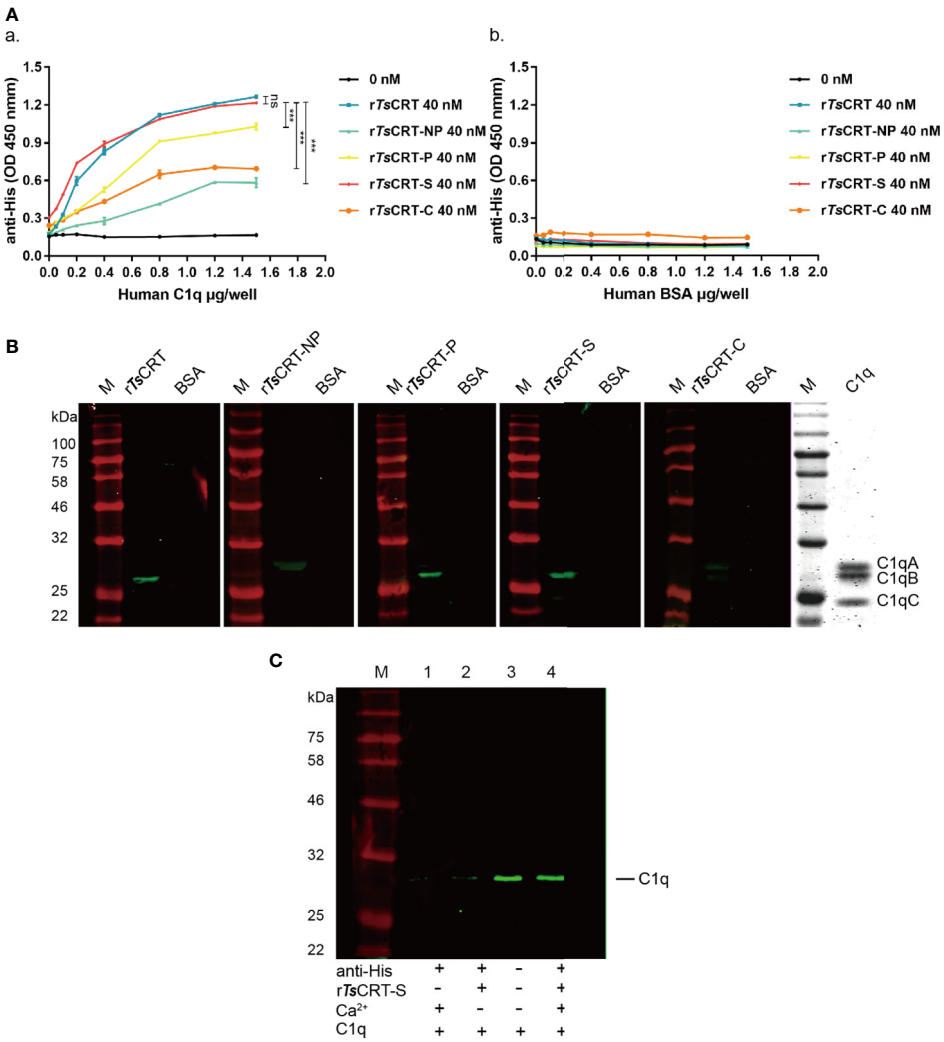

FIGURE 3 | Human C1q binding capacity of different *Ts*CRT fragments. **(A)** ELISA measurement of the binding capacities of different r*Ts*CRT fragments to plates coated with human C1q, detected using anti-His antibody (a). r*Ts*CRT and its fragments did not bind to the BSA control (b). Experiments were repeated three times. Data are shown as the mean ± SEM (***$p < 0.001$). **(B)** Far western blot showing the binding of C1q with r*Ts*CRT and its fragments. 5 μg of C1q and BSA were transferred to nitrocellulose membranes, then incubated with 5 μg/ml r*Ts*CRT, r*Ts*CRT-NP, r*Ts*CRT-P, r*Ts*CRT-S, and r*Ts*CRT-C and probed with anti-His antibody (1:5,000). C1q was separated by gel electrophoresis to assess the relative molecular weights of the A, B, and C chains. **(C)** Ca^{2+}-dependent r*Ts*CRT-S binding to C1q. C1q was pulled down by immunoprecipitation using r*Ts*CRT-S bound on anti-His IgG/ProteinG beads in the buffer with and without Ca^{2+}. Eluted complexes were separated by SDS-PAGE and transferred to a nitrocellulose membrane and then detected using a rabbit anti-C1qA antibody. M, molecular weight marker.

efficiently pulled down by r*Ts*CRT-S immobilized on beads in reaction buffer containing Ca^{2+}. In the absence of Ca^{2+} in the buffer, C1q was barely detectable on the stripped beads, similar to the reaction without r*Ts*CRT-S (**Figure 3C**). These results confirm that r*Ts*CRT-S has similar C1q binding ability to r*Ts*CRT and that the binding reaction requires the native conformation and is Ca^{2+} dependent.

*Ts*CRT-S Inhibits the Classical Complement Activation Pathway Through Binding to C1q

To determine the ability of r*Ts*CRT-S to inhibit C1q-initiated classical complement activation, the IgM-initiated C1q activation intermediate products, C4b and C3b, were measured using an ELISA assay. When 4 μg C1q was pre-incubated with different amounts of r*Ts*CRT-S, similar significant reductions in C4b and C3b products were observed in the reaction when 1 μg of r*Ts*CRT-S or 2 μg of r*Ts*CRT was added (**Figure 4A**).

The hemolysis caused by C1q-initiated classical complement activation was also significantly reduced by addition of r*Ts*CRT-S. As shown in **Figure 4B**, approximately 60% hemolysis occurred when C1q and C1q-D serum were added to sheep red blood cells (SRBCs) sensitized with rabbit anti-SRBC antibody; however, when C1q was pre-incubated with r*Ts*CRT-S, hemolysis was significantly reduced in a dose-dependent fashion. r*Ts*CRT-S as low as 0.5 μg inhibited hemolysis at a similar level to 4 μg r*Ts*CRT. There was no inhibitory effect when

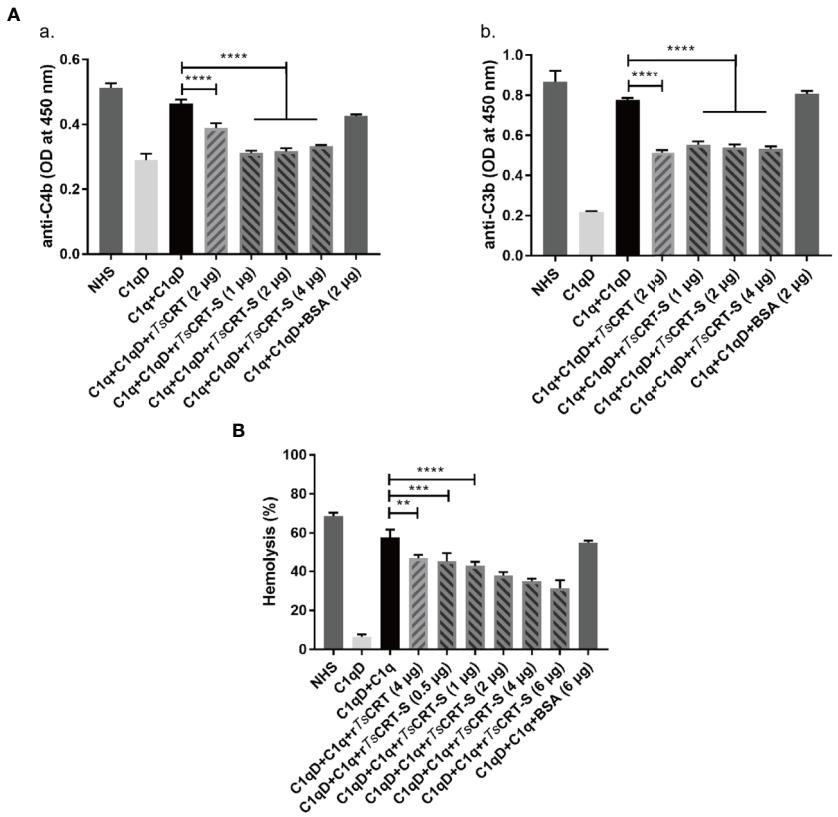

FIGURE 4 | Inhibition of classical complement activation by r*Ts*CRT-S binding to C1q. **(A)** Inhibition of IgM-C1q initiated activation of the intermediary products of classical complement activation, C4b/C3b, as detected by ELISA. C1q (1 μg) was pre-incubated with r*Ts*CRT-S (0, 1, 2, or 4 μg), r*Ts*CRT (2 μg), or BSA (2 μg), then transferred into a 96-well plate coated with human IgM (2 μg/ml). C1q-D serum was supplemented to trigger the IgM-C1q-activated classical pathway, and the generated C4b and C3b detected by anti-C4b and anti-C3b antibodies (1:5,000). **(B)** Sheep red blood cell (SRBC) hemolysis was inhibited in a dose-dependent manner when C1q (1 μg) was incubated with different amounts of r*Ts*CRT-S (0, 0.5, 1, 2, 4, or 6 μg). Each experiment was repeated three times. Data are shown as the mean ± SEM (**$p < 0.01$, ***$p < 0.001$, and ****$p < 0.0001$).

BSA control protein was used. These results indicate that r*Ts*CRT-S has the same, or even stronger, ability as r*Ts*CRT to inhibit the activation of the classical complement pathway by binding to C1q.

r*Ts*CRT-S Inhibits C1q Binding to Neutrophil-Like Cells

HL60 cells were treated with 1 μM ATRA for 5 days to induce differentiation into neutrophil-like cells (34), which was confirmed by the expression of CD11b and CD66a on their surface (data not shown). To investigate whether r*Ts*CRT-S, as well as r*Ts*CRT, could inhibit C1q binding to the C1q receptor on dHL60 cells, C1q was pre-incubated with various concentrations of r*Ts*CRT-S (0, 0.5, 1.0, and 2.0 μM) or 2 μM r*Ts*CRT. C1q binding on dHL60 was effectively inhibited by pre-incubation with r*Ts*CRT-S or r*Ts*CRT. Fluorescence density, measured by High Content Screening, showed that incubation with r*Ts*CRT-S significantly inhibited C1q binding on dHL60 and that 0.5 μM r*Ts*CRT-S induced inhibition at a similar level to that induced by 2 μM r*Ts*CRT (**Figure 5A**). Treatment with r*Ts*CRT-S or r*Ts*-CRT alone, without C1q, yielded no obvious fluorescence detection on cells. This inhibition was also detected by immunofluorescence using an anti-C1q antibody (**Figure 5B**). These results indicate that the binding of r*Ts*CRT-S or r*Ts*CRT to C1q can inhibit C1q binding to the C1q receptor on neutrophil-like dHL60 cells, possibly through competitive binding to C1q sites that bind to dHL60.

r*Ts*CRT-S Inhibits C1q-Induced Neutrophil Activity

To determine whether C1q-induced neutrophil chemotaxis could be suppressed by r*Ts*CRT-S binding, a transwell migration assay was conducted. The results showed that C1q alone attracted dHL60 migration through the inserted membrane; however, C1q-induced migration was significantly inhibited after C1q was incubated with different concentrations of r*Ts*CRT-S (**Figure 6A**). r*Ts*CRT also significantly inhibited C1q-induced neutrophil cell migration. BSA protein did not affect dHL60 cells attraction by C1q.

C1q induced neutrophil secretion of ROS and NE was measured to determine whether r*Ts*CRT-S or r*Ts*CRT interfered with C1q-triggered release of bioactive products by

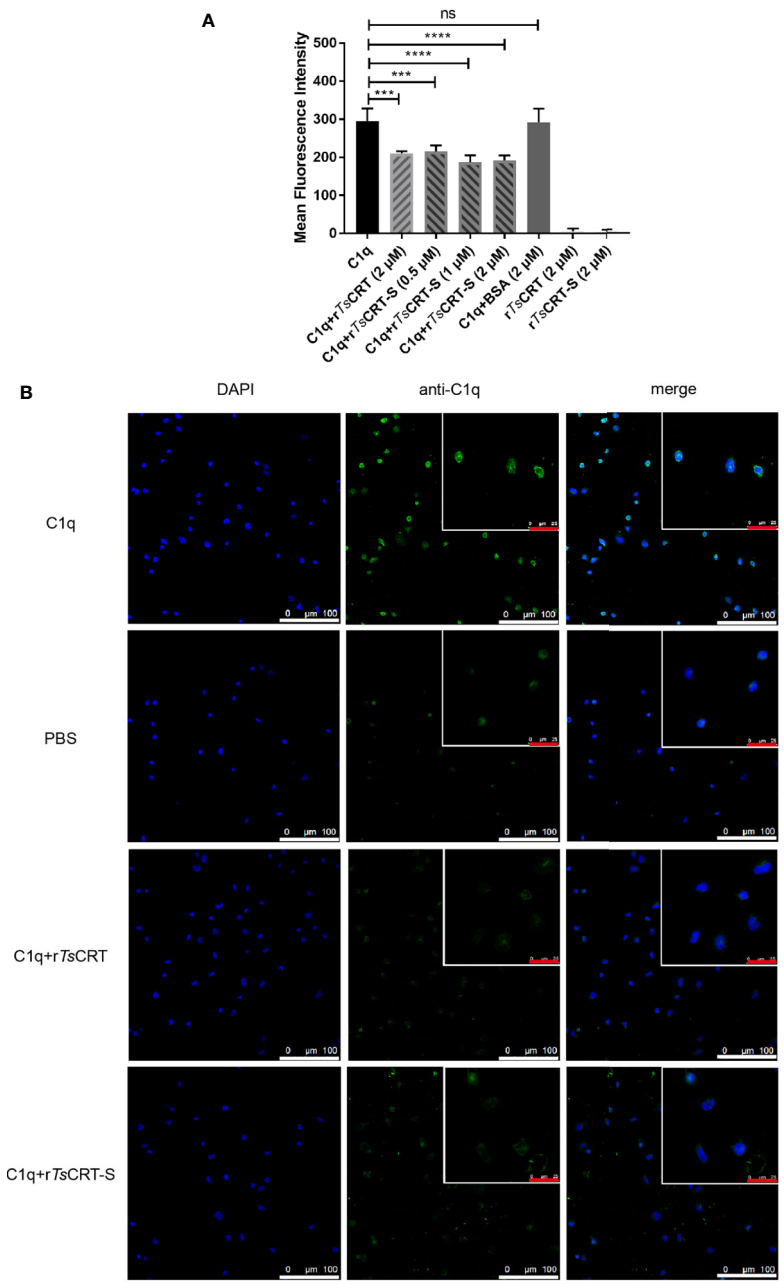

FIGURE 5 | r*Ts*CRT-S inhibited C1q binding to neutrophils. **(A)** C1q binding to neutrophils was inhibited by r*Ts*CRT-S, as detected by high-content screening. ATRA-stimulated dHL60 cells were incubated with C1q (25 nM) that had been pre-incubated with r*Ts*CRT-S (0, 0.5, 1, and 2 μM), r*Ts*CRT (2 μM), or BSA (2 μM). Binding of C1q on dHL60 cells was detected by anti-C1q mAb and DyLight 488-conjugated anti-Rat IgG (green). The experiment was repeated three times. Data are shown as the mean ± SEM (***$p < 0.001$, and ****$p < 0.0001$; ns = no significant difference). **(B)** Inhibition of C1q binding to dHL60 cells by r*Ts*CRT-S shown by confocal photography. Binding of C1q (green) on dHL60 cells is visible at the edge of the cells. Nuclei were stained with DAPI (blue). The white scale bars of the photographs represent 100 μm, and the red scale bars of the cells at the top right corner represent 25 μm.

neutrophils. C1q alone induced significant release of ROS and NE, which act as defense mechanisms to kill invading pathogens (39); however, binding with r*Ts*CRT-S or r*Ts*CRT significantly inhibited C1q stimulation of dHL60 cell release of ROS (**Figure 6B**) and NE (**Figure 6C**). The inhibitory effect was highest when 2 μM r*Ts*CRT-S or r*Ts*CRT was added. No obvious inhibition was detected following incubation of C1q with BSA (2 μM), whereas incubation of the cells with the ROS inhibitor, cysteamine, or the NE inhibitor, SPCK, significantly reduced the detectable levels of ROS and NE, respectively. PMA was used as positive control to stimulate neutrophil release of ROS and NE.

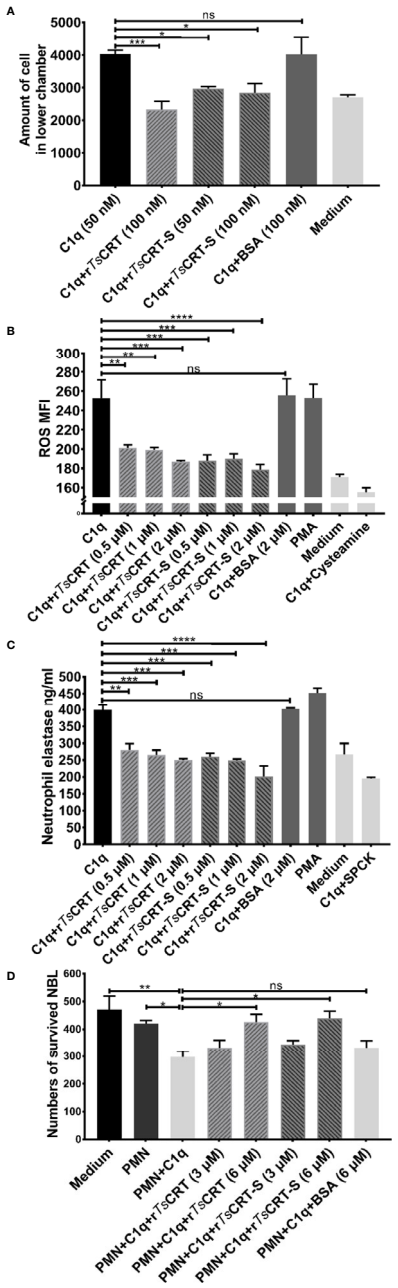

FIGURE 6 | r*Ts*CRT-S inhibited C1q-triggered neutrophil chemotaxis and function. **(A)** C1q-induced neutrophil chemotaxis was inhibited by r*Ts*CRT-S in a transwell migration chamber. The number of cells traversing the membrane was counted. **(B)** r*Ts*CRT-S inhibited dHL60 cell release of ROS and **(C)** neutrophil elastase (NE) through binding to C1q. DCFH-DA was used to probe ROS production, and NE substrate was used to evaluate NE production, which was also quantified as MFI. SPCK was used as an NE inhibitor and cysteamine used as a ROS inhibitor. **(D)** C1q-mediated neutrophil killing of NBL was inhibited by r*Ts*CRT-S. ATP activity was measured as a marker for NBL viability. ATP levels were calculated using a standard curve generated from the ATP levels in untreated control NBL. Each experiment was repeated three times. Data are shown as the mean ± SEM (*$p < 0.05$, **$p < 0.01$, ***$p < 0.001$, and ****$p < 0.0001$; ns = no significant difference).

To investigate the ability of C1q-induced neutrophils to attack NBL, an ATP-based larval viability assay was established. As shown in **Figure 6D**, C1q could directly induce PMN cells to attack and reduce the viability of NBL; however, when C1q was pre-incubated with r*Ts*CRT-S or r*Ts*CRT, C1q-induced PMN-mediated NBL killing was significantly reduced. At 6 μM r*Ts*CRT-S or r*Ts*CRT, C1q-induced PMN killing of NBL was completely inhibited. BSA had no effect on the ability of C1q to induce PMN killing of NBL.

These results indicate that r*Ts*CRT-S has similar effects to r*Ts*CRT in inhibiting C1q-induced neutrophil functions, including chemotaxis, release of bioactive products, and worm killing capacity.

r*Ts*CRT-S Inhibits IC-C1q-Induced NET Formation

To evaluate the effect of r*Ts*CRT-S on NET formation induced by the C1q-initiated classical complement pathway activation, IC (albumin/anti-albumin complex) was used to trigger C1q-induced activation. IC-initiated C1q-dependent complement activation significantly induced PMN to form NET; however, when C1q was pre-incubated with r*Ts*CRT-S, C1q-initiated NETosis was significantly reduced, as characterized by the reduction in free DNA (**Figure 7A**), reduction of extracellular fiber network formation, and reduction in levels of elastase and histone H3 released from the network fibers (**Figure 7B**). r*Ts*CRT-S dose-dependently inhibited the release of free DNA, with the highest inhibition achieved with 0.9 μM r*Ts*CRT-S, similar to the effect of r*Ts*CRT. NETosis was also reduced in dHL60 cells when C1q-initiated complement activation was inhibited by r*Ts*CRT-S binding (data not shown). These findings demonstrate that IC-C1q-initiated complement activation stimulates NETosis of PMN or neutrophil-like dHL60 cells and can be inhibited by r*Ts*CRT-S through binding to C1q.

DISCUSSION

Helminths have developed sophisticated mechanisms to escape host immune attack, particularly by producing molecules to modulate host immune responses, as a survival strategy. Complement is the first line of innate immunity in the defense against pathogen invasion, including with parasitic infections. Activated complement components not only directly attack pathogens by forming a membrane attack complex but also enhance the abilities of antibodies and effector cells (neutrophils, macrophages, and eosinophils, *etc*.) to clear microbes and damaged cells from the infected organism (7). Calreticulin is one such protein secreted by parasitic helminths to evade complement-mediated immune attack (13, 21, 40). The C1 complex, comprising C1q–C1s2–C1r2, is the initiator of the classical complement pathway. C1q is the major binding and effective target of helminth calreticulin in its interference with C1q-initiated classical complement activation, as well as C1q-mediated immune cell functions (4, 8).

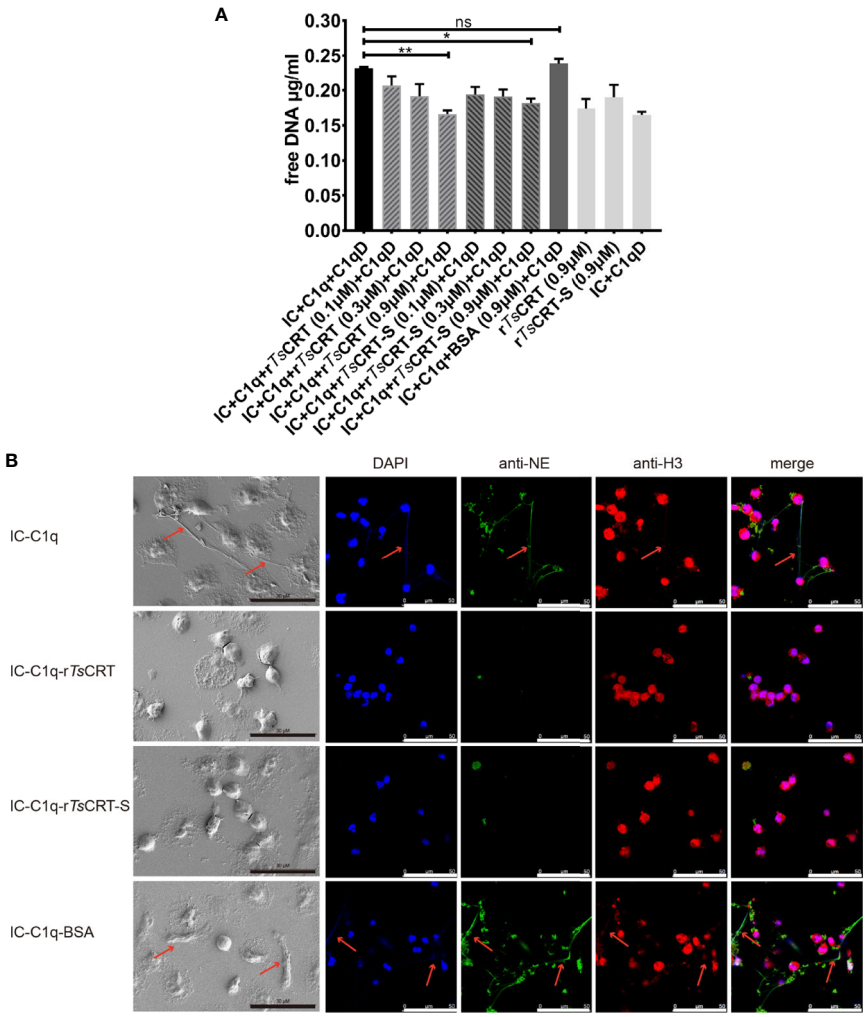

FIGURE 7 | r*Ts*CRT-S inhibits human PMN formation of neutrophil extracellular traps (NETs) through inhibiting C1q-initiated classical complement activation. **(A)** PMN release of free DNA was measured on treatment with C1q (2 μg) pre-incubated with r*Ts*CRT-S or r*Ts*CRT (0, 0.1, 0.3, and 0.9 μM) or BSA (0.9 μM). C1q-D serum and IC were added to activate the classical complement pathway. The free DNA experiment was repeated three times. Data are shown as means ± SEM (*$p < 0.05$, **$p < 0.01$; ns = no significant difference). **(B)** NETosis was visualized using scanning electron microscopy (SEM) and confocal immune fluorescence microscopy (IF). Reduced NETosis, and PMN release of NE and histone H3, were observed when C1q was incubated with r*Ts*CRT-S and r*Ts*CRT, but not the BSA control. The black scale bars of the SEM represent 30 μm, and the white scale bars of the IF represent 50 μm. Arrowheads indicate the NET formation.

In our previous study, we characterized *T. spiralis* calreticulin as a strong C1q binding protein that can inhibit the classical complement pathway and macrophage function (5). To determine the C1q binding site in *Ts*CRT, the 3D structure of *Ts*CRT was predicted, using the crystal structure of human calreticulin arm domains (PDB: 3RG0) as a template.

Molecular docking of *Ts*CRT with human complement C1q showed that amino acids in the C1q head region (particularly ghB and ghC) mainly interacted with the N-domain and P-domain of *Ts*CRT. In general, hydrophobic, electrostatic interactions and hydrogen bonds were formed among *Ts*CRT amino acids and HuC1q. It is also noteworthy that those amino acid residues (Arg^{B108}, Arg^{B109}, Arg^{B114}, His^{B117}, Arg^{C156}) on C1q involved in the C1q–*Ts*CRT interaction are also involved in C1q–IgG, C1q–IgM, and C1q–gC1qR interactions, indicating that *Ts*CRT binding to C1q could competitively block C1q binding to the IC, consequently inhibiting IC–C1q-initiated classical complement activation and other immune cell responses (**Table 2**).

As shown by the protein-protein docking model, r*Ts*CRT-S, which spans the N and P domains, exhibits C1q binding capacity, indicating its importance in the interaction of *Ts*CRT with C1q. This is in accordance with previous publications describing that the C1q binding site in calreticulin was mainly localized to the S-domain (11, 19). Based on this analysis, the *Ts*CRT domain fragments, including the S-domain, were expressed as recombinant proteins in *E. coli*. Binding assays with different *Ts*CRT fragments confirmed that r*Ts*CRT-S has C1q binding capacity similar to that of full-length r*Ts*CRT, and significantly stronger than those of the other fragments (r*Ts*CRT-NP,

r*Ts*CRT-P, and r*Ts*CRT-C). We also demonstrate that C1q binding ability of r*Ts*CRT-S is dependent on the tertiary protein conformation and Ca^{2+} dependent. r*Ts*CRT-S could not bind to C1q under denaturing conditions or in the absence of Ca^{2+}. Hence, our results show that Ca^{2+} binding is not only an intrinsic property of CRT, but also necessary for C1q binding with its ligands that is in accordance with the previous study (37). Far western blotting with C1q transferred onto a membrane and bound to different fragments of *Ts*CRT confirmed that r*Ts*CRT-S bound strongly to C1qB, similar to full-length *Ts*CRT. Surprisingly, r*Ts*CRT-NP primarily bound to C1qA, while r*Ts*CRT-C bound to both C1qA and C1qB. Although *Ts*CRT-S is located within *Ts*CRT-NP, the latter showed lower C1q binding capacity and bound to a different part of the C1q complex C1qA, while r*Ts*CRT-S bound to C1qB. It is possible that r*Ts*CRT-NP exhibits a different tertiary conformational structure compared with r*Ts*CRT-S.

Our results confirm that the C1q binding site in *Ts*CRT is located in *Ts*CRT-S. Further, our study demonstrates that r*Ts*CRT-S shared a comparable capacity with full-length r*Ts*CRT to interfere with human C1q functions through C1q binding. After binding to C1q, r*Ts*CRT-S significantly inhibited the IgM–C1q-initiated classical complement activation pathway, characterized by a reduction in intermediate products (C4b and C3b) and reduced sheep red blood cell hemolysis.

In addition to inhibiting the C1q-initiated classical complement pathway, r*Ts*CRT-S also inhibited C1q binding to its ligands on neutrophils and their consequent functions. Neutrophils express C1q receptor on their surface and C1q induces neutrophil chemotaxis to inflammatory sites and stimulates neutrophil degranulation and production of oxidative and effector products as an immune response to invaded pathogens (14, 15). Surface gC1qR binds to the globular heads of C1q and enhances the chemotactic potency of C1q (14). In this study, we demonstrate that, after being bound with r*Ts*CRT-S, binding of C1q to the surface of ATRA-stimulated dHL60 (neutrophil-like) cells was inhibited, possibly through competitive binding to the C1q receptor on dHL60 cells. Binding with r*Ts*CRT-S not only significantly reduced the chemotaxis effects of C1q on neutrophils (dHL60 cells), as detected by transwell chamber assays, but also significantly reduced dHL60 cells release of NE and ROS.

Neutrophils are often the first cells to be recruited to the site of invaded pathogens, such as parasitic helminths. ROS and granular proteins (NE, *etc.*) are directly involved in killing and clearing infections (41, 42). In early studies to determine the immune mechanisms involved in the expulsion of *T. spiralis* infection, the oxidative products and granular proteins released by neutrophils were identified as toxic to NBL (43, 44). C1q can trigger neutrophil release of toxic ROS and granular proteins by a unique CD18-dependent mechanism (15). Here, we determined that binding with r*Ts*CRT-S significantly reduced the function of C1q, thereby decreasing neutrophil release of ROS and NE. When *T. spiralis* NBL were incubated with PMN isolated from human peripheral blood in the presence of C1q for 48 h, 30% of them died; however after binding with 6 μM r*Ts*CRT-S, C1q induced PMN killing of NBL was completed inhibited, indicating that r*Ts*CRT-S can completely inhibit C1q-induced neutrophil killing of NBL in the same way as full-length r*Ts*CRT, possibly through inhibiting C1q-triggered release of oxidative ROS and NE by neutrophils. Furthermore, eosinophils are also important effector cells involved in the protective immunity against helminth infection, mostly associated with the antibody-dependent cell-mediated cytotoxicity (ADCC) (45). Even though there is no evidence that calreticulin is directly involved in the modification of eosinophil functions, it is worth to explore the possible interference of *Ts*CRT with eosinophils since the C1q receptor is also expressed on eosinophils (46).

In addition to directly releasing anti-microbials (such as ROS and NE) to clear the invaded pathogens, neutrophils also secrete chromatin and granule proteins to form extracellular fibril matrices, NET, which were first described as a strategy by which neutrophils capture and kill extracellular pathogens (24). C1q-initiated classical complement activation is involved in NETosis (26). In this study we demonstrate that NETosis is significantly reduced when C1q is pre-incubated with r*Ts*CRT-S, and IC-C1q-iniated classical complement activation was inhibited, indicating that *T. spiralis* secrets *Ts*CRT to inhibit C1q-induced NETosis as another approach to escape immune attack. In addition to their immune-protective function, NET are involved in a number of diseases with immunological pathology (25). An increasing number of clinical cases show that excessive NET accumulation is associated with atherosclerosis, tumor metastasis, and autoimmune diseases (systemic lupus erythematosus, rheumatoid arthritis, etc.) (25, 29). Therefore, inhibition of NETosis has been targeted to develop therapeutics aimed at mitigating excessive complement activation-induced and NET-related autoimmune diseases (47). Due to its specific inhibition of NETosis through inhibiting C1q-induced complement activation, r*Ts*CRT-S has potential for use as a therapeutic agent to ease NET-related autoimmune diseases. Further, because of their strong immunomodulatory functions, helminth infections and helminth-derived proteins have been successfully used to treat a variety of allergies, autoimmune diseases, and other immune dysregulation disorders, such as type 1 diabetes, systemic lupus erythematosus, rheumatoid arthritis, and inflammatory bowel disease (48–52). Our previous studies have demonstrated that *T. spiralis* infection significantly mitigated collagen-induced arthritis via PD-1 mediated immunomodulation (49), that *T. spiralis*-derived excretory/secretory products ameliorate inflammatory colitis in experimental mouse models (53), and that *T. spiralis* adult extracts have preventive and therapeutic effects on asthma inflammation (54). Since *Ts*CRT is secreted by *T. spiralis* as an immunomodulatory protein to neutralize C1q-induced complement activation as an immune escape strategy, there is potential that *Ts*CRT-S could be developed as a therapeutic agent for complement-involved autoimmune diseases.

Overall, we have determined that the dominant C1q binding site in *Ts*CRT is located within *Ts*CRT-S. The 153 amino acid *Ts*CRT-S functional domain has the same capacity as full-length *Ts*CRT to bind to C1q, inhibit C1q-induced complement activation, and interfere with other C1q-induced immune cell activation and functions. The interaction between *Ts*CRT-S and

C1q not only directly inhibits membrane damage of parasites caused by C1q-iniatiated classic complement activation, but also inhibits C1q-induced neutrophil parasite killing. The findings of this study further elucidate the immune evasion mechanism of *T. spiralis*, which warrants future study as a target for development of therapeutic drugs or preventive vaccines against trichinellosis. As IC-C1q-induced formation of NET was effectively inhibited by *Ts*CRT-S, there is potential for development of *Ts*CRT-S as therapeutic agent to inhibit NET-involved pathologies, such as autoimmune diseases. Since *Ts*CRT-S is a small functional domain, which confers the full complement of modulatory functions of full-length *Ts*CRT, it will be easier to develop this functional domain as vaccine or therapeutic target, rather than the full-length protein.

CONCLUSION

We found that *Ts*CRT binds human complement C1q is mediated by its S-domain. Molecular docking modeling and fragment expression revealed that *Ts*CRT-S is responsible for C1q binding. Similar to the full length of *Ts*CRT, r*Ts*CRT-S expressed in *Escherichia coli* showed the same capacity to bind and therefore inhibit human C1q-induced complement activation. The interaction could also inhibit release of reactive oxygen species and elastase by neutrophil when triggered by C1q, resulting in reduced neutrophil killing of NBL. Lastly, binding of *Ts*CRT-S to C1q also inhibited formation of neutrophil extracellular traps (NET) indicating a potential therapeutical application in treating autoimmune diseases.

DATA AVAILABILITY STATEMENT

The original contributions presented in the study are included in the article/supplementary materials. Further inquiries can be directed to the corresponding author.

ETHICS STATEMENT

The studies involving human participants were reviewed and approved by Institutional Review Board of Capital Medical University (approval number: 2016SY01). The ethics committee waived the requirement of written informed consent for participation. The animal study was reviewed and approved by Capital Medical University Animal Care and Use Committee (approval number: AEEI-2017-133).

AUTHOR CONTRIBUTIONS

XZ and SS conceived and designed the experiments. SS, CH, QZ, LZ, YC, and JH performed the experiments. SS, BZ, and XZ analyzed the data. SS, BZ, and XZ drafted the paper. XZ, BZ, CH, LZ, YC, and JH revised the paper. All authors agreed to be accountable for all aspects of the work in ensuring that questions related to the accuracy or integrity of any part of the work are appropriately investigated and resolved. All authors contributed to the article and approved the submitted version.

FUNDING

This work was supported by a grant from the National Natural Science Foundation of China (81672042).

ACKNOWLEDGMENTS

We thank Ming Xue and Xiaoyi Zhang from Capital Medical University for their help with protein–protein docking modeling. We thank Junfei Wei from Baylor College of Medicine for the suggestions in protein expression. We thank Yuli Cheng, Ximeng Sun, Yuan Gu, Qing Sun, Sha Liu, Zhihui Jia, and Jin Pan from Capital Medical University for all their invaluable efforts and technical assistance.

REFERENCES

1. Dupouy-Camet J. Trichinellosis: a worldwide zoonosis. *Vet Parasitol* (2000) 93(3-4):191–200. doi: 10.1016/s0304-4017(00)00341-1
2. Gottstein B, Pozio E, Nockler K. Epidemiology, diagnosis, treatment, and control of trichinellosis. *Clin Microbiol Rev* (2009) 22(1):127–45. doi: 10.1128/cmr.00026-08.
3. Leid RW. Parasites and complement. *Adv Parasitol* (1988) 27:131–68. doi: 10.1016/s0065-308x(08)60354-1
4. Shao S, Sun X, Chen Y, Zhan B, Zhu X. Complement Evasion: An Effective Strategy That Parasites Utilize to Survive in the Host. *Front Microbiol* (2019) 10:532. doi: 10.3389/fmicb.2019.00532
5. Zhao L, Shao S, Chen Y, Sun X, Sun R, Huang J, et al. Trichinella spiralis Calreticulin Binds Human Complement C1q As an Immune Evasion Strategy. *Front Immunol* (2017) 8:636. doi: 10.3389/fimmu.2017.00636
6. Kishore U, Reid KB. C1q: structure, function, and receptors. *Immunopharmacology* (2000) 49(1-2):159–70. doi: 10.1016/s0162-3109(00)80301-x
7. Nayak A, Ferluga J, Tsolaki AG, Kishore U. The non-classical functions of the classical complement pathway recognition subcomponent C1q. *Immunol Lett* (2010) 131(2):139–50. doi: 10.1016/j.imlet.2010.03.012
8. Thielens NM, Tedesco F, Bohlson SS, Gaboriaud C, Tenner AJ. C1q: A fresh look upon an old molecule. *Mol Immunol* (2017) 89:73–83. doi: 10.1016/j.molimm.2017.05.025
9. Ramirez-Toloza G, Ferreira A. Trypanosoma cruzi Evades the Complement System as an Efficient Strategy to Survive in the Mammalian Host: The Specific Roles of Host/Parasite Molecules and Trypanosoma cruzi Calreticulin. *Front Microbiol* (2017) 8:1667. doi: 10.3389/fmicb.2017.01667
10. Ramirez-Toloza G, Sosoniuk-Roche E, Valck C, Aguilar-Guzman L, Ferreira VP, Ferreira A. Trypanosoma cruzi Calreticulin: Immune Evasion, Infectivity, and Tumorigenesis. *Trends Parasitol* (2020) 36(4):368–81. doi: 10.1016/j.pt.2020.01.007
11. Yadav S, Gupta S, Selvaraj C, Doharey PK, Verma A, Singh SK, et al. In silico and in vitro studies on the protein-protein interactions between Brugia malayi immunomodulatory protein calreticulin and human C1q. *PloS One* (2014) 9(9):e106413. doi: 10.1371/journal.pone.0106413
12. Suchitra S, Joshi P. Characterization of Haemonchus contortus calreticulin suggests its role in feeding and immune evasion by the parasite. *Biochim Biophys Acta* (2005) 1722(3):293–303. doi: 10.1016/j.bbagen.2004.12.020
13. Kasper G, Brown A, Eberl M, Vallar L, Kieffer N, Berry C, et al. A calreticulin-like molecule from the human hookworm Necator americanus interacts with

C1q and the cytoplasmic signalling domains of some integrins. *Parasite Immunol* (2001) 23(3):141–52. doi: 10.1046/j.1365-3024.2001.00366.x
14. Leigh LE, Ghebrehiwet B, Perera TP, Bird IN, Strong P, Kishore U, et al. C1q-mediated chemotaxis by human neutrophils: involvement of gClqR and G-protein signalling mechanisms. *Biochem J* (1998) 330(Pt 1):247–54. doi: 10.1042/bj3300247
15. Goodman EB, Anderson DC, Tenner AJ. C1q triggers neutrophil superoxide production by a unique CD18-dependent mechanism. *J leukocyte Biol* (1995) 58(2):168–76. doi: 10.1002/jlb.58.2.168
16. Kolaczkowska E, Kubes P. Neutrophil recruitment and function in health and inflammation. *Nat Rev Immunol* (2013) 13(3):159–75. doi: 10.1038/nri3399
17. Ghai R, Waters P, Roumenina LT, Gadjeva M, Kojouharova MS, Reid KB, et al. C1q and its growing family. *Immunobiology* (2007) 212(4-5):253–66. doi: 10.1016/j.imbio.2006.11.001
18. Michalak M, Groenendyk J, Szabo E, Gold LI, Opas M. Calreticulin, a multi-process calcium-buffering chaperone of the endoplasmic reticulum. *Biochem J* (2009) 417(3):651–66. doi: 10.1042/bj20081847
19. Stuart GR, Lynch NJ, Lu J, Geick A, Moffatt BE, Sim RB, et al. Localisation of the C1q binding site within C1q receptor/calreticulin. *FEBS Lett* (1996) 397(2-3):245–9. doi: 10.1016/s0014-5793(96)01156-8
20. Stuart GR, Lynch NJ, Day AJ, Schwaeble WJ, Sim RB. The C1q and collectin binding site within C1q receptor (cell surface calreticulin). *Immunopharmacology* (1997) 38(1-2):73–80. doi: 10.1016/s0162-3109(97)00076-3
21. Naresha S, Suryawanshi A, Agarwal M, Singh BP, Joshi P. Mapping the complement C1q binding site in Haemonchus contortus calreticulin. *Mol Biochem Parasitol* (2009) 166(1):42–6. doi: 10.1016/j.molbiopara.2009.02.007
22. Holers VM. Complement and Its Receptors: New Insights into Human Disease. *Annu Rev Immunol* (2014) 32(1):433–59. doi: 10.1146/annurev-immunol-032713-120154
23. Leffler J, Bengtsson AA, Blom AM. The complement system in systemic lupus erythematosus: an update. *Ann Rheum Dis* (2014) 73(9):1601–6. doi: 10.1136/annrheumdis-2014-205287
24. Sollberger G, Tilley DO, Zychlinsky A. Neutrophil Extracellular Traps: The Biology of Chromatin Externalization. *Dev Cell* (2018) 44(5):542–53. doi: 10.1016/j.devcel.2018.01.019
25. Papayannopoulos V. Neutrophil extracellular traps in immunity and disease. *Nat Rev Immunol* (2018) 18(2):134–47. doi: 10.1038/nri.2017.105
26. de Bont CM, Boelens WC, Pruijn GJM. NETosis, complement, and coagulation: a triangular relationship. *Cell Mol Immunol* (2019) 16(1):19–27. doi: 10.1038/s41423-018-0024-0
27. Sorensen OE, Borregaard N. Neutrophil extracellular traps - the dark side of neutrophils. *J Clin Invest* (2016) 126(5):1612–20. doi: 10.1172/jci84538
28. Jorch SK, Kubes P. An emerging role for neutrophil extracellular traps in noninfectious disease. *Nat Med* (2017) 23(3):279–87. doi: 10.1038/nm.4294
29. Lee KH, Kronbichler A, Park DD, Park Y, Moon H, Kim H, et al. Neutrophil extracellular traps (NETs) in autoimmune diseases: A comprehensive review. *Autoimmun Rev* (2017) 16(11):1160–73. doi: 10.1016/j.autrev.2017.09.012
30. Trouw LA, Pickering MC, Blom AM. The complement system as a potential therapeutic target in rheumatic disease. *Nat Rev Rheumatol* (2017) 13(9):538–47. doi: 10.1038/nrrheum.2017.125
31. Rincón E, Rocha-Gregg BL, Collins SR. A map of gene expression in neutrophil-like cell lines. *BMC genomics* (2018) 19(1):573. doi: 10.1186/s12864-018-4957-6
32. Verstuyf A, Mathieu C, Verlinden L, Waer M, Tan BK, Bouillon R. Differentiation induction of human leukemia cells (HL60) by a combination of 1,25-dihydroxyvitamin D3 and retinoic acid (all trans or 9-cis). *J Steroid Biochem Mol Biol* (1995) 53(1-6):431–41. doi: 10.1016/0960-0760(95)00089-i
33. Almzaiel AJ, Billington R, Smerdon G, Moody AJ. Effects of hyperbaric oxygen treatment on antimicrobial function and apoptosis of differentiated HL-60 (neutrophil-like) cells. *Life Sci* (2013) 93(2-3):125–31. doi: 10.1016/j.lfs.2013.06.003
34. Mihara K, Nakayama T, Saitoh H. A Convenient Technique to Fix Suspension Cells on a Coverslip for Microscopy. *Curr Protoc Cell Biol* (2015) 68:4.30.1–4.10. doi: 10.1002/0471143030.cb0430s68
35. Riss TL, Moravec RA, Niles AL, Duellman S, Benink HA, Worzella TJ, et al. Cell Viability Assays. In: GS Sittampalam, A Grossman, K Brimacombe, M Arkin, D Auld, CP Austin, et al., editors. *Assay Guidance Manual*. Bethesda (MD: Eli Lilly & Company and the National Center for Advancing Translational Sciences (2004).
36. Ishiwata K, Watanabe N. Nippostrongylus brasiliensis: reversibility of reduced-energy status associated with the course of expulsion from the small intestine in rats. *Exp Parasitol* (2007) 117(1):80–6. doi: 10.1016/j.exppara.2007.03.019
37. Gaboriaud C, Juanhuix J, Gruez A, Lacroix M, Darnault C, Pignol D, et al. The crystal structure of the globular head of complement protein C1q provides a basis for its versatile recognition properties. *J Biol Chem* (2003) 278(47):46974–82. doi: 10.1074/jbc.M307764200
38. Pednekar L, Pathan AA, Paudyal B, Tsolaki AG, Kaur A, Abozaid SM, et al. Analysis of the Interaction between Globular Head Modules of Human C1q and Its Candidate Receptor gC1qR. *Front Immunol* (2016) 7:567. doi: 10.3389/fimmu.2016.00567
39. Chen Y, Junger WG. Measurement of oxidative burst in neutrophils. *Methods Mol Biol (Clifton NJ)* (2012) 844:115–24. doi: 10.1007/978-1-61779-527-5_8
40. Mendlovic F, Ostoa-Saloma P, Solis CF, Martinez-Ocana J, Flisser A, Laclette JP. Cloning, characterization, and functional expression of Taenia solium calreticulin. *J Parasitol* (2004) 90(4):891–3. doi: 10.1645/ge-3325rn
41. Freudenstein-Dan A, Gold D, Fishelson Z. Killing of schistosomes by elastase and hydrogen peroxide: implications for leukocyte-mediated schistosome killing. *J Parasitol* (2003) 89(6):1129–35. doi: 10.1645/ge-96r
42. Rajamanickam A, Munisankar S, Bhootra Y, Dolla CK, Nutman TB, Babu S. Elevated Systemic Levels of Eosinophil, Neutrophil, and Mast Cell Granular Proteins in Strongyloides Stercoralis Infection that Diminish following Treatment. *Front Immunol* (2018) 9:207. doi: 10.3389/fimmu.2018.00207
43. Bass DA, Szejda P. Mechanisms of killing of newborn larvae of Trichinella spiralis by neutrophils and eosinophils. Killing by generators of hydrogen peroxide in vitro. *J Clin Invest* (1979) 64(6):1558–64. doi: 10.1172/jci109616
44. Venturiello SM, Giambartolomei GH, Costantino SN. Immune killing of newborn Trichinella larvae by human leucocytes. *Parasite immunology* (1993) 15(10):559–64. doi: 10.1111/pim.1993.15
45. Huang L, Appleton JA. Eosinophils in Helminth Infection: Defenders and Dupes. *Trends Parasitol* (2016) 32(10):798–807. doi: 10.1016/j.pt.2016.05.004
46. Kuna P, Iyer M, Peerschke EI, Kaplan AP, Reid KB, Ghebrehiwet B. Human C1q induces eosinophil migration. *Clin Immunol Immunopathol* (1996) 81(1):48–54. doi: 10.1006/clin.1996.0156
47. Barnado A, Crofford LJ, Oates JC. At the Bedside: Neutrophil extracellular traps (NETs) as targets for biomarkers and therapies in autoimmune diseases. *J leukocyte Biol* (2016) 99(2):265–78. doi: 10.1189/jlb.5BT0615-234R
48. Wu Z, Wang L, Tang Y, Sun X. Parasite-Derived Proteins for the Treatment of Allergies and Autoimmune Diseases. *Front Microbiol* (2017) 8:2164. doi: 10.3389/fmicb.2017.02164
49. Cheng Y, Zhu X, Wang X, Zhuang Q, Huyan X, Sun X, et al. Trichinella spiralis Infection Mitigates Collagen-Induced Arthritis via Programmed Death 1-Mediated Immunomodulation. *Front Immunol* (2018) 9:1566. doi: 10.3389/fimmu.2018.01566
50. Lund ME, Greer J, Dixit A, Alvarado R, McCauley-Winter P, To J, et al. A parasite-derived 68-mer peptide ameliorates autoimmune disease in murine models of Type 1 diabetes and multiple sclerosis. *Sci Rep* (2016) 6:37789. doi: 10.1038/srep37789
51. Segal Y, Blank M, Shoenfeld Y. Tuftsin phosphorylcholine-a novel compound harnessing helminths to fight autoimmunity. *Immunol Res* (2018) 66(6):637–41. doi: 10.1007/s12026-018-9051-2
52. Wang M, Wu L, Weng R, Zheng W, Wu Z, Lv Z. Therapeutic potential of helminths in autoimmune diseases: helminth-derived immune-regulators and immune balance. *Parasitol Res* (2017) 116(8):2065–74. doi: 10.1007/s00436-017-5544-5
53. Yang X, Yang Y, Wang Y, Zhan B, Gu Y, Cheng Y, et al. Excretory/secretory products from Trichinella spiralis adult worms ameliorate DSS-induced colitis in mice. *PloS One* (2014) 9(5):e96454. doi: 10.1371/journal.pone.0096454
54. Sun S, Li H, Yuan Y, Wang L, He W, Xie H, et al. Preventive and therapeutic effects of Trichinella spiralis adult extracts on allergic inflammation in an

experimental asthma mouse model. *Parasites Vectors* (2019) 12(1):326. doi: 10.1186/s13071-019-3561-1

Conflict of Interest: The authors declare that the research was conducted in the absence of any commercial or financial relationships that could be construed as a potential conflict of interest.

Advantages of publishing in Frontiers

OPEN ACCESS
Articles are free to read for greatest visibility and readership

FAST PUBLICATION
Around 90 days from submission to decision

HIGH QUALITY PEER-REVIEW
Rigorous, collaborative, and constructive peer-review

TRANSPARENT PEER-REVIEW
Editors and reviewers acknowledged by name on published articles

Frontiers
Avenue du Tribunal-Fédéral 34
1005 Lausanne | Switzerland

Visit us: www.frontiersin.org
Contact us: frontiersin.org/about/contact

REPRODUCIBILITY OF RESEARCH
Support open data and methods to enhance research reproducibility

DIGITAL PUBLISHING
Articles designed for optimal readership across devices

FOLLOW US
@frontiersin

IMPACT METRICS
Advanced article metrics track visibility across digital media

EXTENSIVE PROMOTION
Marketing and promotion of impactful research

LOOP RESEARCH NETWORK
Our network increases your article's readership